UCLA
UCLA Electronic Theses and Dissertations

Title

Total Synthesis of Tubingensin B and Nickel-Catalyzed Methodologies Involving C–O or C–N Bond Activation

Permalink

https://escholarship.org/uc/item/5p24m4dt

Author

Kim, Junyong

Publication Date

2018

Peer reviewed|Thesis/dissertation

eScholarship.org Powered by the California Digital Library
University of California

UNIVERSITY OF CALIFORNIA

Los Angeles

Total Synthesis of Tubingensin B and Nickel-Catalyzed Methodologies Involving C–O or C–N Bond Activation

A dissertation submitted in partial satisfaction of the

requirements for the degree Doctor of Philosophy

in Chemistry

by

Junyong Kim

2018

© Copyright by

Junyong Kim

2018

ABSTRACT OF THE DISSERTATION

Total Synthesis of Tubingensin B and Nickel-Catalyzed Methodologies Involving C–O or C–N Bond Activation

by

Junyong Kim

Doctor of Philosophy in Chemistry

University of California, Los Angeles, 2018

Professor Neil Kamal Garg, Chair

This dissertation describes the total synthesis of tubingensin B and the development of two nickel-catalyzed methods. The two methodologies include the amination of aryl electrophiles in the green solvent 2-methyl-THF and the Suzuki–Miyaura coupling of aliphatic amides via the activation of amide C–N bonds.

Chapter One highlights indole terpenoid natural products as the inspiration for the development of new synthetic methodologies and innovative strategies. This review showcases recent total syntheses of the natural products, penitrem D, emindole SB, paspaline, dixiamycin B, and tubingensins A and B.

Chapter Two pertains to the total synthesis of (–)-tubingensin B. Key steps of the synthesis involves a *B*-alkyl Suzuki–Miyaura reaction, a carbazolyne cyclization, and a radical cyclization to construct the core architecture of the molecule. Key to the synthesis of tubingensin

B was the utilization of a heterocyclic aryne intermediate for the formation of a scaffold bearing vicinal quaternary centers. This synthesis illustrates the capability of aryne methodology in generating stereochemically complex structures.

Chapter Three describes the development of a green variant of a nickel-catalyzed amination reaction. As solvents comprise 85% of pharmaceutical waste, the use of a green solvent provides a considerable benefit for the potential application of the methodology to industrial problems. We developed a method employing 2-Me-THF as a green solvent for the amination of aryl chlorides and sulfamates.

Chapter Four demonstrates the nickel-catalyzed Suzuki–Miyaura coupling of aliphatic amide derivatives. The methodology can be used to activate typically unreactive amide C–N bonds and, in turn, access an array of heterocyclic ketones.

The dissertation of Junyong Kim is approved.

Yi Tang

Jennifer M. Murphy

Neil Kamal Garg, Committee Chair

University of California, Los Angeles

2018

To my parents Changman Kim and Namhee Baek

TABLE OF CONTENTS

ABSTRACT OF THE DISSERTATION ii

COMMITTEE PAGE iv

DEDICATION PAGE v

TABLE OF CONTENTS vi

LIST OF FIGURES x

LIST OF SCHEMES xx

LIST OF TABLES xxi

LIST OF ABBREVIATIONS xxii

ACKNOWLEDGEMENTS xxviii

BIOGRAPHICAL SKETCH xxxiii

CHAPTER ONE: Indole Diterpenoid Natural Products as the Inspiration for New Synthetic Methods and Strategies 1

1.1 Abstract 1

1.2 Introduction 1

1.3 Smith's Total Synthesis of Penitrem D 3

1.4 Pronin's Synthesis of Emindole SB 7

1.5 Johnson's Total Synthesis of Paspaline 10

1.6 Baran's Synthesis of Dixiamycin B 13

1.7 Garg's Total Syntheses of Tubingensins A & B 16

1.8 Conclusion 24

1.9 Notes and References 26

CHAPTER TWO: Total Synthesis of (–)-Tubingensin B Enabled by the Strategic Use of an Aryne Cyclization 31

2.1 Abstract 31

2.2 Introduction 32

2.3 Synthesis of Tubingensin B 33

2.4 Conclusion 42

2.5 Experimental Section 44

2.5.1 Materials and Methods 44

2.5.2 Experimental Procedures 45

2.6 Spectra Relevant to Chapter Two 74

2.7 Notes and References 112

CHAPTER THREE: Nickel-Catalyzed Amination of Aryl Chlorides and Sulfamates in 2-Me-THF 115

3.1 Abstract 115

3.2 Introduction 115

3.3 Optimization and Substrate Scope 116

3.4 Gram-Scale Couplings 123

3.5 Conclusion 124

3.6 Experimental Section 125

3.6.1 Materials and Methods 125

3.6.2 Experimental Procedures 126

3.6.2.1 Syntheses of Aryl Pseudohalide Substrates 126

3.6.2.2 Solvent Optimization and Scope of Electrophile 126

3.6.2.3 Aminations of Aryl Sulfamates and Chlorides 127

3.6.2.4 Isolation Experiments 136

3.7 Spectra Relevant to Chapter Three 140

3.8 Notes and References 162

CHAPTER FOUR: Nickel-Catalyzed Suzuki–Miyaura Coupling of Aliphatic Amides 169

4.1 Abstract 169

4.2 Introduction 169

4.3 Evaluation of Ligand Effects in the Suzuki–Miyaura Coupling 171

4.4 Scope of the Coupling with Hetero-Aliphatic Amides and Hetero-Aryl Boronates 173

4.5 Evaluation of the Coupling with Non-Heterocyclic Aliphatic Amide Substrates 176

4.6 Evaluation of the Coupling with a Benzamide Substrate 177

4.7 Evaluation of the Coupling with Substrates Containing Epimerizable Stereocenters 178

4.8 Gram-Scale Suzuki–Miyaura Coupling and Subsequent Fischer Indolization 179

4.9 Conclusion 180

4.10 Experimental Section 182

4.10.1 Materials and Methods 182

4.10.2 Experimental Procedures 183

4.10.2.1 Syntheses of Amide Substrates 183

4.10.2.2 Initial Survey of Ligands and Relevant Control Experiments .. 188
4.10.2.3 Scope of Methodology 190
4.10.2.4 Verification of Enantiopurity 206
4.10.2.4.1 Synthesis of Racemic Ketone 206
4.10.2.4.2 Chiral SFC Assays for Amide **4.41** and Ketone **4.42** 207
4.10.2.4.3 Erosion of Stereochemistry Control Experiments 210
4.10.2.4.4 Chiral HPLC Assays for Amide **4.41** and Ketone **4.42** 211
4.10.2.4.5 Erosion of Stereochemistry of Ketone **4.42** 213
4.10.2.4.6 Chiral HPLC Assays for Ketone **4.42** 213
4.10.2.5 Robustness Screen 217
4.10.2.6 Gram Scale Suzuki–Miyaura Reaction and Subsequent Fischer Indolization 218
4.11 Spectra Relevant to Chapter Four 220
4.12 Notes and References 284

LIST OF FIGURES

CHAPTER ONE

Figure 1.1. Indole diterpenoids as platforms for discovery 3

Figure 1.2. The indole diterpenoid penitrem D 4

Figure 1.3. Emindole SB and key strategies employed in Pronin's total synthesis 7

Figure 1.4. Paspaline and summary of tactics used by Johnson to achieve the total synthesis.....10

Figure 1.5. Indole diterpenoid alkaloid dixiamycin B 14

Figure 1.6. Tubingensins A & B featuring synthetically challenging vicinal quaternary centers.....17

Figure 1.7. Attempted aryne cyclization to provide undesired adduct **1.32** and successful aryne cyclization to deliver ketone **1.34** en route to tubingensin A 18

Figure 1.8. Carbazolyne cyclization studies toward the total synthesis of tubingensin B ...21

CHAPTER TWO

Figure 2.1. Tubingensins A and B 33

Figure 2.2. Synthesis of coupling fragment **2.7** and assembly of tetrasubstituted alkene **2.13** 36

Figure 2.3. ^{1}H NMR (500 MHz, $CDCl_3$) of compound **2.9** 75

Figure 2.4. Infrared spectrum of compound **2.9** 76

Figure 2.5. ^{13}C NMR (125 MHz, $CDCl_3$) of compound **2.9** 76

Figure 2.6. ^{1}H NMR (500 MHz, $CDCl_3$) of compound **2.10** 77

Figure 2.7. Infrared spectrum of compound **2.10** 78

Figure 2.8. ^{13}C NMR (125 MHz, $CDCl_3$) of compound **2.10** 78

Figure 2.9. ^{1}H NMR (500 MHz, $CDCl_3$) of compound **2.7** 79

Figure 2.10. Infrared spectrum of compound **2.7** 80

Figure 2.11. ^{13}C NMR (125 MHz, $CDCl_3$) of compound **2.7** 80

Figure 2.12. ^{1}H NMR (500 MHz, CD_2Cl_2) of compound **2.26** 81

Figure 2.13. Infrared spectrum of compound **2.26** 82

Figure 2.14. ^{13}C NMR (125 MHz, CD_2Cl_2) of compound **2.26** 82

Figure 2.15. ^{1}H NMR (500 MHz, CD_2Cl_2) of compound **2.14** 83

Figure 2.16. Infrared spectrum of compound **2.14** 84

Figure 2.17. ^{13}C NMR (125 MHz, CD_2Cl_2) of compound **2.14** 84

Figure 2.18. ^{1}H NMR (500 MHz, CD_2Cl_2) of compound **2.15** 85

Figure 2.19. Infrared spectrum of compound **2.15** 86

Figure 2.20. ^{13}C NMR (125 MHz, CD_2Cl_2) of compound **2.15** 86

Figure 2.21. ^{1}H NMR (500 MHz, C_6D_6) of compound **2.16** 87

Figure 2.22. Infrared spectrum of compound **2.16** 88

Figure 2.23. ^{13}C NMR (125 MHz, C_6D_6) of compound **2.16** 88

Figure 2.24. ^{1}H NMR (500 MHz, CD_2Cl_2) of compound **2.17** 89

Figure 2.25. Infrared spectrum of compound **2.17** 90

Figure 2.26. ^{13}C NMR (125 MHz, CD_2Cl_2) of compound **2.17** 90

Figure 2.27. ^{1}H NMR (500 MHz, CD_2Cl_2) of compound **2.18** 91

Figure 2.28. Infrared spectrum of compound **2.18** 92

Figure 2.29. ^{13}C NMR (125 MHz, CD_2Cl_2) of compound **2.18** 92

Figure 2.30. ^{1}H NMR (500 MHz, CD_2Cl_2) of compound **2.19** 93

Figure 2.31. Infrared spectrum of compound **2.19** 94

Figure 2.32. ^{13}C NMR (125 MHz, CD_2Cl_2) of compound **2.19** 94

Figure 2.33. ^{1}H NMR (500 MHz, CD_2Cl_2) of compound **2.20** 95

Figure 2.34. Infrared spectrum of compound **2.20** 96

Figure 2.35. ^{13}C NMR (125 MHz, CD_2Cl_2) of compound **2.20** 96

Figure 2.36. ^{1}H NMR (500 MHz, $CDCl_3$) of compound **2.21** 97

Figure 2.37. Infrared spectrum of compound **2.21** 98

Figure 2.38. ^{13}C NMR (125 MHz, $CDCl_3$) of compound **2.21** 98

Figure 2.39. ^{1}H NMR (500 MHz, C_6D_6) of compound **2.22** 99

Figure 2.40. Infrared spectrum of compound **2.22** 100

Figure 2.41. ^{13}C NMR (125 MHz, C_6D_6) of compound **2.22** 100

Figure 2.42. ^{1}H NMR (500 MHz, C_6D_6) of compound **2.23** 101

Figure 2.43. Infrared spectrum of compound **2.23** 102

Figure 2.44. ^{13}C NMR (125 MHz, C_6D_6) of compound **2.23** 102

Figure 2.45. ^{1}H NMR (500 MHz, C_6D_6) of compound **2.24**. 103

Figure 2.46. Infrared spectrum of compound **2.24** 104

Figure 2.47. ^{13}C NMR (125 MHz, C_6D_6) of compound **2.24** 104

Figure 2.48. ^{1}H NMR (500 MHz, C_6D_6) of compound **2.25** 105

Figure 2.49. Infrared spectrum of compound **2.25** 106

Figure 2.50. ^{13}C NMR (125 MHz, C_6D_6) of compound **2.25** 106

Figure 2.51. ^{1}H NMR (500 MHz, CD_2Cl_2) of compound **2.1** 107

Figure 2.52. Infrared spectrum of compound **2.1** 108

Figure 2.53. ^{13}C NMR (125 MHz, CD_2Cl_2) of compound **2.1** 108

Figure 2.54. ^{1}H NMR (500 MHz, $CDCl_3$) of compound ***epi*-2.1** 109

Figure 2.55. Infrared spectrum of compound ***epi*-2.1** 110

Figure 2.56. ^{13}C NMR (125 MHz, $CDCl_3$) of compound ***epi*-2.1** 110

Figure 2.57. Comparison ^{1}H-NMR spectrum of natural and synthetic (–)-tubingensin B (**2.1**) 111

CHAPTER THREE

Figure 3.1. Amination of (hetero)aryl chlorides and sulfamates in a green solvent using nickel catalysis 116

Figure 3.2. Coupling of (hetero)aryl sulfamates with morpholine in 2-Me-THF 120

Figure 3.3. Coupling of (hetero)aryl chlorides with morpholine in 2-Me-THF 121

Figure 3.4. Scope of amine component in the coupling reaction 122

Figure 3.5. Gram-scale couplings of trifluoromethyl-containing substrates 123

Figure 3.6. Gram-scale couplings of heterocyclic substrates 124

Figure 3.7. ^{1}H NMR (400 MHz, $CDCl_3$) of compound **3.4** 141

Figure 3.8. ^{1}H NMR (500 MHz, $CDCl_3$) of compound **3.6** 142

Figure 3.9. ^{1}H NMR (500 MHz, $CDCl_3$) of compound **3.7** 143

Figure 3.10. ^{1}H NMR (400 MHz, $CDCl_3$) of compound **3.8** 144

Figure 3.11. ^{1}H NMR (400 MHz, $CDCl_3$) of compound **3.9** 145

Figure 3.12. ^{1}H NMR (400 MHz, $CDCl_3$) of compound **3.10** 146

Figure 3.13. ^{1}H NMR (600 MHz, $CDCl_3$) of compound **3.11** 147

Figure 3.14. ^{1}H NMR (400 MHz, $CDCl_3$) of compound **3.12** 148

Figure 3.15. ^{1}H NMR (600 MHz, $CDCl_3$) of compound **3.13** 149

Figure 3.16. ^{1}H NMR (400 MHz, $CDCl_3$) of compound **3.14** 150

Figure 3.17. Infrared spectrum of compound **3.14** 151

Figure 3.18. ^{13}C NMR (100 MHz, $CDCl_3$) of compound **3.14** 151

Figure 3.19. ^{1}H NMR (400 MHz, $CDCl_3$) of compound **3.15** 152

Figure 3.20. Infrared spectrum of compound **3.15** 153

Figure 3.21. ^{13}C NMR (125 MHz, $CDCl_3$) of compound **3.15** 153

Figure 3.22. ^{1}H NMR (400 MHz, $CDCl_3$) of compound **3.16** 154

Figure 3.23. ^{1}H NMR (400 MHz, $CDCl_3$) of compound **3.17** 155

Figure 3.24. Infrared spectrum of compound **3.17** 156

Figure 3.25. ^{13}C NMR (125 MHz, $CDCl_3$) of compound **3.17** 156

Figure 3.26. ^{1}H NMR (600 MHz, $CDCl_3$) of compound **3.18** 157

Figure 3.27. ^{1}H NMR (500 MHz, $CDCl_3$) of compound **3.19** 158

Figure 3.28. ^{1}H NMR (600 MHz, $CDCl_3$) of compound **3.20** 159

Figure 3.29. ^{1}H NMR (500 MHz, $CDCl_3$) of compound **3.21** 160

Figure 3.30. ^{1}H NMR (500 MHz, $CDCl_3$) of compound **3.26** 161

CHAPTER FOUR

Figure 4.1. Suzuki–Miyaura hetero-arylation of aliphatic amides to construct poly-heterocyclic scaffolds 171

Figure 4.2. Scope of the Suzuki–Miyaura coupling with hetero-aliphatic amide substrates and hetero-aryl boronates 175

Figure 4.3. Scope of the coupling with non-heterocyclic aliphatic amide substrates and boronate **4.5** 176

Figure 4.4. Suzuki–Miyaura coupling of amide **4.36** with boronate **4.37** using Ni/SIPr and Ni/Benz-ICy catalyst system..... 177

Figure 4.5. Stereoretentive Suzuki–Miyaura couplings of amide **4.39** and enantioenriched amide **4.41** 179

Figure 4.6. Sequential gram-scale Suzuki–Miyaura coupling and Fischer indolization to forge indolenine **4.47** 180

Figure 4.7. ^{1}H NMR (500 MHz, $CDCl_3$) of compound **4.4** 221

Figure 4.8. Infrared spectrum of compound **4.4** 222

Figure 4.9. ^{13}C NMR (125 MHz, $CDCl_3$) of compound **4.4** 222

Figure 4.10. ^{1}H NMR (500 MHz, $CDCl_3$) of compound **4.50**. 223

Figure 4.11. Infrared spectrum of compound **4.50** 224

Figure 4.12. ^{13}C NMR (125 MHz, $CDCl_3$) of compound **4.50** 224

Figure 4.13. ^{1}H NMR (500 MHz, $CDCl_3$) of compound **4.52**. 225

Figure 4.14. Infrared spectrum of compound **4.52** 226

Figure 4.15. ^{13}C NMR (125 MHz, $CDCl_3$) of compound **4.52** 226

Figure 4.16. ^{1}H NMR (500 MHz, $CDCl_3$) of compound **4.43**. 227

Figure 4.17. Infrared spectrum of compound **4.43** 228

Figure 4.18. ^{13}C NMR (125 MHz, $CDCl_3$) of compound **4.43** 228

Figure 4.19. ^{1}H NMR (500 MHz, $CDCl_3$) of compound **4.55**. 229

Figure 4.20. Infrared spectrum of compound **4.55** 230

Figure 4.21. ^{13}C NMR (125 MHz, $CDCl_3$) of compound **4.55** 230

Figure 4.22. ^{1}H NMR (500 MHz, $CDCl_3$) of compound **4.39**. 231

Figure 4.23. Infrared spectrum of compound **4.39** 232

Figure 4.24. ^{13}C NMR (125 MHz, $CDCl_3$) of compound **4.39** 232

Figure 4.25. ^{1}H NMR (500 MHz, $CDCl_3$) of compound **4.6** 233

Figure 4.26. Infrared spectrum of compound **4.6** 234

Figure 4.27. ^{13}C NMR (125 MHz, $CDCl_3$) of compound **4.6** 234

Figure 4.28. ^{1}H NMR (500 MHz, $CDCl_3$) of compound **4.11**. 235

Figure 4.29. Infrared spectrum of compound **4.11** 236

Figure 4.30. ^{13}C NMR (125 MHz, $CDCl_3$) of compound **4.11** 236

Figure 4.31. ^{1}H NMR (500 MHz, $CDCl_3$) of compound **4.12**. 237

Figure 4.32. ^{1}H NMR (500 MHz, $CDCl_3$) of compound **4.13**. 238

Figure 4.33. Infrared spectrum of compound **4.13** 239

Figure 4.34. ^{13}C NMR (125 MHz, $CDCl_3$) of compound **4.13** 239

Figure 4.35. ^{1}H NMR (500 MHz, $CDCl_3$) of compound **4.14**. 240

Figure 4.36. Infrared spectrum of compound **4.14** 241

Figure 4.37. ^{13}C NMR (125 MHz, $CDCl_3$) of compound **4.14** 241

Figure 4.38. ^{1}H NMR (500 MHz, $CDCl_3$) of compound **4.15**. 242

Figure 4.39. Infrared spectrum of compound **4.15** 243

Figure 4.40. ^{13}C NMR (125 MHz, $CDCl_3$) of compound **4.15** 243

Figure 4.41. ^{1}H NMR (500 MHz, $CDCl_3$) of compound **4.16**. 244

Figure 4.42. Infrared spectrum of compound **4.16** 245

Figure 4.43. ^{13}C NMR (125 MHz, $CDCl_3$) of compound **4.16** 245

Figure 4.44. ^{1}H NMR (500 MHz, $CDCl_3$) of compound **4.17**. 246

Figure 4.45. Infrared spectrum of compound **4.17** 247

Figure 4.46. ^{13}C NMR (125 MHz, $CDCl_3$) of compound **4.17** 247

Figure 4.47. ^{1}H NMR (500 MHz, $CDCl_3$) of compound **4.18**. 248

Figure 4.48. Infrared spectrum of compound **4.18** 249

Figure 4.49. ^{13}C NMR (125 MHz, $CDCl_3$) of compound **4.18** 249

Figure 4.50. ^{1}H NMR (500 MHz, $CDCl_3$) of compound **4.19**. 250

Figure 4.51. Infrared spectrum of compound **4.19** 251

Figure 4.52. ^{13}C NMR (125 MHz, $CDCl_3$) of compound **4.19** 251

Figure 4.53. ^{1}H NMR (500 MHz, $CDCl_3$) of compound **4.20**. 252

Figure 4.54. Infrared spectrum of compound **4.20** 253

Figure 4.55. ^{13}C NMR (125 MHz, $CDCl_3$) of compound **4.20** 253

Figure 4.56. ^{1}H NMR (500 MHz, $CDCl_3$) of compound **4.21**. 254

Figure 4.57. Infrared spectrum of compound **4.21** 255

Figure 4.58. ^{13}C NMR (125 MHz, $CDCl_3$) of compound **4.21** 255

Figure 4.59. ^{1}H NMR (500 MHz, $CDCl_3$) of compound **4.22**. 256

Figure 4.60. Infrared spectrum of compound **4.22** 257

Figure 4.61. ^{13}C NMR (125 MHz, $CDCl_3$) of compound **4.22** 257

Figure 4.62. ^{1}H NMR (500 MHz, $CDCl_3$) of compound **4.23**. 258

Figure 4.63. Infrared spectrum of compound **4.23** 259

Figure 4.64. ^{13}C NMR (125 MHz, $CDCl_3$) of compound **4.23** 259

Figure 4.65. ^{1}H NMR (500 MHz, $CDCl_3$) of compound **4.24** 260

Figure 4.66. Infrared spectrum of compound **4.24** 261

Figure 4.67. ^{13}C NMR (125 MHz, $CDCl_3$) of compound **4.24** 261

Figure 4.68. ^{1}H NMR (500 MHz, $CDCl_3$) of compound **4.25**. 262

Figure 4.69. Infrared spectrum of compound **4.25** 263

Figure 4.70. ^{13}C NMR (125 MHz, $CDCl_3$) of compound **4.25** 263

Figure 4.71. ^{1}H NMR (500 MHz, $CDCl_3$) of compound **4.26**. 264

Figure 4.72. Infrared spectrum of compound **4.26** 265

Figure 4.73. ^{13}C NMR (125 MHz, $CDCl_3$) of compound **4.26** 265

Figure 4.74. ^{1}H NMR (500 MHz, $CDCl_3$) of compound **4.27**. 266

Figure 4.75. ^{1}H NMR (500 MHz, $CDCl_3$) of compound **4.28**. 267

Figure 4.76. ^{1}H NMR (500 MHz, $CDCl_3$) of compound **4.29**. 268

Figure 4.77. ^{1}H NMR (500 MHz, $CDCl_3$) of compound **4.30**. 269

Figure 4.78. ^{1}H NMR (500 MHz, $CDCl_3$) of compound **4.31**. 270

Figure 4.79. ^{1}H NMR (500 MHz, $CDCl_3$) of compound **4.32**. 271

Figure 4.80. Infrared spectrum of compound **4.32**. 272

Figure 4.81. ^{13}C NMR (125 MHz, $CDCl_3$) of compound **4.32** 272

Figure 4.82. ^{1}H NMR (500 MHz, $CDCl_3$) of compound **4.33**. 273

Figure 4.83. ^{1}H NMR (500 MHz, $CDCl_3$) of compound **4.34**. 274

Figure 4.84. ^{1}H NMR (500 MHz, $CDCl_3$) of compound **4.35**. 275

Figure 4.85. ^{1}H NMR (500 MHz, $CDCl_3$) of compound **4.40** 276

Figure 4.86. Infrared spectrum of compound **4.40** 277

Figure 4.87. ^{13}C NMR (125 MHz, $CDCl_3$) of compound **4.40** 277

Figure 4.88. ^{1}H NMR (500 MHz, $CDCl_3$) of compound **4.42** 278

Figure 4.89. Infrared spectrum of compound **4.42** 279

Figure 4.90. ^{13}C NMR (125 MHz, $CDCl_3$) of compound **4.42** 279

Figure 4.91. ^{1}H NMR (500 MHz, $CDCl_3$) of compound **4.45**. 280

Figure 4.92. Infrared spectrum of compound **4.45** 281

Figure 4.93. ^{13}C NMR (125 MHz, $CDCl_3$) of compound **4.45** 281

Figure 4.94. ^{1}H NMR (500 MHz, $CDCl_3$) of compound **4.47**. 282

Figure 4.95. Infrared spectrum of compound **4.47** 283

Figure 4.96. ^{13}C NMR (125 MHz, $CDCl_3$) of compound **4.47** 283

LIST OF SCHEMES

CHAPTER ONE

Scheme 1.1. Smith indole synthesis allows for the coupling of key fragments **1.2** and **1.4** en route to penitrem D.....6

Scheme 1.2. Total synthesis of emindole SB featuring a novel alkenylation reaction to afford **1.10** and an impressive HAT cyclization to furnish **1.14** 9

Scheme 1.3. Enzymatic reduction and C–H functionalization creatively applied toward the total synthesis of paspaline.....11

Scheme 1.4. Gassman indolization and completed synthesis of paspaline.....12

Scheme 1.5. Expedient synthesis of monomeric natural product, xiamycin A 15

Scheme 1.6. Electrochemical oxidation forges key N–N bond of dixiamycin B 16

Scheme 1.7. Challenging *B*-alkyl Suzuki–Miyaura coupling affords tetrasubstituted olefin **1.37**, which was subsequently converted to aryne cyclization substrate **1.38** 20

Scheme 1.8. Carbazolyne cyclization/fragmentation sequence furnished ketone **1.45**.....22

Scheme 1.9. Radical cyclization, deprotection, and late-stage reduction furnishes tubingensin B.....23

CHAPTER TWO

Scheme 2.1. Retrosynthetic analysis of tubingensin B 35

Scheme 2.2. Key aryne cyclization to forge the C20–C11 linkage 38

Scheme 2.3. Radical cyclization and first generation total synthesis of tubingensin B 40

Scheme 2.4. Concise total synthesis of tubingensin B 42

LIST OF TABLES

CHAPTER THREE

Table 3.1. Examination of solvents in the amination of 1-chloronaphthalene 117

Table 3.2. Evaluation of various electrophiles 118

CHAPTER FOUR

Table 4.1. Evaluation of reaction conditions for the coupling of aliphatic amides 173

Table 4.2. Initial survey of ligands and relevant control experiments 189

Table 4.3. Evaluation of impact of reaction components on eronsion of α-stereocenter 213

Table 4.4. Evaluation of functional group compatibility in the Suzuki–Miyaura reaction 217

LIST OF ABBREVIATIONS

9-BBN	9-borabicyclo[3.3.1]nonane
Å	angstrom
$[\alpha]_D$	specific rotation at wavelength of sodium D line
Ac	acetyl, acetate
acac	acetylacetonate
AcOH	acetic acid
AIBN	azobisisobutyronitrile
α	alpha
APCI	atmospheric pressure chemical ionization
app.	apparent
aq.	aqueous
atm	atmosphere
Benz-ICy	1,3-dicyclohexylbenzimidazolium
BINAP	2,2′-Bis(diphenylphosphino)-1,1′-binaphthyl
Bn	benzyl
br	broad
Boc	*tert*-butoxycarbonyl
Bu	butyl
n-Bu	butyl (linear)
t-Bu	*tert*-butyl

s-Bu	*sec*-butyl
c	concentration for specific rotation measurements
°C	degrees Celsius
calcd	calculated
cat.	catalytic
m-CPBA	*meta*-chloroperoxybenzoic acid
CPME	cyclopentyl methyl ether
cod	1,4-cyclooctadiene
Cy	cyclohexyl
d	doublet
DART	direct analysis in real time
dba	dibenzylideneacetone
DMAP	4-dimethylaminopyridine
DME	1,2-dimethoxyethane
DMF	*N*,*N*-dimethylformamide
DMIPS	dimethylisopropylsilyl
DMIPSCl	dimethylisopropylsilyl chloride
DMP	Dess–Martin periodinane
DM-SEGPHOS	5,5′−Bis[di(3,5-xylyl)phosphino]-4,4′-bi-1,3-benzodioxole
DMSO	dimethyl sulfoxide
d.r.	diastereomeric ratio
equiv	equivalent

ESI	electrospray ionization
Et	ethyl
EtOH	ethanol
e.r.	enantiomeric ratio
g	gram(s)
h	hour(s)
HMB	hexamethylbenzene
HMDS	hexamethyldisilane
HMPA	hexamethylphosphoramide
HOBt	hydroxybenzotriazole
HPLC	high performance liquid chromatography
HRMS	high resolution mass spectroscopy
Hz	hertz
IBX	2-iodoxybenzoic acid
ICy	1,3-dicyclohexylimidazolium
IR	infrared (spectroscopy)
J	coupling constant
L	liter
LDA	lithium diisopropylamide
M	molecular mass
m	multiplet or milli
m	meta

m/z	mass to charge ratio
μ	micro
Me	methyl
MsCl	methanesulfonyl chloride
MeOH	methanol
MHz	megahertz
min	minute(s)
mol	mole(s)
MOM	methoxymethyl
MOMCl	methoxymethyl chloride
mp	melting point
MS	molecular sieves
MTBE	methyl *tert*-butyl ether
NBS	*N*-bromosuccinimide
NMR	nuclear magnetic resonance
o	ortho
p	para
Ph	phenyl
pH	hydrogen ion concentration in aqueous solution
PhH	benzene
pin	pinnacol
Piv	pivaloyl

ppm	parts per million
py	pyridine
i-Pr	isopropyl
PSI	pounds per square inch
q	quartet
rac	racemic
rt	room temperature
R_f	retention factor
s	singlet
sat.	saturated
SFC	supercritical fluid chromatography
SIPr	1,3-Bis(2,6-diisopropylphenyl)-4,5-dihydroimidazolium
t	triplet
TBAF	tetrabutylammonium fluoride
TBS	*tert*-butyldimethylsilyl
TBSCl	*tert*-butyldimethylsilyl chloride
TES	triethylsilyl
TESCl	triethylsilyl chloride
Temp.	temperature
Tf	trifluoromethanesulfonyl (trifyl)
TFA	trifluoroacetic acid
THF	tetrahydrofuran

TIPS	triisopropylsilyl
TIPSCl	triisopropylsilyl chloride
TLC	thin layer chromatography
TMS	trimethylsilyl
TMSCl	trimethylsilyl chloride
Ts	*p*-toluenesulfonyl (tosyl)
TsOH	*p*-toluenesulfonic acid
UHP	ultra high purity
UV	ultraviolet
V	voltage
λ	wavelength

ACKNOWLEDGEMENTS

In September of 2013, I flew from Seoul to Los Angeles with just two suitcases to start my graduate school at UCLA. I still remember it as quite an overwhelming experience to be abroad by myself, knowing that Los Angeles was going to be my new home for the next several years. However, I made it through five years with satisfying productivity. My accomplishments would not have been possible without people I met throughout the course. I truly believe that those people helped and influenced me to become the person I am today. Here at the end of my Ph.D., I would like to thank all of them.

First and foremost, I would like to thank my mentor, Professor Neil Garg, for providing an opportunity to join his group and supporting me throughout my Ph.D. It has been a great honor to be a part of the family. He has taught me how to not only be a great chemist, but also a better person. I greatly appreciate all his efforts to support my research, personal development, and funding. His unstoppable enthusiasm toward chemistry and education has always amused me. Teaching undergraduate courses, 14D and 30BL, and developing BACON with him were unique experiences that I did not have with other instructors. His vision in education assured my decision to be a professor and I wish I would be able to pass down the mentorship from Neil to younger generations.

I appreciate two of my inspiring undergraduate advisors, Professors Tae-Lim Choi and David Yu-Kai Chen, for leading me to the world of organic chemistry. Professor Choi, your physical organic chemistry course was one of the best classes that I took in my undergraduate years. It certainly brought back my interest in organic chemistry. Professor Chen, thank you so much for your patience to teach an undergraduate. It was an invaluable experience to learn lab techniques directly from you.

My committee members have guided me through all these years. I appreciate Professors Hosea Nelson, Yi Tang, and Jennifer Murphy for being my mentors. I am grateful to Professor Nelson for teaching me how to use his lab equipment and allowing me to use them. The collaboration with Professor Tang's group was a special experience, from which I could get out of my comfort zone and learn about biochemical research. Thank you Dr. Yang Hai for teaching me about the biosynthesis of the iron carrier alkaloid ferricrocin.

I have worked with an amazing group of people in the Garg lab. The group has been a source of intellectual collaboration as well as friendship. I would like to start by thanking people whom I worked with directly on my dissertation research. Noah Fine Nathel and Liana Hie were my first mentors and coworkers for the nickel-catalyzed "green" amination project. They were very patient and friendly to teach me everything from top to bottom when I joined the group. I would not be able to adapt to the lab easily without their help. Also, I enjoyed being a part of a foodie club with them. Thank you for introducing me to lots of exquisite restaurants in LA. I wish we could have a foodie club reunion and grab a nice dinner together. Next, I spent most of my dissertation research with Michael Corsello on the total synthesis of tubingensin B. It was an incredible three years with him to conquer this beastly molecule. I would not be able to complete this project without you! Also, he started a trend to make numerous nicknames for me. If I recall correctly, the lastest one was 'jun-papito.' After completing the total synthesis of tubingensin B, I came back to a nickel project joining Nick Weires and Tim Boit. When I started in room 5235, I used to work next to Nick's fume hood. Thank you for helping me get situated in the lab. Tim is my first and only mentee during my graduate career. Working with a yourger member was definitely a different experience than working with senior members. It taught me about what leadership means. You have been an awesome coworker and hope for the best in your future

graduate years. Lastly, it was a pleasure to work with my classmate Emma Baker at the end of my school years. Without her help, I might not be able of finish up the last project before my departure. Thank you all my coworkers for your dedication and passion!

Office 5234 has been another home for me during my UCLA years. The culture that my officemates and I have created provided unforgettable memories. Hanging out with them in the lab, I was able to forget about all my burdens from hours of research. Joel Smith, you are such an entertaining speaker. Good luck with your new career at FSU. Tejas Shah, a co-developer of BACON, you have been a great lab technical support. Our lab would not function without you, even after your departure. Thank you for dealing with all computer related problems whenever Jacob and I contacted you. Jesus Moreno, your war against the world on subtleties was one of my favorite parts about you. Hope HR Jesus is doing well at Boston. Jose Medina, as one of the lunch crewmembers, you had been an exemplary member to lead us back to the lab. I always picture you saying "Are you guys ready?" Lucas Morrill, we had created a great culture in 5234 where everyone can sing along without any judgement. Please make sure karaoke 5234 continues. Robert Susick, you are one of the nicest people I have ever met. Your passion for the league of legend gave me a throwback to my college years. One day, you will make it to Gold! Sarah Anthony, I am grateful that you moved to our office and we had a chance to know you better. You are becoming a great scientist. Trust yourself, Sarah! Also, thank you for introducing your brother, Henry. I will never forget hanging out with you and your bother at Cliffs of Id. Jason Chari, it was too short to get to know you better, but your positivity always shed brightness in our office. Maude Giroud, I would like to specially thank our postdoc for being patient to our craziness. You have been a wonderful zookeeper of 5234. I can go on forever, but I need to cut short at this point. Thank you everyone I've met in the Garg group: Grace Chiou, Adam Goetz,

Stephen Ramgren, Amanda Silberstein, Evan Styduhar, Elias Picazo, Joyann Barber, Bryan Simmons, Jacob Dander, Michael Yamano, Jordan Dotson, Melissa Ramirez, Francesca Ippoliti, Rachel Knapp, Yuya Nagato, Travis McMahon, Marie Hoffmann, Sophie Racine, and Evan Darzi. I will miss you a lot.

I also met lots of passionate and inspiring friends outside the Garg lab. As part of a teaching experience, I teamed up with several talented undergraduates to develop an educational program called BACON (Biology and Chemistry Online Notes). Vandan Kasar, Crystal Lin, Krishan Patel, your young and creative minds were essential to the process. You all have been excellent writers, too. Also, whenever I was homesick, there were Korean friends who made me feel like I was at home. Especially, I am pleased that I got to know Jeonghoon Ko. Thank you for organizing all the events for Korean people in the department and hanging out with me whenever I missed Korean food. Woogie Lee, Jung-reem Woo, Juneyoung Lee, Tim Chung, Jin Park, Ga-young Lee, So-yeon Kim, Da-hee Jung, thank you all for helping me feel like at home. I have had terrific roommates over last four years. Ha-seung Kim, Anjan Nandula, Matthew Pagenkopp, Laura Solorzano, Orin Yue, you have been wonderful roommates during my time in graduate school. Your thoughtfulness and cheerfulness always made me feel safe and welcome at home.

Last, but most importantly, I am thankful to my family for their consistent encouragement. Dad, you always have been my inspiration to become a scientist. I was able to pursue my dream because of your support. Mom, I am so proud to be your son. I will always remember your favorite quote: Though thy beginning was small, yet thy latter end should greatly increase. My sisters, Miyeon and Jungeun, you have been an essential part of this family for me. Especially, thank you for Jungeun and Daniel for welcoming me during Thanksgiving and the Christmas season. My first nephew, Rui, it is a true blessing in our family to have you. I am

thrilled to be part of your life on the east coast. I sincerely feel blessed to have such a wonderful group of people to support me during my graduate experience. I will never forget their support and friendship. I believe that this experience will be a precious foundation for my future career. Again, thank you so much.

Biographical Sketch

Education:

University of California, Los Angeles, CA

- Ph.D. in Organic Chemistry, anticipated June 2018
- Current GPA: 3.95/4.00

Seoul National University, Seoul, South Korea

- B.S. in Chemistry - Fall 2012
- Cumulative GPA: 3.80/4.00

Professional and Academic Experience:

Graduate Research Assistant: University of California, Los Angeles, CA

- November 2013 – present; Advisor: Prof. Neil K. Garg.
- Completed the total synthesis of tubingensin B, utilizing a carbazolyne cyclization and a late-stage radical cyclization to construct the core of natural product.
- Developed the amination of aryl sulfamates and chlorides using $NiCl_2$(DME) as an air-stable Ni(II) precatalyst in a green solvent.
- Investigated nickel-catalyzed Suzuki–Miyaura coupling of amides for the construction of C–C bonds to forge ketones containing various heterocycles.

Graduate Teaching Assistant: University of California, Los Angeles, CA

- Undergraduate organic chemistry for life science majors and physical science majors. (Fall 2013, Winter 2014, and Spring 2014)
- Senior level undergraduate organic chemistry laboratory. (Summer 2016)

NMR Instrumental Teaching Assistant: University of California, Los Angeles, CA

- Perform regular maintenance of NMR spectrometers and trained new NMR users. (Summer 2016 – Summer 2017)

Undergraduate Research Assistant: Seoul National University, Seoul, South Korea

- Studied living polymerization of norbornene derived monomers via ring-opening metathesis polymerization (ROMP) and synthesized a series of block copolymers under the supervision of Prof. Tae-Lim Choi (Summer 2011 – Spring 2012).
- Researched the total synthesis of dendrobine under the supervision of Prof. David Y.-K. Chen (Summer 2012 – Spring 2013).

Honors and Awards:

- UCLA Dissertation Year Fellowship, UCLA, 2017–2018
- UCLA Research Showcase Travel Award, UCLA, 2017
- Undergraduate Research Science Scholarship, Seoul National University, 2011– 2013
- National Science & Engineering Scholarship, Seoul National University, 2009–2013

Publications:

– Graduate research

6. **Nickel-Catalyzed Suzuki–Miyaura Coupling of Aliphatic Amides.** Timothy B. Boit,[†] Nicholas A. Weires,[†] Junyong Kim,[†] and Neil K. Garg. *ACS Catal*. **2018**, *8*, 1003–1008. ([†]These authors contributed equally)
5. **Indole Diterpenoid Natural Products as the Inspiration for New Synthetic Methods and Strategies.** Michael A. Corsello,[†] Junyong Kim,[†] and Neil K. Garg. *Chem. Sci*. **2017**, *8*, 5836–5844. ([†]These authors contributed equally)
4. **Total Synthesis of (–)-Tubingensin B Enabled by the Strategic Use of an Aryne Cyclization.** Michael A. Corsello,[†] Junyong Kim,[†] and Neil K. Garg. *Nat. Chem*. **2017**, *9*, 944–949. ([†]These authors contributed equally)
3. **Nickel-Catalyzed Amination of Aryl Chlorides and Sulfamates in 2-Methyl-THF.** Noah F. Fine Nathel, Junyong Kim, Liana Hie, Xingyu Jiang, and Neil K. Garg. *ACS Catal.* **2014**, *4*, 3289–3293.

– Undergraduate research

2. **An Asymmetric Pathway to Dendrobine by a Transition-Metal-Catalyzed Cascade Process.** Yujin Lee, Elise M. Rochette, Junyong Kim, and David Y.-K. Chen. *Angew. Chem., Int. Ed*. **2017**, *56*, 12250–12254.
1. **Living Polymerization of Monomers Containing *endo*-Tricyclo[4.2.2.0^{2,5}]deca-3,9-diene Using Second Generation Grubbs and Hoveyda–Grubbs Catalysts: Approach to Synthesis of Well-Defined Star Polymers.** Kyung Oh Kim, Suyong Shin, Junyong Kim, and Tae-Lim Choi. *Macromolecules* **2014**, *47*, 1351–1359.

Presentations:

8. **Total Synthesis of Tubingensin B.** Junyong Kim,* Michael A. Corsello, and Neil K. Garg. 2017 ACS Graduate Research Symposium, Portland State University, Portland, OR, United States, July 2017 (poster presentation).
7. **Total Synthesis of Tubingensin B.** Junyong Kim,* Michael A. Corsello, and Neil K. Garg. 253rd ACS National Meeting and Exposition, Moscone Center, San Francisco, CA, United States, April 2017 (poster presentation).
6. **Total Synthesis of Tubingensin B.** Junyong Kim,* Michael A. Corsello, and Neil K. Garg. 253rd ACS National Meeting and Exposition, Moscone Center, San Francisco, CA, United States, April 2017 (oral presentation).
5. **Synthetic Efforts Toward the Total Synthesis of Tubingensin B.** Junyong Kim,* Michael A. Corsello, and Neil K. Garg. 30th Annual Glenn T. Seaborg Symposium, University of California, Los Angeles, CA, United States, November 2016 (poster presentation).
4. **Progress Toward the Total Synthesis of Tubingensin B.** Junyong Kim* and Neil K. Garg. University of California Symposium for Chemical Sciences, Lake Arrowhead, CA, United States, March 2016 (oral presentation).
3. **Unified Synthetic Strategy Toward the Tubingensin Alkaloids.** Michael A. Corsello,* Junyong Kim, and Neil K. Garg. 251st ACS National Meeting and Exposition, San Diego Convention Center, San Diego, CA, United States, March 2016 (poster presentation).
2. **Unified Synthetic Strategy Toward the Tubingensin Alkaloids.** Michael A. Corsello,* Junyong Kim, and Neil K. Garg. 29th Annual Glenn T. Seaborg Symposium, University of California, Los Angeles, CA, United States, October 2015 (poster presentation).
1. **Nickel-Catalyzed Coupling in Green Solvents.** Liana Hie,* Noah F. Fine Nathel, Junyong Kim, Xingyu Jiang, and Neil K. Garg. 28th Annual Glenn T. Seaborg Symposium, University of California, Los Angeles, CA, United States, November 2014 (poster presentation).

CHAPTER ONE

Indole Diterpenoid Natural Products as the Inspiration for New Synthetic Methods and Strategies

Michael A. Corsello,[†] Junyong Kim,[†] and Neil K. Garg

Chem. Sci. **2017**, *8*, 5836–5844.

1.1 Abstract

Indole terpenoids comprise a large class of natural products with diverse structural topologies and a broad range of biological activities. Accordingly, indole terpenoids continue to serve as attractive targets for chemical synthesis. Many synthetic efforts over the past few years have focused on a subclass of this family, the indole diterpenoids. This chapter showcases the role indole diterpenoids have played in inspiring the recent development of clever synthetic strategies and new chemical reactions.

1.2 Introduction

Indole terpenoids are a natural product family of paramount importance to biology and chemistry. Several family members have had a tremendous impact on human medicine, such as the dimeric monoterpene indole alkaloids, vincristine and vinblastine, both of which are used to treat numerous types of cancer.[1] Furthermore, indole terpenoids have served as structural platforms for the development of new chemical methods and strategies for many years.[2] From the classic synthesis of lysergic acid[3] by Woodward in 1956, to Boger's development of ingenious cascade reactions toward the *Vinca* alkaloids[4] it is evident that indole terpenoids have played a vital role in spawning innovation in chemical synthesis.

The indole diterpenoids, a subclass of the indole terpenoid family, have recently garnered increased attention from synthetic chemists. The resulting total syntheses, several of which are the focus of this chapter, highlight the impact that indole diterpenoids have had on the development of enabling strategies and methods in chemical synthesis. This chapter, however, is not intended to be comprehensive. There are several elegant syntheses of indole diterpenoids that are not covered herein,[5] including those by Li, who has accomplished impressive syntheses of a number of indole terpenoids, including xiamycin A and tubingensin A.[6]

Specific natural products discussed in this chapter are shown in Figure 1.1. The first topic presented pertains to arguably the most complex member of this natural product family, penitrem D. The synthesis of penitrem D by the Smith group features the use of an innovative fragment coupling/indole synthesis methodology.[7] Next, recent efforts toward the related compounds, emindole SB[8] and paspaline,[9] by Johnson and Pronin, respectively, are discussed. We then highlight the Baran synthesis of dixiamycin B,[10] which has led to the considerable advancement of electrochemical methods in organic synthesis. Finally, we conclude by examining the strategic use of heterocyclic arynes to enable concise total syntheses of tubingensins A and B, as reported by our laboratory.[11]

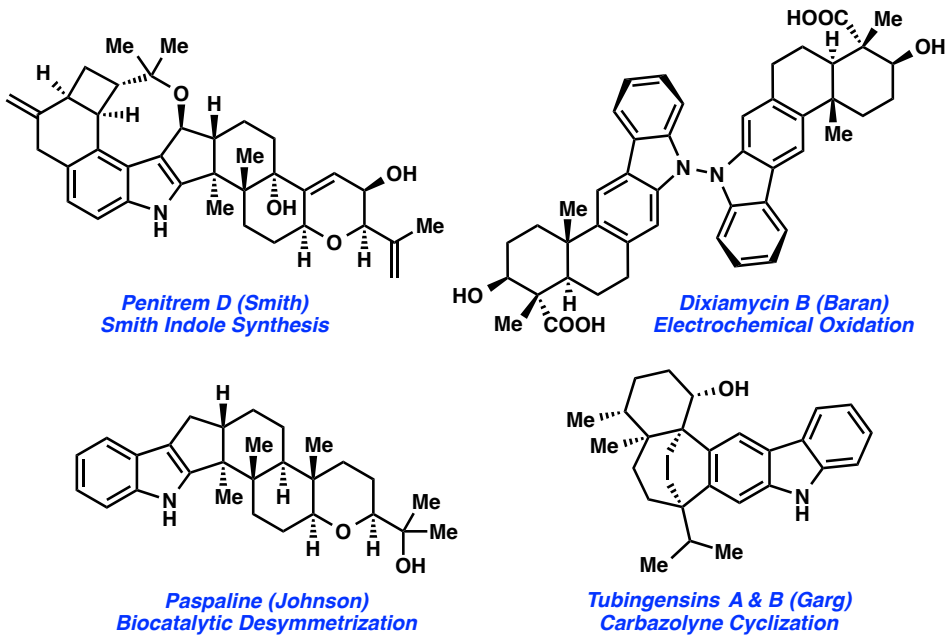

Figure 1.1. Indole diterpenoids as platforms for discovery.

1.3 The Smith Group's Total Synthesis of Penitrem D

Of the groups who have targeted indole diterpenoid natural products, the Smith group has been amongst the most successful. Their work led to the total syntheses of a myriad of indole diterpenoid,[12] including, but not limited to, paspaline,[12a] paspalicine,[12b] and paspalinine.[12b] These efforts set the stage for the pursuit of (–)-penitrem D (**1.1**, Figure 1.2), a tremorgenic alkaloid isolated from *Penicillium crustosum* in 1983.[13] Indole tremorgens are believed to cause neurological disorders in livestock by inhibition of potassium channels.[14]

Penitrem D (**1.1**) is one of the most complex natural products in the indole diterpenoid family. Consequently, the Smith group reported the only total synthesis.[7] The structure contains a staggering nine rings, a highly functionalized indole core, and eleven stereocenters. Of the stereocenters in **1.1**, five are contiguous and two are vicinal quaternary centers. The total synthesis of penitrem D (**1.1**) therefore represents an extraordinary feat in and of itself.

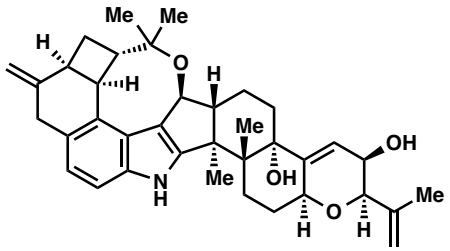

Penitrem D (1.1)
(Smith)

- ***Among the most complex indole diterpenoids***
- ***Inspiration for the development of Smith's Indole Synthesis***

Figure 1.2. The indole diterpenoid penitrem D.

The synthesis of penitrem D (**1.1**) remains the only synthesis of any penitrem alkaloid to date, which highlights the complexity of the penitrem alkaloids. There are many noteworthy features in the total synthesis that are not discussed herein, such as a $Sc(OTf)_3$-promoted cyclization cascade and a novel autoxidation to install the C22 hydroxyl group. Rather, as noted earlier, we focus our discussion of the indole synthesis methodology[15] used to access the natural product. This method is a variant of the Madelung indole synthesis,[16] albeit significantly more mild.

Scheme 1.1 depicts Smith's elegant indole synthesis and its use as a lynchpin in the total synthesis of **1.1**. The transformation begins with the formation of *N*-TMS dianion species **1.3** by treatment of substituted 2-methylaniline **1.2** with *n*-BuLi and TMSCl, followed by *s*-BuLi. This highly reactive intermediate can be generated at low temperature, obviating the need for otherwise harsh conditions required in the Madelung reaction. The reactive intermediate **1.3**, used in excess, is then treated with complex lactone **1.4** to form aminoketone **1.5** via concomitant addition/elimination of the alkyllithium with the lactone. Next, the authors found that subjection

of **1.5** to silica gel led to the smooth formation of the desired 2-substituted indole, **1.6**, in an impressive 81% yield from lactone **1.4**. Thus, the Smith indole synthesis provides a powerful method to unite two fragments of considerable complexity, while also installing the necessary indole heterocycle.

The construction of the indole nucleus set the stage for the completion of the synthesis (Scheme 1.1). After eight additional steps, the Smith group succeeded in elaborating **1.6** to penitrem D (**1.1**). Smith's total synthesis of **1.1**, which relies critically on his methodology for fragment coupling and indole synthesis, stands as one of the greatest feats in indole diterpenoid total synthesis.

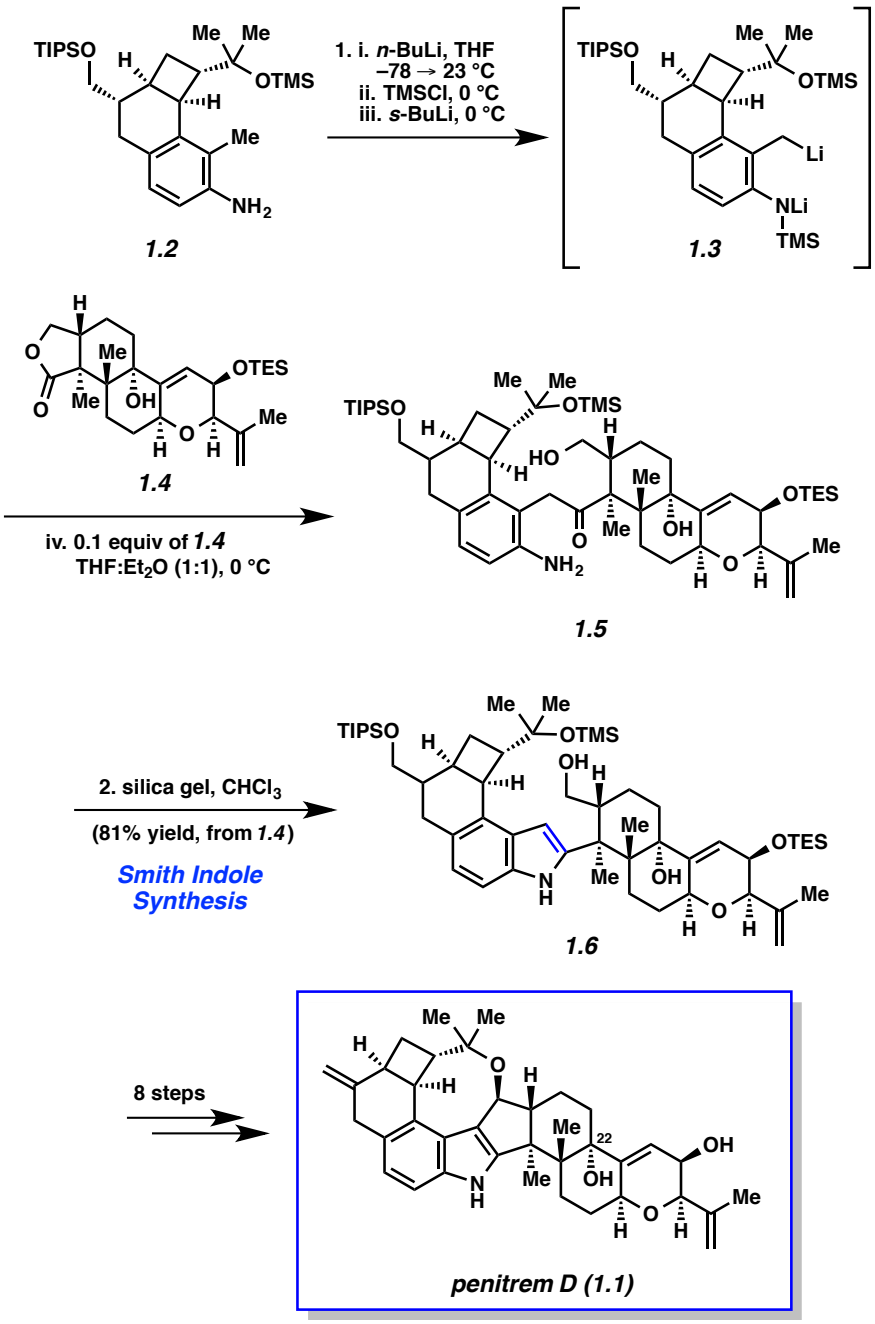

Scheme 1.1. Smith indole synthesis allows for the coupling of key fragments **1.2** and **1.4** en route to penitrem D.

1.4 Pronin's Synthesis of Emindole SB

In 2015, Pronin and co-workers reported the first total synthesis of (±)-emindole SB (**1.7**, Figure 1.3), an indole diterpenoid isolated from the fungus *Emericella striata*,[8,17] that shows promising antiproliferative, antimigratory, and anti-invasive properties against human breast cancer cells.[18] Comparable to penitrem D (**1.1**), the natural product contains an indole unit fused to a tricyclic carbon scaffold. Emindole SB (**1.7**) possesses six contiguous stereocenters, including vicinal quaternary centers on the western cyclohexyl ring. The Pronin group's approach to **1.7** features a novel ketone alkenylation reaction, in addition to a radical cyclization initiated by chemoselective hydrogen atom transfer (HAT) to install the *trans*-hexahydroindene moiety bearing vicinal quaternary centers.

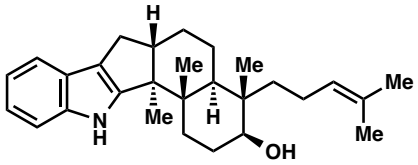

emindole SB (1.7)
(Pronin)

•Ketone alkenylation

•HAT cyclization

Figure 1.3. Emindole SB and key strategies employed in Pronin's total synthesis.

As shown in Scheme 1.2, the synthesis of **1.7** commenced with silyl enol ether **1.8**, which was prepared in one step from commercially available materials. Treatment of **1.8** with substoichiometric amounts of indium(III) bromide in the presence of terminal alkyne **1.9**,[19,20] followed by a mild acidic workup, afforded alkenylated product **1.10** in 50% yield. Notably, an

α-quaternary center was introduced with complete diastereoselectivity, showcasing the utility of this new method.

Ketone **1.10** was then elaborated in three steps to diol **1.11**, an important precursor toward constructing the natural product's *trans*-hexahydroindene moiety (Scheme 1.2). Parikh–Doering oxidation[21] of diol **1.11** provided hemiaminal **1.12** as the substrate for the ensuing key radical cyclization reaction. Using conditions developed independently by Baran and Shenvi, hemiaminal **1.12** was treated with iron(III) acetylacetonate[22] and (isopropoxy)phenylsilane[23] to afford cyclized product **1.14** in 60% yield over two steps (from diol **1.11**, >10:1 *d.r.*). This key radical cyclization, which constructs a new C–C bond and installs vicinal stereocenters, is thought to proceed by formation of tertiary radical intermediate **1.13** via chemoselective hydrogen atom transfer (HAT), followed by 1,4-addition. Of note, restricting the rotation of the radical intermediate by formation of a hemiaminal was crucial for the diasteroselectivity of the radical cyclization step. When the structure was not restricted as a hemiaminal, it resulted in the indiscriminate attack of the enone and poor diastereoselectivity. Nonetheless, pentacycle **1.14** was quickly elaborated to emindole SB (**1.7**) after a final four-step sequence involving cleavage of the hemiaminal fragment, cyclization to forge the final six-membered ring, and installation of the requisite homoprenyl group.

The Pronin approach to emindole SB (**1.7**) provides access to the natural product in only eleven steps from commercially available materials. Critical to the success and brevity of the total synthesis was creative invention. Specifically, the total synthesis of **1.7** was greatly facilitated by the novel alkenylation and diastereoselective radical cyclization reactions highlighted herein.

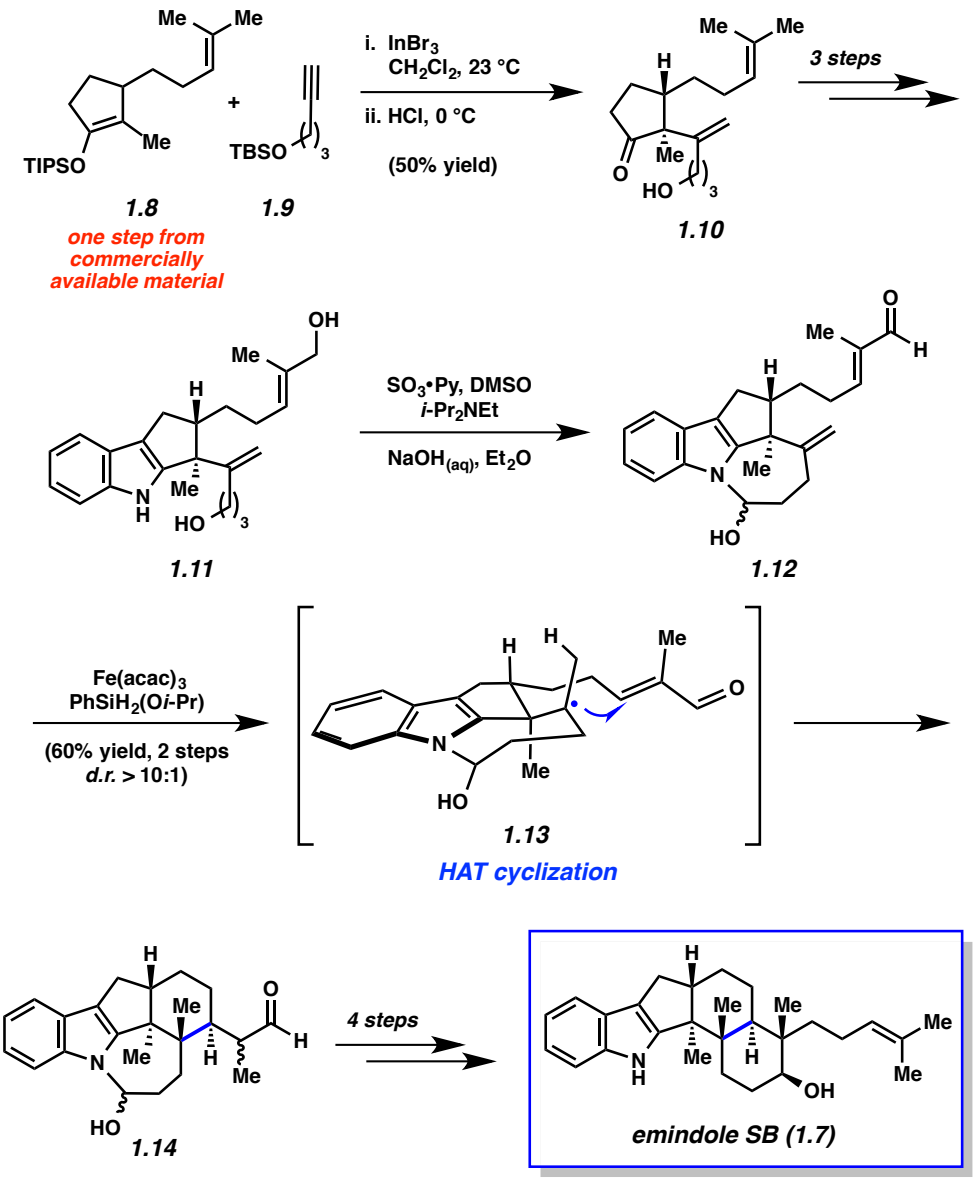

Scheme 1.2. Total synthesis of emindole SB featuring a novel alkenylation reaction to afford **1.10** and an impressive HAT cyclization to furnish **1.14**.

1.5 Johnson's Total Synthesis of Paspaline

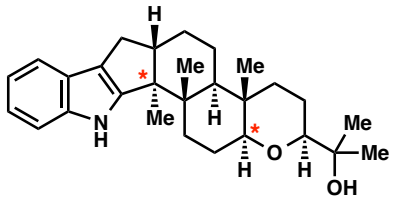

paspaline (1.15)
(Johnson)

- ***Biocatalytic desymmetrization***
- ***Diastereotopic group selective C–H acetoxylation***

Figure 1.4. Paspaline and summary of tactics used by Johnson to achieve the total synthesis.

In 2015, Johnson and coworkers reported an enantioselective total synthesis of (–)-paspaline (**1.15**, Figure 1.4).[9] Paspaline (**1.15**) was isolated from the ergot fungus *Claviceps paspali* in 1966.[24] The natural product's structure and bioactivity profile[18] is similar to that of emindole SB (**1.7**), discussed previously, although **1.15** possesses an additional ring and rests in a higher oxidation state. Johnson's synthesis of paspaline (**1.15**) hinges on two impressive desymmetrization transformations: a biocatalytic desymmetrization and a diastereotopic group selective C–H acetoxylation.

The two desymmetrization reactions utilized in Johnson's synthesis of paspaline (**1.15**) are summarized in Scheme 1.3. The first involved desymmetrization of diketone **1.16**. Biocatalytic reduction with yeast from *Saccharomyces cerevisiae* type 2 (YSC-2) furnished hydroxyketone **1.17** in 66% yield with excellent diastereo- and enantioselectivity.[25] This enzymatic process was essential for the synthesis, as the stereochemistry in alcohol **1.17** would ultimately be transferred to the 2,6-*cis*-tetrahydropyran ring. Alcohol **1.17** was then converted into oxime **1.18**, the substrate for the desired C–H acetoxylation. Inspired by chemistry

developed in the Sanford laboratory,[26] treatment of oxime **1.18** with palladium(II) acetate and iodosobenzene diacetate produced acetate **1.19** in 79% yield (gram-scale) as a single diastereomer. It was hypothesized that the oxime directing group guided the palladium catalyst in proximity to the equatorial methyl group, resulting in diastereotopic, group selective C–H functionalization. This intriguing local desymmetrization approach to install a quaternary stereogenic center allowed access to the *trans*-hexahydroindene moiety present in the natural product.

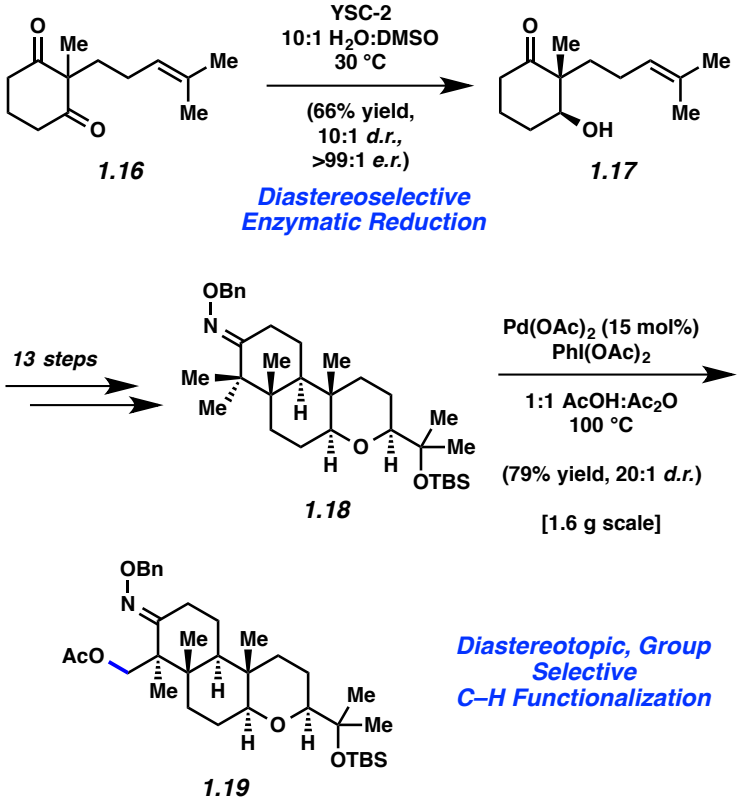

Scheme 1.3. Enzymatic reduction and C–H functionalization creatively applied toward the total synthesis of paspaline.

The endgame of Johnson's total synthesis of paspaline (**1.15**), which utilizes a Gassman indole synthesis,[12a,27] is depicted in Scheme 1.4. Ketone **1.20**, an intermediate derived from oxime **1.19** was first synthesized. Of note, **1.20** contains all the requisite stereocenters of the natural product. An enolate was then generated from ketone **1.20** and trapped with dimethyl disulfide to provide sulfide **1.21** in excellent yield. Next, sulfide **1.21** was treated with *N*-chloroaniline, followed by Raney nickel, to afford aniline **1.22** in 62% yield over two steps. Lastly, aniline **1.22** was treated with mild acid to generate the indole unit thereby completing the total synthesis of **1.15**.

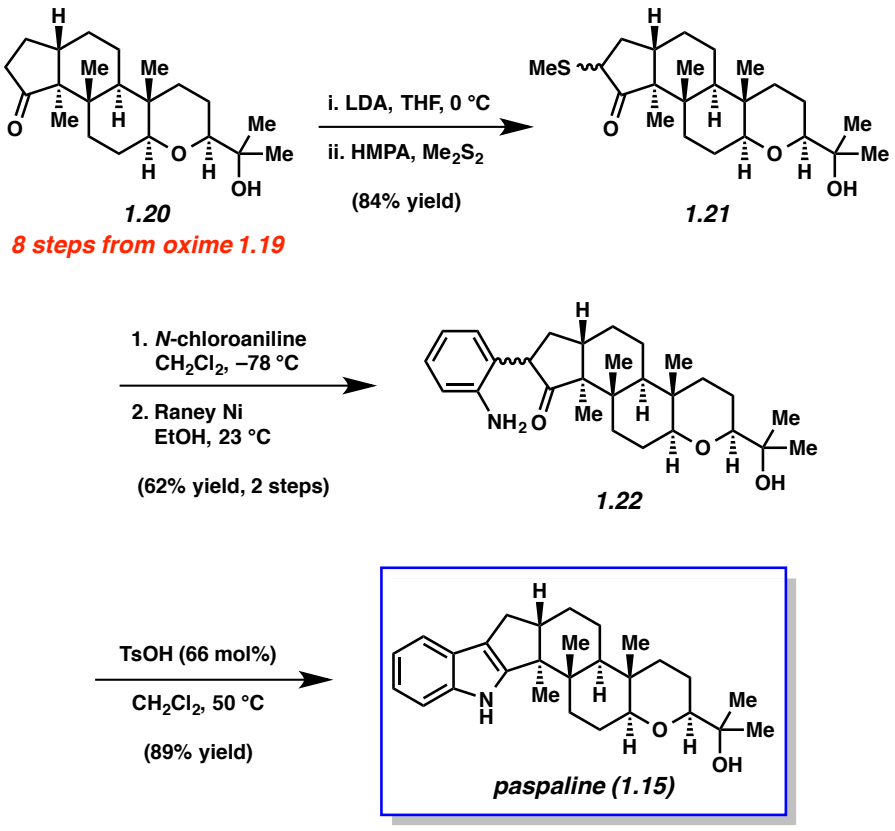

Scheme 1.4. Gassman indolization and completed synthesis of paspaline.

The Johnson synthesis of paspaline (**1.15**) showcases a number of elegant transformations. Central to the success of their approach was the clever utilization of desymmetrization reactions. The early enzymatic desymmetrization established two key stereocenters, including a challenging quaternary center. Subsequently, the judicious application of C–H functionalization chemistry produced a local desymmetrization event and installed another quaternary stereocenter. The execution of these processes not only facilitated the total synthesis of **1.15**, but also underscores innovation prompted by the complexity of an indole diterpenoid.

1.6 Baran Synthesis of Dixiamycin B

Dixiamycin B (**1.23**) is an oligomeric indole alkaloid that was isolated independently by Zhang and Hertweck from *Streptomyces* sp. SCSIO 02999 in 2012.[28] The compound exhibits low μM antibacterial activity against several bacteria, including *E. coli*, *S. auereus*, *B. subtilis*, and *B. thuringensis*. Dixiamycin B (**1.23**) is a dimer of an indole diterpenoid, xiamycin A (**1.27**), which contains a carbazole fused to a *trans*-decalin core with four contiguous stereocenters, three of which are quaternary. In the dimerized natural product, the monomer units are uniquely linked via a N–N bond. Baran's laboratory tackled the total synthesis of dixiamycin B (**1.23**) by implementing a novel application of electrochemical oxidation to form this unusual bond.

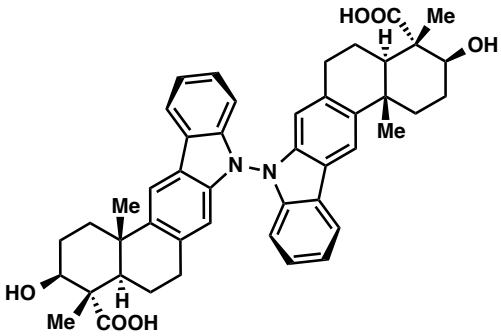

Dixiamycin B (1.23)
(Baran)

- *Oligomeric indole diterpenoid*
- *Expedient synthesis of monomer*

Can dimerization about N–N bond afford natural product?

Figure 1.5. Indole diterpenoid alkaloid dixiamycin B.

To validate their dimerization strategy, the group first tested oxidation methods on a simpler substrate, carbazole, to form the N–N bond. After examining chemical oxidants, which were largely deemed unfruitful, the authors turned to electrochemistry to facilitate the desired oxidative dimerization. Inspired by previous preparative scale carbazole dimerization reactions as well as mechanistic studies,[29] they found that efficient dimerization of carbazole took place using a potential of +1.2 V with a carbon anode (i.e., 63% yield of carbazole dimer).

Armed with these results, they then embarked on the synthesis of the monomeric natural product, xiamycin A (**1.27**), as summarized in Scheme 1.5. The synthesis began with elaboration of epoxide **1.24**, available in >10 g quantity in five steps from geraniol,[30] to carbazole **1.25** in three steps. Boc protection, followed by treatment with BF_3•OEt_2, initiated a cationic polycyclization reaction, which established the core of the natural product. Of note, the product from this transformation, pentacycle **1.26**, possesses the four contiguous stereocenters present in

the natural product. From pentacycle **1.26**, xiamycin A (**1.27**) was accessed in four steps involving removal of the Boc and Bn protecting groups, as well as oxidation to introduce the necessary carboxylic acid.

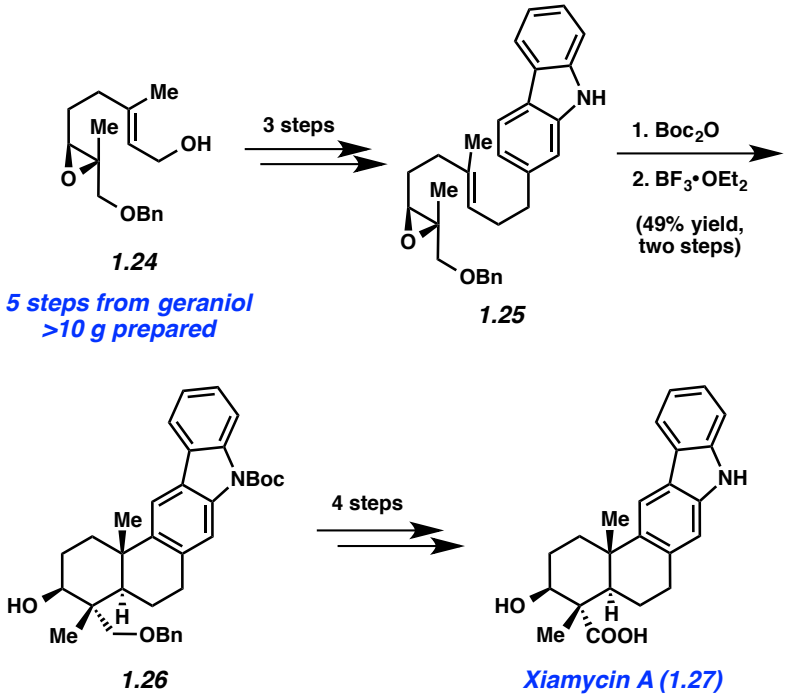

Scheme 1.5. Expedient synthesis of monomeric natural product xiamycin A.

With xiamycin A (**1.27**) in hand, the authors attempted the critical dimerization reaction (Scheme 1.6). Upon subjection of xiamycin A (**1.27**) to electrochemical oxidation conditions involving 1.15 V using a carbon anode, the desired oxidative dimerization took place. Consequently, dixiamycin B (**1.23**) was obtained in 28% yield. The reaction also gave 13% of recovered starting material, along with 17% yield of brominated xiamycin derivative **1.28**.

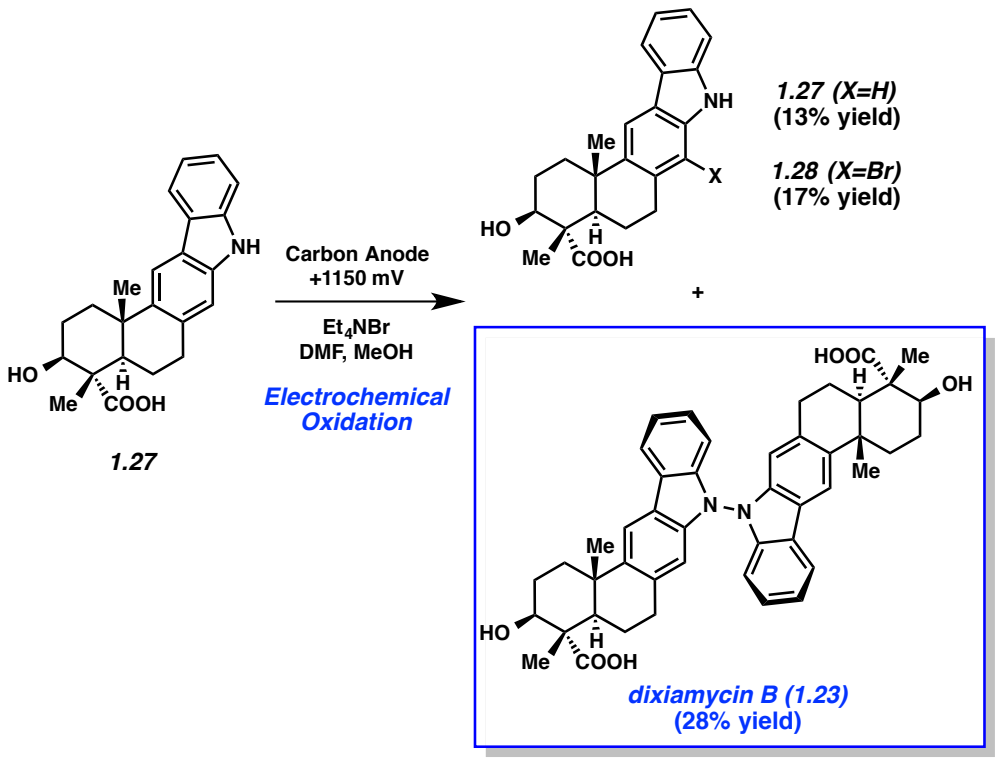

Scheme 1.6. Electrochemical oxidation forges key N–N bond of dixiamycin B.

With the success of the electrochemical dimerization reaction, not only did the Baran laboratory accomplish an expedient synthesis of an unusual natural product, but they also brought forth much deserved attention to the use of electrochemistry as an enabling tool in total synthesis.[31] Numerous advances in electrochemical organic reactions have been disclosed,[32] thus providing exciting tactics for chemists to consider when tackling challenging bond formations.

1.7 Garg's Total Syntheses of Tubingensins A & B

The final natural products highlighted in this chapter are tubingensin A (**1.29**) and tubingensin B (**1.30**) (Figure 1.6). Due to their intriguing structures, these indole diterpenoids have sparked interest from the synthetic community. Both compounds were isolated from the

fungus *Aspergillus tubingensis* by Gloer and coworkers in 1989 and display antiviral, anticancer, and insecticidal activity.[33] Tubingensin A (**1.29**) has been the subject of previous synthetic studies,[34] and has now been synthesized twice. The first synthesis was reported by Li and Nicolaou in 2012.[6c] Two years later, we described an enantiospecific route to the natural product.[11a] Recently, our laboratory completed the first total synthesis of tubingensin B (**1.30**).[11b]

Our lab first became interested in pursuing the total synthesis of the tubingensin alkaloids due to the structural complexity of these targets. Both compounds possess ortho-disubstituted carbazoles fused to intricate ring systems. In the case of tubingensin A (**1.29**), the natural product features four contiguous stereocenters, two of which are vicinal quaternary centers. Regarding tubingensin B (**1.30**), the natural product scaffold is significantly more complex due to the presence of the bicyclo[3.2.2]nonane core. In both cases, we viewed the natural product cores and the presence of quaternary centers as excellent testing grounds for aryne chemistry. Specifically, we questioned if carbazole-derived arynes, or 'carbazolynes' could be used to assemble the stereochemically complex frameworks present in the tubingensin alkaloids.

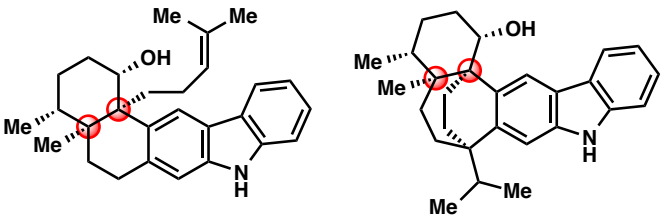

Figure 1.6. Tubingensins A & B featuring synthetically challenging vicinal quaternary centers.

Although the discussion herein will largely focus on tubingensin B (**1.30**), some mention of carbazolyne cyclization studies in the context of tubingensin A (**1.29**) is warranted. In fact,

considerable effort was required to find a substrate prone to undergo the desired carbazolyne cyclization. Two key results are depicted in Figure 1.7. In the first, bromoketone **1.31**, a model substrate lacking the homoprenyl sidechain, was treated with $NaNH_2$/*t*-BuOH.[35] These conditions, which are commonly used to generate arynes by dehydrohalogenation, were intended to facilitate both enolate formation and aryne formation en route to C–C bond construction. However, the major product obtained was tetracyclic ketone **1.32**. This reaction is believed to proceed through the intended intermediate, which underwent formal [2+2] cycloaddition, followed by retro [4+2] reaction.[11a] Ultimately, the desired aryne cyclization was accomplished using TES enol ether **1.33** as the substrate. Exposure to $NaNH_2$/*t*-BuOH furnished the desired pentacyclic ketone **1.34** in a gratifying 84% yield. Ketone **1.34** was then elaborated to the natural product, tubingensin A (**1.29**), in two additional steps.

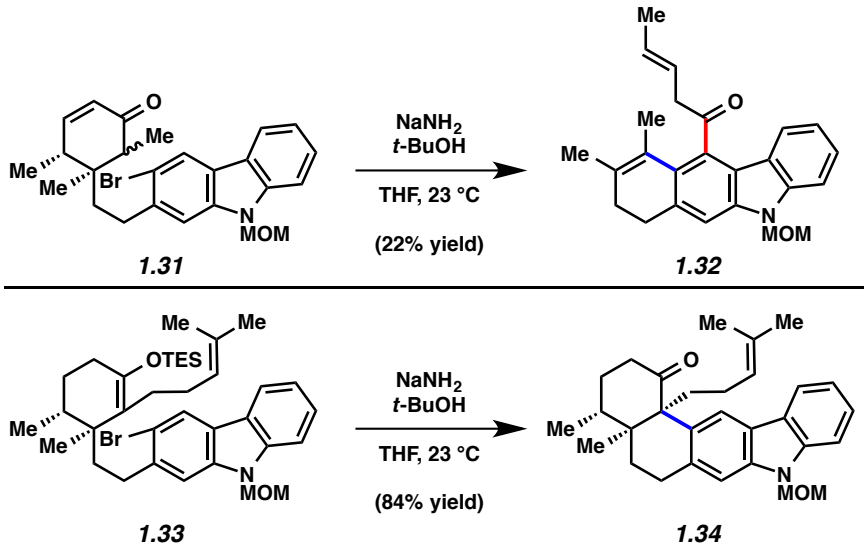

Figure 1.7. Attempted aryne cyclization to provide undesired adduct **1.32** and successful aryne cyclization to deliver ketone **1.34** en route to tubingensin A.

Having established the utility of aryne chemistry for the assembly of the tubingensin A scaffold, we directed our attention to the more complex family member, tubingensin B (**1.30**). In designing our synthesis, we envisioned the use of a carbazolyne cyclization to assemble a 7-membered ring. Aryne cyclizations to construct medium-sized rings are rare[36] and no such examples involving the formation of vicinal quaternary stereocenters were available in the literature.

Our first major hurdle in the total synthesis of tubingensin B (**1.29**) was the construction of an appropriate aryne cyclization precursor. As shown in Scheme 1.7, our strategy involved *B*-alkyl Suzuki–Miyaura coupling of known olefin fragment **1.35** with vinyl iodide **1.36**. Unification of these two fragments was far from trivial due to the congested nature of the tetrasubstituted olefin being formed, which is also positioned ortho to the aryl bromide. The necessary survival of the dimethylisopropylsilyl (DMIPS) enol ether added another layer of complexity to this transformation. After extensive optimization, we found that $Pd_2(dba)_3$ and $AsPh_3$ facilitated the desired bond formation.[37] In three steps, silyl enol ether **1.37** could be further elaborated to α-functionalized TES enol ether **1.38**.

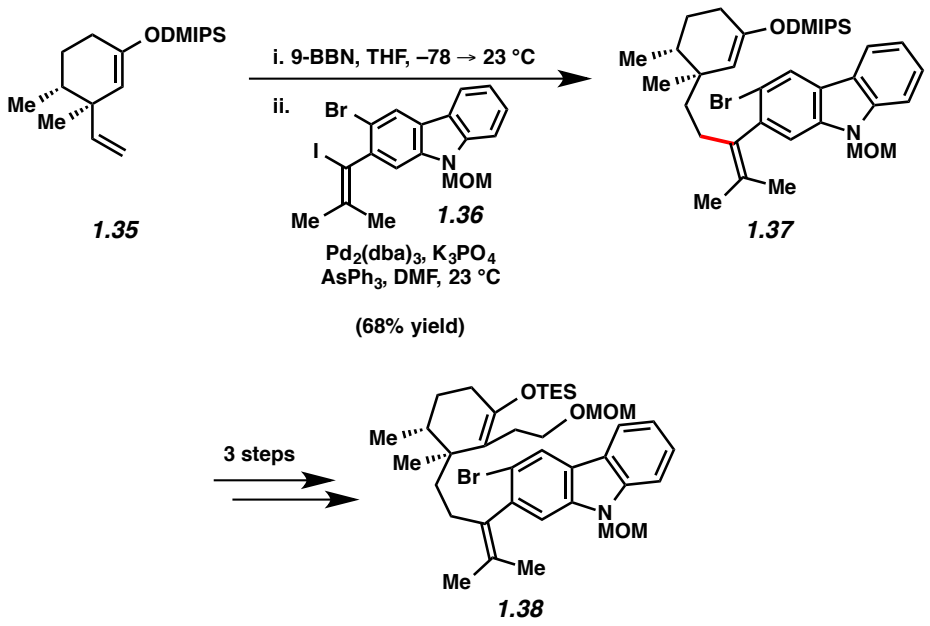

Scheme 1.7. Challenging *B*-alkyl Suzuki–Miyaura coupling affords tetrasubstituted olefin **1.37**, which was subsequently converted to aryne cyclization substrate **1.38**.

With TES enol ether **1.38** in hand, the key carbazolyne cyclization to form the seven-membered ring of the natural product was examined (Figure 1.8). Exposure of **1.38** to $NaNH_2$/*t*-BuOH was expected to result in enolate formation and dehydrohalogenation, with subsequent C–C bond formation. However, rather than obtaining the desired product, cyclobutenol **1.41** was observed. As expected, the desired enolate/aryne is first believed to form and undergo C–C bond formation (see transition structure **1.39**). The resulting carbanion is thought to then cyclize onto the proximal ketone (see **1.40**), thus giving rise to **1.41**, rather than undergo protonation. It was ultimately found, however, that by performing the reaction at higher temperature, the desired product, ketone **1.42**, could be accessed in 58% yield. Presumably, the formal [2+2] cycloaddition still occurs under these conditions, but the resulting intermediate undergoes in situ

fragmentation to eventually give **1.42**. Notably, this carbazolyne cyclization reaction establishes both the pentacyclic core and the vicinal quaternary centers of the natural product.

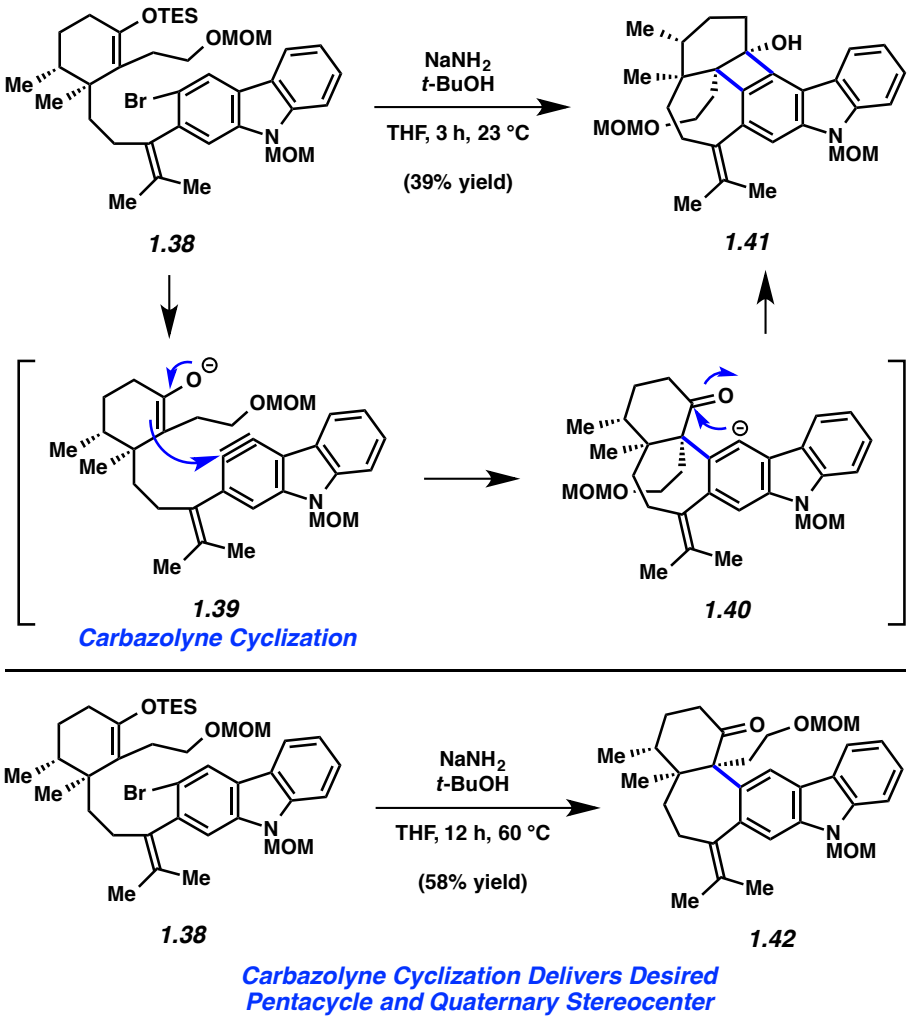

Figure 1.8. Carbazolyne cyclization studies toward the total synthesis of tubingensin B.

We were delighted to find that the carbazolyne cyclization provided access to ketone **1.42** and subsequently focused our efforts on elaborating **1.42** to the natural product. Although we were able to synthesize tubingensin B (**1.30**) from ketone **1.42**, the route required several

functional group interconversions and redox manipulations that we wished to circumvent. Thus, we redesigned our aryne precursor to include a different functional group handle in place of the MOM ether and eventually settled on selenide **1.43** (Scheme 1.8). Exposure of this substrate to $NaNH_2$/*t*-BuOH afforded cyclobutenol **1.44**. Unfortunately, attempts to induce in situ fragmentation by heating the reaction led to elimination of the alkyl selenide. Thus, we turned to the rhodium-catalyzed cyclobutenol ring opening conditions developed by Murakami and coworkers.[38] Gratifyingly, subjection of cyclobutenol **1.44** to catalytic $[Rh(OH)cod]_2$ in toluene at 100 °C led to the appropriate C–C bond cleavage to supply ketone **1.45**.

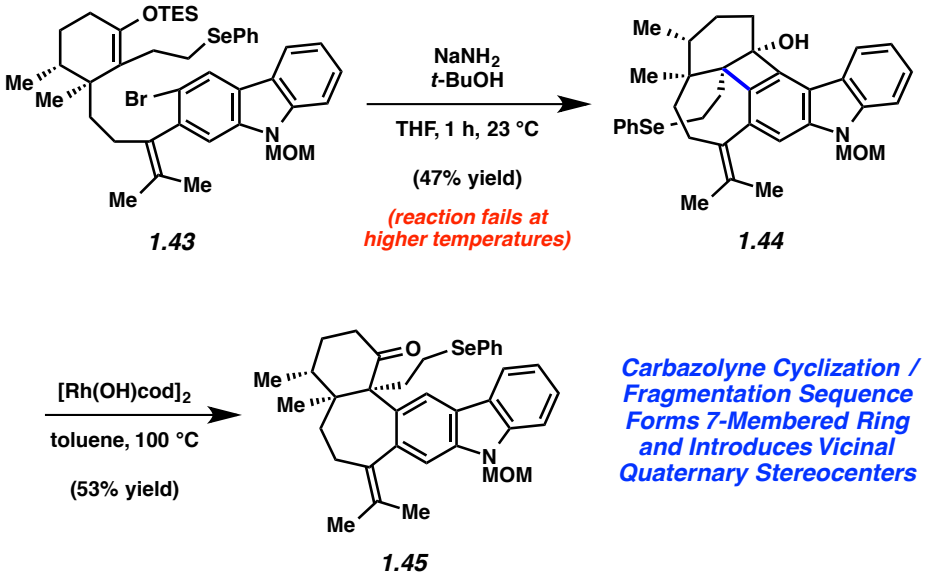

Scheme 1.8. Carbazolyne cyclization/fragmentation sequence furnished ketone **1.45**.

From alkyl selenide **1.45**, completion of the total synthesis of tubingensin B (**1.30**) was achieved using the sequence highlighted in Scheme 1.9. Exposure of selenide **1.45** to tributyltin hydride and AIBN in toluene at 110 °C resulted in the desired radical cyclization[39] to give

product **1.46** in 54% yield. Of note, this reaction installed the bicyclo[3.2.2]nonane core and the final C–C bond of the natural product. From **1.46**, all that remained was deprotection of the carbazole nitrogen and reduction of the ketone. Treatment of *N*-MOM ketone **1.46** with 3 N HCl and ethylene glycol at 55 °C delivered ketone **1.47** in 67% yield. Although diastereoselective ketone reduction proved difficult, an exhaustive survey of conditions led us to identify suitable conditions. Subjection of ketone **1.47** to (*R*)-Ru(OAc)$_2$(DM-SEGPHOS), KOH, and H_2 (1500 psi) gave synthetic tubingensin B (**1.30**).[40]

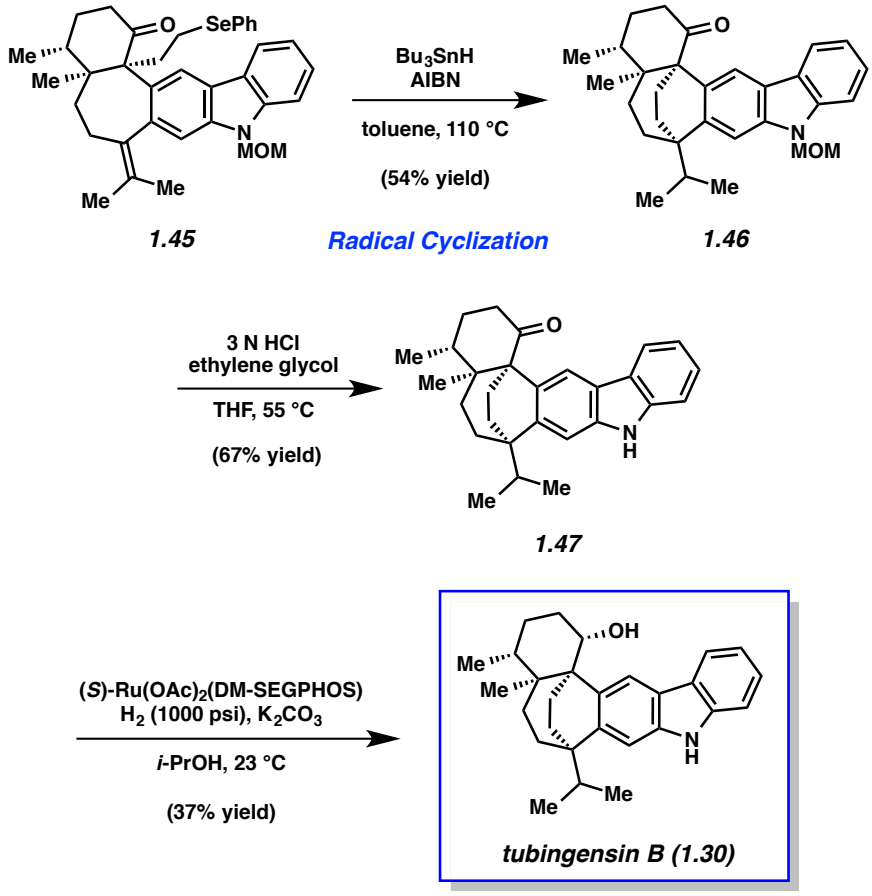

Scheme 1.9. Radical cyclization, deprotection, and late-stage reduction furnishes tubingensin B.

The concise total syntheses of tubingensin A (**1.29**) and tubingensin B (**1.30**) were made possible by the strategic use of aryne chemistry. More specifically, the carbazolyne cyclizations facilitated construction of the pentacyclic cores and installed vicinal quaternary stereocenters of the natural products. The synthesis of tubingensin B (**1.30**) was further enabled by (a) the Rh-catalyzed fragmentation of an unexpected cyclobutenol intermediate and (b) a late-stage radical cyclization stemming from a phenylselenide intermediate to install a final quaternary stereocenter and the [3.2.2]-bridged bicyclic framework of the natural product. These results underscore the fact that arynes, despite often being considered 'too reactive' and therefore undesirable, can be used strategically to access challenging structural motifs, such as medium-sized rings and vicinal quaternary stereocenters.

1.8 Conclusion

In this chapter, we have demonstrated that indole diterpenoid natural products serve as excellent stepping-stones for innovation in chemical synthesis. Penitrem D, arguably the most complex member of this natural product family, featured the Smith indole synthesis, as a means to not only introduce the indole unit, but also to couple two complex fragments. The synthesis of emindole SB from the Pronin group showcased the development of a new ketone alkenylation protocol, as well as an elegant application of hydrogen atom transfer chemistry in total synthesis. Johnson's synthesis of paspaline demonstrated clever use of desymmetrization reactions in the context of an enzymatic reduction and a C–H functionalization to install stereochemical complexity. Moreover, through the synthesis of dixiamycin B, the Baran laboratory has shown that electrochemistry can be a powerful complement to traditional chemical oxidants. Finally, our laboratory's forays toward the tubingensin alkaloids have demonstrated the effectiveness of

heterocyclic aryne chemistry in building stereochemically complex molecules, including vicinal quaternary centers. We envision that indole diterpenoids will continue to foster creativity in chemical synthesis for years to come.

1.9 Notes and References

(1) Jordan, M. A.; Wilson, L. *Nat. Rev. Cancer* **2004**, *4*, 253–265.

(2) For reviews of indole terpenoid synthesis, see: (a) Ishikura, M.; Yamada, K. *Nat. Prod. Rep.* **2009**, *26*, 803–852. (b) Ishikura, M.; Yamada, K.; Abe, T. *Nat. Prod. Rep.* **2010**, *27*, 1630–1680. (c) Ishikura, M.; Abe, T.; Choshib, T.; Hibinob, S. *Nat. Prod. Rep.* **2013**, *30*, 694–752. (d) Marcos, I. S.; Moro, R. F.; Costales, I.; Basabe, P.; Díez, D. *Nat. Prod. Rep.* **2013**, *30*, 1509–1526. (e) Baunach, M.; Franke, J.; Hertweck, C. *Angew. Chem., Int. Ed.* **2015**, *54*, 2604–2626.

(3) Kornfeld, E. C.; Fornefeld, E. J.; Kline, G. B.; Mann, M. J.; Morrison, D. E.; Jones, R. G.; Woodward, R. B. *J. Am. Chem. Soc.* **1956**, *78*, 3087–3114.

(4) Sears, J. E.; Boger, D. L. *Acc. Chem. Res.* **2015**, *48*, 653–662 and references therein.

(5) (a) Enomoto, M.; Morita, A.; Kuwahara, S. *Angew. Chem. Int. Ed.* **2012**, *51*, 12833–12836. (b) Teranishi, T.; Murokawa, T.; Enomoto, M.; Kuwahara, S. *Biosci., Biotechnol., Biochem.* **2015**, *79*, 11–15.

(6) (a) Zhou, S.; Zhang, D.; Sun, Y.; Li, R.; Zhang, W.; Li, A. *Adv. Synth. Catal.* **2014**, *356*, 2867–2872. (b) Xiong, X.; Zhang, D.; Li, J.; Sun, Y.; Zhou, S.; Yang, M.; Shao, H.; Li, A. *Chem. Asian J.* **2015**, *10*, 869–872. (c) Bian, M.; Wang, Z.; Xiong, X.; Sun, Y.; Matera, C.; Nicolaou, K. C.; Li, A. *J. Am. Chem. Soc.* **2012**, *134*, 8078–8081. (d) Sun, Y.; Meng, Z.; Chen, P.; Zhang, D.; Baunach, M.; Hertweck, C.; Li, A. *Org. Chem. Front.* **2016**, *3*, 368–374 and references therein.

(7) (a) Smith, A. B., III; Kanoh, N.; Ishiyama, H.; Hartz, R. A. *J. Am. Chem. Soc.* **2000**, *122,* 11254–11255. (b) Smith, A. B., III; Kanoh, N.; Ishiyama, H.; Minakawa, N.; Rainier, J.; Hartz, R. A.; Cho, Y. S.; Cui, H.; Moser, W. H. *J. Am. Chem. Soc.* **2003**, *125*, 8228–8237.

(8) George, D. T.; Kuenstner, E. J.; Pronin, S. V. *J. Am. Chem. Soc.* **2015**, *137*, 15410–15413.

(9) (a) Sharpe, R. J.; Johnson, J. S. *J. Am. Chem. Soc.* **2015**, *137*, 4968–4971. (b) Sharpe, R. J.; Johnson, J. S. *J. Org. Chem.* **2015**, *80*, 9740–9766.

(10) Rosen, B. R.; Werner, E. W.; O'Brien, A. G.; Baran, P. S. *J. Am. Chem. Soc.* **2014**, *136*, 5571–5574.

(11) (a) Goetz, A. E.; Silberstein, A. L.; Corsello, M. A.; Garg, N. K. *J. Am. Chem. Soc.* **2014**, *136*, 3036–3039. (b) Corsello, M. A.; Kim, J.; Garg, N. K. *Nat. Chem.* **2017**, *9*, 944–949.

(12) (a) Smith, A. B., III; Mewshaw, R. *J. Am. Chem. Soc*. **1985**, *107*, 1769–1771. (b) Smith, A. B., III; Sunazuka, T.; Leenay, T. L.; Kingery-Wood, J. *J. Am. Chem. Soc*. **1990**, *112*, 8197–8198. (c) Smith, A. B., III; Leenay, T. L. *Tetrahedron Lett.* **1988**, *29*, 2787–2790. (d) Smith, A. B., III; Leenay, T. L. *Tetrahedron Lett.* **1988**, *29*, 2791–2792. (e) Mewshaw, R. E.; Taylor, M. D.; Smith, A. B., III. *J. Org. Chem.* **1989**, *54*, 3449–3462. (f) Smith, A. B., III; Leenay, T. L. *J. Am. Chem. Soc.* **1989**, *111*, 5761–5768. (g) Smith, A. B., III; Kingery-Wood, J.; Leenay, T. L.; Nolen, E. G.; Sunazuka, T. J. *J. Am. Chem. Soc.* **1992**, *114*, 1438–1449. (h) Rainier, J. D.; Smith, A. B., III. *Tetrahedron Lett.* **2000**, *41*, 9419–9423. (i) Smith, A. B., III; Cui, H. *Org. Lett.* **2003**, *5*, 587–590. (j) Zou, Y.; Melvin, J. E.; Gonzales, S. S.; Spafford, M. J.; Smith, A. B., III. *J. Am. Chem. Soc.* **2015**, *137*, 7095–7098.

(13) de Jesus, A. E.; Steyn, P. S.; van Heerden, F. R.; Vleggaar, R.; Wessels, P. L.; Hull, W. E. *J. Chem. Soc., Perkin Trans. 1* **1983**, 1847–1856.

(14) Knaus, H.-G.; McManus, O. B.; Lee, S. H.; Schmalhofer, W. A.; Garcia-Calvo, M.; Helms, L. M. H.; Sanchez, M.; Giangiacomo, K.; Reuben, J. P.; Smith, A. B., III; Kaczorowski, G. J.; Garcia, M. L. *Biochemistry* **1994**, *33*, 5819–5828.

(15) Smith, A. B., III; Visnick, M. *Tetrahedron Lett.* **1985**, *26*, 3757–3760.

(16) Madelung, W. *Ber. Dtsch. Chem. Ges.* **1912**, *45*, 1128–1134.

(17) Nozawa, K.; Nakajima, S.; Kawai, K.-i. *J. Chem. Soc. Perkin Trans. 1* **1988**, 2607–2610.

(18) Sallam, A. A.; Houssen, W. E.; Gissendanner, C. R.; Orabi, K. Y.; Foudah, A. I.; El Sayed, K. A. *Med. Chem. Comm.* **2013**, *4*, 1360–1369.

(19) Nishimoto, Y.; Moritoh, R.; Yasuda, M.; Baba, A. *Angew. Chem., Int. Ed.* **2009**, *48*, 4577–4580.

(20) Holmbo, S. D.; Godfrey, N. A.; Hirner, J. J.; Pronin, S. V. *J. Am. Chem. Soc.* **2016**, *138*, 12316–12319.

(21) Parikh, J. R.; Doering, W. E. *J. Am. Chem. Soc.* **1967**, *89*, 5505–5507.

(22) (a) Lo, J. C.; Yabe, Y.; Baran, P. S. *J. Am. Chem. Soc.* **2014**, *136*, 1304–1307. (b) Lo, J. C.; Gui, J.; Yabe, Y.; Pan, C.-M.; Baran, P. S. *Nature* **2014**, *516*, 343–348.

(23) Obradors, C.; Martinez, R. M.; Shenvi, R. A. *J. Am. Chem. Soc.* **2016**, *138*, 4962–4971.

(24) Fehr, T.; Acklin, W. *Helv. Chim. Acta* **1966**, *49*, 1907–1910.

(25) (a) Watanabe, H.; Iwamoto, M.; Nakada, M. *J. Org. Chem.* **2005**, *70*, 4652–4658. (b) Katoh, T.; Mizumoto, S.; Fudesaka, M.; Nakashima, Y.; Kajimoto, T.; Node, M. *Synlett* **2006**, 2176–2182. (c) Katoh, T.; Mizumoto, S.; Fudesaka, M.; Takeo, M.; Kajimoto, T.; Node, M. *Tetrahedron: Asymmetry* **2006**, *17*, 1655–1662.

(26) (a) Desai, L. V.; Hull, K. L.; Sanford, M. S. *J. Am. Chem. Soc.* **2004**, *126*, 9542–9543. (b) Neufeldt, S. R.; Sanford, M. S. *Org. Lett.* **2010**, *12*, 532–535.

(27) Gassman, P. G.; van Bergen, T. J.; Gilbert, D. P.; Cue, B. W., Jr. *J. Am. Chem. Soc*. **1974**, *96*, 5495–5508.

(28) (a) Zhang, Q.; Mańdi, A.; Li, S.; Chen, Y.; Zhang, W.; Tian, X.; Zhang, H.; Li, H.; Zhang, W.; Zhang, S.; Ju, J.; Kurtań, T.; Zhang, C. *Eur. J. Org. Chem.* **2012**, 5256–5262. (b) Xu, Z.; Baunach, M.; Ding, L.; Hertweck, C. *Angew. Chem., Int. Ed.* **2012**, *51*, 10293–10297.

(29) (a) Ambrose, J. F.; Carpenter, L. L.; Nelson, R. F. *J. Electrochem. Soc.* **1975**, *122*, 876–894. (b) Bobbitt, J. M.; Kuljarni, C. L.; Willis, J. P. *Heterocycles* **1981**, *15*, 495–516. (c) Berti, C.; Greci, L.; Andruzzi, R.; Trazza, A. *J. Org. Chem.* **1985**, *50*, 368–373.

(30) Tanis, S. P.; Chuang, Y.-H.; Head, D. B. *J. Org. Chem.* **1988**, *53*, 4929–4938.

(31) (a) Liu, B.; Duan, S.; Sutterer, A. C.; Moeller, K. D. *J. Am. Chem. Soc.* **2002**, *124*, 10101–10111. (b) Mihelcic, J.; Moeller, K. D. *J. Am. Chem. Soc.* **2003**, *125*, 36–37. (c) Hughes, C. C.; Miller, A. K.; Trauner, D. *Org. Lett.* **2005**, *7*, 3425–3428. (d) Xu, H.-C.; Brandt, J. D.; Moeller, K. D. *Tetrahedron Lett.* **2008**, *49*, 3868–3971.

(32) (a) Moeller, K. D. *Tetrahedron* **2000**, *56*, 9527–9554. (b) Horn, E. J.; Rosen, B. R.; Baran, P. S. *ACS Cent. Sci.* **2016**, *2*, 302–308. (c) Ding, H.; DeRoy, P. L.; Perreault, C.; Larivée, A.; Siddiqui, A.; Caldwell, C. G.; Harran, S.; Harran, P. G. *Angew. Chem., Int. Ed.* **2015**, *54*, 4818–4822.

(33) (a) TePaske, M. R.; Gloer, J. B.; Wicklow, D. T.; Dowd, P. F. *J. Org. Chem.* **1989**, *54*, 4743–4746. (b) TePaske, M. R.; Gloer, J. B.; Wicklow, D. T.; Dowd, P. F. *Tetrahedron Lett.* **1989**, *30*, 5965–5968.

(34) Bradshaw, B.; Etxebarria-Jardí, G.; Bonjoch, J. *Org. Biomol. Chem.* **2008**, *6*, 772–778.

(35) Caubere, P. *Acc. Chem. Res.* **1974**, *7*, 301–308.

(36) (a) Tadross, P. M.; Stoltz, B. M. *Chem. Rev.* **2012**, *112*, 3550–3577. (b) Boente, J. M.; Castedo, L.; Rodriguez de Lera, A.; Saá, J. M.; Suau, R.; Vidal, M. C. *Tetrahedron Lett.* **1983**, *24*, 2295–2298. (c) Huters, A. D.; Quasdorf, K. W.; Styduhar, E. D.; Garg, N. K. *J. Am. Chem. Soc.* **2011**, *133*, 15797–15799.

(37) Kojima, A.; Honzawa, S.; Boden, C. D. J.; Shibasaki, M. *Tetrahedron Lett*. **1997**, *38*, 3455–3458.

(38) Ishida, N.; Sawano, S.; Masuda, Y.; Murakami, M. *J. Am. Chem. Soc.* **2012**, *134*, 17502–17504.

(39) Clive, D. L. J.; Cole, D. C.; Tao, Y. *J. Org. Chem.* **1994**, *59*, 1396–1406.

(40) Tang, W.; Zhang, X. *Chem. Rev*. **2003**, *103*, 3029–3069.

CHAPTER TWO

Total Synthesis of (–)-Tubingensin B Enabled by the Strategic Use of an Aryne Cyclization

Michael A. Corsello,[†] Junyong Kim,[†] and Neil K. Garg

Nat. Chem. **2017**, *9*, 944–949.

2.1 Abstract

Tubingensin B is an indole diterpenoid that bears a daunting chemical structure. The natural product presents several challenging structural features, such as a disubstituted carbazole unit, five stereogenic centers, three of which are quaternary, and a decorated [3.2.2]-bridged bicycle that is fused to a 6-membered ring. In this manuscript, we describe our synthetic design toward a concise and enantiospecific total synthesis of tubingensin B, which hinges on the strategic use of a transient aryne intermediate. Although initial studies led to unexpected reaction outcomes, we ultimately implemented a carbazolyne cyclization / Rh-catalyzed fragmentation sequence to install the 7-membered ring and vicinal quaternary stereocenters of the natural product. Coupled with a late-stage radical cyclization to construct the [3.2.2]-bridged bicycle, these efforts have enabled the first total synthesis of tubingensin B. The design and evolution of our succinct total synthesis underscores the utility of long-avoided aryne intermediates for the introduction of structural motifs that have conventionally been viewed as challenging, such as medium-sized rings and vicinal quaternary stereocenters.

2.2 Introduction

Indole alkaloids continue to inspire the development of new chemical transformations and innovative synthetic strategies. The focus of the present study is tubingensin B (**2.1**), an indole diterpenoid that was isolated from the fungus *Aspergillus tubingensis* in 1989 (Figure 2.1).[1] Tubingensin B (**2.1**) is a secondary metabolite that is believed to help protect the producing fungus from natural predators. It exhibits activity against the widespread crop pest *Heliothis zea*, causing 10% mortality in a dietary assay at 125 ppm. In addition, tubingensin B (**2.1**) displays cytotoxicity against cervical cancer cells (HeLa) with an IC_{50} of 4 mg/mL. Lastly, the natural product demonstrates in vitro antiviral activity against herpes simplex virus type 1 (HSV-1) with an IC_{50} of 9 mg/mL. From a structural standpoint, the sheer complexity of tubingensin B (**2.1**) captured our attention. The eastern portion of the natural product possesses a carbazole unit, which, at a glance, is deceptively simple. However, the presence of two adjacent sp^2–sp^3 carbon–carbon (C–C) bond linkages, with quaternary stereocenters stemming from the carbazole, presents a significant hurdle. Further compounding the challenge is the bicyclo[3.2.2]nonane core, which is fused to the carbazole and a densely functionalized 6-membered ring. In total, the natural product possesses five stereogenic centers. Four of these stereocenters are contiguous and three are quaternary, including two vicinal quaternary centers. Although two total syntheses of the related natural product tubingensin A (**2.2**) have been reported (by Li[2] and our own laboratory[3]), a total synthesis of the more daunting family member, tubingensin B (**2.1**), has remained elusive. Herein, we report our synthetic forays toward (–)-**2.1**, which have culminated in a succinct total synthesis of the targeted natural product. Critical to the success of this endeavor is the strategic use of a highly reactive aryne intermediate to rapidly build molecular complexity.

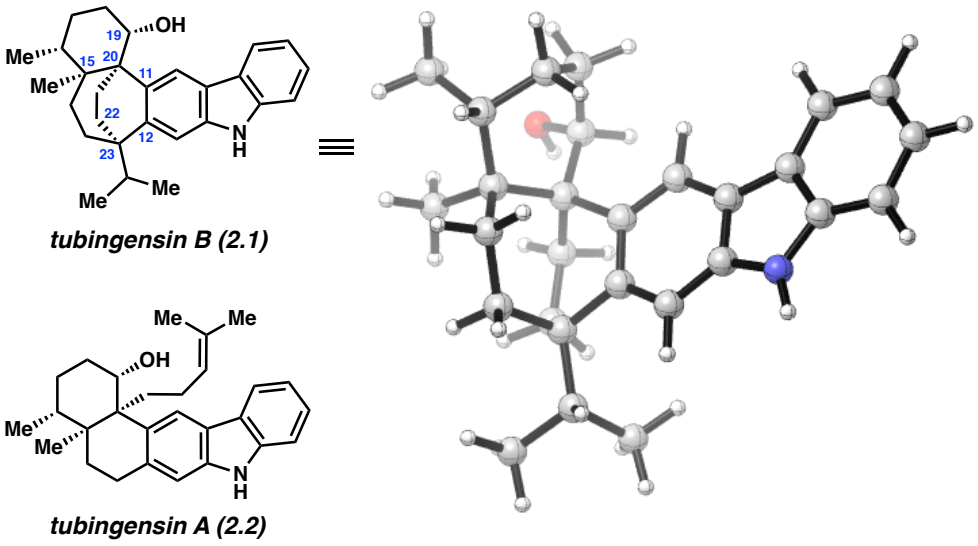

Figure 2.1. Tubingensins A and B.

2.3 Synthesis of Tubingensin B

Our initial retrosynthetic analysis of tubingensin B (**2.1**) is depicted in Scheme 2.1. It was envisioned that the natural product could arise from pentacycle **2.3** via a series of functional group manipulations and a late-stage radical cyclization. In the forward sense, the formation of the C22–C23 linkage using a radical cyclization would provide a suitable entryway to assemble the natural product's bicyclo[3.2.2]nonane core and the C23 quaternary stereocenter. Next, in a critical disconnection, pentacycle **2.3** was thought to be accessible by cyclization of an in situ-generated aryne derivative of a carbazole, known as a carbazolyne (see transition structure **2.4**). In turn, the carbazolyne would ultimately be derived from silyl enol ether **2.5** by C20 functionalization, followed by aryne formation. Although potentially challenging due to the short-lived nature of the highly strained carbazolyne, the success of this step would facilitate installation of the necessary 7-membered ring bearing vicinal quaternary stereocenters. It should

be noted that arynes, despite once being controversial and overlooked by the synthetic community, have recently gained traction in chemical synthesis.[4,5] However, their use as building blocks for the formation of vicinal quaternary stereocenters is limited to one example from our laboratory involving the assembly of a cyclohexyl ring present in tubingensin A.[3] Moreover, aryne cyclizations to form 7-membered rings are kinetically disfavored and especially rare.[5] For example, Castedo and coworkers observed the formation of a 7-membered ring via C–O bond construction as a minor reaction pathway (20% yield) in their synthesis of oxocularine.[6] Likewise, we have previously investigated 7-membered ring formation via enolate-aryne cyclizations in the context of the bridged bicyclic welwitindolinone alkaloids.[7] These efforts led to only modest yields of 7-membered ring-containing products, with competition between C- and O-arylation pathways (33% and 13%, respectively), without the complication of quaternary stereocenter formation in the present endeavor. As such, the desired carbazolyne cyclization to form a 7-membered ring and install vicinal quaternary stereocenters (e.g., **2.4**) challenges the limits of modern aryne chemistry. Nonetheless, to complete our retrosynthesis, we envisioned that enol ether **2.5** could be derived from two simpler fragments, cyclohexyl derivative **2.6** and carbazole **2.7**.

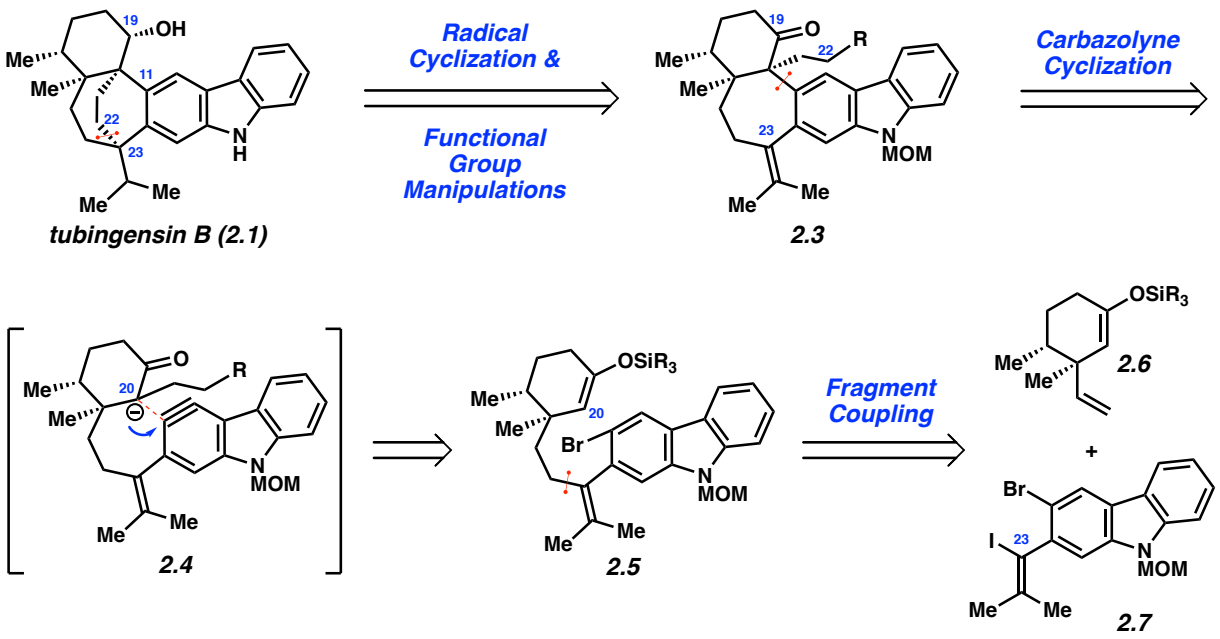

Scheme 2.1. Retrosynthetic analysis of tubingensin B.

We first sought to prepare the carbazole fragment, **2.7** (Figure 2.2a). Known bromotriflate **2.8** (prepared in three steps)[3] was treated with propargyl alcohol in the presence of catalytic $Pd(PPh_3)_4$ and CuI to effect a Sonogashira coupling.[8] The resulting product, alkynol **2.9** was obtained in 84% yield. Of note, this transformation could be performed on >10 g scale and provided an efficient means to homologate the carbazole fragment without disturbing the aryl bromide. Alkynol **2.9** was then subjected to a carbometalation/iodination sequence,[9] which delivered iodoalcohol **2.10** in 71% yield. Lastly, the desired vinyl iodide **2.7** was obtained following a two-step deoxygenation sequence.[10,11]

With vinyl iodide **2.7** available in multigram quantities, we pursued the union of this fragment with an appropriate cyclohexyl building block (Figure 2.2b). Olefin (–)-**2.11**, which is readily accessible from (+)-dihydrocarvone,[3,12] underwent hydroboration to furnish alkyl boron derivative **2.12**. This adduct was directly subjected to Pd-catalyzed Suzuki–Miyaura coupling

with dihalocarbazole **2.7** to afford desired product **2.13** in 76% yield. Several features of this transformation should be emphasized: (a) the use of $AsPh_3$ as the ligand[13] proved critical for catalytic activity, (b) competitive cross-coupling of the aryl bromide was not observed, (c) the DMIPS (dimethyl(isopropyl)silyl) enol ether readily withstood the reaction conditions, and (d) the formation of **2.13** provides an uncommon example of a $C(sp^2)$–$C(sp^3)$ cross-coupling to access a tetrasubstituted olefin.

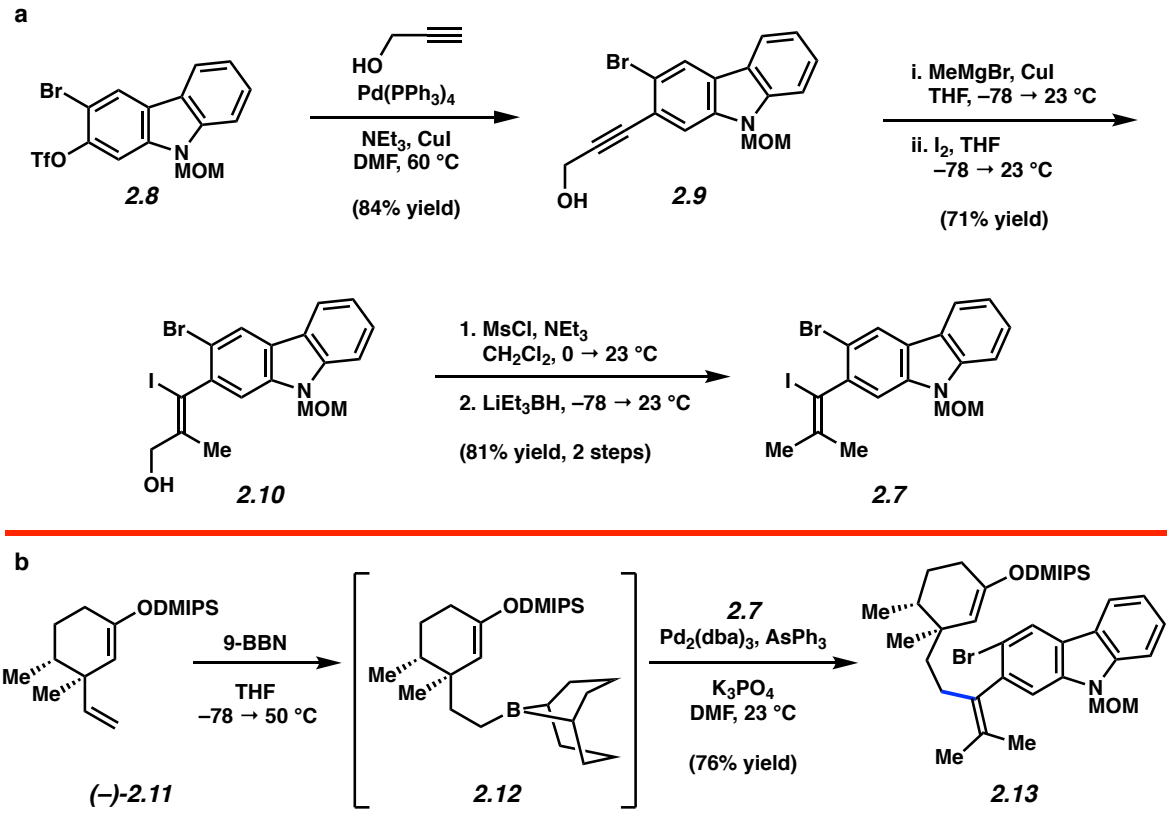

Figure 2.2. Synthesis of coupling fragment **2.7** and assembly of tetrasubstituted alkene **2.13**.

With rapid access to silyl enol ether **2.13**, we turned our attention to the critical aryne cyclization, with the hope of assembling the 7-membered ring and vicinal quaternary centers of the natural product (Scheme 2.2). However, it was first necessary to functionalize C20 with a

two-carbon unit adorned with a functional group handle. This goal was achieved using a three-step sequence involving Eschenmoser methenylation[14] of the labile dimethyl(isopropyl)silyl enol ether (**2.13→2.14**), followed by conjugate addition using the cuprate prepared in situ from $MOMOCH_2SnBu_3$.[15] Direct trapping of the resulting enolate with TESCl delivered C20-functionalized silyl enol ether **2.15**. Given our prior success in forging a 6,6-fused ring system in our total synthesis of tubingensin A,[3] we were hopeful that treatment of **2.15** with sodium amide/*t*-butanol[16] at ambient temperature would lead to dehydrohalogenation and enolate formation, with subsequent carbazolyne cyclization to forge the medium-sized ring. However, in this crucial reaction, the desired pentacyclic ketone was not observed. Rather, the major product isolated was cyclobutenol **2.16** as a single diastereomer, which presumably arises from formal [2+2] cycloaddition.[17] Although not the desired reaction outcome, the formation of strained hexacycle **2.16** underscores the power of aryne chemistry for the assembly of intricate molecular scaffolds (see 3D rendering[18]) through the formation of two C–C bonds and two fully substituted stereocenters. Not to be deterred, we explored the possibility of converting cyclobutenol **2.16** to the intended carbazolyne cyclization product.[17] Ultimately, it was found that such a ring fragmentation could be achieved using basic reaction conditions at elevated temperatures. Thus, we attempted the carbazolyne cyclization of **2.15** at 60 °C and were delighted to obtain the desired pentacyclic product **2.17**, bearing the key C20 quaternary stereocenter, in 58% yield. Of note, this reaction proceeded with complete diastereoselectivity, presumably guided by the adjacent C15 stereocenter, and allowed us to access the challenging 7-membered ring and vicinal quaternary stereocenters of the natural product scaffold.

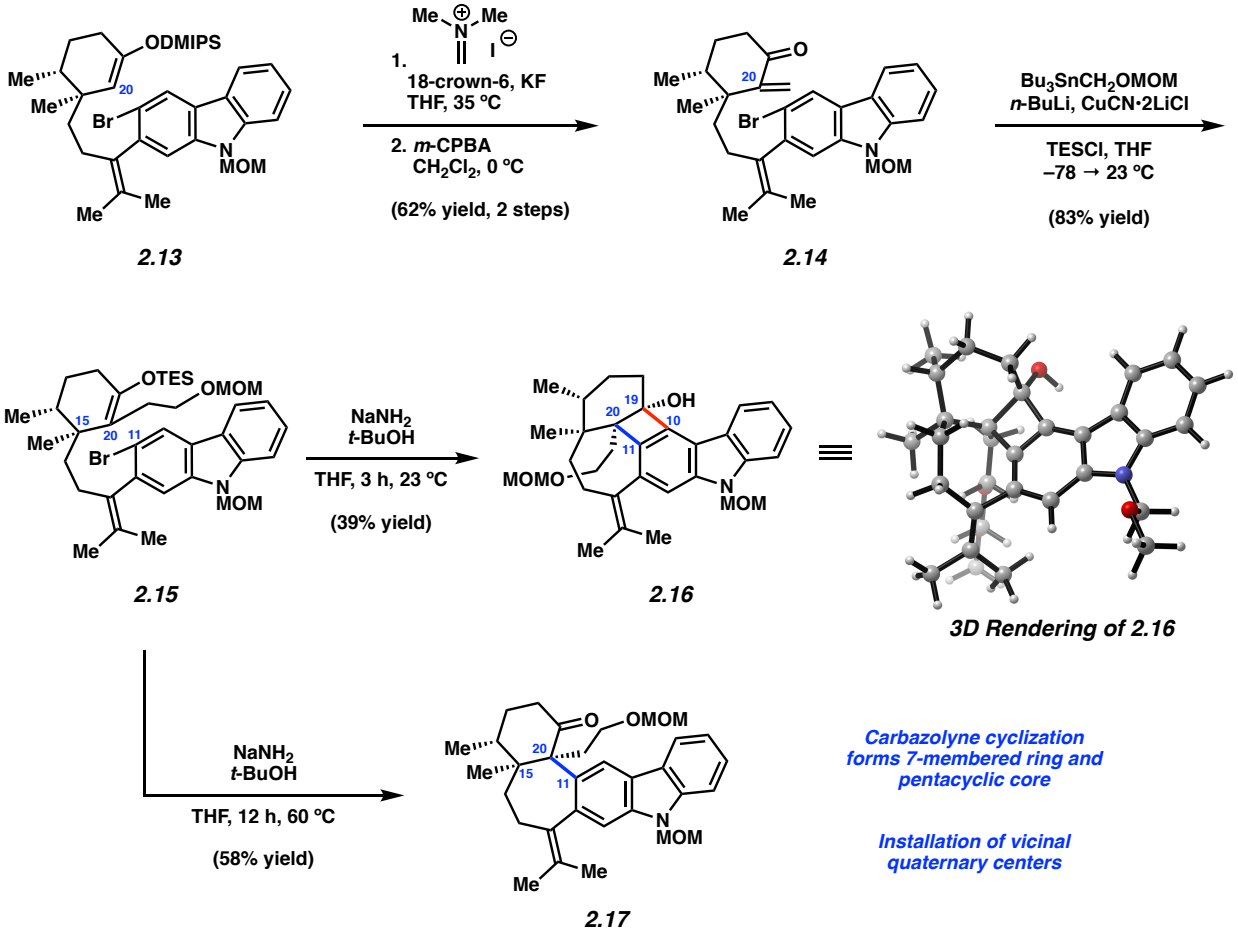

Scheme 2.2. Key aryne cyclization to forge the C20–C11 linkage.

With pentacycle **2.17** in hand, we turned our attention to construction of the bicyclo[3.2.2]nonane core (Scheme 2.3). Initial efforts to directly elaborate **2.17** to a suitable radical cyclization precursor were thwarted due to the incompatibility of the C19 ketone. Thus, a more circuitous route was pursued, which involved initial reduction of ketone **2.17**, followed by silyl protection of the resulting alcohol to give **2.18**. Unfortunately, reduction of the C19 ketone occurred exclusively from the α-face of **2.17**, regardless of the reducing agent employed, and exhaustive attempts to invert the stereochemical configuration failed. As such, the C19 stereochemistry would require correction at a later point in our synthesis. Nonetheless, removal

of the MOM protecting group of **2.18**,[19] followed by treatment of the resulting alcohol under Appel conditions,[20] delivered iodide **2.19**. Gratifyingly, exposure of iodide **2.19** to tributyltin hydride and AIBN in toluene at 110 °C delivered bridged bicycle **2.20** in 89% yield.[21] This radical cyclization constructs the final C–C bond needed for the total synthesis (i.e, C22–C23), in addition to the final quaternary stereocenter at C23. Of note, the conversion of **2.19** to **2.20** provides a rare example of a radical cyclization being used to forge a quaternary stereocenter from a primary alkyl halide and an electron-rich olefin.[21,22] From bicycle **2.20**, all that remained to complete the total synthesis was the removal of protecting groups and inversion of the C19 stereocenter. Although TIPS cleavage proceeded readily using TBAF, exhaustive attempts to achieve the critical stereochemical inversion proved fruitless. Thus, following TIPS cleavage, we performed a straightforward alcohol oxidation, followed by acid-mediated cleavage of the MOM protecting group, to furnish the penultimate ketone intermediate **2.21**. A myriad of reducing agents, such as hydride donors, single-electron donors, and heterogeneous hydrogenation catalysts were evaluated for the final step of the total synthesis. However, all efforts to reduce the hindered ketone of **2.21** led exclusively to the undesired C19 epimer of the natural product, *epi*-tubingensin B (*epi*-**2.1**). With few options remaining, we evaluated catalyst-controlled reduction conditions and ultimately found that treatment of ketone **2.21** with (*S*)-$Ru(OAc)_2$(BINAP) under Noyori reduction conditions[23,24] delivered a 1:4 ratio of tubingensin B (**2.1**) and *epi*-tubingensin B (*epi*-**2.1**) in quantitative yield. Although the yield of **2.1** was modest, this effort provided our first synthetic sample of the natural product.

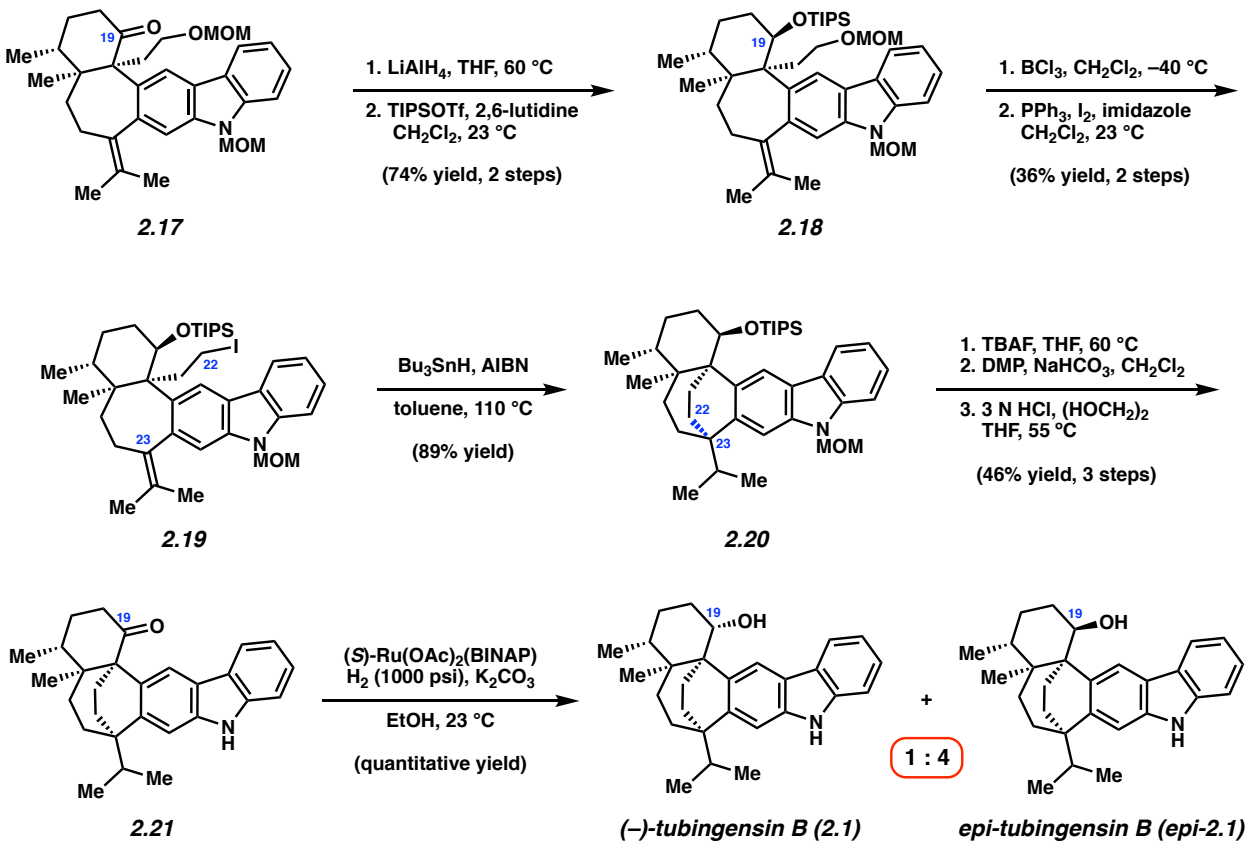

Scheme 2.3. Radical cyclization and first generation total synthesis of tubingensin B.

Having accessed tubingensin B (**2.1**) and validated several critical elements of our synthetic design, such as the carbazolyne and radical cyclizations, we sought to streamline our total synthesis. We reasoned that the ideal endgame would avoid lengthy manipulations pertaining to the C19 ketone and the elaboration of the MOM-protected alcohol to a suitable radical precursor (see Scheme 2.3). After pursuing several unsuccessful strategies toward this end, we uncovered the concise route to tubingensin B (**2.1**) depicted in Scheme 2.4. The early stages of our total synthesis remain unchanged, which allowed access to gram quantities of enone **2.14** in three steps from (–)-**2.11** and **2.7**. Enone **2.14** was treated with phenylselenomethyl lithium[25] in the presence of CuCN•2LiCl and TESCl in THF to generate phenylselenide **2.22** in

61% yield. This seemingly simple tactic was intended to serve as a synthetic lynchpin, as we envisioned the phenylselenide motif would be sufficiently stable to be carried through subsequent steps and later used directly as a radical precursor. We next tested the carbazolyne cyclization for assembly of the 7-membered ring and vicinal quaternary stereocenters. Unfortunately, when this key step was carried out at elevated temperatures, which we had previously deemed necessary to surpass cyclobutenol formation (see Scheme 2.2), decomposition of the phenylselenide was observed. We thus had to perform the cyclization at ambient temperature, which provided cyclobutenol **2.23** as a single diastereomer, without disturbing the phenylselenide. In order to fragment the unnecessary C10–C19 bond of **2.23**, we turned to the mild rhodium-catalyzed ring opening methodology pioneered by Murakami.[26] To our delight, exposure of cyclobutenol **2.23** to catalytic $[Rh(OH)cod]_2$ in toluene at 100 °C led to rupture of the desired C–C bond to supply ketone **2.24**. To forge the last carbon–carbon bond and final quaternary stereocenter of the natural product, ketone **2.24** was treated with tributyltin hydride and AIBN in toluene at 110 °C to furnish bridged bicycle **2.25** in 54% yield. This complexity-generating step provides a rare example of a phenylselenide radical precursor being used in total synthesis, particularly to form a quaternary center.[27] Following cleavage of the MOM protecting group under acidic conditions (**2.25→2.21**), the only challenge that remained was the diastereoselective reduction of the ketone. After evaluating a variety of chiral ligands, it was found that exposure of ketone **2.21** to (*R*)-$Ru(OAc)_2$(DM-SEGPHOS),[23] KOH, and H_2 (1500 psi) led to a notably improved 1:1.3 ratio of tubingensin B (**2.1**) and *epi*-**2.1** (see Scheme 2.3 for previous reduction, which gave 1:4 ratio of **2.1** to *epi*-**2.1**). Given that the undesired epimer could be recycled to **2.21** using a straightforward Dess–Martin oxidation, while also considering the brevity of our synthesis, we viewed this final transformation as a viable solution to

introducing the troublesome C19 stereocenter. Spectroscopic analysis of synthetic material and comparisons to an authentic sample validated our successful total synthesis of tubingensin B (**2.1**).

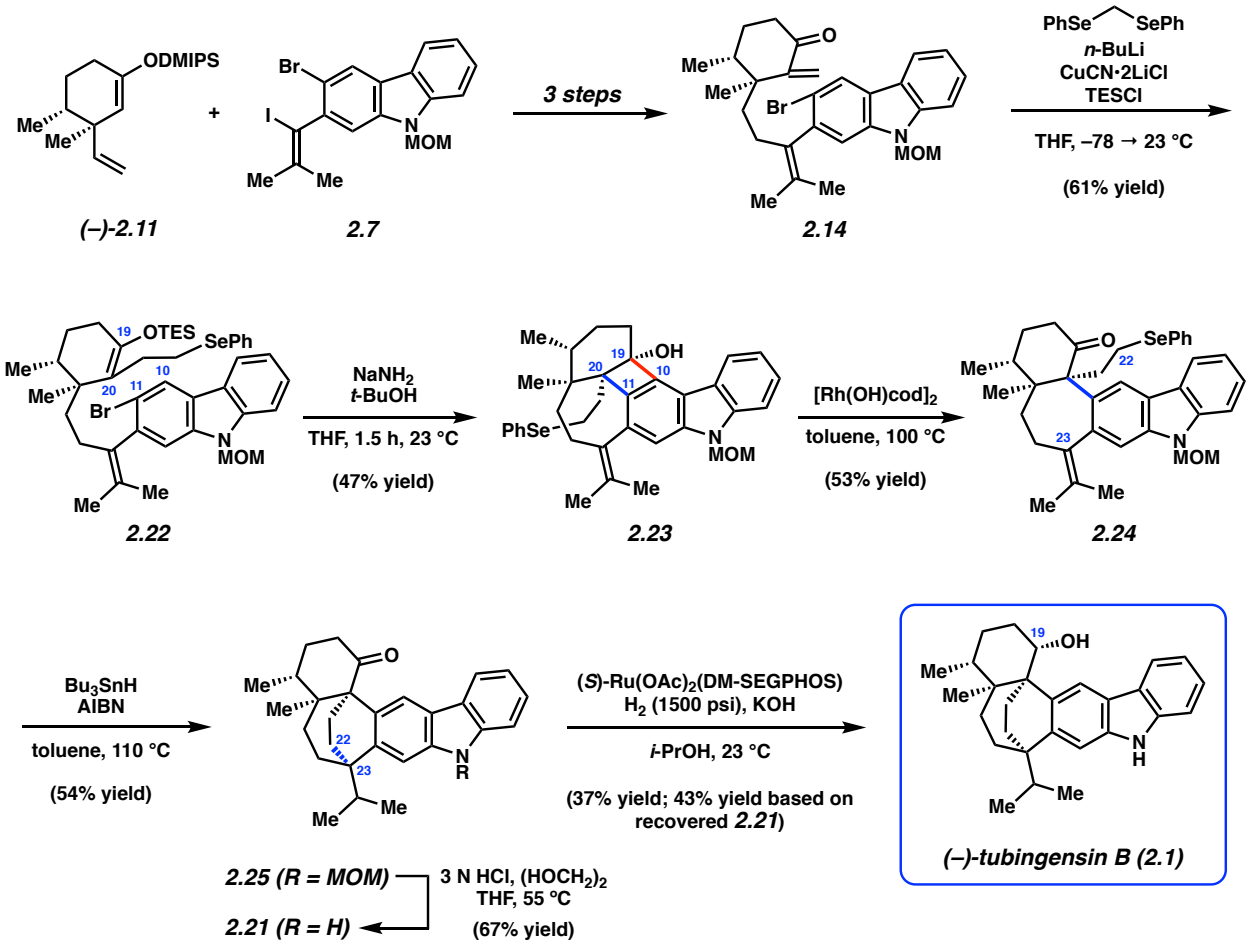

Scheme 2.4. Concise total synthesis of tubingensin B.

2.4 Conclusion

We have achieved the first total synthesis of the structurally complex indole diterpenoid tubingensin B (**2.1**). Following validation of our initial approach, we uncovered a concise enantiospecific route that features a number of key steps, including: (a) a *B*-alkyl Suzuki–

Miyaura coupling to access a tetrasubstituted olefin and unite readily available cyclohexyl and carbazole fragments, (b) a carbazolyne cyclization to construct the 7-membered ring and install vicinal quaternary stereocenters, (c) a Rh-catalyzed fragmentation of a fortuitously formed cyclobutenol ring, (d) and a late-stage radical cyclization stemming from a phenylselenide intermediate to install a final quaternary stereocenter and the [3.2.2]-bridged bicyclic framework of the natural product.

Of the strategic advances that enabled our synthesis, the carbazolyne cyclization is worthy of further emphasis and reflection. Arynes have a rich history, as alluded to earlier, including decades where even the existence of such species was questioned. Additionally, their high reactivity has seemingly steered chemists away from using them to assemble stereochemically complex scaffolds. The present study, on the other hand, provides an opposing perspective. Our results demonstrate that arynes can and should be used strategically to enable the synthesis of complex molecules with motifs that have conventionally been viewed as challenging, such as medium-sized rings and vicinal quaternary stereocenters.

2.5 Experimental Section

2.5.1 Materials and Methods. Unless stated otherwise, reactions were conducted in flame-dried glassware under an atmosphere of nitrogen using anhydrous solvents (either freshly distilled or passed through activated alumina columns). All commercially obtained reagents were used as received unless otherwise specified. The following reagents were distilled prior to use: chlorotriethylsilane (TESCl, distilled over CaH_2), chlorodimethylisopropylsilane (DMIPSCl), hexamethylphosphoramide (HMPA, distilled over CaH_2 and stored over 4Å molecular sieves), isopropyl alcohol (*i*-PrOH, distilled over CaO after refluxing overnight), and MsCl (distilled over P_2O_5). Dess–Martin periodinane (DMP) was prepared following literature precedent.[28] 18-Crown-6 was recrystallized from acetonitrile and stored in a glovebox. Triphenylarsine was recrystallized from EtOH and stored in a glovebox. *N,N*-Dimethylmethyleneiminium iodide, CuI, and CuCN were purchased from Sigma–Aldrich and stored inside a glovebox. $Pd(PPh_3)_3$, $Pd_2(dba)_3$, (*S*)-$Ru(OAc)_2$(BINAP), and (*S*)-$Ru(OAc)_2$(dm-segphos) were purchased from Strem and stored inside a glovebox at –20 °C. Reaction temperatures were controlled using an IKAmag temperature modulator, and unless stated otherwise, reactions were performed at room temperature (rt, approximately 23 °C). Thin-layer chromatography (TLC) was conducted with EMD gel 60 F254 pre-coated plates (0.25 mm) and visualized using a combination of UV, anisaldehyde, iodine, vanillin, ninhydrin, and potassium permanganate staining. Silicycle P60 (particle size 0.040–0.063 mm) silica gel was used for flash column chromatography. ^{1}H NMR spectra were recorded on Bruker spectrometers (at 300 MHz or 500 MHz) and are reported relative to deuterated solvent signals (7.26 ppm for $CDCl_3$, 7.16 ppm for C_6D_6, and 5.32 ppm for CD_2Cl_2). Data for ^{1}H NMR spectra are reported as follows: chemical shift (δ ppm), multiplicity, coupling constant (Hz), and integration. ^{13}C NMR spectra were recorded on Bruker

spectrometers (at 75 or 125 MHz) and are reported relative to deuterated solvent signals (77.16 ppm for $CDCl_3$, 128.06 ppm for C_6D_6, and 53.84 ppm for CD_2Cl_2). Data for ^{13}C NMR spectra are reported in terms of chemical shift, and when necessary, multiplicity, coupling constant (Hz) and carbon type. IR spectra were recorded on a Perkin-Elmer 100 spectrometer and are reported in terms of frequency of absorption (cm^{-1}). High resolution mass spectra were obtained from the UC Irvine Mass Spectrometry Facility and the UCLA Molecular Instrumentation Center using TOF mass analyzer and a Thermo Fisher Scientific Exactive Plus with IonSense ID-CUBE DART source, respectively. Melting points were determined using a DigiMelt MPA160 melting point apparatus. Images in Figures 2.1 & Scheme 2.2 were created using CYLview.[18]

2.5.2 Experimental Procedures

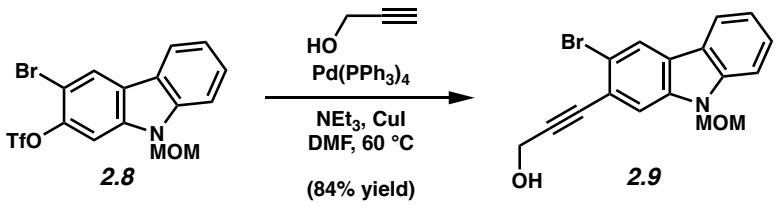

Propargyl Alcohol 2.9. To a flask charged with triflate **2.8**[3] (3.0 g, 6.84 mmol, 1 equiv) was added $Pd(PPh_3)_4$ (791 mg, 0.68 mmol, 0.10 equiv) and CuI (260 mg, 1.36 mmol, 0.2 equiv) in the glovebox. The flask was removed from the glovebox and propargyl alcohol (515 mL, 8.89 mmol, 1.3 equiv) was added, followed by NEt_3 (1.43 mL, 10.27 mmol, 1.5 equiv) and DMF (46 mL). The reaction mixture was sparged with N_2 for 10 min, and stirred at 60 °C for 16 h. The reaction was allowed to cool to room temperature and quenched with sat. aq. NH_4Cl (100 mL), then diluted with H_2O (100 mL) and EtOAc (200 mL). The layers were separated, and the aqueous layer was extracted with EtOAc (3 x 150 mL). The combined organic layers were

washed with brine (2 x 100 mL) and dried over Na_2SO_4. Evaporation under reduced pressure afforded the crude product, which was purified by flash chromatography (7:3 Hexanes:EtOAc) to provide propargyl alcohol **2.9** (1.9 g, 84% yield) as a white solid. Mp: 132–136 °C; R_f 0.20 (7:3 Hexanes:EtOAc); ^{1}H NMR (500 MHz, $CDCl_3$): δ 8.26 (s, 1H), 8.01 (d, J = 7.8, 1H), 7.70 (s, 1H), 7.49–7.55 (m, 2H), 7.28–7.31 (m, 1H), 5.63 (s, 2H), 4.61 (d, J = 5.8, 2H), 3.29 (s, 3H), 1.74 (t, J = 6.0, 1H); ^{13}C NMR (500 MHz, $CDCl_3$): δ 141.6, 139.1, 127.4, 125.2, 123.9, 122.0, 121.1, 120.82, 120.76, 116.0, 114.3, 109.6, 91.2, 85.4, 74.3, 56.3, 51.9; IR (film): 3379, 2931, 1600, 1468, 1451, 1429, 1337, 1241, 1110, 1060, 1035, 1024 cm^{-1}; HRMS-APCI (*m/z*) $[M]^{\bullet+}$ calcd for $C_{17}H_{14}BrNO_2$, 343.0202; found, 343.0190.

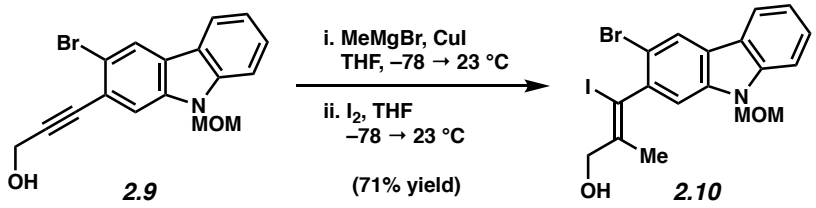

Hydroxyiodide 2.10. To a flask charged with propargyl alcohol **2.9** (3.0 g, 8.75 mmol, 1 equiv) was added CuI (1.67 g, 8.75 mmol, 1 equiv) in the glovebox. The flask was removed from the glovebox, THF (32 mL) was added, and the reaction mixture was cooled to –78 °C. MeMgBr (3.0 M in Et_2O, 14.6 mL, 43.8 mmol, 5 equiv) was then added dropwise over 5 min and the reaction was stirred for 2 h at room temperature. The reaction was re-cooled to –78 °C and I_2 (11.1 g, 43.8 mmol, 5 equiv) was added dropwise over 1 min as a solution in THF (40 mL). The reaction mixture was allowed to warm to room temperature and was stirred for 1 h. Next, it was cooled to 0 °C, and then quenched with sat. aq. NH_4Cl (90 mL). The mixture was diluted with

sat. aq. $Na_2S_2O_3$ (90 mL) and EtOAc (200 mL). The layers were separated and the aqueous layer was extracted with EtOAc (3 x 90 mL). The combined organic layers were washed with brine (90 mL), and dried over Na_2SO_4. Evaporation under reduced pressure afforded the crude product, which was purified by flash chromatography (7:3 Hexanes:EtOAc) to provide hydroxyiodide **2.10** (3.0 g, 71% yield) as an off-white foam. Mp: 59.5–61.2 °C; R_f 0.32 (7:3 Hexanes:EtOAc); ^{1}H NMR (500 MHz, $CDCl_3$): δ 8.25 (s, 1H), 8.02 (d, *J* = 7.8, 1H), 7.49–7.55 (m, 2H), 7.41 (s, 1H), 7.28–7.31 (m, 1H), 5.66 (d, *J* = 11.5, 1H), 5.63 (d, *J* = 11.5, 1H), 4.49 (d, *J* = 4.8, 2 H), 3.31 (s, 3H), 1.75 (s, 3 H); ^{13}C NMR (500 MHz, $CDCl_3$): δ 143.5, 141.5, 140.7, 139.6, 127.1, 124.9, 124.5, 122.1, 120.7, 120.7, 113.1, 110.2, 109.5, 94.5, 74.3, 72.0, 56.3, 17.4; IR (film): 3370, 2925, 1599, 1467, 1447, 1422, 1332, 1242, 1110, 1059, 1026, 1011 cm^{-1}; HRMS-APCI (*m/z*) $[M]^{\bullet+}$ calcd for $C_{18}H_{17}BrINO_2$, 484.9482; found, 484.9482.

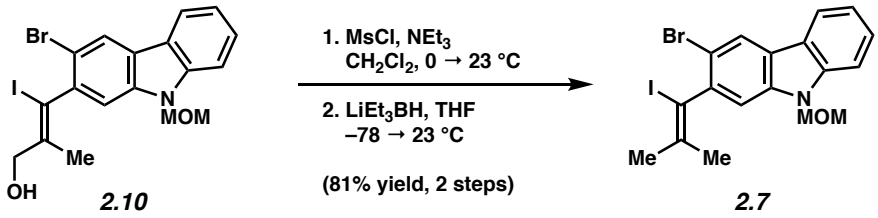

Vinyliodide 2.7. To a flask charged with hydroxyiodide **2.10** (2.79 g, 5.75 mmol, 1 equiv) was added NEt_3 (2.4 mL, 17.2 mmol, 3 equiv) and CH_2Cl_2 (29 mL). The mixture was cooled to 0 °C and MsCl (1.7 g, 17.2 mmol, 3 equiv) was added. The reaction was warmed to room temperature and stirred for 20 h. The reaction was quenched with sat. aq. $NaHCO_3$ (100 mL), then diluted with EtOAc (100 mL). The layers were separated and the aqueous layer was extracted with EtOAc (3 x 100 mL). The combined organic layers were washed with brine (100 mL) and dried

over Na_2SO_4. Evaporation under reduced pressure afforded the crude product, which was purified by flash chromatography (4:1 Hexanes:EtOAc) to provide the corresponding chloride (2.35 g, 81% yield) as an off-white foam.

To a flask containing the chloride intermediate (3.06 g, 6.06 mmol, 1 equiv) was added THF (30 mL). The resulting mixture was cooled to 0 °C. $LiEt_3BH$ (1.0 M in THF, 30.3 mL, 30.3 mmol, 5 equiv) was added dropwise over 10 min and the reaction was stirred for 5 min. The reaction was then quenched at 0 °C with H_2O (5 mL). The reaction mixture was transferred to a separatory funnel and diluted with 6 M NaOH (10 mL), H_2O (80 mL) and EtOAc (50 mL). The layers were separated and the aqueous layer was extracted with EtOAc (3 x 50 mL). The combined organic layers were washed with sat. aq. NH_4Cl (30 mL), brine (30 mL), and dried over $MgSO_4$. Evaporation under reduced pressure afforded the crude product, which was purified by flash chromatography (5:1 Hexanes:EtOAc) to provide vinyliodide **2.7** (2.85 g, quantitative yield) as an off-white foam. R_f 0.66 (4:1 Hexanes:EtOAc); ^{1}H NMR (500 MHz, $CDCl_3$): δ 8.23 (s, 1H), 8.00 (d, *J* = 7.4, 1H), 7.50 (m, 2H), 7.41 (s, 1H), 7.28 (m, 1H), 5.65 (d, *J* = 11.5, 1H), 5.62 (d, *J* = 11.5, 1H), 3.30 (s, 3H), 2.16 (s, 3H), 1.66 (s, 3H); ^{13}C NMR (500 MHz, $CDCl_3$): δ 141.7, 141.6, 141.4, 139.7, 127.0, 124.6, 124.4, 122.2, 120.6, 113.9, 110.6, 109.5, 93.4, 74.3, 56.3, 29.9, 20.7; IR (film): 2924, 1599, 1468, 1447, 1422, 1332, 1242, 1112, 1066, 1026, 782, 748, 552 cm^{-1}; HRMS-APCI (*m/z*) $[M]^{\bullet+}$ calcd for $C_{18}H_{17}BrINO$, 468.9533; found, 468.9530.

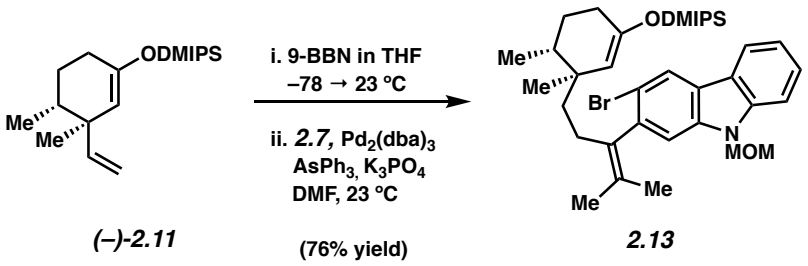

(–)-2.11 *2.13*

Silyl Enol Ether 2.13. To a vial charged with olefin **2.11**[3] (140 mg, 0.553 mmol, 2 equiv) at –78 °C was added 9-BBN (0.5 M in THF, 1.3 mL, 0.664 mmol, 2.4 equiv) dropwise over 2 min as a solution in THF. The reaction was allowed to warm to room temperature and stirred for 5 h. To a separate vial was added $Pd_2(dba)_3$ (50.6 mg, 0.055 mmol, 0.2 equiv) and $AsPh_3$ (33.9 mg, 0.111 mmol, 0.4 equiv) in the glovebox. The vial was removed from the glovebox, K_3PO_4 (88.2 mg, 0.415 mmol, 1.5 equiv), vinyliodide **2.7** (130 mg, 0.277 mmol, 1 equiv), and DMF (1.1 mL) were added. The solution was sparged with N_2 for 10 min. The THF solution was then added to the DMF mixture and the reaction was stirred at room temperature for 48 h. The reaction was quenched with NEt_3 (1 mL) and H_2O (5 mL) and then diluted with EtOAc (5 mL). The layers were separated and the aqueous layer was extracted with EtOAc (3 x 5 mL). The combined organic layers were washed with brine (5 mL), dried over Na_2SO_4, and concentrated under reduced pressure. The crude product was purified by flash chromatography (5:1 Hexanes:EtOAc) to provide silyl enol ether **2.13** (124.6 mg, 76% yield) as a yellow oil. R_f 0.40 (9:1 Hexanes:EtOAc).

*Note: An analytical sample of silyl enol ether **2.13** was unattainable despite extensive purification efforts. As a result, the structure of **2.13** was, in part, corroborated after conversion to the corresponding ketone **2.26**.*

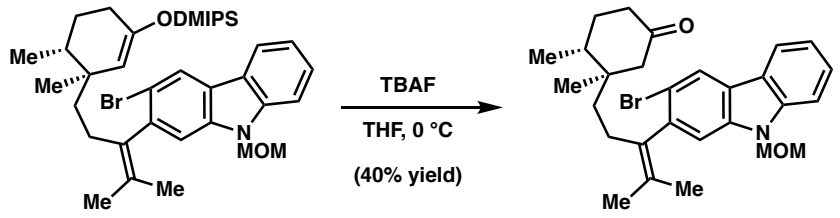

2.13 ***2.26***

Ketone 2.26. To a vial charged with silyl enol ether **2.13** (20.5 mg, 0.034 mmol, 1 equiv) was added THF (170 μL). The mixture was cooled to 0 °C and TBAF (1.0 M in THF, 52 μL, 0.052 mmol, 1.5 equiv) was added. The reaction was stirred for 5 min and then allowed to warm to room temperature. The solution was then quenched with H_2O (2 mL) and diluted with EtOAc (2 mL). The layers were separated and the aqueous layer was extracted with EtOAc (3 x 2 mL). The combined organic layers were washed with brine (2 mL), dried over Na_2SO_4, and concentrated under reduced pressure. The crude product was purified by preparative thin layer chromatography (7:3 Hexanes:EtOAc) to provide ketone **2.26** (6.7 mg, 40% yield, unoptimized) as a colorless oil. R_f 0.50 (7:3 Hexanes:EtOAc); ^{1}H NMR (500 MHz, CD_2Cl_2): δ 8.29 (d, *J* = 2.5, 1H), 8.03 (app. dd, *J* = 7.8, 0.7, 1H), 7.55 (d, *J* = 8.2, 1H), 7.47–7.51 (m, 1H), 7.27–7.30 (m, 2H), 5.63–5.69 (m, 2H), 3.27 (d, *J* = 1.3, 3H), 2.44–2.55 (m, 1H), 2.21–2.29 (m, 4H), 1.95 (ddd, *J* =, 30.5, 13.3, 1.95, 1H), 1.88 (d, *J* = 5.8, 3H), 1.77–1.86 (m, 2H), 1.49–1.57 (m, 3H), 1.47 (s, 3H), 1.30–1.46 (m, 3H), 0.80–0.93 (m, 1H), 0.78 (app. dd, *J* = 6.7, 59.7, 3H), 0.68–0.69 (d, *J* = 6.5, 3H); ^{13}C NMR (500 MHz, CD_2Cl_2): δ 211.7, 211.6, 141.5, 141.1, 141.0, 139.9, 134.6, 134.5, 129.5, 129.4, 126.4, 123.9, 123.8, 123.4, 122.29, 122.27, 120.29, 120.25, 114.8, 114.7, 111.33, 111.25, 109.47, 109.45, 74.22, 74.20, 56.0, 52.0, 51.9, 40.8, 40.7, 40.3, 40.2, 39.2, 39.1, 36.4, 36.3, 30.5, 29.7, 27.7, 27.5, 21.83, 21.81, 19.29, 19.25, 18.81, 18.77, 14.5, 14.3; IR (film): 2927,

1709, 1600, 1469, 1449, 1425, 1336, 1242, 1112, 1066 cm^{-1}; HRMS-APCI (*m/z*) $[M]^{\bullet+}$ calcd for $C_{28}H_{34}BrNO_2$, 495.1767; found, 495.1762. $[\alpha]^{21}_D$ +5.06 ° (*c* = 1.0, $CHCl_3$).

*Note: Ketone **2.26** was obtained as a mixture of conformers. These data represent empirically observed chemical shifts and coupling constants from the ^1H and ^{13}C NMR spectra.*

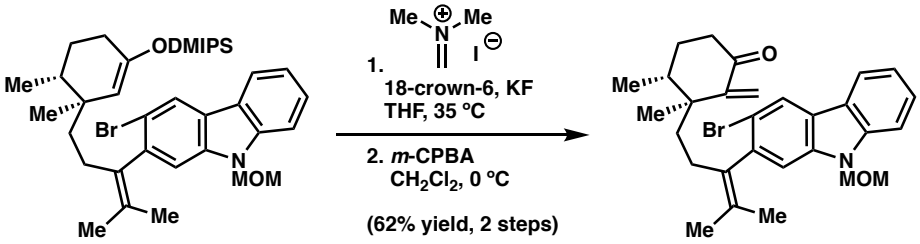

2.13 ***2.14***

Enone 2.14. To a vial charged with silyl enol ether **2.13** (69 mg, 0.116 mmol, 1 equiv) was added 18-crown-6 (122 mg, 0.462 mmol, 4 equiv), Eschenmoser's salt (214 mg, 1.16 mmol, 10 equiv), and KF (27 mg, 0.462 mmol, 4 equiv) inside the glovebox. The vial was removed from the glovebox, THF (2.9 mL) was added, and the mixture was warmed to 35 °C and stirred for 48 h. The reaction was then cooled to room temperature, quenched with H_2O (12 mL), and diluted with EtOAc (12 mL). The layers were separated and the aqueous layer was extracted with EtOAc (3 x 12 mL). The combined organic layers were washed with brine (10 mL) and dried over Na_2SO_4. Evaporation under reduced pressure afforded the crude adduct, which was used without further purification.

The crude adduct was dissolved in CH_2Cl_2 (7.7 mL) and cooled to 0 °C. *m*-CPBA (77%, 40.0 mg, 0.231 mmol, 2 equiv) was added and the reaction was stirred for 30 min at 0 °C. The reaction was allowed to warm to room temperature. Next, it was quenched with sat. aq. $NaHCO_3$

(20 mL) and diluted with EtOAc (20 mL). The layers were separated, and the aqueous layer was extracted with EtOAc (2 x 20 mL). The combined organic layers were washed with brine (20 mL), dried over Na_2SO_4, and concentrated under reduced pressure to afford the crude product. Purification by flash chromatography (5:1 Hexanes:EtOAc) provided enone **2.14** (58.8 mg, 62% yield, 2 steps) as an off-white foam. R_f 0.60 (4:1 Hexanes:EtOAc); ^{1}H NMR (500 MHz, CD_2Cl_2): δ 8.28 (s, 1H), 8.02 (d, *J* = 7.6, 1H), 7.55–7.53 (m, 1H), 7.48 (t, *J* = 7.8, 1H) 7.27 (t, *J* = 7.5, 1H), 7.24 (d, *J* = 2.3, 2H), 5.67–5.60 (m, 3H), 4.91 (app. dd, *J* = 46.0, 1.3, 1H), 3.24 (d, *J* = 1.5, 3H), 2.50–2.16 (m, 5H), 1.97–1.79 (m, 2H), 1.84 (d, *J* = 5.2, 3H), 1.64–1.48 (m, 5H), 1.45 (d, *J* = 1.0, 3H), 0.89 (app. dd, *J* = 31.7, 6.8, 3H); ^{13}C NMR (500 MHz, CD_2Cl_2): δ 203.0, 202.9, 153.6, 153.5, 141.4, 141.3, 141.07, 141.06, 139.91, 139.87, 134.5, 134.3, 129.53, 129.48, 126.4, 123.9, 123.8, 123.4, 122.3, 120.28, 120.27, 117.7, 117.4, 114.9, 114.7, 111.3, 111.2, 109.49, 109.47, 74.2, 56.0, 43.7, 43.5, 37.4, 37.3, 36.9, 36.8, 34.7, 34.5, 28.1, 27.7, 26.6, 26.5, 21.84, 21.79, 21.6, 19.4, 19.3, 14.83, 14.76. IR (film): 2928, 1691, 1601, 1468, 1449, 1425, 1335, 1242, 1112, 1066 cm^{-1}; HRMS-APCI (*m/z*) $[M]^{\bullet+}$ calcd for $C_{29}H_{34}BrNO_2$, 507.1767; found, 507.1760. $[\alpha]^{21}_D$ +13.6 ° (*c* = 1.0, $CHCl_3$).

*Note: Enone **2.14** was obtained as a mixture of conformers. These data represent empirically observed chemical shifts and coupling constants from the ^{1}H and ^{13}C NMR spectra.*

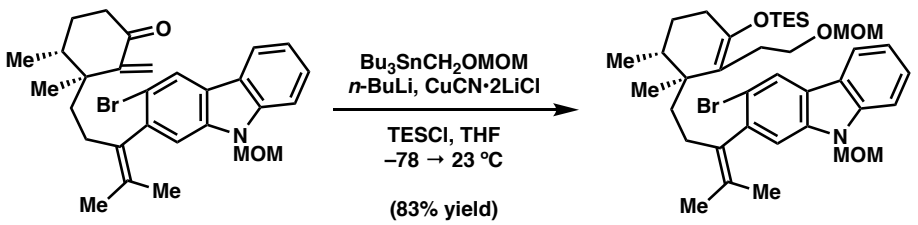

2.14 *2.15*

***O*-MOM Ether 2.15.** A vial was charged with CuCN (44.8 mg, 0.5 mmol) and LiCl (42.4 mg, 1.0 mmol) inside the glovebox. The vial was removed from the glovebox and THF (1.0 mL) was added. The resulting mixture was stirred until all solids were dissolved, thus affording a solution of CuCN•2LiCl (0.50 M in THF). A separate flask was charged with Bu_3SnCH_2MOM[29] (208.7 mg, 0.571 mmol, 3 equiv) and purged with N_2 for 5 min. THF (1.9 mL) was then added and the mixture was cooled to –78 °C. To the stannane solution was added *n*-BuLi (2.38M in Hexanes, 0.240 mL, 0.571 mmol, 3 equiv) dropwise over 1 min and the reaction was stirred for 5 min. The CuCN•2LiCl solution (0.5 M in THF, 0.57 mL, 0.280 mmol, 1.5 equiv) was then added dropwise over 1 min to the lithiate solution. The reaction was stirred at –78 °C for 30 min. A separate flask was charged with enone **2.14** (96.9 mg, 0.190 mmol, 1 equiv), TESCl (64 µL, 0.381 mmol, 2 equiv), and THF (1.9 mL). This mixture was then added dropwise over 2 min to the above solution and the reaction was stirred for 10 min at –78 °C. It was then allowed to warm to room temperature and stirred for 10 min. The reaction was quenched with a 9:1 mixture of sat. aq. NH_4Cl and sat. aq. NH_4OH (10 mL), then diluted with H_2O (5 mL) and EtOAc (15 mL). The layers were separated and the aqueous layer was extracted with EtOAc (3 x 15 mL). The combined organic layers were washed with a 9:1 mixture of sat. aq. NH_4Cl and sat. aq. NH_4OH (5 mL), followed by brine (5 mL), then dried over $MgSO_4$. Evaporation under reduced pressure afforded the crude product, which was purified by flash chromatography (95:5 Hexanes:EtOAc)

to provide *O*-MOM ether **2.15** (111.2 mg, 83% yield) as a colorless oil. R_f 0.57 (4:1 Hexanes:EtOAc); ^{1}H NMR (500 MHz, CD_2Cl_2): δ 8.27 (s, 1H), 8.02 (d, *J* = 7.7, 1H), 7.54 (d, *J* = 8.2, 1H), 7.47 (t, *J* = 7.6, 1H), 7.26 (dd, *J* = 8.2, 6.7, 2H), 5.62–5.68 (m, 2H), 4.48 (s, 1H), 4.30 (s, 1H), 3.66–3.44 (app. dddd, *J* = 85.3, 11.0, 9.3, 5.8, 1H), 3.37–3.10 (m, 8H), 2.51–2.38 (app. dtd, *J* = 30.0, 12.7, 5.8, 1H), 2.24–2.15 (m, 2H), 2.12–2.07 (m, 1H), 1.95–1.91 (m, 3H), 1.85 (s, 3H), 1.74–1.61 (m, 2H), 1.53–1.32 (m, 8H), 0.97 (dt, *J* = 19.8, 7.9, 10H), 0.77–0.61 (m, 13 H); ^{13}C NMR (500 MHz, CD_2Cl_2): δ 147.3, 141.0, 139.92, 139.89, 135.3, 135.2, 128.8, 128.6, 126.3, 123.8, 123.7, 123.3, 122.4, 122.3, 120.2, 117.2, 117.1, 114.9, 111.3, 111.1, 109.5, 109.4, 96.3, 96.1, 74.21, 74.19, 67.1, 66.9, 55.9, 54.7, 54.5, 40.3, 40.2, 35.2, 35.0, 33.3, 33.2, 30.4, 30.3, 28.7, 28.6, 27.1, 26.9, 26.7, 21.8, 21.2, 19.4, 19.3, 15.7, 15.6, 6.7, 5.8, 5.7; IR (film): 2955, 1657, 1469, 1336, 1241, 1197, 1150, 1111, 1068 cm^{-1}; HRMS-APCI (*m/z*) $[M]^{\bullet+}$ calcd for $C_{38}H_{56}BrNO_4Si$, 697.3156; found, 697.3122. $[\alpha]^{21}_D$ –21.66 ° (*c* = 1.0, $CHCl_3$).

*Note: O-MOM ether **2.15** was obtained as a mixture of conformers. These data represent empirically observed chemical shifts and coupling constants from the ^{1}H and ^{13}C NMR spectra.*

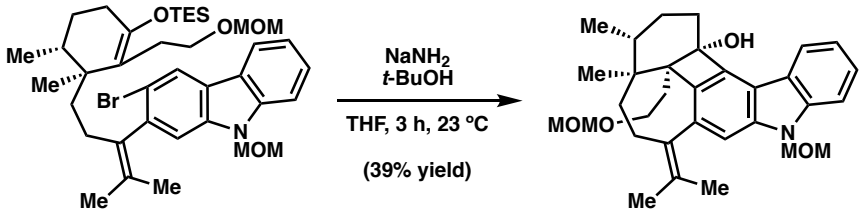

2.15 ***2.16***

Cyclobutenol 2.16. A vial was charged with powdered $NaNH_2$ (36 mg, 0.940 mmol, 55 equiv) in the glovebox. The vial was removed and THF (0.85 mL) was added followed by *t*-BuOH (28 μL, 0.300 mmol, 17.5 equiv). The reaction was stirred at 40 °C for 1 h. The mixture was allowed

to cool to room temperature, and then a solution of silyl enol ether **2.15** (12 mg, 0.017 mmol, 1 equiv) in THF (85 μL) was added. The reaction was stirred for 3 h at room temperature, quenched with sat. aq. NH_4Cl (3 mL), and then diluted with H_2O (3 mL) and EtOAc (6 mL). The layers were separated and the aqueous layer was extracted with EtOAc (3 x 6 mL). The combined organic layers were washed with brine (3 mL) and dried over $NaSO_4$. Evaporation under reduced pressure afforded the crude product, which was purified by preparative thin layer chromatography (4:1 Hexanes:EtOAc) to provide cyclobutenol **2.16** (3.4 mg, 39% yield) as a colorless oil. R_f 0.44 (4:1 Hexanes:EtOAc); ^{1}H NMR (500 MHz, C_6D_6): δ 8.45 (d, *J* = 7.6, 1H), 7.30 (ddd, *J* = 8.2, 7.0, 1.2, 1H), 7.26 (d, *J* = 8.0, 1H), 7.24 (s, 1H), 7.22 (ddd, *J* = 7.9, 6.7, 0.9, 1H), 5.61 (s, 1H), 5.18 (d, *J* = 11.5, 1H), 5.10 (d, *J* = 11.5, 1H), 3.76 (d, *J* = 6.7, 1H), 3.52 (d, *J* = 6.7, 1H), 3.40 (dt, *J* = 9.5, 3.5, 1H), 3.34 (ddd, *J* = 11.5, 9.7, 1.8, 1H), 2.89–2.84 (m, 1H), 2.83 (s, *J* = 2.9, 3H), 2.57–2.51 (m, 2H), 2.49 (ddd, *J* = 15.6, 12.3, 3.4, 1H), 2.35 (s, 3H), 1.97–1.88 (m, 5H), 1.75 (s, 3H), 1.71–1.69 (m, 1H), 1.56–1.48 (m, 2H), 1.38–1.32 (m, 1H), 1.30–1.24 (m, 1H), 0.85 (s, 3H), 0.49 (d, *J* = 6.7, 3H); ^{13}C NMR (500 MHz, C_6D_6): δ 142.7, 141.33, 141.30, 137.4, 136.5, 134.2, 126.0, 125.6, 122.9, 121.9, 120.4, 116.7, 109.0, 108.5, 95.9, 79.8, 73.8, 66.2, 63.2, 55.2, 54.1, 40.2, 37.8, 29.6, 27.8, 27.4, 27.0, 25.5, 21.8, 19.4, 16.4, 15.9; IR (film): 3420, 2924, 2853, 1633, 1611, 1555, 1468, 1428, 1384, 1342, 1259, 1150, 1097 cm^{-1}; HRMS-APCI (*m/z*) $[M]^{\bullet+}$ calcd for $C_{32}H_{41}NO_4$, 503.3030; found, 503.3007. $[\alpha]^{21}_D$ +72.0 ° (*c* = 0.1, $CHCl_3$).

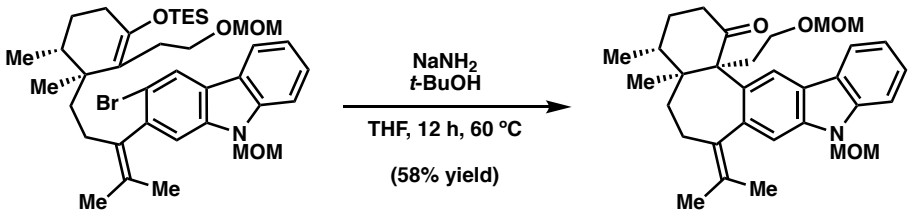

2.15 *2.17*

Ketone 2.17. A Schlenk tube was charged with powdered $NaNH_2$ (146 mg, 3.73 mmol, 11 equiv) in the glovebox. The tube was removed and THF (3.4 mL) was added followed by *t*-BuOH (113 μL, 1.19 mmol, 3.5 equiv). The reaction was stirred at 40 °C for 1 h. The mixture was allowed to cool to room temperature, and then a solution of silyl enol ether **2.15** (237.6 mg, 0.340 mmol, 1 equiv) in THF (3.4 mL) was added. The reaction was then heated to 60 °C and stirred for 12 h. The reaction was quenched with sat. aq. NH_4Cl (10 mL), and then diluted with H_2O (10 mL) and EtOAc (20 mL). The layers were separated and the aqueous layer was extracted with EtOAc (3 x 20 mL). The combined organic layers were washed with brine (20 mL) and dried over $MgSO_4$. Evaporation under reduced pressure afforded the crude product, which was purified by flash chromatography (5:1 Hexanes:EtOAc) to provide ketone **2.17** (100.5 mg, 58% yield) as a colorless oil. R_f 0.38 (4:1 Hexanes:EtOAc); ^{1}H NMR (500 MHz, CD_2Cl_2): δ 7.99 (d, *J* = 7.8, 1H), 7.53 (d, *J* = 8.2, 1H), 7.45 (ddd, *J* = 8.2, 7.1, 1.0, 1H), 7.39 (s, 1H), 7.26–7.23 (m, 2H), 5.66 (d, *J* = 11.6, 1H), 5.61 (d, *J* = 11.6, 1H), 4.39 (d, *J* = 6.4, 1H), 4.29 (d, *J* = 6.4, 1H), 3.54 (ddd, *J* = 11.5, 8.9, 4.5, 1H), 3.36–3.27 (m, 4H), 3.14 (s, 3H), 2.79 (ddd, *J* = 13.4, 5.5, 2.2, 1H), 2.54–2.49 (m, 1H), 2.45–2.40 (ddd, *J* = 11.0, 8.9, 5.6, 1H), 2.28–2.17 (m, 3H), 2.13–2.06 (m, 1H), 1.96–1.91 (m, 1H), 1.90 (s, 3H), 1.82 (app. dd, *J* = 14.4, 3.9, 1H), 1.69–1.53 (m, 5H), 0.80 (d, *J* = 6.8, 3H), 0.78 (s, 3H); ^{13}C NMR (500 MHz, CD_2Cl_2): δ 215.4, 143.2, 141.5, 139.4, 137.0, 130.6, 127.9, 126.2, 123.7, 123.0, 121.3, 120.41, 120.38, 111.7, 109.7, 96.7, 74.6,

67.2, 66.5, 56.4, 55.1, 44.8, 40.3, 37.4, 31.8, 30.9, 29.5, 27.3, 22.2, 19.9, 19.4, 15.8; IR (film): 2926, 1699, 1604, 1493, 1469, 1390, 1342, 1240, 1149, 1112, 1064, 1043 cm^{-1}; HRMS-APCI (*m/z*) $[M]^{\bullet+}$ calcd for $C_{32}H_{41}NO_4$, 503.3030; found, 503.3001. $[\alpha]^{21}_D$ +32.9 ° (*c* = 1.0, $CHCl_3$).

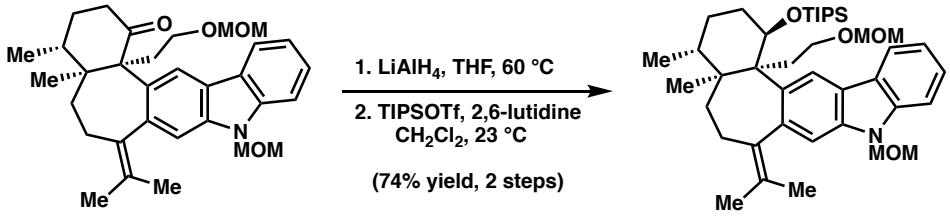

2.17 ***2.18***

Silyl Ether 2.18. To a vial charged with ketone **2.17** (61.7 mg, 0.12 mmol, 1 equiv) was added THF (2.5 mL, 0.05 M). A solution of $LiAlH_4$ (1.0 M in THF, 1.2 mL, 1.2 mmol, 10 equiv) was then added dropwise over 2 min. The reaction was heated to 60 °C, stirred for 5 min, and then allowed to cool to room temperature. The mixture was then quenched with a sat. aq. solution of Rochelle's salt (5 mL), and then diluted with H_2O (5 mL) and EtOAc (10 mL). The layers were separated and the aqueous layer was extracted with EtOAc (3 x 10 mL). The organic layers were combined, washed with brine (10 mL), and dried over Na_2SO_4. Evaporation under reduced pressure afforded the crude product, which was purified by flash chromatography (4:1 Hexanes:EtOAc) to provide the intermediate alcohol as a colorless oil.

To a vial charged with intermediate alcohol (15 mg, 0.033 mmol, 1 equiv) was added CH_2Cl_2 (300 μL) and 2,6-lutidine (11 μL, 0.098 mmol, 3 equiv). TIPSOTf (17 μL, 0.065 mmol, 2 equiv) was then added and the reaction was stirred for 23 h at room temperature. The reaction was quenched with sat. aq. $NaHCO_3$ (2 mL) and diluted with H_2O (1 mL) and EtOAc (3 mL). The layers were separated and the aqueous layer was extracted with EtOAc (3 x 3 mL). The

organic layers were combined, washed with brine (3 mL), and dried over Na_2SO_4. Evaporation under reduced pressure afforded the crude product, which was purified by flash chromatography (4:1 Hexanes:EtOAc) to provide the silyl ether **2.18** (17.7 mg, 74% yield, 2 steps) as a colorless oil. R_f 0.55 (4:1 Hexanes:EtOAc); ^{1}H NMR (500 MHz, CD_2Cl_2): δ 8.88 (app. d, *J* = 256, 1H), 7.95 (t, *J* = 7.6, 1H), 7.50 (d, *J* = 8.1, 1H), 7.40 (t, *J* = 7.6, 1H), 7.22–7.19 (m, 1H), 7.14 (d, *J* = 21.4, 1H), 5.68–5.55 (m, 2H), 4.76–4.18 (m, 3H), 3.91–3.76 (m, 1H), 3.30 (s, 3H), 3.14 (d, *J* = 22.5, 3H), 2.84–2.74 (m, 1H), 2.69–2.56 (m, 3H), 2.43–2.12 (m, 2H), 2.02–1.91 (m, 1H), 1.83–1.56 (m, 10H), 1.54–1.33 (m, 3H), 1.25–1.12 (m, 18H), 1.03–0.94 (m, 18H), 0.64 (t, *J* = 6.7, 3H); ^{13}C NMR (500 MHz, CD_2Cl_2): δ 139.9, 138.2, 136.4, 130.8, 127.3, 125.2, 123.8, 123.0, 119.9, 119.82, 119.79, 119.7, 112.3, 110.4, 109.2, 109.1, 96.3, 96.1, 82.7, 79.9, 74.04, 74.01, 67.5, 67.4, 56.3, 54.9, 54.7, 52.3, 44.6, 41.8, 40.0, 39.1, 38.9, 34.4, 31.1, 30.0, 29.3, 27.6, 27.5, 22.7, 21.8, 20.5, 19.5, 19.0, 18.4, 18.2, 17.6, 16.5, 16.1, 13.9, 13.8, 12.5, 12.1; IR (film): 2926, 1489, 1462, 1052 cm^{-1}; HRMS-APCI (*m/z*) $[M]^{\bullet+}$ calcd for $C_{41}H_{63}NO_4Si$, 661.4521; found, 661.4507. $[\alpha]^{21}_D$ +35.0 ° (*c* = 1.0, $CHCl_3$).

*Note: NMR data for silyl ether **2.18** were acquired at –40 °C and showed a mixture of conformers. These data represent empirically observed chemical shifts and coupling constants from the ^{1}H and ^{13}C NMR spectra.*

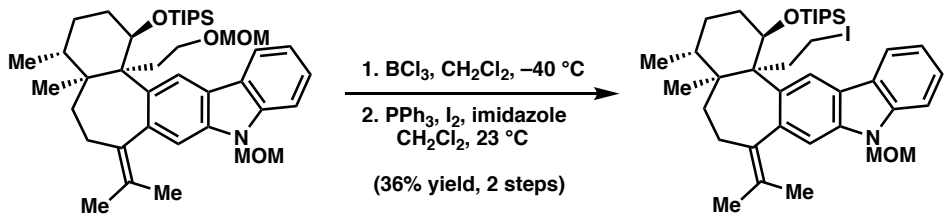

2.18 ***2.19***

Iodide 2.19. To a vial charged with silyl ether **2.18** (9.5 mg, 0.018 mmol, 1 equiv) in CH_2Cl_2 (330 μL) at –78 °C, was added BCl_3 (1.0 M solution in CH_2Cl_2, 18.0 μL, 0.018 mmol, 1.3 equiv). The mixture was allowed to warm to –40 °C and stirred for 40 min. The reaction was quenched at –40 °C with MeOH (1 mL) and sat. aq. $NaHCO_3$ (2 mL), and then allowed to warm to room temperature. Next, the mixture was diluted with H_2O (1 mL) and EtOAc (3 mL). The layers were separated and the aqueous layer was extracted with EtOAc (3 x 3 mL). The combined organic layers were washed with brine (3 mL) and dried over Na_2SO_4. Concentration under reduced pressure afforded the crude product, which was purified by flash chromatography (4:1 Hexanes:EtOAc) to provide the intermediate alcohol (4.3 mg, 48% yield) and recovered silyl ether **2.18** (1.7 mg, 18% yield) as colorless oils.

To a flask charged with the intermediate alcohol (27.3 mg, 0.044 mmol, 1 equiv) was added triphenylphosphine (57.9 mg, 0.022 mmol, 5 equiv) and imidazole (15.0 mg, 0.022 mmol, 5 equiv). The flask was purged with N_2 for 5 min and then CH_2Cl_2 (4 mL) was added. The solution was cooled to 0 °C and a solution of I_2 (44.8 mg, 0.177 mmol, 4 equiv) in CH_2Cl_2 (0.4 mL) was added dropwise over 2 min. The reaction was allowed to warm to room temperature and stirred for an additional 30 min. It was then quenched with sat. aq. $NaHCO_3$ (10 mL) and diluted with H_2O (5 mL) and EtOAc (15 mL). The layers were separated and the aqueous layer was extracted with EtOAc (3 x 15 mL). The combined organic layers were washed with brine

(15 mL), dried over $MgSO_4$. Concentration under reduced pressure afforded the crude product, which was purified by flash chromatography (9:1 Hexanes:EtOAc) to provide iodide **2.19** as a colorless oil (24.0 mg, 36% yield, 2 steps). R_f 0.59 (4:1 Hexanes:EtOAc); ^{1}H NMR (500 MHz, CD_2Cl_2): δ (major conformer) 8.63 (s, 1H), 7.94 (d, *J* = 7.7, 1H), 7.51 (d, *J* = 8.0, 1H), 7.41 (t, *J* = 7.3, 1H), 7.23 (d, *J* = 7.6, 1H), 7.20 (s, 1H), 5.67 (d, *J* = 11.7, 1H), 5.58 (d, *J* = 11.7, 1H), 4.41 (dd, *J* = 12.8, 5.6, 1H), 3.50 (sep, *J* = 4.3), 3.29 (s, 3H), 2.93 (td, *J* = 13.6, 4.0, 1H), 2.75–2.61 (m, 2H), 2.50 (dd, *J* = 12.9, 9.0, 3.8, 1H), 2.43–2.41 (d, *J* = 17.1, 1H), 2.14–2.12 (m, 1H), 2.04 (td, *J* = 13.7, 4.4, 1H), 1.85–1.81 (m, 6H), 1.70–1.65 (m, 2H), 1.46–1.34 (m, 3H), 1.25 (d, *J* = 6.6, 1H), 1.19 (d, *J* = 6.9, 10H), 1.16–1.10 (m, 6H), 1.02 (d, *J* = 7.1, 10H), 0.92 (s, 3H), (d, *J* = 6.7, 3H); δ (minor conformer) [11/63 protons were discernible] 9.14 (s, 1H), 7.29 (t, *J* = 7.3, 1H), 7.15 (s, 1H), 4.76 (dd, *J* = 12.6, 4.8, 1H), 3.39 (s, 3H), 2.86 (dd, *J* = 13.6, 3.9, 1H), 2.25 (ddd, *J* = 13.1, 8.6, 4.5, 1H) 1.95–1.90 (m, 2H); ^{13}C NMR (500 MHz, CD_2Cl_2): δ (major conformer) 140.5, 139.5, 138.2, 136.3, 129.0, 128.0, 127.8, 127.6, 125.2, 123.6, 123.4, 120.0, 119.7, 112.3, 109.1, 83.0, 73.9, 56.2, 55.9, 46.3, 41.8, 38.9, 38.7, 34.3, 29.0, 27.4, 22.7, 20.4, 18.3, 18.0, 16.2, 13.9, 12.2; IR (film): 2940, 2866, 1461, 1338, 1240, 1115 cm^{-1}; HRMS-APCI (*m/z*) $[M]^{\bullet+}$ calcd for $C_{39}H_{58}INO_2Si$, 727.3276; found, 727.3306. $[\alpha]^{21}_D$ +51.2 ° (*c* = 0.5, $CHCl_3$).

*Note: NMR data for iodide **2.19** were acquired at –40 °C and showed a mixture of conformers with a ratio of 7:1. These data represent empirically observed chemical shifts and coupling constants from the ^{1}H and ^{13}C NMR spectra. The ^{13}C NMR spectrum of the minor conformer was indiscernible.*

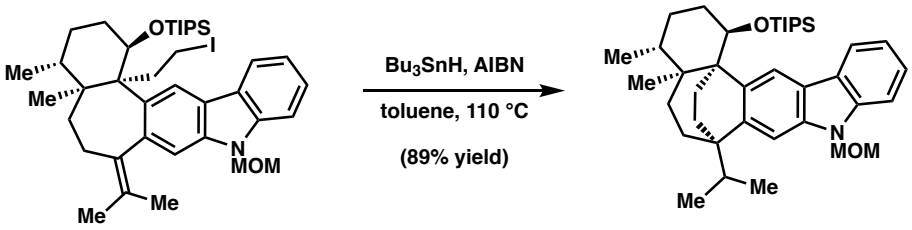

2.19 *2.20*

Cyclized product 2.20. To a solution of iodide **2.19** (24 mg, 0.033 mmol, 1 equiv) in toluene (2.9 mL) was added *n*-Bu_3SnH (88 μL, 0.33 mmol, 10 equiv). AIBN (5.4 mg, 0.033 mmol, 1 equiv) was then added as a solution in toluene (0.4 mL). The vial was sealed with a Teflon-lined screw cap and stirred at 110 °C for 4 h. The reaction was then cooled to room temperature and additional AIBN (5.4 mg, 0.033 mmol, 1 equiv) was added as a solution in toluene (0.4 mL). The vial was again sealed with a Teflon-lined screw cap and stirred at 110 °C for 4 h. The reaction was cooled to room temperature and concentrated under reduced pressure to afford the crude product, which was purified by preparative thin layer chromatography (9:1:EtOAc) to provide cyclized product **2.20** (17.7 mg, 89% yield) as a colorless oil. R_f 0.57 (9:1 Hexanes:EtOAc); ^{1}H NMR (500 MHz, CD_2Cl_2): δ 8.50 (s, 1H), 7.97 (ddd, *J* = 7.7, 1.1, 0.7, 1H), 7.50 (d, *J* = 8.2, 1H), 7.39 (ddd, *J* = 8.3, 7.2, 1.2, 1H), 7.36 (d, *J* = 3.6, 1H), 7.21 (m, 1H), 5.69 (d, *J* = 11.5, 1H), 5.64 (d, *J* = 11.5, 1H), 4.08 (dd, *J* = 12.5, 6.5, 1H), 3.32 (s, 3H), 2.70–2.59 (m, 1H), 2.49 (sept, *J* = 6.3, 1H), 2.27–2.18 (m, *2*H), 1.97 (ddd, *J* = 14.4, 10.4, 6.3, 1H), 1.82 (td, *J* = 13.6, 4.2, 1H), 1.73 (ddd, *J* = 12.7, 10.0, 3.8, 1H), 1.48–1.41 (m, 4H), 1.31–1.20 (m, 4H), 1.20–1.15 (m, 2H), 1.11 (d, *J* = 6.9, 3H), 1.07–1.05 (m, 10H), 0.98–0.96 (m, 10H), 0.92 (s, 3H), 0.63 (d, *J* = 6.9, 3H), 0.22 (td, *J* = 13.8, 4.6, 1H); ^{13}C NMR (500 MHz, CD_2Cl_2): δ 144.1, 141.1, 139.0, 133.4, 125.1, 124.6, 121.9, 120.0, 119.9, 119.4, 109.4, 105.2, 76.7, 74.6, 56.4, 50.3, 43.2, 41.8, 38.5, 38.3, 36.9, 35.5, 35.1, 29.2, 27.6, 19.5, 18.6, 18.5, 17.1, 16.7, 13.4, 13.2; IR (film): 2928, 2864, 1464, 1260, 1240,

1100, 1083, 1066, 1014 cm^{-1}; HRMS-APCI (*m/z*) $[M]^{\bullet+}$ calcd for $C_{39}H_{59}NO_2Si$, 601.4310; found, 601.4310. $[\alpha]^{21}_D$ +32.33 ° (*c* = 0.20, $CHCl_3$).

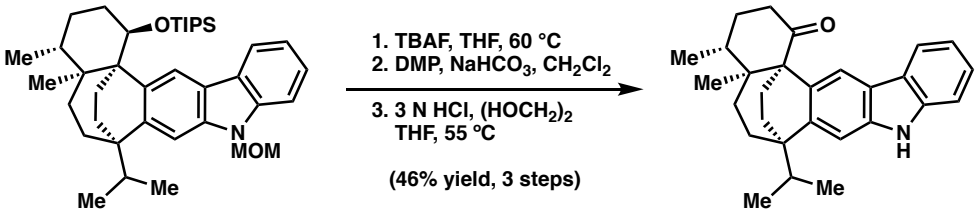

2.20 ***2.21***

Ketone 2.21. To a solution of cyclized product **2.20** (10 mg, 0.017 mmol, 1 equiv) in THF (1.7 mL) was added a solution of TBAF (1.0 M in THF, 0.83 mL, 0.83 mmol, 50 equiv). The vial was sealed with a Teflon-lined screw cap and stirred at 60 °C for 8 h. The reaction was then cooled to room temperature, quenched with H_2O (10 mL), and then diluted with EtOAc (5 mL). The layers were separated, and the aqueous layer was extracted with EtOAc (3 x 5 mL). The combined organic layers were washed with brine (10 mL) and dried over Na_2SO_4. Evaporation under reduced pressure afforded the crude product, which was purified by preparative thin layer chromatography (4:1 Hexanes:EtOAc) to provide intermediate alcohol (5.1 mg, 69% yield) as a colorless oil.

To a solution of the intermediate alcohol (5.1 mg, 0.011 mmol, 1 equiv) in CH_2Cl_2 (1.2 mL) was added Dess-Martin periodinane (10.4 mg, 0.023 mmol, 2 equiv) and $NaHCO_3$ (6.2 mg, 0.068 mmol, 6 equiv) in one portion. The reaction was stirred at room temperature for 15 min, quenched with sat. aq. $Na_2S_2O_3$ (1 mL), and then diluted with H_2O (5 mL) and EtOAc (5 mL). The layers were separated, and the aqueous layer was extracted with EtOAc (3 x 5 mL). The

combined organic layers were dried over Na_2SO_4 and concentrated under reduced pressure to provide the crude product, which was purified by preparative thin layer chromatography (4:1 Hexanes:EtOAc) to provide *N*-MOM ketone **2.25** (5.0 mg, quantitative yield) as a colorless oil.

To a solution of *N*-MOM ketone **2.25** (5.0 mg, 0.011 mmol, 1 equiv) in THF (0.9 mL) was added ethylene glycol (45.0 μL, 0.81 mmol, 72 equiv) and 3 N HCl (110 μL, 0.33 mmol, 30 equiv). The vial was sealed with a Teflon-lined screw cap and stirred at 55 °C for 20 h. The reaction was allowed to cool to room temperature, and was then diluted with Et_2O (5 mL) and sat. aq. $NaHCO_3$ (5 mL). The layers were separated, and the aqueous layer was extracted with Et_2O (3 x 5 mL). The combined organic layers were dried over Na_2SO_4 and concentrated under reduced pressure to provide the crude product, which was purified by preparative thin layer chromatography (4:1 Hexanes:EtOAc) to provide ketone **2.21** (3.0 mg, 46% yield, 3 steps) as a colorless oil. R_f 0.51 (4:1 Hexanes:EtOAc); ^{1}H NMR (500 MHz, CD_2Cl_2): δ 8.13 (s, 1H), 8.00 (d, *J* = 7.7, 1H), 7.52 (s, 1H), 7.44 (d, *J* = 8.0, 1H), 7.40–7.34 (m, 2H), 7.18 (td, *J* = 7.0, 0.9, 1H), 2.87–2.77 (m, 2H), 2.45 (sept, *J* = 6.6, 1H), 2.17–2.03 (m, 2H), 1.92–1.82 (m, 2H), 1.81–1.72 (m, 4H), 1.43–1.33 (m, 1H), 1.22 (ddd, *J* = 14.0, 4.7, 2.7, 1H), 1.10 (d, *J* = 6.6, 3H), 1.09 (s, 3H), 1.05 (d, *J* = 6.9, 3H), 0.73 (d, *J* = 6.1, 3H), 0.16 (td, J = 13.5, 5.2, 1H); ^{13}C NMR (500 MHz, $CDCl_3$): δ 218.9, 140.8, 139.8, 138.7, 133.5, 125.4, 123.6, 120.3, 120.2, 119.4, 118.8, 110.6, 107.4, 61.8, 42.9, 41.2, 40.0, 38.8, 36.6, 36.2, 34.8, 27.9, 27.4, 25.8, 19.5, 17.0, 16.4, 14.4; IR (film): 3368, 2927, 1685, 1611, 1493, 1464, 1386, 1331, 1251 cm^{-1}; HRMS-APCI (*m/z*) $[M]^{\bullet+}$ calcd for $C_{28}H_{33}NO$, 399.2557; found, 399.2533; $[\alpha]^{21}_D$ –11.67 ° (*c* = 0.24, $CHCl_3$).

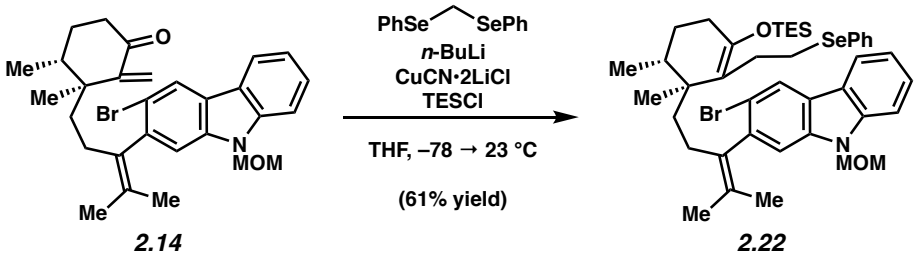

2.14 *2.22*

Silyl Enol Ether 2.22. A vial was charged with CuCN (44.8 mg, 0.5 mmol) and LiCl (42.4 mg, 1.0 mmol) inside the glovebox. The vial was removed from the glovebox and THF (1.0 mL) was added. The resulting mixture was stirred until all solids had dissolved to afford a solution of CuCN•2LiCl (0.50 M in THF). A separate vial was charged with $(PhSe)_2CH_2$[30] (136 mg, 0.417 mmol, 4 equiv) and purged with N_2 for 5 min. THF (1.0 mL) was then added and the mixture was cooled to –78 °C. To the selenide solution was added *n*-BuLi (2.52M in Hexanes, 165 µL, 0.417 mmol, 4 equiv) dropwise over 1 min and the reaction was stirred for 5 min. The CuCN•2LiCl solution (0.50 M in THF, 0.42 mL, 0.21 mmol, 2 equiv) was then added dropwise over 1 min to the lithiate solution. The reaction was stirred at –78 °C for 30 min. A separate vial was charged with enone **2.14** (53 mg, 0.104 mmol, 1 equiv), TESCl (47 mg, 0.313 mmol, 3 equiv), and THF (1.0 mL). This mixture was then added dropwise over 2 min to the above mentioned solution. The reaction was stirred for 10 min at –78 °C, followed by an additional 1 h at room temperature. The reaction was quenched with a 9:1 mixture of sat. aq. NH_4Cl and sat. aq. NH_4OH solution (1.0 mL), and then diluted with H_2O (5 mL) and EtOAc (5 mL). The layers were separated and the aqueous layer was extracted with EtOAc (3 x 5 mL). The combined organic layers were washed with 9:1 sat. aq. NH_4Cl : sat. aq. NH_4OH (5 mL) and brine (5 mL), then dried over Na_2SO_4. Evaporation under reduced pressure afforded the crude product, which was purified by preparative thin layer chromatography (95:5 Hexanes:NEt_3) to provide silyl enol

ether **2.22** (50.4 mg, 61% yield) as a yellow oil. R_f 0.64 (4:1 Hexanes:EtOAc); ^{1}H NMR (500 MHz, C_6D_6): δ 8.33 (d, *J* = 4.5, 2H), 7.78–7.71 (m, 2H), 7.53–7.47 (m, 2H), 7.34–7.26 (m, 6H), 7.23 (d, *J* = 8.2, 2H), 7.13 (d, *J* = 7.5, 2H), 7.01–6.91 (m, 4H), 6.90–6.86 (m, 2H), 5.22–5.02 (m, 4H), 3.43 (ddd, *J* = 12.6, 11.4, 5.0, 1H), 3.24 (ddd, *J* = 12.4, 11.1, 5.1, 1H), 3.06–2.99 (m, 1H), 2.90 (d, *J* = 2.6, 6H), 2.88–2.80 (m, 2H), 2.63 (td, *J* = 13.4, 5.3, 1H), 2.52 (td, *J* = 13.3, 5.0, 1H), 2.44 (t, *J* = 8.6, 2H), 2.34 (td, *J* = 12.9, 4.2, 1H), 2.21 (td, *J* = 13.1, 3.0, 1H), 2.09 (td, *J* = 13.0, 4.3, 1H), 2.05–1.90 (m, 4H), 1.88 (d, *J* = 1.2, 6H), 1.76–1.63 (m, 4H), 1.61 (d, *J* = 9.8, 6H), 1.55–1.48 (m, 1H), 1.41–1.22 (m, 6H), 1.01 (dt, *J* = 27.8, 8.0, 18H), 0.83–0.77 (m, 6H), 0.75 (s, 2H), 0.69–0.56 (m, 15H); ^{13}C NMR (500 MHz, C_6D_6): δ 135.0, 135.8, 133.3, 133.0, 129.2, 129.1, 129.0, 128.9, 126.7, 126.64, 126.61, 126.4, 124.71, 124.66, 124.3, 124.1, 122.9, 121.33, 121.30, 120.9, 120.8, 120.61, 120.57, 115.4, 111.6, 111.5, 109.8, 109.7, 74.2, 74.1, 55.68, 55.67, 41.0, 40.8, 35.7, 35.5, 33.7, 33.5, 30.8, 30.7, 29.4, 29.3, 28.9, 28.2, 27.2, 27.0, 22.4, 22.3, 22.0, 19.8, 19.7, 16.1, 16.0, 7.3, 7.2, 6.3, 6.2; IR (film): 3059, 2956, 2926, 1658, 1467, 1448, 1425, 1334, 1241, 1186, 1114, 1066 cm^{-1}; HRMS-APCI (*m/z*) $[M]^{\bullet+}$ calcd for $C_{42}H_{56}BrNO_2SeSi$, 793.2423; found, 793.2400. $[\alpha]^{21}_D$ –10.59 ° (*c* = 0.34, $CHCl_3$).

*Note: Silyl enol ether **2.22** was obtained as a mixture of conformers. These data represent empirically observed chemical shifts and coupling constants from the ^{1}H and ^{13}C NMR spectra.*

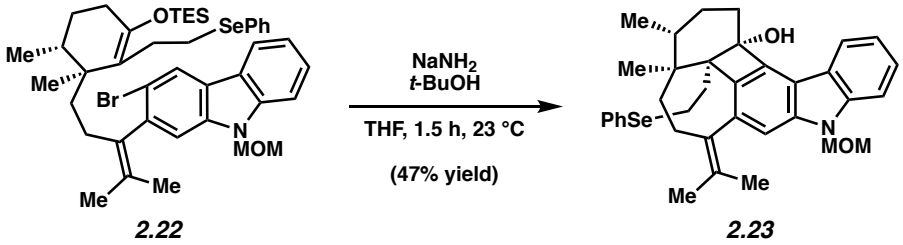

2.22 *2.23*

Cyclobutenol 2.23. A vial was charged with powdered $NaNH_2$ (65 mg, 1.67 mmol, 27.5 equiv) in the glovebox. The vial was removed and THF (3.0 mL) was added, followed by *t*-BuOH (51.0 µL, 0.533 mmol, 8.8 equiv). The reaction was stirred at room temperature for 1 h. A solution of silyl enol ether **2.22** (48.1 mg, 0.060 mmol, 1 equiv) in THF (3.0 mL) was then added. The reaction was stirred at room temperature for 1.5 h. The reaction was quenched with sat. aq. NH_4Cl (1 mL), and then diluted with H_2O (5 mL) and EtOAc (5 mL). The layers were separated and the aqueous layer was extracted with EtOAc (3 x 5 mL). The combined organic layers were washed with brine (5 mL) and dried over Na_2SO_4. Evaporation under reduced pressure afforded the crude product, which was purified by preparative thin layer chromatography (4:1 Hexanes:EtOAc) to provide cyclobutenol **2.23** (17.0 mg, 47% yield) as a yellow oil. R_f 0.39 (4:1 Hexanes:EtOAc); ^{1}H NMR (500 MHz, C_6D_6): δ 8.20 (d, *J* = 7.5, 1H), 7.46–7.42 (m, 2H), 7.34 (ddd, *J* = 8.1, 7.0, 1.0, 1H), 7.30–7.22 (m, 3H), 6.98–6.88 (m, 3H), 5.15 (d, *J* = 11.5, 1H), 5.07 (d, *J* = 11.5, 1H), 2.90 (td, *J* = 11.9, 6.1, 1H), 2.84 (s, 3H), 2.74 (td, *J* = 10.9, 5.4, 1H), 2.59–2.36 (m, 4H), 1.96 (ddd, *J* = 14.3, 11.3, 8.1, 1H), 1.87 (s, 3H), 1.85–1.80 (m, 1H), 1.79–1.72 (m, 4H), 1.45–1.35 (m, *2*H), 1.34–1.26 (m, 1H), 1.26–1.16 (m, 1H), 1.06 (dtd, *J* = 14.3, 11.3, 2.9, 1H), 0.69 (s, 3H), 0.40 (d, *J* = 6.8, 3H); ^{13}C NMR (500 MHz, C_6D_6): δ 141.8, 141.7, 140.2, 137.7, 137.3, 134.4, 132.3, 131.9, 129.3, 126.9, 126.4, 126.1, 122.98, 122.97, 120.6, 116.9, 109.6, 109.5, 80.3, 74.4, 63.5, 55.8, 40.5, 38.2, 31.2, 30.0, 28.0, 27.3, 27.2, 25.7, 22.2, 19.8, 16.8, 16.0;

IR (film): 3391, 2924, 2854, 1554, 1468, 1386, 1341, 1260, 1063 cm^{-1}; HRMS-APCI (*m/z*) $[M]^{\bullet+}$ calcd for $C_{36}H_{41}NO_2Se$, 599.2297; found, 599.2268. $[\alpha]^{21}_D$ +42.5 ° (*c* = 0.16, $CHCl_3$).

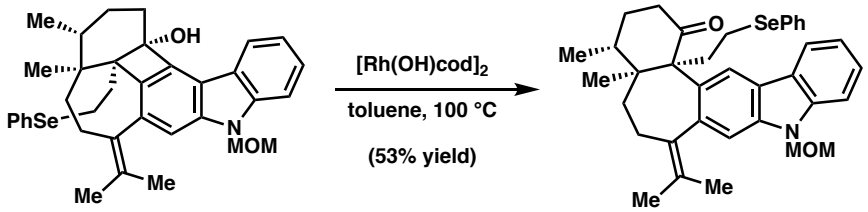

2.23 ***2.24***

Selenide 2.24. To a vial charged with cyclobutenol **2.23** (14.5 mg, 0.024 mmol, 1 equiv) was added $[Rh(OH)cod]_2$ (1.1 mg, 0.002 mmol, 10 mol%) and toluene (2.4 mL) in a glovebox. The vial was sealed with a Teflon-lined screw cap, removed from the glovebox, and stirred at 100 °C for 2 h. The reaction was allowed to cool to room temperature, and was then diluted with H_2O (5 mL) and Et_2O (5 mL). The layers were separated and the aqueous layer was extracted with Et_2O (3 x 5 mL). The combined organic layers were washed with brine (5 mL) and dried over Na_2SO_4. Evaporation under reduced pressure afforded the crude product, which was purified by preparative thin layer chromatography (25:1 benzene:MeCN) to provide selenide **2.24** (7.7 mg, 53% yield) as a colorless oil. R_f 0.54 (4:1 Hexanes:EtOAc); ^1H NMR (500 MHz, C_6D_6): δ 7.71–7.67 (m, 2H), 7.66 (s, 1H), 7.64 (d, *J* = 7.3, 1H), 7.30 (ddd, *J* = 8.3, 7.3, 1.2, 1H), 7.24 (d, *J* = 8.2, 1H), 7.16 (s, 1H), 7.10–7.08 (m, 1H), 6.96 (t, *J* = 7.5, 2H), 6.84 (tt, *J* = 7.4, 1.1, 1H), 5.12 (d, *J* = 11.2, 1H), 5.02 (d, *J* = 11.2, 1H), 3.64 (td, *J* = 12.6, 4.1, 1H), 3.16 (ddd, *J* = 14.8, 12.0, 9.5, 1H), 2.80 (s, 3H), 2.69 (td, *J* = 13.2, 4.4, 1H), 2.56–2.43 (m, 3H), 2.09–2.01 (m, 2H), 2.00–1.93 (m, 1H), 1.73 (s, 3H), 1.70–1.65 (m, 1H), 1.50 (s, 3H), 1.43 (dd, *J* = 14.2, 5.4, 1H), 1.34–1.25 (m, 2H), 1.15 (ddd, *J* = 14.2, 9.1, 4.4, 1H), 0.54 (s, 3H), 0.43 (d, *J* = 6.7, 3H); ^{13}C NMR (500

MHz, C_6D_6): δ 213.9, 142.5, 141.3, 139.0, 136.7, 131.5, 131.3, 129.8, 128.9, 125.9, 125.7, 123.5, 123.4, 121.6, 120.3, 120.2, 111.4, 109.2, 73.7, 68.6, 55.3, 44.3, 39.8, 36.7, 31.51, 31.49, 30.2, 26.9, 24.5, 21.9, 19.3, 18.9, 15.2; IR (film): 2954, 2926, 1698, 1605, 1467, 1438, 1340, 1260, 1241, 1112, 1063, 1021 cm^{-1}; HRMS-APCI (*m/z*) $[M+H]^+$ calcd for $C_{36}H_{42}NO_2Se$, 600.2375; found, 600.2357. $[\alpha]^{21}_D$ +41.67 ° (*c* = 0.20, $CHCl_3$).

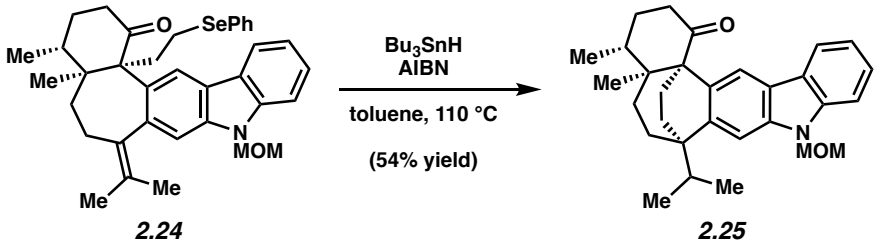

2.24 *2.25*

***N*-MOM Ketone 2.25.** To a solution of selenide **2.24** (2.5 mg, 0.004 mmol, 1 equiv) in toluene (320 µL) was added *n*-Bu_3SnH (3.4 µL, 0.012 mmol, 3 equiv) as a solution in toluene (50.0 µL). AIBN (0.34 mg, 0.002 mmol, 0.5 equiv) was then added as a solution in toluene (50.0 µL). The vial was sealed with a Teflon-lined screw cap and stirred at 110 °C for 12 h. The reaction was cooled to room temperature and concentrated under reduced pressure to afford the crude product, which was purified by preparative thin layer chromatography (4:1 Hexanes:EtOAc) to provide *N*-MOM ketone **2.25** (1.0 mg, 54% yield) as a colorless oil. R_f 0.54 (4:1 Hexanes:EtOAc); ^1H NMR (500 MHz, C_6D_6): δ 7.92 (s, 1H), 7.87 (d, *J* = 7.74, 1H), 7.44 (s, 1H), 7.37–7.30 (m, 2H), 7.15–7.13 (m, 1H), 5.29 (d, *J* = 11.6, 1H), 5.19 (d, *J* = 11.6, 1H), 2.91 (s, 3H), 2.79–2.65 (m, 3H), 2.36 (sept, *J* = 6.5, 1H), 2.00 (ddd, *J* = 14.2, 10.2, 3.9, 1H), 1.74–1.62 (m, 3H), 1.54 (ddd, *J* = 13.2, 10.2, 6.2, 1H), 1.48–1.34 (m, 3H), 1.30–1.24 (m, 1H), 1.02 (d, *J* = 6.5, 3H), 0.99 (d, *J* = 6.5, 3H), 0.80 (s, 3H), 0.53 (d, *J* = 6.7, 3H), 0.31 (td, J = 13.4, 5.3, 1H); ^{13}C NMR (500 MHz,

C_6D_6): δ 215.0, 141.5, 141.1, 140.0, 134.5, 125.8, 124.1, 120.8, 120.7, 120.2, 119.1, 109.4, 106.5, 74.1, 61.7, 55.7, 43.2, 41.5, 41.0, 38.5, 37.0, 36.7, 35.0, 27.7, 27.1, 26.1, 19.4, 17.1, 16.5, 14.3; IR (film): 2926, 2875, 1693, 1607, 1556, 1463, 1387, 1332, 1243, 1116, 1063 cm^{-1}; HRMS-APCI (*m/z*) $[M]^{\bullet+}$ calcd for $C_{30}H_{37}NO_2$, 443.2819; found, 443.2788. $[\alpha]^{21}_D$ +1.30 ° (*c* = 0.36, $CHCl_3$).

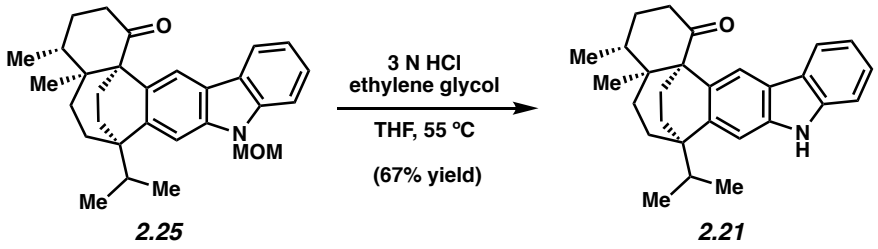

Ketone 2.21. To a solution of *N*-MOM ketone **2.25** (5.0 mg, 0.011 mmol, 1 equiv) in THF (0.9 mL) was added ethylene glycol (45.0 µL, 0.810 mmol, 72 equiv) and 3 N HCl (110 µL, 0.330 mmol, 30 equiv). The vial was sealed with a Teflon-lined screw cap and stirred at 55 °C for 20 h. The reaction was cooled to room temperature, diluted with Et_2O (5 mL), and quenched with sat. aq. $NaHCO_3$ (5 mL). The layers were separated, and the aqueous layer was extracted with Et_2O (3 x 5 mL). The combined organic layers were then dried over Na_2SO_4. Concentration under reduced pressure provided the crude product, which was purified by preparative thin layer chromatography (4:1 Hexanes:EtOAc) to afford ketone **2.21** (3.0 mg, 67% yield) as a colorless oil. Spectral data for ketone **2.21** match those reported above.

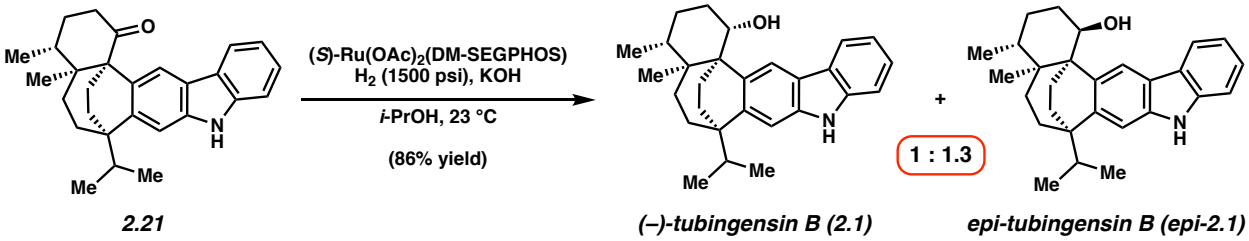

Tubingensin B (2.1) and *epi*-tubingensin B (*epi*-2.1). To a vial charged with ketone **2.21** (7.0 mg, 0.017 mmol, 1 equiv) was added (*S*)-Ru(OAc)$_2$(dm-segphos) (16.5 mg, 0.017 mmol, 1 equiv), KOH (7.8 mg, 0.140 mmol, 8 equiv), and *i*-PrOH (0.2 mL) in a glovebox. The vial was removed from the glovebox, and placed into a 50 mL stainless steel Parr reactor. The vessel was purged with hydrogen (3 x) and then a hydrogen pressure of 1500 psi was introduced. The reaction was stirred at 23 °C for 72 h. The hydrogen was released and the vial was removed from the reaction vessel. The reaction mixture was filtered through a pad of silica gel and the solvent was removed under reduced pressure. The crude product was purified by preparative thin layer chromatography (50:1 benzene:MeCN) to provide ketone **2.21** (0.9 mg, 13% yield), tubingensin B (**2.1**) (2.6 mg, 37% yield) and *epi*-tubingensin B (***epi*-2.1**) (3.2 mg, 49% yield) as colorless oil. Tubingensin B (**2.1**): R_f 0.27 (50:1 benzene:MeCN); ^{1}H NMR (500 MHz, CD_2Cl_2): δ 8.10 (s, 1H), 8.07 (s, 1H), 8.04 (d, *J* = 7.9, 1H), 7.44 (d, *J* = 8.0, 1H), 7.39–7.29 (m, 2H), 7.20 (td, *J* = 7.9, 1.0, 1H), 4.32 (t, *J* = 3.1, 1H), 2.73–2.65 (m, 1H), 2.62 (ddd, *J* = 14.0, 10.3, 3.4, 1H), 2.44 (sept, *J* = 6.5, 1H), 2.17–2.02 (m, 1H), 1.85 (td, *J* = 13.8, 4.6, 1H), 1.81–1.67 (m, 2H), 1.66–1.61 (m, 1H), 1.46–1.35 (m, 2H), 1.33–1.23 (m, 2H), 1.21 (ddd, *J* = 12.6, 6.9, 3.1, 1H), 1.14 (s, 3H), 1.11 (d, *J* = 6.7, 3H), 1.00 (d, *J* = 6.5, 3H), 0.71 (d, *J* = 6.7, 3H), 0.16 (td, *J* = 14.0, 5.0, 1H); ^{13}C NMR (500 MHz, CD_2Cl_2): δ 142.6, 140.1, 138.4, 135.4, 125.4, 124.0, 120.02, 119.97, 119.5, 117.3, 110.9, 107.8, 76.6, 48.0, 42.8, 41.0, 39.3, 38.8, 38.5, 35.4, 34.3, 28.1, 26.04, 26.00, 19.6, 17.2, 17.0, 14.1; IR (film): 3412, 3298, 2954, 2876, 1611, 1493, 1466, 1388, 1246, 1215, 1095

cm^{-1}; HRMS-APCI (*m/z*) $[M]^{\bullet+}$ calcd for $C_{28}H_{35}NO$, 401.2713; found, 401.2713. $[\alpha]^{21}_D$–16.44 ° (*c* = 0.58, $CHCl_3$). *Epi*-tubingensin B (***epi*-2.1**): R_f 0.17 (50:1 benzene:MeCN); ^1H NMR (500 MHz, $CDCl_3$): δ 8.34 (s, 1H), 8.06 (d, *J* = 7.7, 1H), 7.97 (s, 1H), 7.41 (d, *J* = 8.1, 1H), 7.37 (td, *J* = 7.0, 0.9, 1H), 7.36 (s, 1H), 7.21 (td, *J* = 8.0, 1.0, 1H), 3.85 (td, *J* = 12.9, 6.6, 1H), 2.58–2.47 (m, 1H), 2.42 (sept, *J* = 6.7, 1H), 2.26 (ddd, *J* = 13.4, 6.7, 3.8, 1H), 2.18 (ddd, *J* = 14.7, 12.1, 4.5, 1H), 2.09–1.99 (m, 2H), 1.84–1.72 (m, 2H), 1.64–1.58 (m, 1H), 1.52–1.45 (m, 2H), 1.44–1.38 (m, 1H), 1.35 (dd, *J* = 15.0, 7.0, 1H), 1.19 (dt, *J* = 14.1, 3.7, 1H), 1.10 (d, *J* = 6.7, 3H), 1.01 (d, *J* = 6.6, 3H), 0.94 (s, 3H), 0.65 (d, *J* = 6.7, 3H), 0.14 (td, *J* = 13.9, 4.9, 1H); ^{13}C NMR (500 MHz, $CDCl_3$): δ 143.9, 139.8, 138.1, 131.8, 125.3, 123.7, 120.1, 119.8, 119.4, 119.0, 110.6, 108.1, 75.4, 49.5, 42.7, 41.5, 37.9, 37.8, 37.4, 34.9, 34.8, 28.8, 27.8, 26.2, 19.5, 17.1, 16.7, 12.9; IR (film): 3410, 3310, 2954, 2924, 1633, 1608, 1466, 1386, 1248, 1091 cm^{-1}; HRMS-APCI (*m/z*) $[M]^{\bullet+}$ calcd for $C_{28}H_{35}NO$, 401.2713; found, 401.2690; observed for natural sample $[\alpha]^{21}_D$ –6.7 ° (*c* = 0.80, $CHCl_3$)[1], observed for synthetic sample $[\alpha]^{21}_D$ –23.15 ° (*c* = 0.23, $CHCl_3$).

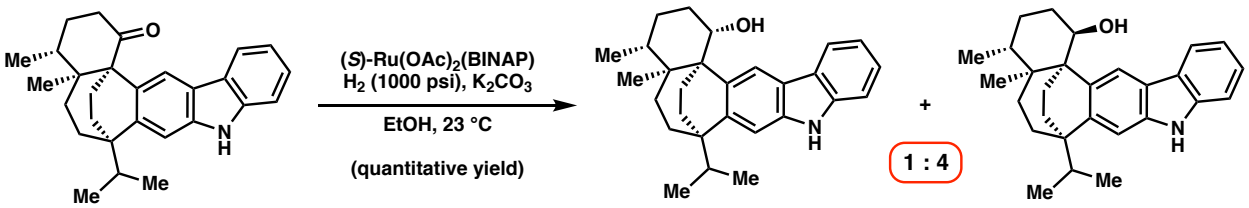

2.21 ***(–)-tubingensin B (2.1)*** ***epi-tubingensin B (epi-2.1)***

Tubingensin B (2.1) and *epi*-tubingensin B (*epi*-2.1). A stock solution of (*S*)-$Ru(OAc)_2$(BINAP) (5.9 mg) and K_2CO_3 (3.9 mg) in EtOH (2.9 mL) was prepared in the glovebox and stirred for 5 min at room temperature. The resulting stock solution containing (*S*)-$Ru(OAc)_2$(BINAP) (0.59 mg, 0.001 mmol, 0.5 equiv), K_2CO_3 (0.39 mg, 0.003 mmol, 2 equiv) in

EtOH (0.29 mL) was then transferred to a separate vial containing ketone **2.21** (1.4 mg, 3.5 μmol, 1 equiv) in the glovebox. The vial was removed from the glovebox, and placed into a 50 mL stainless steel Parr reactor. The vessel was flushed with hydrogen (3 x) and then a hydrogen pressure of 1000 psi was introduced. The reaction was stirred at 23 °C for 48 h. The hydrogen was released and the vial was removed from the reaction vessel. The reaction mixture was filtered through a pad of silica gel and the solvent was removed under reduced pressure to provide a mixture of tubingensin B (**2.1)** and *epi*-tubingensin B (***epi*-2.1**) (1.4 mg, quantitative yield) as a colorless oil. The ratio of tubingensin B (**2.1)** and *epi*-tubingensin B (***epi*-2.1**) was determined by analysis of the crude ^{1}H-NMR spectrum.

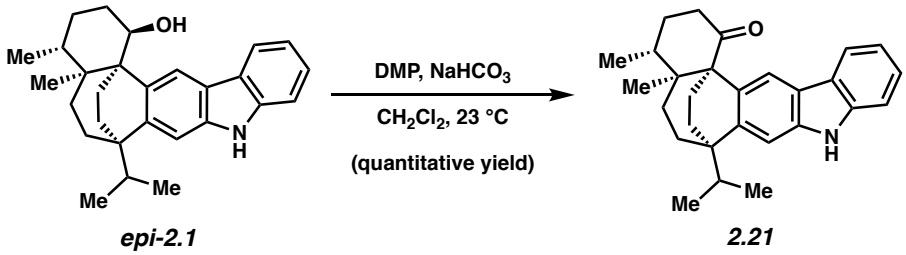

epi-2.1 *2.21*

Ketone 2.21. To a solution of *epi*-tubingensin B (***epi*-2.1)** (2.1 mg, 0.004 mmol, 1 equiv) in CH_2Cl_2 (0.47 mL) was added Dess-Martin periodinane (4.0 mg, 9 mmol, 2 equiv) and $NaHCO_3$ (2.4 mg, 28.0 mmol, 6 equiv). The mixture was allowed to stir at room temperature for 15 min. The reaction was then quenched with sat. aq. $Na_2S_2O_3$ (1 mL) and diluted with H_2O (5 mL) and EtOAc (5 mL). The layers were separated, and the aqueous layer was extracted with EtOAc (3 x 5 mL). The combined organic layers were dried over Na_2SO_4. Evaporation under reduced pressure provided the crude product, which was purified by preparative thin layer

chromatography (4:1 Hexanes:EtOAc) to provide ketone **2.21** (2.1 mg, quantitative yield) as a colorless oil. Spectral data for ketone **2.21** match those reported above.

2.6 Spectra Relevant to Chapter Two

Total Synthesis of (–)-Tubingensin B Enabled by the Strategic Use of an Aryne Cyclization

Michael A. Corsello,[†] Junyong Kim,[†] and Neil K. Garg

Nat. Chem. **2017**, *9*, 944–949.

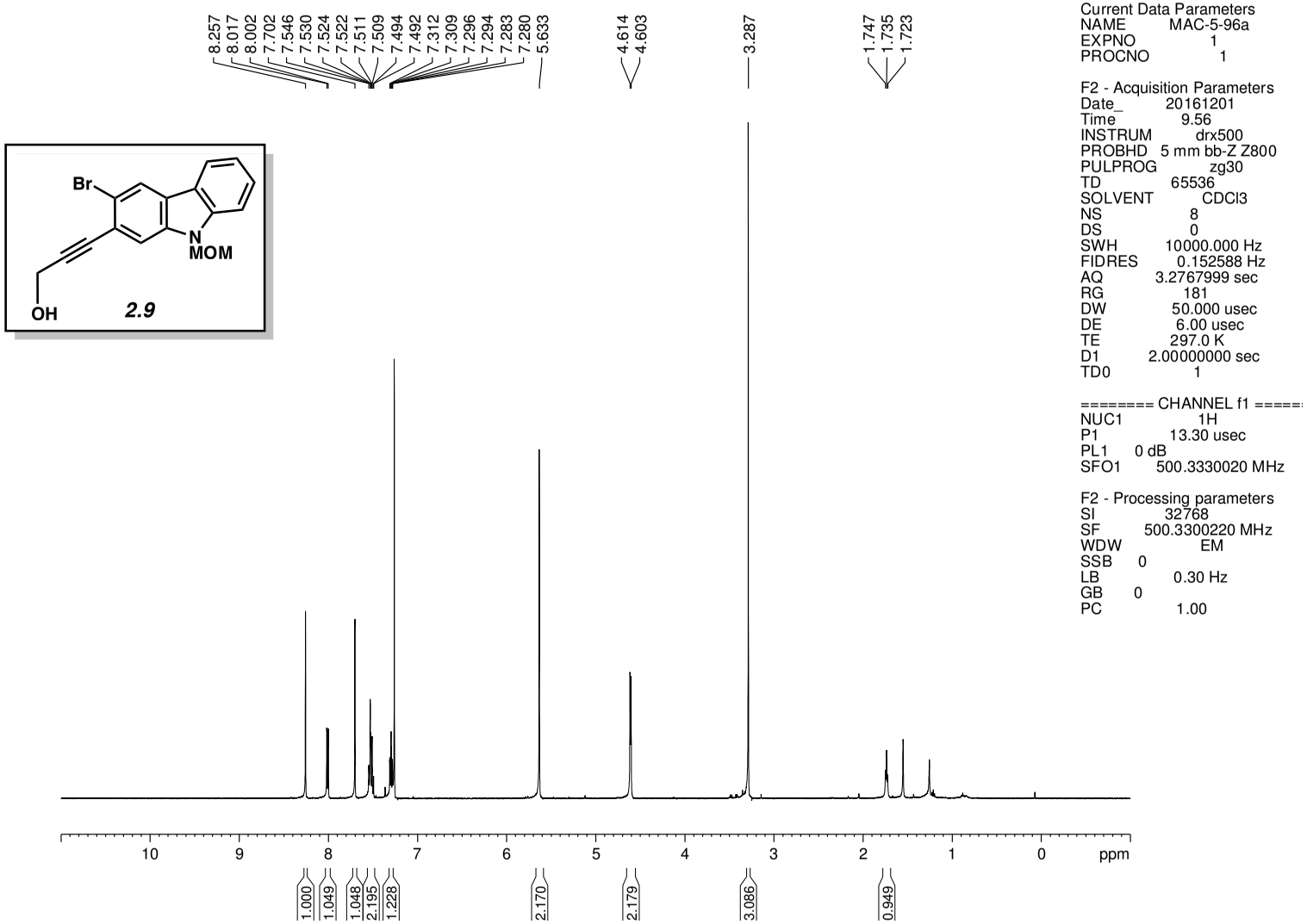

Figure 2.3 ^{1}H NMR (500 MHz, $CDCl_3$) of compound **2.9**.

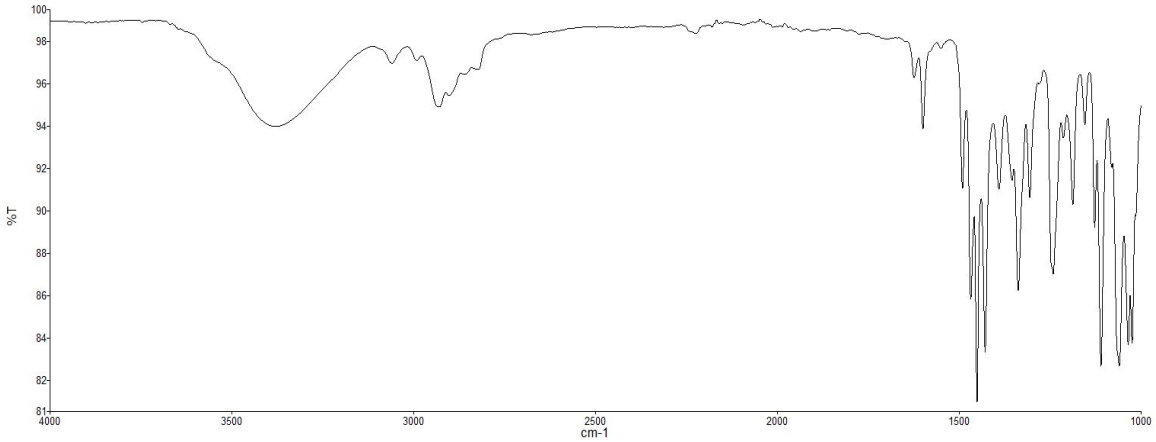

Figure 2.4 Infrared spectrum of compound **2.9**.

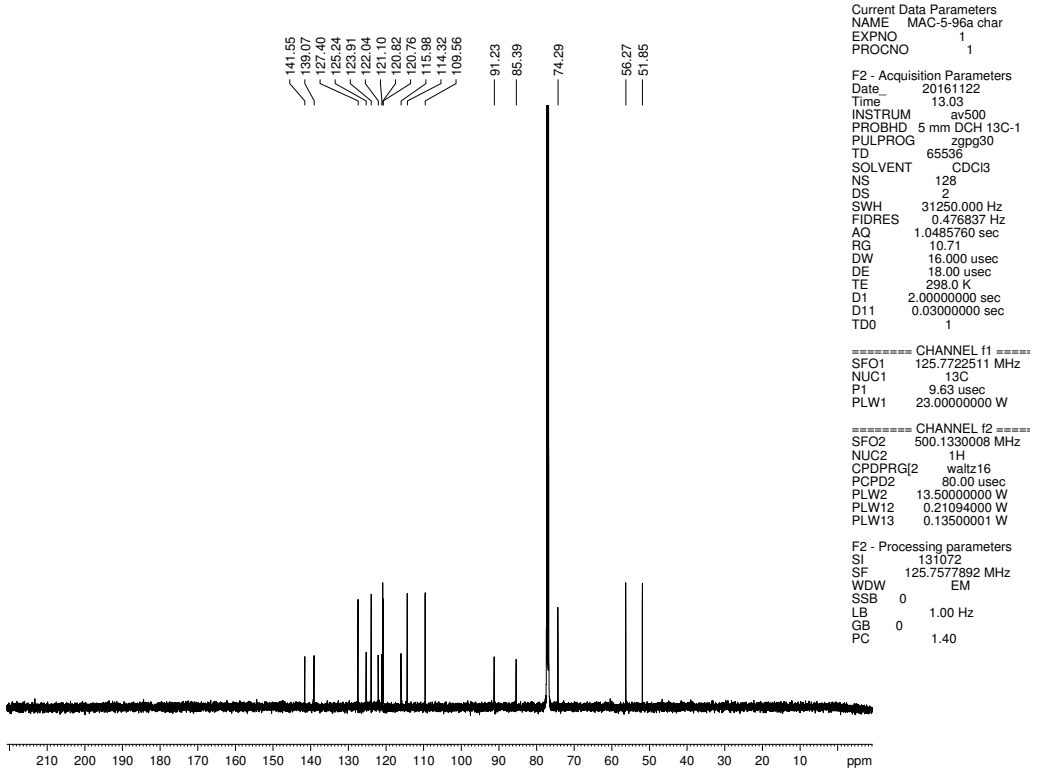

Figure 2.5 ^{13}C NMR (125 MHz, $CDCl_3$) of compound **2.9**.

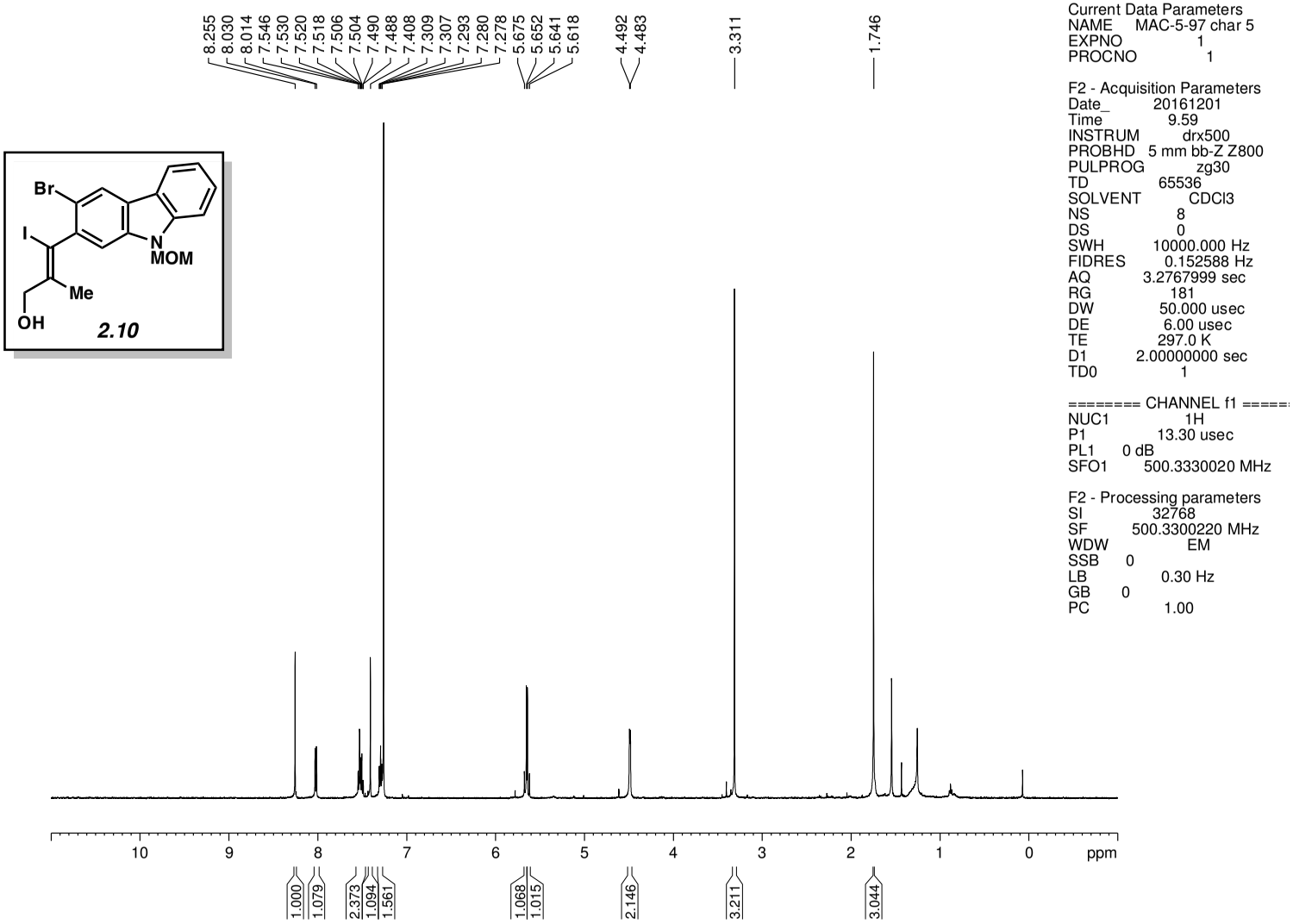

Figure 2.6 ^{1}H NMR (500 MHz, $CDCl_3$) of compound **2.10**.

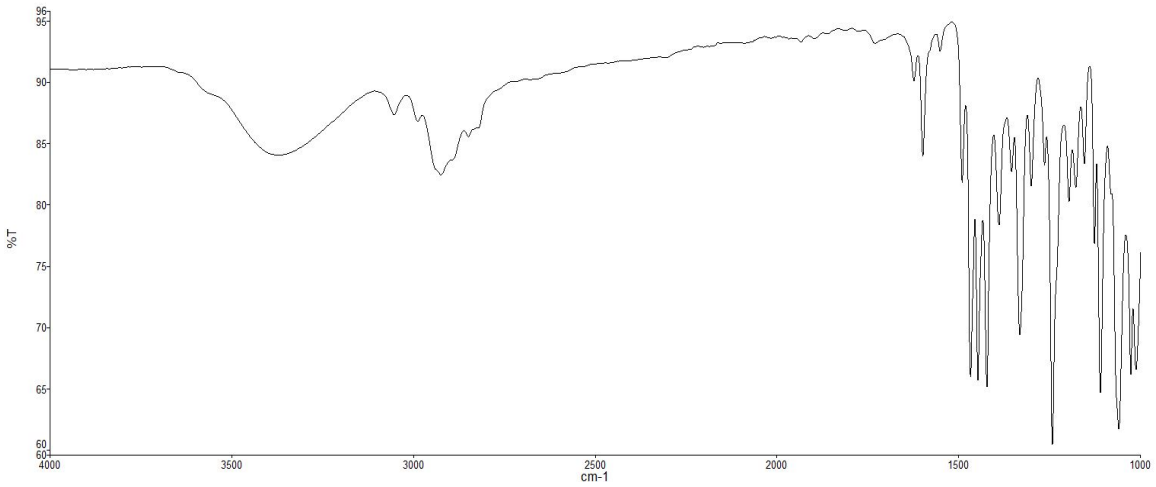

Figure 2.7 Infrared spectrum of compound **2.10**.

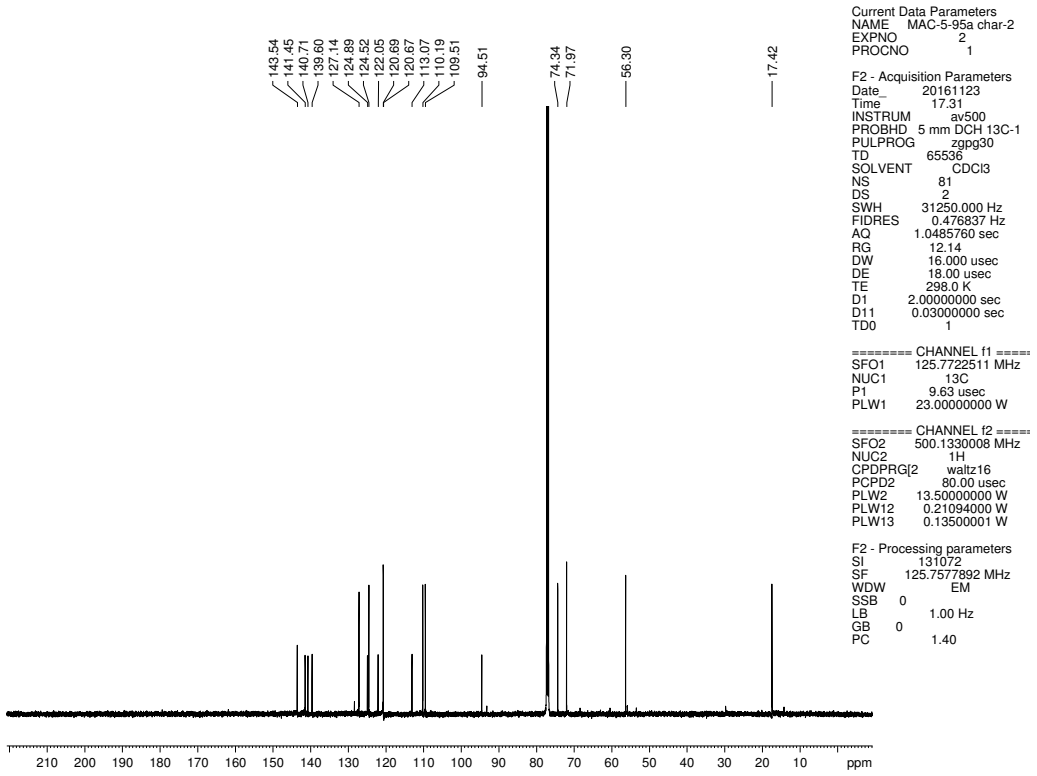

Figure 2.8 ^{13}C NMR (125 MHz, $CDCl_3$) of compound **2.10**.

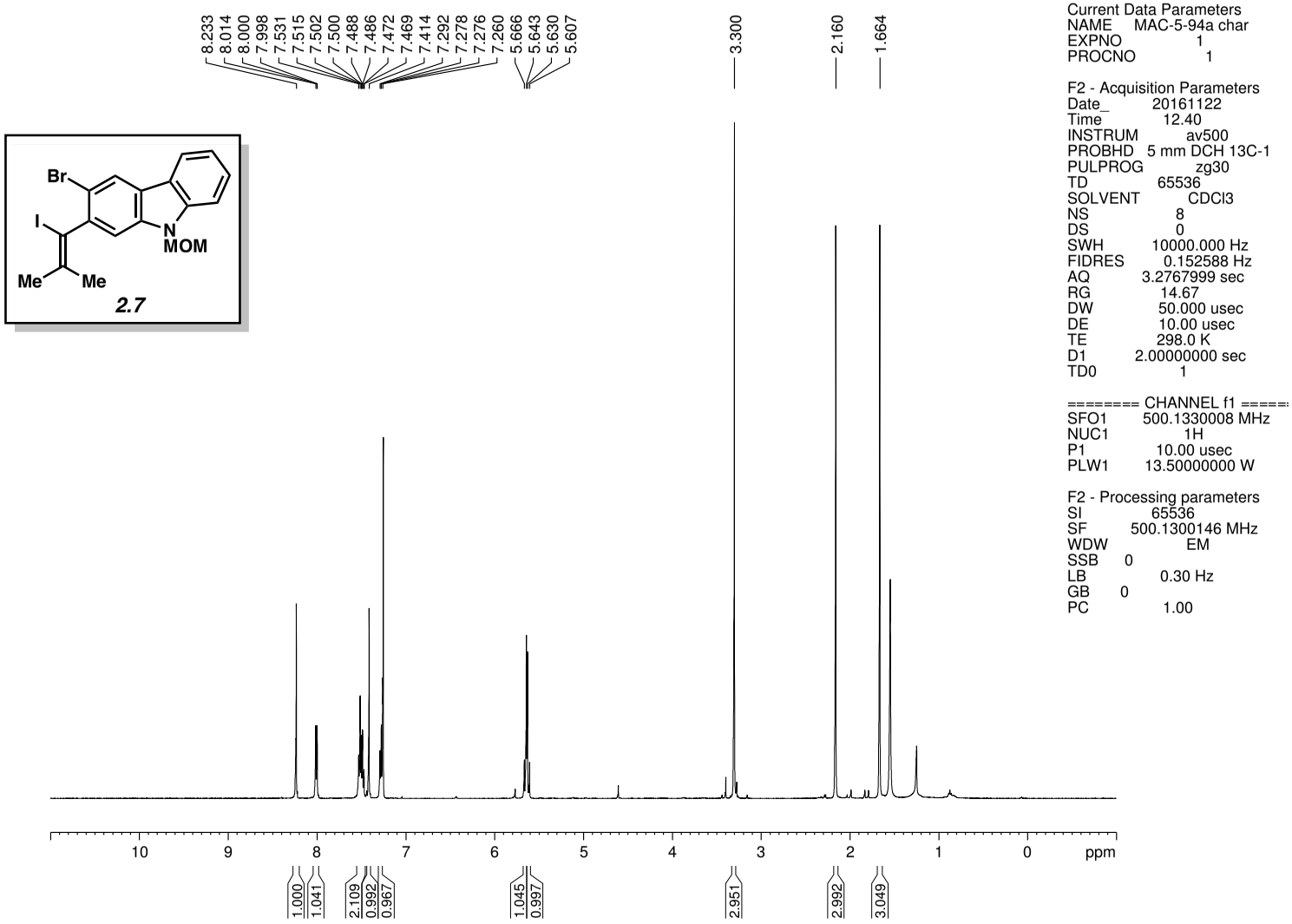

Figure 2.9 ^{1}H NMR (500 MHz, $CDCl_3$) of compound **2.7**.

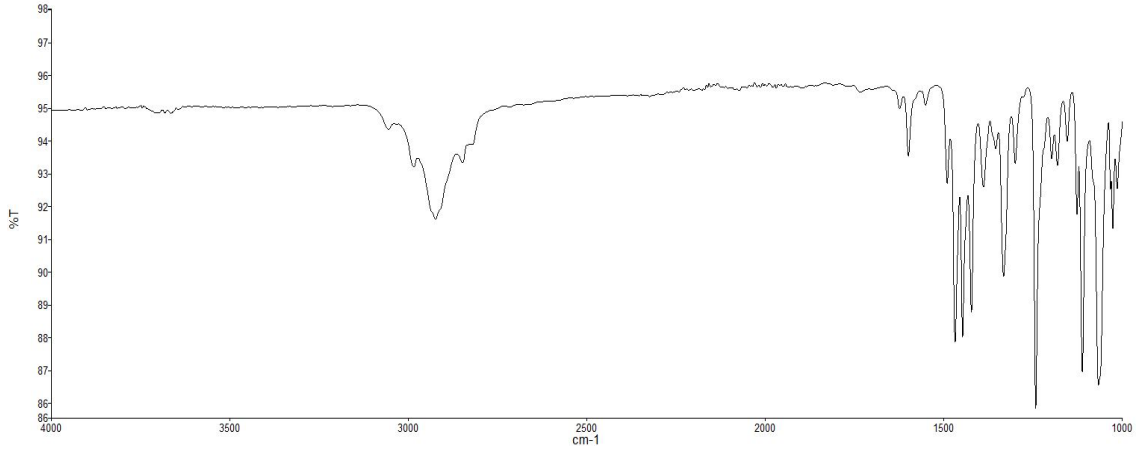

Figure 2.10 Infrared spectrum of compound **2.7**.

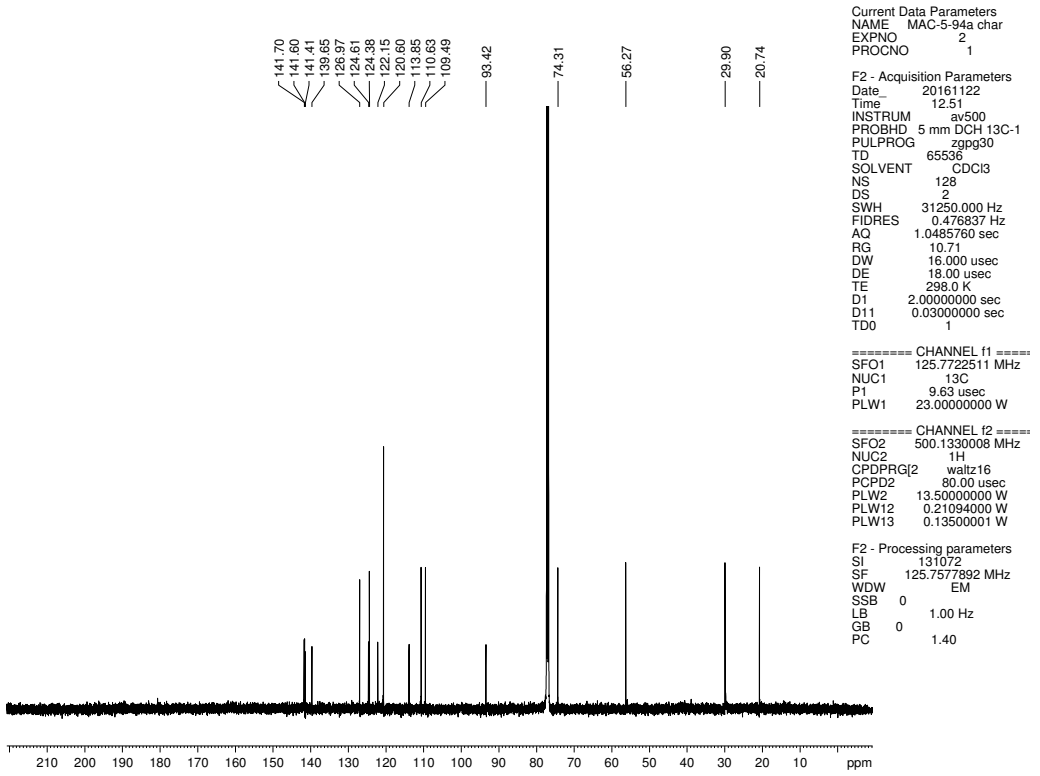

Figure 2.11 ^{13}C NMR (125 MHz, $CDCl_3$) of compound **2.7**.

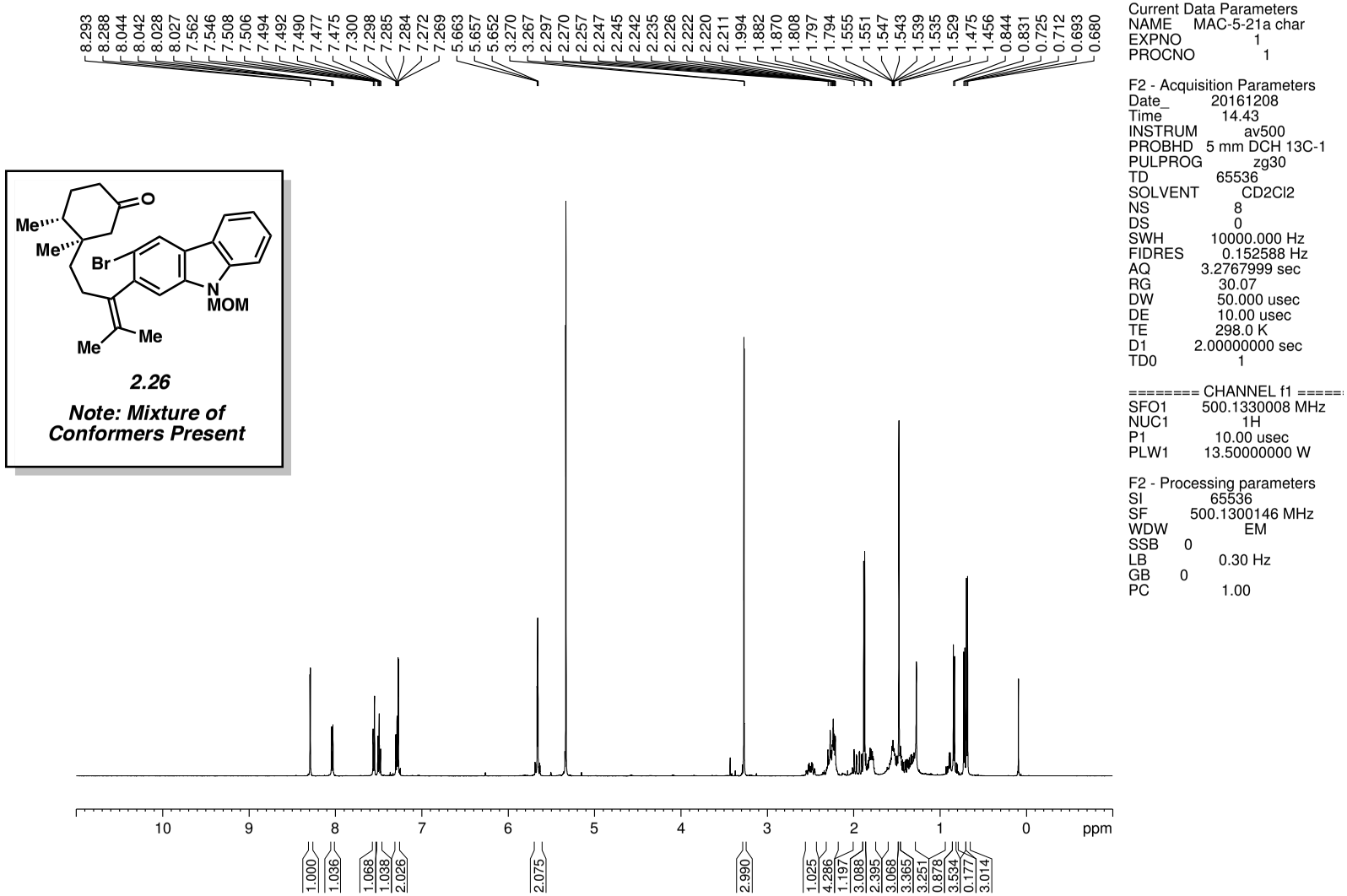

Figure 2.12 ^{1}H NMR (500 MHz, CD_2Cl_2) of compound **2.26**.

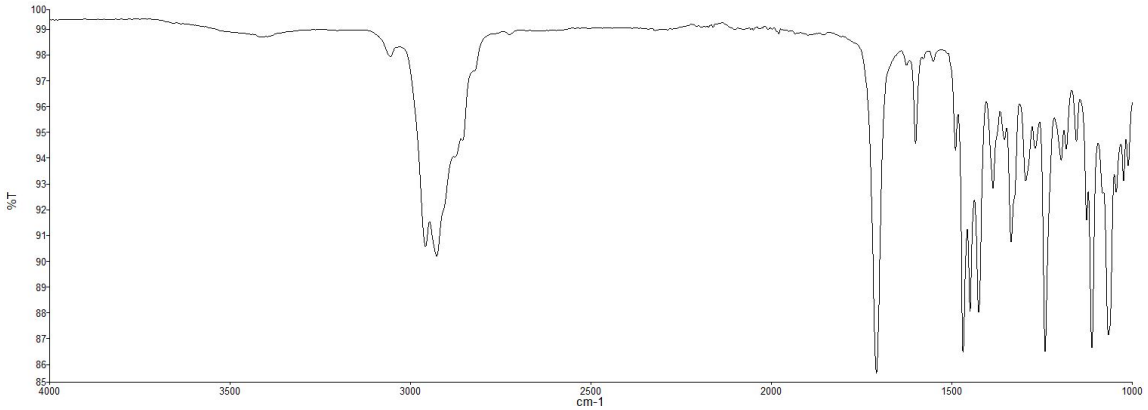

Figure 2.13 Infrared spectrum of compound **2.26**.

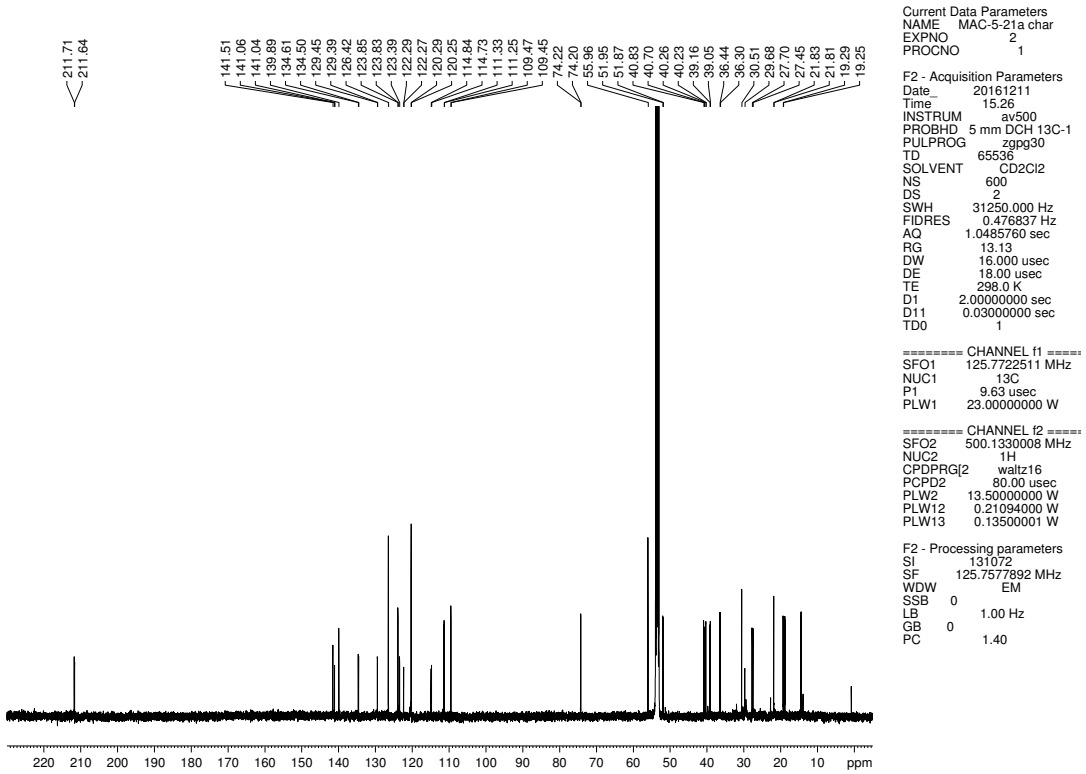

Figure 2.14 ^{13}C NMR (125 MHz, CD_2Cl_2) of compound **2.26**.

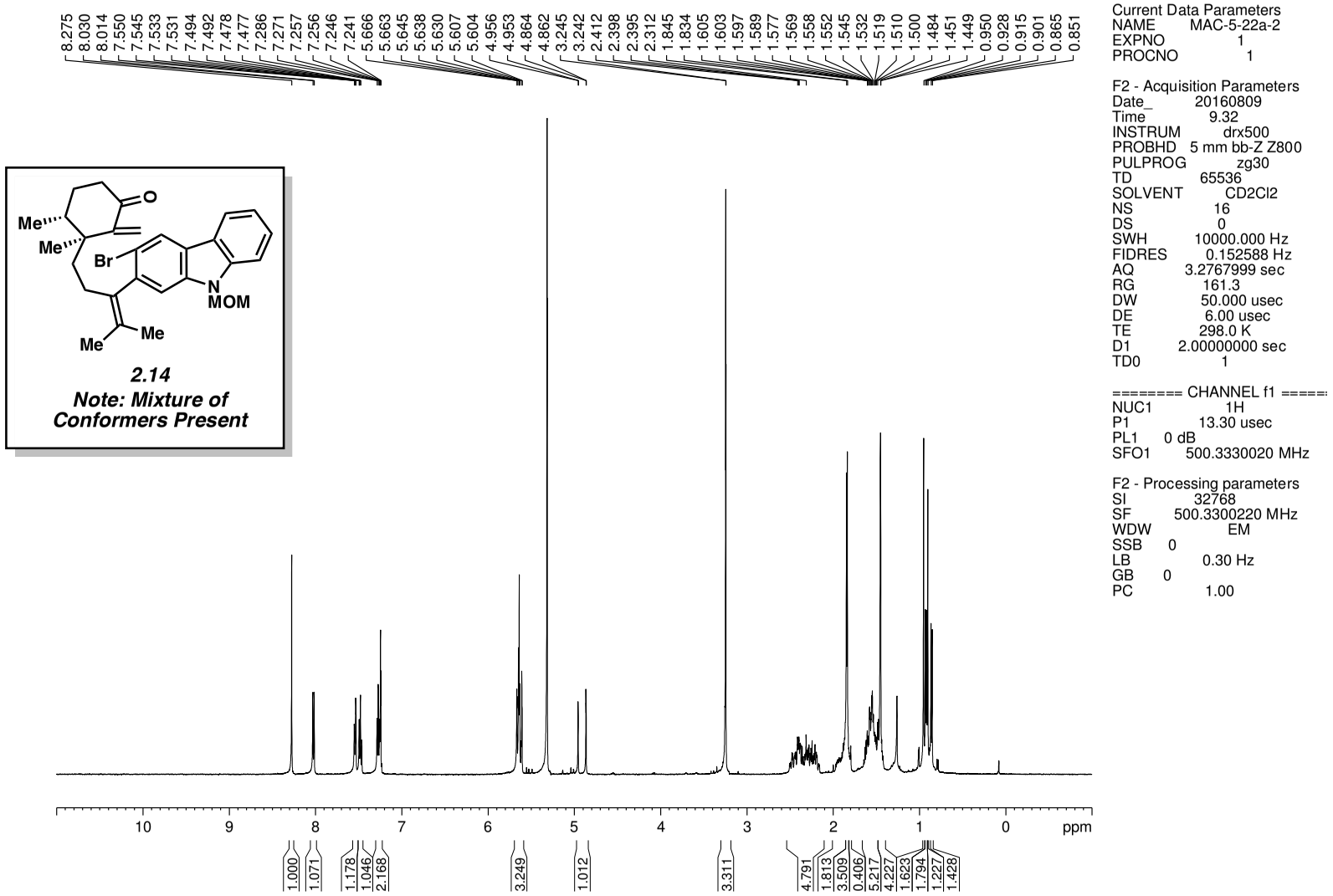

Figure 2.15 ^{1}H NMR (500 MHz, CD_2Cl_2) of compound **2.14**.

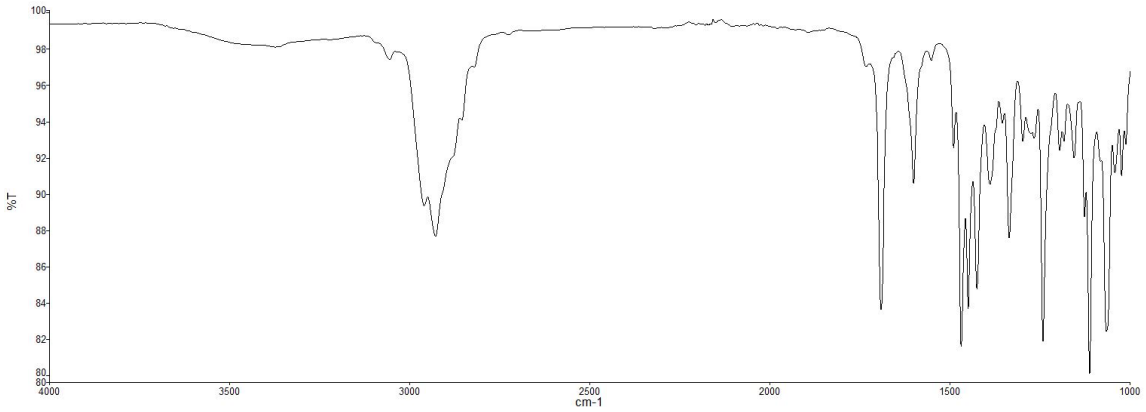

Figure 2.16 Infrared spectrum of compound **2.14**.

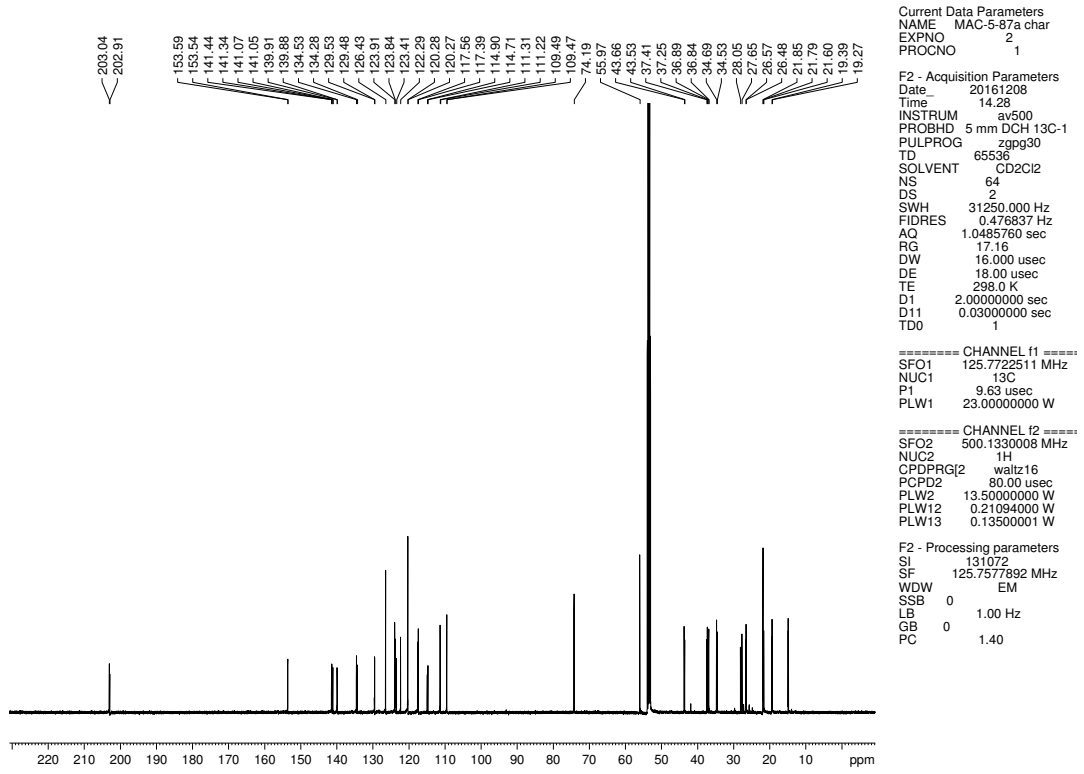

Figure 2.17 ^{13}C NMR (125 MHz, CD_2Cl_2) of compound **2.14**.

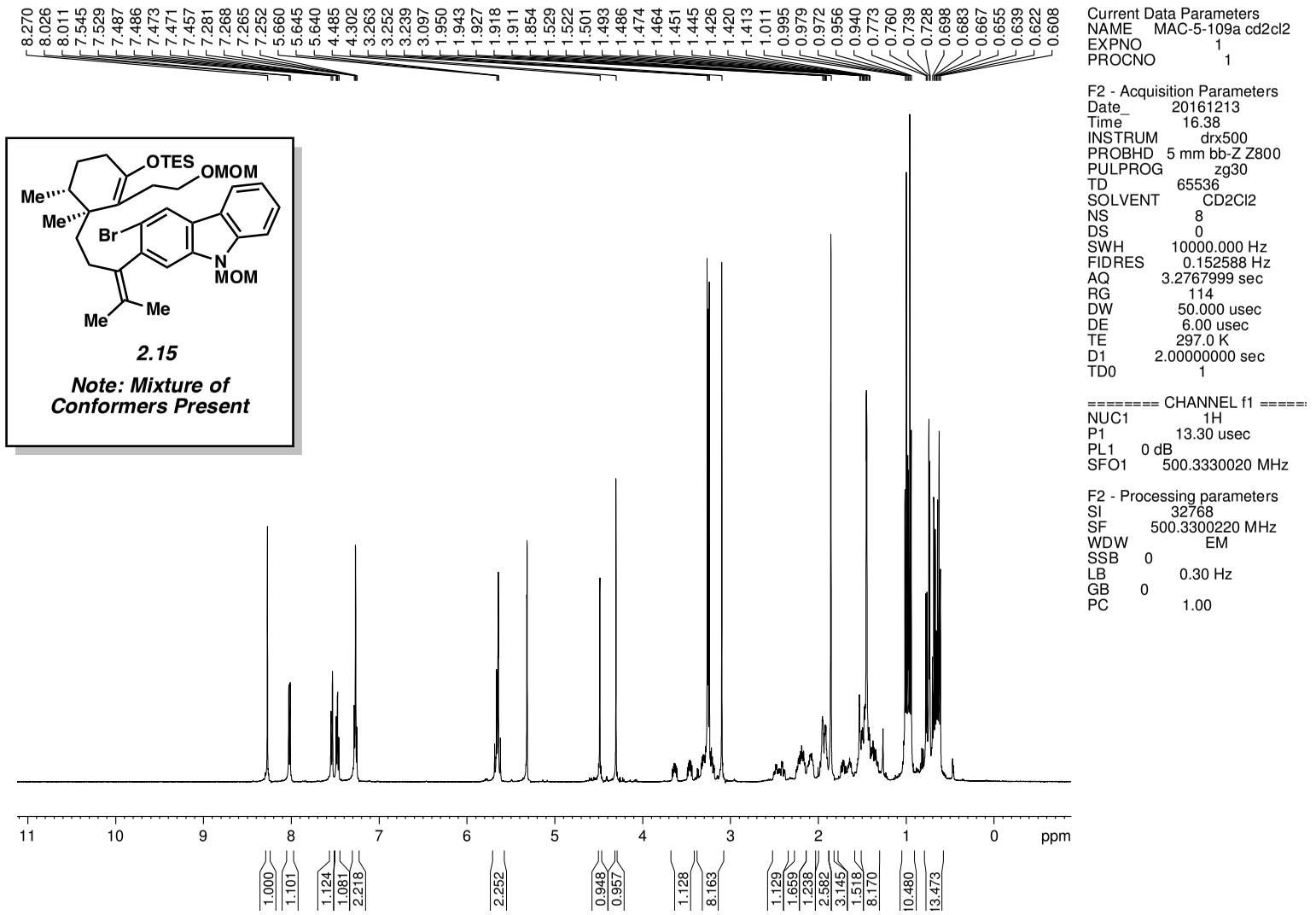

Figure 2.18 ^{1}H NMR (500 MHz, CD_2Cl_2) of compound **2.15**.

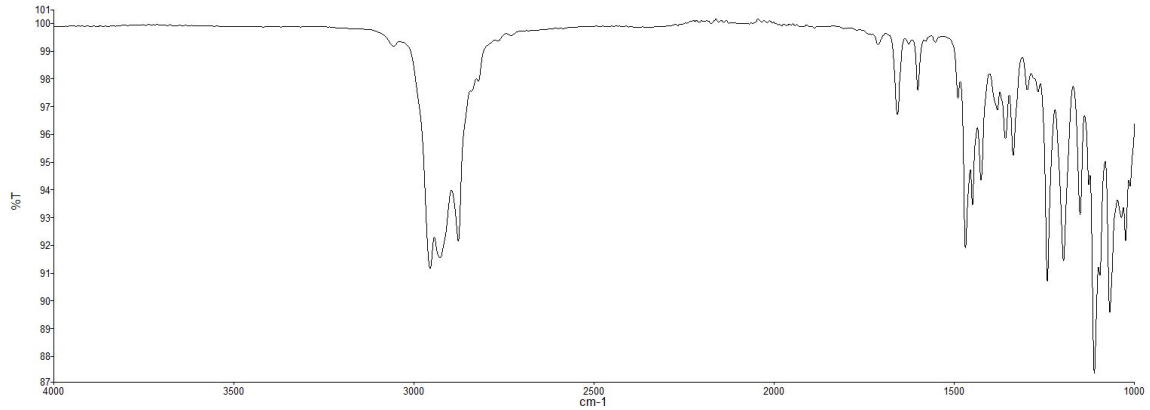

Figure 2.19 Infrared spectrum of compound **2.15**.

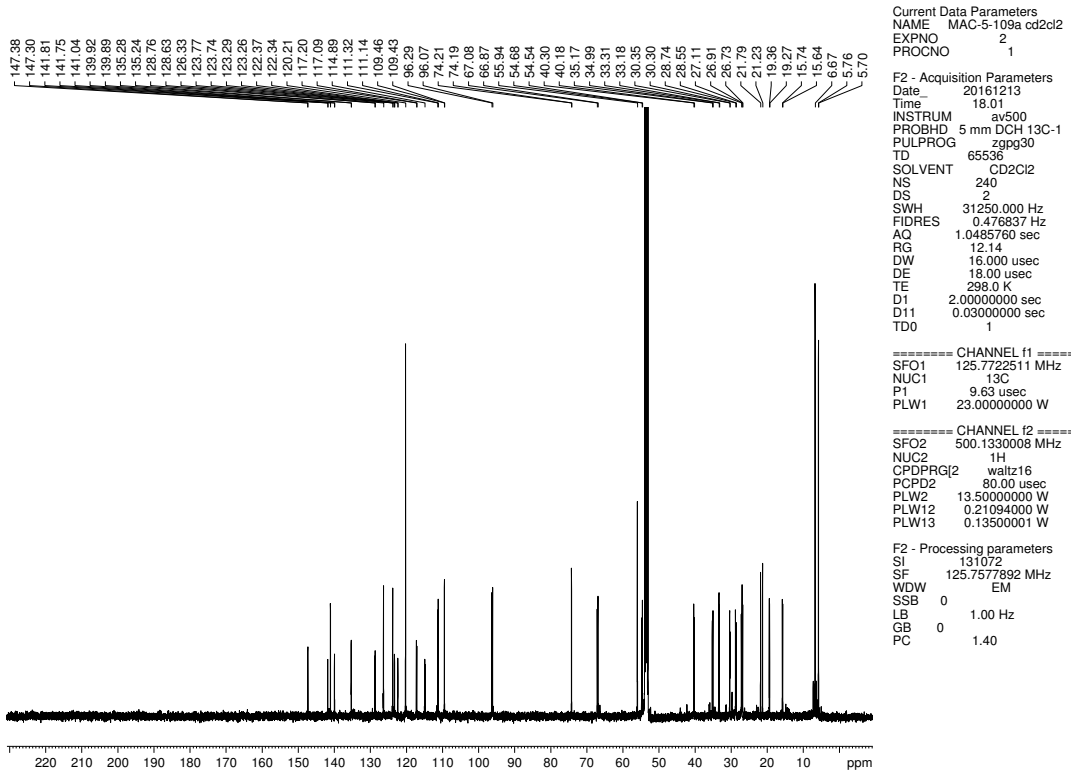

Figure 2.20 ^{13}C NMR (125 MHz, CD_2Cl_2) of compound **2.15**.

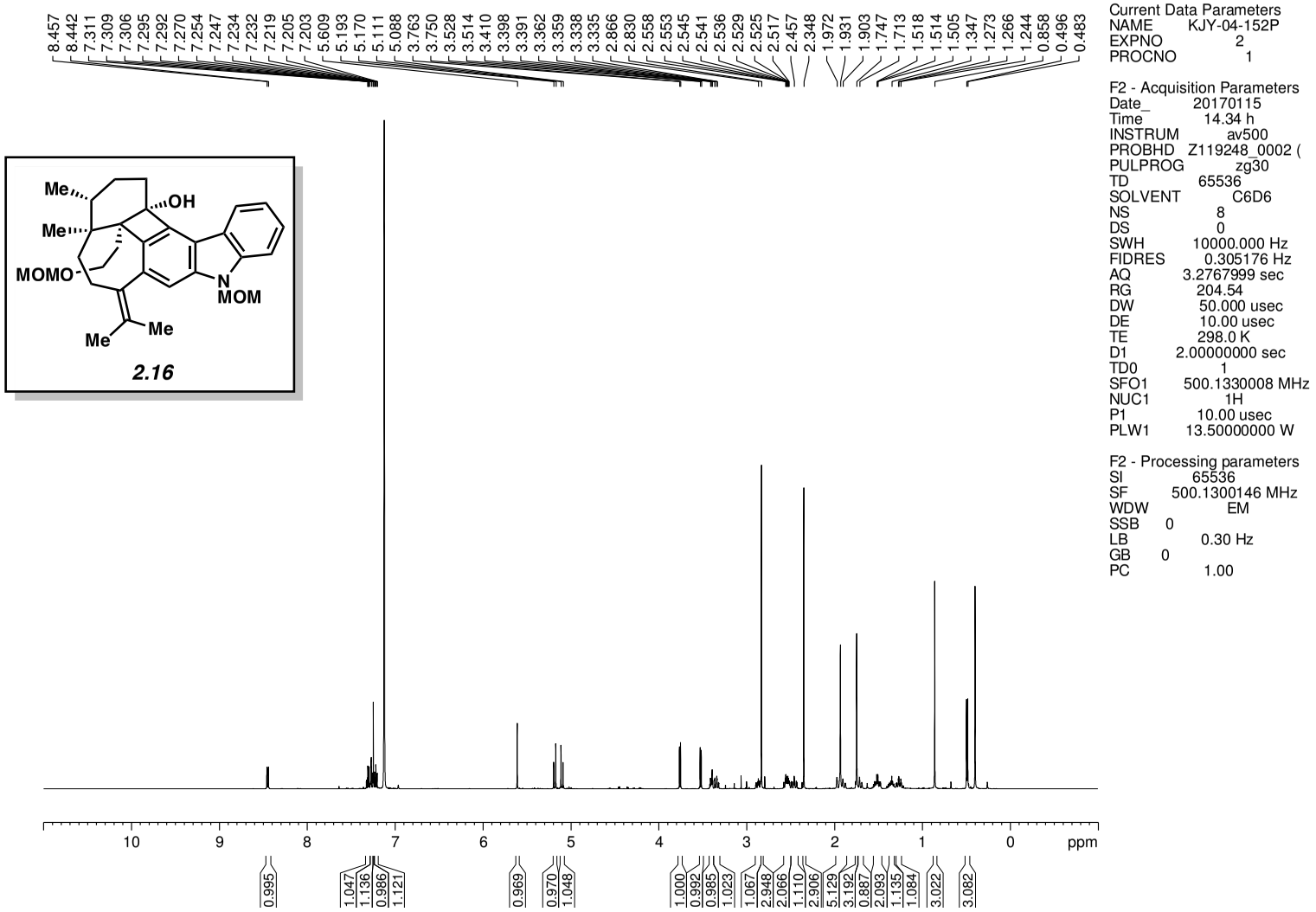

Figure 2.21 ^{1}H NMR (500 MHz, C_6D_6) of compound **2.16**.

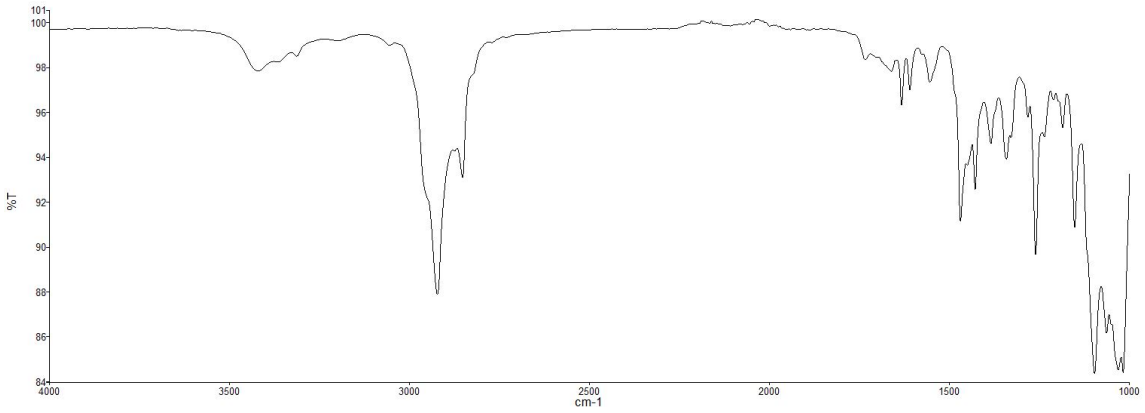

Figure 2.22 Infrared spectrum of compound **2.16**.

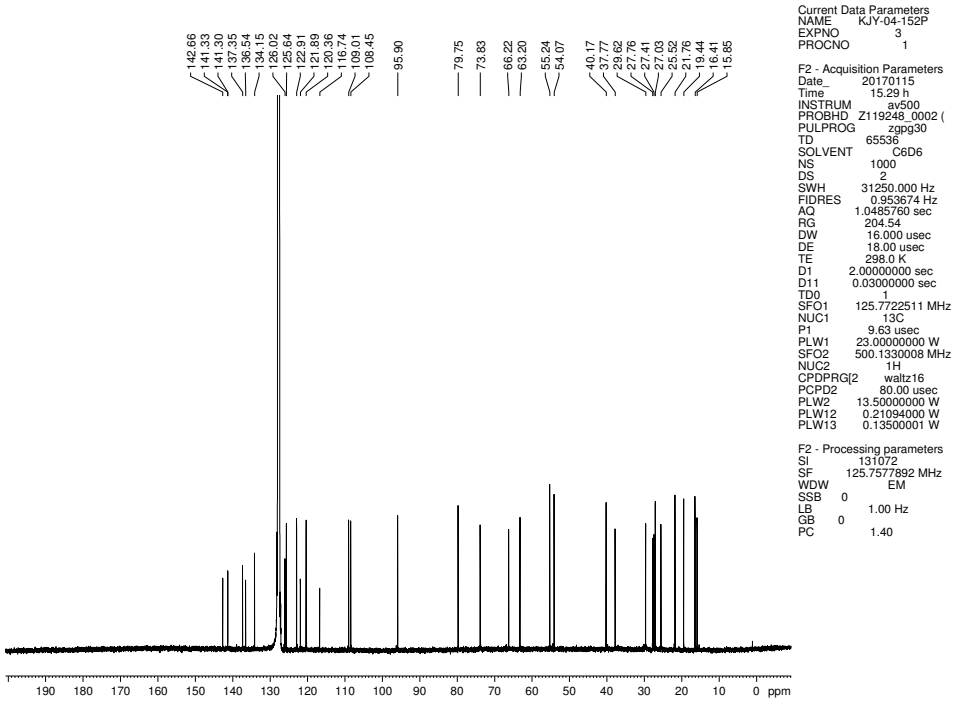

Figure 2.23 ^{13}C NMR (125 MHz, C_6D_6) of compound **2.16**.

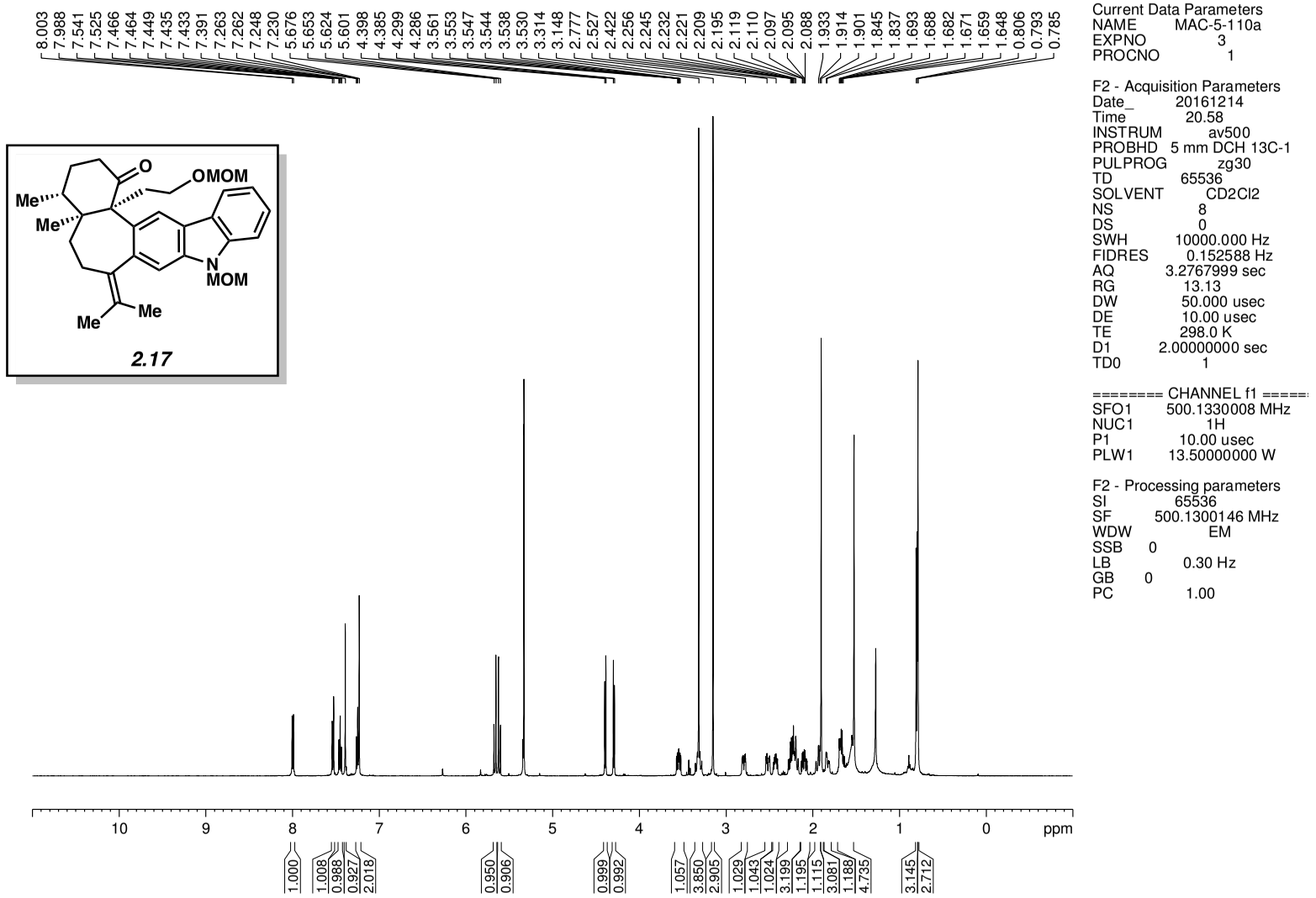

Current Data Parameters
NAME MAC-5-110a
EXPNO 3
PROCNO 1

F2 - Acquisition Parameters
Date_ 20161214
Time 20.58
INSTRUM av500
PROBHD 5 mm DCH 13C-1
PULPROG zg30
TD 65536
SOLVENT CD2Cl2
NS 8
DS 0
SWH 10000.000 Hz
FIDRES 0.152588 Hz
AQ 3.2767999 sec
RG 13.13
DW 50.000 usec
DE 10.00 usec
TE 298.0 K
D1 2.00000000 sec
TD0 1

======== CHANNEL f1 ======
SFO1 500.1330008 MHz
NUC1 1H
P1 10.00 usec
PLW1 13.50000000 W

F2 - Processing parameters
SI 65536
SF 500.1300146 MHz
WDW EM
SSB 0
LB 0.30 Hz
GB 0
PC 1.00

Figure 2.24 ^{1}H NMR (500 MHz, CD_2Cl_2) of compound **2.17**.

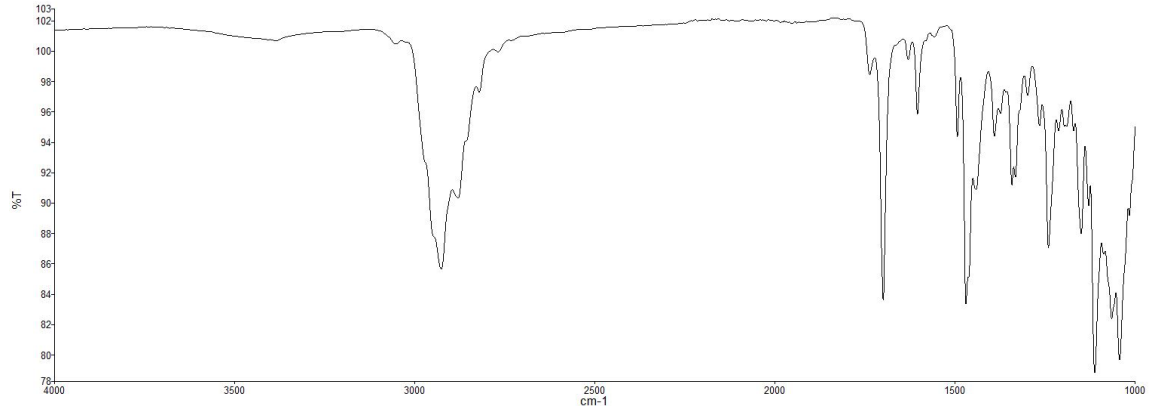

Figure 2.25 Infrared spectrum of compound **2.17**.

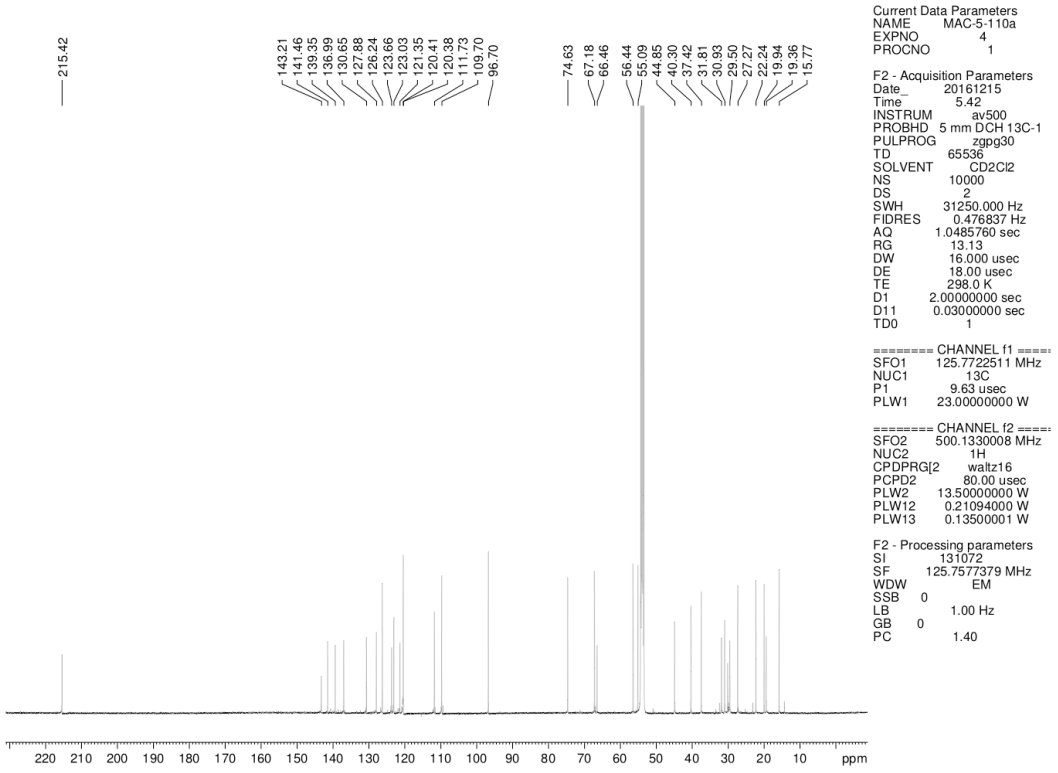

Figure 2.26 ^{13}C NMR (125 MHz, CD_2Cl_2) of compound **2.17**.

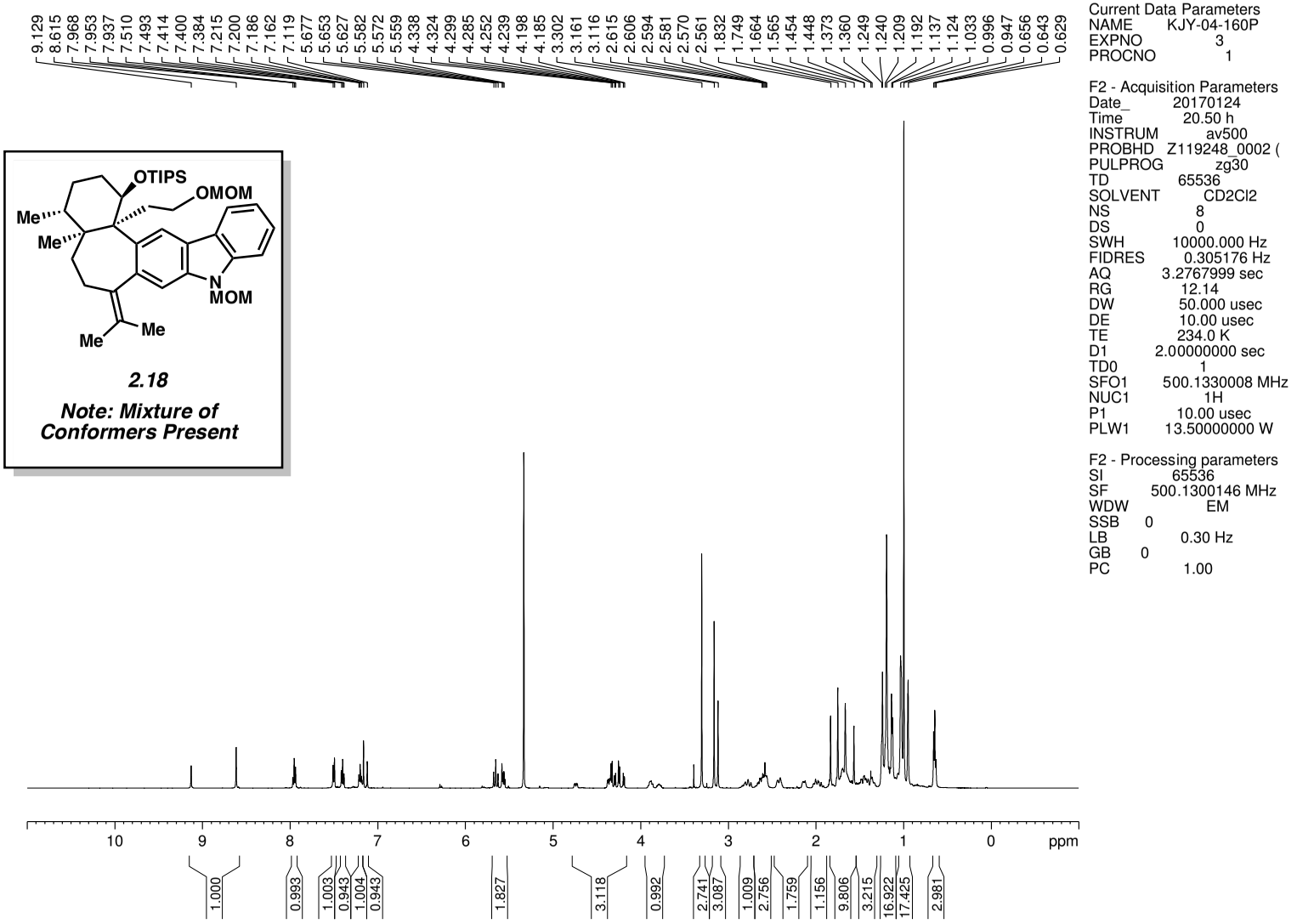

Figure 2.27 ^{1}H NMR (500 MHz, CD_2Cl_2) of compound **2.18**.

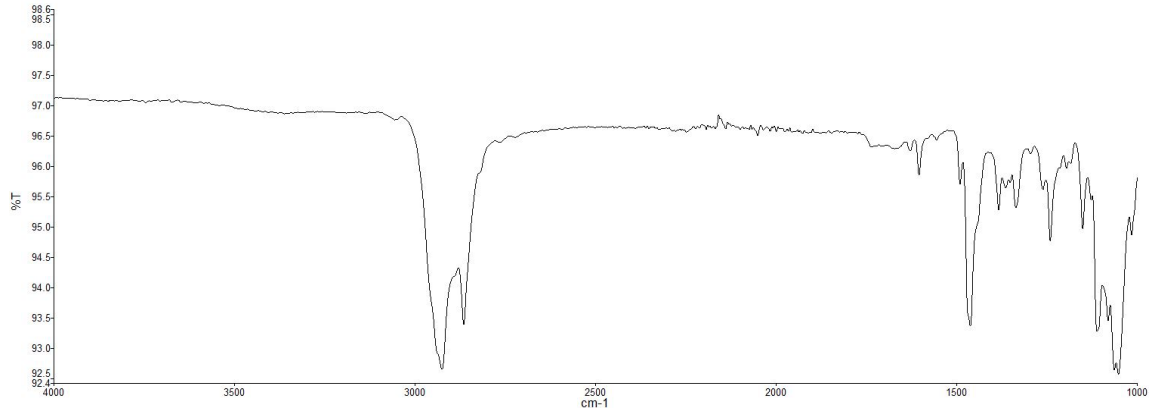

Figure 2.28 Infrared spectrum of compound **2.18**.

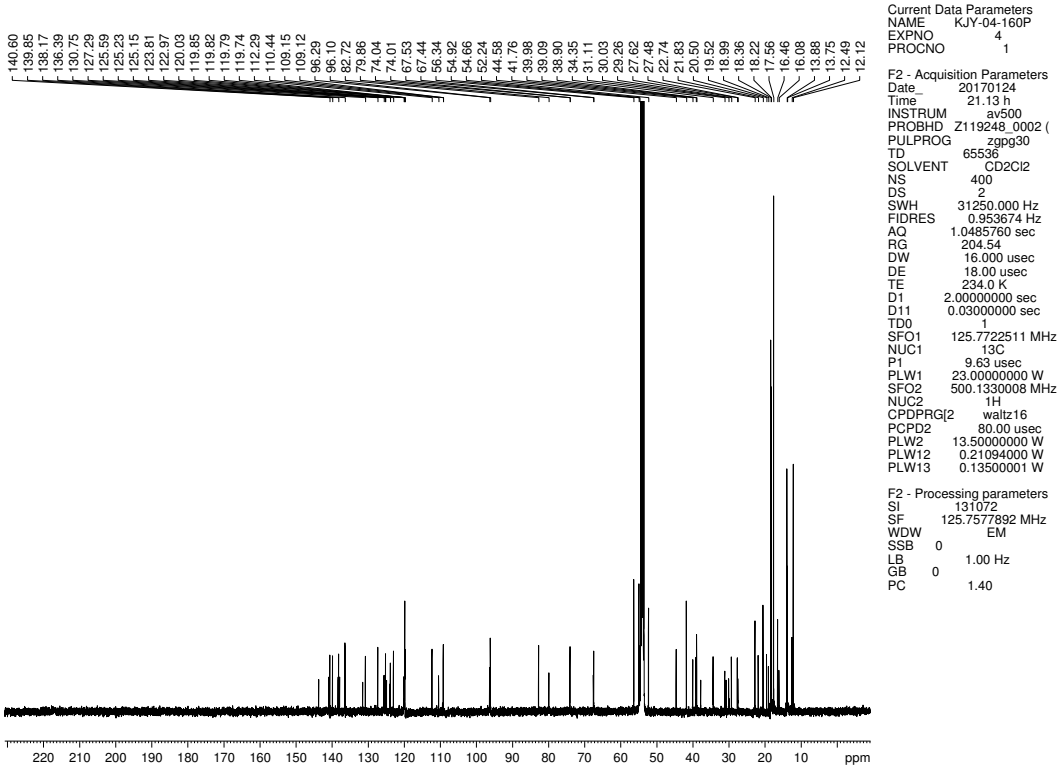

Figure 2.29 ^{13}C NMR (125 MHz, CD_2Cl_2) of compound **2.18**.

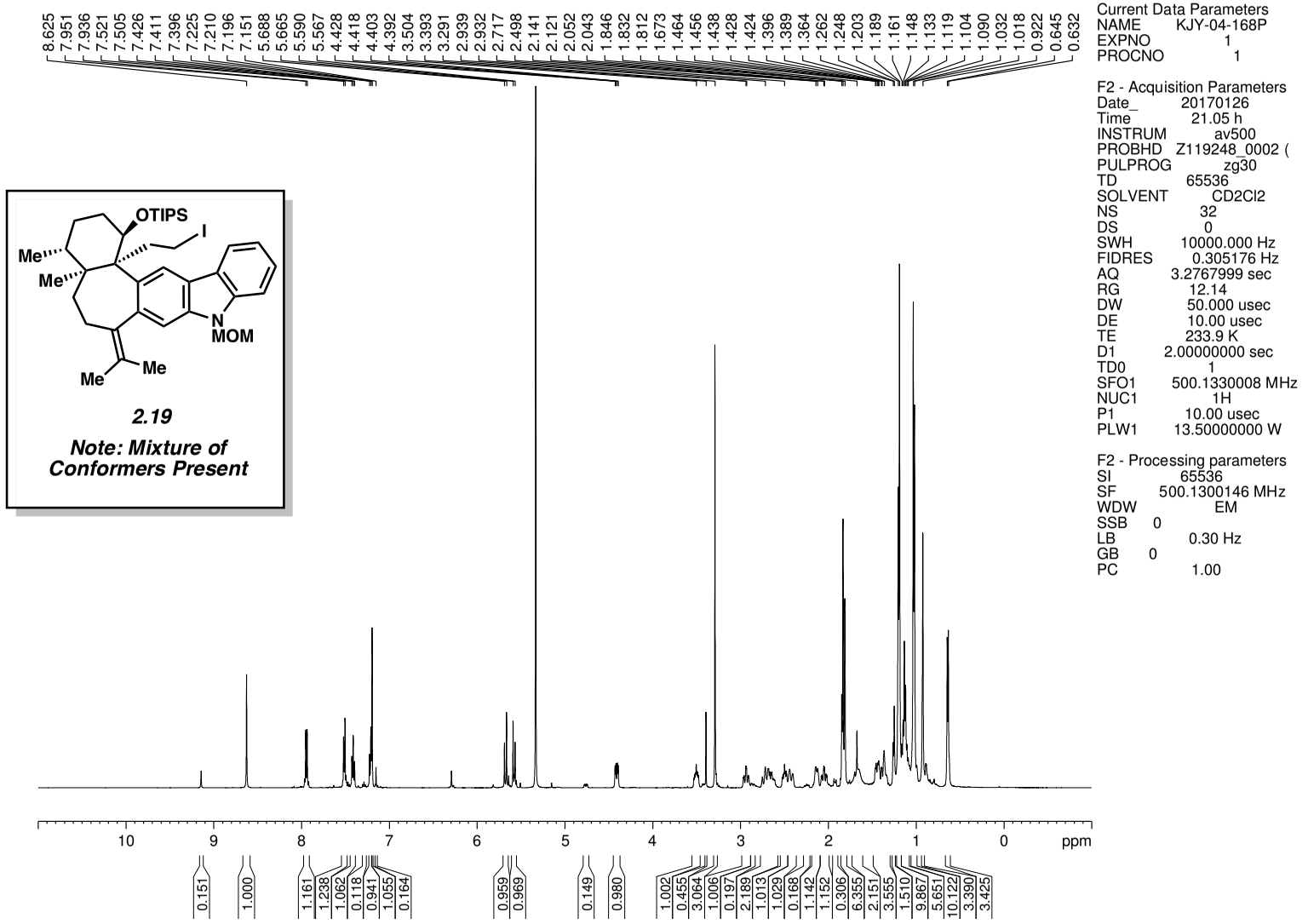

Figure 2.30 ^{1}H NMR (500 MHz, CD_2Cl_2) of compound **2.19**.

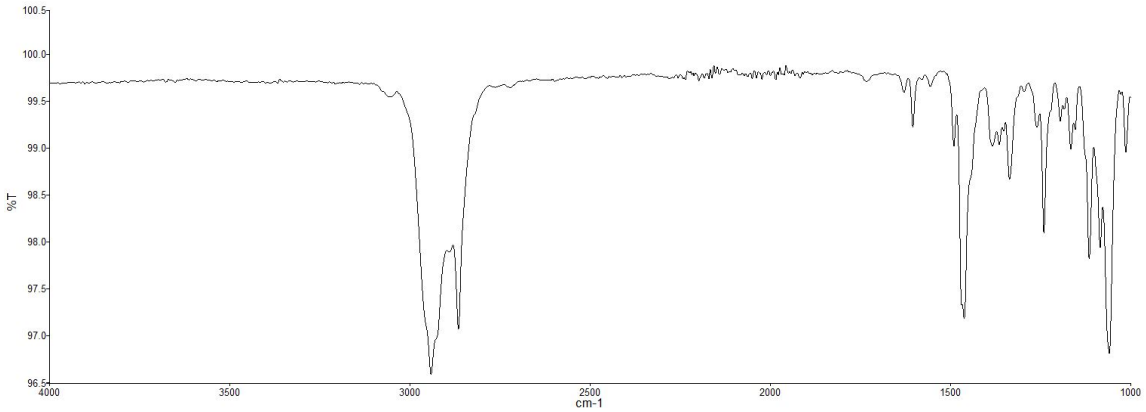

Figure 2.31 Infrared spectrum of compound **2.19**.

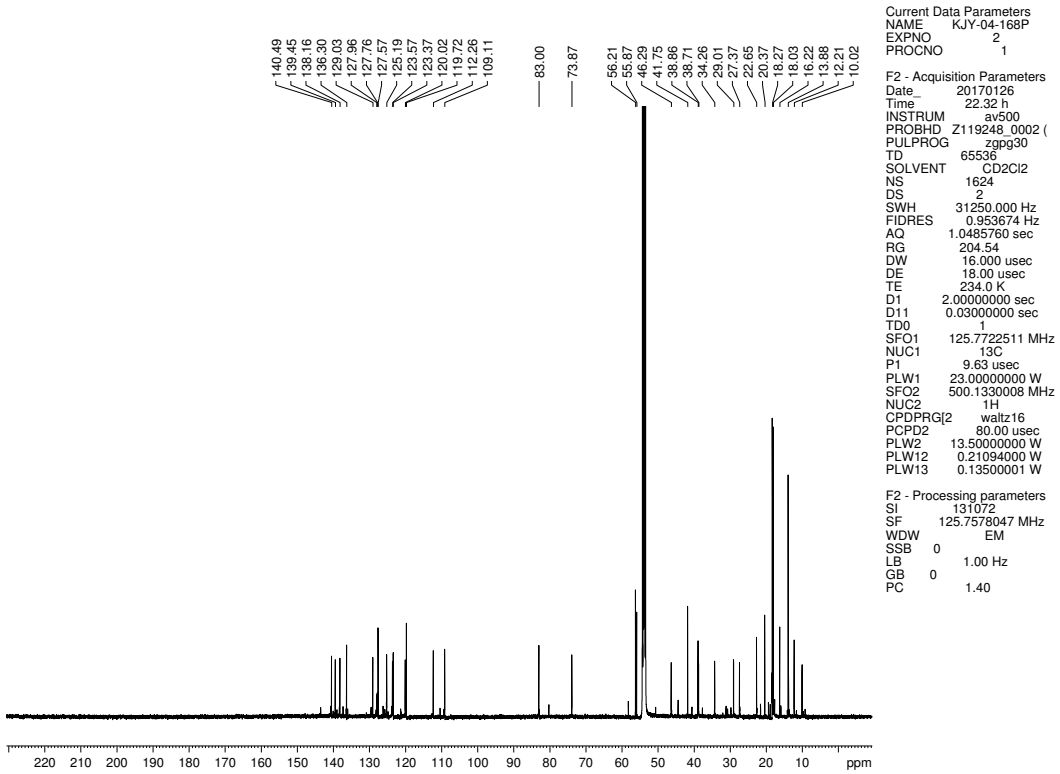

Figure 2.32 ^{13}C NMR (125 MHz, CD_2Cl_2) of compound **2.19**.

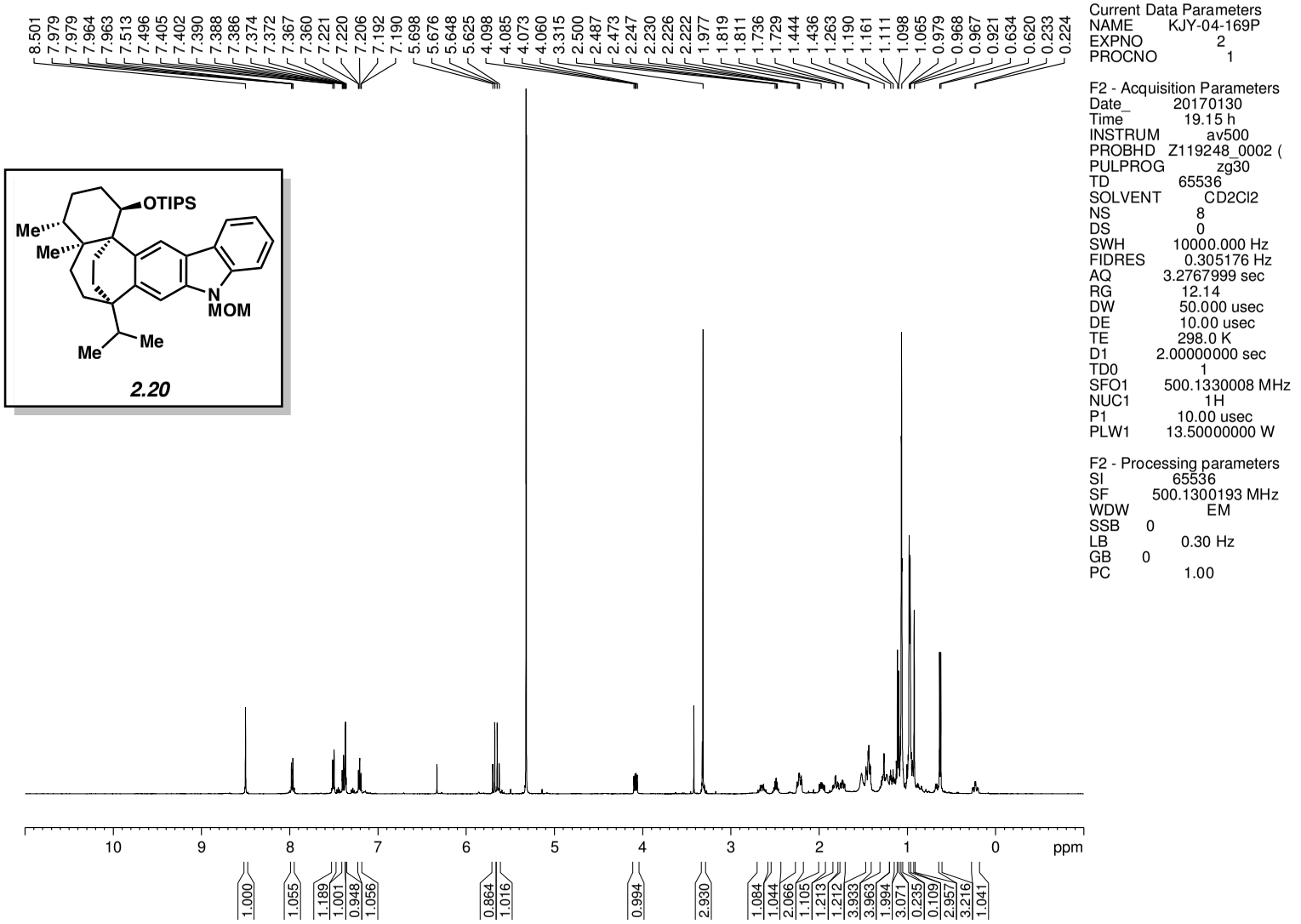

Figure 2.33 ^{1}H NMR (500 MHz, CD_2Cl_2) of compound **2.20**.

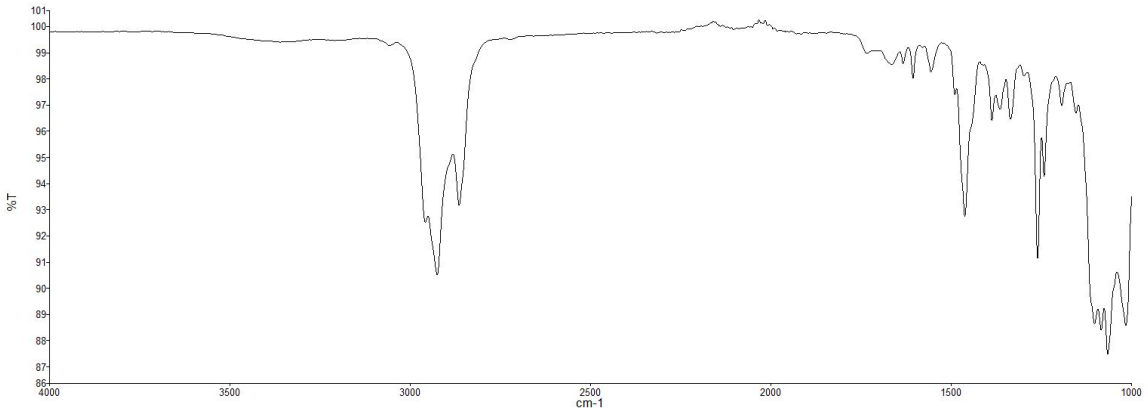

Figure 2.34 Infrared spectrum of compound **2.20**.

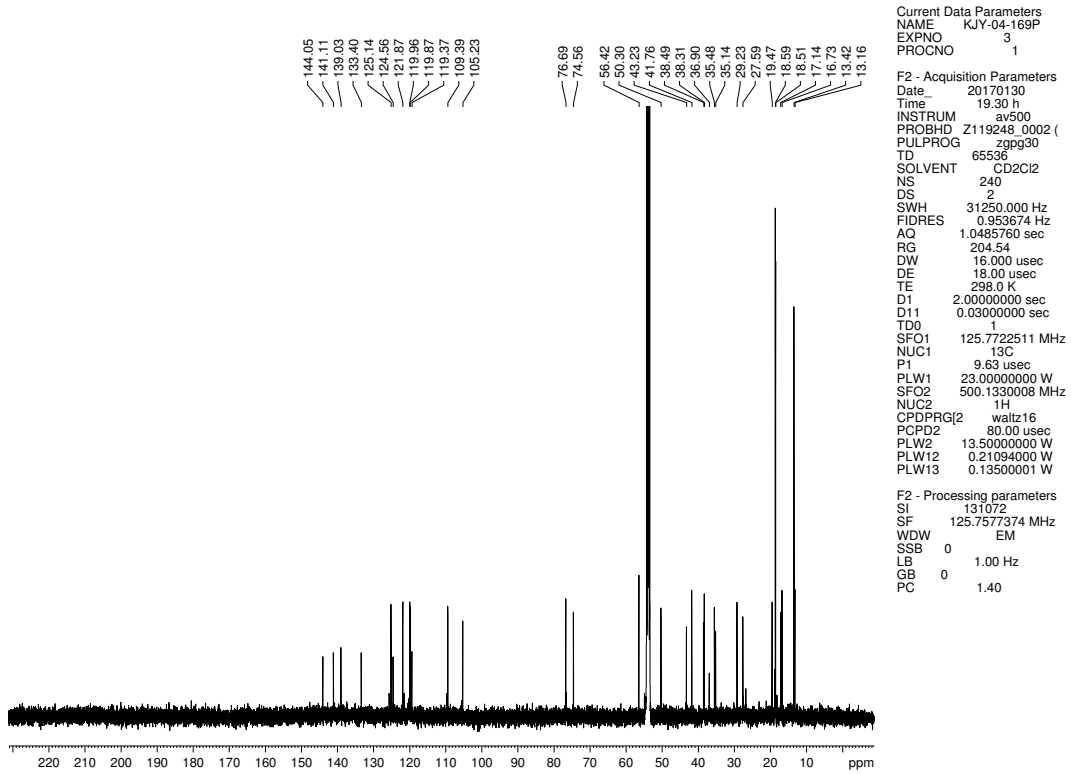

Figure 2.35 ^{13}C NMR (125 MHz, CD_2Cl_2) of compound **2.20**.

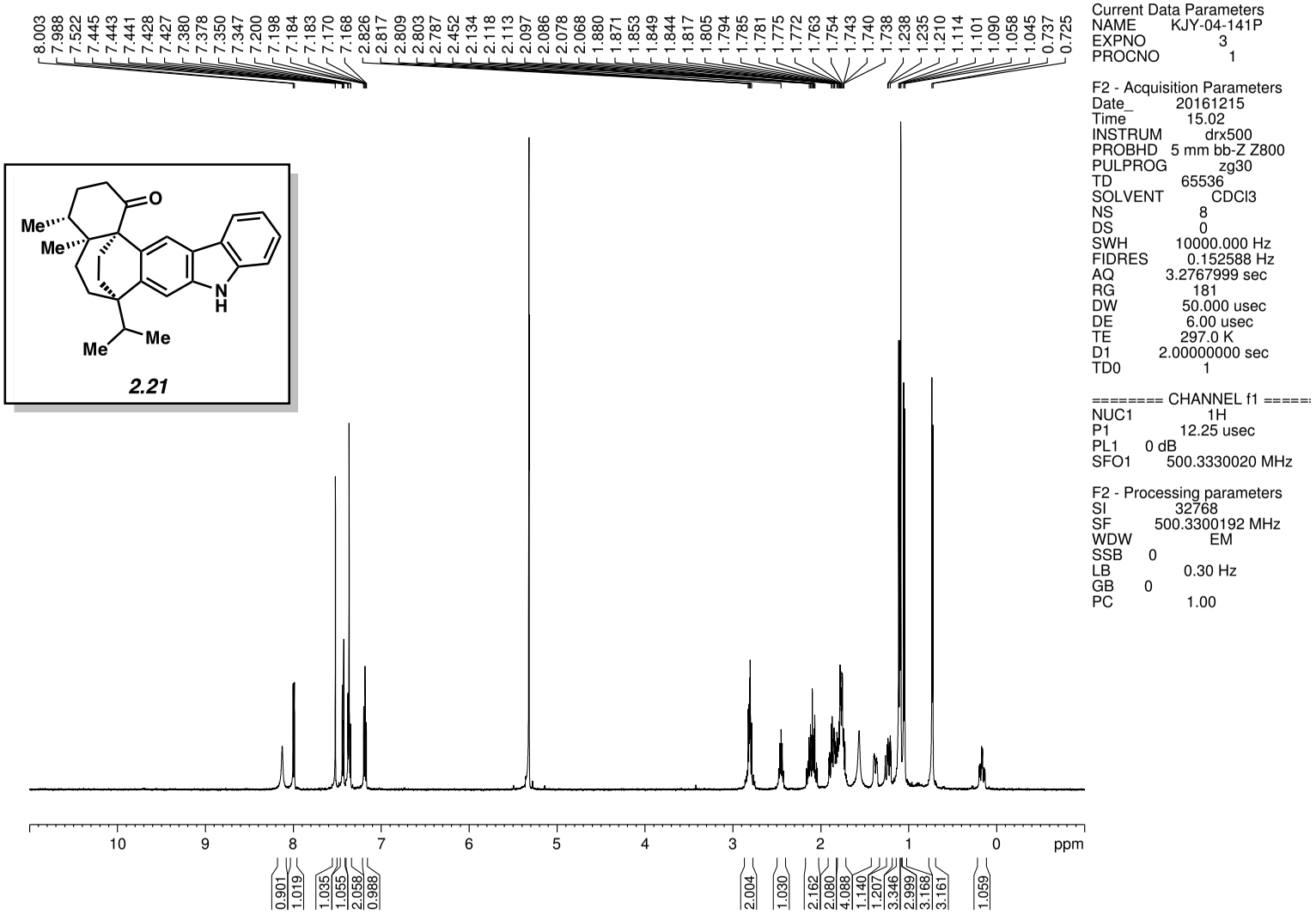

Figure 2.36 ^{1}H NMR (500 MHz, $CDCl_3$) of compound **2.21**.

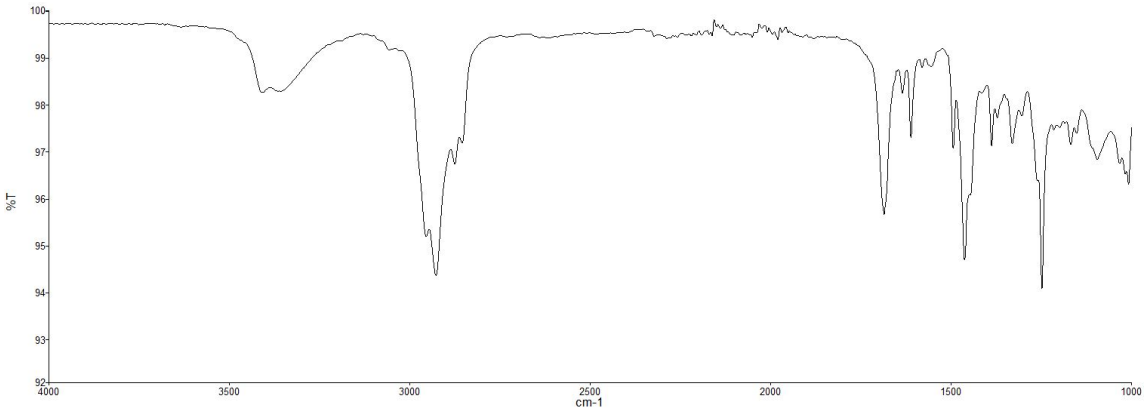

Figure 2.37 Infrared spectrum of compound **2.21**.

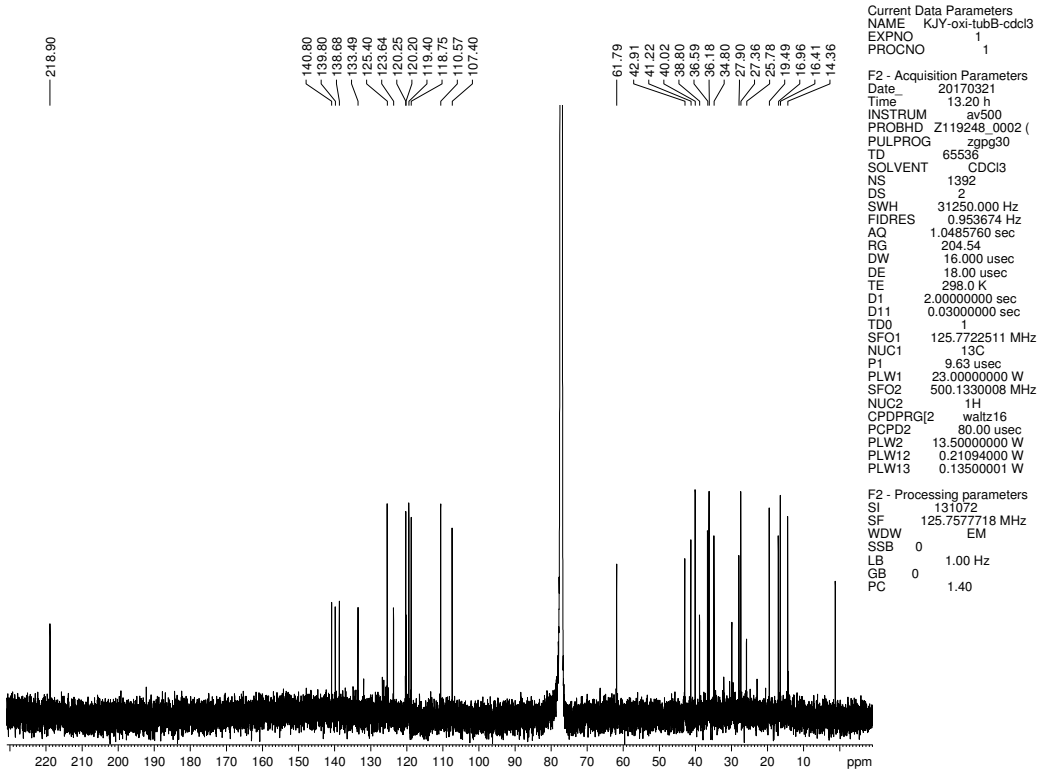

Figure 2.38 ^{13}C NMR (125 MHz, $CDCl_3$) of compound **2.21**.

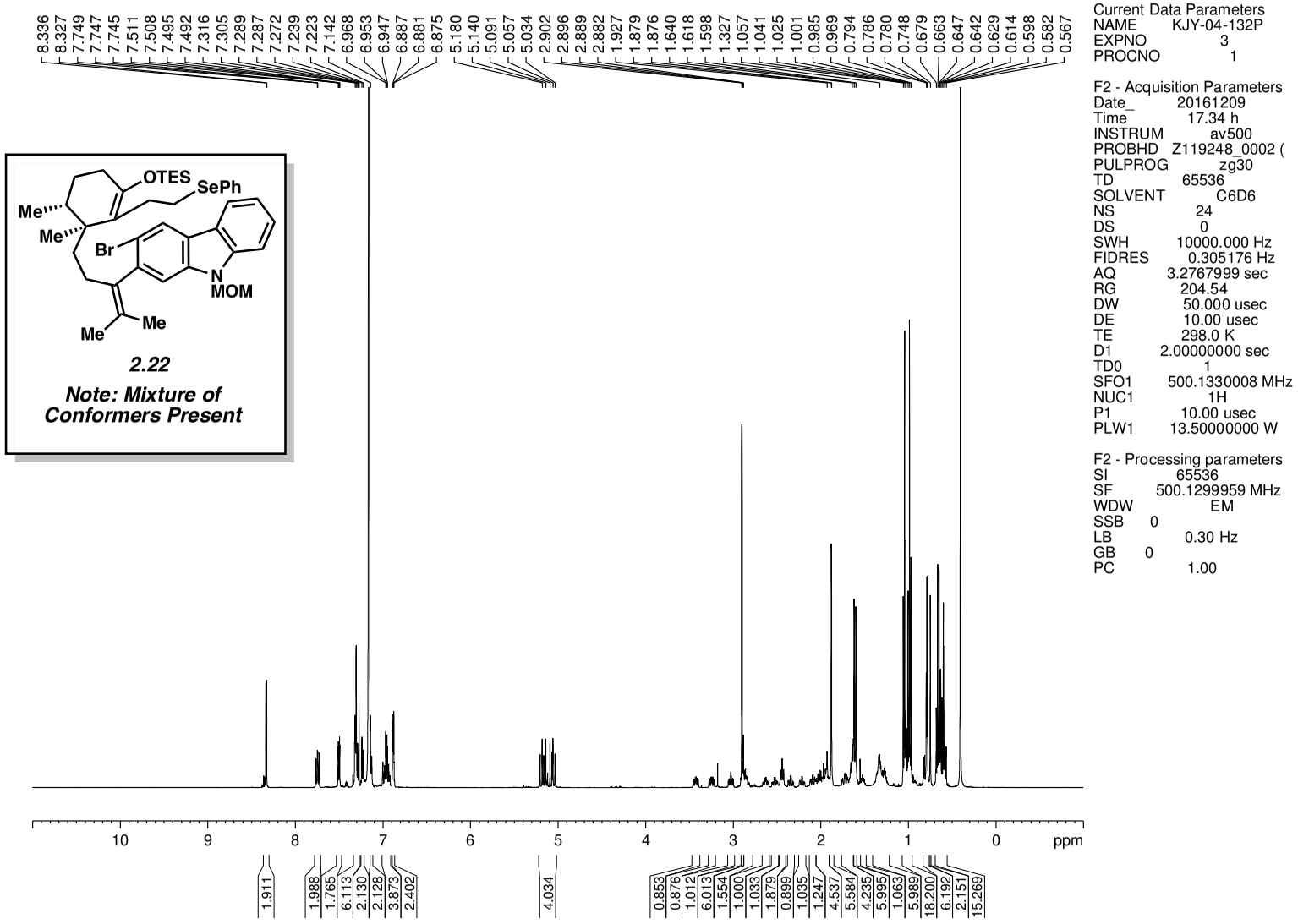

Figure 2.39 ^{1}H NMR (500 MHz, C_6D_6) of compound **2.22**.

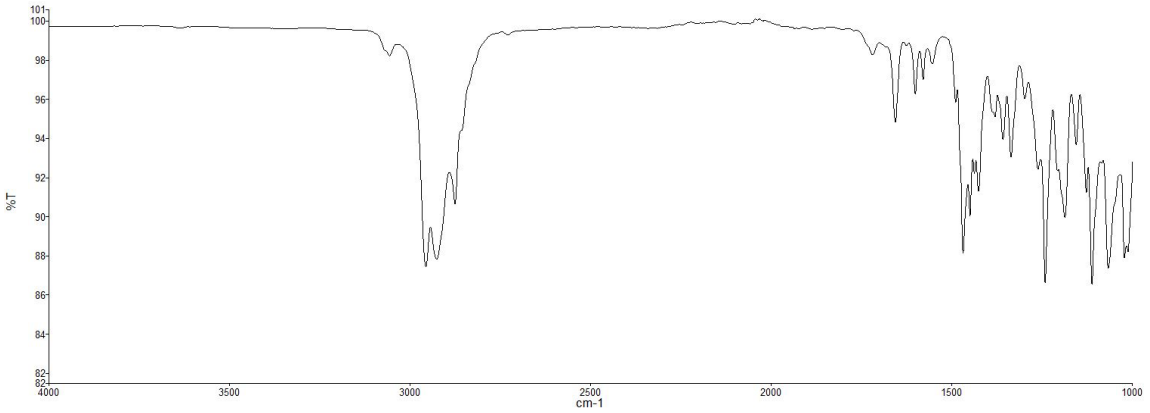

Figure 2.40 Infrared spectrum of compound **2.22**.

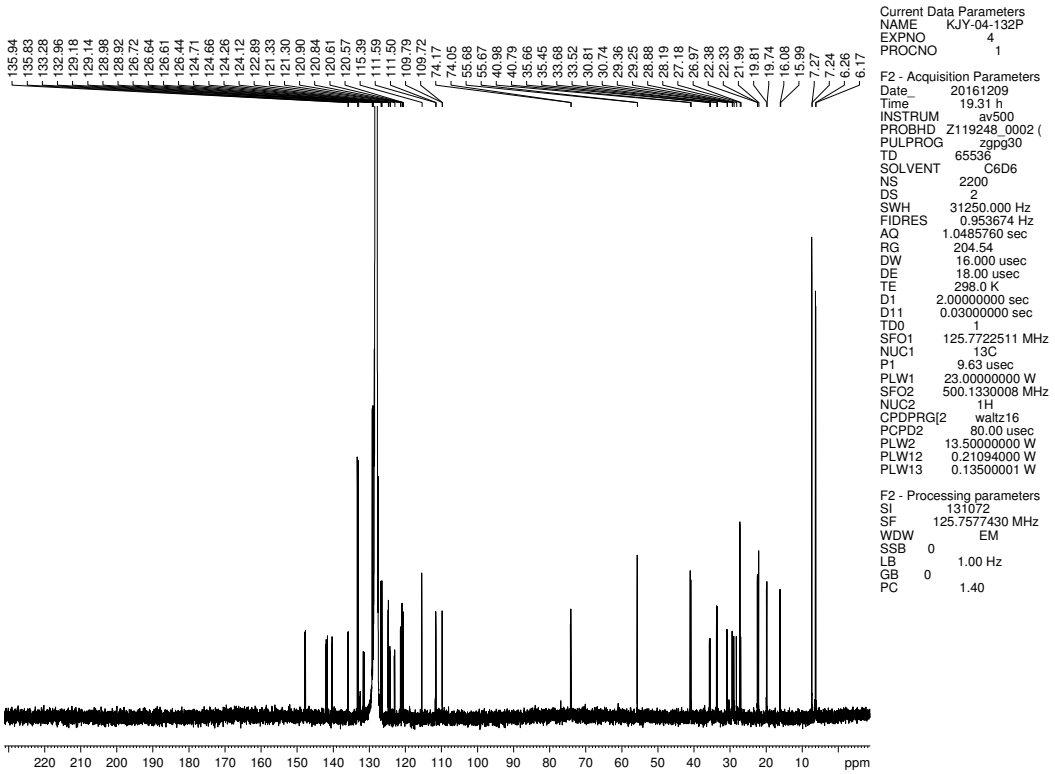

Figure 2.41 ^{13}C NMR (125 MHz, C_6D_6) of compound **2.22**.

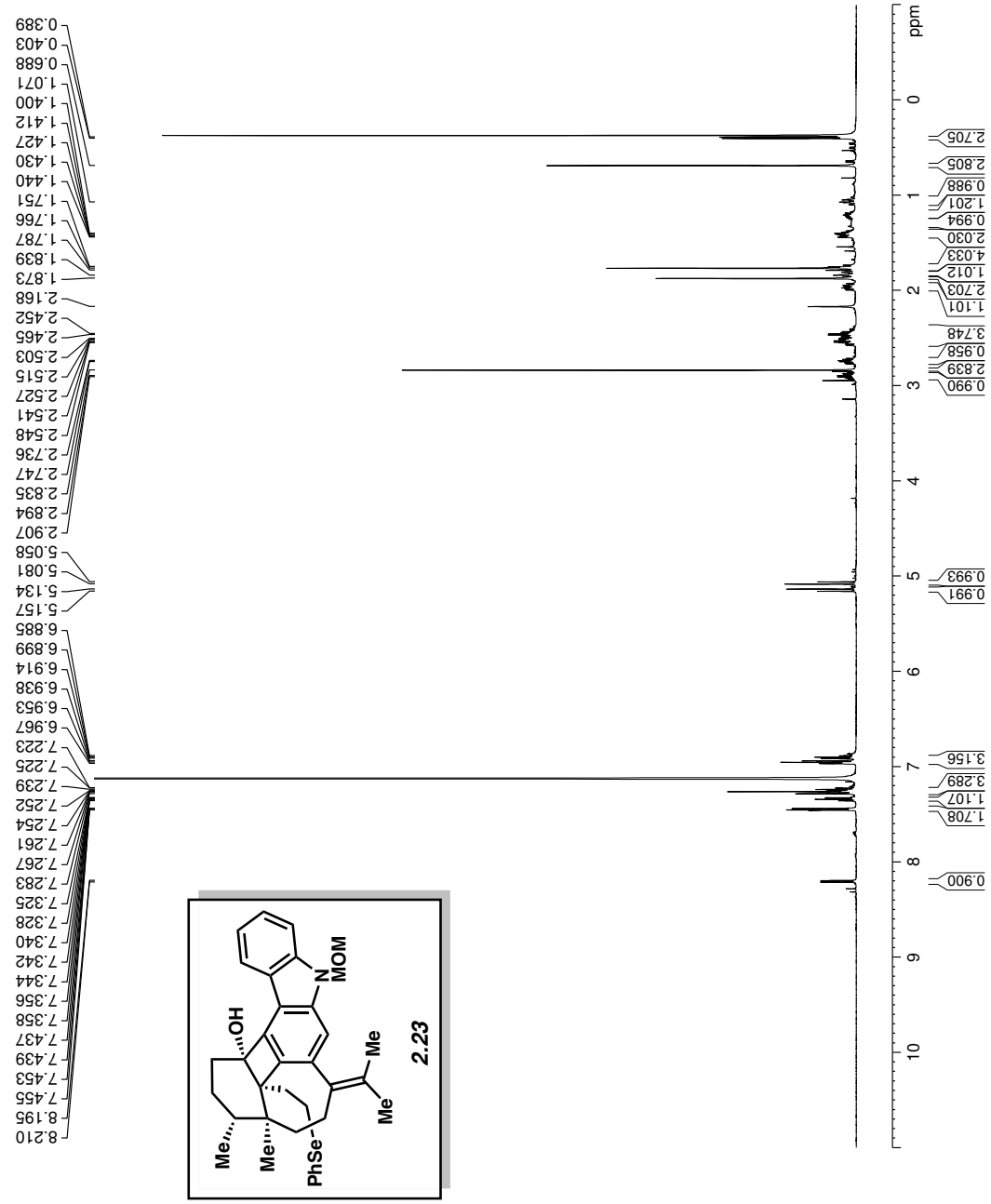

Figure 2.42 ^{1}H NMR (500 MHz, C_6D_6) of compound **2.23**.

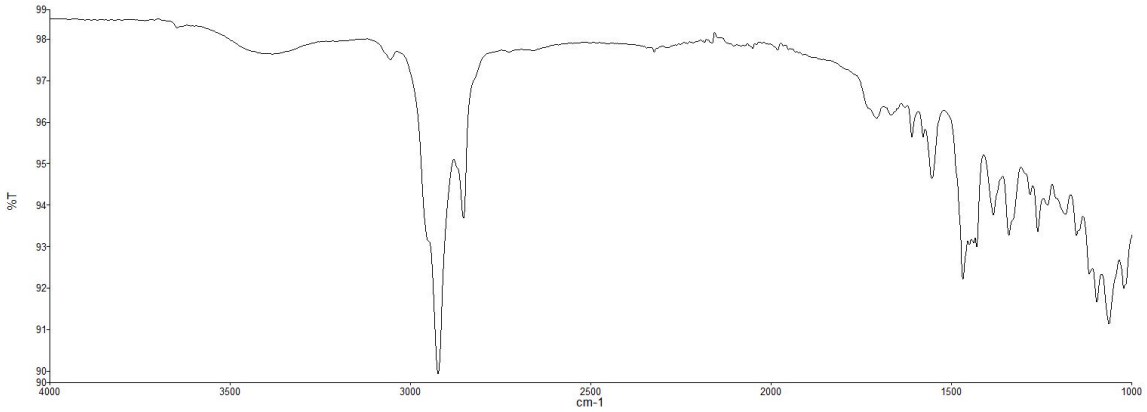

Figure 2.43 Infrared spectrum of compound **2.23**.

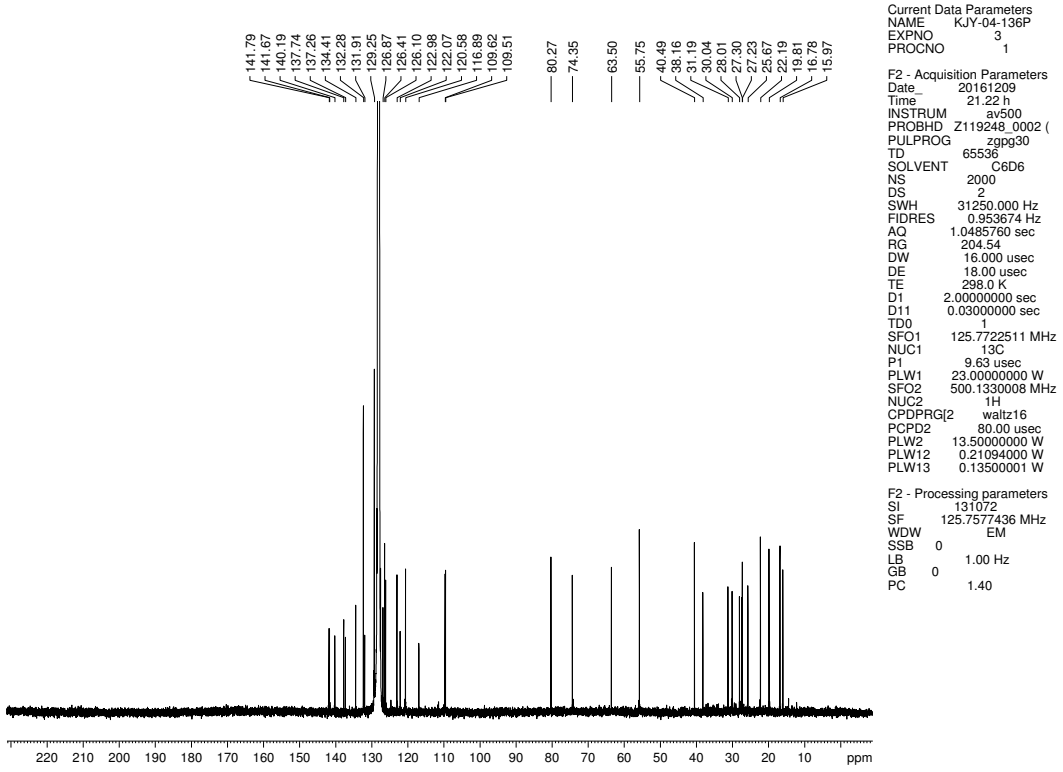

Figure 2.44 ^{13}C NMR (125 MHz, C_6D_6) of compound **2.23**.

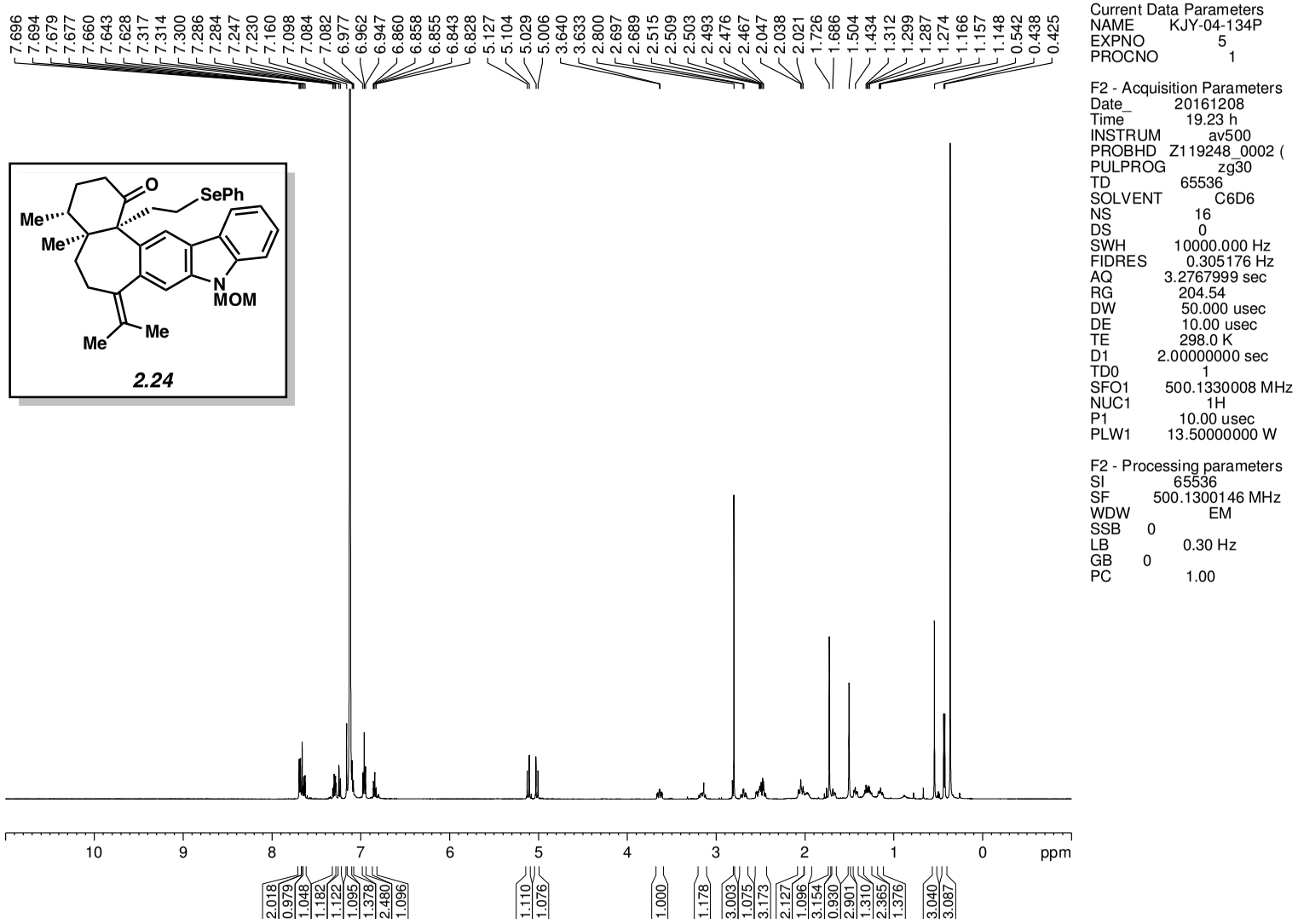

Figure 2.45 ^{1}H NMR (500 MHz, C_6D_6) of compound **2.24**.

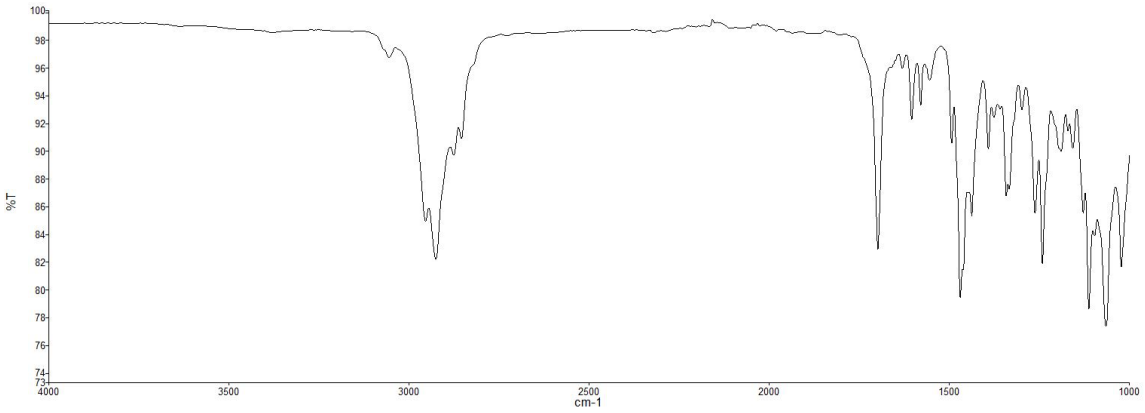

Figure 2.46 Infrared spectrum of compound **2.24**.

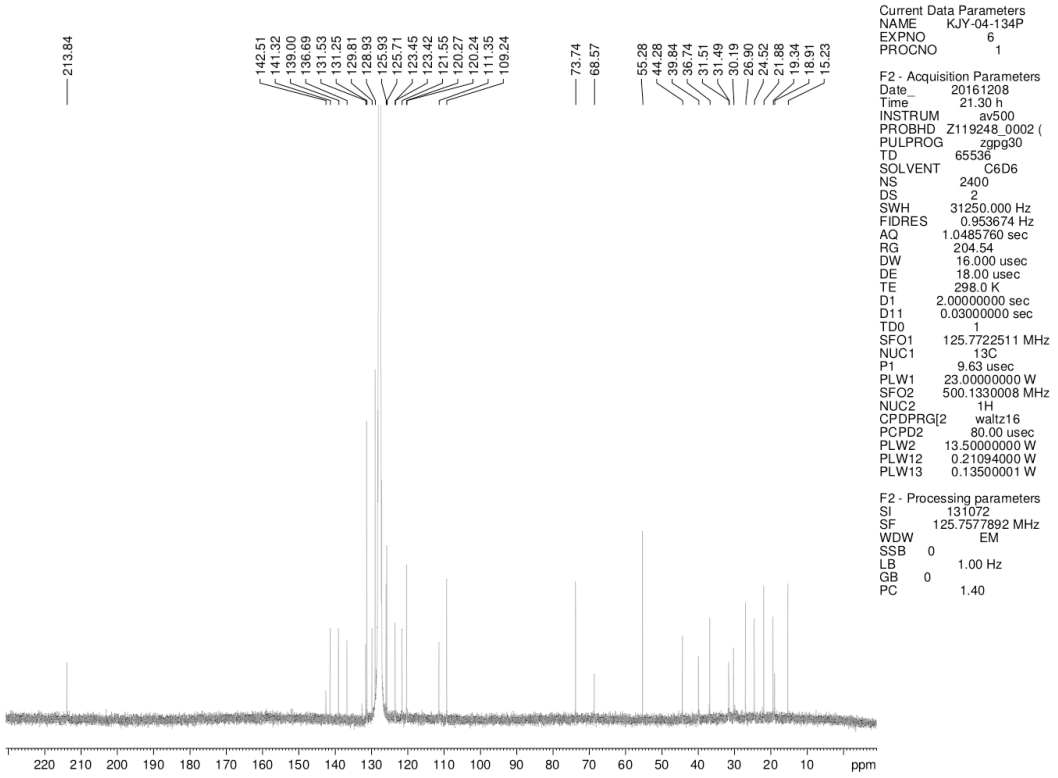

Figure 2.47 ^{13}C NMR (125 MHz, C_6D_6) of compound **2.24**.

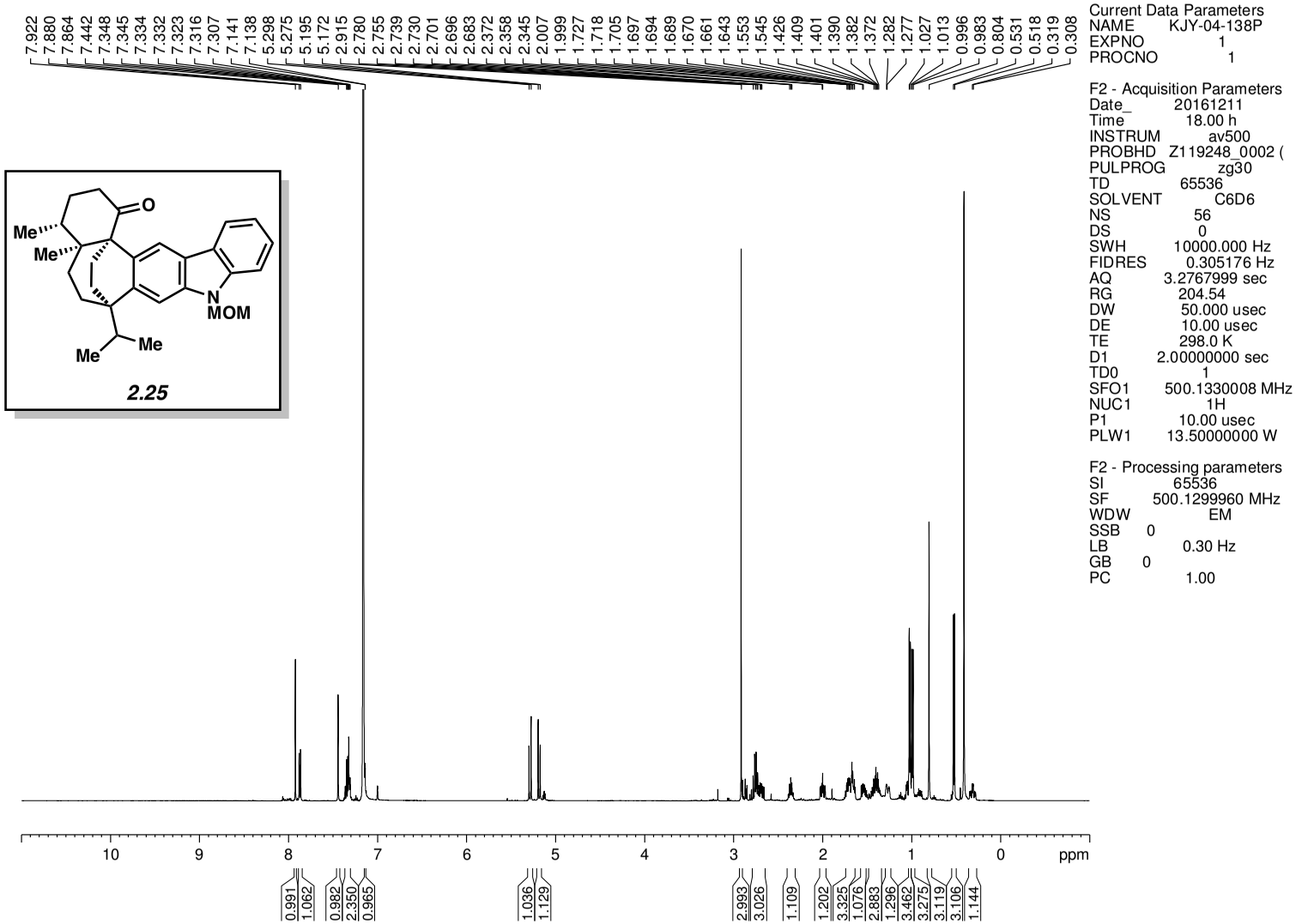

Figure 2.48 ^{1}H NMR (500 MHz, C_6D_6) of compound **2.25**.

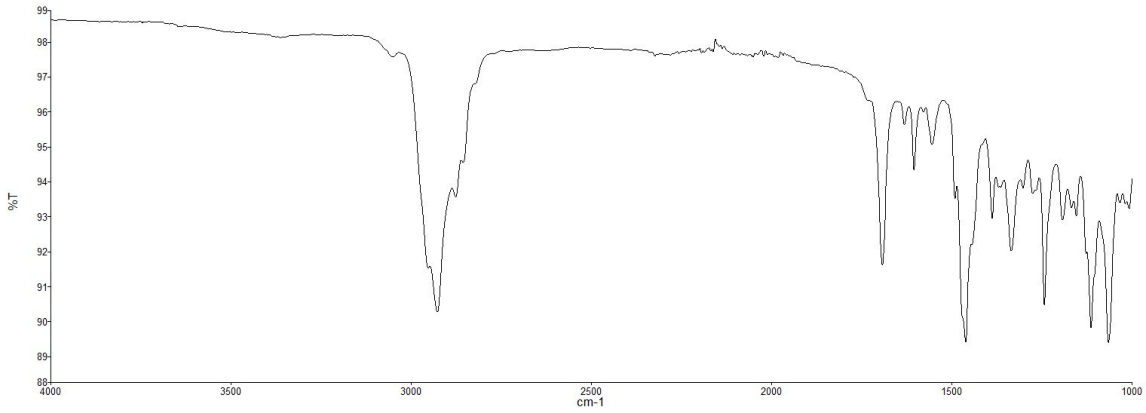

Figure 2.49 Infrared spectrum of compound **2.25**.

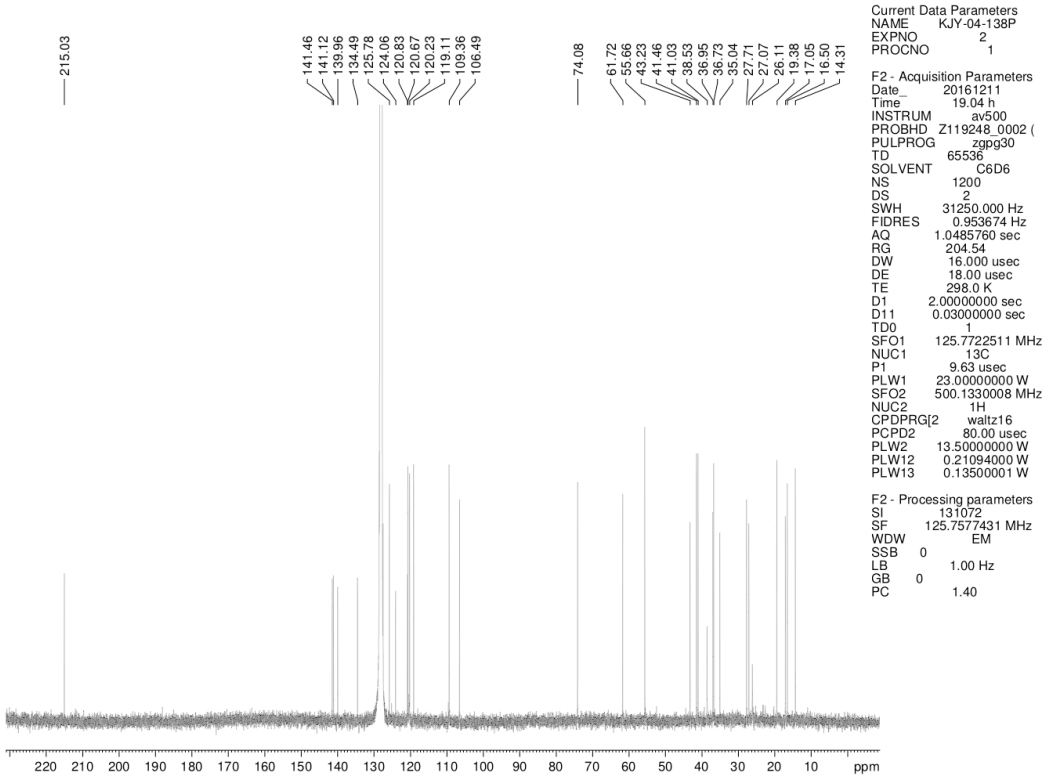

Figure 2.50 ^{13}C NMR (125 MHz, C_6D_6) of compound **2.25**.

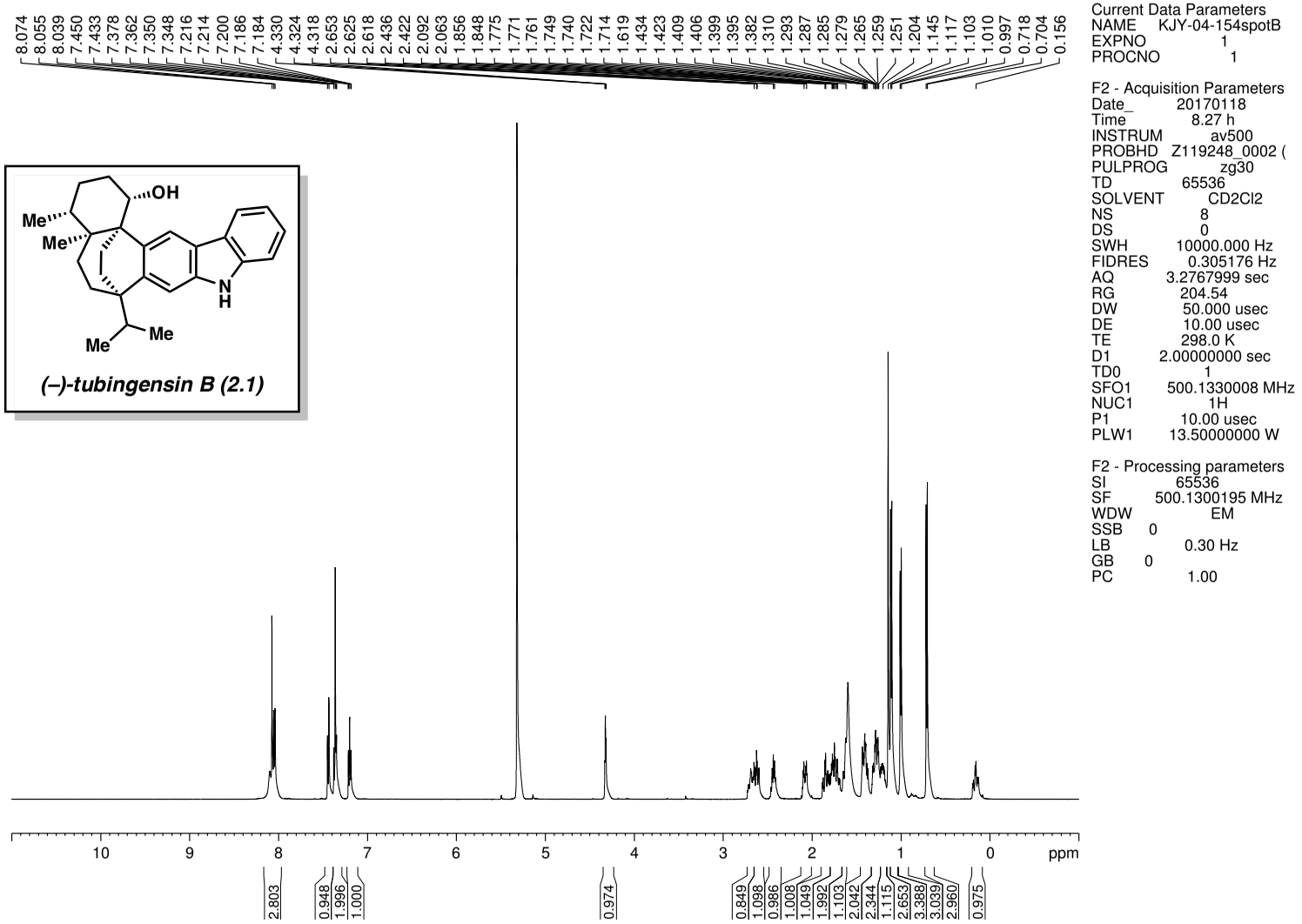

Figure 2.51 ^{1}H NMR (500 MHz, CD_2Cl_2) of compound **2.1**.

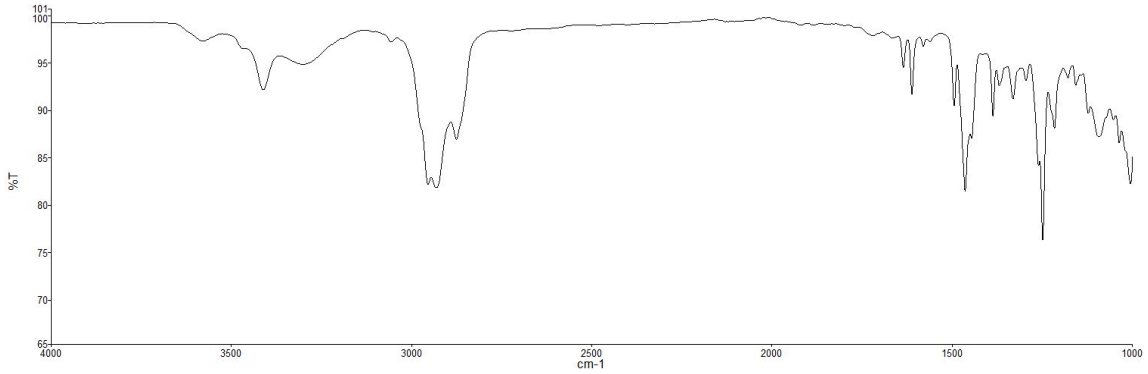

Figure 2.52 Infrared spectrum of compound **2.1**.

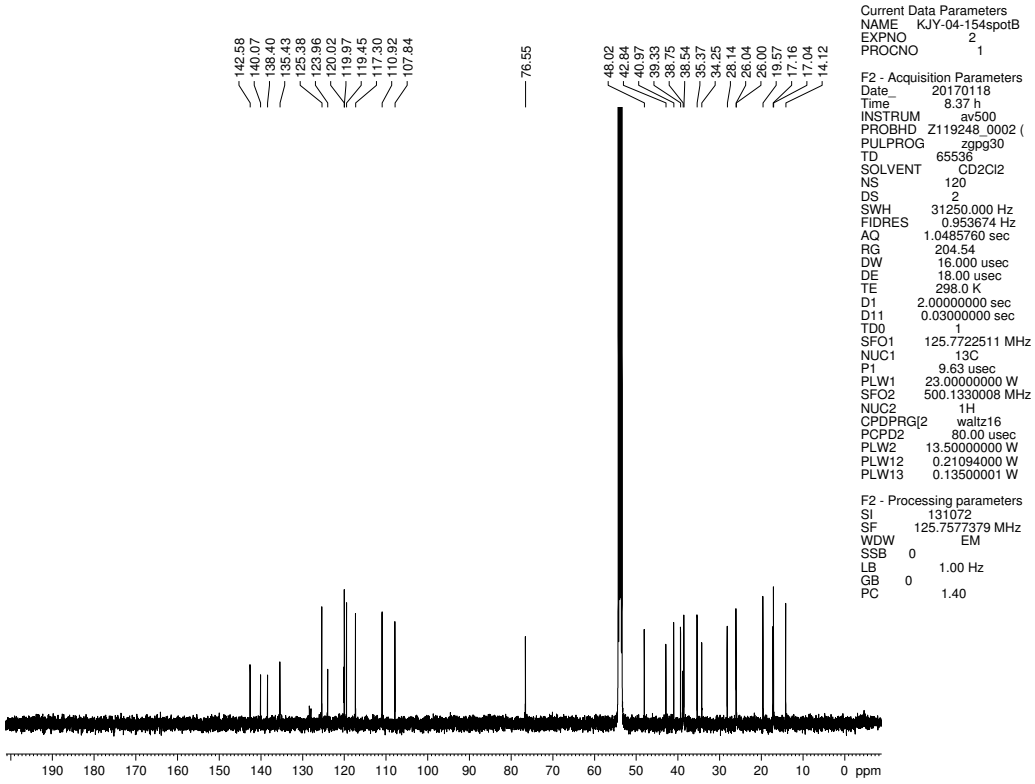

Figure 2.53 ^{13}C NMR (125 MHz, CD_2Cl_2) of compound **2.1**.

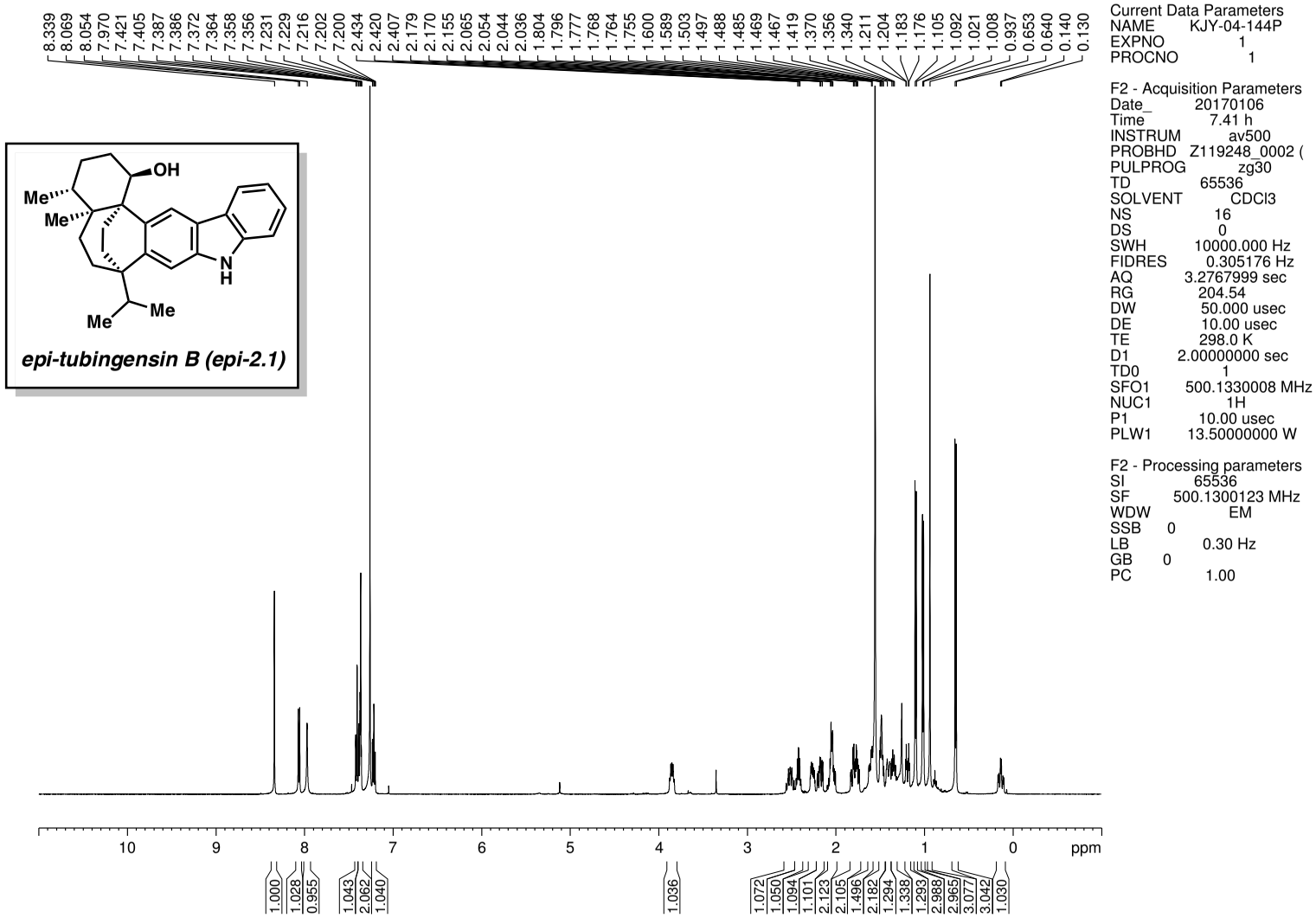

Figure 2.54 ^{1}H NMR (500 MHz, $CDCl_3$) of compound ***epi*-2.1**.

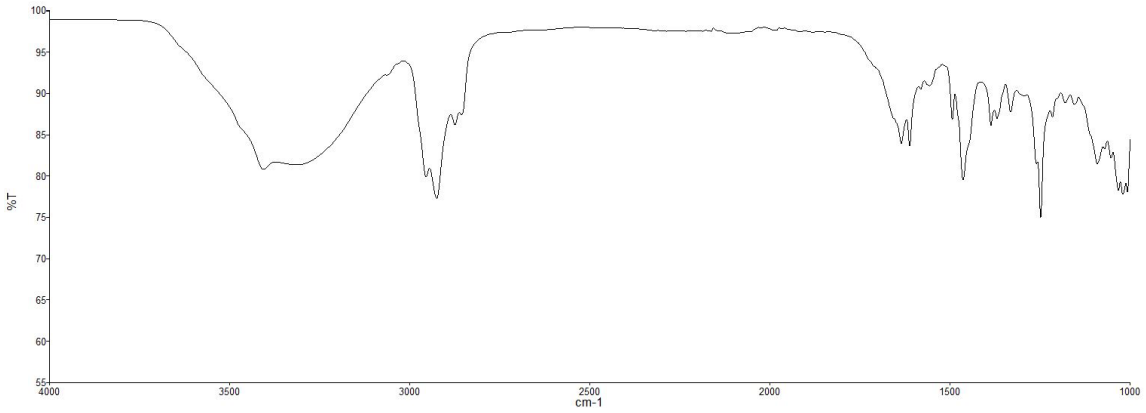

Figure 2.55 Infrared spectrum of compound ***epi*-2.1**.

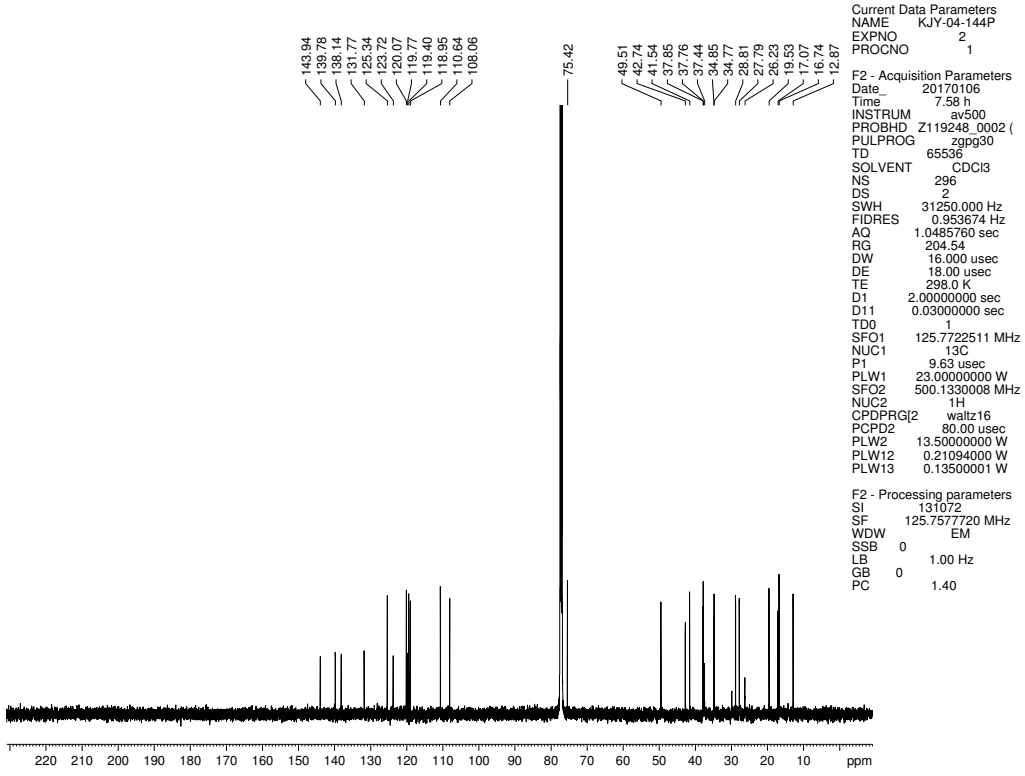

Figure 2.56 ^{13}C NMR (125 MHz, $CDCl_3$) of compound ***epi*-2.1**.

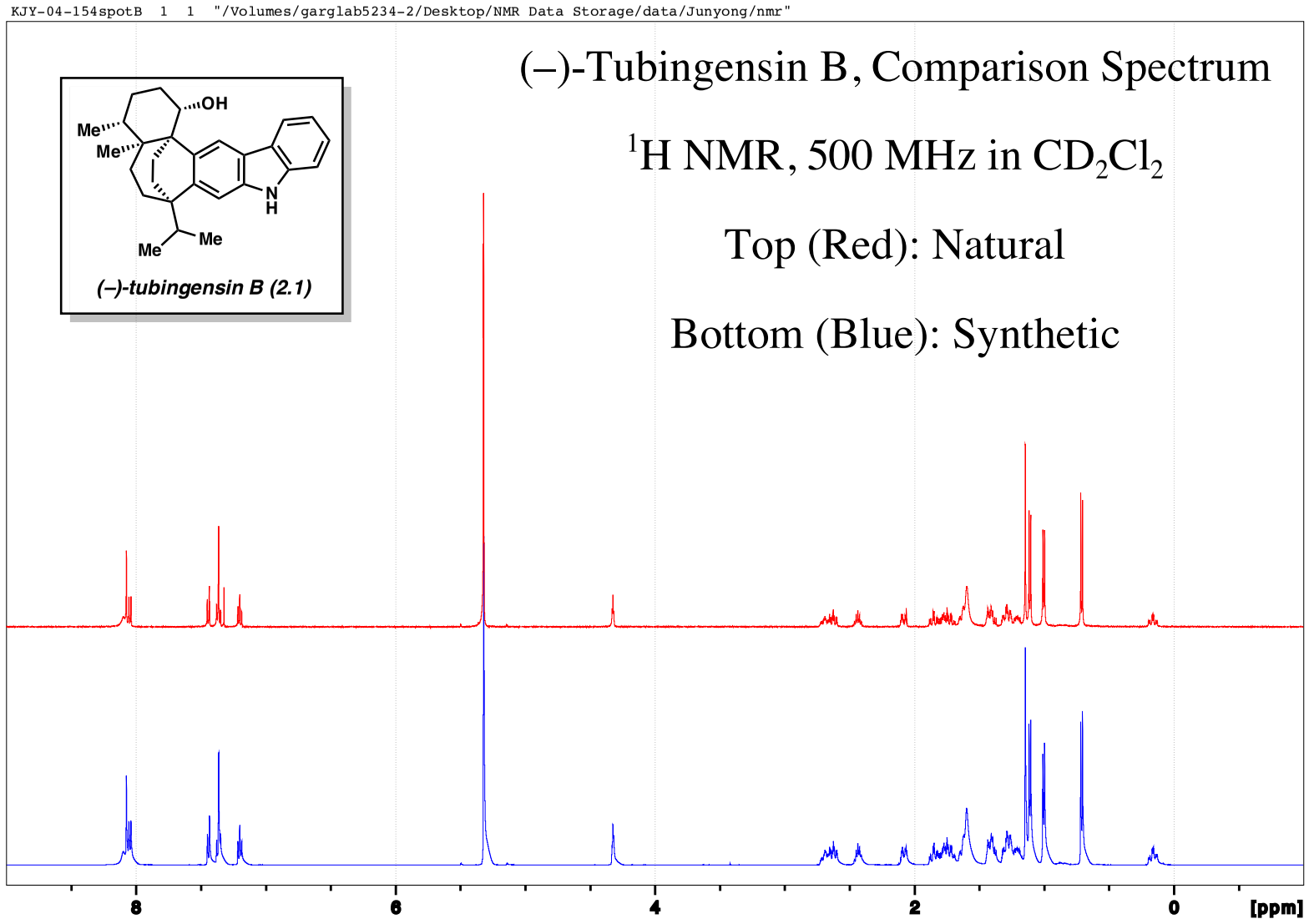

Figure 2.57 Comparison ^{1}H-NMR spectrum of natural and synthetic (–)-tubingensin B (**2.1**)

2.7 Notes and References

(1) TePaske, M. R.; Gloer, J. B.; Wicklow, D. T.; Dowd, P. F. *Tetrahedron Lett.* **1989**, *30*, 5965–5968.

(2) Bian, M.; Wang, Z.; Xiong, X.; Sun, Y.; Matera, C.; Nicolaou, K. C.; Li, A. *J. Am. Chem. Soc.* **2012**, *134*, 8078–8081.

(3) Goetz, A. E.; Silberstein, A. L.; Corsello, M. A.; Garg, N. K. *J. Am. Chem. Soc.* **2014**, *136*, 3036–3039.

(4) Goetz, A. E.; Shah, T. K.; Garg, N. K. *Chem. Commun.* **2015**, *51*, 34–45.

(5) Tadross, P. M.; Stoltz, B. M. *Chem. Rev.* **2012**, *112*, 3550–3577.

(6) Boente, J. M.; Castedo, L.; Rodriguez de Lera, A.; Saá, J. M.; Suau, R.; Vidal, M. C. *Tetrahedron Lett.* **1983**, *24*, 2295–2298.

(7) Huters, A. D.; Quasdorf, K. W.; Styduhar, E. D.; Garg, N. K. *J. Am. Chem. Soc.* **2011**, *133*, 15797–15799.

(8) Skorobogatyi, M. V.; Ustinov, A. V.; Stepanova, I. A.; Pchelintseva, A. A.; Petrunina, A. L.; Andronova, V. L.; Galegov, G. A.; Malakhov, A. D.; Korshun, V. A. *Org. Biomol. Chem.* **2006**, *4*, 1091–1096.

(9) Tummatorn, J.; Dudley, G. B. *Org. Lett.* **2011**, *13*, 1572–1575.

(10) Gulías, M.; Durán, J.; López, F.; Castedo, L.; Mascareñas, J. L. *J. Am. Chem. Soc.* **2007**, *129*, 11026–11027.

(11) Freeman, F.; Robarge, K. D. *J. Org. Chem*. **1989**, *54*, 346–359.

(12) White, J. D.; Grether, U. M.; Lee, C.-S. *Org. Synth.* **2005**, *82*, 108–114.

(13) Kojima, A.; Honzawa, S.; Boden, C. D. J.; Shibasaki, M. *Tetrahedron Lett*. **1997**, *38*, 3455–3458.

(14) Dudley, G. B.; Tan, D. S.; Kim, G.; Tanski, J. M.; Danishefsky, S. J. *Tetrahedron Lett*. **2001**, *42*, 6789–6791.

(15) Schwartz, B. D.; Denton, J. R.; Lian, Y.; Davies, H. W. L.; Williams, C. M. *J. Am. Chem. Soc*. **2009**, *131*, 8329–8332.

(16) Caubere, P. *Acc. Chem. Res*. **1974**, *7*, 301–308.

(17) Gregoire, B.; Carre, M.-C.; Caubere, P. *J. Org. Chem*. **1986**, *51*, 1419–1427.

(18) Legault, C. Y. CYLview, 1.0b; Université de Sherbrooke: Quebec, Montreal, Canada, 2009; http://www.cylview.org.

(19) Lipomi, D. J.; Langille, M. F.; Panek, J. S. *Org. Lett*. **2004**, *6*, 3533–3536.

(20) Szpilman, A. M.; Cereghetti, D. M.; Wurtz, N. R.; Manthorpe, J. M.; Carreira, E. M. *Angew. Chem., Int. Ed*. **2008**, *47*, 4335–4338.

(21) Uyehara, T.; Murayama, T.; Sakai, K.; Ueno, M.; Sato, T. *Tetrahedron Lett*. **1996**, *37*, 7295–7298.

(22) Uyehara, T.; Murayama, T.; Sakai, K.; Onda, K.; Ueno, M.; Sato, T. *Bull. Chem. Soc. Jpn.* **1998**, *71*, 231–242.

(23) Tang, W.; Zhang, X. *Chem. Rev*. **2003**, *103*, 3029–3069.

(24) Tranchier, J.-P.; Ratovelomanana-Vidal, V.; Genêt, J.-P.; Tong, S.; Cohen, T. *Tetrahedron Lett*. **1997**, *38*, 2951–2954.

(25) Reich, H. J.; Chow, F.; Shah, S. K. *J. Am. Chem. Soc*. **1979**, *101*, 6638–6648.

(26) Ishida, N.; Sawano, S.; Masuda, Y.; Murakami, M. *J. Am. Chem. Soc.* **2012**, *134*, 17502–17504.

(27) Clive, D. L. J.; Cole, D. C.; Tao, Y. *J. Org. Chem.* **1994**, *59*, 1396–1406.

(28) Niu, C.; Pettersson, T.; Miller, M. J. *J. Org. Chem.* **1996**, *61*, 1014–1022.

(29) Danheiser, R. L.; Romines, K. R.; Koyama, H.; Gee, S. K.; Johnson, C. R.; Medich, J. R. *Org. Synth*. **1993**, *71*, 133–139.

(30) Ajiki, K.; Hirano, M.; Tanaka, K. *Org. Lett*. **2005**, *7*, 4193–4195.

CHAPTER THREE

Nickel-Catalyzed Amination of Aryl Chlorides and Sulfamates in 2-Me-THF

Noah F. Fine Nathel, Junyong Kim, Liana Hie, Xingyu Jiang, and Neil K. Garg

ACS Catal. **2014**, *4*, 3289–3293.

3.1 Abstract

The nickel-catalyzed amination of aryl *O*-sulfamates and chlorides using the green solvent 2-methyl-THF is reported. This methodology employs the commercially available and air-stable pre-catalyst $NiCl_2$(DME), is broad in scope, and provides access to aryl amines in synthetically useful yields. The utility of this methodology is underscored by examples of gram-scale couplings conducted with catalyst loadings as low as 1 mol % nickel. Moreover, the nickel-catalyzed amination described is tolerant of heterocycles and should prove useful in the synthesis of pharmaceutical candidates and other heteroatom-containing compounds.

3.2 Introduction

Transition metal-catalyzed cross-couplings have had a profound impact on chemical synthesis.[1] As mild and useful alternatives to classical fragment couplings, cross-couplings have become one of the most frequently employed transformations for the construction of carbon–carbon (C–C) and carbon–heteroatom (C–X) bonds in both academic and industrial settings.[1] Although palladium-catalyzed couplings dominate the field, there has been growing interest in the development of related couplings that employ non-precious metals.[2] Nickel, in particular, is very attractive in part due to its wide availability and low cost.[2d–h] Additionally, certain nickel

catalysts have the unique ability to activate a wide range of electrophilic coupling partners, well beyond the scope of traditional cross-couplings that use palladium catalysis.[2d–h] Moreover, in addition to cost and reactivity benefits, nickel catalysis has shown great promise for operating under green reaction conditions,[3] particularly in green solvents.[4]

Our research group and others have developed new protocols for aryl C–C and C–N bond formation[5] using nickel catalysis.[2d–h,4,6,7,8] These procedures not only enable the desired bond formations, but also utilize air and moisture stable Ni(II) precatalysts that do not require glove box handling. To render these transformations more practical, we have recently focused our efforts on developing greener variants. This has led to a general nickel-catalyzed Suzuki–Miyaura coupling procedure that takes place in a variety of green solvents, is scalable at low catalyst loadings, and possesses an unusually broad substrate scope.[4] Herein, we report a complementary procedure for the efficient formation of aryl C–N bonds that proceeds in a green solvent using nickel catalysis (Figure 3.1).

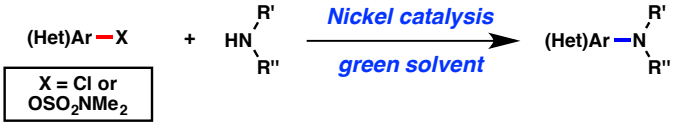

Figure 3.1. Amination of (hetero)aryl chlorides and sulfamates in a green solvent using nickel catalysis.

3.3 Optimization and Substrate Scope

Having previously established the nickel-catalyzed amination of aryl sulfamates,[7g,j] albeit not in a green solvent, we sought to first develop the corresponding coupling of aryl chlorides. We chose naphthyl chloride **3.1** for our studies and tested its coupling with morpholine (**3.2**)

using nickel catalysis (Table 3.1). Indeed, upon exposure of **3.1** and **3.2** to our previously disclosed sulfamate amination conditions,[7g,7j,9,10] product **3.4** was obtained when toluene was used as the solvent (entry 1). Other solvents that are considered environmentally attractive were also tested.[11,12] The use of DMF, which ranks favorably with regard to safety and some environmental considerations,[11] gave **3.4** in 50% yield (entry 2). We also examined alcohol solvents. Although the desired coupling did not take place when *n*-butanol was employed (entry 3), we found that the use of *t*-amyl alcohol gave the aminated product in good yield (entry 4). Ethereal solvents were also tested. Fortunately, the use of THF, MTBE, CPME,[13] or 2-Me-THF (entries 5–8, respectively) uniformly furnished **3.4** in excellent yield.

Table 3.1. Examination of Solvents in the Amination of 1-Chloronaphthalene.[a]

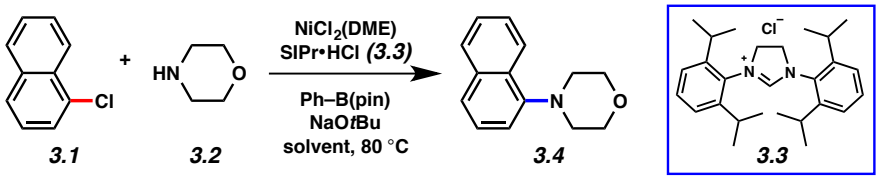

3.1 *3.2* *3.4* *3.3*

Entry	Solvent	Yield[b]	Entry	Solvent	Yield[b]
1	toluene	95%	5	THF	88%
2	DMF	50%	6	MTBE	96%
3	*n*-BuOH	0%	7	CPME	100%
4	*t*-amyl alcohol	78%	8	2-Me-THF	95%

[a] Reactions were carried out with $NiCl_2$(DME) (5 mol %), SIPr•HCl (***3.3***, 10 mol %), Ph-B(pin) (0.55 equiv), substrate (***3.1***, 0.5 mmol, 1.00 equiv), morpholine (***3.2***, 1.80 equiv), NaOtBu (1.85 equiv), hexamethylbenzene (0.10 equiv), and solvent (used as received, 2.5 mL), for 3 h. [b] Yields were determine using hexamethylbenzene as an internal standard.

Of the solvents surveyed, we elected to focus on the use of 2-Me-THF for our subsequent studies.[14] 2-Me-THF has gained attention as a promising solvent for industrial applications[15] due to several salient features, including that: a) it is not easily oxidized; b) it readily phase-separates from aqueous layers (in contrast to THF); c) it is obtained from furfural, which, in turn comes

from renewable feedstock; d) it has a higher boiling point compared to THF, which can be advantageous in some instances; and e) it poses minimal health risks.

After establishing suitable reaction conditions for the amination of **3.1** with morpholine (**3.2**) we probed the use of other 1-naphthyl-based electrophilic coupling partners **3.5** in this methodology (Table 3.2). We were delighted to find that 1-bromonaphthalene could also be employed (entry 2). However, the corresponding iodide and triflate substrates gave only modest yields of **3.4** (entries 3 and 4). The use of a tosylate coupling partner, on the other hand, led to the desired product in 71% yield (entry 5). Finally, whereas the pivalate ester substrate failed (entry 6), we found that the corresponding carbamate and sulfamate substrates could be employed in the methodology (entries 7 and 8). Overall, the chloride and sulfamate substrates gave the best yields of product **3.4**; thus, we elected to evaluate the scope of the methodology for these two types of electrophiles.[16,17]

Table 3.2. Evaluation of Various Electrophiles.[a]

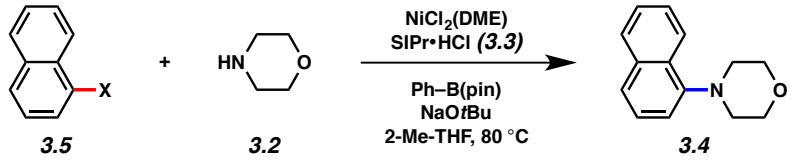

3.5 *3.2* *3.4*

Entry	*X*	*Yield*[b]	*Entry*	*X*	*Yield*[b]
1	Cl	95%	5	OTs	71%
2	Br	62%	6	OPiv	4%
3	I	27%	7	$OC(O)NEt_2$	76%
4	OTf	6%	8	OSO_2NMe_2	87%

[a] Reactions were carried out with $NiCl_2$(DME) (5 mol %), SIPr•HCl (***3.3***, 10 mol %), Ph–B(pin) (0.55 equiv), substrate (***3.5***, 0.5 mmol, 1.00 equiv), morpholine (***3.2***, 1.80 equiv), NaOtBu (1.85 equiv), hexamethylbenzene (0.10 equiv), and solvent (used as received, 2.5 mL), for 3 h. [b] Yields were determine using hexamethylbenzene as an internal standard.

Figure 3.2 highlights the scope of the methodology with regard to the coupling of aryl sulfamate substrates using morpholine (**3.2**) as the amine partner and 2-Me-THF as solvent. Simple aryl hydrocarbon substrates, such as naphthyl and phenyl sulfamates, were readily aminated as demonstrated by the high yielding formation of **3.4** and **3.6**, respectively. Additionally, the generation of products **3.7**–**3.10** in good yields shows the methodology's tolerance of electron-donating, electron-withdrawing, and ortho substituents. Given the prevalence of heterocycles in pharmaceuticals, where amination reactions are widely employed, we also tested several heterocyclic sulfamate substrates. 2- and 3-substituted pyridines were well tolerated, as demonstrated by the formation of products **3.11** and **3.12**, respectively. Moreover, indole-, isoquinoline-, and dihydrobenzofuran-containing substrates were suitable coupling partners, as judged by the formation of **3.13**–**3.15** in synthetically useful yields.

Figure 3.2. Coupling of (hetero)aryl sulfamates with morpholine in 2-Me-THF.[a]

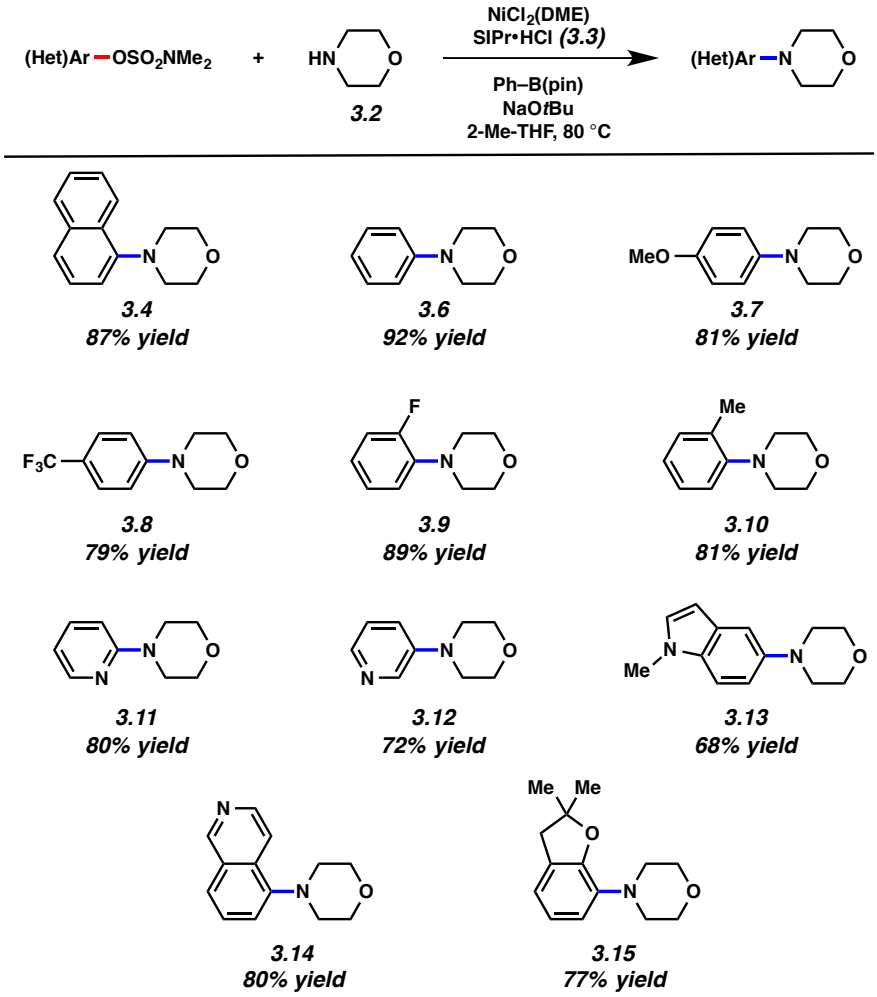

[a] Reactions were carried out with $NiCl_2$(DME) (5–15 mol %), SIPr•HCl (***3.3***, 10–30 mol %), Ph–B(pin) (0.30–0.45 equiv), substrate (0.5 mmol, 1.00 equiv), morpholine (***3.2***, 1.80 equiv), NaO*t*Bu (2.25–2.55 equiv), hexamethylbenzene (0.10 equiv), and solvent (used as received, 2.5 mL), for 3 h. Yields were determine using hexamethylbenzene as an internal standard.

Similarly, an array of aryl chlorides underwent the nickel-catalyzed amination reaction with morpholine (**3.2**) in 2-Me-THF (Figure 3.3). Non-heterocyclic substrates, including those containing electronically or sterically biasing substituents, coupled smoothly, as shown by the formation of adducts **3.4** and **3.7**–**3.10**. Of note, commercially available heterocyclic aryl

chlorides could also be employed, thus giving rise to products **3.11**, **3.12**, **3.16**, and **3.17**. The tolerance of the methodology to pyridines, quinolines, and benzothiophenes suggests the utility of our coupling conditions for applications in drug discovery.

Figure 3.3. Coupling of (hetero)aryl chlorides with morpholine in 2-Me-THF.[a]

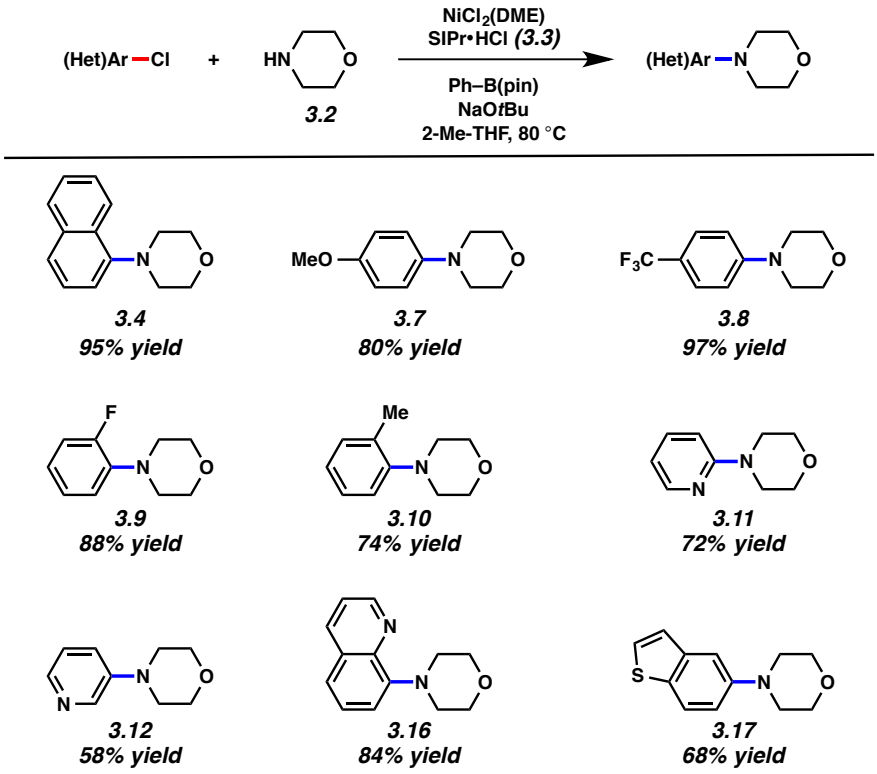

[a] Reactions were carried out with $NiCl_2$(DME) (5–15 mol %), SIPr•HCl (***3.3***, 10–30 mol %), Ph–B(pin) (0.35–0.70 equiv), substrate (0.5 mmol, 1.00 equiv), morpholine (***3.2***, 1.80 equiv), NaOtBu (2.25–2.70 equiv), hexamethylbenzene (0.10 equiv), and solvent (used as received, 2.5 mL), for 3 h. Yields were determine using hexamethylbenzene as an internal standard.

As shown in Figure 3.4, the scope of this amination methodology is not limited to the use of morpholine as the amine coupling partner. For example, pyrrolidine could be employed to give aminated product **3.18**. As demonstrated by the formation of **3.19**, the acyclic amine n-methylbutylamine was also tolerated in this methodology. Additionally, we found that 2,6-

dimethylaniline, despite its steric hindrance, underwent the desired amination to give the unsymmetrical biaryl amine product **3.20**. We were also delighted to find that a piperazine nucleophile bearing a pyridine ring coupled smoothly to give product **3.21** in 94% yield.

Figure 3.4. Scope of amine component in the coupling reaction.[a]

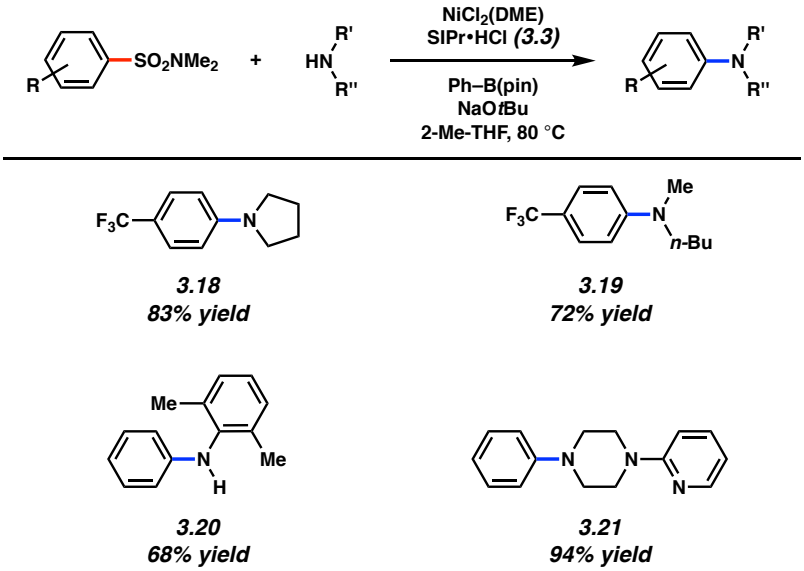

[a] Reactions were carried out with $NiCl_2$(DME) (5–15 mol %), SIPr•HCl (***3.3***, 10–30 mol %), Ph–B(pin) (0.35–0.75 equiv), substrate (0.5 mmol, 1.00 equiv), amine (1.20–2.40 equiv), NaOtBu (2.10–3.45 equiv), hexamethylbenzene (0.10 equiv), and solvent (used as received, 2.5 mL), for 3 h. Yields were determined using hexamethylbenzene as an internal standard.

3.4 Gram-Scale Couplings

One general limitation pertaining to nickel-catalyzed cross-couplings is the frequent use of high catalyst loadings (i.e., often >10%).[2d–h] Whereas progress has been made in rendering nickel-catalyzed Suzuki–Miyaura couplings more efficient,[4,6i] corresponding achievements in nickel-mediated amination reactions have been lacking. To address this challenge, we tested the coupling of trifluoromethyl-containing sulfamate and chloride substrates **3.22** and **3.23**, respectively, in the amination reaction with **3.2** using 2-Me-THF as solvent (Figure 3.5). Using 3 and 1 mol% Ni, respectively, we found that gram-scale couplings could be achieved to give the arylated morpholine product **3.8** in excellent yields.

Figure 3.5. Gram-scale couplings of trifluoromethyl-containing substrates.

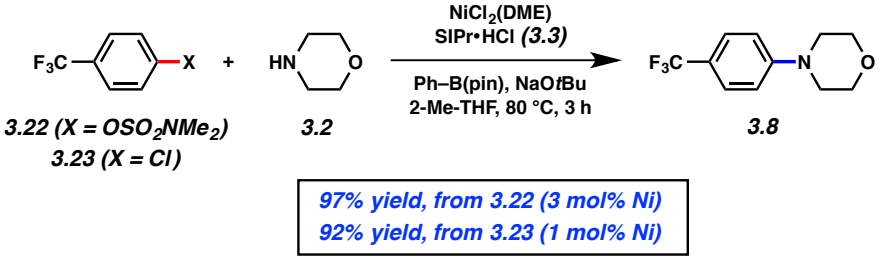

As noted earlier, the amination of heterocyclic substrates in 2-Me-THF provides a promising tool for the synthesis of pharmaceutical candidates. To further probe this notion, we tested the gram-scale couplings of heterocycle-containing substrates, as shown in Figure 3.6. Chloroquinoline **3.24** underwent facile coupling with morpholine (**3.2**) to generate aminated product **3.16** in 94% yield. This coupling was performed on gram-scale using 3 mol % Ni. Finally, we tested the gram-scale coupling of trifluoromethylated aryl chloride **3.23** with pyridyl piperazine derivative **3.25**. This reaction provided adduct **3.26** in 88% yield; of note, **3.26**

contains two heterocycles and a trifluoromethyl group, all of which are motifs commonly seen in pharmaceuticals.

Figure 3.6. Gram-scale couplings of heterocyclic substrates.

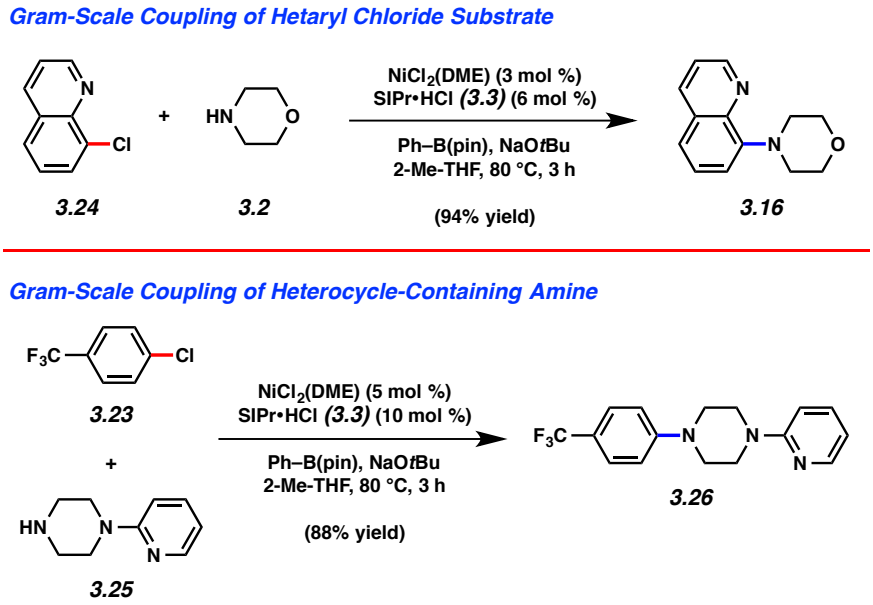

3.5 Conclusion

In summary, we have developed the nickel-catalyzed coupling of a variety of electrophilic substrates (e.g., halides and pseudohalides) with amines using the attractive, green solvent 2-Me-THF. The couplings of aryl *O*-sulfamates and aryl chlorides proceed in the highest yields, and may be achieved using an air-stable nickel precatalyst. The methodology has a broad scope and is tolerant of electronically biasing substituents, sterics, and even pharmaceutically-relevant heterocycles. The scalability of the nickel-catalyzed amination in 2-Me-THF using low catalyst loading bodes well for future synthetic applications in drug discovery and other arenas.

3.6 Experimental Section

3.6.1 Materials and Methods

Unless stated otherwise, reactions were conducted in flame-dried glassware under an atmosphere of nitrogen and commercially obtained reagents were used as received. Amines were purified by filtration over basic Brockmann Grade I 58 Å Alumina (Activity 1), followed by distillation over calcium hydride prior to use. $NiCl_2$(DME) was obtained from Strem Chemicals. NaO*t*Bu, the amines, SIPr•HCl, and Ph–B(pin) were obtained from Sigma-Aldrich and Alfa Aesar. Halogenated substrates were obtained from Combi-Blocks, Sigma-Aldrich, and Oakwood Products, Inc. 2-Me-THF was obtained from Acros Organics [2-Methyltetrahydrofuran, 99+%, pure, stabilized] and used without further purification. Reaction temperatures were controlled using an IKAmag temperature modulator, and unless stated otherwise, reactions were performed at room temperature (rt, approximately 23 °C). Thin-layer chromatography (TLC) was conducted with EMD gel 60 F254 pre-coated plates (0.25 mm for analytical chromatography and 0.5 mm for preparative chromatography) and visualized using a combination of UV, anisaldehyde, ceric ammonium molybdate, iodine, vanillin, and potassium permanganate staining. Silicycle Siliaflash P60 (particle size 0.040–0.063 mm) was used for flash column chromatography. ^{1}H NMR spectra were recorded on Bruker spectrometers (at 400, 500, and 600 MHz) and are reported relative to residual solvent signals. Data for ^{1}H NMR spectra are reported as follows: chemical shift (δ ppm), multiplicity, coupling constant (Hz), integration and are referenced to the residual solvent peak 7.26 ppm for $CDCl_3$. Data for ^{13}C NMR are reported in terms of chemical shift (at 100 and 125 MHz) and are referenced to the residual solvent peak 77.16 for $CDCl_3$. IR spectra were recorded on a Perkin-Elmer 100 spectrometer and are reported in terms of frequency absorption (cm^{-1}). Uncorrected melting points were measured using a Digimelt

MPA160 melting point apparatus. High-resolution mass spectra were obtained from the UCLA Mass Spectrometry Facilities.

3.6.2 Experimental Procedures

3.6.2.1 Syntheses of Aryl Pseudohalide Substrates

Note: Experimental procedures for the syntheses of the aryl triflates,[18] tosylates,[19] pivalates,[20] carbamates,[21] and sulfamates[21a,22] shown in Table 3.2 and Figures 3.2, 3.4, and 3.5 have previously been reported.

3.6.2.2 Solvent Optimization and Scope of Electrophile

Representative Procedure for Amination of Electrophiles from Table 3.1 (coupling of naphthyl chloride 3.1 is used as an example). A 4 mL reaction vial with a magnetic stir bar was charged with Ph–B(pin) (57.5 mg, 0.275 mmol, 0.55 equiv), anhydrous powdered NaO*t*Bu (88.9 mg, 0.925 mmol, 1.85 equiv), $NiCl_2$(DME) (5.5 mg, 0.025 mmol, 5 mol %), hexamethylbenzene (8.1 mg, 0.050 mmol, 0.1 equiv), and SIPr•HCl (21.7 mg, 0.0506 mmol, 10 mol %). Subsequently, toluene (2.5 mL), naphthyl chloride **3.1** (81.3 mg, 0.500 mmol, 1.0 equiv), and morpholine (87.1 μL, 0.900 mmol, 1.8 equiv) were added sequentially. The resulting heterogenous mixture was stirred for 1 min while purging with N_2, and the vial was sealed with a Teflon-lined screw cap. The mixture was stirred at 23 °C for 1 h, and then at 80 °C for 3 h in a preheated aluminum block. The reaction vessel was allowed to cool to 23 °C and the mixture was filtered by passage through a plug of silica gel (EtOAc eluent, 5 mL), and then concentrated under reduced pressure. The yield was determined by ^{1}H NMR analysis with hexamethylbenzene as an internal standard. Spectral data match those previously reported.[23]

3.6.2.3 Aminations of Aryl Sulfamates and Chlorides

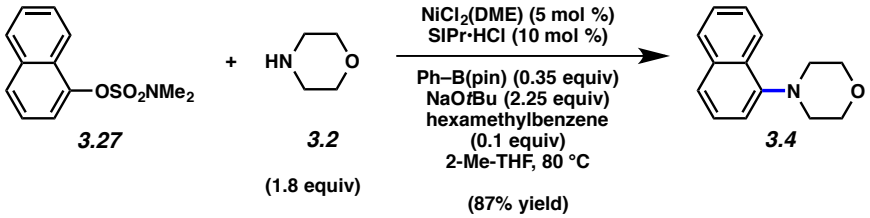

Representative Procedure (coupling of naphthylsulfamate 3.27 is used as an example). A 4 mL reaction vial with a magnetic stir bar was charged with Ph–B(pin) (36.6 mg, 0.175 mmol, 0.35 equiv), anhydrous powdered NaO*t*Bu (108.1 mg, 1.125 mmol, 2.25 equiv), $NiCl_2$(DME) (5.5 mg, 0.025 mmol, 5 mol %), hexamethylbenzene (8.1 mg, 0.050 mmol, 0.1 equiv), and SIPr•HCl (21.7 mg, 0.0506 mmol, 10 mol %). Subsequently, 2-Me-THF (2.5 mL), naphthylsulfamate **3.27** (125.7 mg, 0.5002 mmol, 1.0 equiv), and morpholine (87.1 μL, 0.900 mmol, 1.8 equiv) were added, sequentially. The resulting heterogenous mixture was stirred for 1 min while purging with N_2, and the vial was sealed with a Teflon-lined screw cap. The mixture was stirred at 23 °C for 1 h, and then at 80 °C for 3 h in a preheated aluminum heating block. The reaction vessel was allowed to cool to 23 °C and the mixture was filtered by passage over a plug of silica gel (EtOAc eluent, 5 mL), and then concentrated under reduced pressure. The yield was determined by ^{1}H NMR analysis with hexamethylbenzene as an internal standard. Spectral data match those previously reported.[23]

Any modifications of the conditions shown in the representative procedure above are specified in the following schemes, which depict all of the results shown in Figures 3.2–3.4.

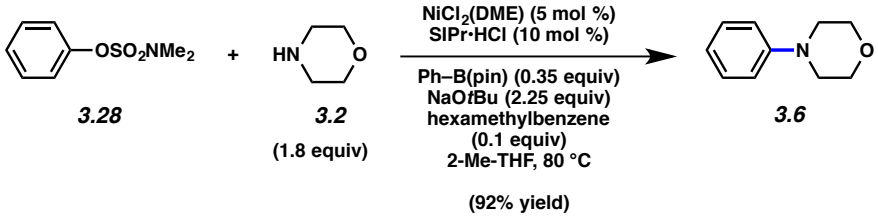

3.28 *3.2* (1.8 equiv) *3.6*

3.6 (Figure 3.2). The yield was determined by ^{1}H NMR analysis with hexamethylbenzene as an internal standard. Spectral data match those previously reported.[24]

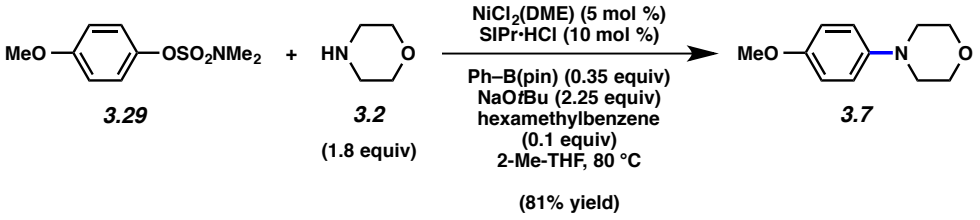

3.29 *3.2* (1.8 equiv) *3.7*

3.7 (Figure 3.2). The yield was determined by ^{1}H NMR analysis with hexamethylbezene as an internal standard. Spectral data match those previously reported.[25]

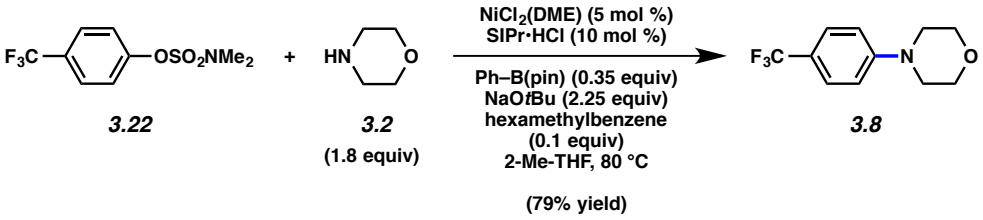

3.22 *3.2* (1.8 equiv) *3.8*

3.8 (Figure 3.2). The yield was determined by ^{1}H NMR analysis with hexamethylbenzene as an internal standard. Spectral data match those previously reported.[26]

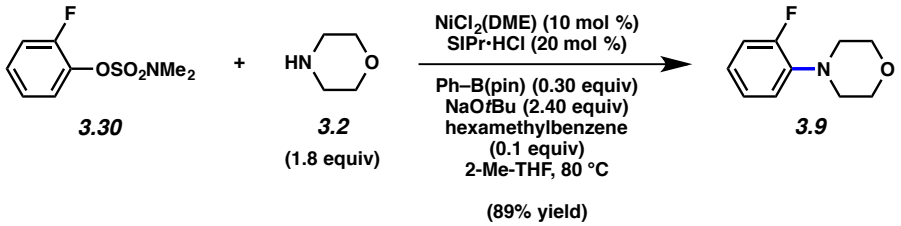

3.9 (Figure 3.2). The yield was determined by ^{1}H NMR analysis with hexamethylbenzene as an internal standard. Spectral data match those previously reported.[27]

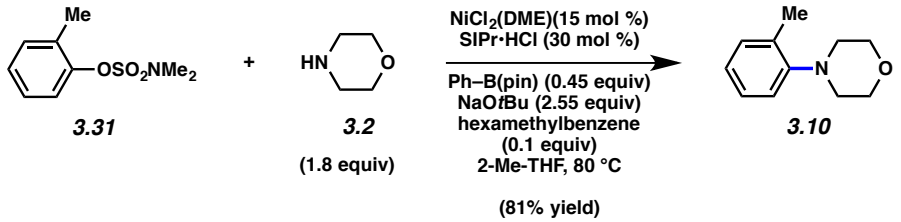

3.10 (Figure 3.2). The yield was determined by ^{1}H NMR analysis with hexamethylbenzene as an internal standard. Spectral data match those previously reported.[10e]

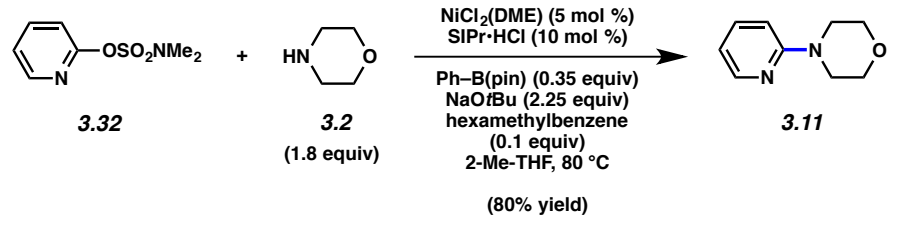

3.11 (Figure 3.2). The yield was determined by ^{1}H NMR analysis with hexamethylbenzene as an internal standard. Spectral data match those previously reported.[28]

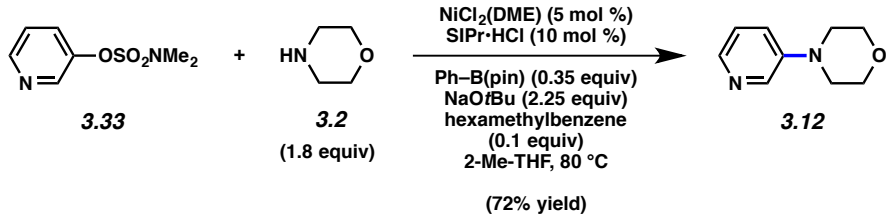

3.33 + *3.2* (1.8 equiv) → *3.12*

3.12 (Figure 3.2). The yield was determined by ^{1}H NMR analysis with hexamethylbenzene as an internal standard. Spectral data match those previously reported.[28]

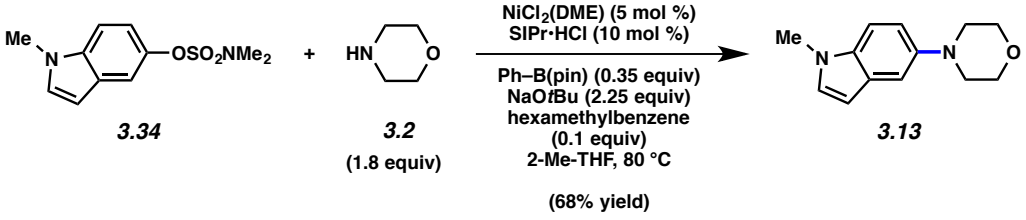

3.34 + *3.2* (1.8 equiv) → *3.13*

3.13 (Figure 3.2). The yield was determined by ^{1}H NMR analysis with hexamethylbenzene as an internal standard. Spectral data match those previously reported.[29]

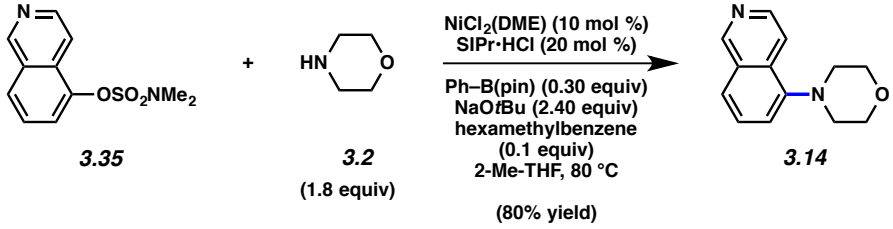

3.35 + *3.2* (1.8 equiv) → *3.14*

3.14 (Figure 3.2). The yield was determined by ^{1}H NMR analysis with hexamethylbenzene as an internal standard. An analytic sample of **3.14** was prepared by filtration of the reaction mixture through a plug of silica gel (EtOAc eluent, 5 mL), evaporation of the solvent under reduced pressure, and purification of an aliquot of the crude residue by preparative thin-layer chromatography (5:1 Hexanes:EtOAc, 20x20 cm). R_f 0.18 (1:1 Hexanes:EtOAc); ^{1}H NMR: (400

MHz, $CDCl_3$): δ 9.23 (s, 1H), 8.53 (d, *J* = 6.0, 1H), 7.93 (d, *J* = 6.0, 1H), 7.68 (d, *J* = 8.0, 1H), 7.54 (app t, *J* = 8.0, 1H), 7.27 (t, *J* = 7.5, 1H), 3.99 (t, *J* = 4.5, 4H), 3.11 (t, *J* = 4.5, 4H); ^{13}C NMR (100 MHz, $CDCl_3$): δ 152.1, 147.6, 141.8, 130.8, 129.1, 126.5, 122.0, 117.7, 115.5, 66.4, 52.4; IR (film): 2966, 2825, 1617, 1582, 1489, 1454, 1433, 1387, 1263, 1115, 1055, 1033 cm^{-1}; HRMS-ESI (*m/z*) $[M+H]^+$ calcd for $C_{13}H_{15}N_2O$, 215.11789; found 215.11741.

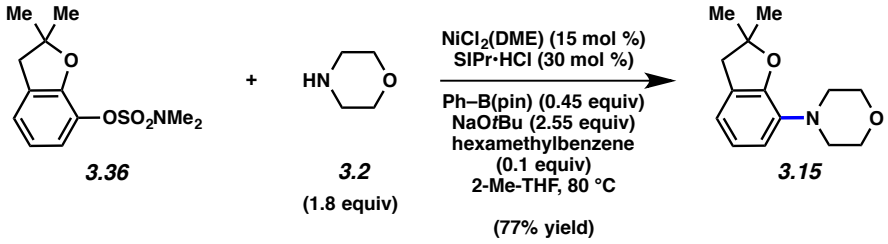

3.15 (Figure 3.2). The yield was determined by ^1H NMR analysis with hexamethylbenzene as an internal standard. An analytic sample of **3.15** was prepared by filtration of the reaction mixture through a plug of silica gel (EtOAc eluent, 5 mL), evaporation of the solvent under reduced pressure, and purification of an aliquot of the crude residue by preparative thin-layer chromatography (5:1 Hexanes:EtOAc, 20x20 cm). R_f 0.27 (9:1 Hexanes:EtOAc); ^1H NMR: (400 MHz, $CDCl_3$): δ 6.81–6.77 (m, 2H), 6.68 (dd, *J* = 6.7, 2.2, 1H), 3.88 (t, *J* = 4.5, 4H), 3.13 (t, *J* = 4.5, 4H), 2.99 (s, 2H), 1.49 (s, 6H); ^{13}C NMR (125 MHz, $CDCl_3$): δ 150.1, 136.4, 128.0, 120.7, 118.6, 115.3, 86.8, 67.1, 50.0, 43.2, 28.4; IR (film): 2968, 2854, 1608, 1455, 1269, 1119, 1006 cm^{-1}; HRMS-ESI (*m/z*) $[M+H]^+$ calcd for $C_{14}H_{20}NO_2$, 234.14886; found 234.14766.

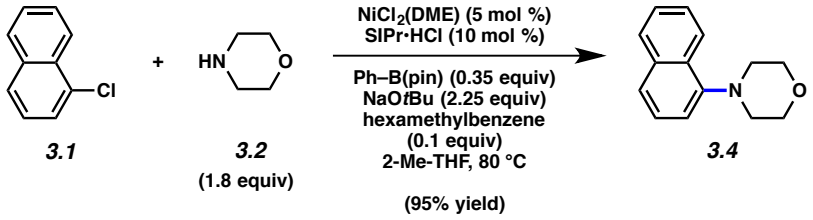

3.4 (Figure 3.3). The yield was determined by ^{1}H NMR analysis with hexamethylbenzene as an internal standard. Spectral data match those previously reported.[23]

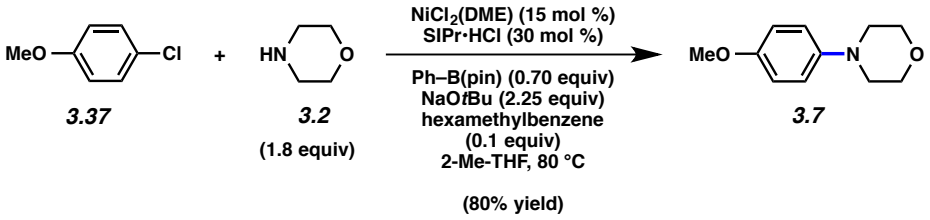

3.7 (Figure 3.3). The yield was determined by 1H NMR analysis with hexamethylbenzene as an internal standard. Spectral data match those previously reported.[25]

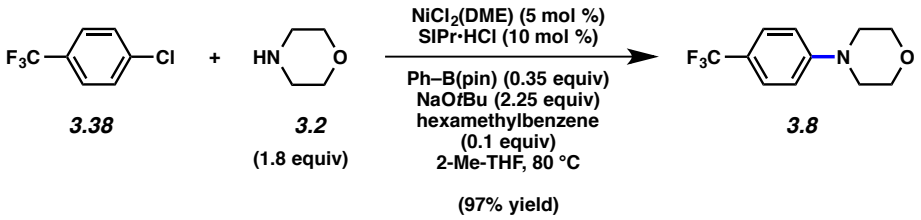

3.8 (Figure 3.3). The yield was determined by ^{1}H NMR analysis with hexamethylbenzene as an internal standard. Spectral data match those previously reported.[26]

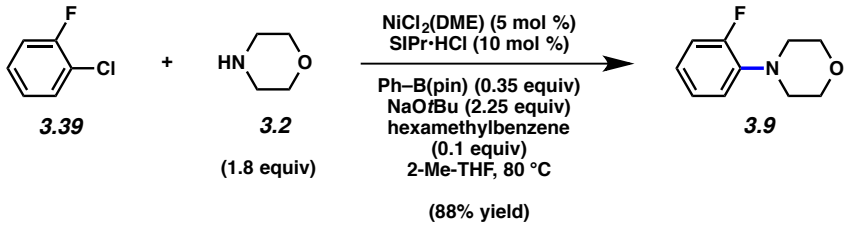

3.9 (Figure 3.3). The yield was determined by ^{1}H NMR analysis with hexamethylbenzene as an internal standard. Spectral data match those previously reported.[27]

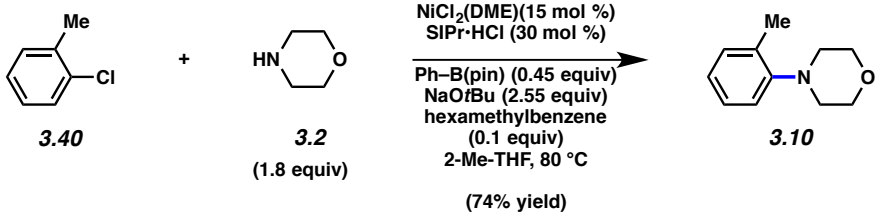

3.10 (Figure 3.3). The yield was determined by ^{1}H NMR analysis with hexamethylbenzene as an internal standard. Spectral data match those previously reported.[10e]

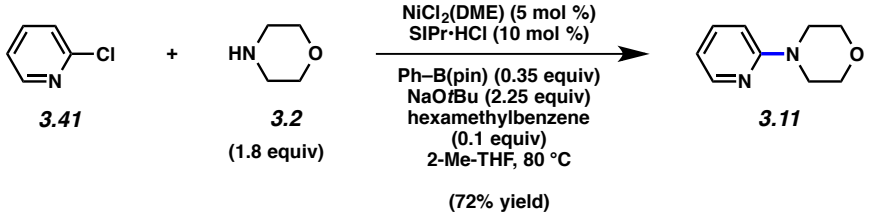

3.11 (Figure 3.3). The yield was determined by ^{1}H NMR analysis with hexamethylbenzene as an internal standard. Spectral data match those previously reported.[28]

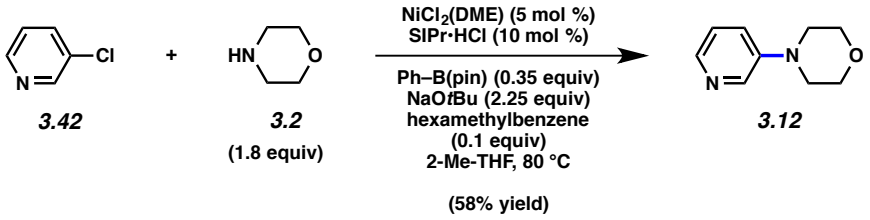

3.12 (Figure 3.3). The yield was determined by ^{1}H NMR analysis with hexamethylbenzene as an internal standard. Spectral data match those previously reported.[28]

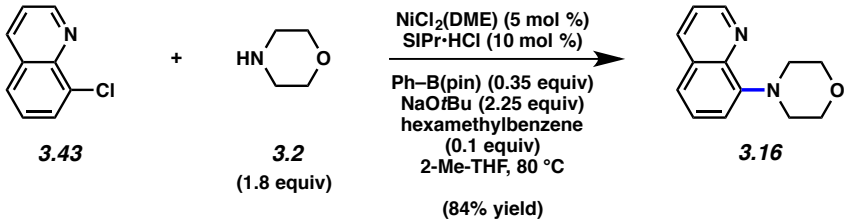

3.16 (Figure 3.3). The yield was determined by ^{1}H NMR analysis with hexamethylbenzene as an internal standard. Spectral data match those previously reported.[30]

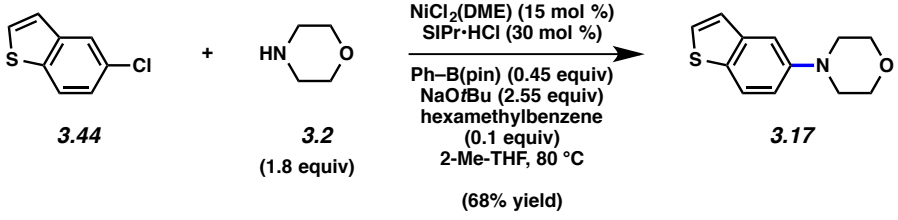

3.17 (Figure 3.3). The yield was determined by ^{1}H NMR analysis with hexamethylbenzene as an internal standard. An analytic sample of **3.17** was prepared by filtration of the reaction mixture through a plug of silica gel (EtOAc eluent, 5 mL), evaporation of the solvent under reduced pressure, and purification of an aliquot of the crude residue by preparative thin-layer chromatography (5:1 Hexanes:EtOAc, 20x20 cm). R_f 0.21 (9:1 Hexanes:EtOAc); ^{1}H NMR: (400

MHz, $CDCl_3$): δ 7.75 (d, J = 8.8, 1H), 7.41 (d, J = 5.4, 1H), 7.29 (br s, 1H), 7.24 (d, J = 5.4, 1H), 7.07 (dd, J = 8.8, 2.2, 1H), 3.90 (t, J = 4.5, 4H), 3.20 (t, J = 4.5, 4H); ^{13}C NMR (125 MHz, $CDCl_3$): δ 149.2, 140.8, 132.3, 127.3, 123.8, 123.0, 116.3, 109.7, 67.1, 50.8; IR (film): 2966, 2909, 2829, 1595, 1444, 1262, 1233, 1120 cm^{-1}; HRMS-ESI (*m/z*) $[M+H]^+$ calcd for $C_{12}H_{14}SNO$, 220.07906; found 220.07835.

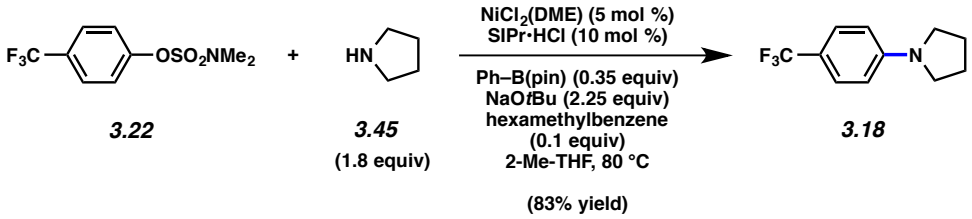

3.18 (Figure 3.4). The yield was determined by ^{1}H NMR analysis with hexamethylbenzene as an internal standard. Spectral data match those previously reported.[31]

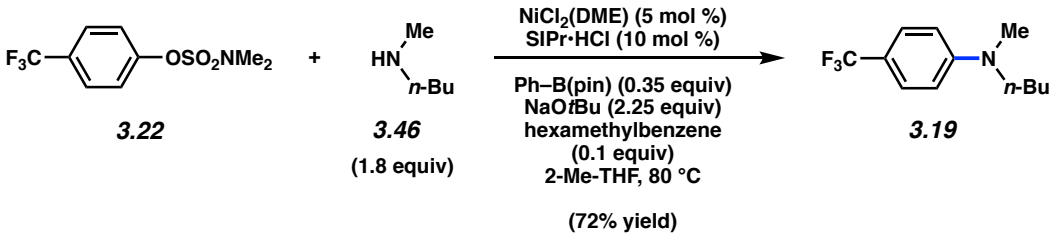

3.19 (Figure 3.4). The yield was determined by ^{1}H NMR analysis with hexamethylbenzene as an internal standard. Spectral data match those previously reported.[29]

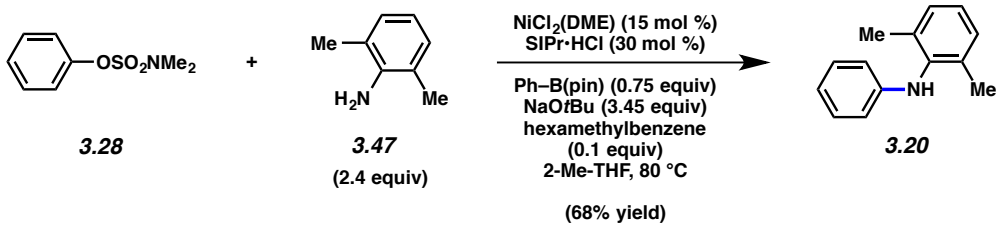

3.20 (Figure 3.4). The yield was determined by ^{1}H NMR analysis with hexamethylbenzene as an internal standard. Spectral data match those previously reported.[10e]

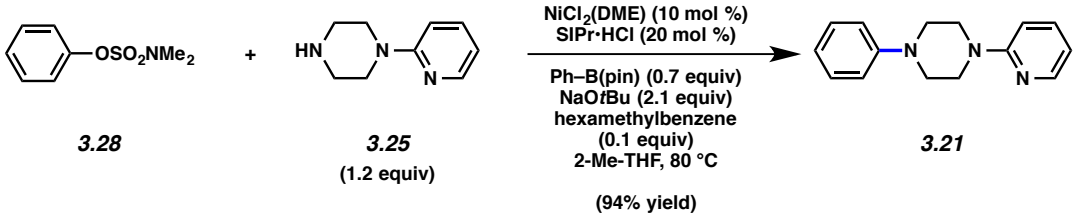

3.21 (Figure 3.4). The yield was determined by ^{1}H NMR analysis with hexamethylbenzene as an internal standard. Spectral data match those previously reported.[7e]

3.6.2.4 Isolation Experiments

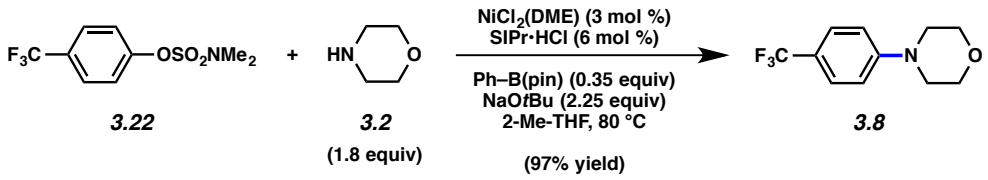

3.8 (Figure 3.5). A 100 mL round bottom flask with a magnetic stir bar was charged with Ph–B(pin) (271.5 mg, 1.30 mmol, 0.35 equiv), anhydrous powdered NaO*t*Bu (802.2 mg, 8.35 mmol, 2.25 equiv), $NiCl_2$(DME) (24.5 mg, 0.11 mmol, 3 mol %), and SIPr•HCl (95.5 mg, 0.22 mmol, 6 mol %). Subsequently, 2-Me-THF (18.6 ml), trifluorobenzosulfamate **3.22** (1.0 g, 3.71 mmol, 1.0

equiv), and morpholine (578 μL, 6.69 mmol, 1.8 equiv) were added, sequentially. The resulting heterogenous mixture was stirred for 1 min while purging with N_2, and then under an atmosphere of N_2 for 1 h. The reaction was then equipped with a reflux condenser and placed in an oil bath, preheated to 80 °C, for 3 h. The reaction flask was allowed to cool to 23 °C and the mixture was filtered by passage over a plug of silica gel (EtOAc eluent, 5 mL). After concentration under reduced pressure, the crude residue was purified by flash chromatography (4:1 Hexanes:EtOAc) to yield amine **3.8** (832.1 mg, 97% yield) as a white solid. Spectral data match those previously reported.[26]

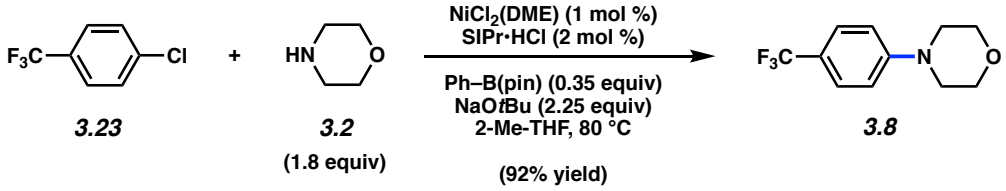

3.8 (Figure 3.5). A 100 mL round bottom flask with a magnetic stir bar was charged with Ph–B(pin) (405.4 mg, 1.94 mmol, 0.35 equiv), anhydrous powdered NaO*t*Bu (1.20 g, 12.47 mmol, 2.25 equiv), $NiCl_2$(DME) (12.2 mg, 0.06 mmol, 1 mol %), and SIPr•HCl (47.5 mg, 0.111 mmol, 2 mol %). Subsequently, 2-Me-THF (27.7 ml), trifluorobenzochloride **3.23** (1.0 g, 5.54 mmol, 1.0 equiv), and morpholine (863 μL, 9.97 mmol, 1.8 equiv) were added, sequentially. The resulting heterogenous mixture was stirred for 1 min while purging with N_2, and then under an atmosphere of N_2 at 23 °C for 1 h. The reaction was then equipped with a reflux condenser and placed in an oil bath, preheated to 80 °C, for 3 h. The reaction flask was allowed to cool to 23 °C and the mixture was filtered by passage through a plug of silica gel (EtOAc eluent, 5 mL). After concentration under reduced pressure, the crude residue was purified by flash

chromatography (4:1 Hexanes:EtOAc) to yield amine **3.8** (1.18 g, 92% yield) as a white solid. Spectral data match those previously reported.[26]

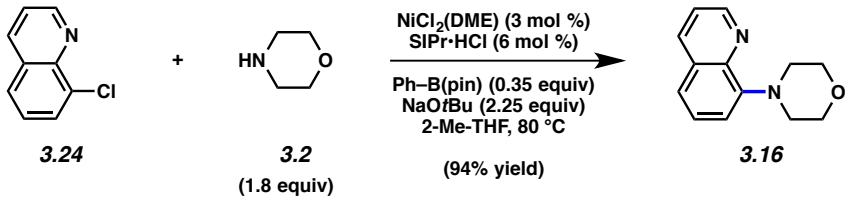

3.16 (Figure 3.6). A 100 mL round bottom flask was charged with a magnetic stir bar, flame-dried under reduced pressure, and allowed to cool under N_2. The flask was then charged with Ph–B(pin) (447.1 mg, 2.14 mmol, 0.35 equiv), anhydrous powdered NaO*t*Bu (1.32 g, 13.8 mmol, 2.25 equiv), $NiCl_2$(DME) (40.2 mg, 0.183 mmol, 3 mol %), and SIPr•HCl (157.3 mg, 0.367 mmol, 6 mol %). Subsequently, 2-Me-THF (30.6 mL), chloroquinoline **3.24** (1.0 g, 6.11 mmol, 1.0 equiv), and morpholine (95.1 μL, 11.0 mmol, 1.8 equiv) were added, sequentially. The resulting heterogenous mixture was stirred for 1 min while purging with N_2, and then under an atmosphere for 1 h. The reaction was then equipped with a reflux condenser and placed in an oil bath, preheated to 80 °C, for 3 h. The reaction flask was allowed to cool to 23 °C and the mixture was filtered by passage through a plug of silica gel (EtOAc eluent, 5 mL). After concentration under reduced pressure, the crude residue was purified by flash chromatography (2:1 Hexanes:EtOAc) to yield morpholino quinoline **3.16** (1.23 g, 94% yield) as a clear viscous oil. Spectral data match those previously reported.[30]

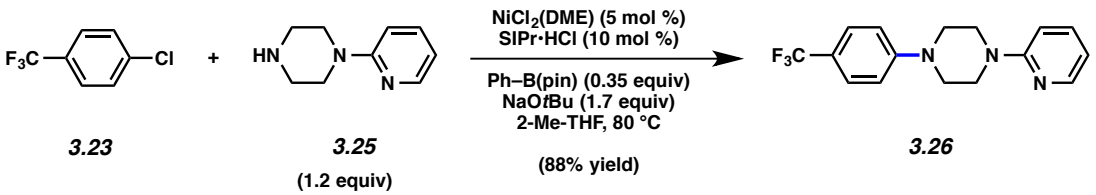

3.26 (Figure 3.6). A 100 mL round bottom flask was charged with a magnetic stir bar, flame-dried under reduced pressure, and allowed to cool under N_2. The flask was then charged with Ph–B(pin) (426.0 mg, 1.94 mmol, 0.35 equiv), anhydrous powdered NaO*t*Bu (904.9 mg, 9.42 mmol, 1.7 equiv), $NiCl_2$(DME) (60.9 mg, 0.277 mmol, 5 mol %), and SIPr•HCl (237.7 mg, 0.554 mmol, 10 mol %). Subsequently, 2-Me-THF (27.7 ml), chloride **3.23** (1.0 g, 5.54 mmol, 1.0 equiv), and 1-(2-pyridyl)piperizine (1.01 mL, 6.65 mmol, 1.2 equiv) were added, sequentially. The resulting heterogenous mixture was stirred for 1 min while purging with N_2, and then under an atmosphere of N_2 for 1 h. The reaction was then equipped with a reflux condenser and placed in an oil bath, preheated to 80 °C, for 3 h. The reaction flask was allowed to cool to 23 °C and the mixture was filtered by passage through a plug of silica gel (EtOAc eluent, 5 mL). After concentration under reduced pressure, the crude residue was purified by flash chromatography (8:1 Hexanes:EtOAc) to yield piperizine **3.26** (1.49 g, 88% yield) as an off-white solid. Spectral data match those previously reported.[32]

3.7 Spectra Relevant to Chapter Three

Nickel-Catalyzed Amination of Aryl Chlorides and Sulfamates in 2-Me-THF

Noah F. Fine Nathel, Junyong Kim, Liana Hie, Xingyu Jiang, and Neil K. Garg

ACS Catal. **2014**, *4*, 3289–3293.

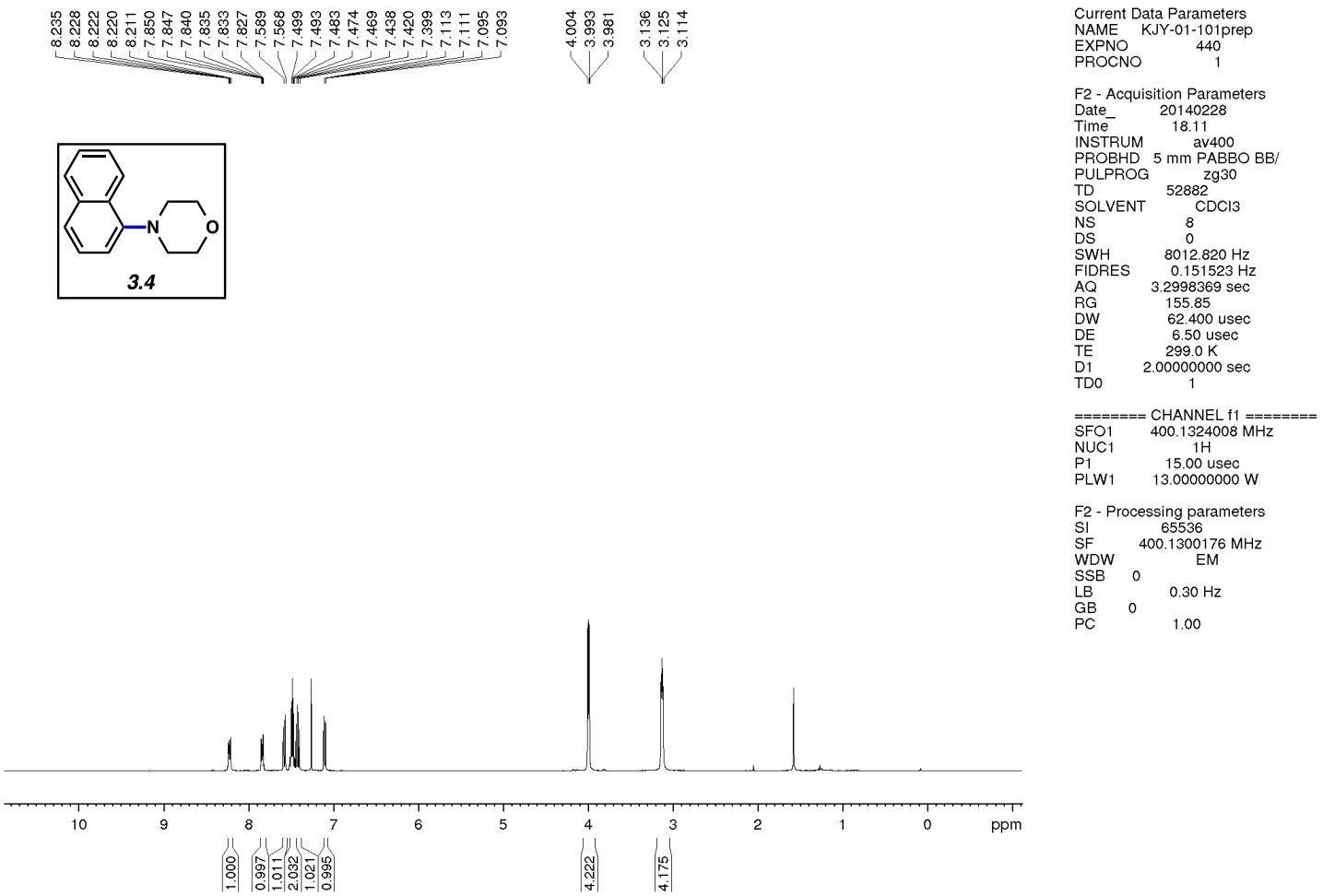

Figure 3.7 ^{1}H NMR (400 MHz, $CDCl_3$) of compound **3.4**.

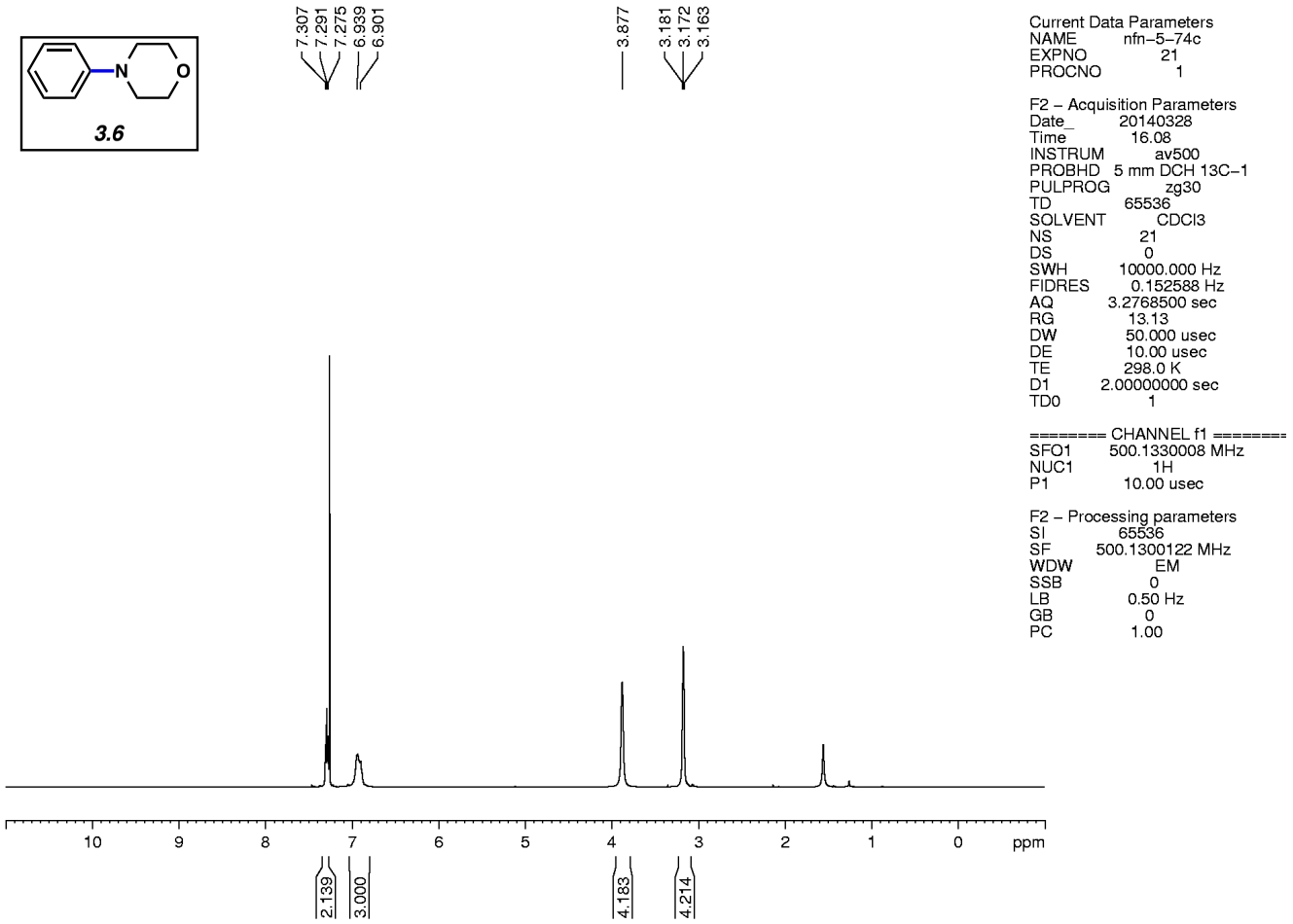

Figure 3.8 ^{1}H NMR (500 MHz, $CDCl_3$) of compound **3.6**.

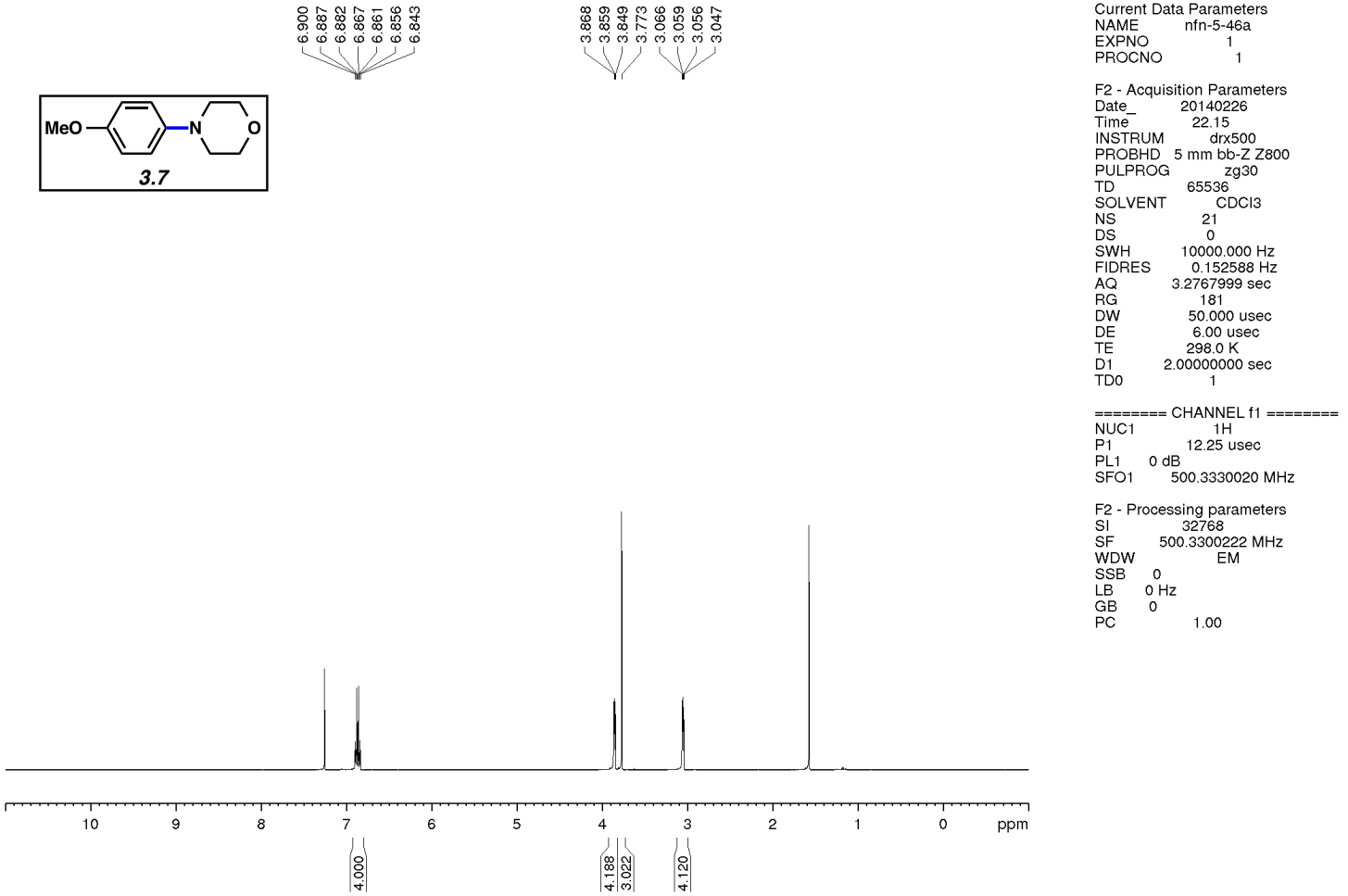

Figure 3.9 ^{1}H NMR (500 MHz, $CDCl_3$) of compound **3.7**.

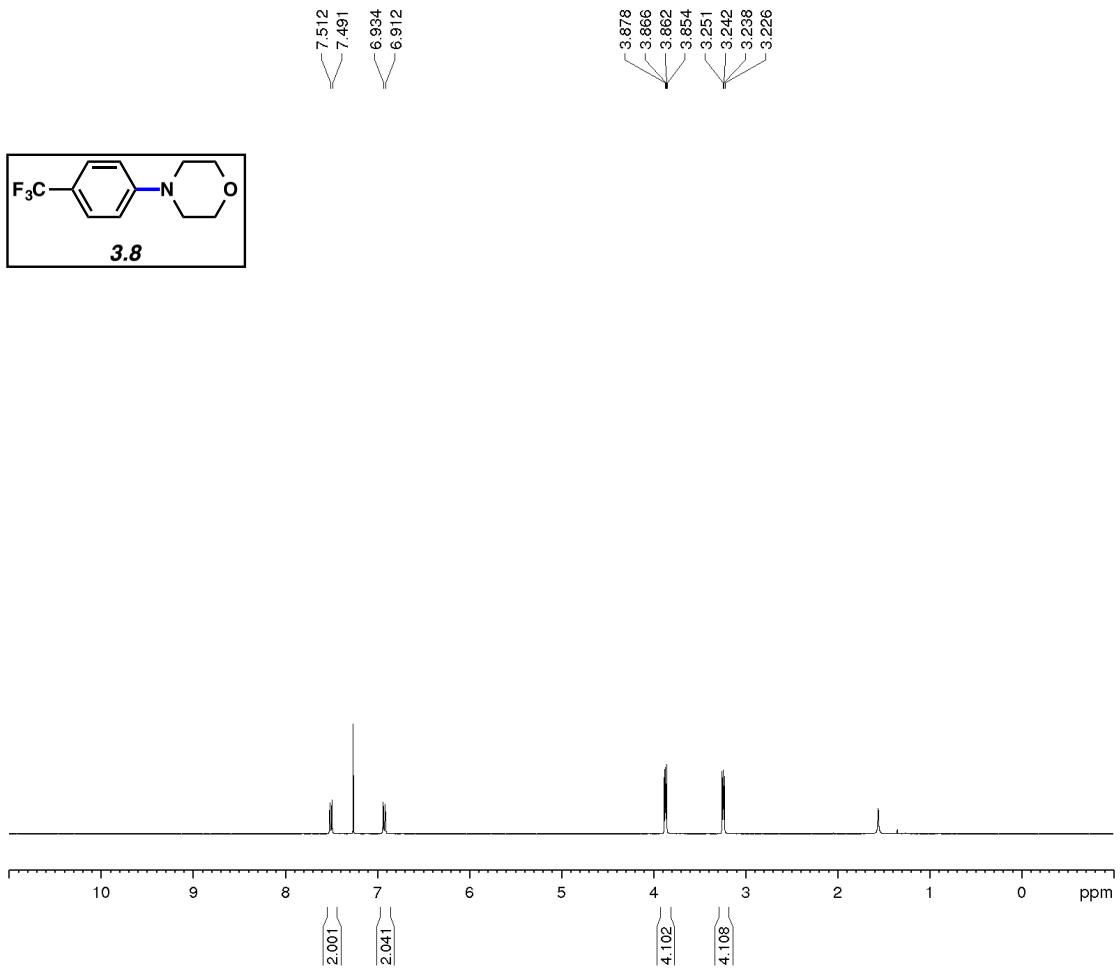

Current Data Parameters
NAME KJY-01-095
EXPNO 650
PROCNO 1

F2 - Acquisition Parameters
Date_ 20140227
Time 19.55
INSTRUM av400
PROBHD 5 mm PABBO BB/
PULPROG zg30
TD 52882
SOLVENT CDCl3
NS 8
DS 0
SWH 8012.820 Hz
FIDRES 0.151523 Hz
AQ 3.2998369 sec
RG 155.85
DW 62.400 usec
DE 6.50 usec
TE 299.0 K
D1 2.00000000 sec
TD0 1

======== CHANNEL f1 ========
SFO1 400.1324008 MHz
NUC1 1H
P1 15.00 usec
PLW1 13.00000000 W

F2 - Processing parameters
SI 65536
SF 400.1300176 MHz
WDW EM
SSB 0
LB 0.30 Hz
GB 0
PC 1.00

Figure 3.10 ^{1}H NMR (400 MHz, $CDCl_3$) of compound **3.8**.

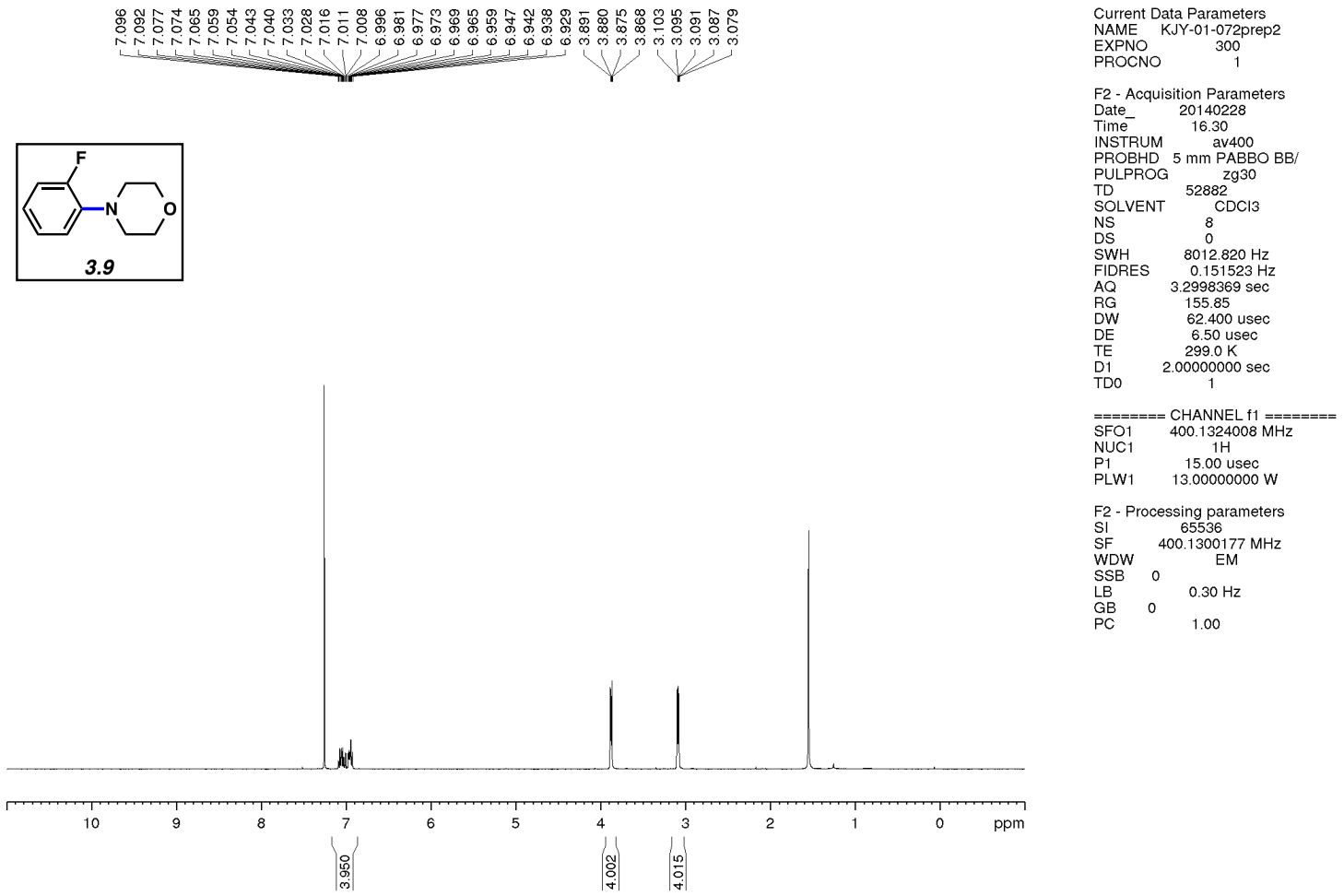

Figure 3.11 ^{1}H NMR (400 MHz, $CDCl_3$) of compound **3.9**.

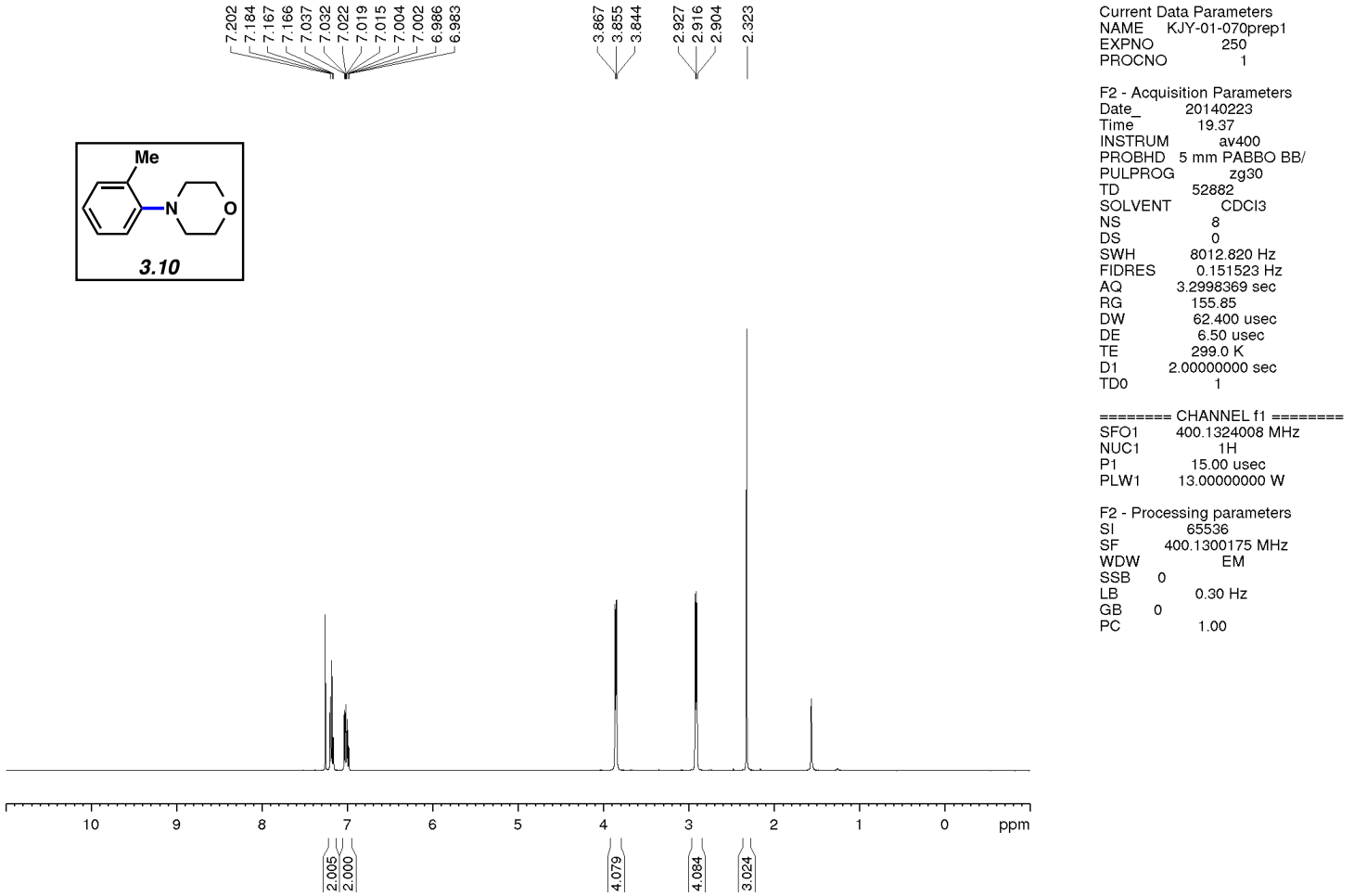

Figure 3.12 ^{1}H NMR (400 MHz, $CDCl_3$) of compound **3.10**.

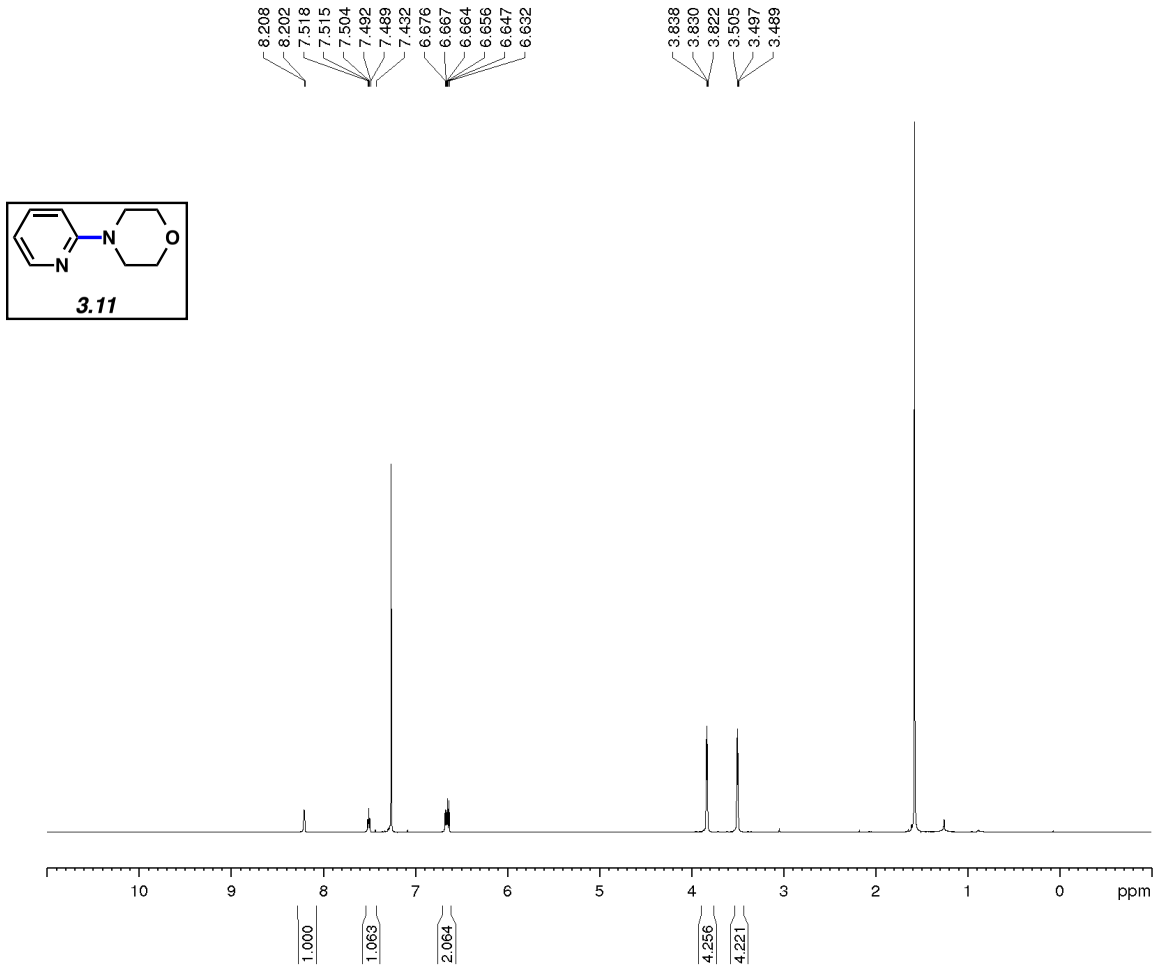

Current Data Parameters
NAME nfn-5-36c
EXPNO 2
PROCNO 1

F2 - Acquisition Parameters
Date_ 20140226
Time 18.07
INSTRUM av600
PROBHD 5 mm TBI5
PULPROG zg30
TD 65536
SOLVENT CDCl3
NS 8
DS 0
SWH 12376.237 Hz
FIDRES 0.188846 Hz
AQ 2.6476543 sec
RG 256
DW 40.400 usec
DE 6.50 usec
TE 680.7 K
D1 2.00000000 sec
TD0 1

======== CHANNEL f1 ========
NUC1 1H
P1 9.50 usec
PL1 -2.00 dB
PL1W 39.81071854 W
SFO1 600.1336008 MHz

F2 - Processing parameters
SI 65536
SF 600.1300297 MHz
WDW EM
SSB 0
LB 1.00 Hz
GB 0
PC 1.00

Figure 3.13 ^{1}H NMR (600 MHz, $CDCl_3$) of compound **3.11**.

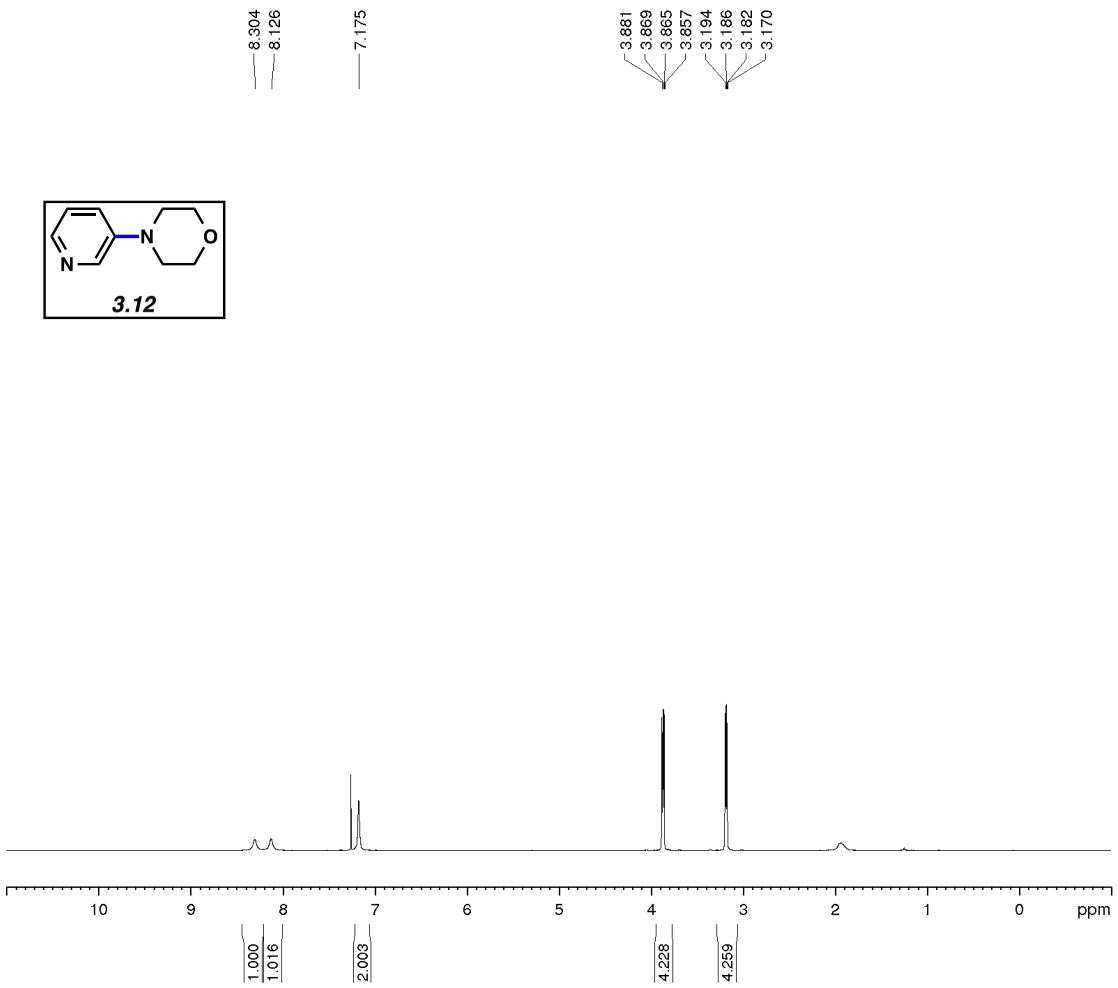

Current Data Parameters
NAME KJY-01-100prep
EXPNO 400
PROCNO 1

F2 - Acquisition Parameters
Date_ 20140304
Time 21.01
INSTRUM av400
PROBHD 5 mm PABBO BB/
PULPROG zg30
TD 52882
SOLVENT CDCl3
NS 8
DS 0
SWH 8012.820 Hz
FIDRES 0.151523 Hz
AQ 3.2998369 sec
RG 155.85
DW 62.400 usec
DE 6.50 usec
TE 299.0 K
D1 2.00000000 sec
TD0 1

======== CHANNEL f1 ========
SFO1 400.1324008 MHz
NUC1 1H
P1 15.00 usec
PLW1 13.00000000 W

F2 - Processing parameters
SI 65536
SF 400.1300174 MHz
WDW EM
SSB 0
LB 0.30 Hz
GB 0
PC 1.00

Figure 3.14 ^{1}H NMR (400 MHz, $CDCl_3$) of compound **3.12**.

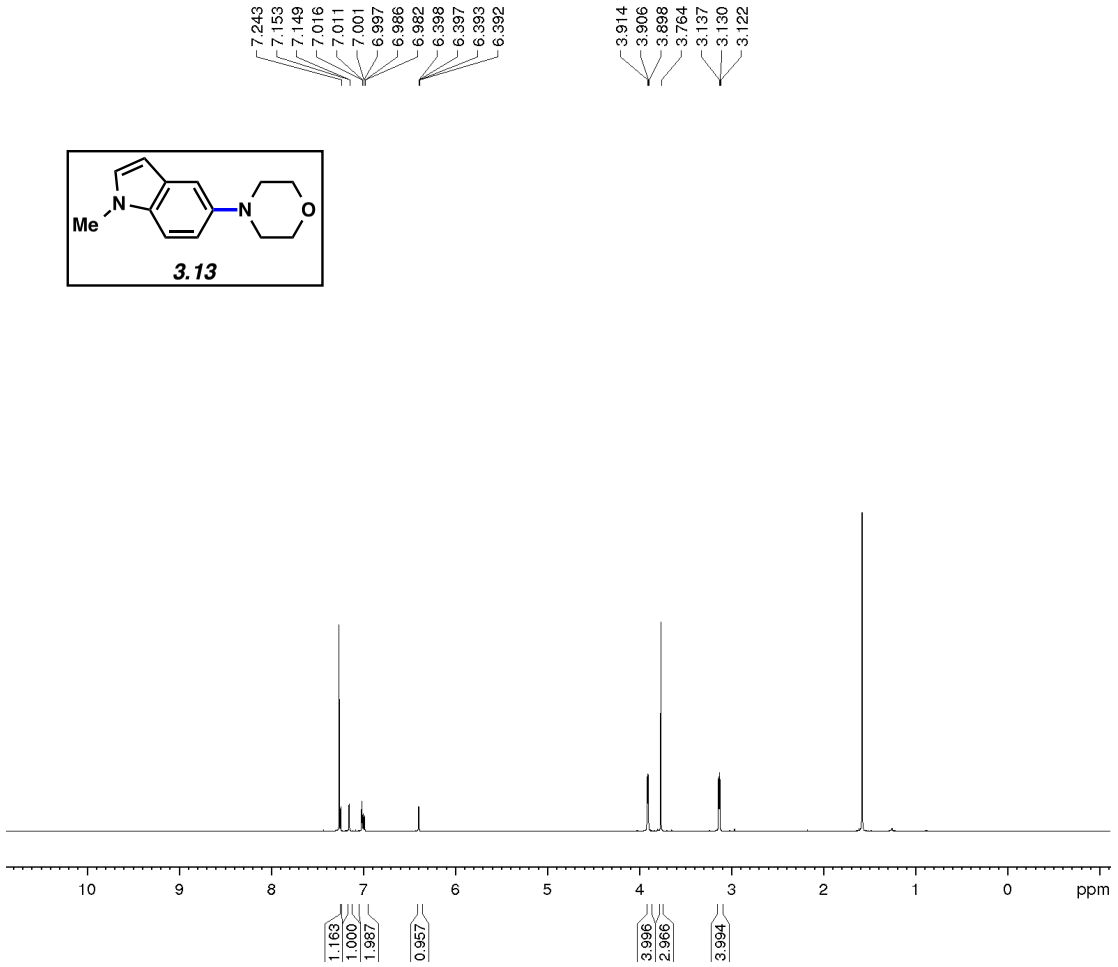

Current Data Parameters
NAME nfn-5-37c
EXPNO 2
PROCNO 1

F2 - Acquisition Parameters
Date_ 20140226
Time 17.44
INSTRUM av600
PROBHD 5 mm TBI5
PULPROG zg30
TD 65536
SOLVENT CDCl3
NS 8
DS 0
SWH 12376.237 Hz
FIDRES 0.188846 Hz
AQ 2.6476543 sec
RG 256
DW 40.400 usec
DE 6.50 usec
TE 680.7 K
D1 2.00000000 sec
TD0 1

======== CHANNEL f1 ========
NUC1 1H
P1 9.50 usec
PL1 -2.00 dB
PL1W 39.81071854 W
SFO1 600.1336008 MHz

F2 - Processing parameters
SI 65536
SF 600.1300297 MHz
WDW EM
SSB 0
LB 0.30 Hz
GB 0
PC 1.00

Figure 3.15 ^{1}H NMR (600 MHz, $CDCl_3$) of compound **3.13**.

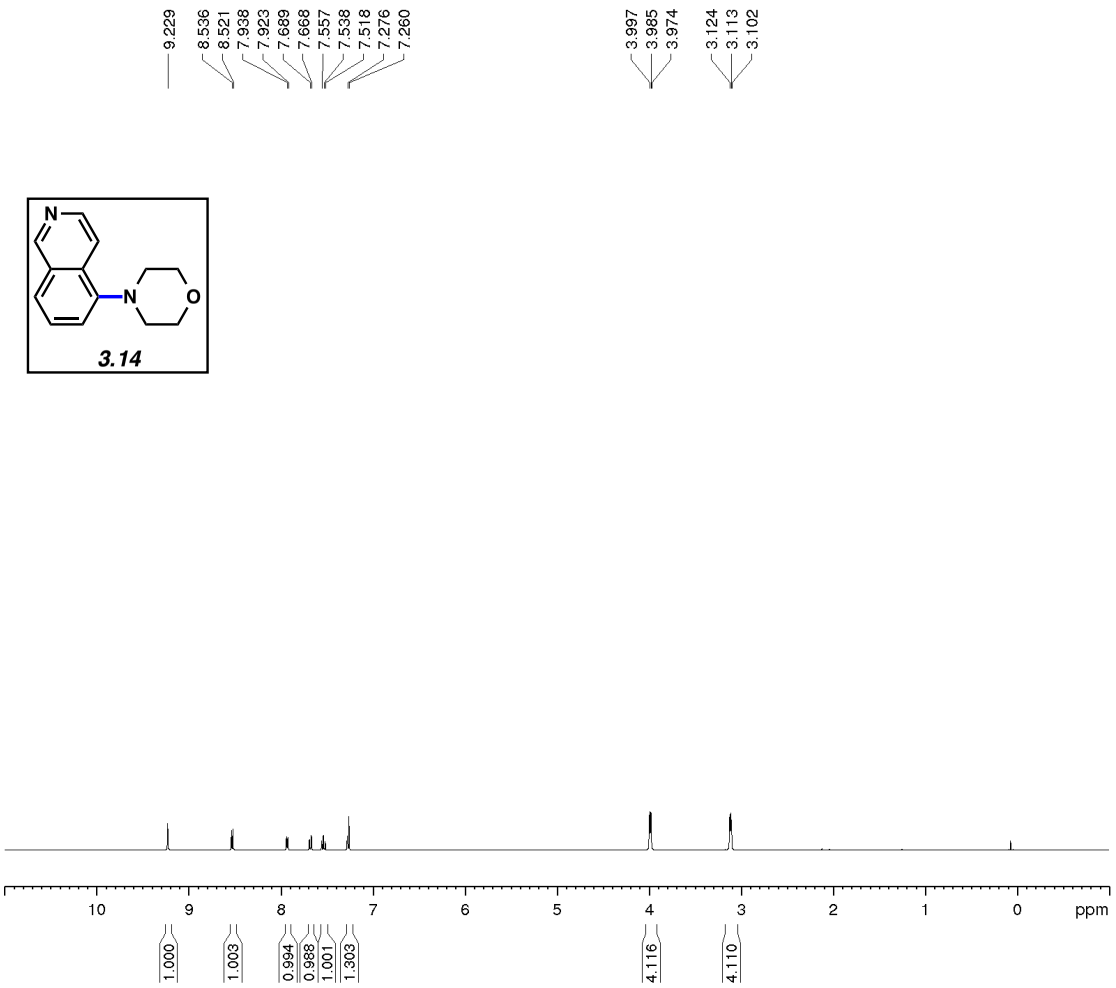

Figure 3.16 ^{1}H NMR (400 MHz, $CDCl_3$) of compound **3.14**.

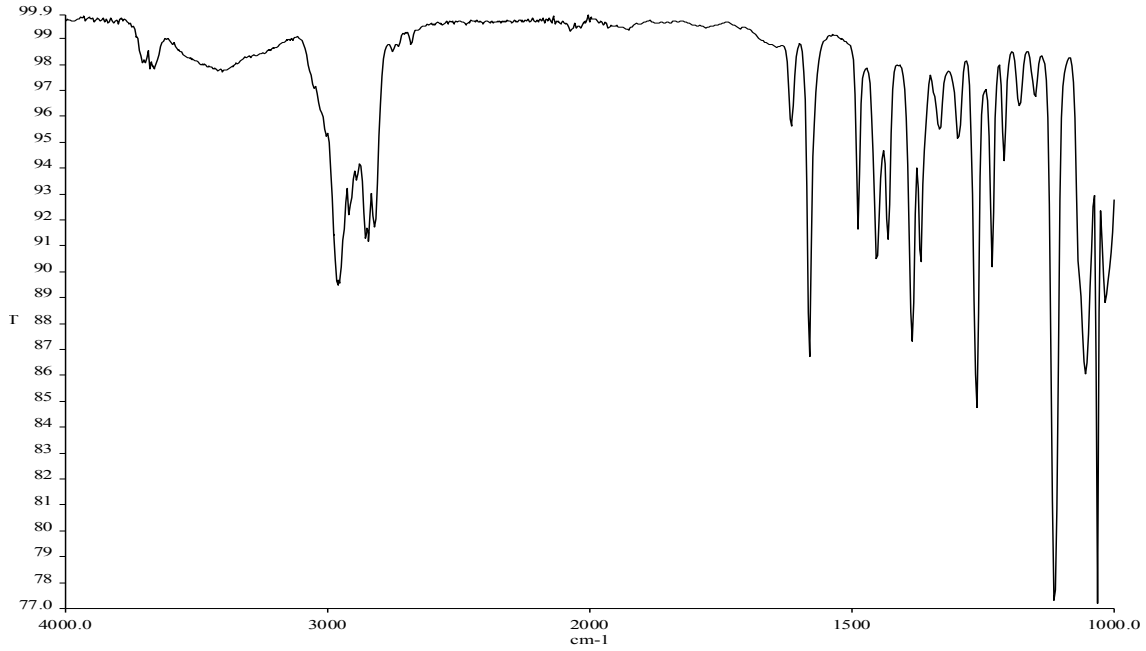

Figure 3.17 Infrared spectrum of compound **3**.**14**.

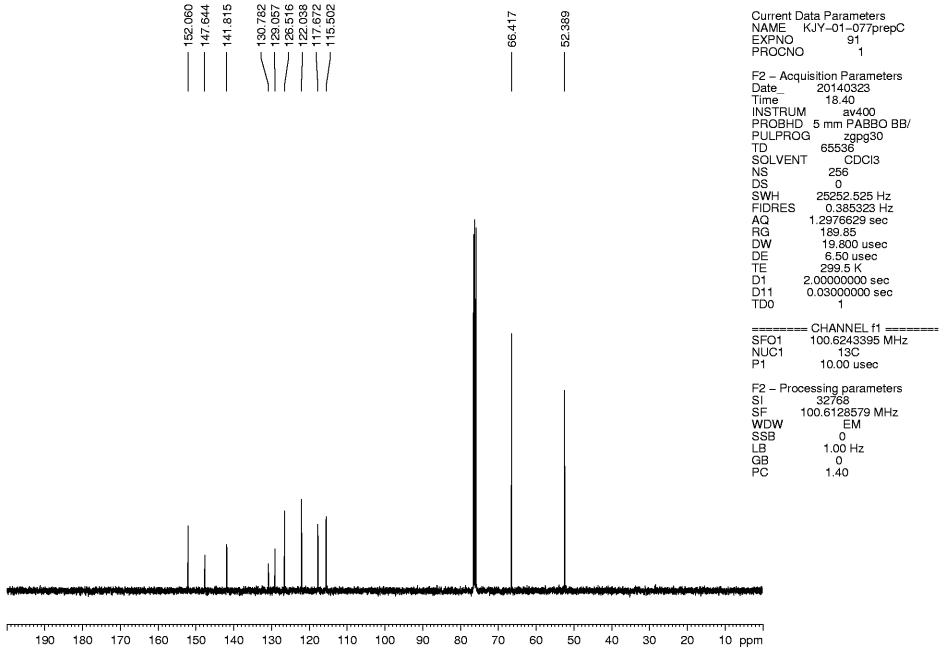

Figure 3.18 ^{13}C NMR (100 MHz, $CDCl_3$) of compound **3.14**.

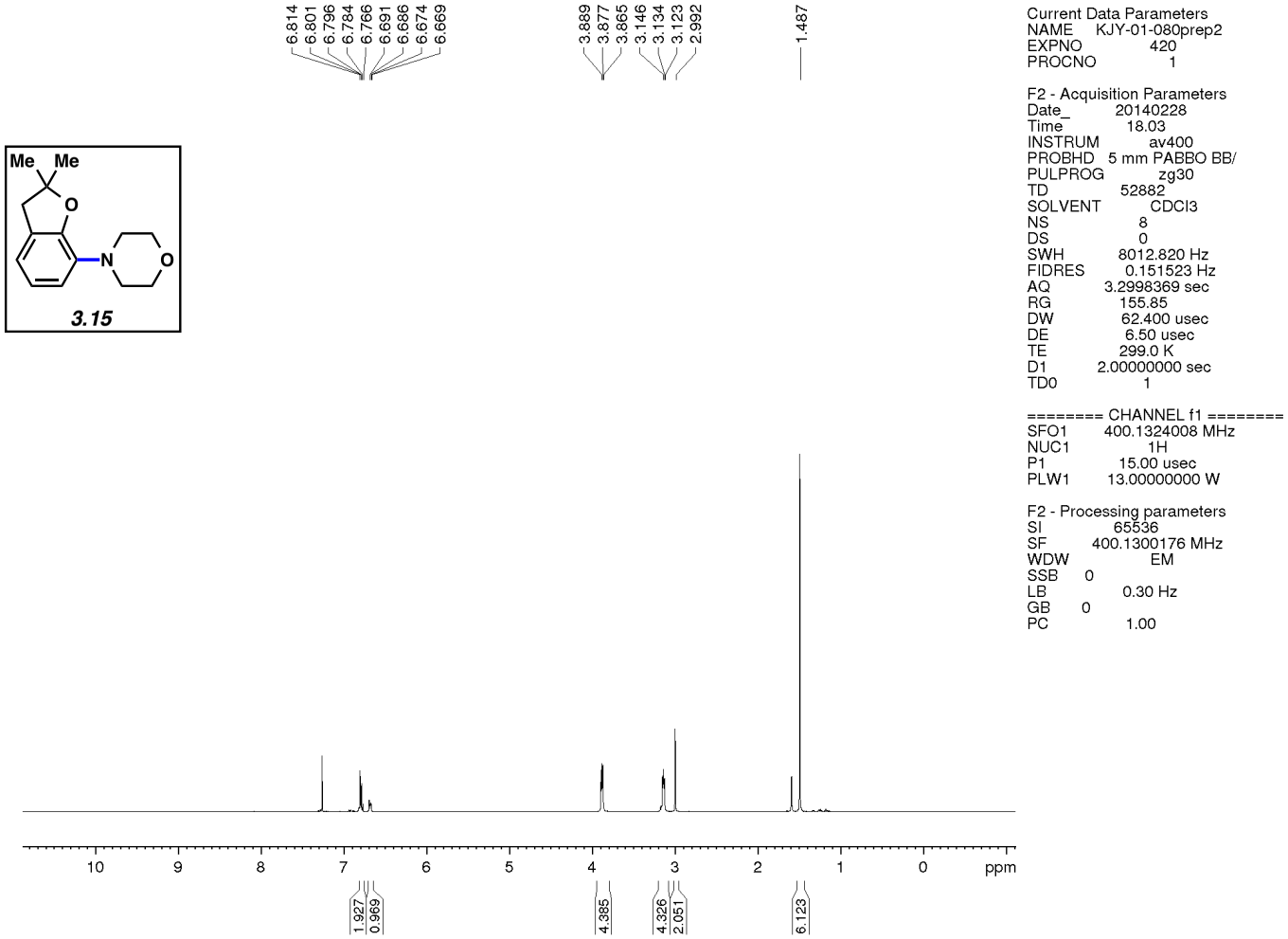

Figure 3.19 ^{1}H NMR (400 MHz, $CDCl_3$) of compound **3.15**.

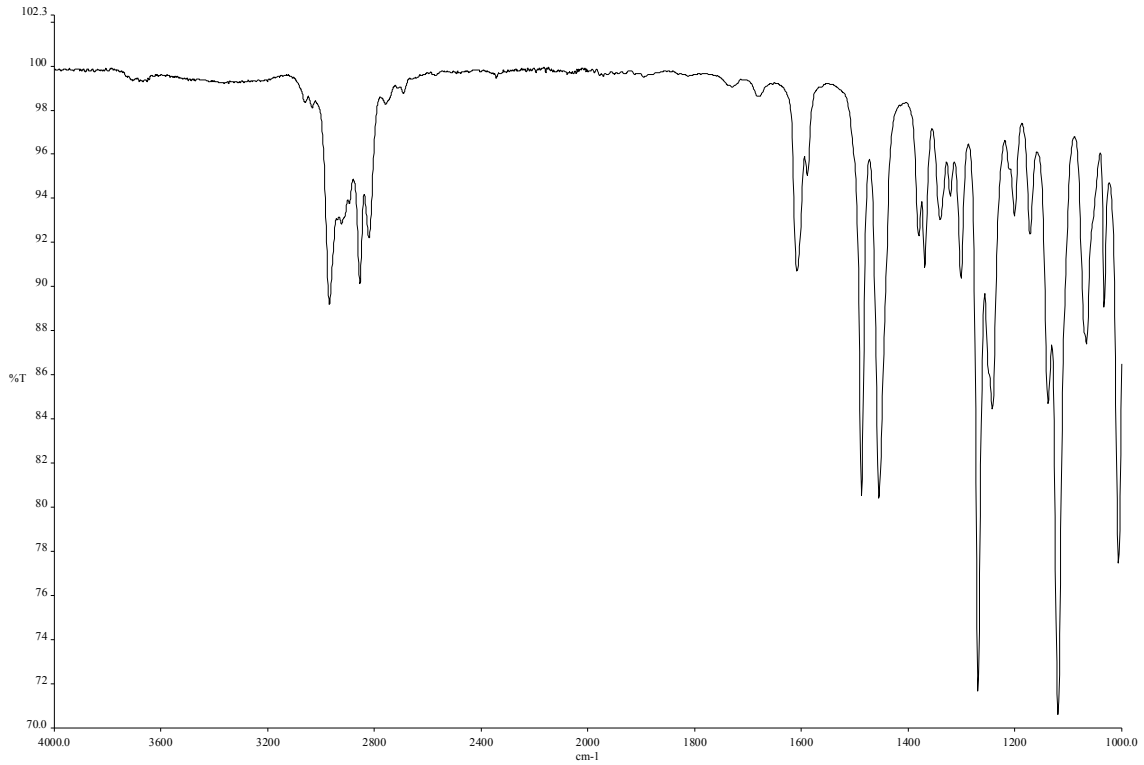

Figure 3.20 Infrared spectrum of compound **3.15**.

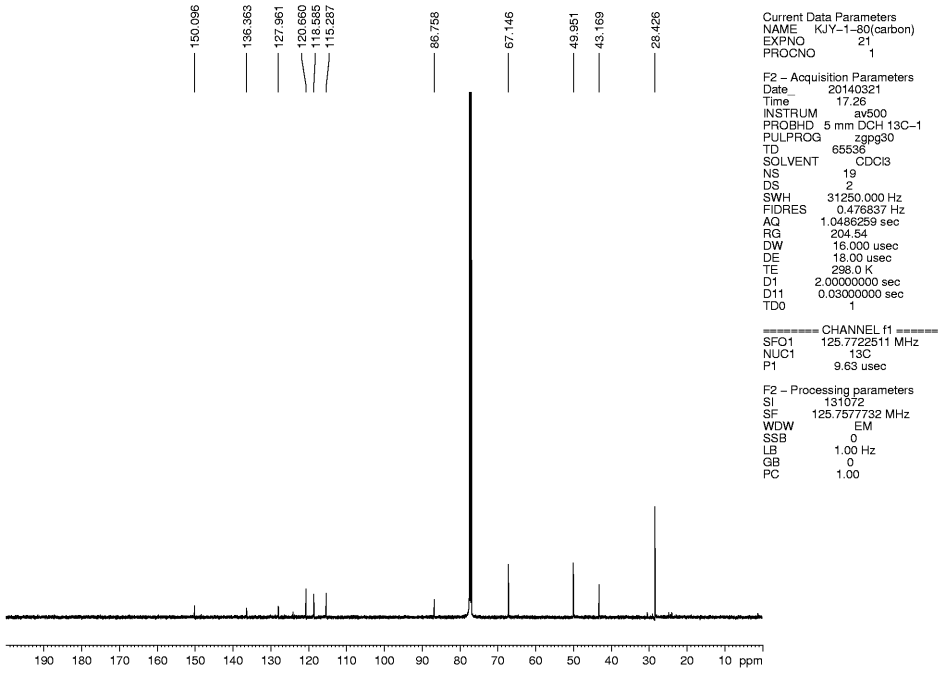

Figure 3.21 ^{13}C NMR (125 MHz, $CDCl_3$) of compound **3.15**.

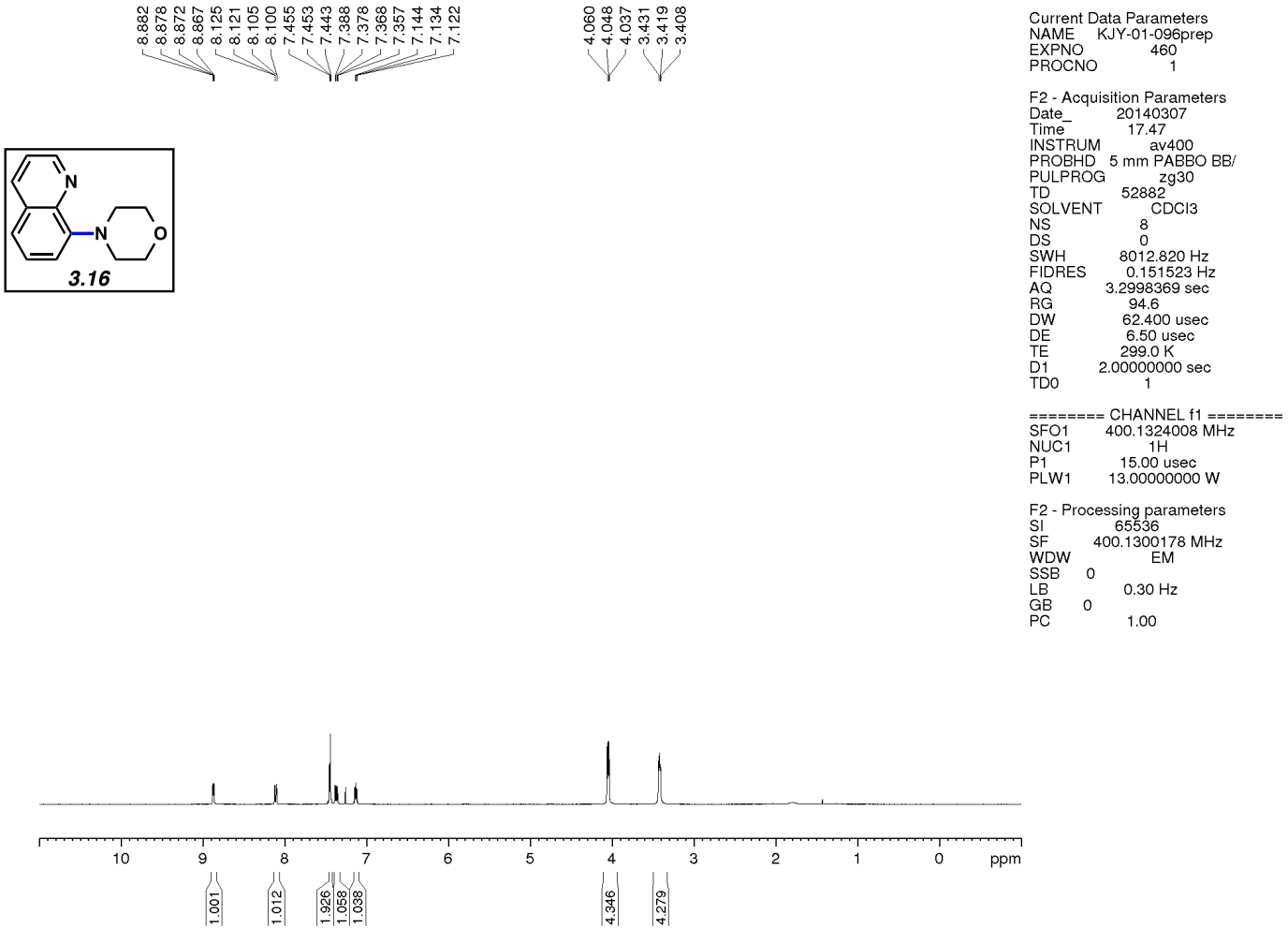

Figure 3.22 ^{1}H NMR (400 MHz, $CDCl_3$) of compound **3.16**.

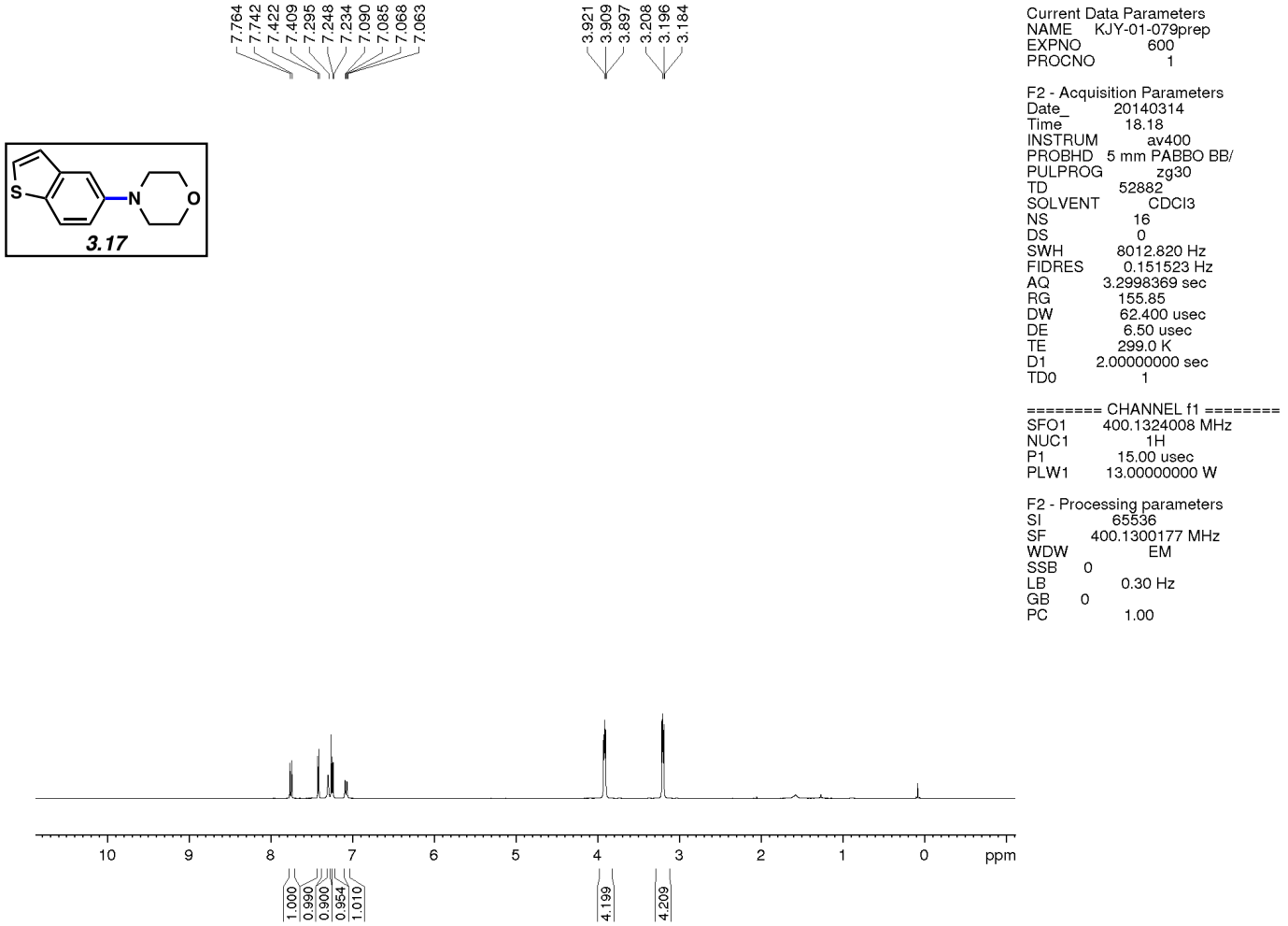

Figure 3.23 ^{1}H NMR (400 MHz, $CDCl_3$) of compound **3.17**.

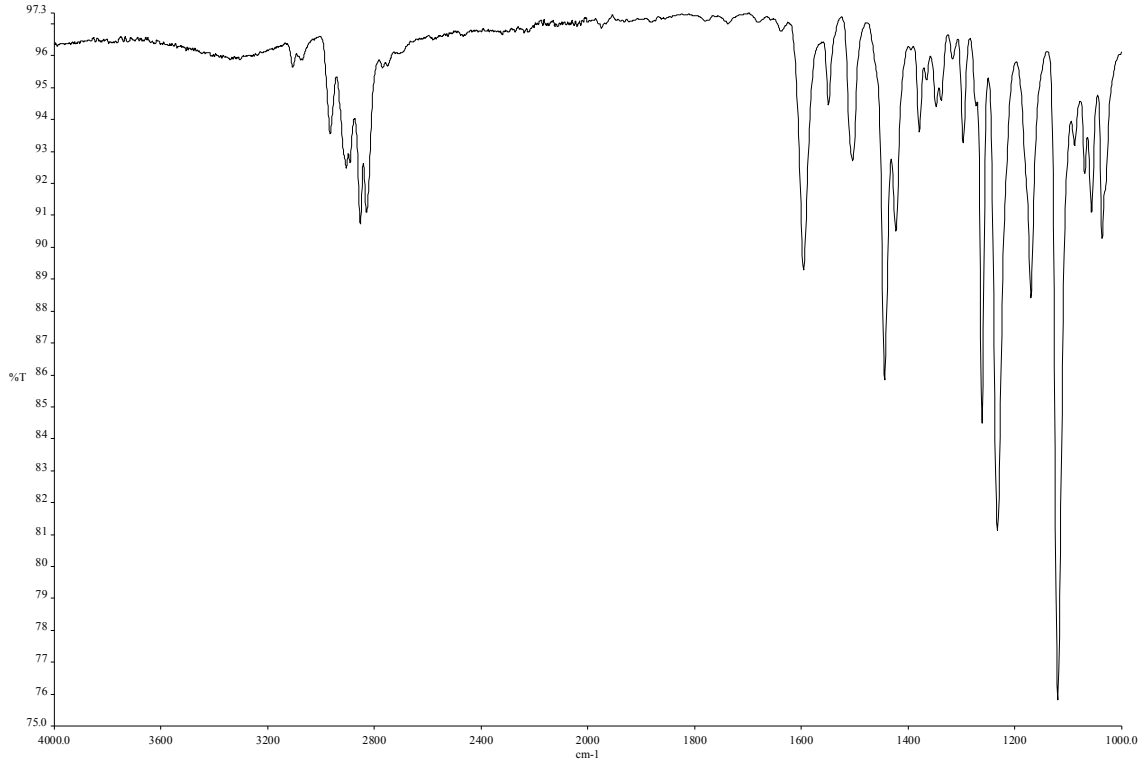

Figure 3.24 Infrared spectrum of compound **3.17**.

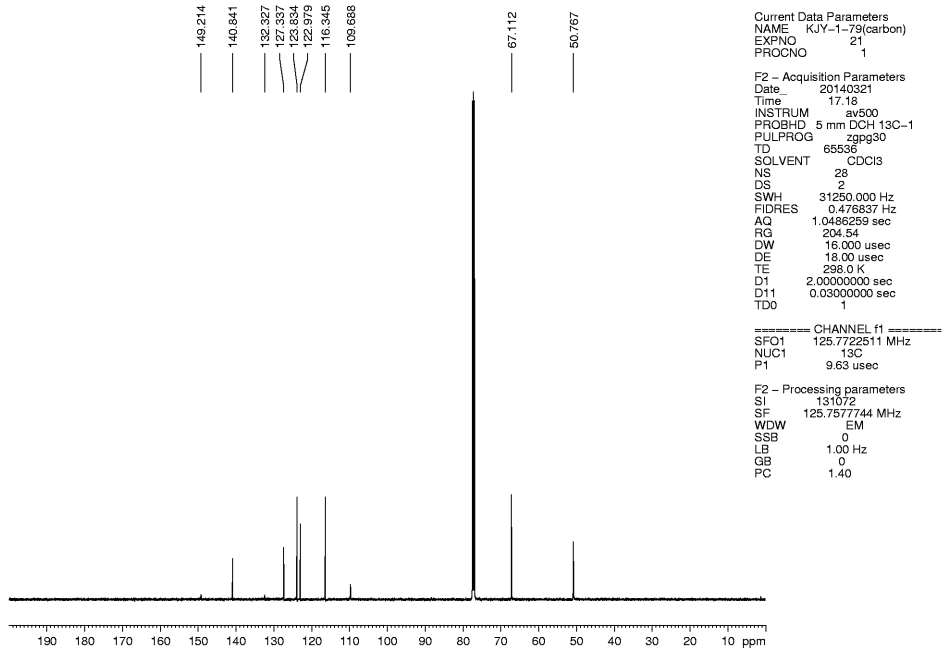

Figure 3.25 ^{13}C NMR (125 MHz, $CDCl_3$) of compound **3.17**.

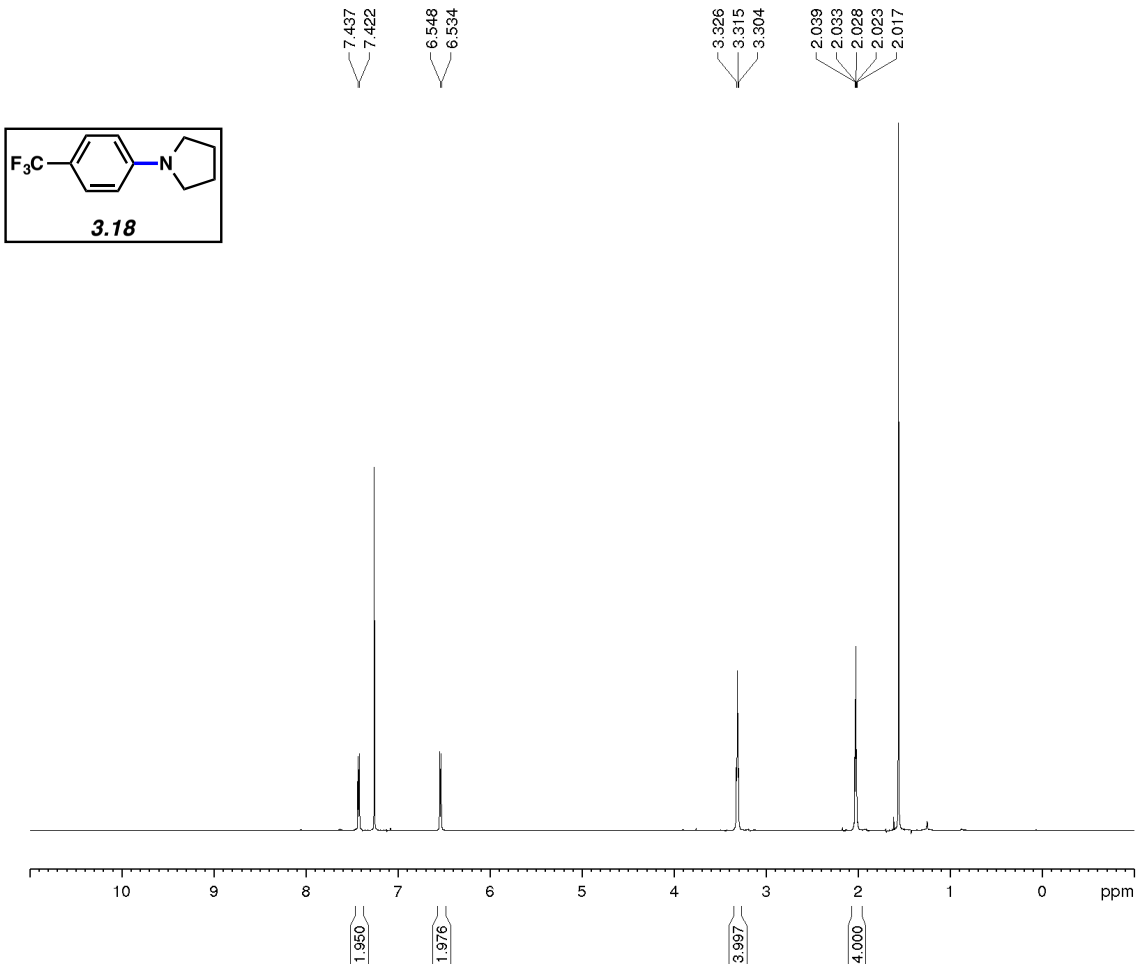

Current Data Parameters
NAME nfn-5-41c
EXPNO 2
PROCNO 1

F2 - Acquisition Parameters
Date_ 20140226
Time 17.59
INSTRUM av600
PROBHD 5 mm TBI5
PULPROG zg30
TD 65536
SOLVENT CDCl3
NS 8
DS 0
SWH 12376.237 Hz
FIDRES 0.188846 Hz
AQ 2.6476543 sec
RG 256
DW 40.400 usec
DE 6.50 usec
TE 680.7 K
D1 2.00000000 sec
TD0 1

======== CHANNEL f1 ========
NUC1 1H
P1 9.50 usec
PL1 -2.00 dB
PL1W 39.81071854 W
SFO1 600.1336008 MHz

F2 - Processing parameters
SI 65536
SF 600.1300297 MHz
WDW EM
SSB 0
LB 1.00 Hz
GB 0
PC 1.00

Figure 3.26 ^{1}H NMR (600 MHz, $CDCl_3$) of compound **3.18**.

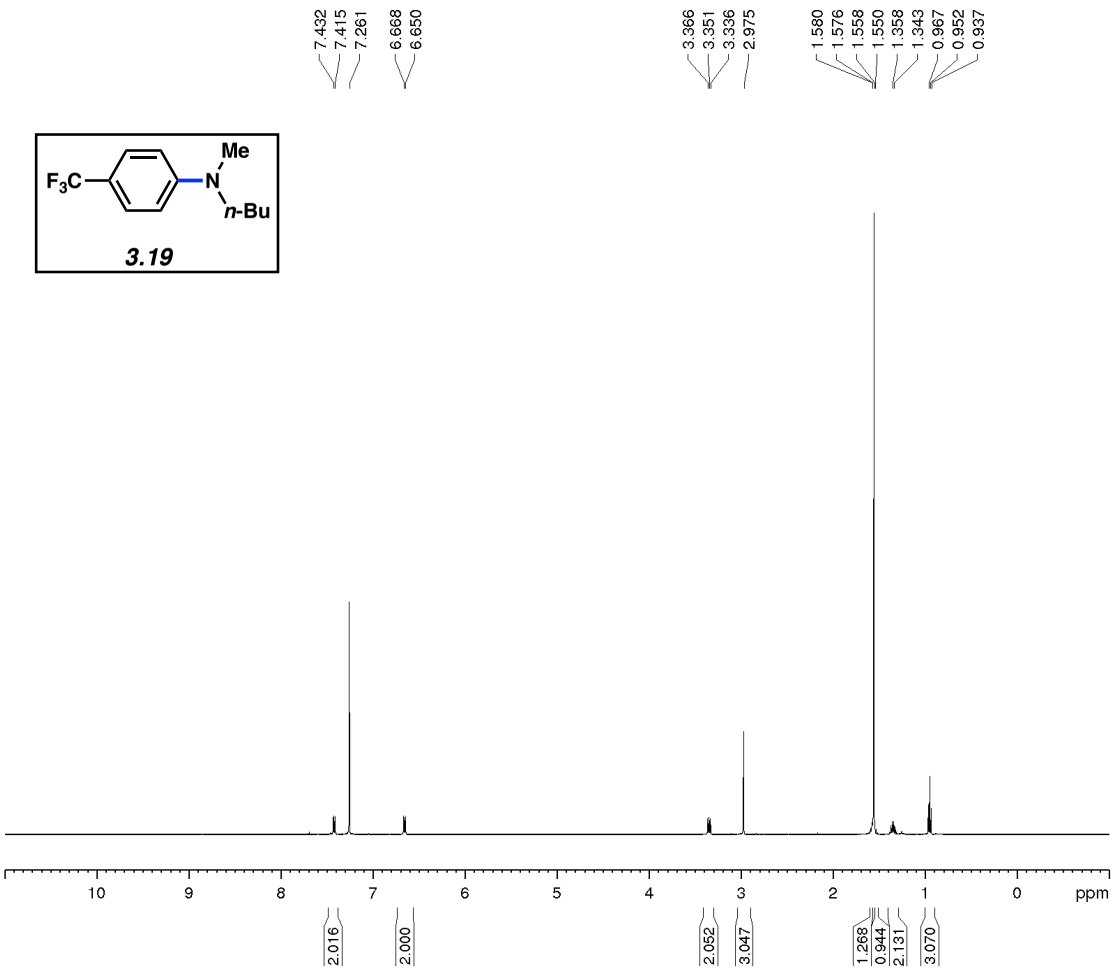


```
Current Data Parameters
NAME       nfn-5-42c2p2
EXPNO              1
PROCNO             1

F2 - Acquisition Parameters
Date_        20140227
Time           20.14
INSTRUM        drx500
PROBHD  5 mm bb-Z Z800
PULPROG         zg30
TD             65536
SOLVENT        CDCl3
NS               24
DS               0
SWH        10000.000 Hz
FIDRES      0.152588 Hz
AQ         3.2767999 sec
RG              181
DW           50.000 usec
DE            6.00 usec
TE            297.3 K
D1         2.00000000 sec
TD0              1

======== CHANNEL f1 ========
NUC1               1H
P1            12.25 usec
PL1      0 dB
SFO1       500.3330020 MHz

F2 - Processing parameters
SI              32768
SF         500.3300219 MHz
WDW               EM
SSB      0
LB       0 Hz
GB       0
PC             1.00
```

Figure 3.27 ^{1}H NMR (500 MHz, $CDCl_3$) of compound **3.19**.

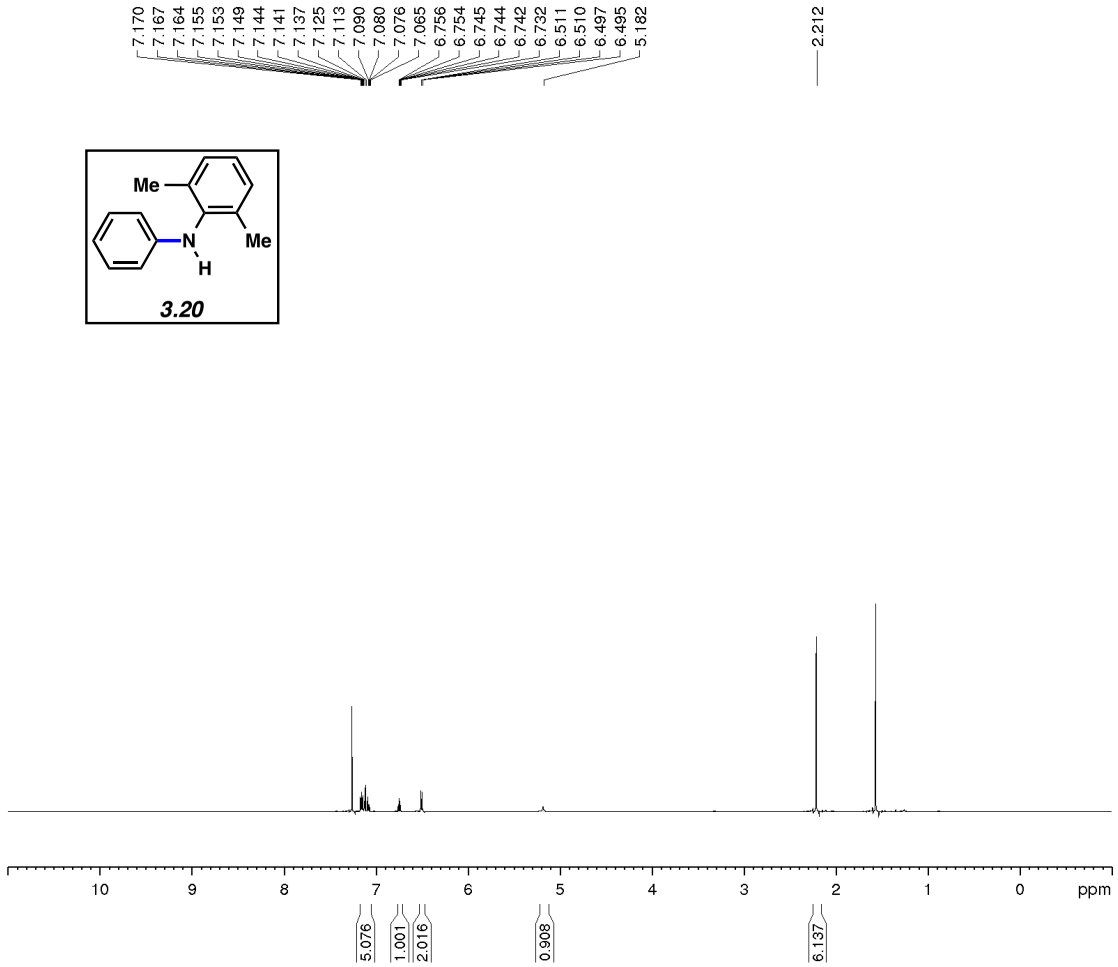

Current Data Parameters
NAME nfn-5-38c
EXPNO 2
PROCNO 1

F2 - Acquisition Parameters
Date_ 20140226
Time 17.37
INSTRUM av600
PROBHD 5 mm TBI5
PULPROG zg30
TD 65536
SOLVENT CDCl3
NS 8
DS 0
SWH 12376.237 Hz
FIDRES 0.188846 Hz
AQ 2.6476543 sec
RG 256
DW 40.400 usec
DE 6.50 usec
TE 680.9 K
D1 2.00000000 sec
TD0 1

======== CHANNEL f1 ========
NUC1 1H
P1 9.50 usec
PL1 -2.00 dB
PL1W 39.81071854 W
SFO1 600.1336008 MHz

F2 - Processing parameters
SI 65536
SF 600.1300297 MHz
WDW EM
SSB 0
LB 0.30 Hz
GB 0
PC 1.00

Figure 3.28 ^{1}H NMR (600 MHz, $CDCl_3$) of compound **3.20**.

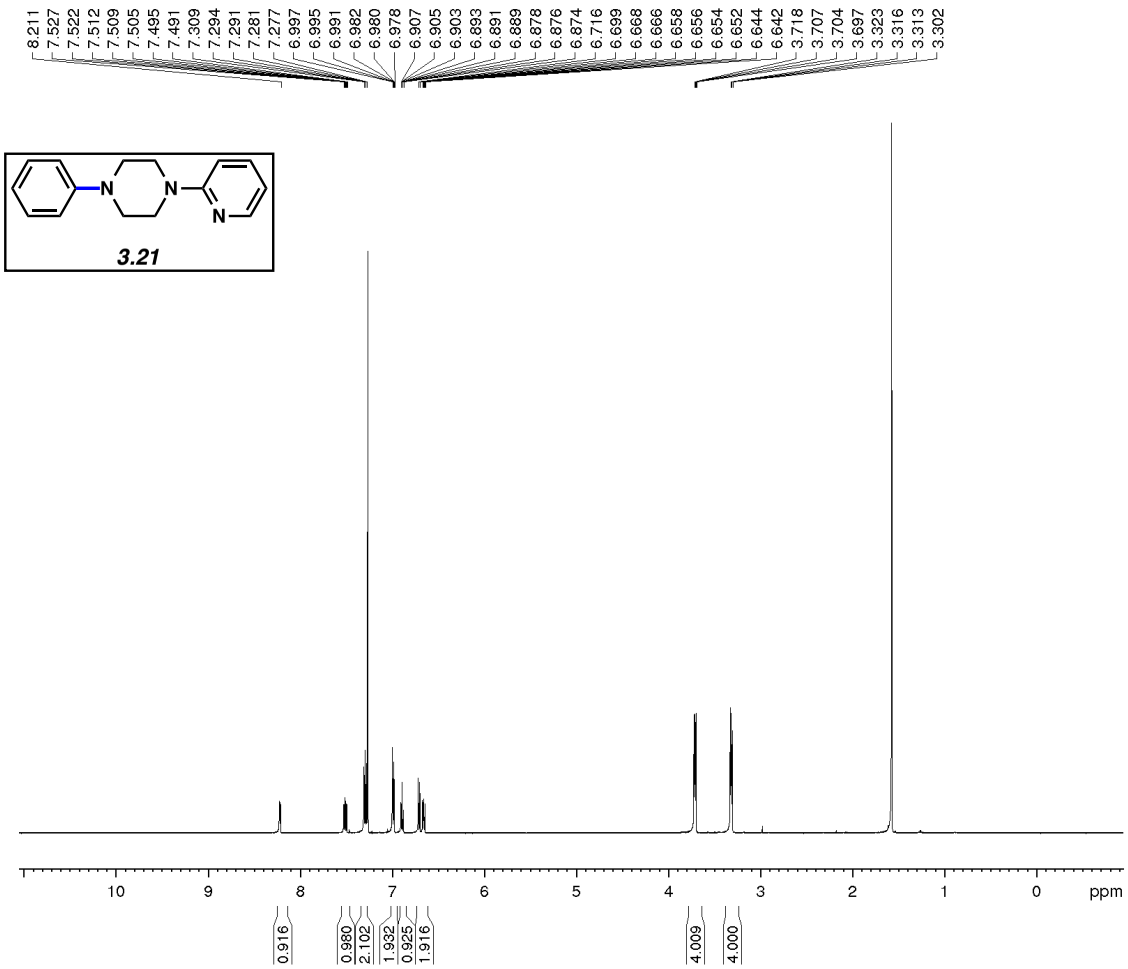

Current Data Parameters
NAME nfn-5-47a
EXPNO 1
PROCNO 1

F2 - Acquisition Parameters
Date_ 20140226
Time 22.31
INSTRUM drx500
PROBHD 5 mm bb-Z Z800
PULPROG zg30
TD 65536
SOLVENT CDCl3
NS 31
DS 0
SWH 10000.000 Hz
FIDRES 0.152588 Hz
AQ 3.2767999 sec
RG 181
DW 50.000 usec
DE 6.00 usec
TE 298.0 K
D1 2.00000000 sec
TD0 1

======== CHANNEL f1 ========
NUC1 1H
P1 12.25 usec
PL1 0 dB
SFO1 500.3330020 MHz

F2 - Processing parameters
SI 32768
SF 500.3300219 MHz
WDW EM
SSB 0
LB 0 Hz
GB 0
PC 1.00

Figure 3.29 ^{1}H NMR (500 MHz, $CDCl_3$) of compound **3.21**.

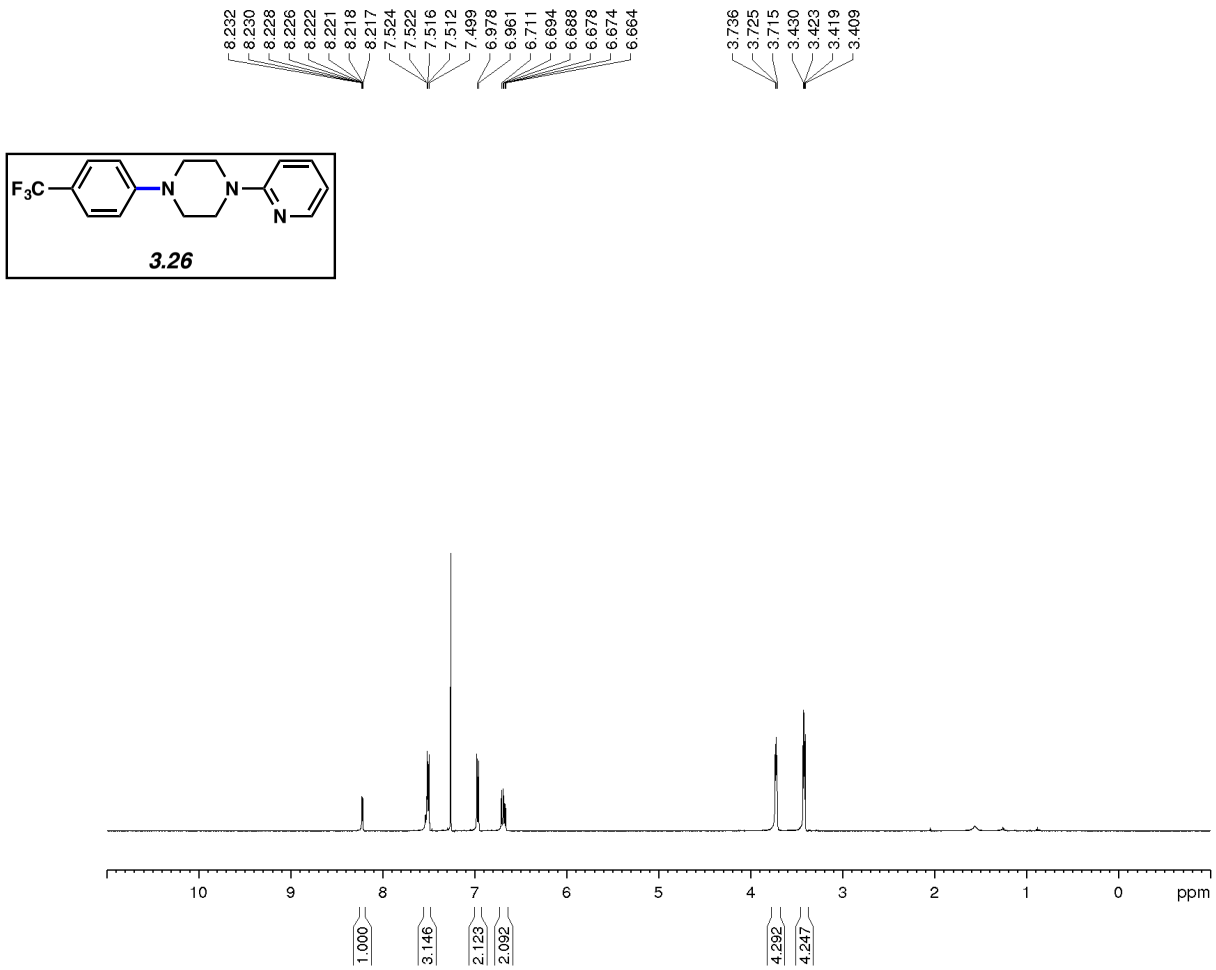

Current Data Parameters
NAME nfn-5-50b
EXPNO 1
PROCNO 1

F2 - Acquisition Parameters
Date_ 20140302
Time 21.05
INSTRUM drx500
PROBHD 5 mm bb-Z Z800
PULPROG zg30
TD 65536
SOLVENT CDCl3
NS 23
DS 0
SWH 10000.000 Hz
FIDRES 0.152588 Hz
AQ 3.2767999 sec
RG 181
DW 50.000 usec
DE 6.00 usec
TE 297.1 K
D1 2.00000000 sec
TD0 1

======== CHANNEL f1 ========
NUC1 1H
P1 12.25 usec
PL1 0 dB
SFO1 500.3330020 MHz

F2 - Processing parameters
SI 32768
SF 500.3300219 MHz
WDW EM
SSB 0
LB 0 Hz
GB 0
PC 1.00

Figure 3.30 ^{1}H NMR (500 MHz, $CDCl_3$) of compound **3.26**.

3.8 Notes and References

(1) (*a*) Hassan, J.; Sévignon, M.; Gozzi, C.; Schulz, E.; Lemaire, M. *Chem. Rev*. **2002**, *102*, 1359–1470. (*b*) Muci, A. R.; Buchwald, S. L. In *Topics in Current Chemistry*; Miyaura, N., Ed.; Springer Verlag: New York, 2002; Vol. 219, pp 131–209. (*c*) Jiang, L.; Buchwald, S. L. In *Metal-Catalyzed Cross-Coupling Reactions*, 2nd ed.; Meijere, A., Diederich, F., Eds.; Wiley-VCH: Weinheim, 2004; pp 699–760. (*d*) Corbet, J. P.; Mignani, G. *Chem. Rev*. **2006**, *106*, 2651–2710. (*e*) Negishi, E. *Bull. Chem. Soc. Jpn*. **2007**, *80*, 233–257. (*f*) Shen, H. C. In *Application of Transition Metal Catalysis in Drug Discovery and Development: An Industrial Perspective*; Crawley, M. L., Trost, B. M., Eds.; John Wiley & Sons, Inc.: Hoboken, NJ, 2012; pp 25–96.

(2) (*a*) Bolm, C.; Legros, J.; Le Paih, J.; Zani, L. *Chem. Rev*. **2004**, *104*, 6217–6254. (*b*) Enthaler, S.; Junge, K.; Beller, M. *Angew. Chem., Int. Ed*. **2008**, *47*, 3317–3321. (*c*) Bauer, E. B. *Curr. Org. Chem*. **2008**, *12*, 1341–1369. (*d*) Yu, D.-G.; Li, B.-J.; Shi, Z.-J. *Acc. Chem. Res*. **2010**, *43*, 1486–1495. (*e*) Rosen, B. M.; Quasdorf, K. W.; Wilson, D. A.; Zhang, N.; Resmerita, A.-M.; Garg, N. K.; Percec, V. *Chem. Rev*. **2011**, *111*, 1346–1416. (*f*) Li, B.-J.; Yu, D.-G.; Sun, C.-L.; Shi, Z.-J. *Chem. Eur. J*. **2011**, *17*, 1728–1759. (*g*) Mesganaw, T.; Garg, N. K. *Org. Process Res. Dev*. **2013**, *17*, 29–39. (*h*) Tasker, S. Z.; Standley, E. A.; Jamison, T. F. *Nature* **2014**, *509*, 299–309.

(3) (*a*) Anastas, P. T.; Warner, J. C. *Green Chemistry: Theory and Practice*; Oxford University Press: New York, 1998. (*b*) Anastas, P. T.; Kirchhoff, M. M. *Acc. Chem. Res*. **2002**, *35*, 686–694.

(4) (*a*) Ramgren, S. D.; Hie, L.; Ye, Y.; Garg, N. K. *Org. Lett*. **2013**, *15*, 3950–3953. (*b*) Hie, L.; Chang, J. J.; Garg, N. K. *J. Chem. Educ.* **2015**, *92*, 571–574.

(5) For reviews on Buchwald–Hartwig cross-couplings, see: (*a*) Wolfe, J. P.; Wagaw, S.; Marcoux, J.-F.; Buchwald, S. L. *Acc. Chem. Res*. **1998**, *31*, 805–818. (*b*) Hartwig, J. F. *Angew. Chem., Int. Ed*. **1998**, *37*, 2046–2067. (*c*) Anderson, K. W.; Tundel, R. E.; Ikawa, T.; Altman, R. A.; Buchwald, S. L. *Angew. Chem., Int. Ed*. **2006**, *45*, 6523–6527. (*d*) Kienle, M.; Dubbaka, S. R.; Brade, K.; Knochel, P. *Eur. J. Org. Chem*. **2007**, 4166–4176. (*e*) Surry, D. S.; Buchwald, S. L. *Angew. Chem., Int. Ed*. **2008**, *47*, 6338–6361. (*f*) Hartwig, J. F. *Acc. Chem. Res*. **2008**, *41*, 1534–1544; see also ref. 1b.

(6) For select recent examples of Ni-catalyzed aryl C–C bond couplings, see: (*a*) Guan, B.-T.; Wang, Y.; Li, B.-J.; Yu, D.; Shi, Z.-J. *J. Am. Chem. Soc*. **2008**, *130*, 14468–14470. (*b*) Quasdorf, K. W.; Tian, X.; Garg, N. K. *J. Am. Chem. Soc*. **2008**, *130*, 14422–14423. (*c*) Tobisu, M.; Shimasaki, T.; Chatani N. *Angew. Chem., Int. Ed*. **2008**, *47*, 4866–4869. (*d*) Quasdorf, K. W.; Riener, M.; Petrova, K. V.; Garg, N. K. *J. Am. Chem. Soc*. **2009**, *131*, 17748–17749. (*e*) Antoft-Finch, A.; Blackburn, T.; Snieckus, V. *J. Am. Chem. Soc*. **2009**, *131*, 17750–17752. (*f*) Xi, L.; Li, B.-J.; Wu, Z.-H.; Lu, X.-Y.; Guan, B.-T.; Wang, B.-Q.; Zhao, K.-Q.; Shi, Z.-J. *Org. Lett*. **2010**, *12*, 884–887. (*g*) Quasdorf, K. W.; Antoft-Finch, A.; Liu, P.; Silberstein, A. L.; Komaromi, A.; Blackburn, T.; Ramgren, S. D.; Houk, K. N.; Snieckus, V.; Garg, N. K. *J. Am. Chem. Soc*. **2011**, *133*, 6352–6363. (*h*) Zhang, N.; Hoffman, D. J.; Gutsche, N.; Gupta, J.; Percec, V. *J. Org. Chem*. **2012**, *77*, 5956–5964. (*i*) Ge, S.; Hartwig, J. F. *Angew. Chem., Int. Ed*. **2012**, *51*, 12837–12841; see also ref. 4.

(7) For select recent examples of Ni-catalyzed aryl C–N bond couplings, see: (*a*) Ogata, T.; Hartwig, J. F. *J. Am. Chem. Soc*. **2008**, *130*, 13848–13849. (*b*) Gao, C.-Y.; Yang, L.-M. *J. Org. Chem*. **2008**, *73*, 1624–1627. (*c*) Fors, B. P.; Watson, D. A.; Biscoe, M. R.; Buchwald, S. L. *J. Am. Chem. Soc*. **2008**, *130*, 13552–13554 (*d*) Tobisu, M.; Shimasaki, T.; Chatani, N. *Chem. Lett*. **2009**, *38*, 710–711. (*e*) Shimasaki, T.; Tobisu, M.; Chatani, N. *Angew. Chem., Int. Ed*. **2010**, *49*, 2929–2932. (*f*) Mesganaw, T.; Silberstein, A. L.; Ramgren, S. D.; Fine Nathel, N. F.; Hong, X.; Liu, P.; Garg, N. K. *Chem. Sci*. **2011**, *2*, 1766–1771. (*g*) Ramgren, S. D.; Silberstein, A. L.; Yang, Y.; Garg, N. K. *Angew. Chem., Int. Ed*. **2011**, *50*, 2171–2173. (*h*) Ackermann, L.; Sandmann, R.; Song, W. *Org. Lett*. **2011**, *13*, 1784–1786. (*i*) Huang, J.-H.; Yang L.-M. *Org. Lett*. **2011**, *13*, 3750–3753. (*j*) Hie, L.; Ramgren, S. D.; Mesganaw, T.; Garg, N. K. *Org. Lett*. **2012**, *14*, 4182–4185.

(8) For select seminal studies on aryl C–C and C–N bond coupling using Ni catalysis, see: (*a*) Sengupta, S.; Leite, M.; Raslan, D. S.; Quesnelle, C.; Snieckus, V. *J. Org. Chem*. **1992**, *57*, 4066–4068. (*b*) Wolfe, J. P.; Buchwald, S. L. *J. Am. Chem. Soc*. **1997**, *119*, 6054–6058. (*c*) Hamann, B. C.; Hartwig, J. F. *J. Am. Chem. Soc*. **1998**, *120*, 7369–7370. (*d*) Brenner, E.; Fort, Y. *Tetrahedron Lett*. **1998**, *39*, 5359–5362. (*e*) Wehn, P. M.; Du Bois, J. *Org. Lett*. **2005**, *7*, 4685–4688.

(9) The addition of Ph–B(pin) is believed to be instrumental in reducing the Ni(II) precatalyst to an active Ni(0) species.

(10) For nickel catalyzed amination methodologies that use Ni(II) precatalysts with Zn or hydrides as reducing agents, see: (*a*) Fan, X.-H.; Li, G.; Yang, L.-M. *J. Organomet. Chem*. **2011**, *696*, 2482–2484. (*b*) Gao, C.-Y.; Cao, X.; Yang, L.-M. *Org. Biomol. Chem*. **2009**, *7*,

3922–3925. (*c*) Manolikakes, G.; Gavryushin, A.; Knochel, P. *J. Org. Chem*. **2008**, *73*, 1429–1434. (*d*) Omar-Amrani, R.; Thomas, A.; Brenner, E.; Schneider, R.; Fort, Y. *Org. Lett*. **2003**, *5*, 2311–2314. (*e*) Desmarets, C.; Schneider, R.; Fort, Y. *J. Org. Chem*. **2002**, *67*, 3029–3036. (*f*) Gradel, B.; Brenner, E.; Schneider, R.; Fort, Y. *Tetrahedron Lett*. **2001**, *42*, 5689–5692.

(11) Solvents were selected from the ACS Green Chemistry Institute Roundtable Solvent Selection Guide. **http://www.acs.org/content/dam/acsorg/greenchemistry/industriainnovation/roundtable/acs-gci-pr-solvent-selection-guide.pdf.**

(12) For solvent selection guides in medicinal chemistry, see: (*a*) Alfonsi, K.; Colberg, J.; Dunn, P. J.; Fevig, T.; Jennings, S.; Johnson, T. A.; Kleine, H. P.; Knight, C.; Nagy, M. A.; Perry, D. A.; Stefaniak, M. *Green Chem*. **2008**, *10*, 31–36. (*b*) Henderson, R. K.; Jiménez-González, C.; Constable, D. J. C.; Alston, S. R.; Inglis, G. G. A.; Fisher, G.; Sherwood, J.; Binks, S. P.; Curzons, A. D. *Green Chem*. **2011**, *13*, 854– 862.

(13) For a discussion on CPME, see: (*a*) Watanabe, K.; Yamagiwa, N.; Torisawa, Y. *Org. Process Res. Dev*. **2007**, *11*, 251–258. (*b*) Antonucci, V.; Coleman, J.; Ferry, J. B.; Johnson, N.; Mathe, M.; Scott, J. P.; Xu, J. *Org. Process Res. Dev*. **2011**, *15*, 939–941.

(14) *Tert*-Amyl alcohol was also considered an especially promising solvent for the amination reaction; however, it was found to be less generally useful compared to 2-Me-THF in attempts to couple various other substrates.

(15) For discussion on 2-Me-THF, see: (*a*) Aycock, D. F. *Org. Process Res. Dev*. **2007**, *11*, 156–159. (*b*) Pace, V.; Hoyos, P.; Castoldi, L.; Domínguez de María, P.; Alcántara, A. R. *ChemSusChem* **2012**, *5*, 1369–1379; see also ref. 13b.

(16) Aryl chlorides are attractive substrates as they are often available commercially or are easily synthesized. Additionally, aryl chlorides are often robust enough to be carried through multiple synthetic operations.

(17) Aryl sulfamates bear many notable features. They are easily synthesized from their corresponding phenols, which are often commercially available, and are generally stable to acidic and basic reaction conditions. Moreover, aryl sulfamates may be used to direct arene functionalization through electrophilic aromatic substitution or *ortho*-lithiation processes. For a discussion of these features, see: (*a*) Snieckus, V. *Chem. Rev*. **1990**, *90*, 879–933. (*b*) Hartung, C. G.; Snieckus V. In *Modern Arene Chemistry*; Astruc, D., Ed.; Wiley-VCH: New York, 2002; pp. 330–367. (*c*) Macklin, T. K., Snieckus, V. *Org. Lett*. **2005**, *7*, 2519–2522. (*d*) Snieckus, V.; Macklin, T. In *Handbook of C-H Transformations*; Dyker G., Ed.; Wiley-VCH: New York, 2005; Vol. 1, pp 106–118; see also ref. 6d.

(18) Piel, I.; Steinmetz, M.; Hirano, K.; Frohlich, R.; Grimme, S.; Glorius, F. *Angew. Chem., Int. Ed.* **2011**, *50*, 4983–4987.

(19) Civicos, J. F.; Alonso, D. A.; Najera, C. *Adv. Synth. Catal.* **2012**, *354*, 2771–2776.

(20) Quasdorf, K. W.; Tian, X.; Garg, N. K. *J. Am. Chem. Soc.* **2008**, *130*, 14422–14423.

(21) (*a*) Quasdorf, K. W.; Riener, M.; Petrova, K. V.; Garg, N. K. *J. Am. Chem. Soc.* **2009**, *131*, 17748–17749. (*b*) Antoft-Finch, A.; Blackburn, T.; Snieckus, V. *J. Am. Chem. Soc.* **2009**, *131*, 17750–17752.

(22) (*a*) King, J. F.; Lee. T. M. *Can. J. Chem.* **1981**, *59*, 356–361. (*b*) Ramgren, S. D.; Silberstein, A. L.; Yang, Y.; Garg, N. K. *Angew. Chem., Int. Ed.* **2011**, *50*, 2171–2173. (*c*) Leowanawat, P.; Zhang, N.; Resmerita, A.-M.; Rosen, B. M.; Percec, V. *J. Org. Chem.* **2011**, *76*, 9946–9955. **(***d*) Quasdorf, K. W.; Antoft-Finch, A.; Liu, P.; Silberstein, A. L.; Komaromi, A.; Blackburn, T.; Ramgren, S. D.; Houk, K. N.; Snieckus, V.; Garg, N. K. *J. Am. Chem. Soc.* **2011**, *133*, 6352–6363. (*e*) Agrawal, T.; Cook, S. P. *Org. Lett.* **2013**, *15*, 96–99. (*f*) Molander, G. A.; Shin, I. *Org. Lett.* **2013**, *15*, 2534–2537.

(23) Desmarets, C.; Champagne, B.; Walcarius, A.; Bellouard, C.; Omar-Amrani, R.; Ahajji, A.; Fort, Y.; Schneider, R. *J. Org. Chem*. **2006**, *71*, 1351–1361.

(24) Barker, T. J.; Jarvo, E. R. *J. Am. Chem. Soc.* **2009**, *131*, 15598–15599.

(25) Wolfe, J. P.; Buchwald, S. L. *J. Org. Chem.* **1996**, *61*, 1133–1135.

(26) Guo, D.; Huang, H.; Xu, J.; Jiang, H.; Liu, H. *Org. Lett.* **2008**, *10*, 4513–4516.

(27) Fasani, E.; Tilocca, F.; Protti, S.; Merli, D.; Albini, A. *Org. Biomol. Chem.* **2008**, *6*, 4634–4642.

(28) Wagaw, S.; Buchwald, S. L. *J. Org. Chem.* **1996**, *61*, 7240–7241.

(29) Mesganaw, T.; Silberstein, A. L.; Ramgren, S. D.; Fine Nathel, N. F.; Hong, X.; Liu, P.; Garg, N. K. *Chem. Sci.* **2011**, *2*, 1766–1771.

(30) Tobisu, M.; Yasutome, A.; Yamakawa, K.; Shimasaki, T.; Chatani, N. *Tetrahedron* **2012**, *68*, 5157–5161.

(31) Brenner, E.; Schneider, R.; Fort, Y. *Tetrahedron* **1999**, *55*, 12829–12842.

(32) Zhu, F.; Wang, Z.-X. *Adv. Synth. Catal.* **2013**, *355*, 3694–3702.

CHAPTER FOUR

Nickel-Catalyzed Suzuki–Miyaura Coupling of Aliphatic Amides

Timothy B. Boit,[†] Nicholas A. Weires,[†] Junyong Kim,[†] and Neil K. Garg

ACS Catal. **2018**, *8*, 1003–1008.

4.1 Abstract

We report the Ni-catalyzed Suzuki–Miyaura coupling of aliphatic amide derivatives. Prior studies have shown that aliphatic amide derivatives can undergo Ni-catalyzed carbon–heteroatom bond formation, but Ni-mediated C–C bond formation using aliphatic amide derivatives has remained difficult. The coupling disclosed herein is tolerant of considerable variation with respect to both the amide-based substrate and the boronate coupling partner, and proceeds in the presence of heterocycles and epimerizable stereocenters. Moreover, a gram-scale Suzuki–Miyaura coupling / Fischer indolization sequence demonstrates the ease with which unique poly-heterocyclic scaffolds can be constructed, particularly by taking advantage of the enolizable ketone functionality present in the cross-coupled product. The methodology provides an efficient means to form C–C bonds from aliphatic amide derivatives using non-precious metal catalysis and offers a general platform for the hetero-arylation of aliphatic acyl electrophiles.

4.2 Introduction

The facile unification of molecular fragments via C–C bond formation represents an important and challenging objective in transition metal catalysis.[1] Although the field has been largely dominated by the coupling of aryl electrophiles, there has been a recent resurgence in

developing analogous methods using stable acyl electrophiles. More specifically, esters and amides have emerged as useful synthetic building blocks in a variety of acyl cross-coupling manifolds. Recent breakthroughs in the area include the Suzuki–Miyaura coupling of phenyl esters reported independently by Newman and Szostak, which proceeds using palladium catalysis,[2,3] in addition to numerous amide C–N bond activation studies using either palladium or nickel.[4,5,6,7,8,9]

We and others have been especially interested in using nickel catalysis to enable facile C–C bond formation from amide derivatives. Such methods provide new strategies for the synthesis of ketones which complement Weinreb's methodology,[10] but importantly avoid the use of highly basic or pyrophoric reagents. Previously, we have shown that nickel catalysis can promote the cross-coupling of Ts- or Boc- activated benzamide derivatives in C–C bond forming reactions.[4b,4d,4k] These cross-coupling platforms have allowed for the efficient coupling of *aryl* amide electrophiles, however, the corresponding activation of *aliphatic* amides is more challenging. Prior computational studies suggest that the use of aliphatic amides is inherently more difficult because of the high kinetic barrier of activation associated with oxidative addition into the resonance-stabilized C–N bond.[4a] Indeed, achievements in cross-couplings of aliphatic amides using Ni catalysis is limited to carbon-heteratom bond formation.[4h,o] Molander and coworkers have also reported an elegant coupling of *N*-acyl succinimides with alkyl trifluoroborate salts employing a dual-metal photoredox approach using nickel and an iridium photocatalyst,[9] which nicely complements the method described herein.[11,12]

With the aim of developing a general cross-coupling manifold to build C–C bonds from aliphatic amides, we targeted the Suzuki–Miyaura coupling shown in Figure 4.1. From the outset, we opted to focus our efforts on the coupling of heterocyclic fragments due to their

prevalence in bioactive molecules. Certain heterocycles can be challenging to employ in metal-mediated cross couplings as they are known to ligate metal catalysts and inhibit reactivity.[1b] Moreover, only a handful of isolated examples of hetero-arylative Suzuki–Miyaura couplings of aliphatic acyl electrophiles exist[13] (i.e., anhydrides,[13a,b] thioesters,[13c,d] acid chlorides[13e,f]), and a general platform for the hetero-arylation of aliphatic acyl electrophiles has not been developed. In this manuscript, we describe the nickel-catalyzed Suzuki–Miyaura coupling of aliphatic amide derivatives. Importantly, this methodology provides rapid access to functionalizable heterocyclic scaffolds, while expanding the scope of synthetically useful transformations involving amide derivatives and non-precious metal catalysis.

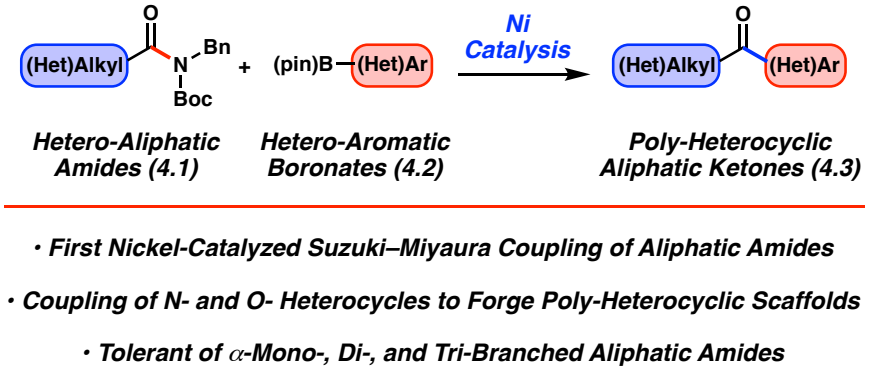

Figure 4.1. Suzuki–Miyaura hetero-arylation of aliphatic amides to construct poly-heterocyclic scaffolds.

4.3 Evaluation of Ligand Effects in the Suzuki–Miyaura Coupling

To initiate our study, we examined the coupling of piperidine derivative **4.4**[14] with *N*-methylpyrrole-2-boronic acid pinacol ester (**4.5**) as shown in Table 4.1. Our initial attempts to employ the *N*-heterocyclic carbene (NHC) ligand SIPr (**4.7**), which we had previously shown to be competent in the Suzuki–Miyaura coupling of aromatic amide derivatives,[4b] were met with

difficulty, as no trace of the desired ketone product **4.6** was formed at 50 °C (entry 1). Moreover, increasing the temperature to 120 °C only led to partial decomposition of substrate **4.4** (entry 2). Next, we screened several ligand frameworks that have been used in the context of nickel-catalyzed couplings. Interestingly, efforts to utilize the ligand terpyridine (**4.8**), which had been shown to facilitate the nickel-catalyzed esterification of aliphatic amide derivatives,[4h] were also unfruitful (entry 3). Gratifyingly, however, use of the NHC precursor ICy•HBF_4 (**4.9**) was found to promote the desired Suzuki–Miyaura coupling, and delivered ketone **4.6** in 95% yield (entry 4). Ligand **4.9** has been used in other nickel-catalyzed processes,[5b,5f,15] including in the Heck reaction of benzamide derivatives.[4k] Finally, the related NHC precursor Benz-ICy•HCl (**4.10**) was evaluated and found to give similarly useful results (entry 5). As NHC precursor **4.10** was found to be broadly effective in subsequent scouting experiments, it was used in our further studies.[16] Lastly, although we focus on the use of *N*-Bn,Boc amides in this study, it should be noted that the methodology is not limited to the use of the *N*-benzyl group. For example, coupling of *N*-*i*Pr,Boc cyclohexamide with boronate **4.5** under the optimized conditions gave the corresponding ketone in 72% yield.

Table 4.1. Evaluation of reaction conditions for the coupling of aliphatic amides.[a]

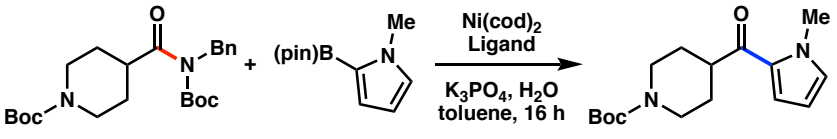

4.4 | *4.5* (2.5 equiv) | *4.6*

Entry	*Temp.*	*Ni(cod)$_2$*	*Ligand*	*Remaining 4.4*	*Yield of 4.6*
1	50 °C	5 mol%	*4.7* (10 mol%)	100%	0%
2	120 °C	5 mol%	*4.7* (10 mol%)	52%	0%
3	120 °C	5 mol%	*4.8* (10 mol%)	50%	0%
4	120 °C	5 mol%	*4.9* (10 mol%)	0%	95%
5	120 °C	5 mol%	*4.10* (10 mol%)	0%	95%

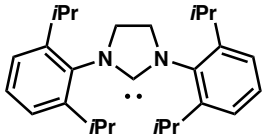

SIPr (4.7)

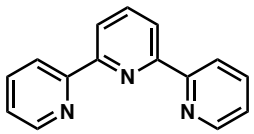

terpyridine (4.8)

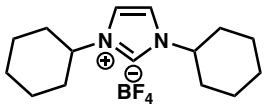

ICy·HBF$_4$ (4.9)

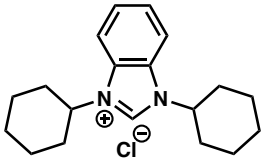

Benz-ICy·HCl (4.10)

[a] Conditions: Ni(cod)$_2$ (5 mol%), **4.7**–**4.10** (10 mol%), substrate **4.4** (1.0 equiv), boronate **4.5** (2.5 equiv), K_3PO_4 (4.0 equiv), toluene (1.0 M), and H_2O (2.0 equiv) heated at the indicated temperature for 16 h. Yields were determined by ^{1}H NMR analysis using hexamethylbenzene as an internal standard.

4.4 Scope of the Coupling with Hetero-Aliphatic Amides and Hetero-Aryl Boronates

With optimized conditions in hand, we explored the scope of the coupling with respect to both the hetero-aliphatic amide-derived substrate and the hetero-aryl boronate, producing a variety of bis-heterocyclic ketone products (Figure 4.2). The reaction was found to be widely tolerant of *N*-heterocyclic boronate nucleophiles, including pyrrole, quinoline, indole, pyrazole, and morpholino-pyridine moieties, as demonstrated by the formation of **4.6** and **4.11**–**4.16**, all in

good yields. Moreover, an isomeric piperidine amide substrate could be utilized, allowing for the formation of pyrrolo- and pyrazolo-ketones **4.17** and **4.18**, respectively. Alternatively, the pyrrolidine heterocycle could also be employed to generate ketones **4.19** and **4.20** in 82% and 90% yields, respectively. Finally, substrates derived from both 4- and 3-isomers of tetrahydropyran carboxylic acid were shown to be competent in the coupling, furnishing ketones **4.21**–**4.25** in good to excellent yields. The formation of **4.25** highlights the use of an oxygen-containing heterocyclic boronate in the coupling reaction. It is also worth noting that non-heterocyclic aryl boronates, such as 2-naphthyl and phenyl boronic esters, could be employed in the Suzuki–Miyaura coupling as demonstrated by the formation of **4.26** and **4.27**, respectively. In addition, *o*-Me, *p*-CF_3, and *p*-CO_2Me substituents were tolerated on the phenyl boronate, giving rise to ketones **4.28**–**4.30**, respectively.[17]

Figure 4.2. Scope of the Suzuki–Miyaura coupling with hetero-aliphatic amide substrates and hetero-aryl boronates.

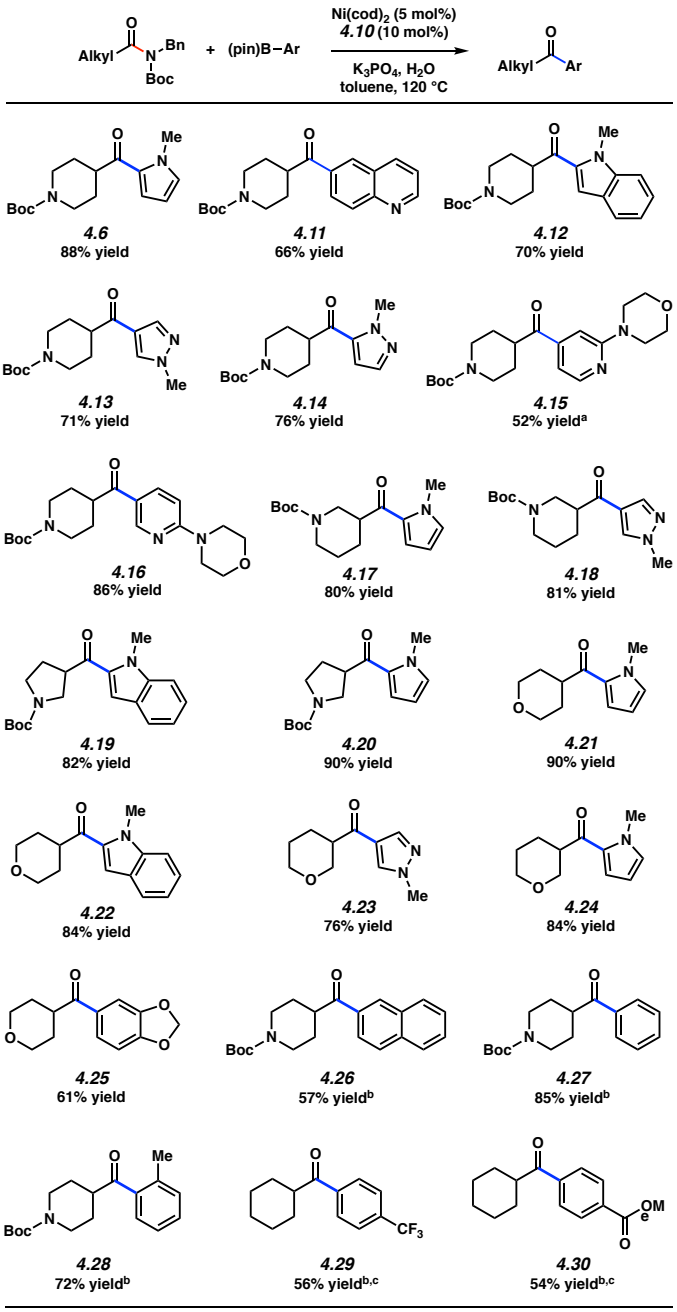

Conditions: $Ni(cod)_2$ (5 mol%), **4.10** (10 mol%), substrate (1.0 equiv), boronate (2.5 equiv), K_3PO_4 (4.0 equiv), toluene (1.0 M), and H_2O (2.0 equiv) heated at 120 °C for 16 h. Yields reflect the average of two isolation experiments. [a] The reaction was run using 3.3 equiv of the boronate. [b] Yield determined by ^1H NMR analysis using hexamethylbenzene as an external standard. [c] The reaction was run for 24 h using 5.0 equiv of the boronate.

4.5 Scope of the Coupling with Non-Heterocyclic Aliphatic Amide Substrates

The scope of the hetero-arylative coupling with boronate **4.5** was also evaluated with respect to several non-heterocyclic aliphatic amide derivatives (Figure 4.3). Substrates derived from dihydrocinnamic and decanoic acids coupled in high yields to furnish ketones **4.31** and **4.32**, respectively. Additionally, α-branched carbocyclic amides also underwent efficient couplings, providing pyrrolo-ketones **4.33** and **4.34**. Lastly, sterically encumbered carboxamides could also be employed in the coupling, as demonstrated by the production of *tert*-butyl ketone **4.35** in excellent yield.

Figure 4.3. Scope of the coupling with non-heterocyclic aliphatic amide substrates and boronate **4.5**.

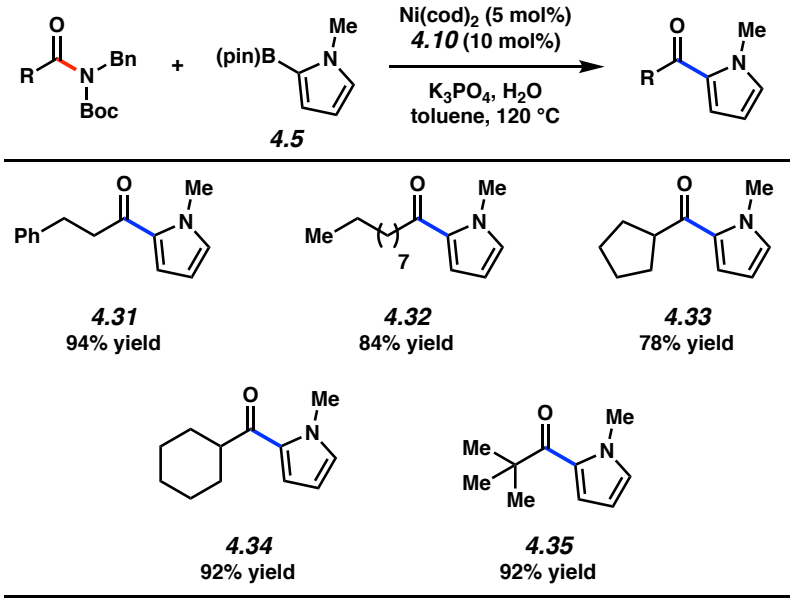

Conditions: $Ni(cod)_2$ (5 mol%), **4.10** (10 mol%), substrate (1.0 equiv), boronate **4.5** (2.5 equiv), K_3PO_4 (4.0 equiv), toluene (1.0 M), and H_2O (2.0 equiv) heated at 120 °C for 16 h. Yields reflect the average of two isolation experiments.

4.6 Evaluation of the Coupling with a Benzamide Substrate

Although our manuscript focuses on *aliphatic* amides for the reasons mentioned earlier, we were curious if our optimal reaction conditions could be applied to a benzamide substrate (Figure 4.4). We have reported earlier the coupling of *N*-Bn,Boc benzamide **4.36** with phenylboronic acid pinacol ester **4.37** using a Ni/SIPr system at 50 ºC. This gives ketone **4.38** in 96% yield (entry 1).[4b] We performed the corresponding coupling of **4.36** and **4.37** using the Ni/Benz-ICy catalyst system. At 50 °C, we obtained only a 14% yield of the cross-coupled product **4.38** (entry 2). We also performed the cross-coupling using the Ni/Benz-ICy catalyst system at 120 ºC, which furnished **4.38** in 60% yield (entry 3).[18] As such, for practioners of this methodology, we recommend the use of Ni/SIPr at 50 °C to achieve the Suzuki–Miyaura coupling of benzamide-type substrates[4b] and the use of the conditions reported herein (i.e., Ni/Benz-ICy at 120 °C) for aliphatic amides.

Figure 4.4. Suzuki–Miyaura coupling of amide **4.36** with boronate **4.37** using Ni/SIPr and Ni/Benz-ICy catalyst systems.

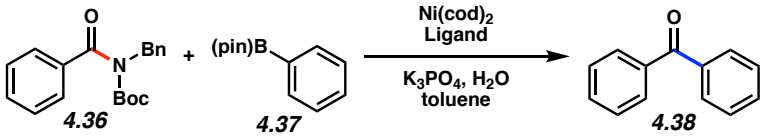

Entry	*Temp.*	*Mol % Ni*	*Ligand (mol%)*	*Yield of 4.38*
1[a]	50 °C	5 mol%	*SIPr* (*4.7*, 5 mol%)	96%
2[b,c]	50 °C	5 mol%	*Ben-ICy·HCl* (*4.10*, 10 mol%)	14%
3[b,c]	120 °C	5 mol%	*Ben-ICy·HCl* (*4.10*, 10 mol%)	60%

Conditions: [a] $Ni(cod)_2$ (5 mol%), **4.7** (5 mol%), substrate (1.0 equiv), boronate **4.5** (1.2 equiv), K_3PO_4 (2.0 equiv), toluene (1.0 M), and H_2O (2.0 equiv) heated at 50 ºC for 24 h. [b] $Ni(cod)_2$ (5 mol%), **4.10** (10 mol%), substrate (1.0 equiv), boronate **4.5** (2.5 equiv), K_3PO_4 (4.0 equiv), toluene (1.0 M), and H_2O (2.0 equiv) heated at the indicated temperature for 16 h. [c] Yields reflect the average of two experiments; yields were determined by ^1H NMR analysis using hexamethylbenzene as an external standard.

4.7 Evaluation of the Coupling with Substrates Containing Epimerizable Stereocenters

We also questioned if the methodology would be amenable to the coupling of an amide substrate containing a defined chiral center *α* to the carbonyl. As such, we attempted the coupling between amide **4.39** and boronate **4.5** (Figure 4.5). Although the use of standard conditions (i.e., 120 ºC for 16 h), gave the desired ketone product **4.40** in 68% yield, roughly 20% epimerization was also observed. We found that by carrying out the reaction at 90 ºC for 2 h, the epimerization could be avoided. Thus, ketone **4.40** was obtained in 70% yield, without observable formation of the *syn* diastereomer. Moreover, the tolerance of the ester (and other functional groups)[19] underscores the complementarity of this methodology to the Weinreb ketone synthesis,[10] where such electrophilic functional groups typically do not withstand the use of highly basic and nucleophilic organometallic reagents. Importantly, this result provides the first example of an amide or ester Suzuki–Miyaura coupling that proceeds smoothly in the presence of an epimerizable stereocenter *α* to the amide carbonyl. The tolerance of the method to defined stereocenters *α* to the carbonyl was also evaluated using enantioenriched cyclohexenyl amide **4.41**. Using standard conditions (i.e., 120 ºC for 16 h), the desired ketone **4.42** was obtained in 81% yield, but only in 14% *ee*. By lowering the temperature of the reaction to 70 ºC, the desired coupling of **4.41** with boronate **4.5** proceeded in good yield and with significant preservation of stereochemical information. We hypothesize that the observed epimerization stems from the basicity of the deprotonated Benz-ICy•HCl (**4.10**). In fact, subjection of enantioenriched **4.42** to the free NHC in toluene at 120 ºC for 4 h led to complete racemization of the substrate. In contrast, the corresponding experiments performed with Benz-ICy•HCl (**4.10**) or K_3PO_4 led to no or minimal observable loss in *ee*, respectively. It should also be noted that ketone product **4.42** was observed to racemize more readily than amide **4.41** under the standard reaction

conditions. Nonetheless, these results demonstrate the mildness of the reaction conditions and bode well for future synthetic applications.

Figure 4.5. Stereoretentive Suzuki–Miyaura couplings of amide **4.39** and enantioenriched amide **4.41**.

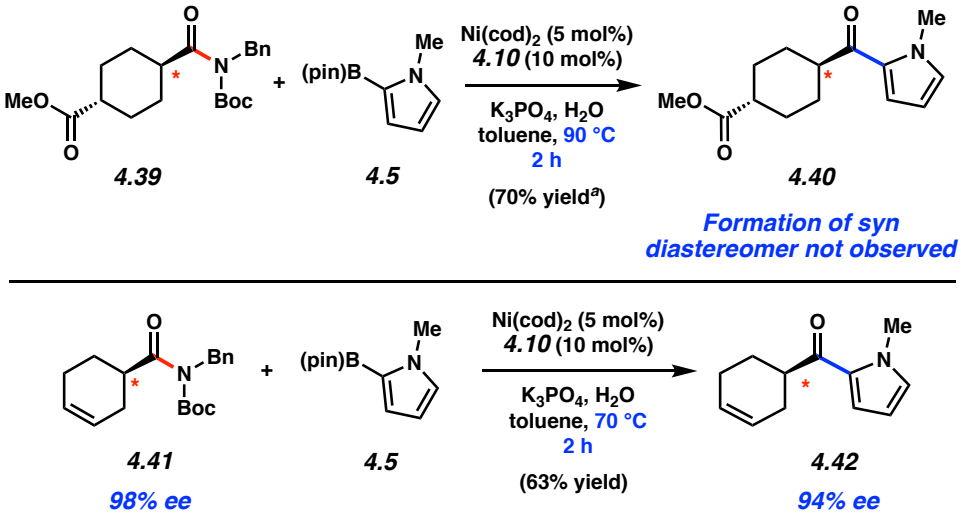

Conditions: $Ni(cod)_2$ (5 mol%), **4.10** (10 mol%), substrate (1.0 equiv), boronate **4.5** (2.5 equiv), K_3PO_4 (4.0 equiv), toluene (1.0 M), and H_2O (2.0 equiv) heated at 70 °C for 2 h. Yield reflects the average of two isolation experiments. [a] Reaction was run at 90 ºC for 2 h; yield was determined by ^1H NMR analysis using hexamethylbenzene as an external standard.

4.8 Gram-Scale Suzuki–Miyaura Coupling and Subsequent Fischer Indolization

In comparison to more classical aryl-aryl couplings, the products obtained from this methodology possess enolizable ketones, which serve as valuable synthetic handles. As a demonstration of this benefit, we performed a gram-scale Suzuki–Miyaura coupling and subsequent Fischer indolization reaction to construct a poly-heterocyclic spiroindolenine scaffold (Figure 4.6). Spiroindolenines are commonly seen in bioactive molecules[20] and also serve as valuable synthetic intermediates.[21] In the event, Suzuki–Miyaura coupling of tetrahydropyran carboxamide **4.43** with boronate **4.44** took place on gram scale under conditions employing

reduced boronate, catalyst, and ligand loadings (1.2 equiv, 2.5 and 5 mol%, respectively) to furnish ketone **4.45** in 82% yield. Next, ketone **4.45** was transformed into spirocycle **4.47** in 61% yield by reaction with phenylhydrazine (**4.46**) in the presence of TFA by way of a Fischer indolization.[22] The rapid construction of poly-heterocyclic spiroindolenine **4.47**,[23] hinging upon the classical reactivity of enolizable ketones, underscores the utility of the Suzuki–Miyaura coupling of aliphatic amides and further demonstrates the ease with which a variety of unique heterocyclic compounds can be fashioned.

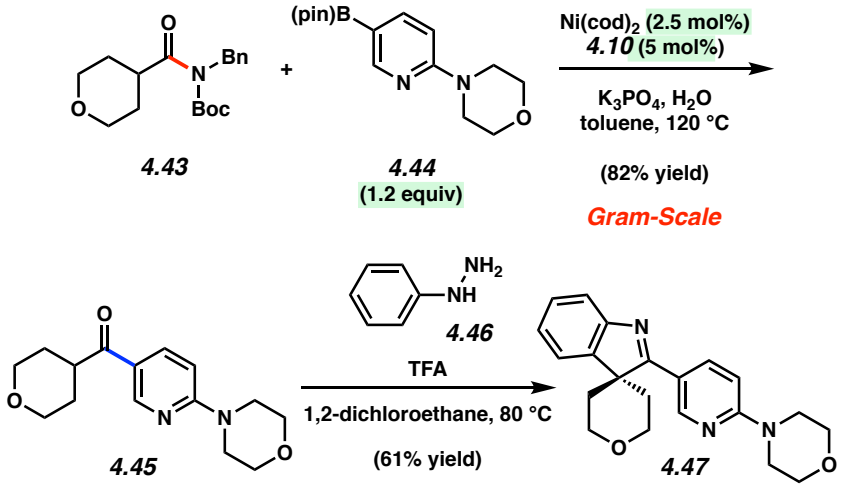

Figure 4.6. Sequential gram-scale Suzuki–Miyaura coupling and Fischer indolization to forge indolenine **4.47**.

4.9 Conclusion

We have developed the nickel-catalyzed Suzuki–Miyaura coupling of aliphatic amides. The coupling was found to be tolerant of variation in both coupling partners, and can be employed in the presence of heterocycles, epimerizable stereocenters, and sensitive functional groups (e.g., esters). The synthetic utility of this methodology was further demonstrated on

gram-scale via a Suzuki–Miyaura coupling / Fischer indolization sequence to form poly-heterocyclic spiroindolenine **4.47**. These studies offer a general platform for the hetero-arylation of aliphatic acyl electrophiles, while contributing to the repertoire of synthetic transformations involving amide derivatives and non-precious metal catalysis. Moreover, given their stability towards a variety of conditions, we view amides as having significant potential utility as synthons in the derivatization of biomolecules and multistep synthetic efforts.

4.10 Experimental Section

4.10.1 Materials and Methods

Unless stated otherwise, reactions were conducted in flame-dried glassware under an atmosphere of nitrogen or argon and commercially obtained reagents were used as received. Non-commercially available substrates were synthesized following protocols specified in Section A in the Experimental Procedures. Prior to use, toluene was purified by distillation and taken through five freeze-pump-thaw cycles, and phenylhydrazine (**4.46**) was passed over a plug of basic alumina. Benzylamine was obtained from Sigma–Aldrich. Boronate esters **4.5**, **4.37, 4.44, 4.57**, **4.58**, **4.59**, **4.61**, **6.61**, **4.63**, **4.64**, **4.66**, **4.67** and carboxylic acids **4.48**, **4.49**, **4.51**, **4.53**, **4.54**, **4.56** were obtained from Combi-Blocks. Boronate ester **4.62**[24] was prepared according to literature procedures. $Ni(cod)_2$, SIPr (**4.7**), terpyridine (**4.8**), ICy•HBF_4 (**4.9**), and Benz-ICy•HCl (**4.10**) were obtained from Strem Chemicals. K_3PO_4 was obtained from Acros. Reaction temperatures were controlled using an IKAmag temperature modulator, and unless stated otherwise, reactions were performed at room temperature (approximately 23 °C). Thin-layer chromatography (TLC) was conducted with EMD gel 60 F254 pre-coated plates (0.25 mm for analytical chromatography and 0.50 mm for preparative chromatography) and visualized using a combination of UV, anisaldehyde, iodine, and potassium permanganate staining techniques. Silicycle Siliaflash P60 (particle size 0.040–0.063 mm) was used for flash column chromatography. ^{1}H NMR spectra were recorded on Bruker spectrometers (at 300, 400 and 500 MHz) and are reported relative to residual solvent signals. Data for ^{1}H NMR spectra are reported as follows: chemical shift (δ ppm), multiplicity, coupling constant (Hz), integration. Data for ^{13}C NMR are reported in terms of chemical shift (at 75 and 125 MHz). IR spectra were recorded on a Perkin-Elmer UATR Two FT-IR spectrometer and are reported in terms of frequency absorption

(cm^{-1}). DART-MS spectra were collected on a Thermo Exactive Plus MSD (Thermo Scientific) equipped with an ID-CUBE ion source and a Vapur Interface (IonSense Inc.). Both the source and MSD were controlled by Excalibur software v. 3.0. The analyte was spotted onto OpenSpot sampling cards (IonSense Inc.) using $CHCl_3$ as the solvent. Ionization was accomplished using UHP He plasma with no additional ionization agents. The mass calibration was carried out using Pierce LTQ Velos ESI (+) and (–) Ion calibration solutions (Thermo Fisher Scientific). Determination of enantiopurity was carried out using either a Mettler Toledo SFC (supercritical fluid chromatography) or Agilent HPLC using a Daicel ChiralPak OJ-H column. Optical rotations were measured with a Rudolph Autopol III Automatic Polarimeter.

4.10.2 Experimental Procedures

4.10.2.1 Syntheses of Amide Substrates

Representative Procedure for the synthesis of amide substrates from Tables 4.1, 4.2, and 4.3 and Figures 4.2, 4.3, 4.4, 4.5, and 4.6 (synthesis of amide 4.4 is used as an example).

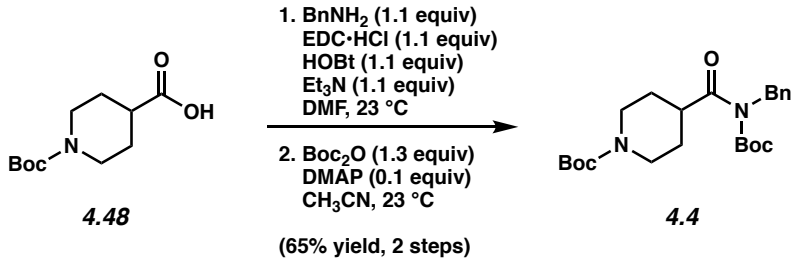

To a mixture of carboxylic acid **4.48** (3.00 g, 13.1 mmol, 1.0 equiv), EDC•HCl (2.76 g, 14.4 mmol, 1.1 equiv), HOBt (1.94 g, 14.4 mmol, 1.1 equiv), triethylamine (1.99 mL, 14.4 mmol, 1.1 equiv) and DMF (131 mL, 0.1 M) was added benzylamine (1.57 mL, 14.4 mmol, 1.1 equiv). The resulting mixture was stirred at 23 °C for 16 h, and then diluted with deionized water (250 mL) and transferred to a separatory funnel with EtOAc (150 mL) and brine (50 mL). The

aqueous layer was extracted with EtOAc (3 x 150 mL), then the organic layers were combined and washed with deionized water (3 x 125 mL), dried over Na_2SO_4, and evaporated under reduced pressure. The resulting crude solid material was used in the subsequent step without further purification.

To a flask containing the crude material from the previous step was added DMAP (148 mg, 1.21 mmol, 0.1 equiv) followed by acetonitrile (60.0 mL, 0.2 M). Boc_2O (3.43 g, 15.7 mmol, 1.3 equiv) was added in one portion and the reaction vessel was flushed with N_2, then the reaction mixture was allowed to stir at 23 °C for 16 h. The reaction was quenched by addition of saturated aqueous $NaHCO_3$ (200 mL), transferred to a separatory funnel with EtOAc (200 mL) and H_2O (200 mL), and extracted with EtOAc (3 x 100 mL). The organic layers were combined, dried over Na_2SO_4, and evaporated under reduced pressure. The resulting crude residue was purified by flash chromatography (9:1 Hexanes:EtOAc) to yield amide **4.4** (3.59 g, 65% yield, over two steps) as white solid. Amide **4.4**: mp: 83–85 ºC; R_f 0.39 (5:1 Hexanes:EtOAc); ^{1}H NMR (500 MHz, $CDCl_3$): δ 7.31–7.26 (m, 2H), 7.24–7.18 (m, 3H), 4.86 (s, 2H), 4.12 (br s, 2H), 3.59 (tt, *J* = 11.2, 3.6, 1H), 2.88–2.70 (m, 2H), 1.91–1.79 (m, 2H), 1.65 (qd, *J* = 12.2, 4.0, 2H), 1.45 (s, 9H), 1.40 (s, 9H); ^{13}C NMR (125 MHz, $CDCl_3$): δ 178.2, 154.8, 153.1, 138.4, 128.5, 127.5, 127.2, 83.5, 79.6, 47.8, 43.8, 43.0, 29.0, 28.6, 28.0; IR (film): 2976, 2932, 2861, 1731, 1689 cm^{-1}; HRMS-APCI (*m/z*) $[M + H]^+$ calcd for $C_{23}H_{35}N_2O_5$, 419.25405; found 419.25413.

Note: Supporting information for the syntheses of some amides shown in Figures 4.2, 4.3, 4.4 and 4.5 have previously been reported: **4.65**,[25] **4.68**,[25] **4.69**,[25] **4.70**,[25] **4.71**,[25] **4.36**,[26] **4.41**,[27] **rac-4.41**,[27] and **4.72**.[27] Syntheses for the remaining substrates shown in Figures 4.2, 4.3, 4.5, and 4.6 are as follows:

Any modifications of the conditions shown in the representative procedure above are specified in the following schemes.

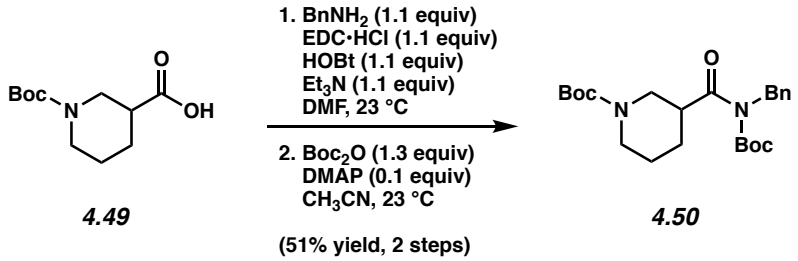

Amide 4.50. Purification by flash chromatography (9:1 Hexanes:EtOAc) generated amide **4.50** (51% yield, over two steps) as a white solid. Amide **4.50**: mp: 73–75 ºC; R_f 0.43 (5:1 Hexanes:EtOAc); ^{1}H NMR (500 MHz, $CDCl_3$): δ 7.31–7.26 (m, 2H), 7.24–7.19 (m, 3H), 4.92–4.78 (m, 2H), 4.26–3.94 (m, 2H), 3.51 (tt, J = 10.6, 3.6, 1H), 2.99 (dd, J = 12.5, 11.0, 1H), 2.75 (br s, 1H), 2.10 (br s, 1H), 1.74–1.68 (m, 1H), 1.62–1.48 (m, 2H), 1.45 (s, 9H), 1.40 (s, 9H); ^{13}C NMR (125 MHz, $CDCl_3$, 15 of 17 observed): δ 177.2, 154.8, 152.9, 138.3, 128.5, 127.5, 127.3, 83.6, 79.7, 47.7, 43.5, 28.7, 28.6, 28.0, 24.7; IR (film): 2977, 2935, 2862, 1732, 1687 cm^{-1}; HRMS-APCI (*m/z*) $[M + H]^+$ calcd for $C_{23}H_{35}N_2O_5$, 419.25405; found 419.25304.

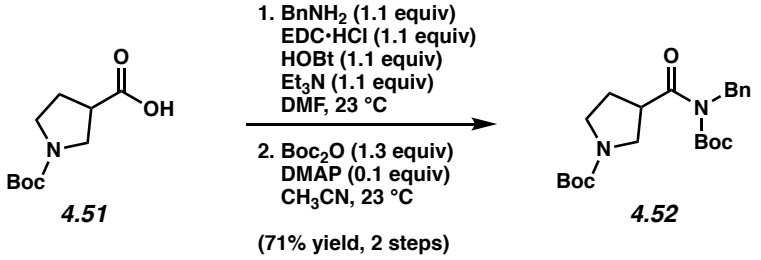

Amide 4.52. Purification by flash chromatography (9:1 Hexanes:EtOAc) generated amide **4.52** (71% yield, over two steps) as a colorless oil. Amide **4.52**: R_f 0.47 (5:1 Hexanes:EtOAc); ^{1}H

NMR (500 MHz, $CDCl_3$): δ 7.32–7.27 (m, 2H), 7.25–7.19 (m, 3H), 4.88 (s, 2H), 4.08 (quint, *J* = 7.1, 1H), 3.67 (br s, 1H), 3.56 (dd, *J* = 10.8, 6.3, 1H), 3.53–3.45 (m, 1H), 3.43–3.33 (m, 1H), 2.15 (br s, 2H), 1.46 (s, 9H), 1.42 (s, 9H); ^{13}C NMR (125 MHz, $CDCl_3$, 15 of 16 observed): δ 176.2, 154.6, 153.2, 138.3, 128.5, 127.6, 127.4, 83.8, 79.4, 49.3, 48.0, 45.6, 29.4, 28.7, 28.1; IR (film): 2979, 2887, 1731, 1693, 1366, 1143 cm^{-1}; HRMS-APCI (*m/z*) $[M + H]^+$ calcd for $C_{22}H_{33}N_2O_5$, 405.23840; found 405.23794.

Note: ^1H and ^{13}C NMR spectra of amide **4.52** *were obtained at 57 °C.*

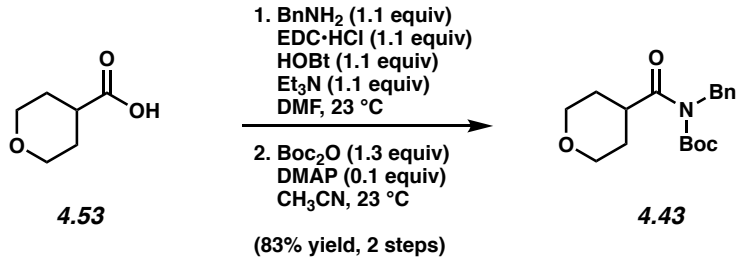

Amide 4.43. Purification by flash chromatography (14:1 Hexanes:EtOAc) generated amide **4.43** (83% yield, over two steps) as a white solid. Amide **4.43**: mp: 52–54 ºC; R_f 0.59 (5:1 Hexanes:EtOAc); ^1H NMR (500 MHz, $CDCl_3$): δ 7.32–7.27 (m, 2H), 7.25–7.19 (m, 3H), 4.87 (s, 2H), 4.03–3.97 (m, 2H), 3.74–3.65 (m, 1H), 3.48 (td, *J* = 11.5, 2.4, 2H), 1.91–1.75 (m, 4H), 1.40 (s, 9H); ^{13}C NMR (125 MHz, $CDCl_3$): δ 178.1, 153.1, 138.4, 128.5, 127.5, 127.3, 83.4, 67.5, 47.8, 42.2, 29.7, 28.0; IR (film): 2962, 2842, 1728, 1688, 1366, 1143 cm^{-1}; HRMS-APCI (*m/z*) $[M + H]^+$ calcd for $C_{18}H_{26}NO_4$, 320.18563; found 320.18538.

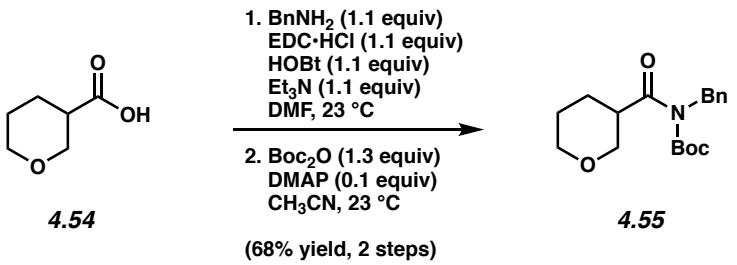

Amide 4.55. Purification by flash chromatography (14:1 Hexanes:EtOAc) generated amide **4.55** (68% yield, over two steps) as a white solid. Amide **4.55**: mp: 49–50 ºC; R_f 0.38 (5:1 Hexanes:EtOAc); ^{1}H NMR (500 MHz, $CDCl_3$): δ 7.31–7.26 (m, 2H), 7.25–7.18 (m, 3H), 4.87 (d, *J* = 14.9, 1H), 4.81 (d, *J* = 14.9, 1H), 4.10–4.01 (m, 1H), 3.95–3.87 (m, 1H), 3.72–3.63 (m, 1H), 3.55 (t, *J* = 10.4, 1H), 3.44 (td, *J* = 10.8, 3.4, 1H), 2.13–2.04 (m, 1H), 1.81–1.63 (m, 3H), 1.42 (s, 9H); ^{13}C NMR (125 MHz, $CDCl_3$): δ 176.7, 153.0, 138.3, 128.5, 127.6, 127.3, 83.7, 70.1, 68.4, 47.7, 44.0, 28.0, 27.3, 25.3; IR (film): 2977, 2847, 1732, 1685, 1371, 1146 cm^{-1}; HRMS-APCI (*m/z*) $[M + H]^+$ calcd for $C_{18}H_{26}NO_4$, 320.18563; found 320.18577.

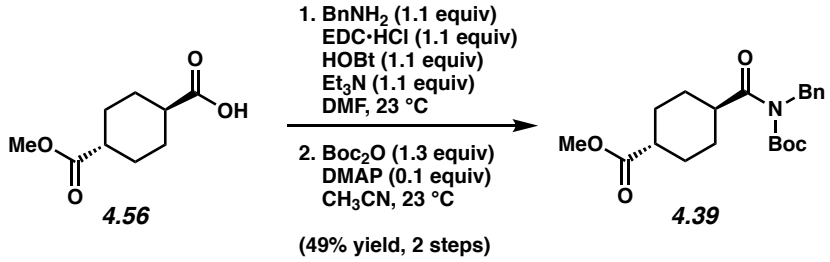

Amide 4.39. Purification by flash chromatography (9:1 Hexanes:EtOAc) generated amide **4.39** (49% yield, over two steps) as a white solid. Amide **4.39**: mp: 65–67 ºC; R_f 0.49 (5:1 Hexanes:EtOAc); ^{1}H NMR (500 MHz, $CDCl_3$): δ 7.31–7.26 (m, 2H), 7.24–7.20 (m, 3H), 4.85 (s, 2H), 3.67 (s, 3H), 3.43–3.36 (m, 1H), 2.37–2.0 (m, 1H), 2.10–1.96 (m, 4H), 1.58–1.46 (m, 4H), 1.41 (s, 9H); ^{13}C NMR (125 MHz, $CDCl_3$): δ 179.1, 176.2, 153.1, 138.5, 128.5, 127.6, 127.2,

83.4, 51.7, 47.8, 44.1, 42.8, 29.0, 28.4, 28.0; IR (film): 2977, 2946, 2865, 1728, 1689 cm^{-1}; HRMS-APCI (*m/z*) $[M + H]^+$ calcd for $C_{21}H_{30}NO_5$, 376.21185; found 376.21140.

4.10.2.2. Initial Survey of Ligands and Relevant Control Experiments

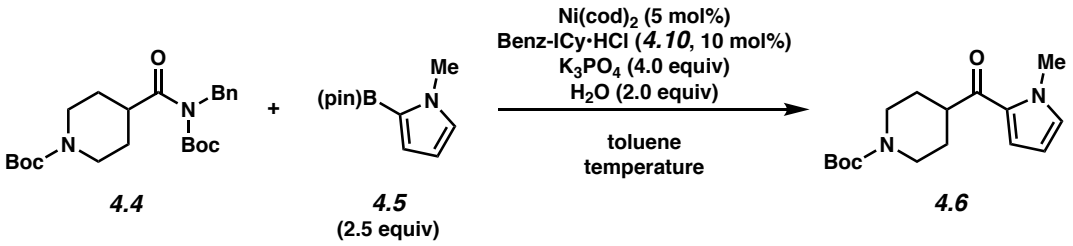

Representative Procedure for Suzuki–Miyaura Reactions from Table 4.2 (coupling of amide 4.4 and *N*-methylpyrrole-2-boronic acid pinacol ester (4.5) is used as an example). A 1-dram vial was charged with anhydrous powdered K_3PO_4 (170 mg, 0.800 mmol, 4.0 equiv) and a magnetic stir bar. The vial and contents were flame-dried under reduced pressure, then allowed to cool under N_2. Amide substrate **4.4** (83.8 mg, 0.200 mmol, 1.0 equiv), *N*-methylpyrrole-2-boronic acid pinacol ester (**4.5**) (104 mg, 0.500 mmol, 2.5 equiv), and hexamethylbenzene (9.6 mg, 0.59 mmol, 0.30 equiv) were added. The vial was flushed with N_2, then water (7.2 μL, 0.400 mmol, 2.0 equiv), which had been sparged with N_2 for 10 min, was added. The vial was taken into a glove box and charged with $Ni(cod)_2$ (2.8 mg, 0.010 mmol, 5 mol%) and Benz-ICy•HCl (**4.10**, 6.4 mg, 0.020 mmol, 10 mol%). Subsequently, toluene (0.20 mL, 1.0 M) was added. The vial was sealed with a Teflon-lined screw cap, removed from the glove box, and stirred vigorously (800 rpm) at 120 °C for 16 h. After cooling to 23 °C, the mixture was diluted with hexanes (0.5 mL) and filtered over a plug of silica gel (10 mL of EtOAc eluent). The volatiles were removed under reduced pressure, and the yield was determined by ^1H NMR analysis with hexamethylbenzene as an internal standard.

Any modifications of the conditions shown in the representative procedure above are specified below in Table 4.2.

Table 4.2. Initial Survey of Ligands and Relevant Control Experiments[a]

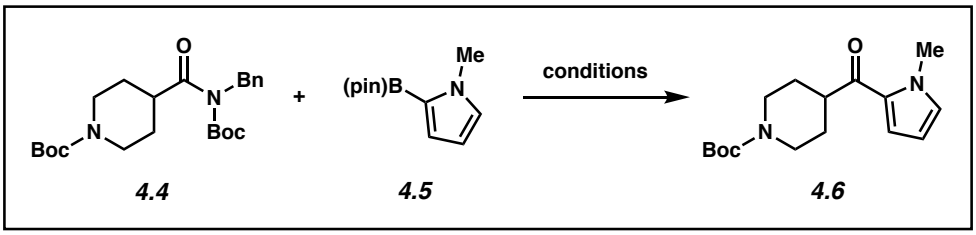

4.4 *4.5* *4.6*

Reaction Conditions	*Experimental Results* *4.4*	*4.6*
4.5 (2.5 equiv), K_3PO_4 (4.0 equiv), H_2O (2.0 equiv) $Ni(cod)_2$ (5 mol%), SIPr (*4.7*,10 mol%), toluene (1.0 M), 50 °C, 16 h	100%	0%
4.5 (2.5 equiv), K_3PO_4 (4.0 equiv), H_2O (2.0 equiv) $Ni(cod)_2$ (5 mol%), SIPr (*4.7*,10 mol%), toluene (1.0 M), 120 °C, 16 h	52%[b]	0%
4.5 (2.5 equiv), K_3PO_4 (4.0 equiv), H_2O (2.0 equiv) $Ni(cod)_2$ (5 mol%), terpyridine (*4.8*,10 mol%), toluene (1.0 M), 120 °C, 16 h	50%[b]	0%
4.5 (2.5 equiv), K_3PO_4 (4.0 equiv), H_2O (2.0 equiv) $Ni(cod)_2$ (5 mol%), ICy·HBF_4 (*4.9*,10 mol%), toluene (1.0 M), 120 °C, 16 h	0%	95%
4.5 (2.5 equiv), K_3PO_4 (4.0 equiv), H_2O (2.0 equiv) $Ni(cod)_2$ (5 mol%), Benz-ICy·HCl (*4.10*,10 mol%), toluene (1.0 M), 120 °C, 16 h	0%	95%
Control Experiments:		
4.5 (2.5 equiv), K_3PO_4 (4.0 equiv), H_2O (2.0 equiv) toluene (1.0 M), 120 °C, 16 h	25%[b]	0%
4.5 (2.5 equiv), K_3PO_4 (4.0 equiv), H_2O (2.0 equiv) Benz-ICy·HCl (*4.10*,10 mol%), toluene (1.0 M), 120 °C, 16 h	25%[b]	0%
4.5 (2.5 equiv), K_3PO_4 (4.0 equiv), H_2O (2.0 equiv) $Ni(cod)_2$ (5 mol%), toluene (1.0 M), 120 °C, 16 h	5%[b]	0%

[a] Yields were determined by ^1H NMR analysis using hexamethylbenzene as an internal standard.
[b] Substantial amounts of the corresponding Boc-cleavage product (des-Boc amide starting material) were observed due to the elevated reaction temperature.

4.10.2.3. Scope of Methodology

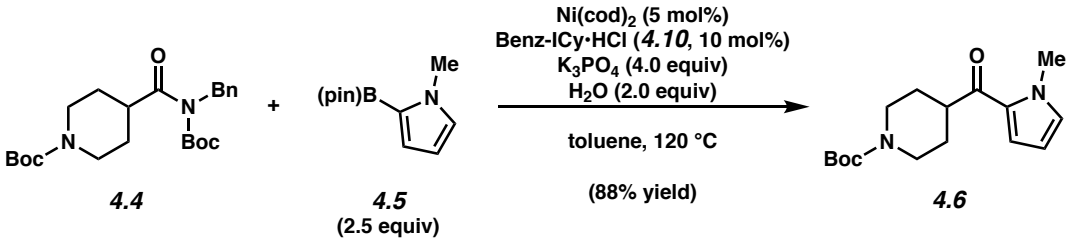

Representative Procedure (coupling of amide 4.4 and *N*-methylpyrrole-2-boronic acid pinacol ester (4.5) is used as an example). Ketone 4.6. A 1-dram vial was charged with anhydrous powdered K_3PO_4 (170 mg, 0.800 mmol, 4.0 equiv) and a magnetic stir bar. The vial and contents were flame-dried under reduced pressure, then allowed to cool under N_2. Amide substrate **4.4** (83.8 mg, 0.200 mmol, 1.0 equiv) and *N*-methylpyrrole-2-boronic acid pinacol ester (**4.5**) (104 mg, 0.500 mmol, 2.5 equiv) were added. The vial was flushed with N_2, then water (7.2 μL, 0.400 mmol, 2.0 equiv), which had been sparged with N_2 for 10 min, was added. The vial was taken into a glove box and charged with $Ni(cod)_2$ (2.8 mg, 0.010 mmol, 5 mol%) and Benz-ICy•HCl (**4.10**, 6.4 mg, 0.020 mmol, 10 mol%). Subsequently, toluene (0.20 mL, 1.0 M) was added. The vial was sealed with a Teflon-lined screw cap, removed from the glove box, and stirred vigorously (800 rpm) at 120 °C for 16 h. After cooling to 23 °C, the mixture was diluted with hexanes (0.5 mL) and filtered over a plug of silica gel (10 mL of EtOAc eluent). The volatiles were removed under reduced pressure, and the crude residue was purified by flash chromatography (19:1 Hexanes:EtOAc → 14:1 Hexanes:EtOAc → 9:1 Hexanes:EtOAc) to yield ketone product **4.6** (88% yield, average of two experiments) as a white solid. Ketone **4.6**: mp: 77–80 ºC; R_f 0.18 (5:1 Hexanes:EtOAc); ^{1}H NMR (500 MHz, $CDCl_3$): δ 7.00–6.95 (m, 1H), 6.85–6.80 (m, 1H), 6.16–6.11 (m, 1H), 4.18 (br s, 2H), 3.93 (s, 3H), 3.20–3.10 (m, 1H), 2.93–2.70 (m, 2H), 1.85–1.66 (m, 4H), 1.46 (s, 9H); ^{13}C NMR (125 MHz, $CDCl_3$): δ 193.1, 154.9,

131.6, 129.8, 118.9, 108.1, 79.7, 44.8, 43.6, 38.0, 29.1, 28.6; IR (film): 2929, 2859, 1686, 1646, 1408, 1168 cm^{-1}; HRMS-APCI (*m/z*) $[M + H]^+$ calcd for $C_{16}H_{25}N_2O_3$, 293.18597; found 293.18535.

Any modifications of the conditions shown in the representative procedure above are specified in the following schemes, which depict all of the results shown in Figures 4.2, 4.3, 4.4, 4.5, and 4.6.

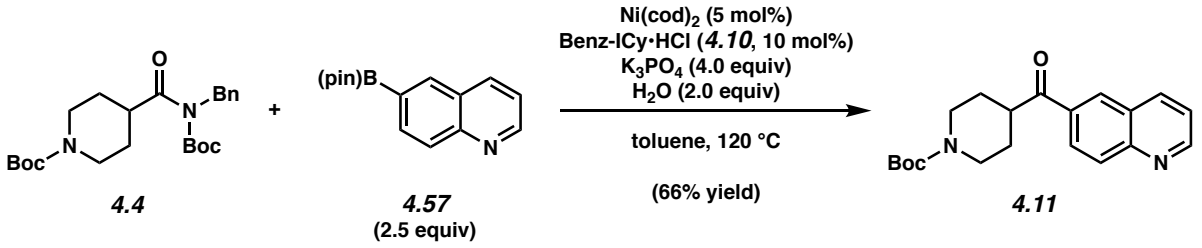

Ketone 4.11. Purification by flash chromatography (1:1 Hexanes:EtOAc → 1:2 Hexanes:EtOAc) generated ketone **4.11** (66% yield, average of two experiments) as a clear oil. Ketone **4.11**: R_f 0.33 (1:1 Hexanes:EtOAc); ^1H NMR (500 MHz, $CDCl_3$): δ 9.02 (dd, *J* = 4.2, 1.7, 1H), 8.44 (d, *J* = 1.9, 1H), 8.29 (dd, *J* = 8.3, 1.3, 1H), 8.23 (dd, *J* = 8.8, 1.9, 1H), 8.18 (d, *J* = 8.8, 1H), 7.50 (dd, *J* = 8.3, 4.2, 1H), 4.20 (br s, 2H), 3.56 (tt, *J* = 11.1, 3.7, 1H), 3.04–2.85 (m, 2H), 1.98–1.84 (m, 2H), 1.82–1.74 (m, 2H), 1.47 (s, 9H); ^{13}C NMR (125 MHz, $CDCl_3$, 14 of 16 observed): δ 201.6, 154.8, 152.8, 150.2, 137.7, 133.8, 130.5, 129.6, 128.0, 127.7, 122.2, 79.9, 43.9, 28.6; IR (film): 2972, 2859, 1676, 1423, 1366, 1161 cm^{-1}; HRMS-APCI (*m/z*) $[M + H]^+$ calcd for $C_{20}H_{25}N_2O_3$, 341.18597; found 341.18465.

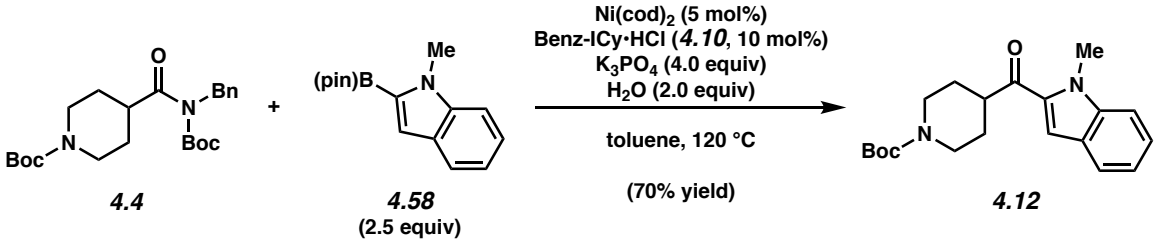

Ketone 4.12. Purification by flash chromatography (19:1 Hexanes:EtOAc → 14:1 Hexanes:EtOAc → 9:1 Hexanes:EtOAc) generated ketone **4.12** (70% yield, average of two experiments) as a white solid. Ketone **4.12**: R_f 0.25 (5:1 Hexanes:EtOAc). Spectral data match those previously reported.[27]

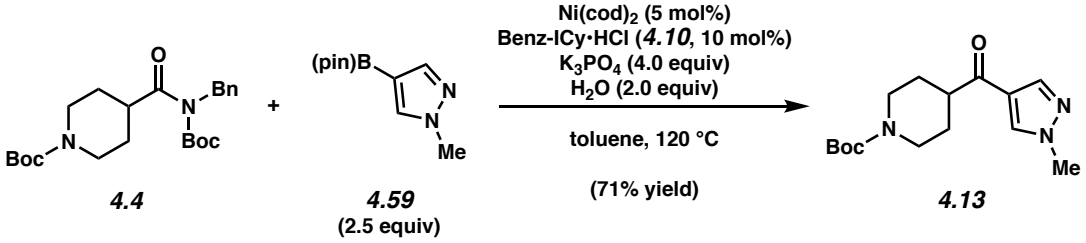

Ketone 4.13. Purification by flash chromatography (49:1 PhH:CH_3CN → 19:1 PhH:CH_3CN → 1:1 Hexanes:EtOAc → 1:3 Hexanes:EtOAc) generated ketone **4.13** (71% yield, average of two experiments) as a white solid. Ketone **4.13**: mp: 99–101 ºC; R_f 0.24 (1:3 Hexanes:EtOAc); ^{1}H NMR (500 MHz, $CDCl_3$): δ 7.89 (s, 1H), 7.88 (s, 1H), 4.15 (br s, 2H), 3.94 (s, 3H), 3.27 (tt, J = 11.1, 3.9, 1H), 2.93–2.73 (m, 2H), 1.93–1.63 (m, 4H), 1.46 (s, 9H); ^{13}C NMR (125 MHz, $CDCl_3$, 10 of 11 observed): δ 196.4, 154.8, 140.4, 132.8, 123.0, 79.8, 46.3, 39.6, 28.6, 28.4; IR (film): 2977, 2937, 2859, 1671, 1540, 1168 cm^{-1}; HRMS-APCI (*m/z*) $[M + H]^+$ calcd for $C_{15}H_{24}N_3O_3$, 294.18122; found 294.18073.

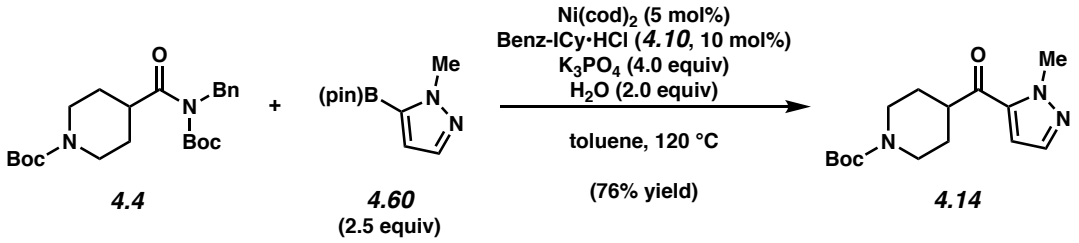

Ketone 4.14. Purification by flash chromatography (4:1 Hexanes:EtOAc → 3:1 Hexanes:EtOAc) generated ketone **4.14** (76% yield, average of two experiments) as a clear oil. Ketone **4.14**: R_f 0.42 (2:1 Hexanes:EtOAc); ^{1}H NMR (500 MHz, $CDCl_3$): δ 7.48 (d, J = 2.1, 1H), 6.84 (d, J = 2.1, 1H), 4.16 (s, 5H), 3.12 (tt, J = 11.3, 3.7, 1H), 2.93–2.75 (m, 2H), 1.89–1.76 (m, 2H), 1.75–1.66 (m, 2H), 1.46 (s, 9H); ^{13}C NMR (125 MHz, $CDCl_3$, 9 of 11 observed): δ 193.5, 154.8, 137.8, 137.6, 111.2, 79.9, 46.3, 40.6, 28.6; IR (film): 2955, 2860, 1677, 1423, 1366, 1321, 1169 cm^{-1}; HRMS-APCI (*m/z*) $[M + H]^+$ calcd for $C_{15}H_{24}N_3O_3$, 294.18122; found 294.18035.

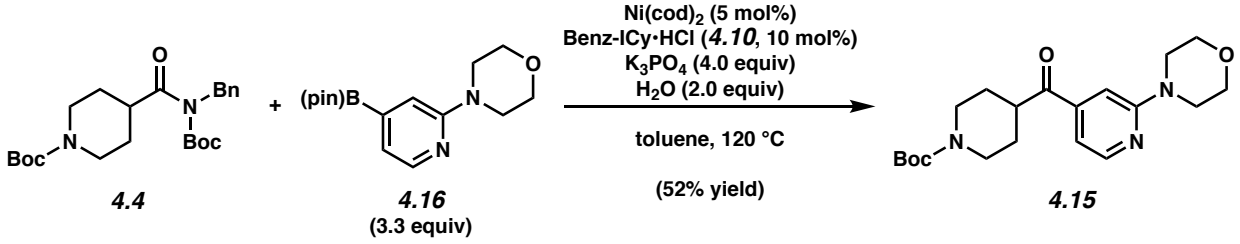

Ketone 4.15. Purification by flash chromatography (2:1 Hexanes:EtOAc) generated ketone **4.15** (52% yield, average of two experiments) as a yellow oil. Ketone **4.15**: R_f 0.31 (2:1 Hexanes:EtOAc); ^{1}H NMR (500 MHz, $CDCl_3$): δ 8.33 (dd, J = 5.1, 0.8, 1H), 7.03 (s, 1H), 7.00 (dd, J = 5.2, 1.2, 1H), 4.13 (br s, 2H), 3.85–8.80 (m, 4H), 3.59–3.54 (m, 4H), 3.27 (tt, J = 11.1, 3.6, 1H), 2.97–2.80 (m, 2H), 1.91–1.77 (m, 2H), 1.70–1.60 (m, 2H); ^{13}C NMR (125 MHz, $CDCl_3$, 13 of 14 observed): δ 202.5, 160.5, 154.8, 149.3, 144.1, 111.1, 104.7, 79.9, 66.8, 45.6, 44.2, 28.6, 28.2; IR (film): 2969, 2854, 1688, 1426, 1241, 1166 cm^{-1}; HRMS-APCI (*m/z*) $[M + H]^+$ calcd for $C_{20}H_{30}N_3O_4$, 376.22308; found 376.22152.

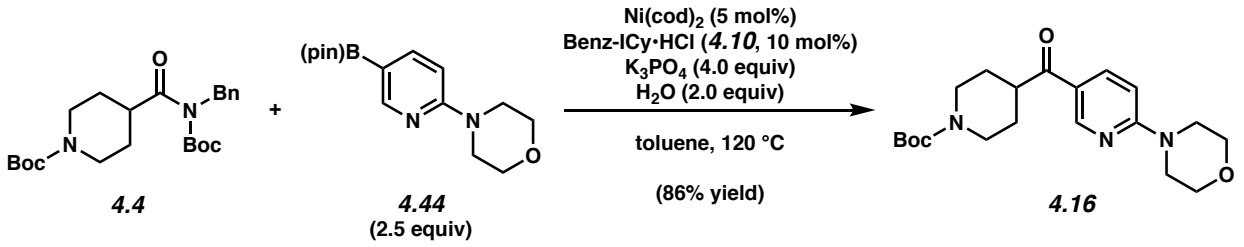

Ketone 4.16. Purification by flash chromatography (5:1 Hexanes:EtOAc → 9:1 CH_2Cl_2:MeOH) generated ketone **4.16** (86% yield, average of two experiments) as a white solid. Ketone **4.16**: mp: 131–133 ºC; R_f 0.52 (1:3 Hexanes:EtOAc); ^{1}H NMR (500 MHz, $CDCl_3$): δ 8.82–8.72 (m, 1H), 3.26 (dd, *J* = 9.1, 2.5, 1H), 6.69–6.58 (m, 1H), 4.17 (br s, 2H), 3.86–3.77 (m, 4H), 3.73–3.64 (m, 4H), 3.27 (tt, *J* = 11.1, 3.8, 1H), 2.99–2.71 (m, 2H), 1.94–1.64 (m, 4H), 1.46 (s, 9H); ^{13}C NMR (125 MHz, $CDCl_3$, 12 of 14 observed): δ 199.4, 160.9, 154.9, 150.4, 137.9, 121.5, 105.9, 79.8, 66.7, 45.0, 43.3, 28.6; IR (film): 2969, 2857, 1686, 1593, 1418, 1216, 1168 cm^{-1}; HRMS-APCI (*m/z*) $[M + H]^+$ calcd for $C_{20}H_{30}N_3O_4$, 376.22308; found 376.22247.

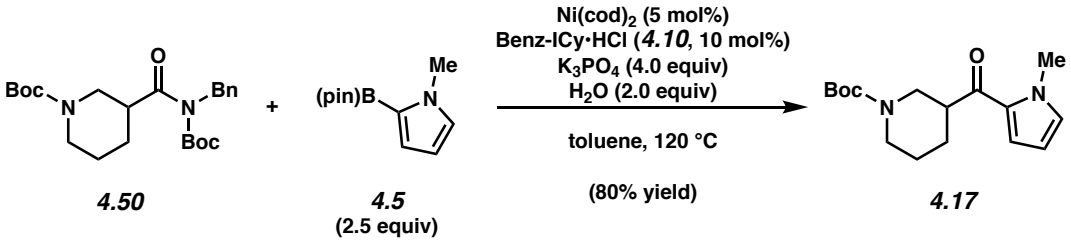

Ketone 4.17. Purification by flash chromatography (19:1 Hexanes:EtOAc → 14:1 Hexanes:EtOAc → 9:1 Hexanes:EtOAc) generated ketone **4.17** (80% yield, average of two experiments) as a white solid. Ketone **4.17**: mp: 86–88 ºC; R_f 0.19 (5:1 Hexanes:EtOAc); ^{1}H NMR (500 MHz, $CDCl_3$): δ 7.08–7.02 (m, 1H), 6.82 (br s, 1H), 6.17–6.12 (m, 1H), 4.40–4.00 (m, 2H), 3.93 (s, 3H), 3.22–3.09 (m, 1H), 2.99–2.78 (m, 1H), 2.76–2.61 (m, 1H), 2.02–1.92 (m, 1H), 1.78–1.69 (m, 2H), 1.57–1.50 (m, 1H), 1.47 (s, 9H); ^{13}C NMR (125 MHz, $CDCl_3$): δ 192.0,

154.9, 131.7, 129.9, 119.5, 108.3, 79.7, 47.8, 47.1, 45.3, 44.0, 37.9, 28.6, 28.4, 24.8; IR (film): 2937, 2862, 1690, 1645, 1408 cm^{-1}; HRMS-APCI (*m/z*) $[M + H]^+$ calcd for $C_{16}H_{25}N_2O_3$, 293.18597; found 293.18458.

*Note: Ketone **4.17** was obtained as a mixture of conformers. These data represent empirically observed chemical shifts from the ^{13}C NMR spectrum.*

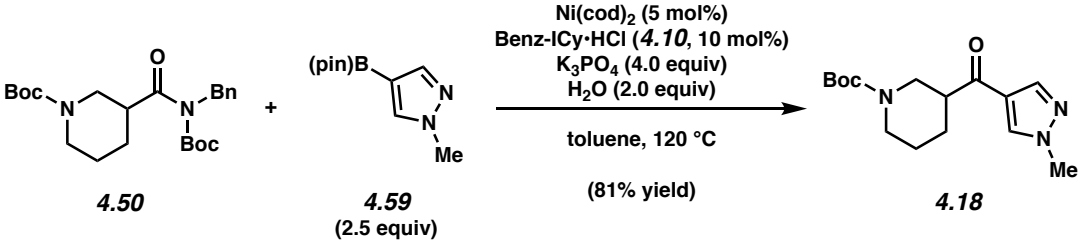

Ketone 4.18. Purification by flash chromatography (9:1 Hexanes:EtOAc → 5:1 Hexanes:EtOAc → 2:1 Hexanes:EtOAc → 1:1 Hexanes:EtOAc) generated ketone **4.18** (81% yield, average of two experiments) as a white solid. Ketone **4.18**: mp: 96–97 ºC; R_f 0.19 (1:1 Hexanes:EtOAc); ^1H NMR (500 MHz, $CDCl_3$): δ 7.93 (s, 1H), 7.91 (br s, 1H), 4.40–4.01 (m, 2H), 3.94 (s, 3H), 3.05–2.65 (m, 3H), 2.03–1.95 (m, 1H), 1.79–1.64 (m, 2H), 1.55–1.43 (m, 10H); ^{13}C NMR (125 MHz, $CDCl_3$): δ 195.3, 154.8, 140.6, 132.8, 123.1, 79.9, 46.7, 45.0, 43.9, 39.5, 28.6, 27.8, 24.8; IR (film): 2939, 2862, 1683, 1663, 1540, 1148 cm^{-1}; HRMS-APCI (*m/z*) $[M + H]^+$ calcd for $C_{15}H_{24}N_3O_3$, 294.18122; found 294.17877.

*Note: Ketone **4.18** was obtained as a mixture of conformers. These data represent empirically observed chemical shifts from the ^{13}C NMR spectrum.*

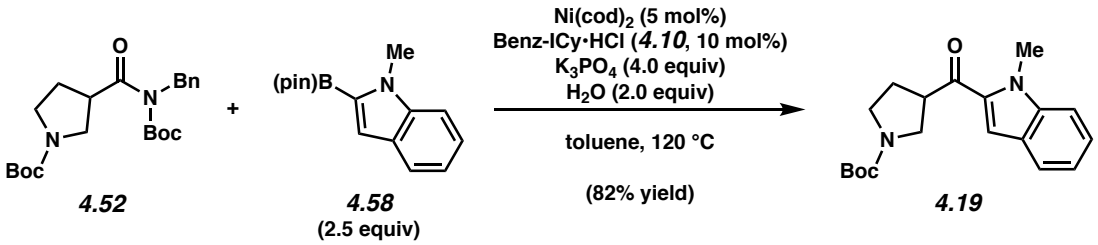

Ketone 4.19. Purification by flash chromatography (4:1 Hexanes:EtOAc) generated ketone **4.19** (82% yield, average of two experiments) as a clear oil. Ketone **4.19**: R_f 0.26 (4:1 Hexanes:EtOAc); ^{1}H NMR (500 MHz, $CDCl_3$): δ 7.70 (br s, 1H), 7.39 (br s, 2H), 7.33 (br s, 1H), 7.17 (br s, 1H), 4.08 (s, 3H), 4.04–3.91 (m, 1H), 3.82–3.65 (m, 1H), 3.65–3.39 (m, 3H), 2.35–2.12 (m, 2H), 1.47 (s, 9H); ^{13}C NMR (125 MHz, $CDCl_3$): δ 193.1, 192.9, 154.5, 140.5, 134.2, 126.4, 125.9, 123.1, 121.1, 112.0, 110.6, 79.5, 49.0, 48.9, 47.3, 46.3, 45.8, 45.6, 32.4, 29.7, 29.4, 28.6; IR (film): 2974, 2882, 1688, 1658, 1393, 1166, 1118 cm^{-1}; HRMS-APCI (*m/z*) $[M + H]^+$ calcd for $C_{19}H_{25}N_2O_3$, 329.18597; found 329.18463.

*Note: Ketone **4.19** was obtained as a mixture of conformers. These data represent empirically observed chemical shifts from the ^{13}C NMR spectrum.*

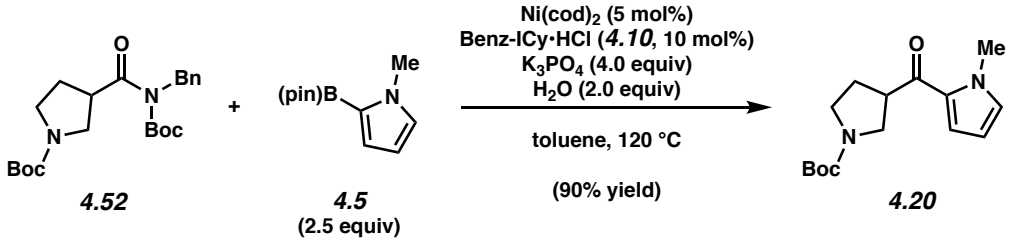

Ketone 4.20. Purification by flash chromatography (4:1 Hexanes:EtOAc) generated ketone **4.20** (90% yield, average of two experiments) as a clear oil. Ketone **4.20**: R_f 0.18 (4:1 Hexanes:EtOAc); ^{1}H NMR (500 MHz, $CDCl_3$): δ 6.97 (br s, 1H), 6.83 (br s, 1H), 6.14 (br s, 1H), 3.93 (s, 3H), 3.83–3.44 (m, 4H), 3.38 (br s, 1H), 2.28–2.12 (m, 1H), 2.08 (br s, 1H), 1.45 (s, 9H); ^{13}C NMR (125 MHz, $CDCl_3$): δ 189.9, 189.7, 154.5, 131.9, 130.2, 119.6, 108.4, 79.4, 49.0, 48.9,

46.4, 45.9, 45.6, 45.5, 37.9, 29.5, 29.4, 28.6; IR (film): 2977, 2882, 1686, 1643, 1401, 1366, 1118 cm^{-1}; HRMS-APCI (*m/z*) $[M + H]^+$ calcd for $C_{15}H_{23}N_2O_3$, 279.17032; found 279.17976.

*Note: Ketone **4.20** was obtained as a mixture of conformers. These data represent empirically observed chemical shifts from the ^{13}C NMR spectrum.*

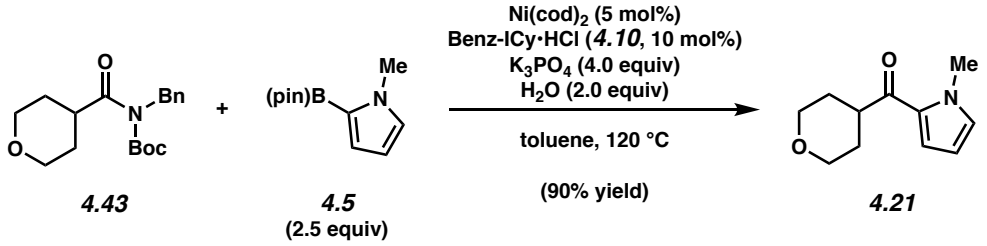

Ketone 4.21. Purification by flash chromatography (5:1 Hexanes:EtOAc) generated ketone **4.21** (90% yield, average of two experiments) as a white solid. Ketone **4.21**: mp: 72–74 ºC; R_f 0.21 (4:1 Hexanes:EtOAc); ^1H NMR (500 MHz, $CDCl_3$): δ 7.00–6.95 (m, 1H), 6.82 (s, 1H), 6.15–6.10 (m, 1H), 4.09–4.00 (m, 2H), 3.94 (s, 3H), 3.51 (t, *J* = 11.8, 2H), 3.26 (tt, *J* = 11.5, 3.8, 1H), 1.91 (qd, *J* = 12.4, 4.3, 2H), 1.70 (d, *J* = 13.4, 2H); ^{13}C NMR (125 MHz, $CDCl_3$): δ 192.9, 131.6, 129.8, 118.9, 108.1, 67.6, 43.8, 38.0, 29.7; IR (film): 2952, 2847, 1642, 1408, 1306, 1094 cm^{-1}; HRMS-APCI (*m/z*) $[M + H]^+$ calcd for $C_{11}H_{16}NO_2$, 194.11756; found 194.11707.

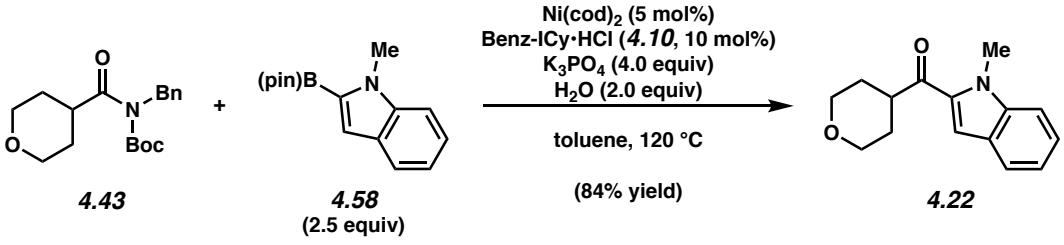

Ketone 4.22. Purification by flash chromatography (5:1 Hexanes:EtOAc) generated ketone **4.22** (84% yield, average of two experiments) as a white solid. Ketone **4.22**: mp: 63–66 ºC; R_f 0.35 (4:1 Hexanes:EtOAc); ^1H NMR (500 MHz, $CDCl_3$): δ 7.70 (d, *J* = 8.1, 1H), 7.39 (d, *J* = 3.6,

2H), 7.33 (s, 1H), 7.19–7.14 (m, 1H), 4.12–4.09 (m, 1H), 4.07 (s, 4H), 3.57 (t, J = 11.7, 2H), 3.48 (tt, J = 11.5, 3.6, 1H), 1.96 (qd, J = 12.4, 4.2, 2H), 1.81 (d, J = 13.2, 2H); ^{13}C NMR (125 MHz, $CDCl_3$): δ 196.0, 140.4, 133.8, 126.1, 125.9, 123.0, 120.9, 111.1, 110.6, 67.5, 44.7, 32.4, 29.8; IR (film): 2954, 2844, 1656, 1511, 1386, 1118 cm^{-1}; HRMS-APCI (*m/z*) $[M + H]^+$ calcd for $C_{15}H_{18}NO_2$, 244.13321; found 244.13264.

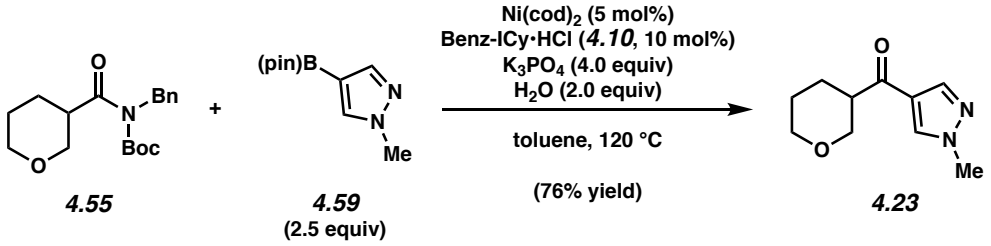

Ketone 4.23. Purification by flash chromatography (1:2 Hexanes:EtOAc) generated ketone **4.23** (76% yield, average of two experiments) as a yellow solid. Ketone **4.23**: mp: 83–84 ºC; R_f 0.25 (1:2 Hexanes:EtOAc); ^{1}H NMR (500 MHz, $CDCl_3$): δ 7.89 (s, 1H), 7.87 (s, 1H), 4.04 (d, J = 11.1, 1H), 3.96–3.86 (m, 4H), 3.50 (t, J = 10.9, 1H), 3.43–3.34 (m, 1H), 3.20–3.11 (m, 1H), 1.97 (d, J = 12.7, 1H), 1.86–1.73 (m, 1H), 1.73–1.63 (m, 2H); ^{13}C NMR (125 MHz, $CDCl_3$): δ 195.2, 140.4, 132.8, 123.3, 69.8, 68.2, 47.2, 39.5, 26.6, 25.2; IR (film): 2947, 2852, 1656, 1541, 1401, 1188, 1080 cm^{-1}; HRMS-APCI (*m/z*) $[M + H]^+$ calcd for $C_{10}H_{15}N_2O_2$, 165.11280; found 165.11223.

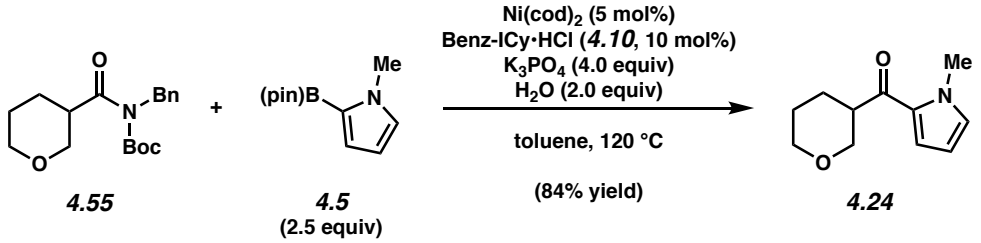

Ketone 4.24. Purification by flash chromatography (4:1 Hexanes:EtOAc) generated ketone **4.24** (84% yield, average of two experiments) as a clear oil. Ketone **4.24**: R_f 0.30 (4:1 Hexanes:EtOAc); ^{1}H NMR (500 MHz, $CDCl_3$): δ 7.04–7.00 (m, 1H), 6.81 (s, 1H), 6.15–6.10 (m, 1H), 4.09–4.02 (m, 1H), 3.98–3.92 (m, 1H), 3.91 (s, 3H), 3.52 (t, J = 10.9, 1H), 3.44–3.33 (m, 2H), 2.00–1.93 (m, 1H), 1.84 (qd, J = 12.1, 4.3, 1H), 1.78–1.65 (m, 2H); ^{13}C NMR (125 MHz, $CDCl_3$): δ 191.8, 131.7, 130.1, 119.5, 108.2, 70.6, 68.3, 45.7, 37.9, 27.1, 25.4; IR (film): 2947, 2849, 1638, 1406, 1201, 1065 cm^{-1}; HRMS-APCI (*m/z*) [M + H]$^+$ calcd for $C_{11}H_{16}NO_2$, 194.11756; found 194.11699.

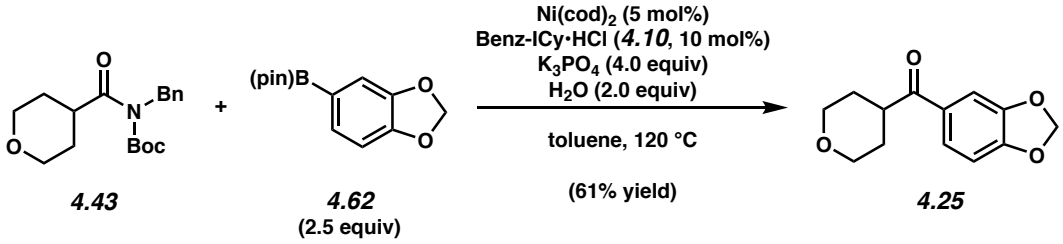

Ketone 4.25. Purification by flash chromatography (30:15:1 Hexanes:EtOAc:TEA) generated ketone **4.25** (61% yield, average of two experiments) as a white solid. Ketone **4.25**: mp: 97–98 ºC; R_f 0.35 (2:1 Hexanes:EtOAc); ^{1}H NMR (500 MHz, $CDCl_3$): δ 7.55 (dd, J = 8.2, 1.8, 1H), 7.42 (d, J = 1.8, 1H), 6.86 (d, J = 8.2, 1H), 6.04 (s, 2H), 4.05 (ddd, J = 11.4, 4.0, 2.4, 2H), 3.54 (td, J = 11.7, 2.2, 2H), 3.40 (tt, J = 11.2, 3.8, 1H), 1.92–1.83 (m, 2H), 1.77–1.72 (m, 2H); ^{13}C NMR (125 MHz, $CDCl_3$): δ 200.0, 151.9, 148.5, 130.7, 124.5, 108.3, 108.1, 102.0, 67.5, 42.6,

29.4; IR (film): 2955, 2847, 1670, 1440, 1258, 1241, 1114 cm^{-1}; HRMS-APCI (*m/z*) $[M + H]^+$ calcd for $C_{13}H_{15}O_4$, 235.09649; found 235.09592.

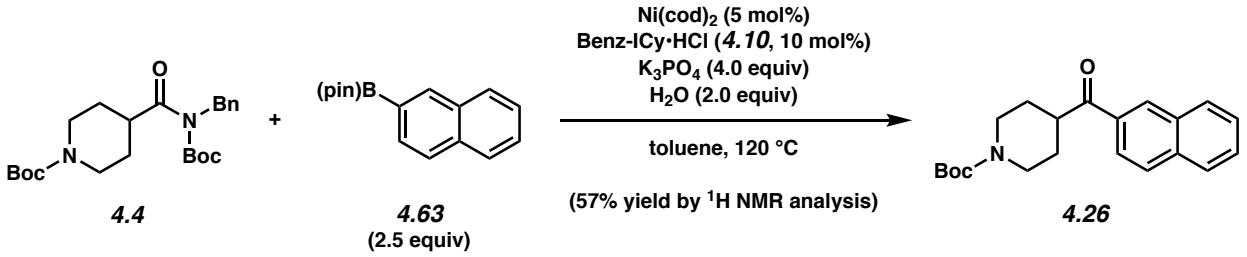

Ketone 4.26. ^1H NMR analysis of the crude reaction mixture indicated a 57% yield of ketone **4.26** relative to hexamethylbenzene internal standard. Purification by preparative thin-layer chromatography (4:1 Hexanes:EtOAc) provided an analytical sample of ketone **4.26** as a white amorphous solid. Ketone **26**: R_f 0.29 (4:1 Hexanes:EtOAc); ^1H NMR (500 MHz, $CDCl_3$): δ 8.45 (s, 1H), 8.02–7.96 (m, 2H), 7.93–7.86 (m, 2H), 7.63–7.54 (m, 2H), 4.20 (br s, 2H), 3.58 (tt, *J* = 11.1, 3.7, 1H), 3.04–2.87 (m, 2H), 1.97–1.84 (m, 2H), 1.82–1.71 (m, 2H), 1.48 (s, 9H); ^{13}C NMR (125 MHz, $CDCl_3$): δ 202.2, 154.9, 135.7, 133.3, 132.7, 129.8, 129.7, 128.8, 128.7, 127.9, 127.0, 124.3, 79.8, 43.7, 43.3, 28.7, 28.6; IR (film): 3060, 2975, 2930, 2858, 1682 cm^{-1}; HRMS-APCI (*m/z*) $[M + H]^+$ calcd for $C_{21}H_{26}NO_3$, 340.19072; found 340.19041.

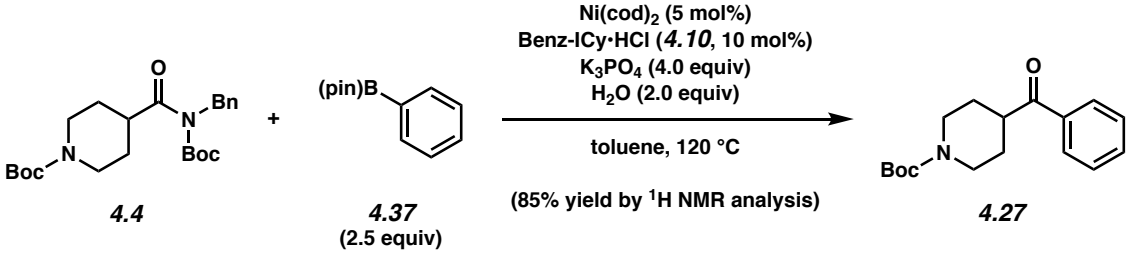

Ketone 4.27. ^1H NMR analysis of the crude reaction mixture indicated an 85% yield of ketone **4.27** relative to hexamethylbenzene internal standard. Purification by preparative thin-layer

chromatography (3:1 Hexanes:EtOAc) provided an analytical sample of ketone **4.27** as a white amorphous solid. Ketone **27**: R_f 0.21 (5:1 Hexanes:EtOAc). Spectral data match those previously reported.[28]

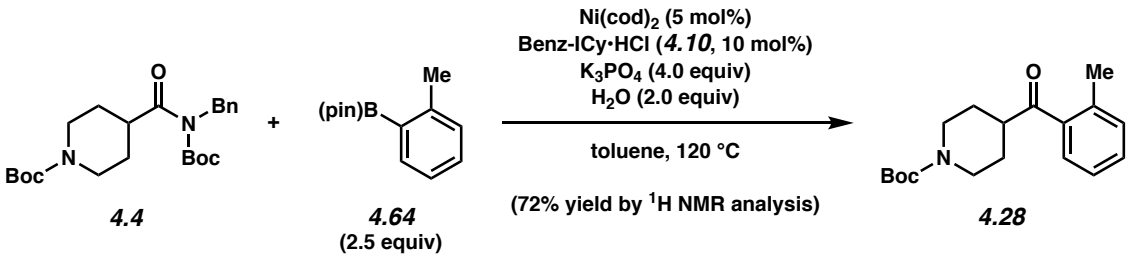

Ketone 4.28. ^{1}H NMR analysis of the crude reaction mixture indicated a 72% yield of ketone **4.28** relative to hexamethylbenzene internal standard. Purification by preparative thin-layer chromatography (4:1 Hexanes:EtOAc) provided an analytical sample of ketone **4.28** as a clear oil. Ketone **4.28**: R_f 0.42 (3:1 Hexanes:EtOAc). Spectral data match those previously reported.[27]

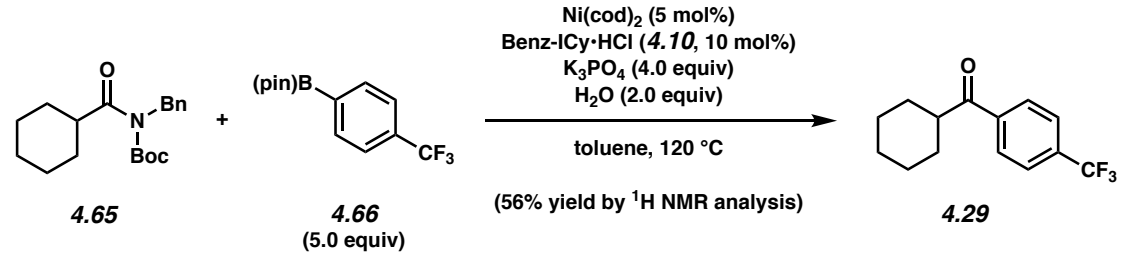

Ketone 4.29. ^{1}H NMR analysis of the crude reaction mixture indicated a 56% yield of ketone 4.**29** relative to hexamethylbenzene internal standard. Purification by preparative thin-layer chromatography (9:1 Hexanes:EtOAc) provided an analytical sample ketone **4.29** as a white solid. Ketone **4.29**: R_f 0.56 (9:1 Hexanes:EtOAc). Spectral data match those previously reported.[29]

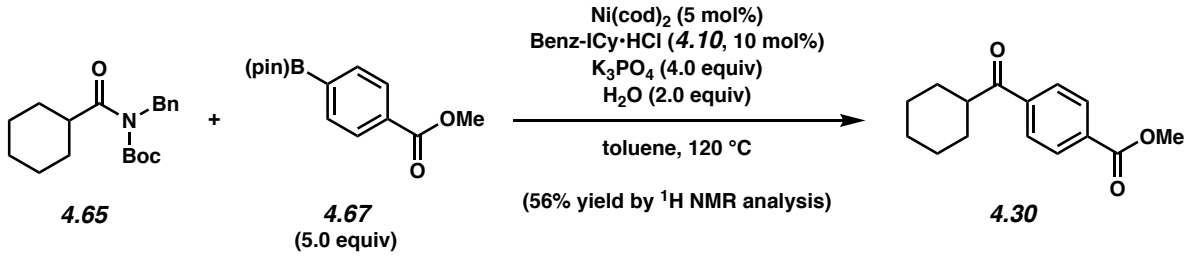

Ketone 4.30. ^{1}H NMR analysis of the crude reaction mixture indicated a 38% yield of ketone **4.30** relative to hexamethylbenzene internal standard. Purification by preparative thin-layer chromatography (9:1 Hexanes:EtOAc) provided an analytical sample of ketone **4.30** as a white solid. Ketone **4.30**: R_f 0.39 (9:1 Hexanes:EtOAc). Spectral data match those previously reported.[30]

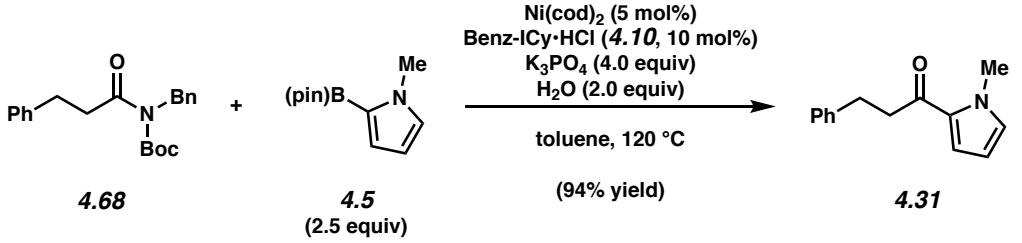

Ketone 4.31. Purification by flash chromatography (19:1 Hexanes:EtOAc → 14:1 Hexanes:EtOAc → 9:1 Hexanes:EtOAc) generated ketone **4.31** (94% yield, average of two experiments) as a clear oil. Ketone **4.31**: R_f 0.43 (5:1 Hexanes:EtOAc). Spectral data match those previously reported.[31]

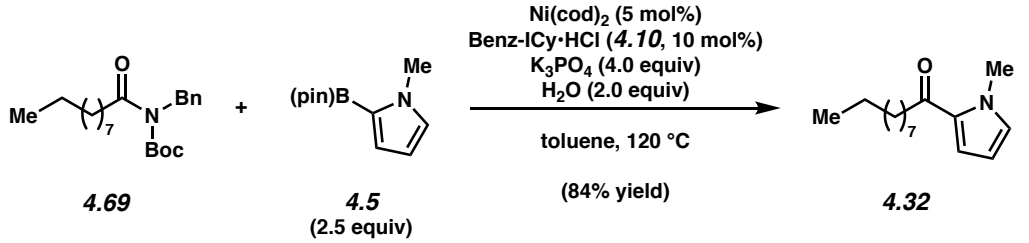

Ketone 4.32. Purification by flash chromatography (24:1 Hexanes:EtOAc) generated ketone **4.32** (84% yield, average of two experiments) as a clear oil. Ketone **4.32**: R_f 0.52 (5:1 Hexanes:EtOAc); ^{1}H NMR (500 MHz, $CDCl_3$): δ 6.95 (dd, J = 4.1, 1.7, 1H), 6.80–6.77 (m, 1H), 6.11 (dd, J = 4.1, 2.5, 1H), 3.94 (s, 3H), 2.77–2.73 (m, 2H), 1.69 (quint, J = 7.5, 2H), 1.39–1.20 (m, 12H), 0.88 (t, J = 7.1, 3H); ^{13}C NMR (125 MHz, $CDCl_3$): δ 192.0, 131.0, 130.9, 119.0, 107.9, 39.3, 37.9, 32.0, 29.7, 29.633, 29.627, 29.5, 25.5, 22.8, 14.3; IR (film): 2955, 2923, 2853, 1649, 1528 cm^{-1}; HRMS-APCI (*m/z*) $[M + H]^+$ calcd for $C_{15}H_{26}NO$, 236.20089; found 236.20080.

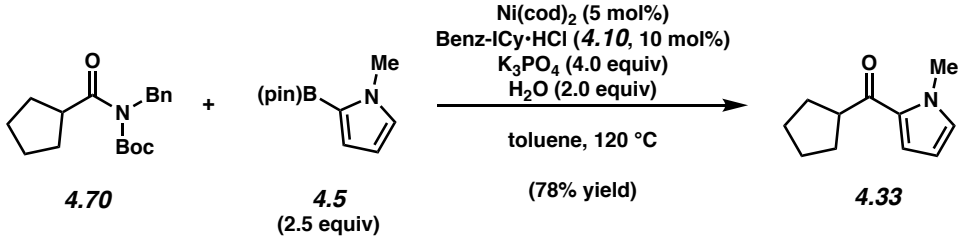

Ketone 4.33. Purification by flash chromatography (24:1 Hexanes:EtOAc → 19:1 Hexanes:EtOAc) generated ketone **4.33** (78% yield, average of two experiments) as a clear oil. Ketone **4.33**: R_f 0.50 (5:1 Hexanes:EtOAc). Spectral data match those previously reported.[32]

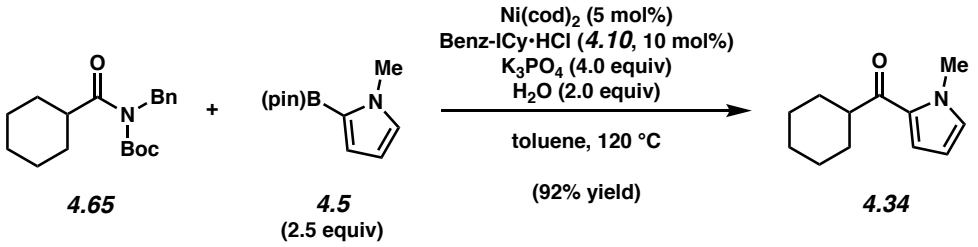

Ketone 4.34. Purification by flash chromatography (14:1 Hexanes:EtOAc) generated ketone **4.34** (92% yield, average of two experiments) as a clear oil. Ketone **4.34**: R_f 0.28 (14:1 Hexanes:EtOAc). Spectral data match those previously reported.[33]

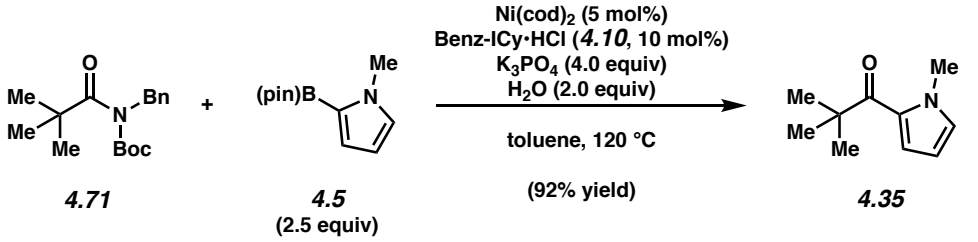

Ketone 4.35. Purification by flash chromatography (19:1 Hexanes:EtOAc) generated ketone **4.35** (92% yield, average of two experiments) as a clear oil. Ketone **4.35**: R_f 0.66 (4:1 Hexanes:EtOAc). Spectral data match those previously reported.[34]

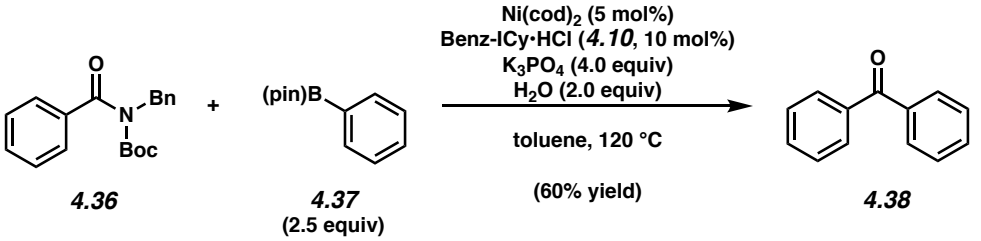

Ketone 4.38. Purification by thin-layer chromatography (5:1 Hexanes:EtOAc) generated ketone **4.38** (the reported yield was based on ^{1}H NMR analysis using hexamethylbenzene as an external standard) as a white solid. Ketone **4.38**: R_f 0.56 (5:1 Hexanes:EtOAc). Spectral data match those previously reported.[26]

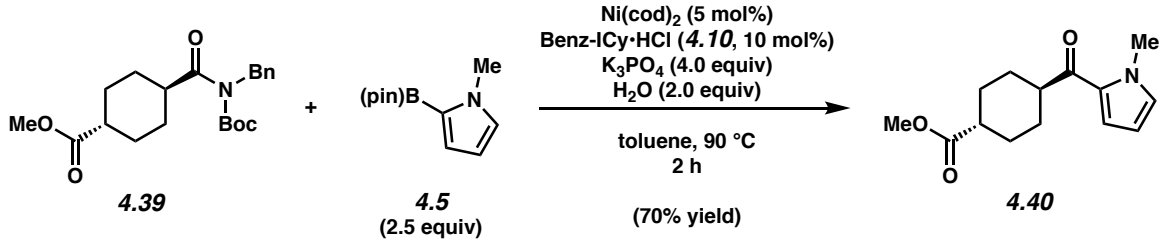

Ketone 4.40. Purification by flash chromatography (49:1 $CHCl_3$:CH_3CN) generated ketone **4.40** (the reported yield was based on ^{1}H NMR analysis using hexamethylbenzene as an external standard) as a white solid. Ketone **4.40**: R_f 0.48 (19:1 $CHCl_3$:CH_3CN); ^{1}H NMR (500 MHz, $CDCl_3$): δ 6.97 (dd, J = 4.1, 1.7, 1H), 6.83–6.80 (m, 1H), 6.13 (dd, J = 4.1, 2.5, 1H), 3.93 (s, 3H), 3.68 (s, 3H), 3.06–2.99 (m, 1H), 2.38–2.30 (m, 1H), 2.14–2.05 (m, 2H), 1.98–1.88 (m, 2H), 1.63–1.49 (m, 4H); ^{13}C NMR (125 MHz, $CDCl_3$): δ 194.3, 176.3, 131.5, 130.0, 118.9, 108.0, 51.7, 45.9, 42.7, 37.9, 29.0, 28.5; IR (film): 2942, 2862, 1730, 1645, 1408, 1251 cm^{-1}; HRMS-APCI (m/z) $[M + H]^+$ calcd for $C_{14}H_{20}NO_3$, 250.14377; found 250.14273.

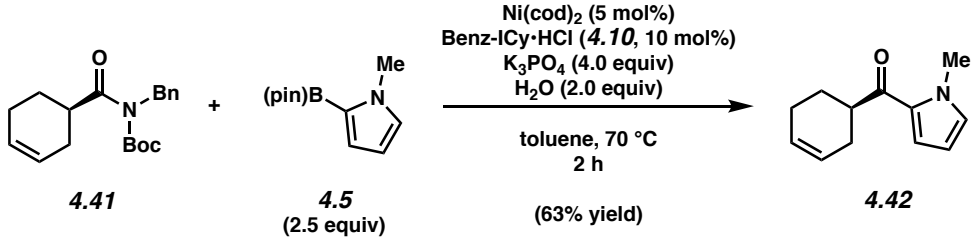

Ketone 4.42. Purification by flash chromatography (19:1 Hexanes:EtOAc → 14:1 Hexanes:EtOAc) generated ketone **4.42** (63% yield, average of two experiments) as a clear oil. Ketone **4.42**: R_f 0.46 (5:1 Hexanes:EtOAc); ^{1}H NMR (500 MHz, $CDCl_3$): δ 6.99 (dd, J = 4.1, 1.6, 1H), 6.83–6.80 (m, 1H), 6.13 (dd, J = 4.1, 2.4, 1H), 5.79–5.70 (m, 2H), 3.95 (s, 3H), 3.32–3.25 (m, 1H), 2.39–2.30 (m, 1H), 2.20–2.11 (m, 3H), 1.96–1.90 (m, 1H), 1.79–1.69 (m, 1H); ^{13}C NMR (125 MHz, $CDCl_3$): δ 194.8, 131.3, 130.3, 126.6, 126.2, 119.0, 108.0, 42.7, 38.0, 28.6,

26.4, 25.2; IR (film): 3107, 3023, 2931, 2838, 1643, 1527 cm^{-1}; HRMS-APCI (*m/z*) $[M + H]^+$ calcd for $C_{12}H_{16}NO$, 190.12264; found 190.12245. $[\alpha]^{20.7}_D$ –6.20 ° (*c* = 1.00, $CHCl_3$).

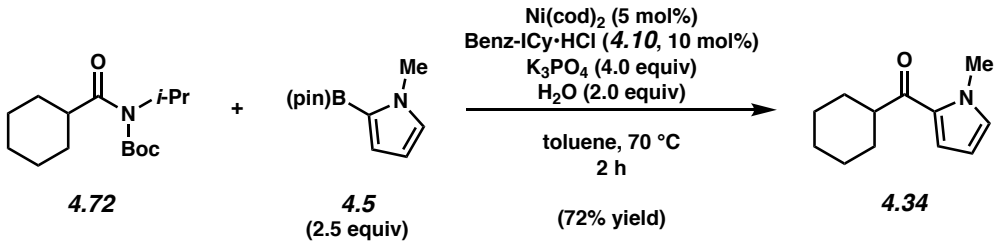

Ketone 4.34. Purification by column chromatography (49:1 Hexanes:EtOAc) generated ketone **4.34** (the reported yield was based on ^1H NMR analysis using hexamethylbenzene as an external standard) as a clear oil. Ketone **4.34**: R_f 0.28 (14:1 Hexanes:EtOAc). Spectral data match those previously reported.[33]

4.10.2.4. Verification of Enantiopurity

4.10.2.4.1. Synthesis of Racemic Ketone

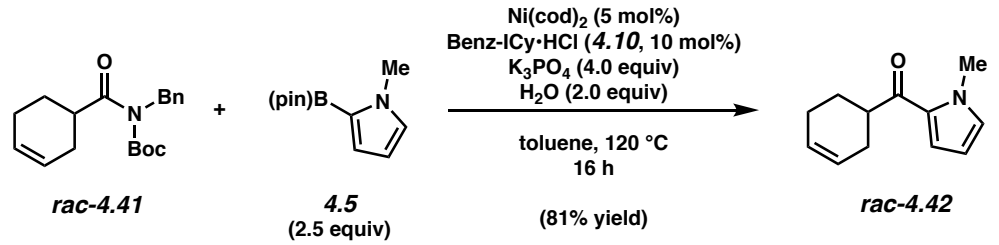

Ketone rac-4.42. Purification by flash chromatography (19:1 Hexanes:EtOAc → 14:1 Hexanes:EtOAc) generated ketone **rac-4.42** (81% yield, average of two experiments) as a clear oil.

4.10.2.4.2. Chiral SFC Assays for Amide 4.41 and Ketone 4.42

Compound	Method Column/Temp.	Solvent	Method Flow Rate	Retention Times (min)	Enantiomeric Ratio (er)
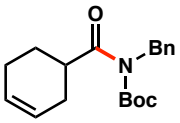 *rac-4.41*	Daicel ChiralPak OJ-H/35 °C	1% isopropanol in CO_2	1 mL/min	9.29/10.63	50:50
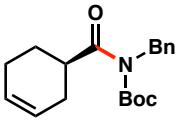 *4.41*	Daicel ChiralPak OJ-H/35 °C	1% isopropanol in CO_2	1 mL/min	9.57/10.54	99:1

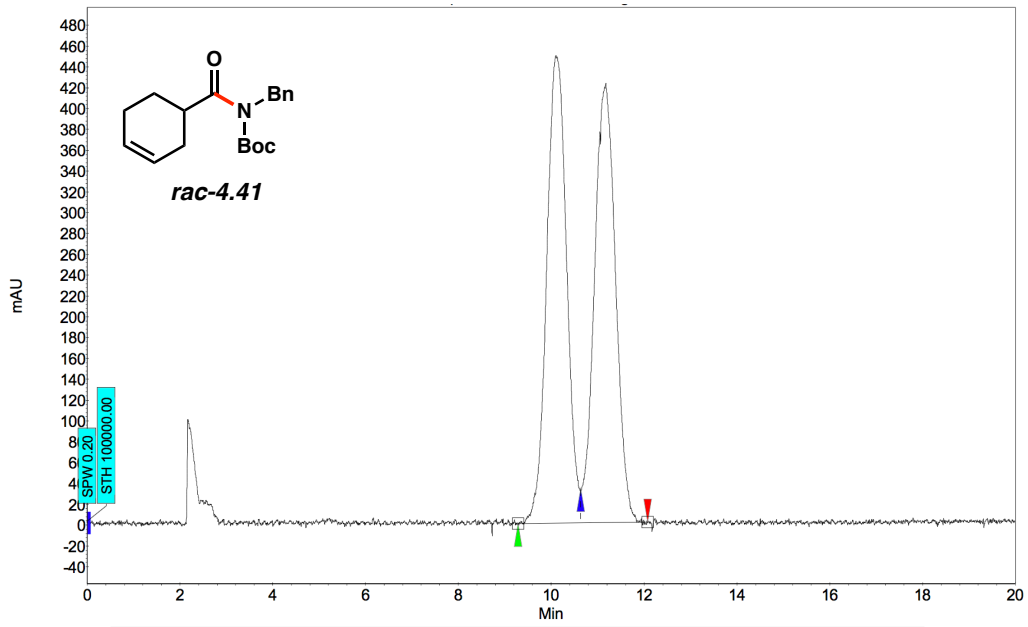

Index	Name	Start	Time	End	RT Offset	Quantity	Height	Area	Area
		[Min]	[Min]	[Min]	[Min]	[% Area]	[µV]	[µV.Min]	[%]
1	UNKNOWN	9.29	10.10	10.63	0.00	50.11	449.1	223.3	50.106
2	UNKNOWN	10.63	11.18	12.08	0.00	49.89	422.0	222.4	49.894
Total						100.00	871.2	445.7	100.000

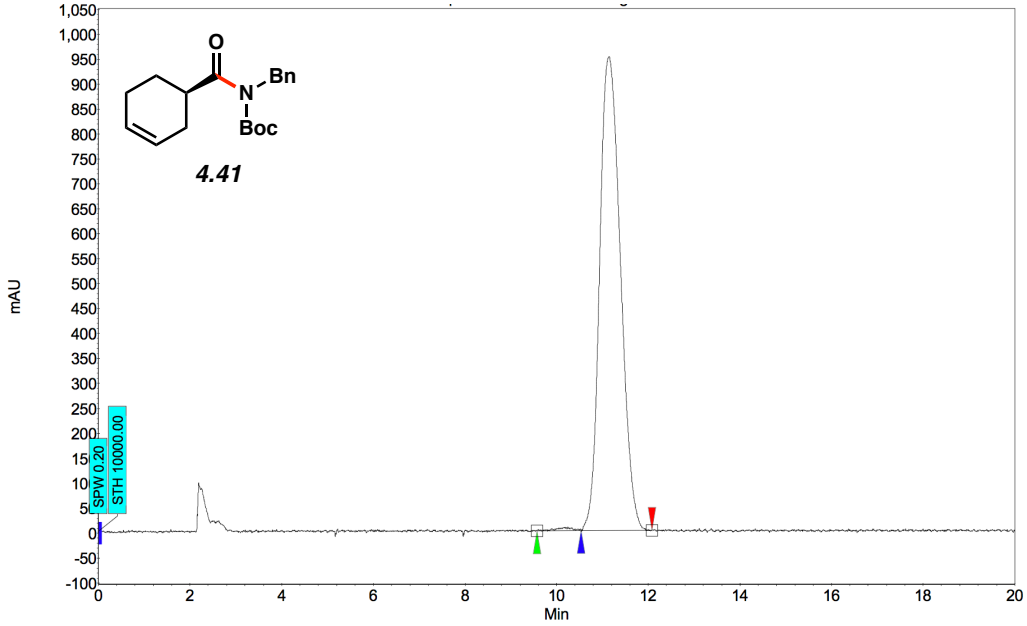

Index	Name	Start	Time	End	RT Offset	Quantity	Height	Area	Area
		[Min]	[Min]	[Min]	[Min]	[% Area]	[µV]	[µV.Min]	[%]
1	UNKNOWN	9.57	10.18	10.54	0.00	0.56	7.1	2.8	0.556
2	UNKNOWN	10.54	11.15	12.08	0.00	99.44	950.0	498.7	99.444
Total						100.00	957.2	501.5	100.000

Compound	Method Column/Temp.	Solvent	Method Flow Rate	Retention Times (min)	Enantiomeric Ratio (er)
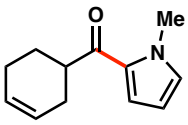 *rac-4.42*	Daicel ChiralPak OJ-H/35 °C	5% isopropanol in CO_2	2 mL/min	6.72/7.33	50:50
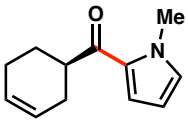 *4.42*	Daicel ChiralPak OJ-H/35 °C	5% isopropanol in CO_2	2 mL/min	6.69/7.12 6.82/7.29	99:2 96:4

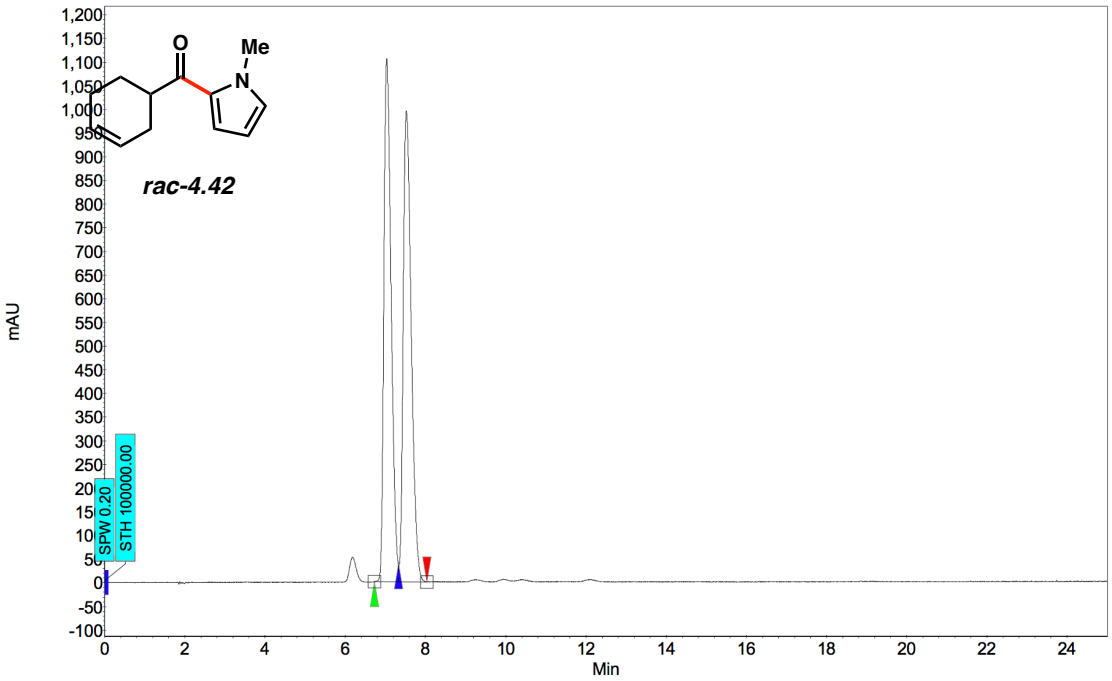

Index	Name	Start	Time	End	RT Offset	Quantity	Height	Area	Area
		[Min]	[Min]	[Min]	[Min]	[% Area]	[µV]	[µV.Min]	[%]
1	UNKNOWN	6.72	7.03	7.33	0.00	50.11	1104.5	231.5	50.113
2	UNKNOWN	7.33	7.52	8.04	0.00	49.89	994.7	230.5	49.887
Total						100.00	2099.2	462.0	100.000

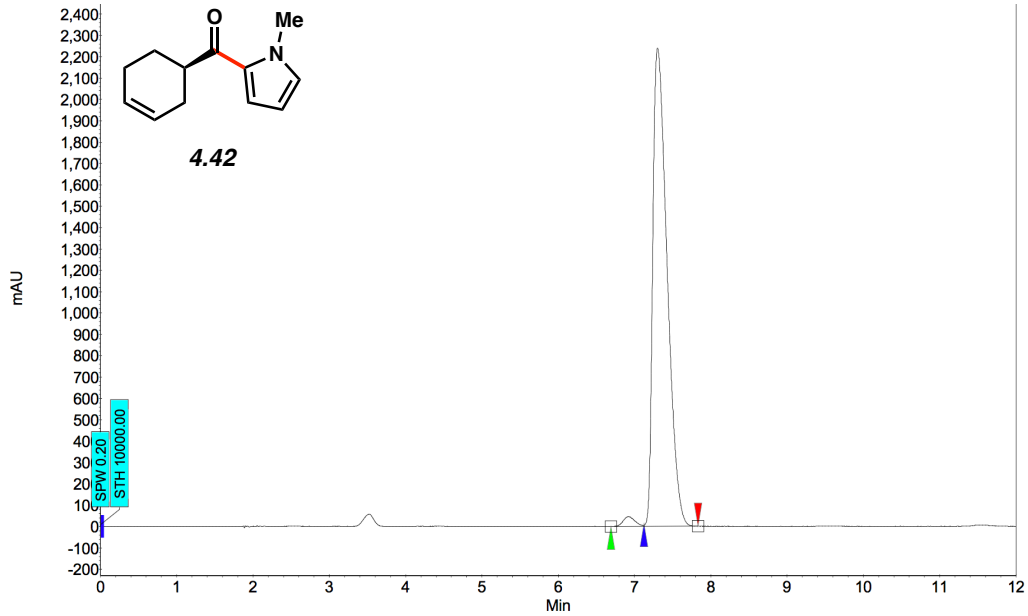

Index	Name	Start	Time	End	RT Offset	Quantity	Height	Area	Area
		[Min]	[Min]	[Min]	[Min]	[% Area]	[µV]	[µV.Min]	[%]
1	UNKNOWN	6.69	6.92	7.12	0.00	1.66	46.1	8.2	1.656
2	UNKNOWN	7.12	7.30	7.83	0.00	98.34	2239.4	485.6	98.344
Total						100.00	2285.5	493.8	100.000

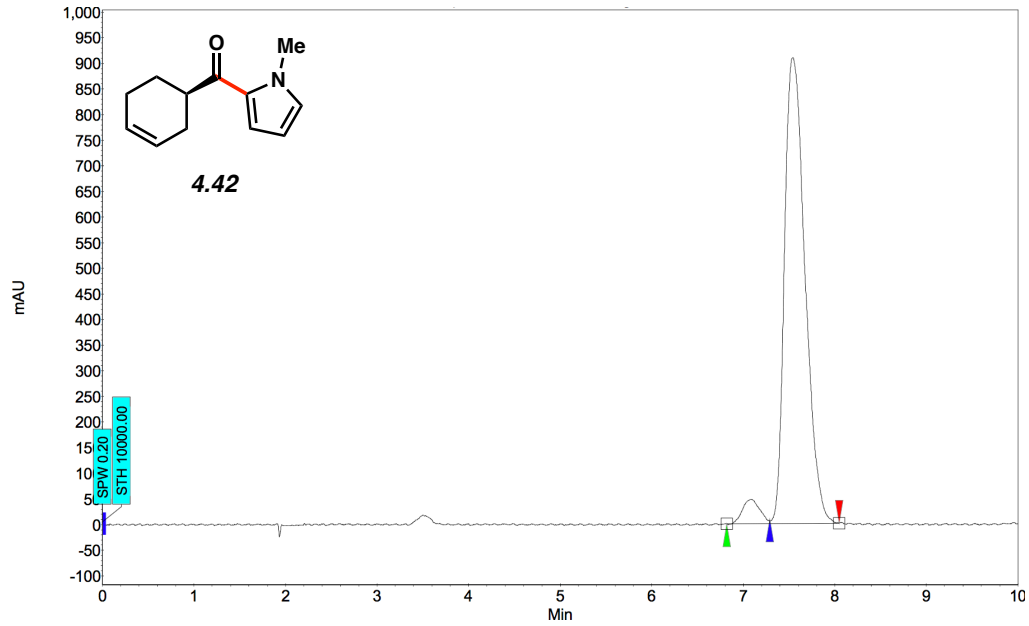

Index	Name	Start	Time	End	RT Offset	Quantity	Height	Area	Area
		[Min]	[Min]	[Min]	[Min]	[% Area]	[µV]	[µV.Min]	[%]
1	UNKNOWN	6.82	7.08	7.29	0.00	4.17	47.1	10.2	4.168
2	UNKNOWN	7.29	7.54	8.05	0.00	95.83	908.7	235.6	95.832
Total						100.00	955.8	245.9	100.000

4.10.2.4.3. Erosion of Stereochemistry Control Experiments

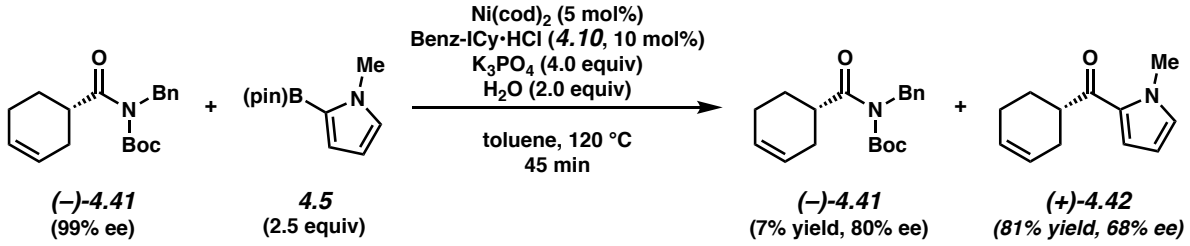

Amide 4.41 & Ketone 4.42. Purification by flash chromatography (Hexanes → 49:1 Hexanes:EtOAc → 24:1 Hexanes:EtOAc → 16:1 Hexanes:EtOAc) afforded recovered amide substrate **4.41** in 80% ee and ketone **4.42** in 68% ee (the reported yield was based on ^{1}H NMR analysis using hexamethylbenzene as an external standard) as clear oils.

4.10.2.4.4. Chiral HPLC Assays for Amide 4.41 and Ketone 4.42

Compound	Method Column/Temp.	Solvent	Method Flow Rate	Retention Times (min)	Enantiomeric Ratio (er)
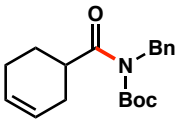 *rac-4.41*	Daicel ChiralPak OJ-H/23 °C	1% isopropanol in hexanes	1 mL/min	14.51/16.14	50:50
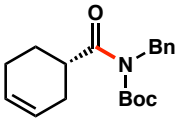 *(–)-4.41*	Daicel ChiralPak OJ-H/23 °C	1% isopropanol in hexanes	1 mL/min	14.08/15.61	90:10

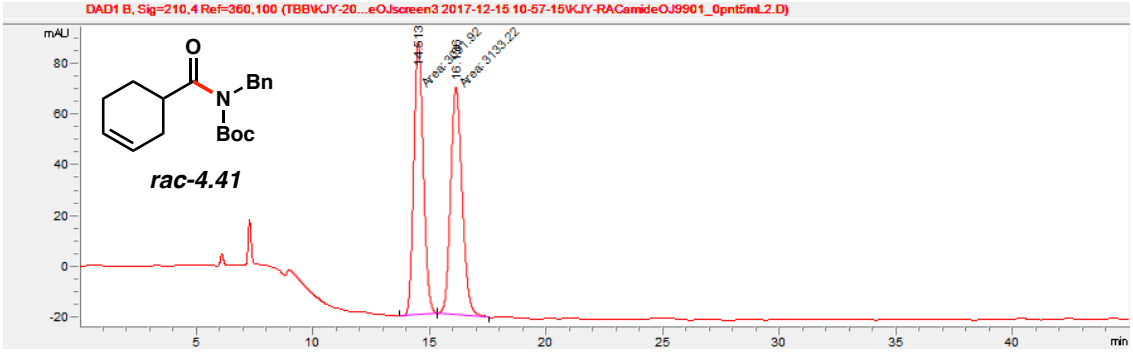

#	Time	Area	Height	Width	Area%	Symmetry
1	14.513	3091.9	108.2	0.4765	49.668	0.859
2	16.136	3133.2	90.2	0.5787	50.332	0.827

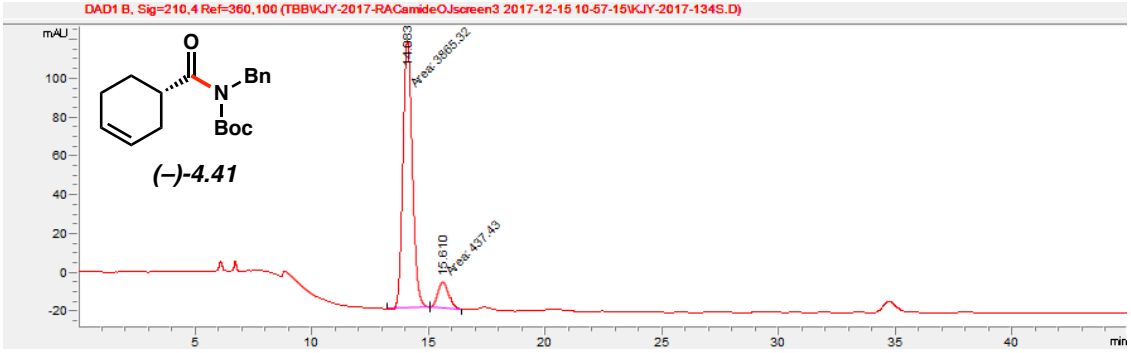

#	Time	Area	Height	Width	Area%	Symmetry
1	14.083	3865.3	138.1	0.4666	89.834	0.841
2	15.61	437.4	13.6	0.5372	10.166	0.848

Compound	Method Column/Temp.	Solvent	Method Flow Rate	Retention Times (min)	Enantiomeric Ratio (er)
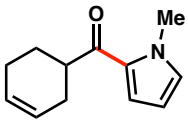 ***rac-4.42***	Daicel ChiralPak OJ-H/23 °C	10% isopropanol in hexanes	1 mL/min	6.04/6.43	50:50
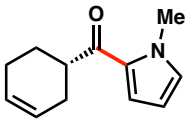 ***(+)-4.42***	Daicel ChiralPak OJ-H/23 °C	10% isopropanol in hexanes	1 mL/min	6.05/6.46	84:16

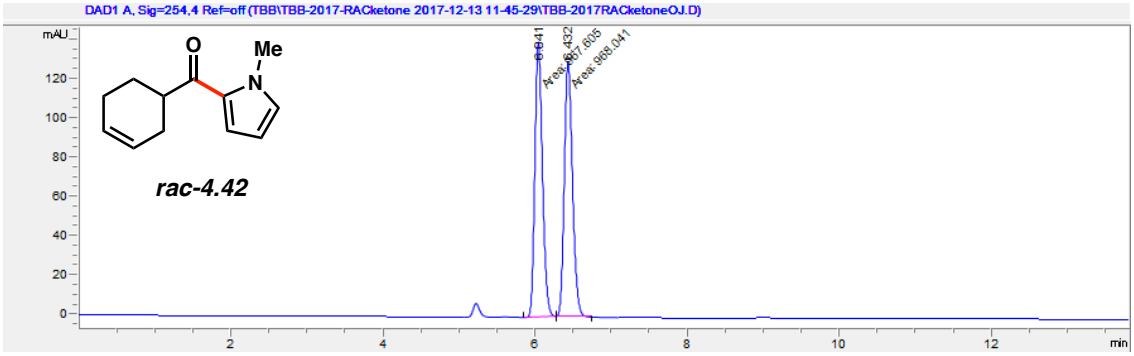

#	Time	Area	Height	Width	Area%	Symmetry
1	6.041	967.6	140.3	0.1149	49.989	0.799
2	6.432	968	129.5	0.1246	50.011	0.805

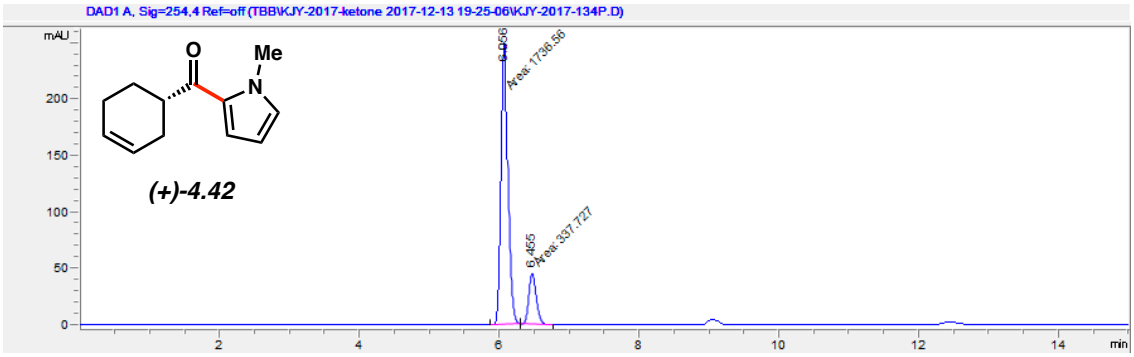

#	Time	Area	Height	Width	Area%	Symmetry
1	6.056	1736.6	249.8	0.1159	83.718	0.788
2	6.455	337.7	45.3	0.1243	16.282	0.807

4.10.2.4.5. Erosion of Stereochemistry of Ketone 4.42

Table 4.3. Evaluation of Impact of Reaction Components on Erosion of *a*-Stereocenter[a]

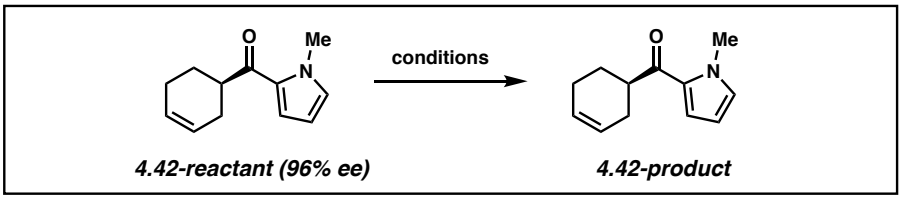

4.42-reactant (96% ee) *4.42-product*

Entry	*Control Experiment Conditions*	*Experimental Results ee of 4.42-product*
1	K_3PO_4 (4.0 equiv), H_2O (2.0 equiv) toluene (1.0 M), 120 °C, 4 h	88%
2	$Ni(cod)_2$ (5 mol%) toluene (1.0 M), 120 °C, 16 h	92%
3	Benz-ICy·HCl (*4.10*, 10 mol%) toluene (1.0 M), 120 °C, 4 h	96%
4	$Ni(cod)_2$ (5 mol%), Benz-ICy·HCl (*4.10*, 10 mol%), NaOtBu (9 mol%) toluene (1.0 M), 120 °C, 4 h	51%[a]
5	Benz-ICy·HCl (*4.10*, 10 mol%), NaOtBu (9 mol%) toluene (1.0 M), 120 °C, 4 h	0%[b]

[a] $Ni(cod)_2$, Benz-ICy·HCl (*4.10*), and NaOtBu were stirred for 1 h in toluene at 23 °C to generate active catalyst prior to addition to ketone substrate. [b] Benz-ICy·HCl and NaOtBu were stirred for 1 h in toluene at 23 °C to generate free NHC prior to addition to ketone substrate.

4.10.2.4.6. Chiral HPLC Assays for Ketone 4.42

Compound	Entry	Method Column/ Temp.	Solvent	Method Flow Rate	Retention Times (min)	Enantiomeric Ratio (er)
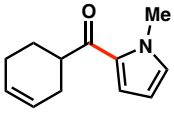 *rac-4.42*	-	Daicel ChiralPak OJ-H/23 °C	10% isopropanol in hexanes	1 mL/min	6.041/6.432	50:50
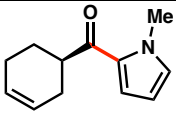 *4.42*	1	Daicel ChiralPak OJ-H/23 °C	10% isopropanol in hexanes	1 mL/min	6.063/6.455	6:94
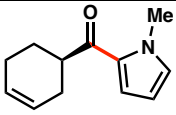 *4.42*	2	Daicel ChiralPak OJ-H/23 °C	10% isopropanol in hexanes	1 mL/min	6.064/6.456	4:96

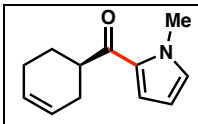 *4.42*	3	Daicel ChiralPak OJ-H/23 °C	10% isopropanol in hexanes	1 mL/min	6.073/6.464	2:98
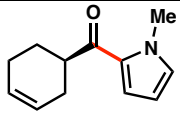 *4.42*	4	Daicel ChiralPak OJ-H/23 °C	10% isopropanol in hexanes	1 mL/min	6.074/6.466	24:76
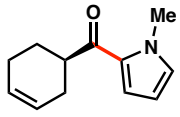 *4.42*	5	Daicel ChiralPak OJ-H/23 °C	10% isopropanol in hexanes	1 mL/min	6.092/6.488	50:50

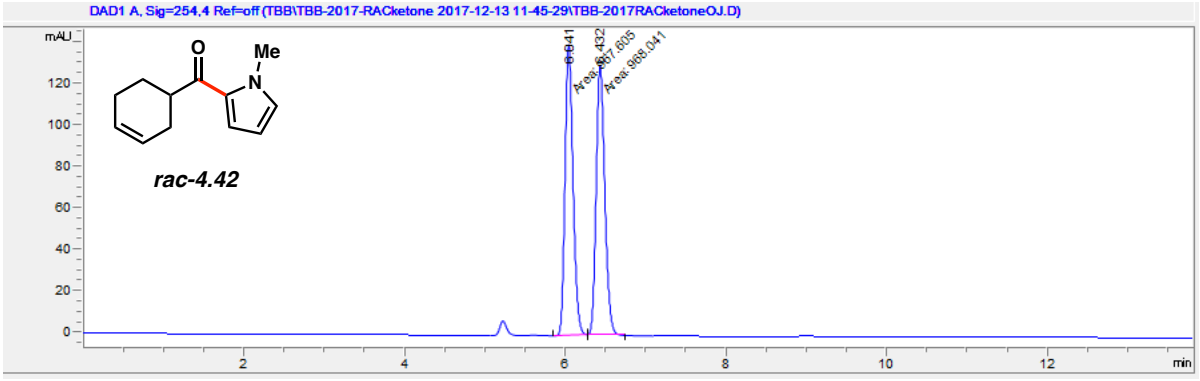

#	Time	Area	Height	Width	Area%	Symmetry
1	6.041	967.6	140.3	0.1149	49.989	0.799
2	6.432	968	129.5	0.1246	50.011	0.805

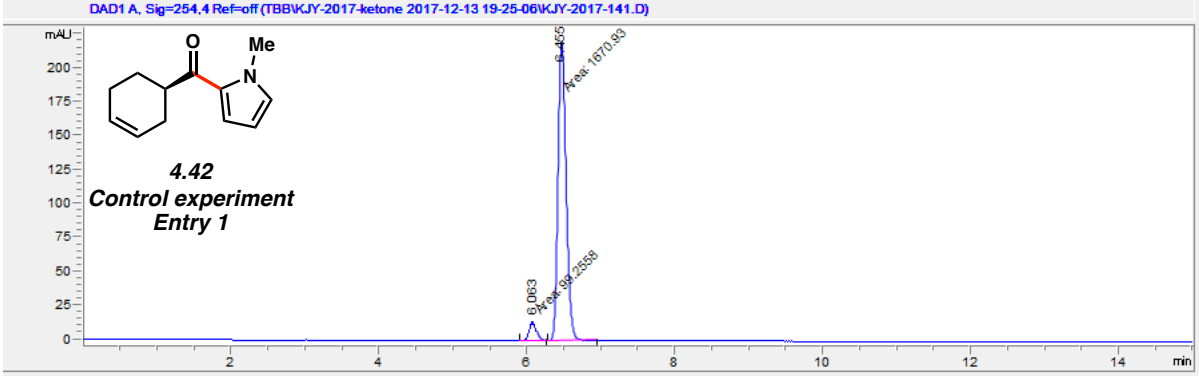

#	Time	Area	Height	Width	Area%	Symmetry
1	6.063	99.3	14.1	0.1172	5.607	0.819
2	6.455	1670.9	219.9	0.1267	94.393	0.799

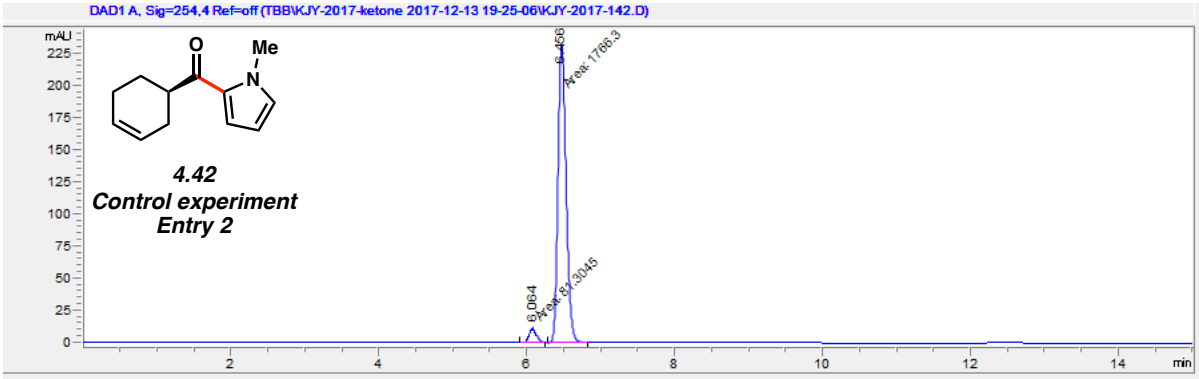

#	Time	Area	Height	Width	Area%	Symmetry
1	6.064	81.3	11.6	0.1168	4.401	0.798
2	6.456	1766.3	232.5	0.1266	95.599	0.798

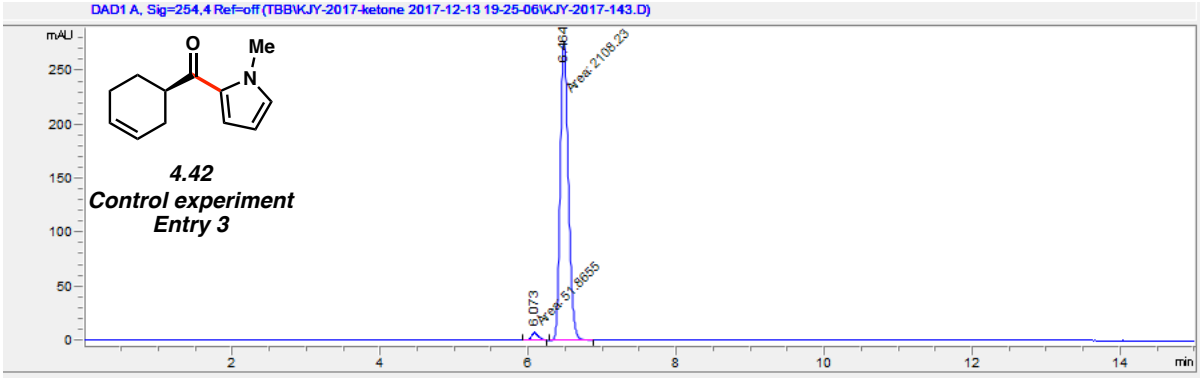

#	Time	Area	Height	Width	Area%	Symmetry
1	6.073	51.9	7.6	0.1144	2.401	0.839
2	6.464	2108.2	276.1	0.1273	97.599	0.796

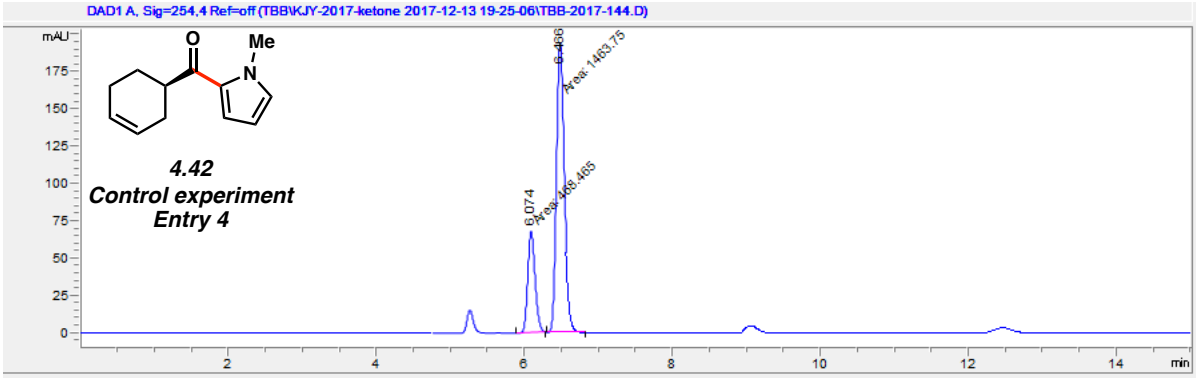

#	Time	Area	Height	Width	Area%	Symmetry
1	6.074	468.5	67.7	0.1154	24.245	0.808
2	6.466	1463.8	193.6	0.126	75.755	0.799

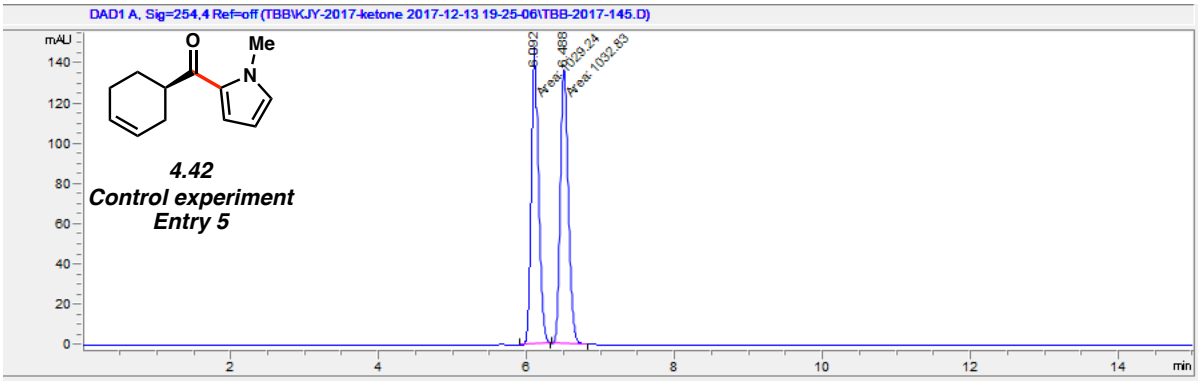

#	Time	Area	Height	Width	Area%	Symmetry
1	6.092	1029.2	147.7	0.1161	49.913	0.796
2	6.488	1032.8	136.8	0.1259	50.087	0.801

4.10.2.5. Robustness Screen

Table 4.4. Evaluation of Functional Group Compatibility in the Suzuki–Miyaura Reaction[a]

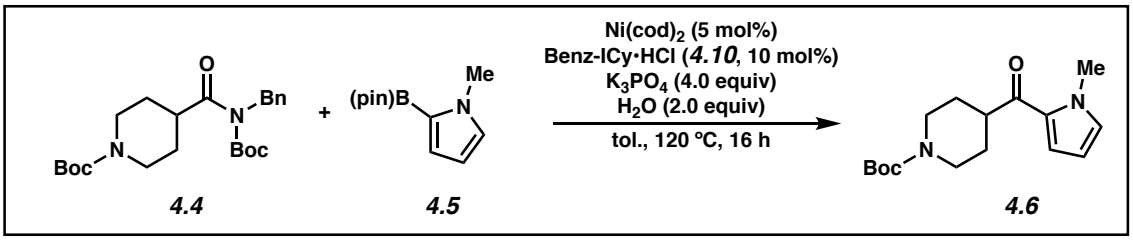

Entry	Additive	Yield of *4.6* (%)	Additive Remaining (%)	*4.4* Remaining (%)
1	None	95	N.D.	0
2	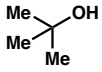	70	N.D.[b]	0
3	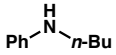	58	73	0
4	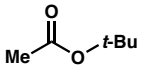	66	N.D.[b]	0
5	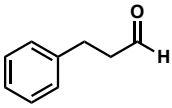	0	8	46
6	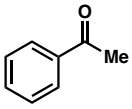	67	73	0
7		0	N.D.[b]	0
8	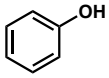	0	42	0
9	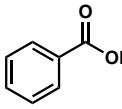	68	0	0
10	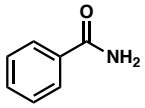	0	30	0
11	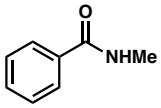	66	66	0
12	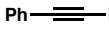	71	4	0
13		26	N.D.[b]	0

[a] Conditions: $Ni(cod)_2$ (5 mol%), Benz-ICy·HCl (*4.10*, 10 mol%), substrate (*4.4*, 1.0 equiv), boronate (*4.5*, 2.5 equiv), K_3PO_4 (4.0 equiv), toluene (1.0 M), H_2O (2.0 equiv), and additive (1.0 equiv) at 120 °C for 16 h. Yields of coupled product, remaining additive, and remaining starting material were determined by ^1H NMR analysis using hexamethylbenzene as an internal standard. [b] Not determined due to low boiling point.

4.10.2.6. Gram Scale Suzuki–Miyaura Reaction and Subsequent Fischer Indolization

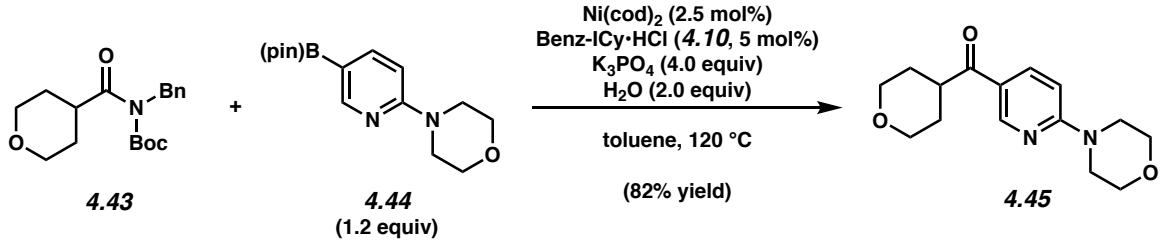

Ketone 4.45. A 20 mL scintillation vial was charged with anhydrous powdered K_3PO_4 (2.66 g, 12.5 mmol, 4.0 equiv) and a magnetic stir bar. The vial and contents were flame-dried under reduced pressure, then allowed to cool under N_2. Amide substrate **4.43** (1.00 g, 3.14 mmol, 1.0 equiv) and 2-morpholinopyridine-5-boronic acid pinacol ester (**4.44**) (1.09 g, 3.76 mmol, 1.2 equiv) were added. The vial was flushed with N_2, then water (113 μL, 6.27 mmol, 2.0 equiv), which had been sparged with N_2 for 10 min, was added. The vial was taken into a glove box and charged with $Ni(cod)_2$ (21.6 mg, 0.0784 mmol, 2.5 mol%) and Benz-ICy•HCl (**10**, 50.0 mg, 0.157 mmol, 5 mol%). Subsequently, toluene (3.14 mL, 1.0 M) was added. The vial was sealed with a Teflon-lined screw cap, removed from the glove box, and stirred vigorously (800 rpm) at 120 °C for 16 h. After cooling to 23 °C, the mixture was diluted with hexanes (7 mL) and filtered over a plug of silica gel (100 mL of EtOAc eluent). The volatiles were removed under reduced pressure, and the crude residue was purified by flash chromatography (3:1 Hexanes:EtOAc → 19:1 CH_2Cl_2:MeOH) to yield ketone product **4.45** (707 mg, 82% yield) as an off-white solid. Ketone **4.45**: mp: 122–124 ºC; R_f 0.36 (4:1 PhH:CH_3CN); ^{1}H NMR (500 MHz, $CDCl_3$): δ 8.79 (d, *J* = 2.2, 1H), 8.06 (dd, *J* = 9.1, 2.4, 1H), 6.63 (d, *J* = 9.1, 1H), 4.09–4.02 (m, 2H), 3.84–3.78 (m, 4H), 3.71–3.65 (m, 4H), 3.54 (td, *J* = 11.7, 2.2, 2H), 3.37 (tt, *J* = 11.2, 3.8, 1H), 1.96–1.84 (m, 2H), 1.79–1.71 (m, 2H); ^{13}C NMR (125 MHz, $CDCl_3$): δ 199.2, 160.7, 150.4, 137.9, 121.5,

105.9, 67.5, 66.7, 45.0, 42.4, 29.3; IR (film): 2955, 2920, 2850, 1663, 1596 cm^{-1}; HRMS-APCI (*m/z*) $[M + H]^+$ calcd for $C_{15}H_{21}N_2O_3$, 277.15467; found 277.15256.

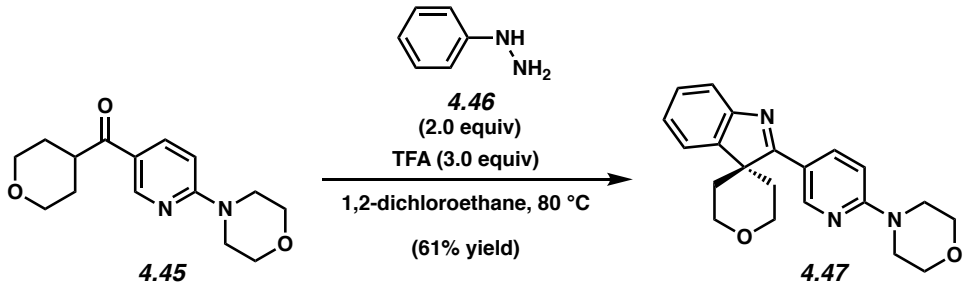

Indolenine 4.47. A 20 mL scintillation vial was charged with ketone **4.45** (707 mg, 2.56 mmol, 1.0 equiv) and a magnetic stir bar. Subsequently, 1,2-dichloroethane (12.0 mL, 0.21 M), phenylhydrazine **4.46** (503 µL, 5.12 mmol, 2.0 equiv), and TFA (588 µL, 7.69 mmol, 3.0 equiv) were added. The vial was sealed with a Teflon-lined screw cap and stirred at 80 °C for 16 h. After cooling to 23 °C, the volatiles were removed under reduced pressure, and the crude residue was purified by flash chromatography (3:1 Hexanes:EtOAc → 1:1 Hexanes:EtOAc → 100% EtOAc) to yield indolenine **4.47** (546 mg, 61% yield) as a tan solid. Indolenine **4.47**: mp: 186–189 ºC; R_f 0.26 (4:1 PhH:CH_3CN); ^{1}H NMR (500 MHz, $CDCl_3$): δ 9.11 (d, *J* = 2.2, 1H), 8.49 (dd, *J* = 9.1, 2.5, 1H), 7.92 (d, *J* = 7.4, 1H), 7.69 (d, *J* = 7.3, 1H), 7.41 (td, *J* = 7.6, 1.1, 1H), 7.22 (td, *J* = 7.5, 1.1, 1H), 6.73 (d, *J* = 9.1, 1H), 4.23–4.08 (m, 4H), 3.87–3.81 (m, 4H), 3.70–3.64 (m, 4H), 2.77–2.67 (m, 2H), 1.36 (d, *J* = 14.1, 2H); ^{13}C NMR (125 MHz, $CDCl_3$): δ 179.2, 159.5, 154.1, 148.9, 145.9, 138.2, 128.3, 124.8, 123.6, 121.2, 118.4, 106.4, 66.8, 64.0, 54.5, 45.2, 31.6; IR (film): 2960, 2921, 2858, 1596, 1499 cm^{-1}; HRMS-APCI (*m/z*) $[M + H]^+$ calcd for $C_{21}H_{24}N_3O_2$, 350.18630; found 350.18529.

4.11 Spectra Relevant to Chapter Four:

Nickel-Catalyzed Suzuki–Miyaura Coupling of Aliphatic Amides

Timothy B. Boit,[†] Nicholas A. Weires,[†] Junyong Kim,[†] and Neil K. Garg

ACS Catal. **2018**, *8*, 1003–1008.

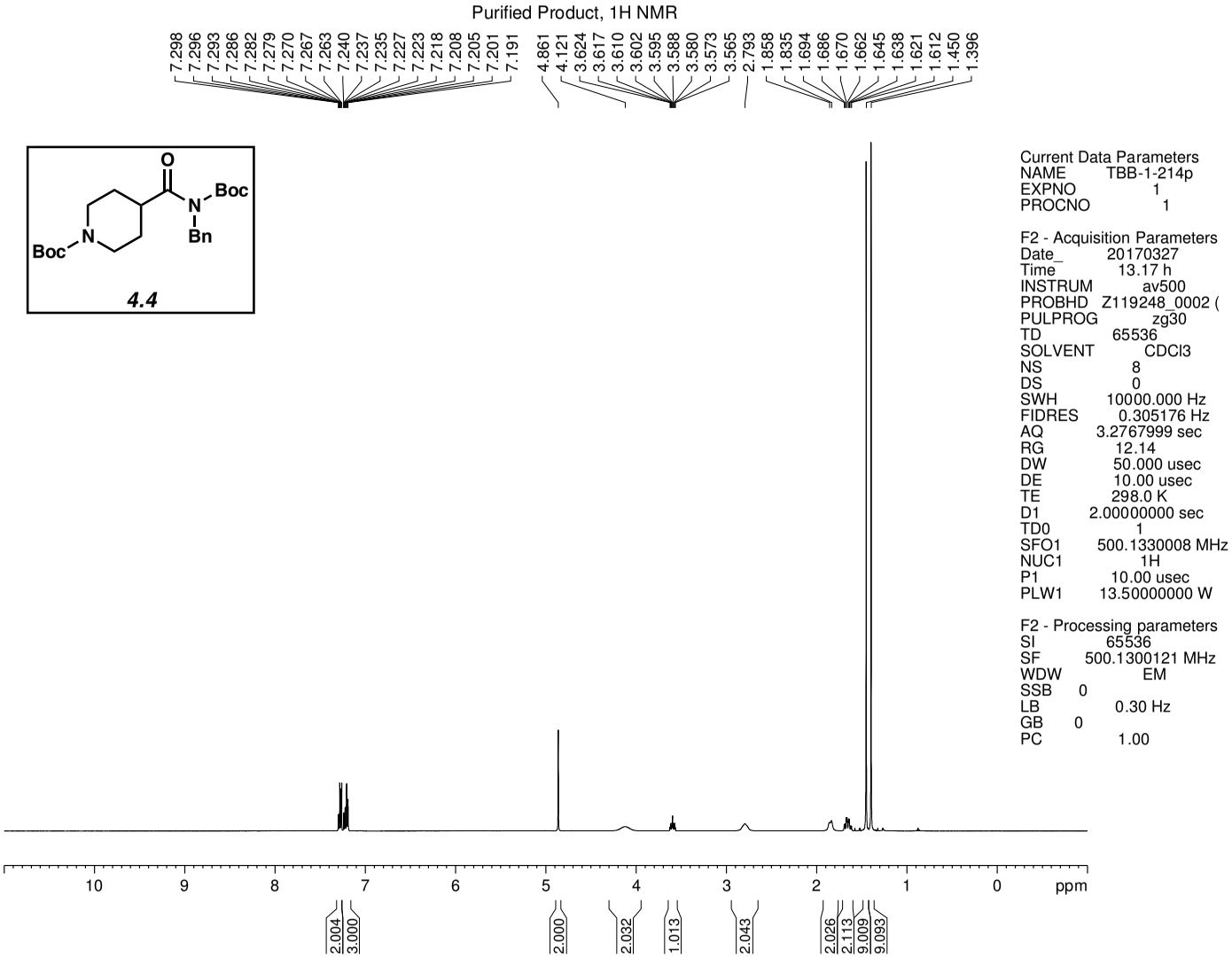

Figure 4.7 ^{1}H NMR (500 MHz, $CDCl_3$) of compound **4.4**.

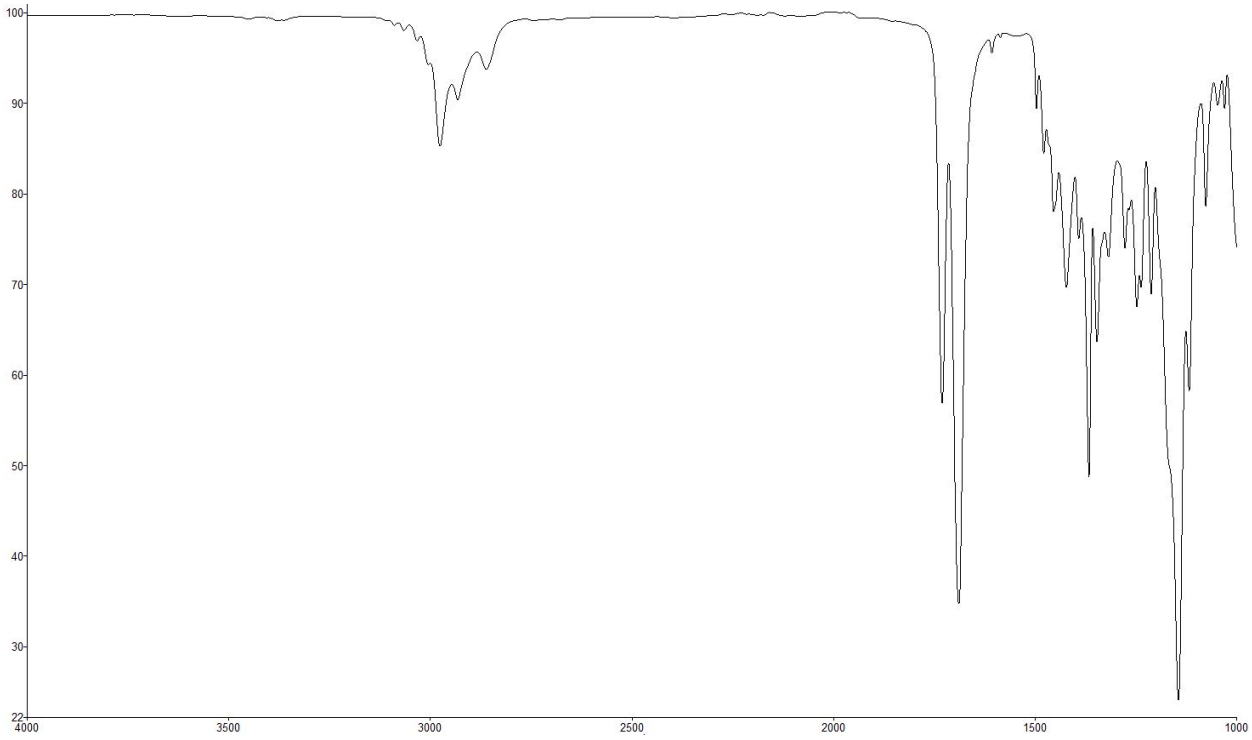

Figure 4.8 Infrared spectrum of compound **4.4**.

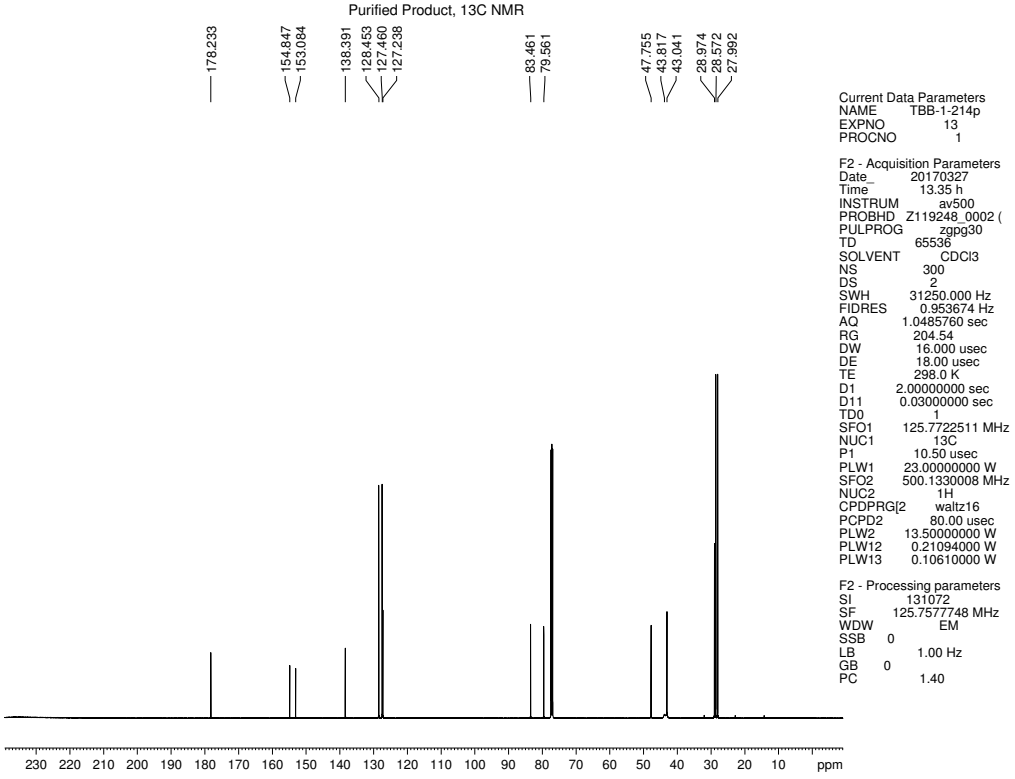

Figure 4.9 ^{13}C NMR (125 MHz, $CDCl_3$) of compound **4.4**.

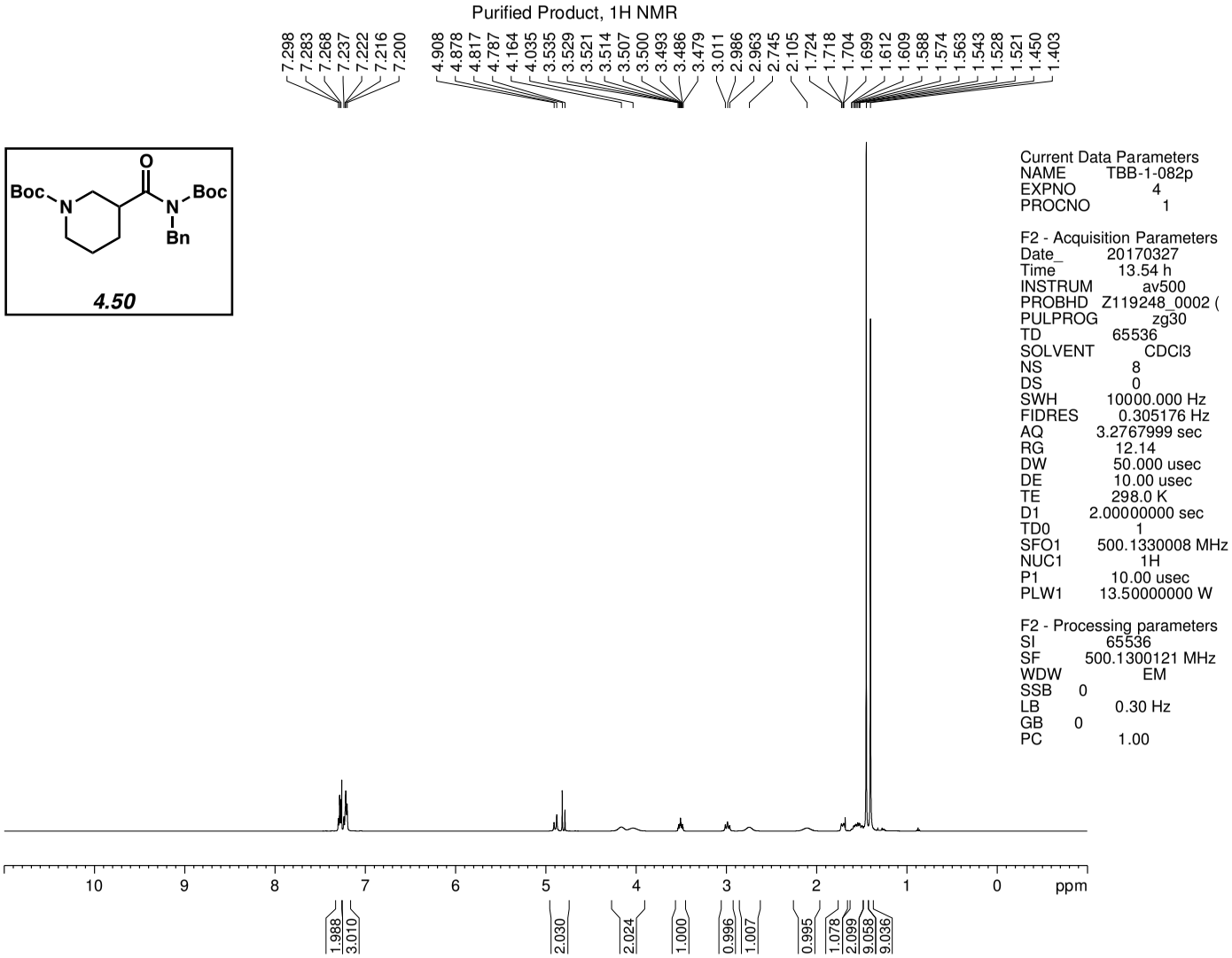

Figure 4.10 ^{1}H NMR (500 MHz, $CDCl_3$) of compound **4.50**.

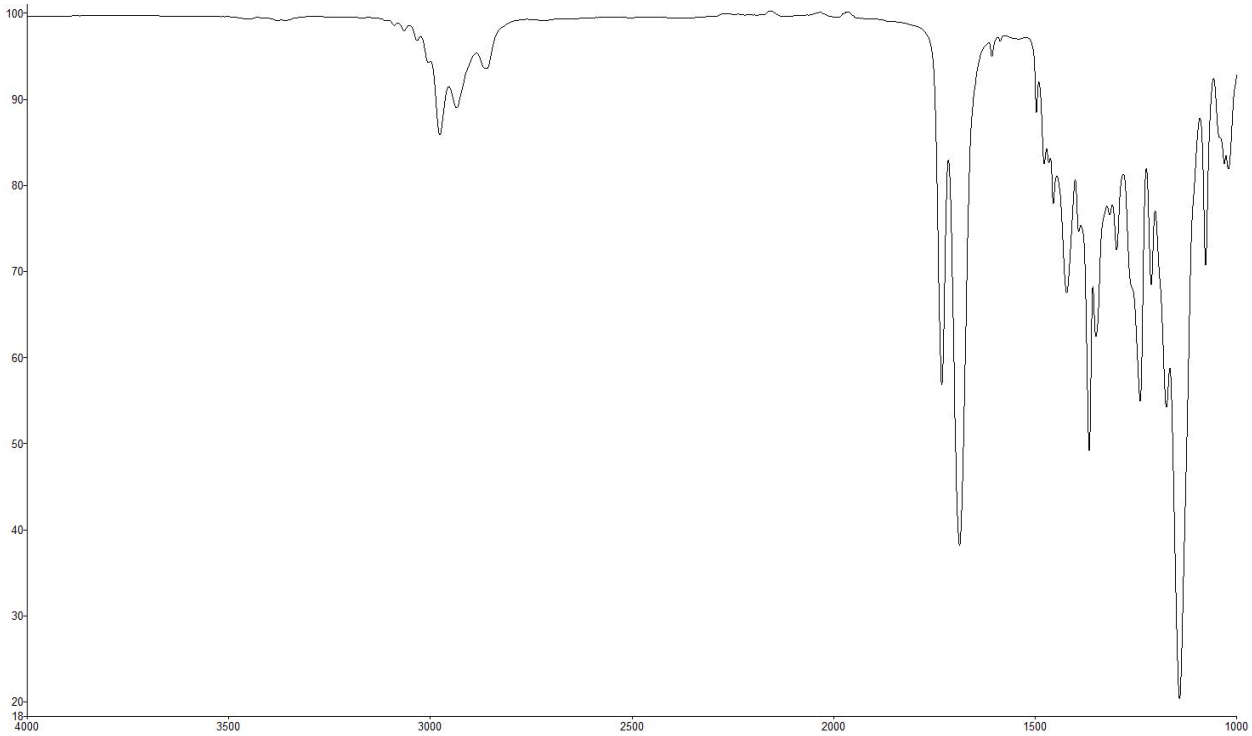

Figure 4.11 Infrared spectrum of compound **4.50**.

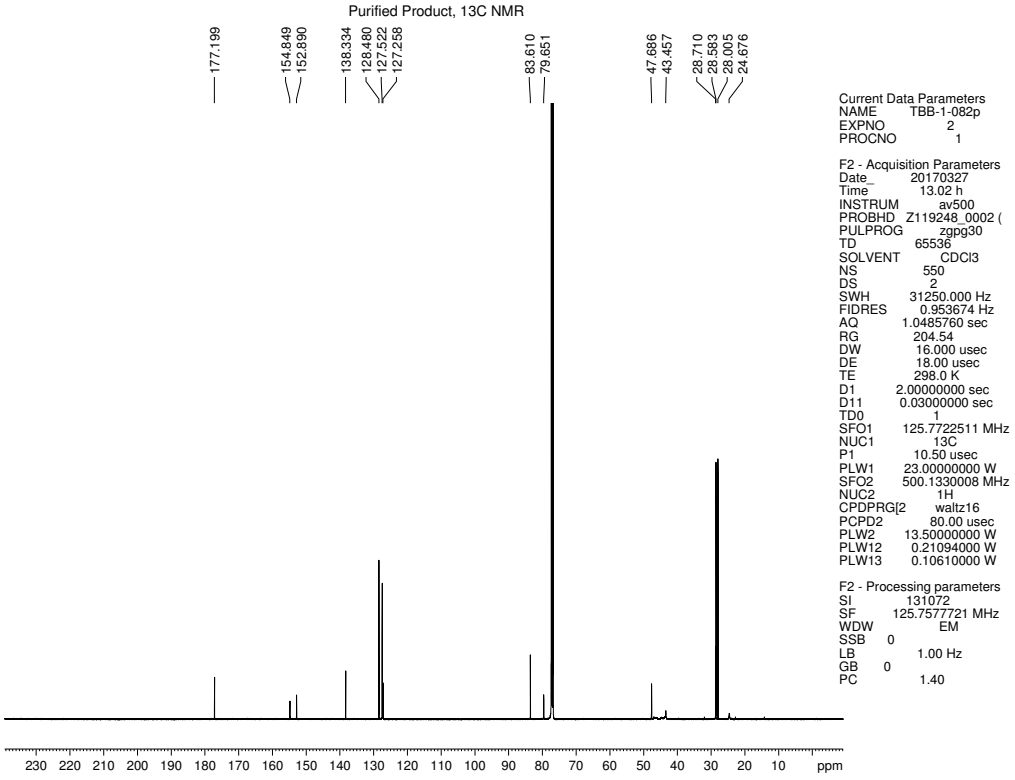

Figure 4.12 ^{13}C NMR (125 MHz, $CDCl_3$) of compound **4.50**.

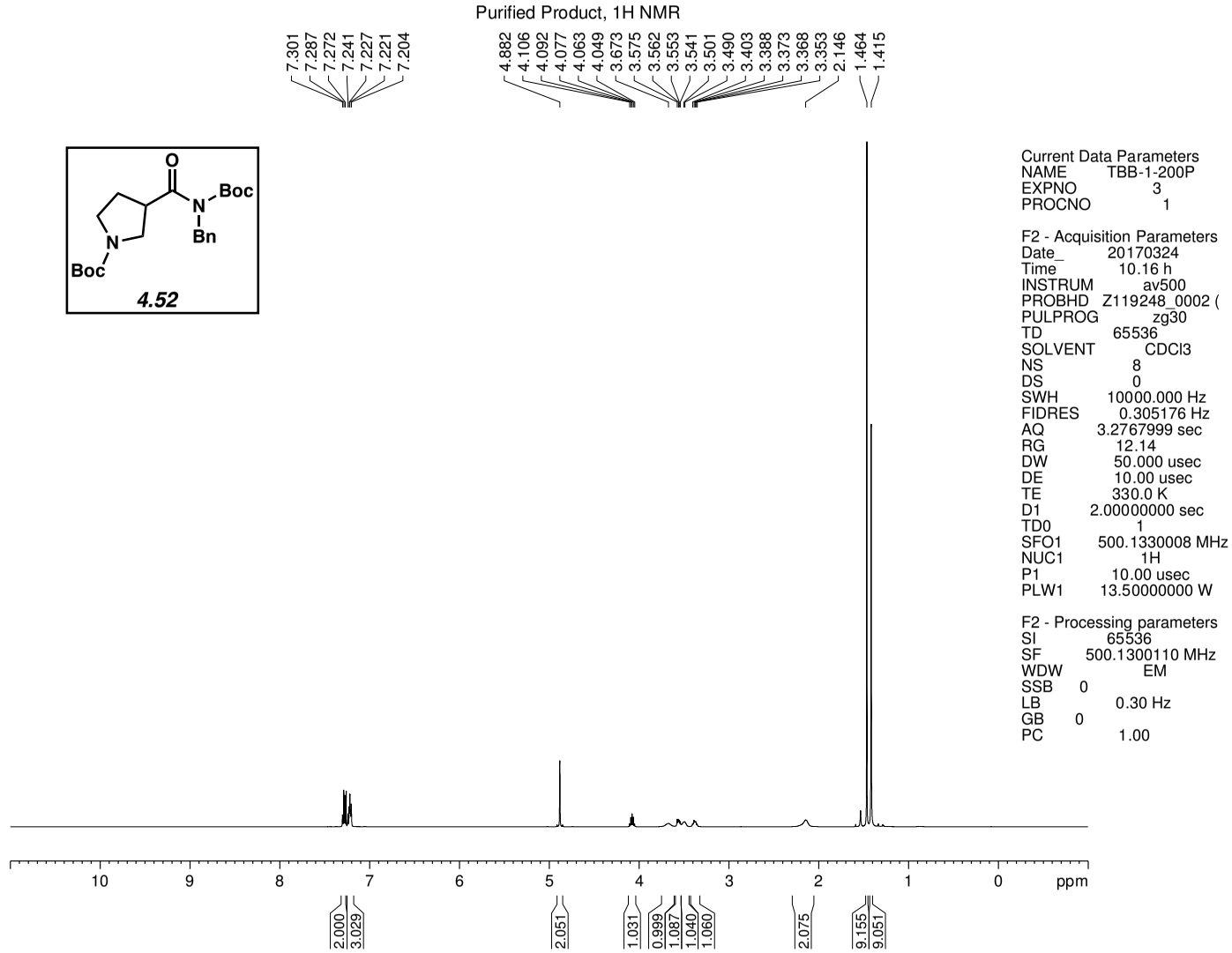

Figure 4.13 ^{1}H NMR (500 MHz, $CDCl_3$) of compound **4.52**.

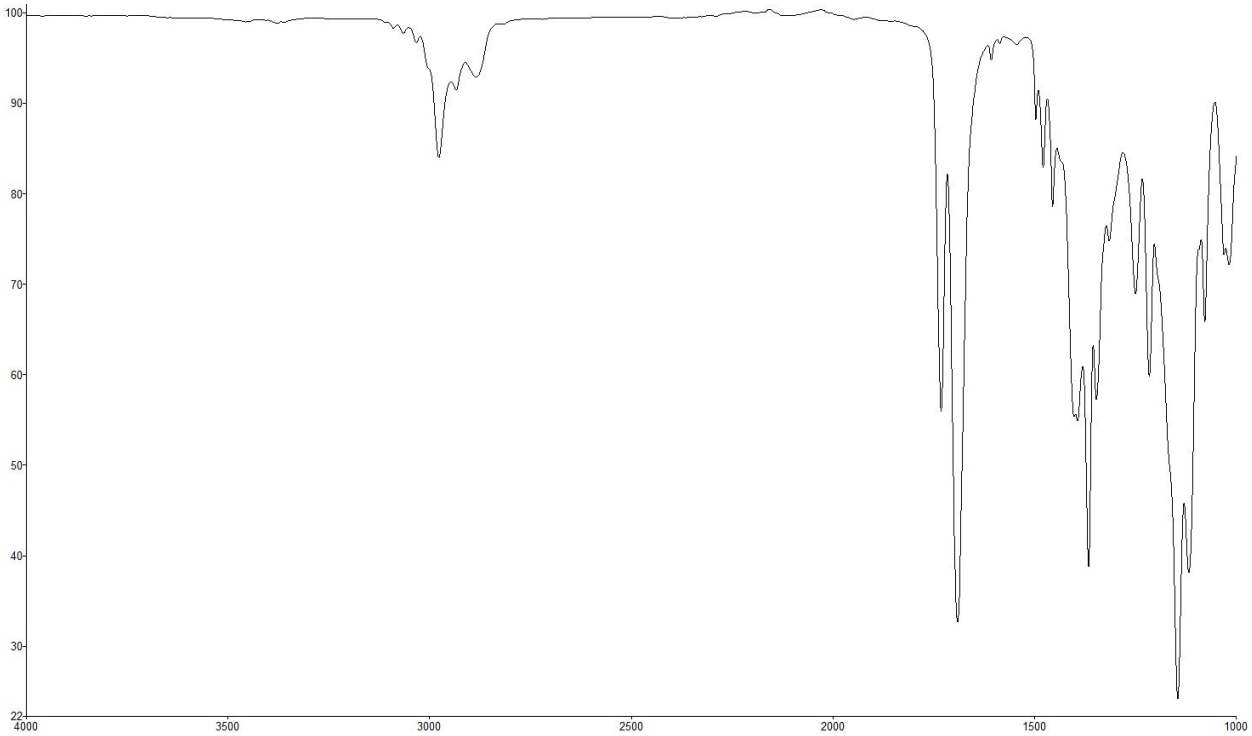

Figure 4.14 Infrared spectrum of compound **4.52**.

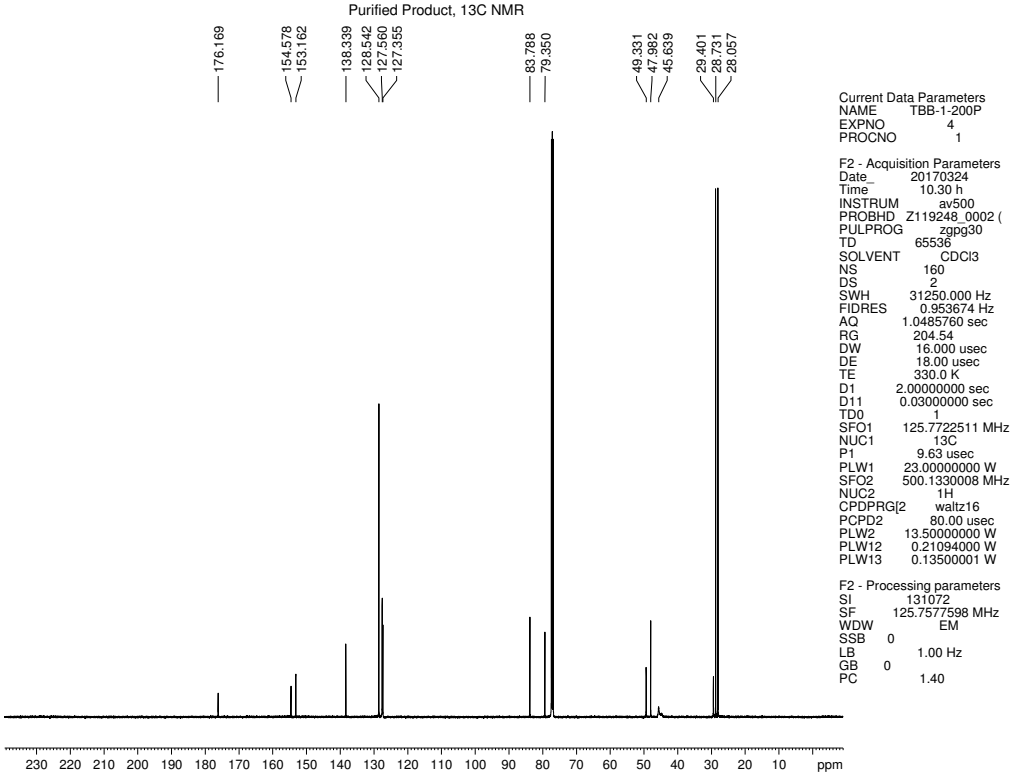

Figure 4.15 ^{13}C NMR (125 MHz, $CDCl_3$) of compound **4.52**.

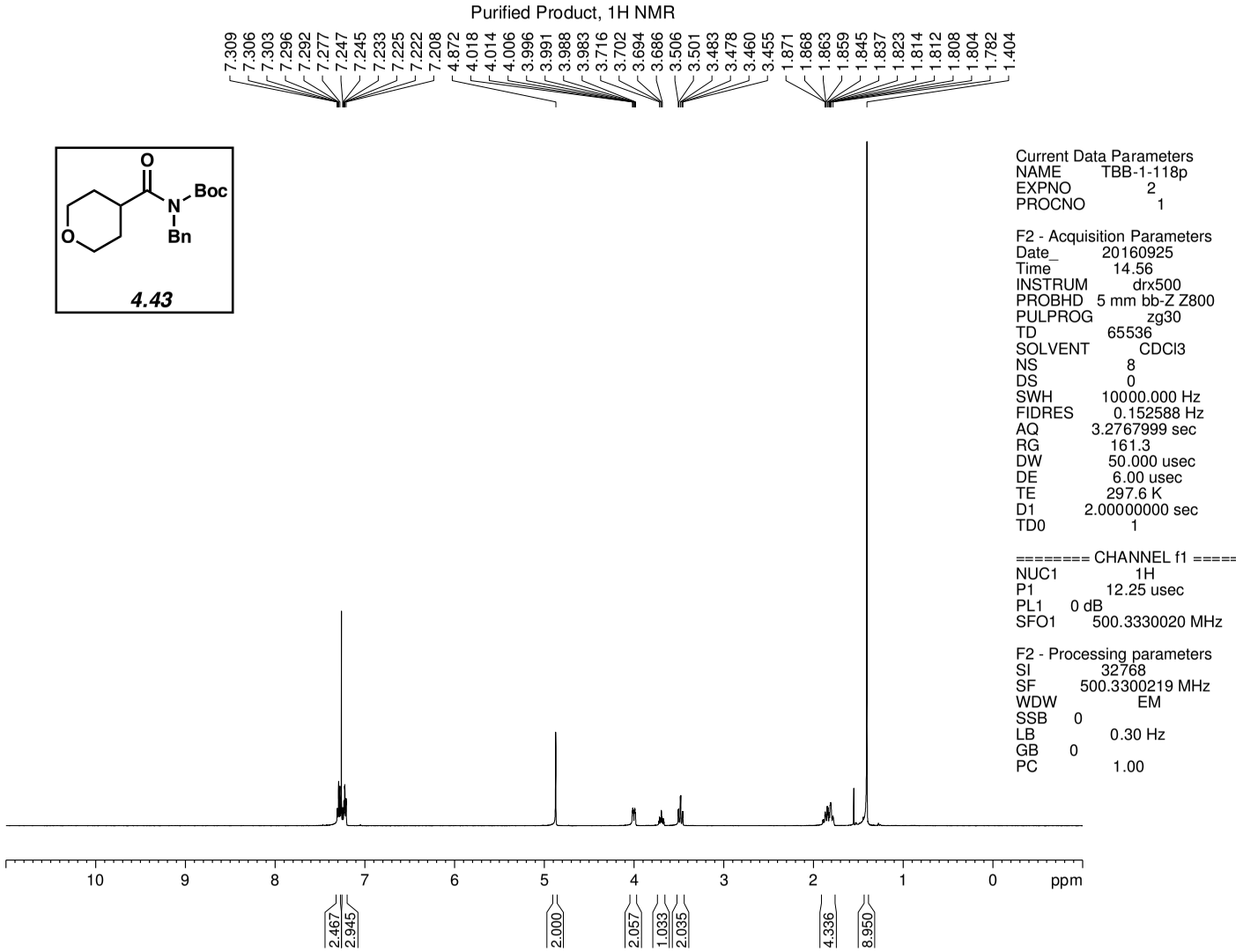

Figure 4.16 ^{1}H NMR (500 MHz, $CDCl_3$) of compound **4.43**.

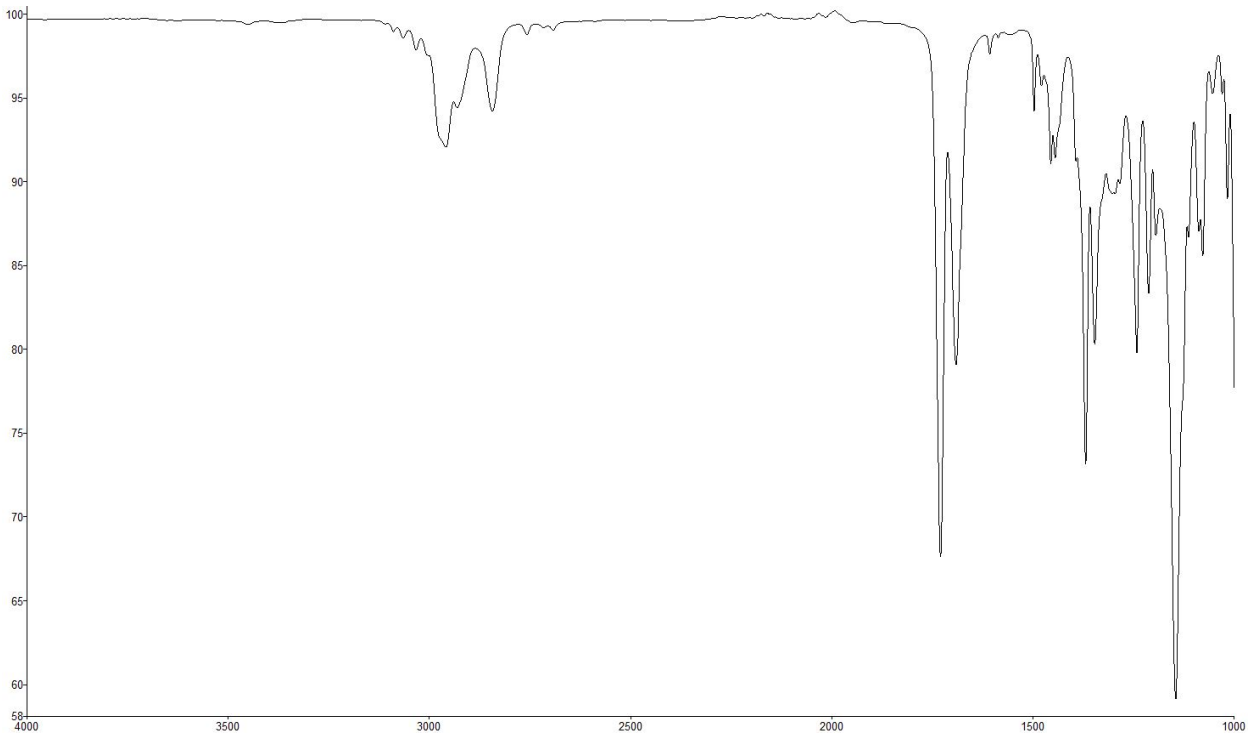

Figure 4.17 Infrared spectrum of compound **4.43**.

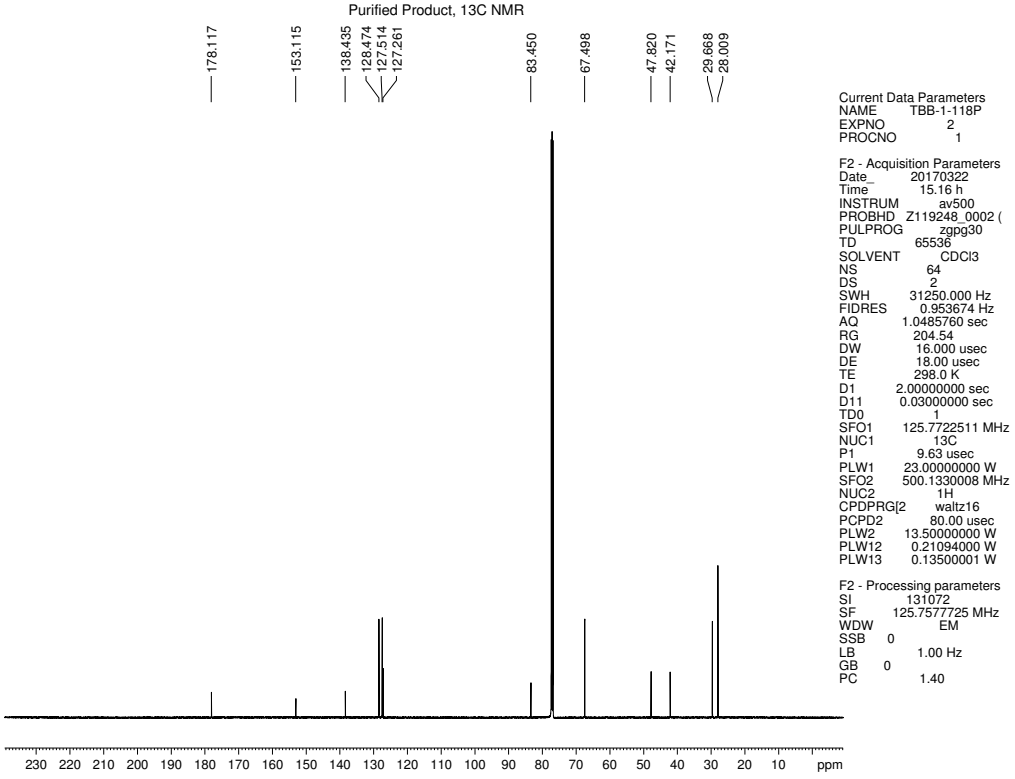

Figure 4.18 ^{13}C NMR (125 MHz, $CDCl_3$) of compound **4.43**.

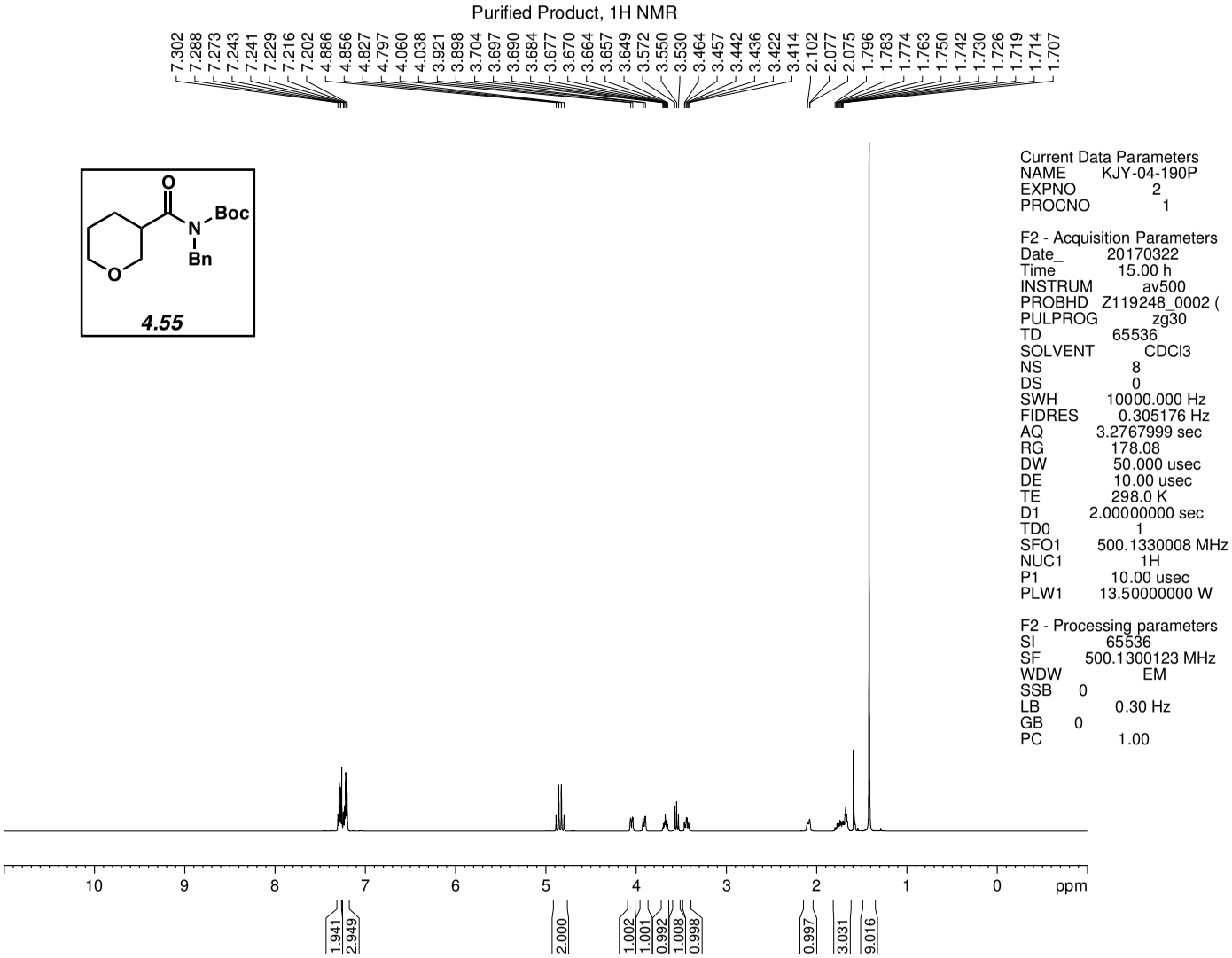

Figure 4.19 ^{1}H NMR (500 MHz, $CDCl_3$) of compound **4.55**.

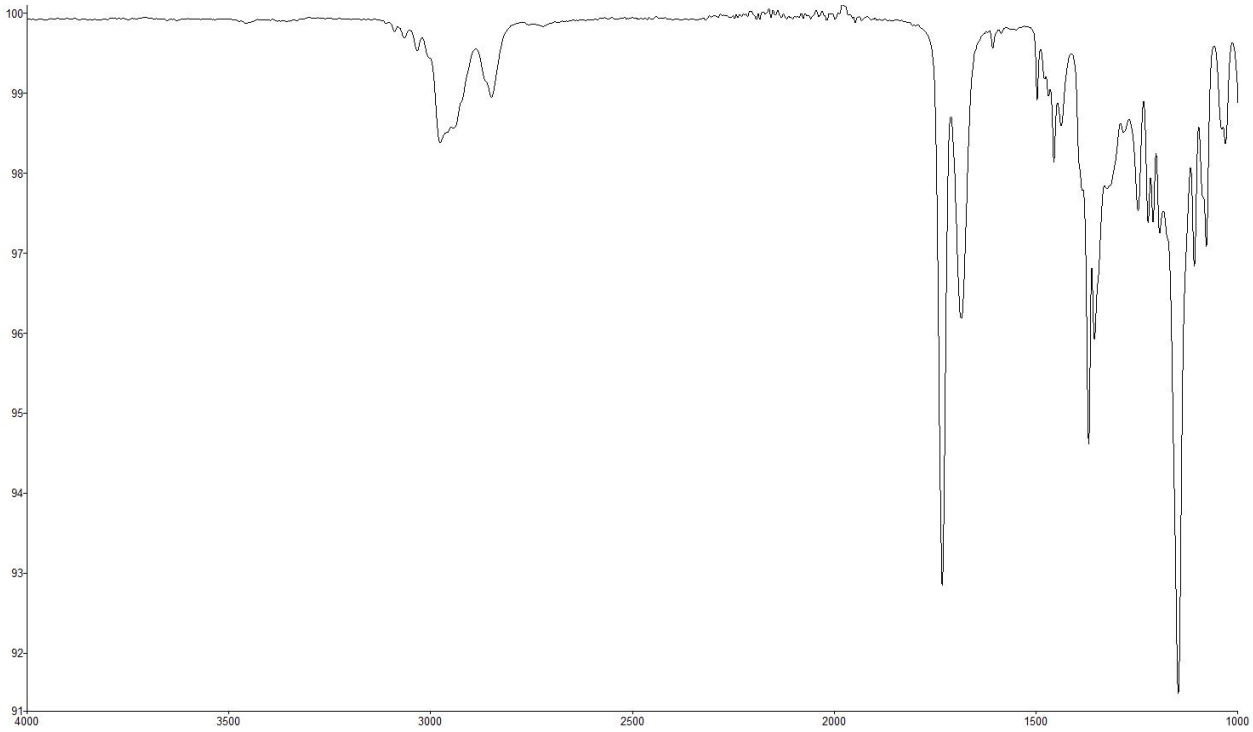

Figure 4.20 Infrared spectrum of compound **4.55**.

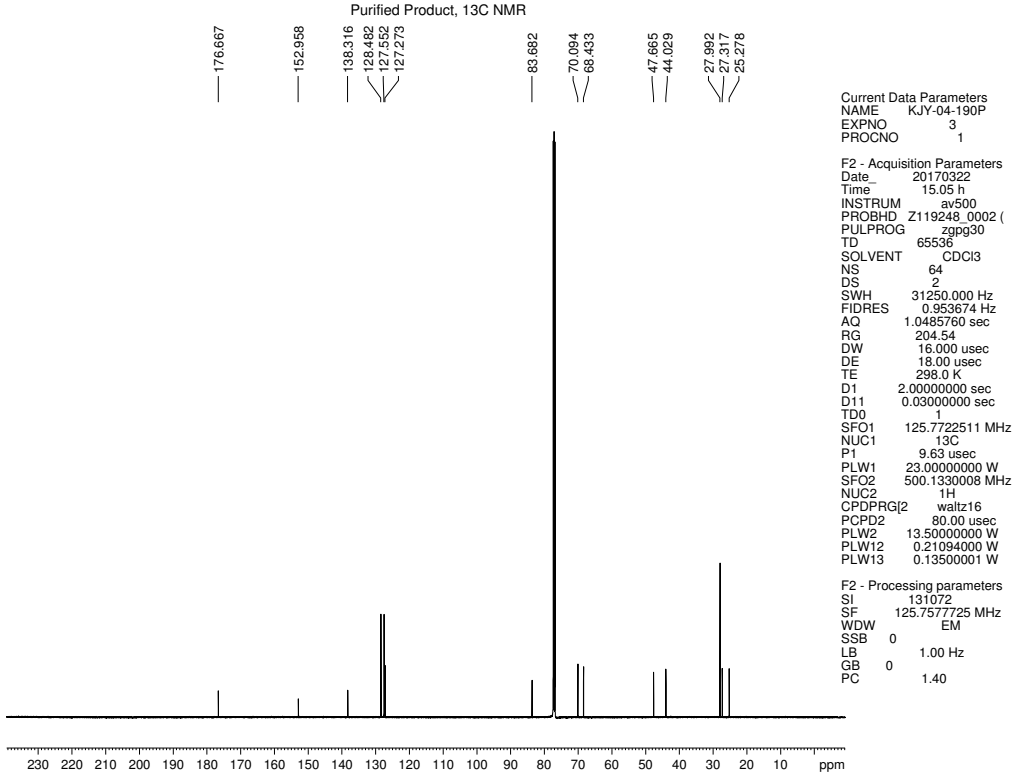

Figure 4.21 ^{13}C NMR (125 MHz, $CDCl_3$) of compound **4.55**.

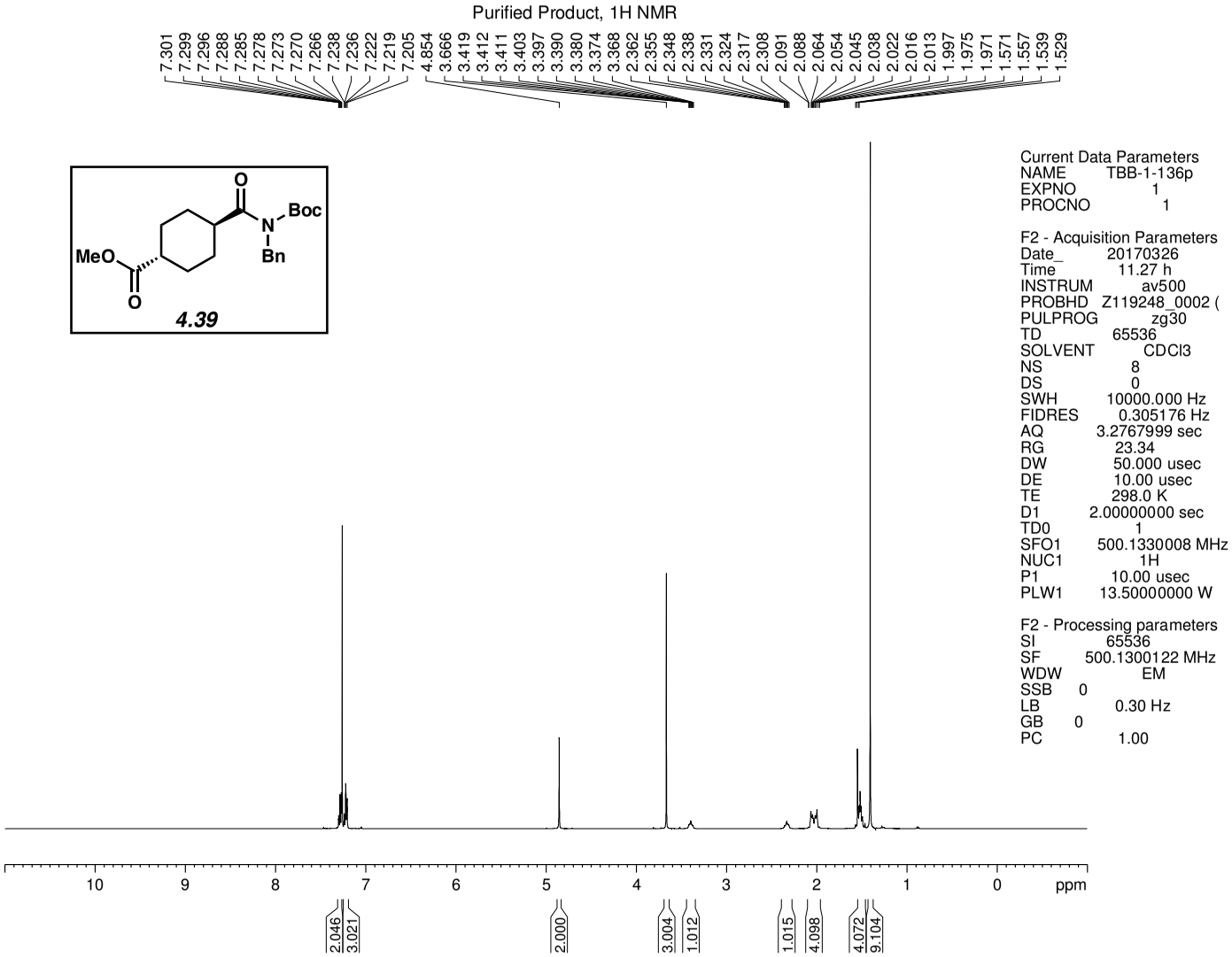

Figure 4.22 ^{1}H NMR (500 MHz, $CDCl_3$) of compound **4.39**.

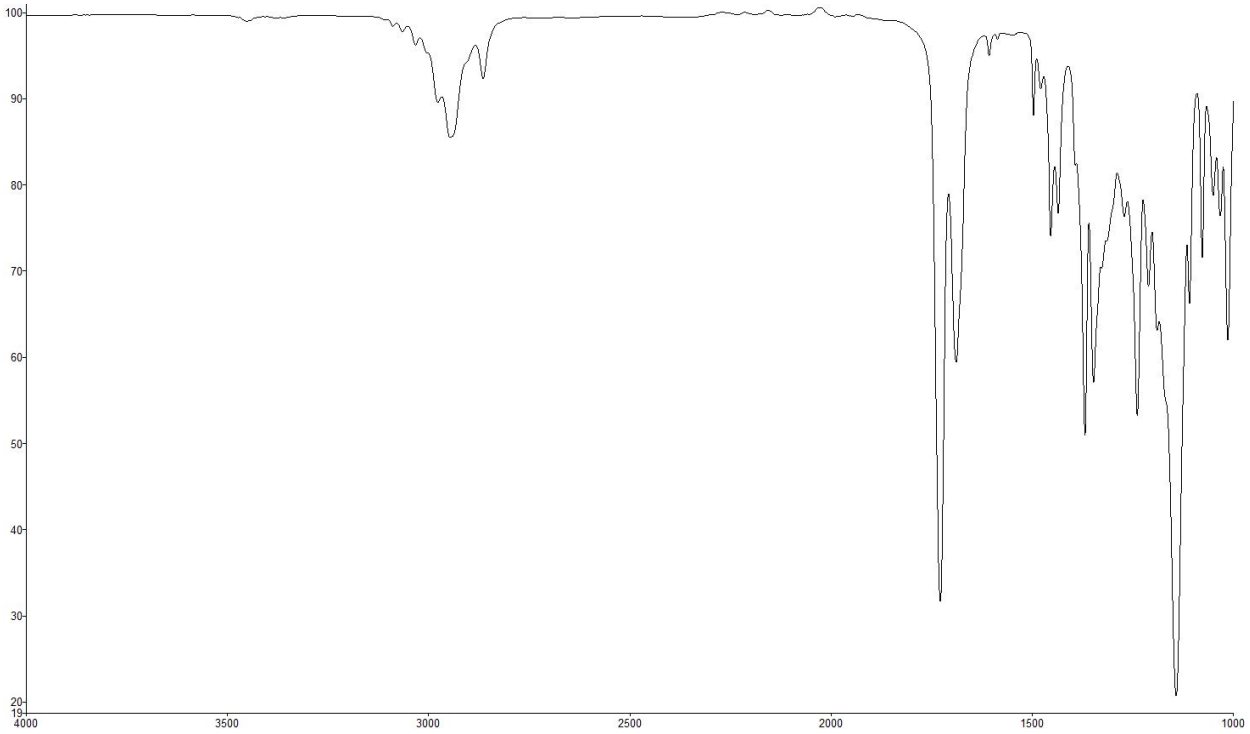

Figure 4.23 Infrared spectrum of compound **4.39**.

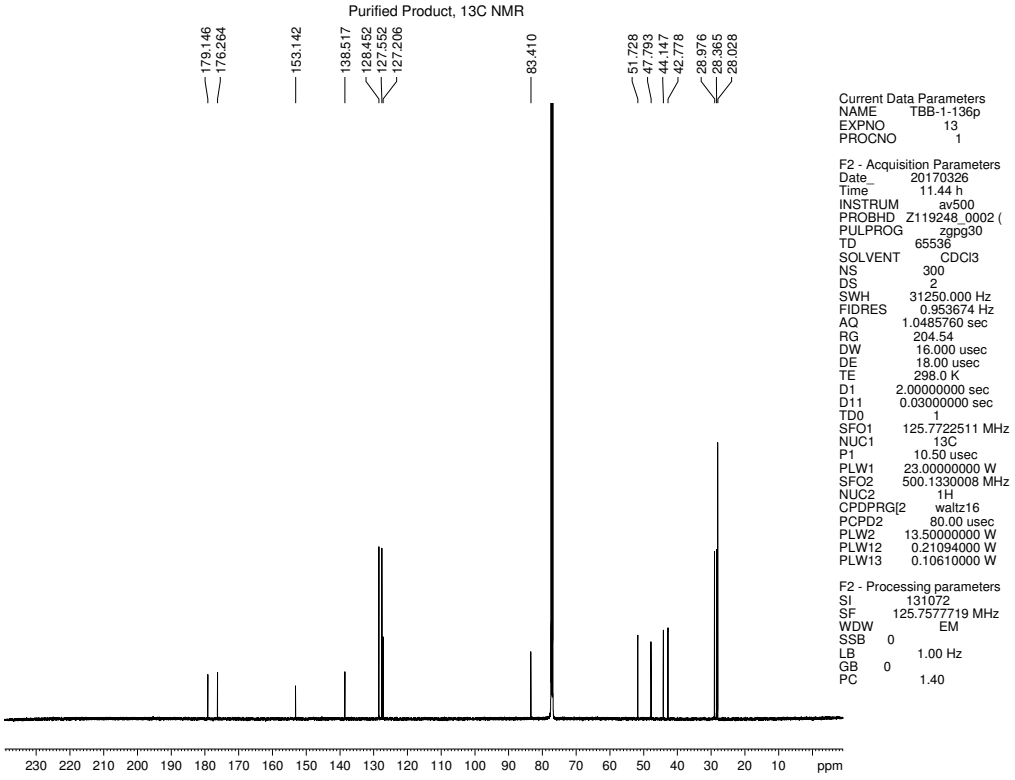

Figure 4.24 ^{13}C NMR (125 MHz, $CDCl_3$) of compound **4.39**.

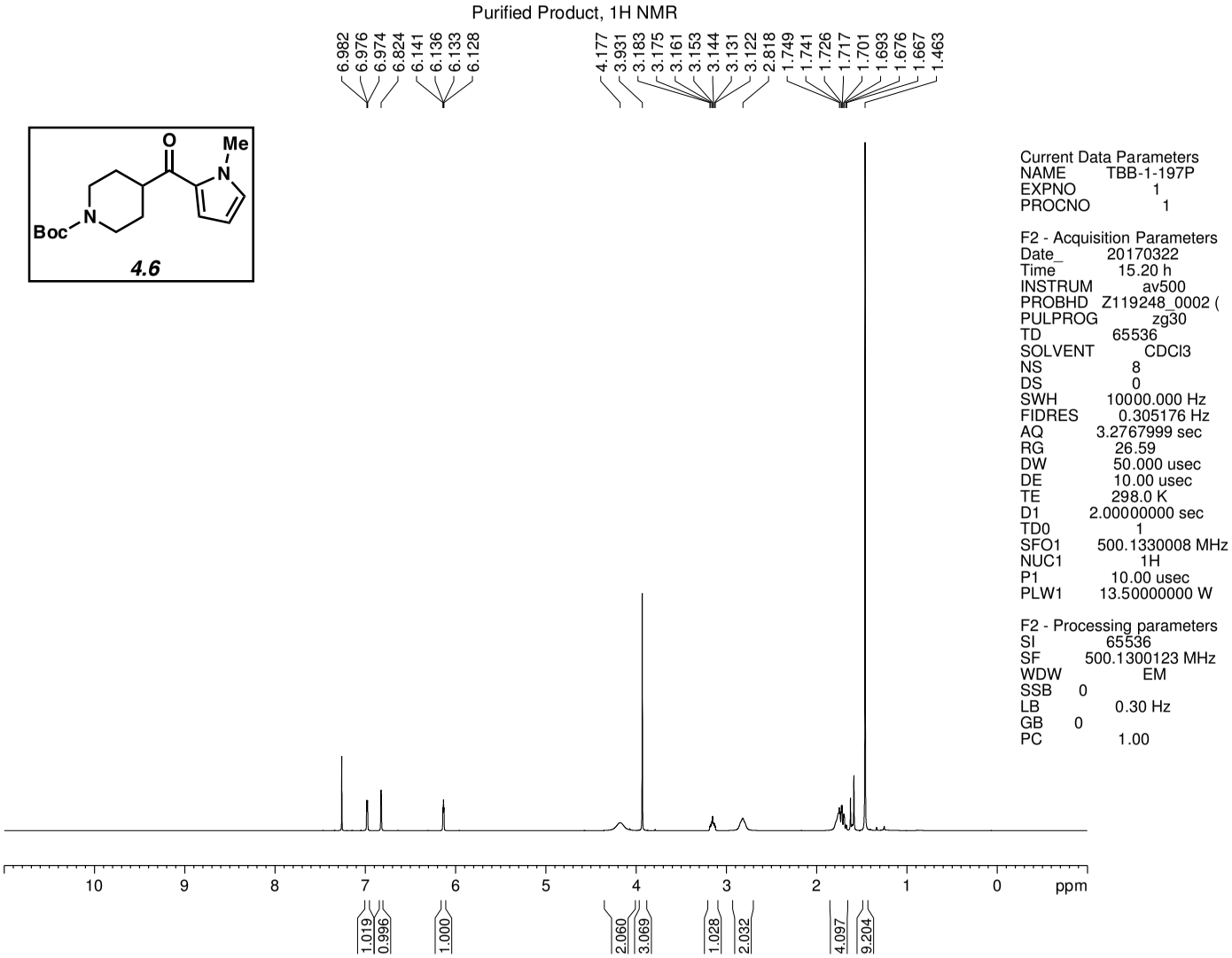

Figure 4.25 ^{1}H NMR (500 MHz, $CDCl_3$) of compound **4.6**.

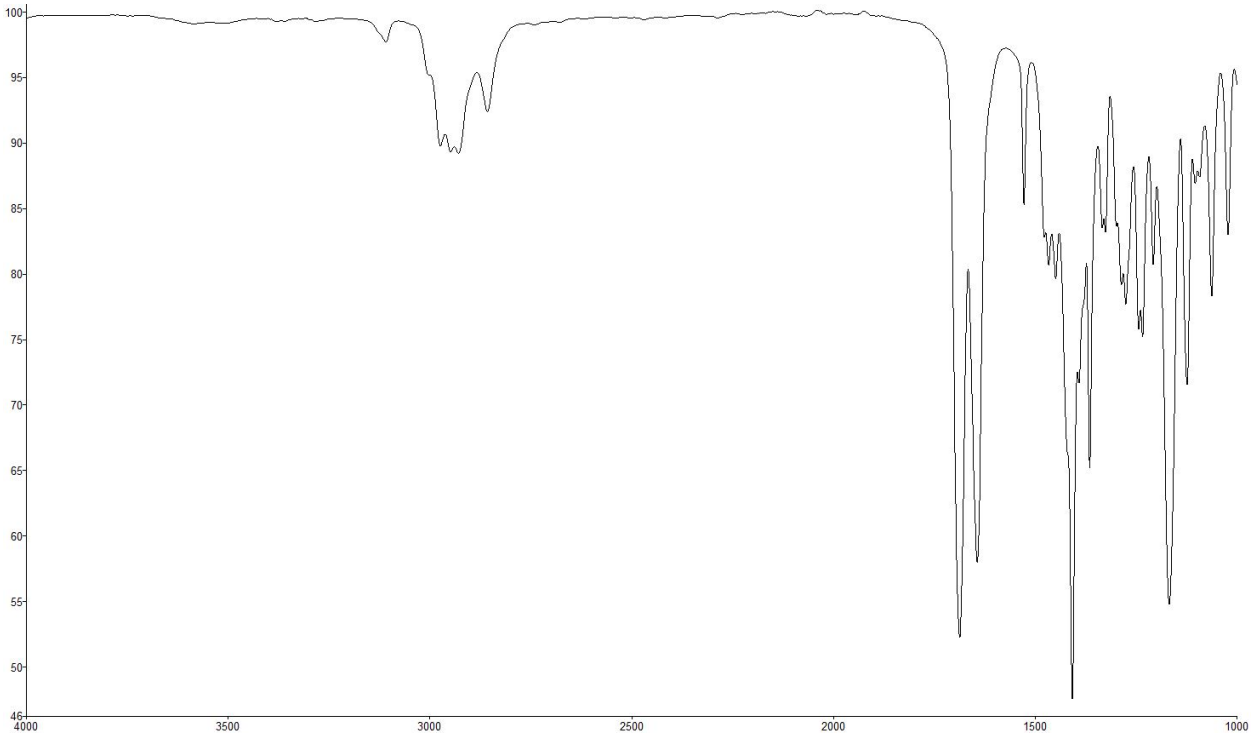

Figure 4.26 Infrared spectrum of compound **4.6**.

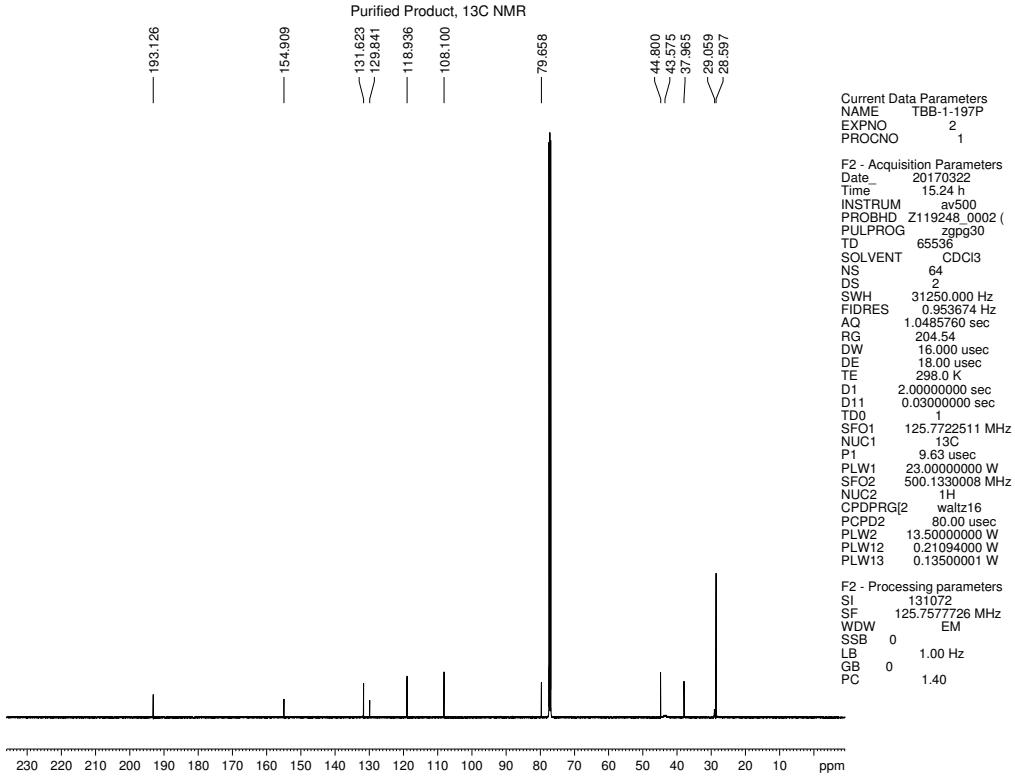

Figure 4.27 ^{13}C NMR (125 MHz, $CDCl_3$) of compound **4.6**.

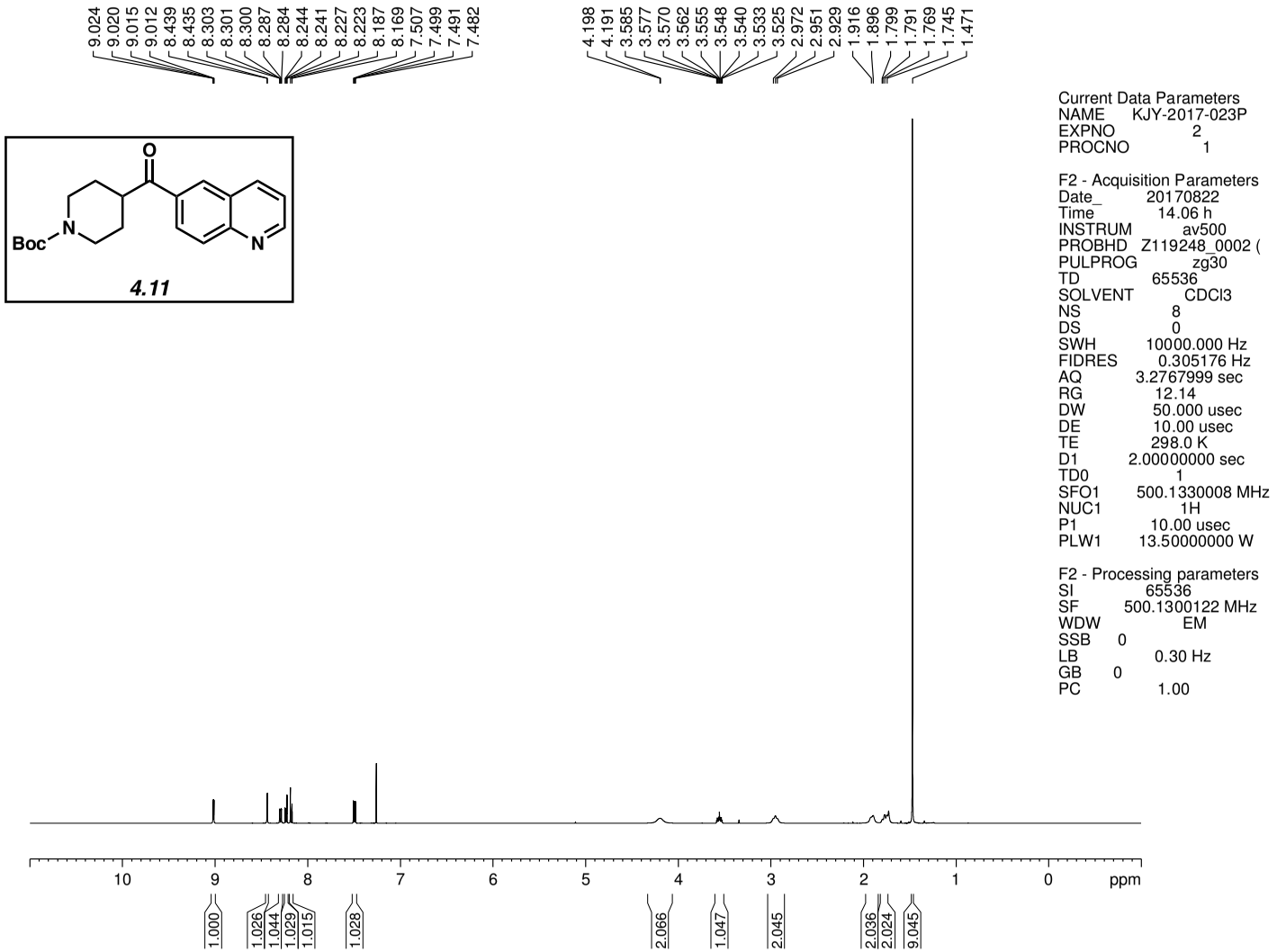

Figure 4.28 ^{1}H NMR (500 MHz, $CDCl_3$) of compound **4.11.**

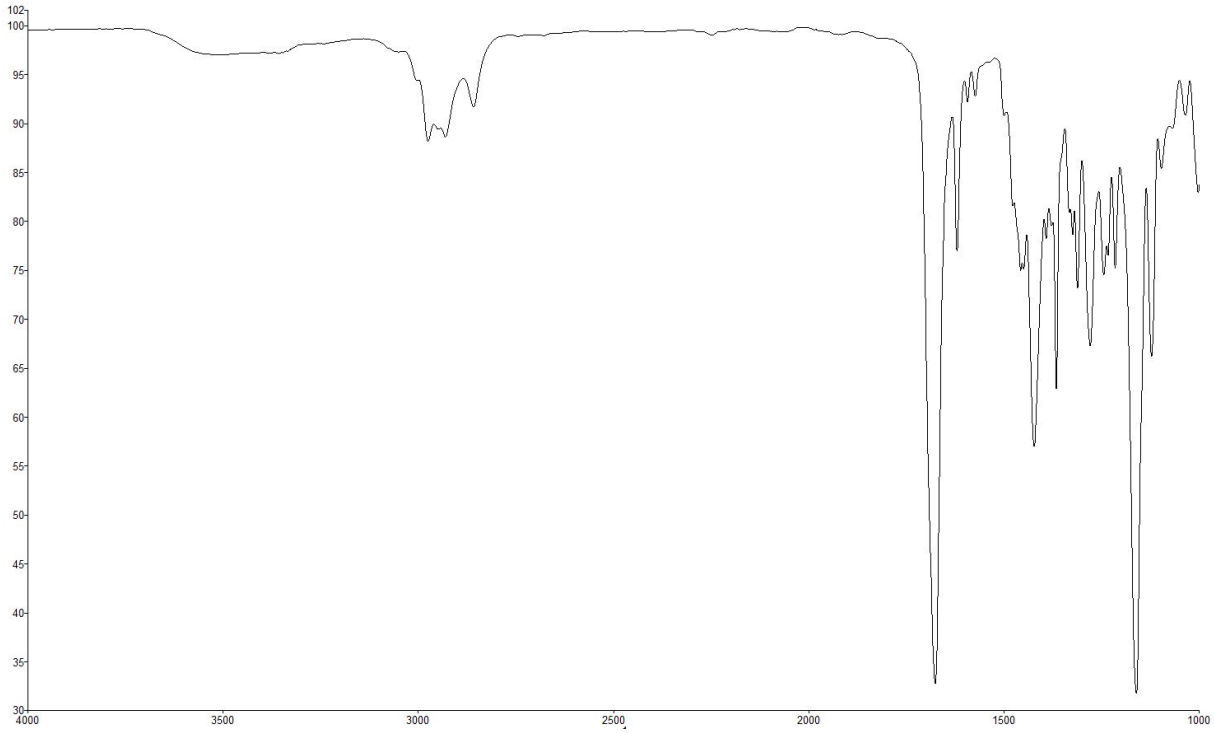

Figure 4.29 Infrared spectrum of compound **4.11**.

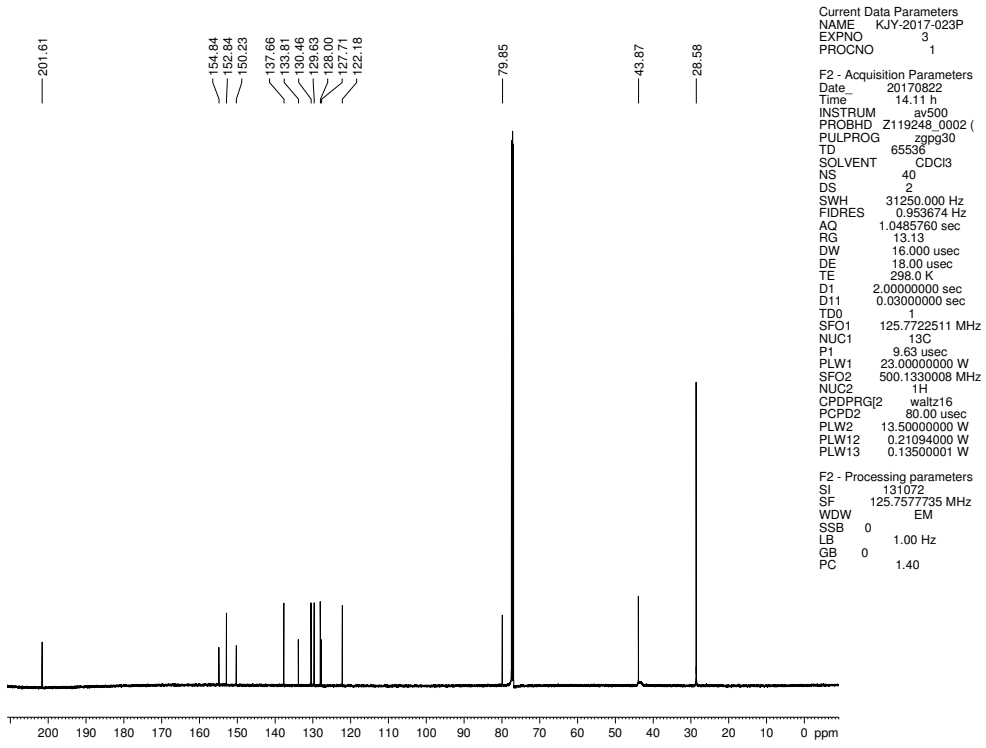

Figure 4.30 ^{13}C NMR (125 MHz, $CDCl_3$) of compound **4.11**.

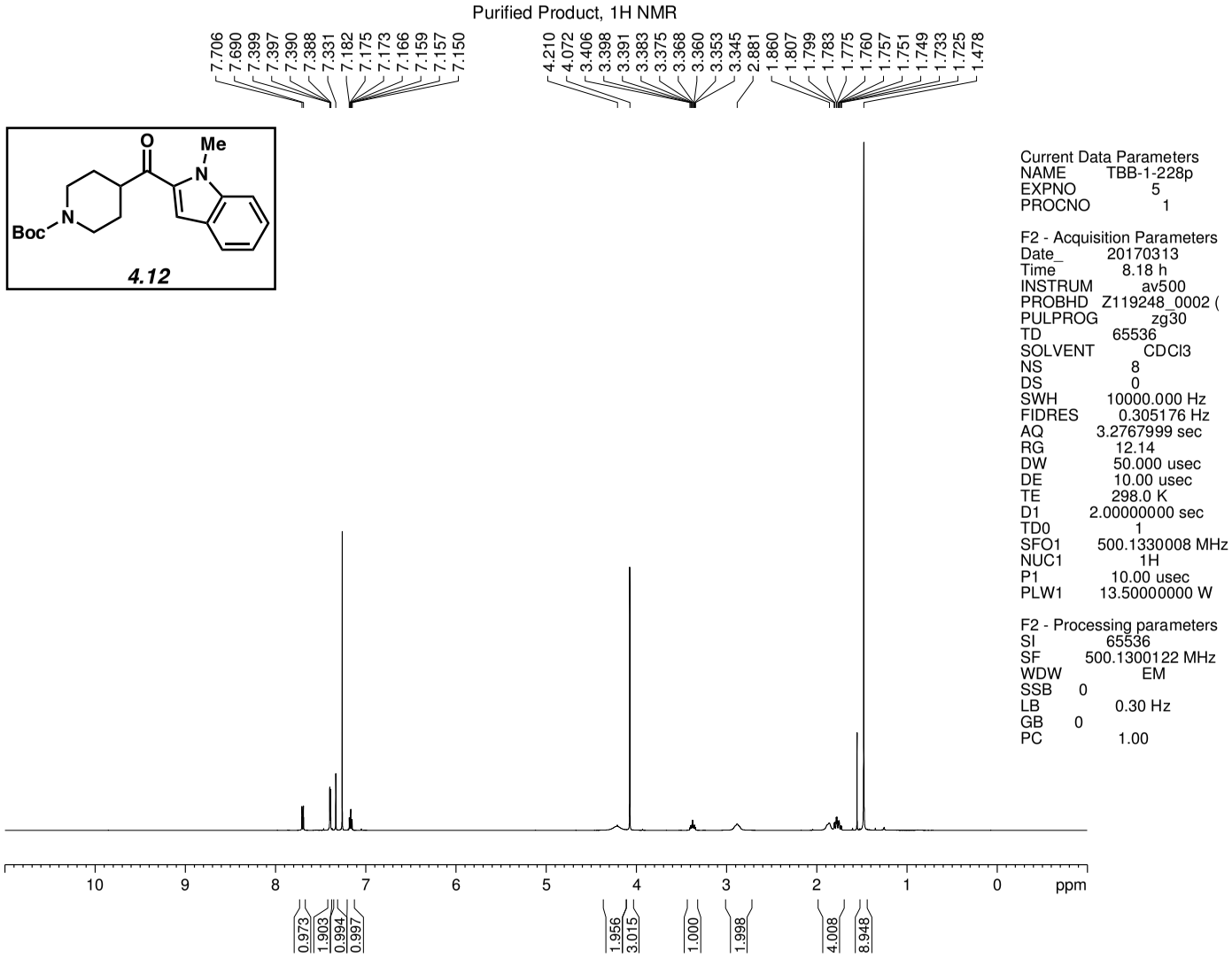

Figure 4.31 ^{1}H NMR (500 MHz, $CDCl_3$) of compound **4.12**.

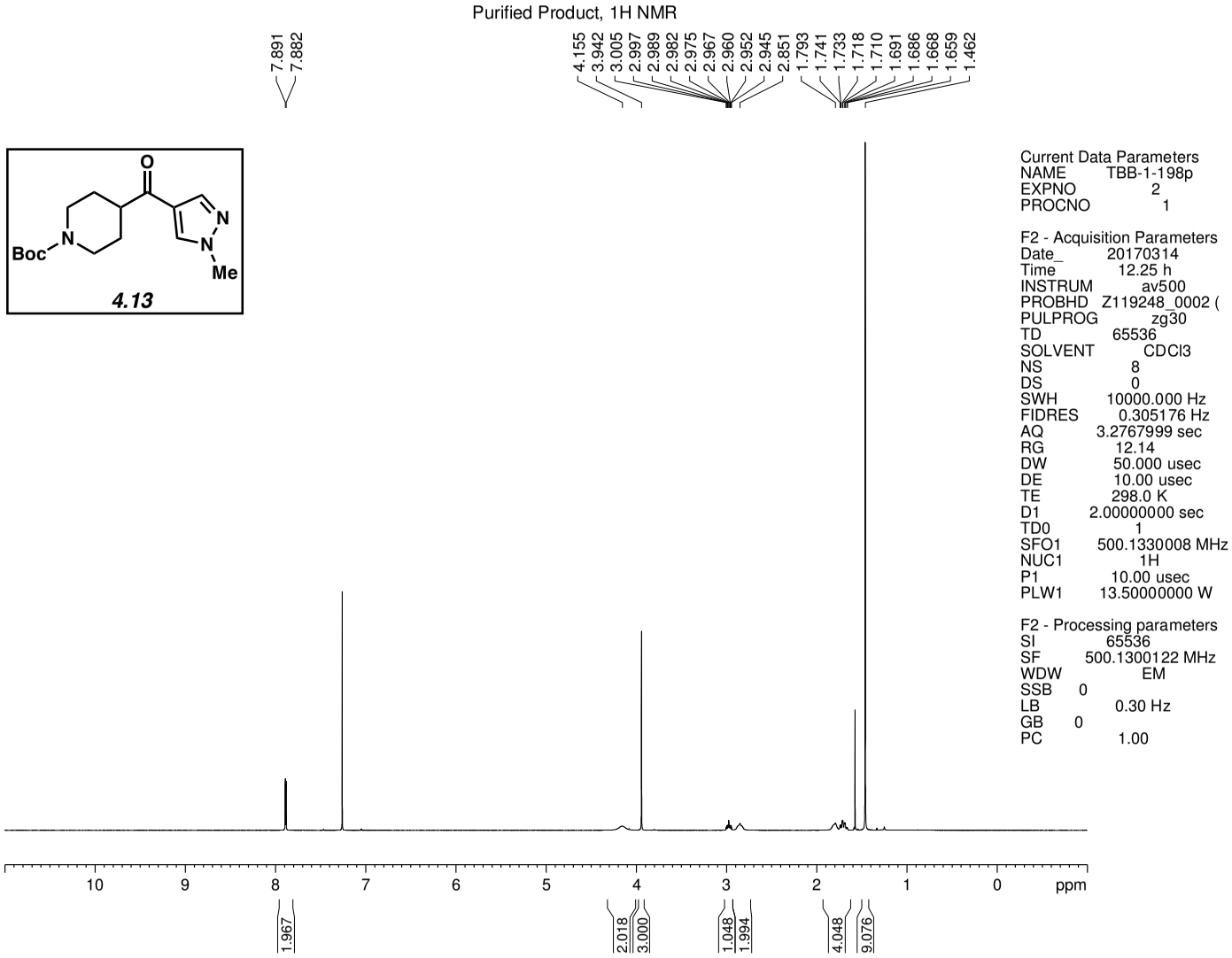

Figure 4.32 ^{1}H NMR (500 MHz, $CDCl_3$) of compound **4.13**.

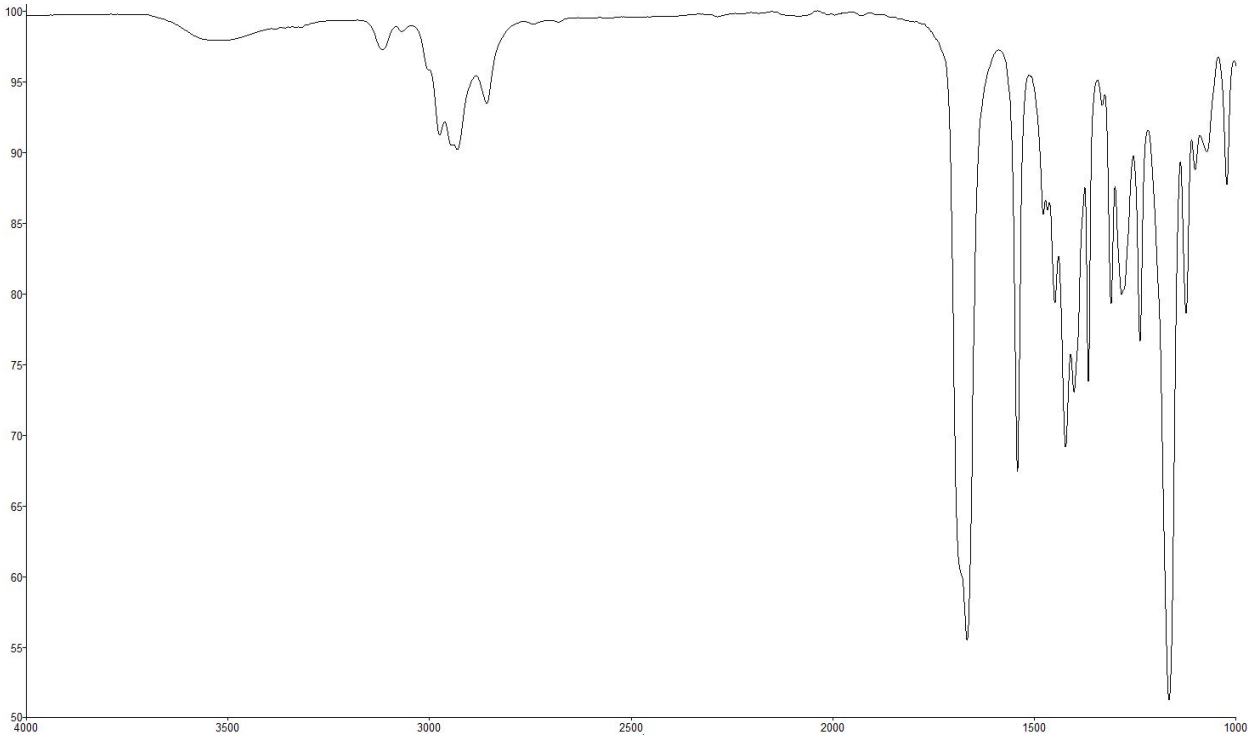

Figure 4.33 Infrared spectrum of compound **4.13**.

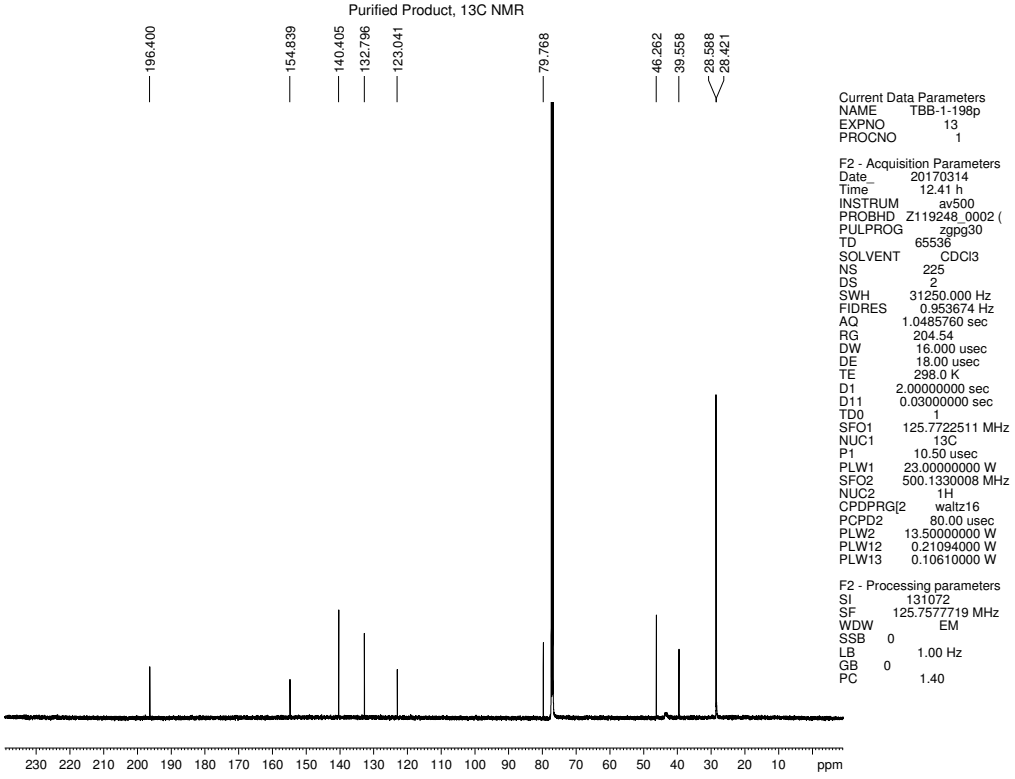

Figure 4.34 ^{13}C NMR (125 MHz, $CDCl_3$) of compound **4.13**.

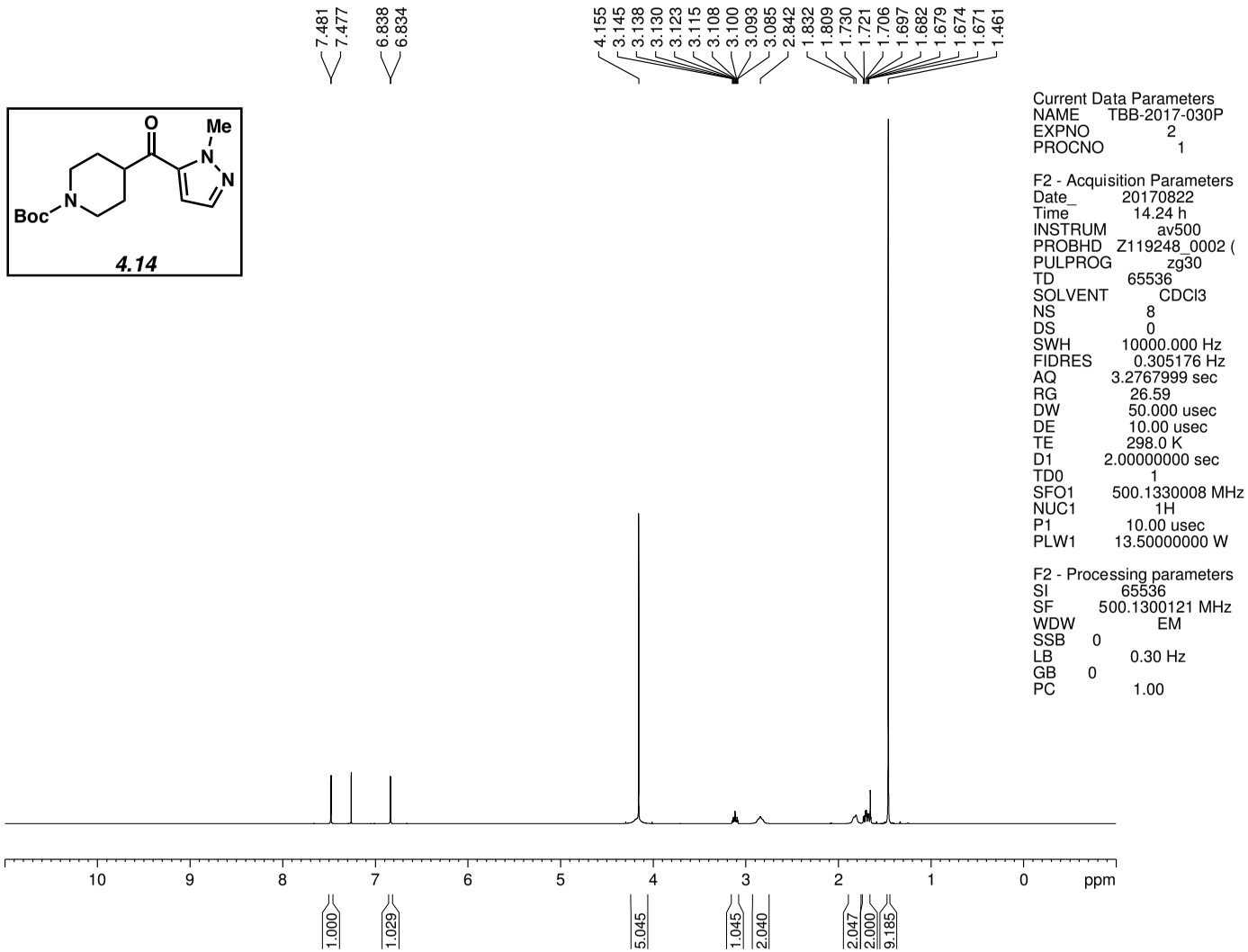

Figure 4.35 ^{1}H NMR (500 MHz, $CDCl_3$) of compound **4.14**.

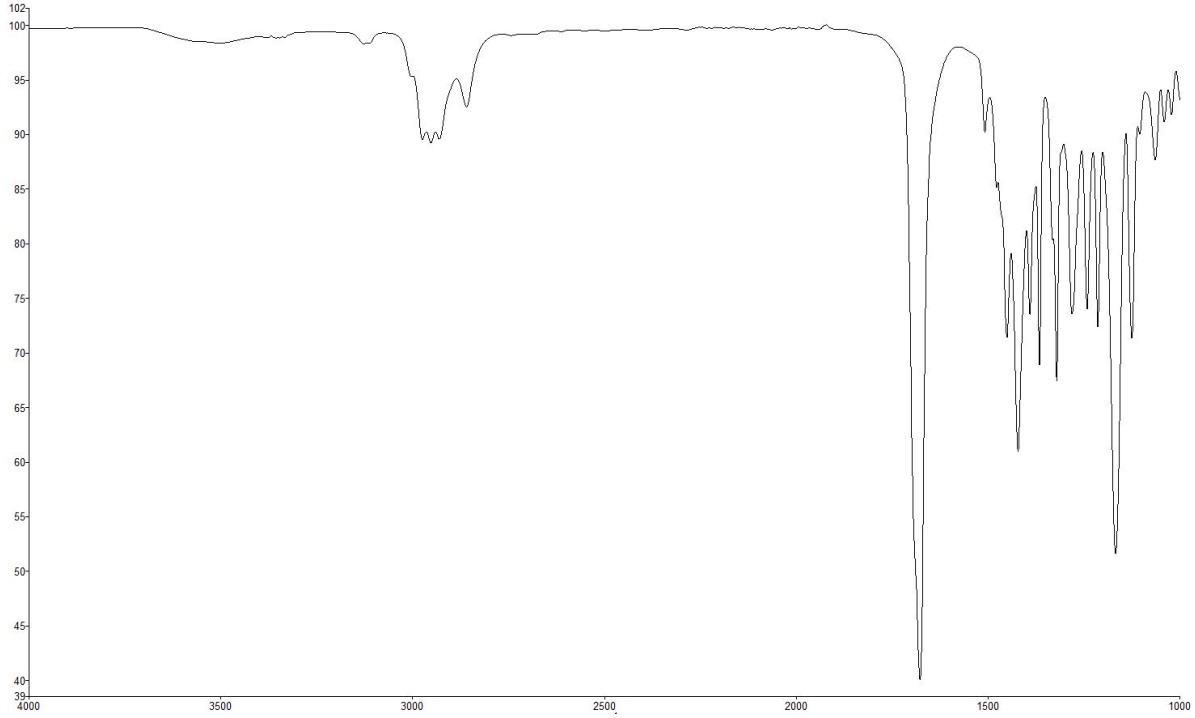

Figure 4.36 Infrared spectrum of compound **4.14**.

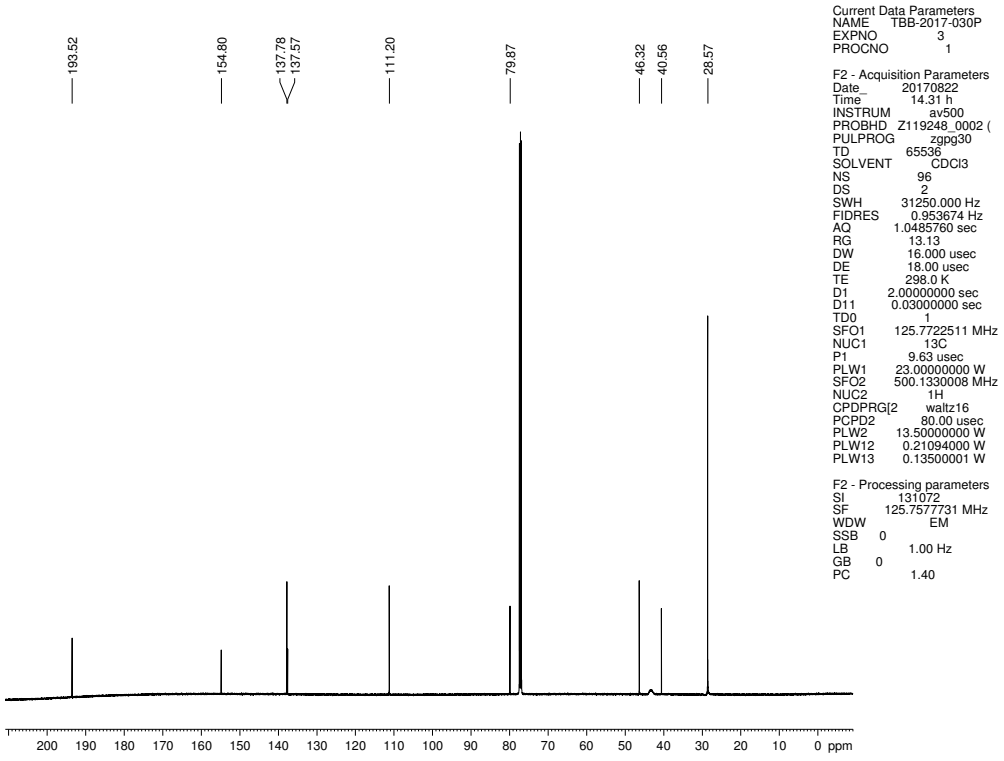

Figure 4.37 ^{13}C NMR (125 MHz, $CDCl_3$) of compound **4.14**.

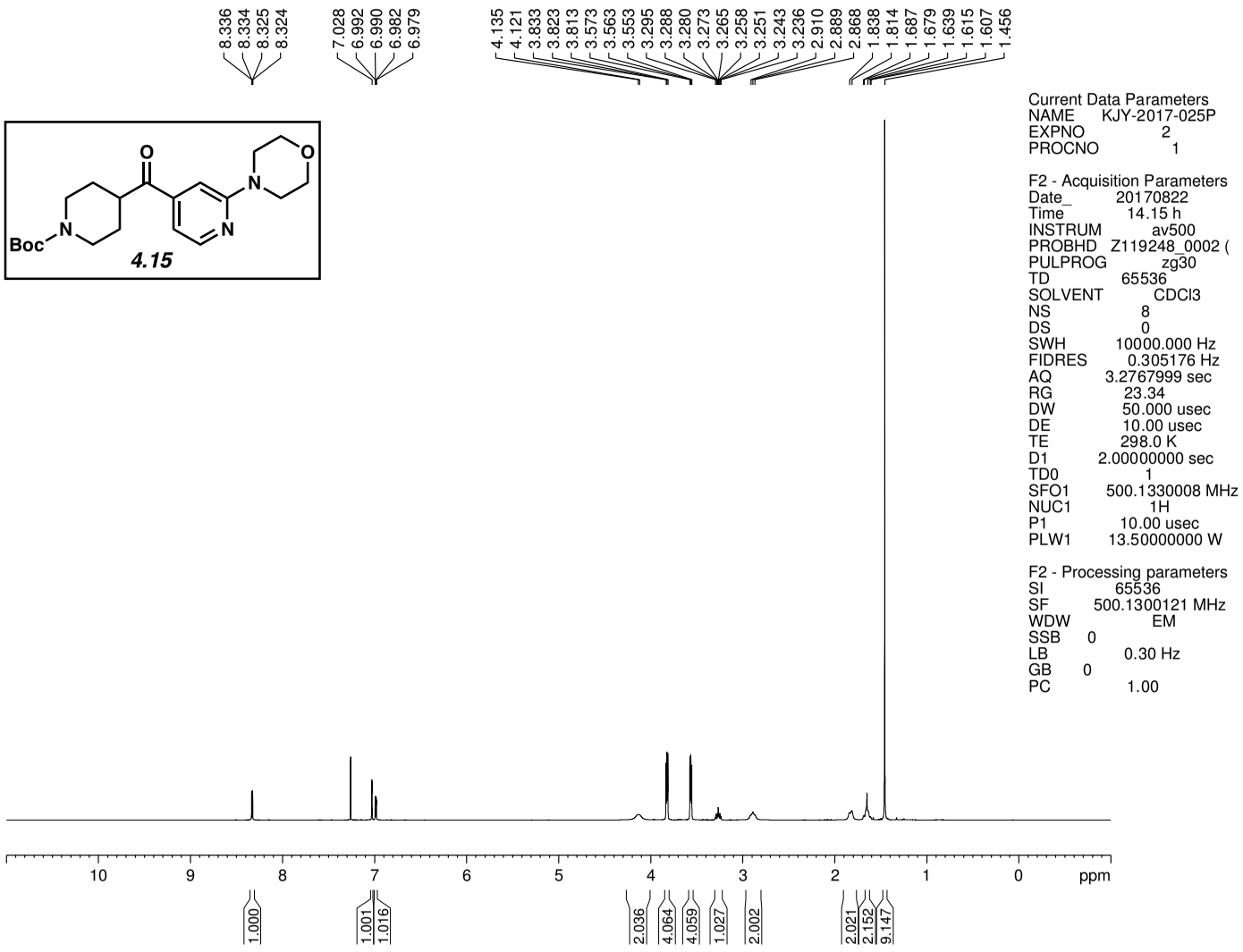

Figure 4.38 ^{1}H NMR (500 MHz, $CDCl_3$) of compound **4.15**.

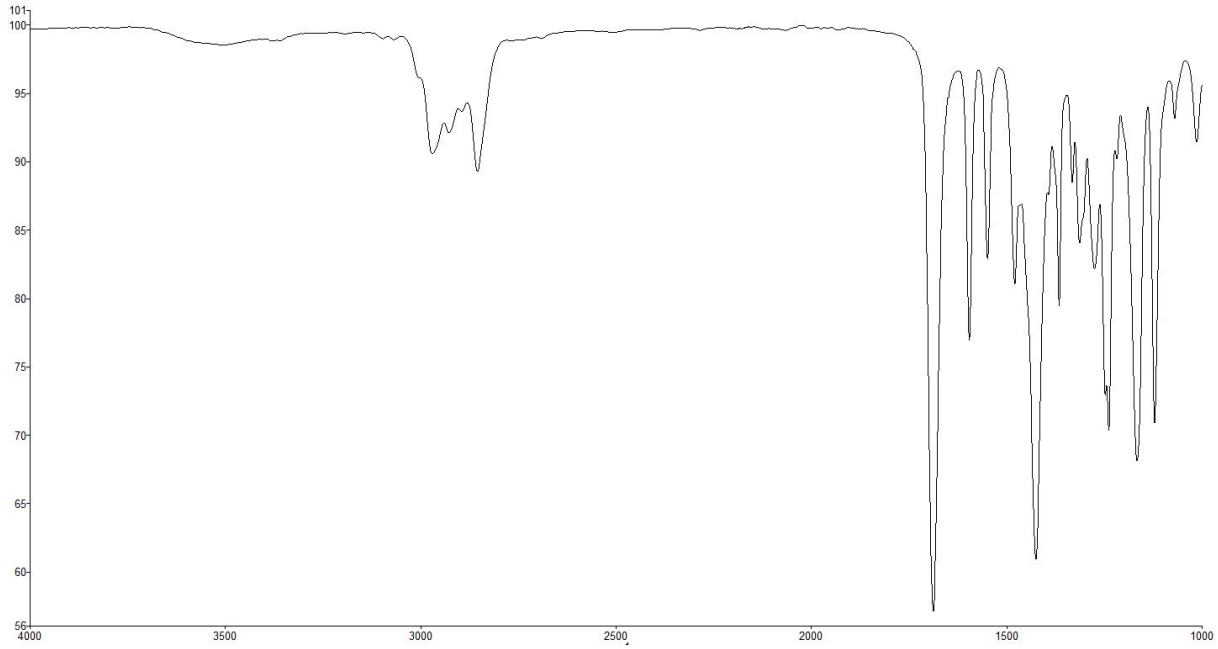

Figure 4.39 Infrared spectrum of compound **4.15**.

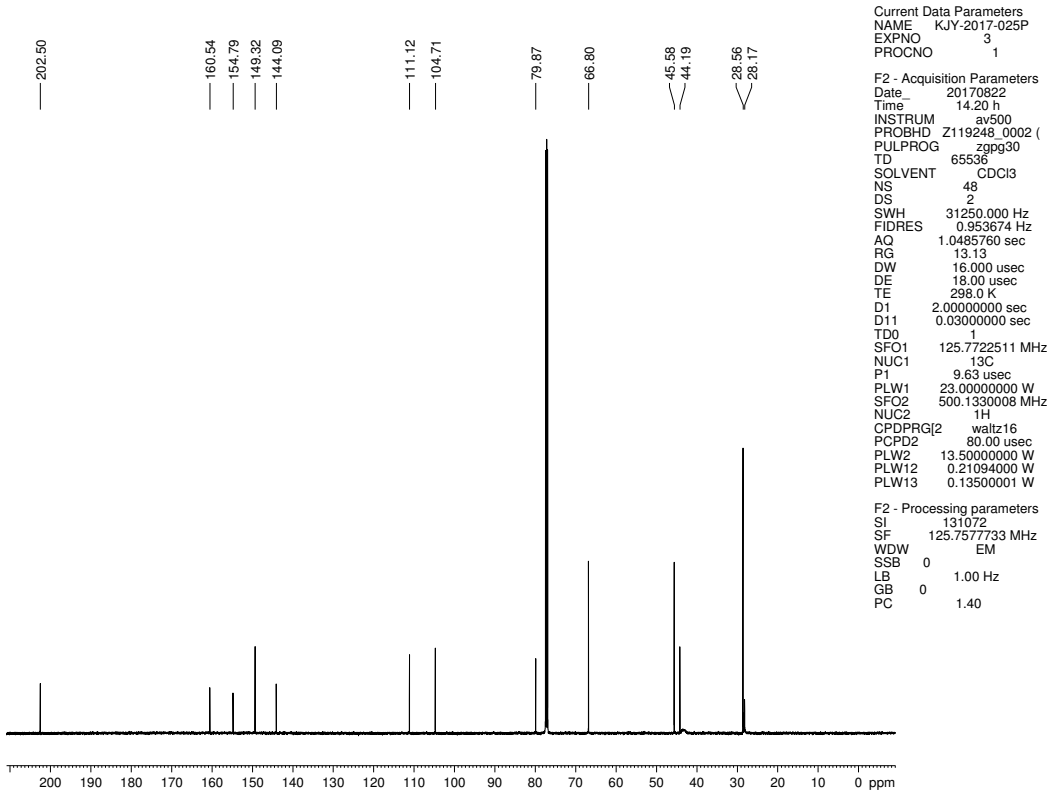

Figure 4.40 ^{13}C NMR (125 MHz, $CDCl_3$) of compound **4.15**.

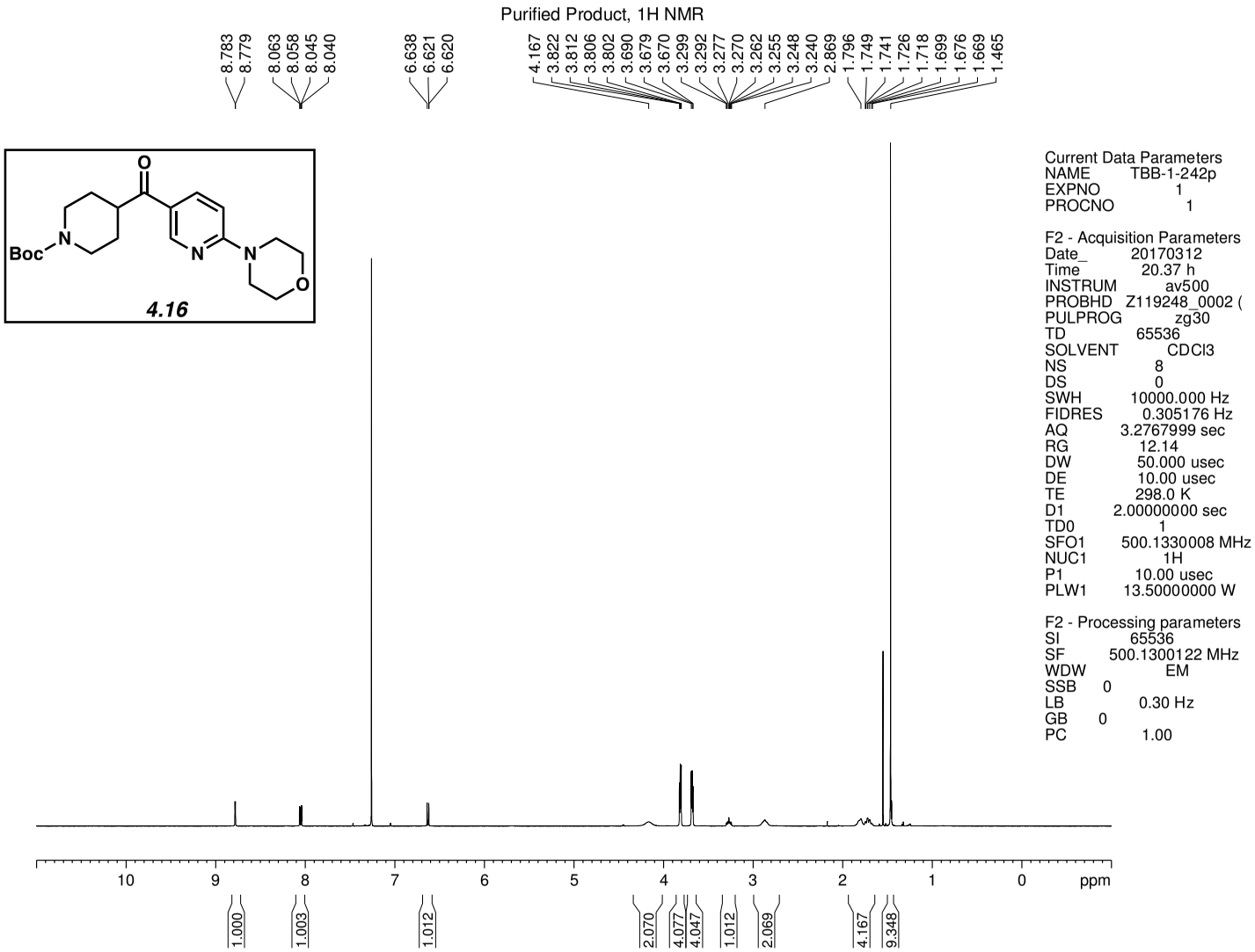

Figure 4.41 ^{1}H NMR (500 MHz, $CDCl_3$) of compound **4.16**.

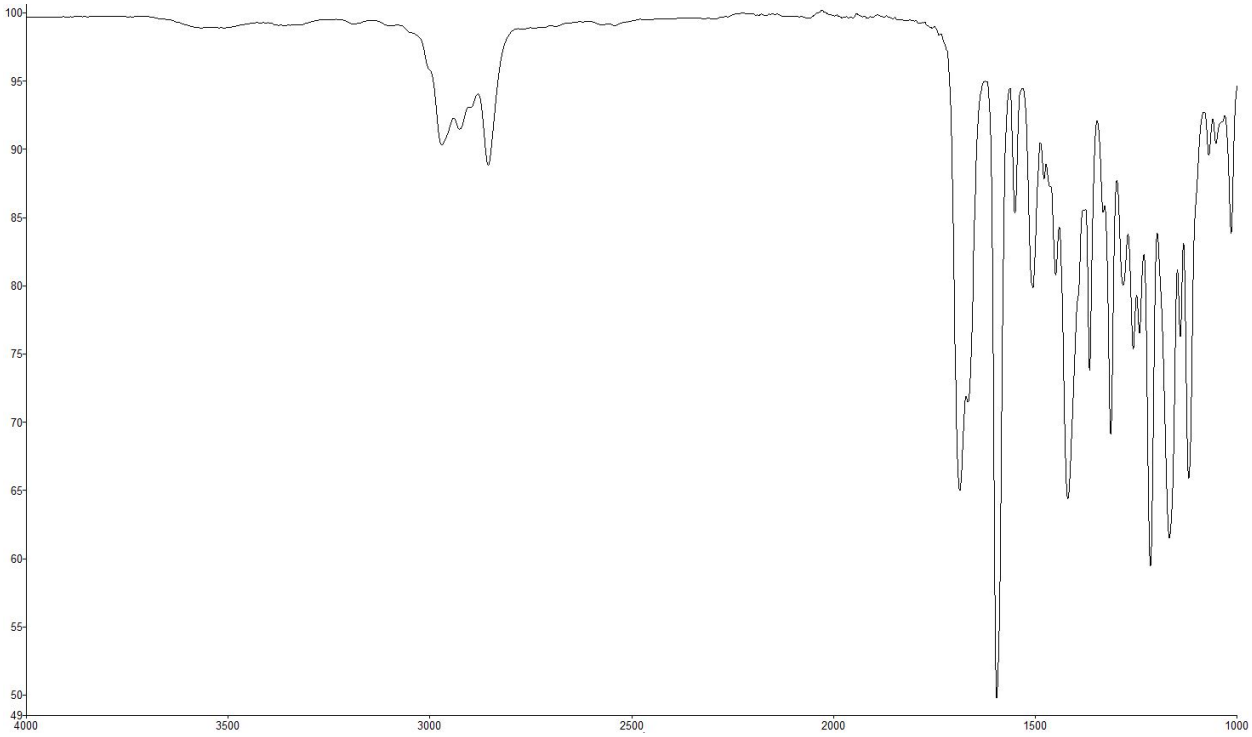

Figure 4.42 Infrared spectrum of compound **4.16**.

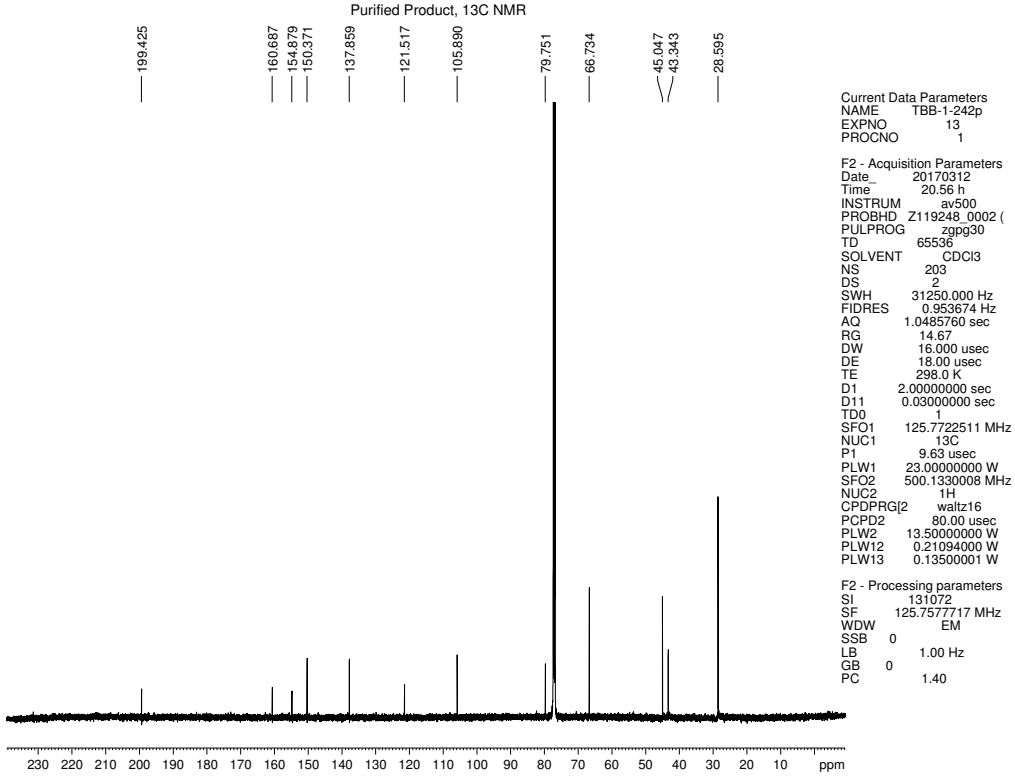

Figure 4.43 ^{13}C NMR (125 MHz, $CDCl_3$) of compound **4.16**.

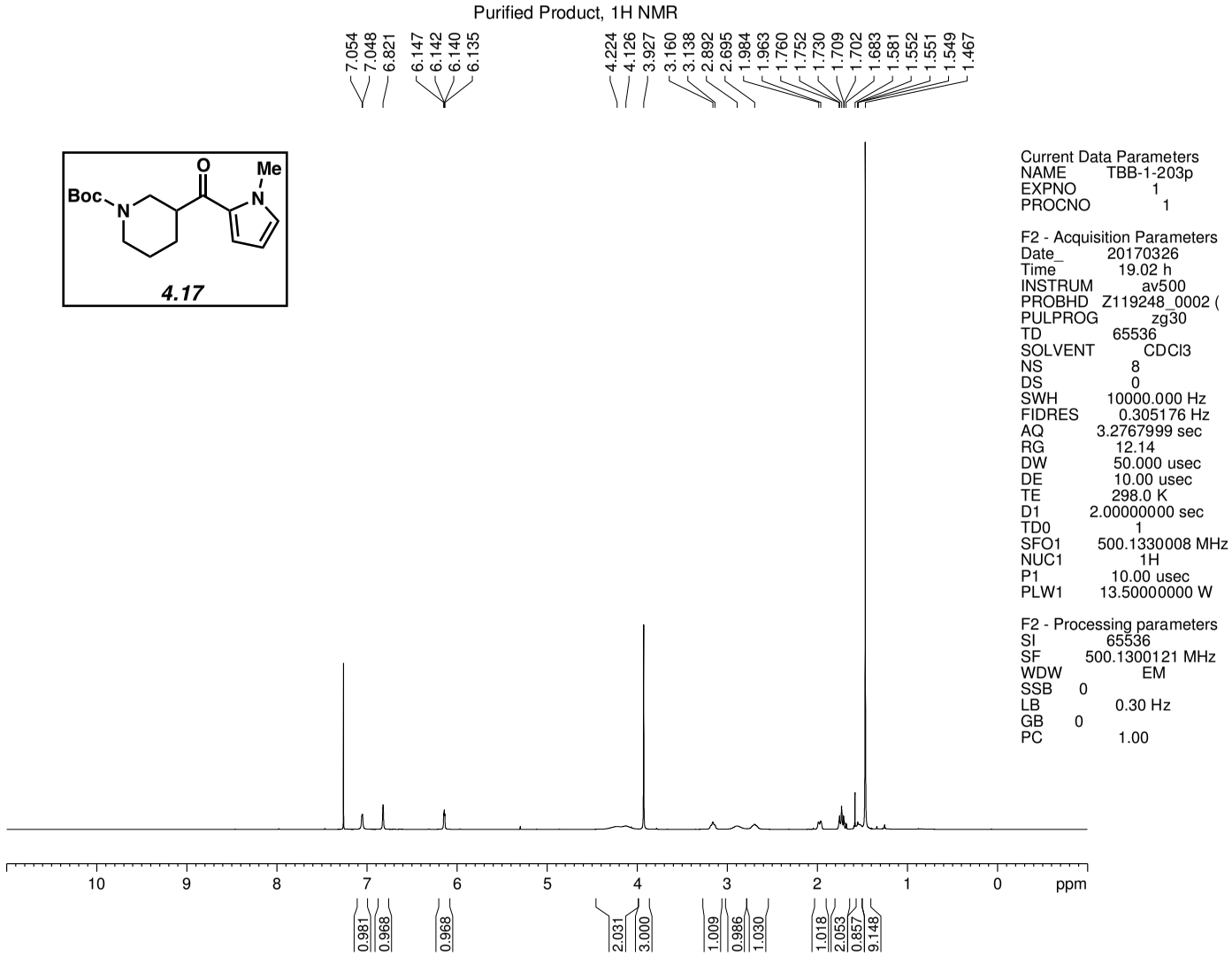

Figure 4.44 ^{1}H NMR (500 MHz, $CDCl_3$) of compound **4.17**.

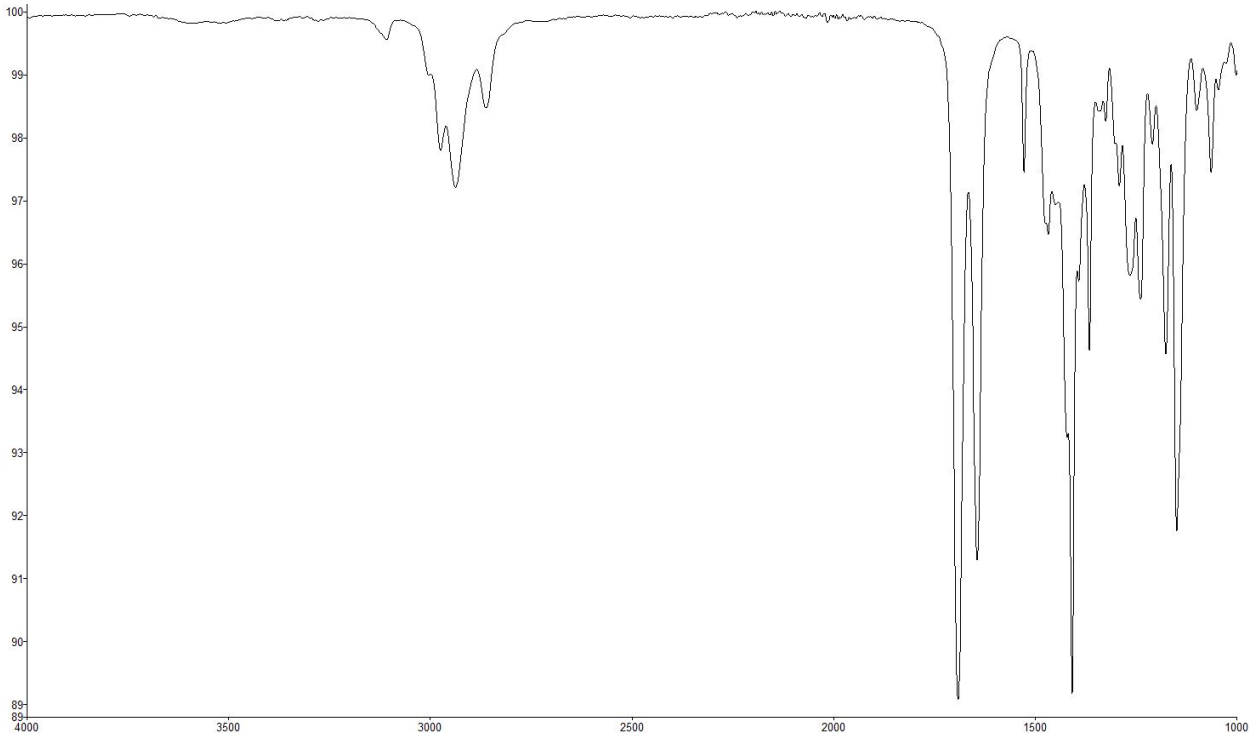

Figure 4.45 Infrared spectrum of compound **4.17**.

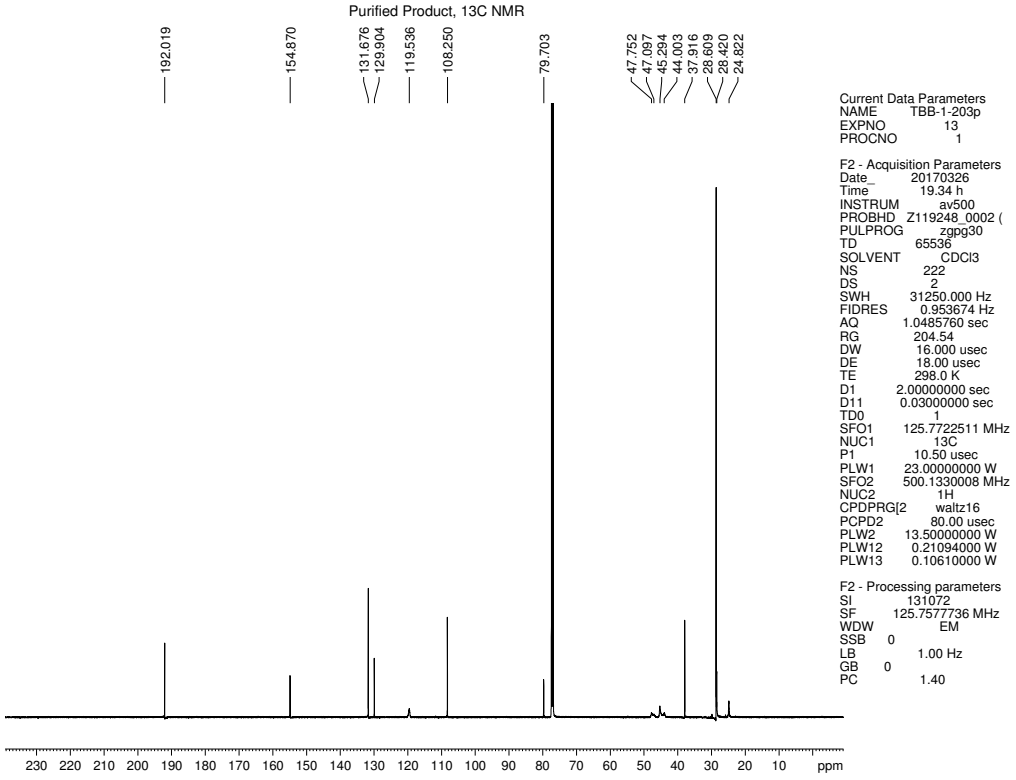

Figure 4.46 ^{13}C NMR (125 MHz, $CDCl_3$) of compound **4.17**.

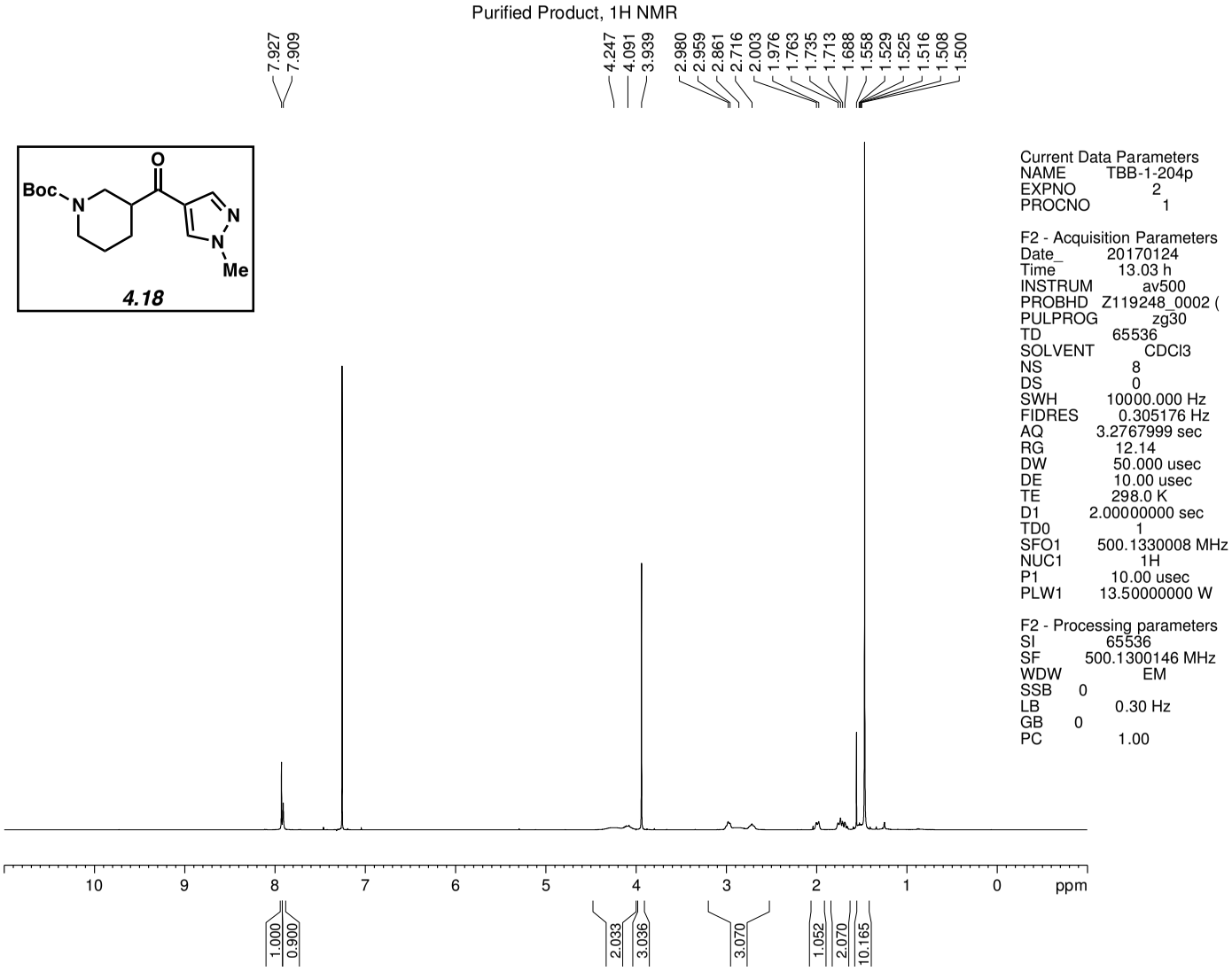

Figure 4.47 ^{1}H NMR (500 MHz, $CDCl_3$) of compound **4.18**.

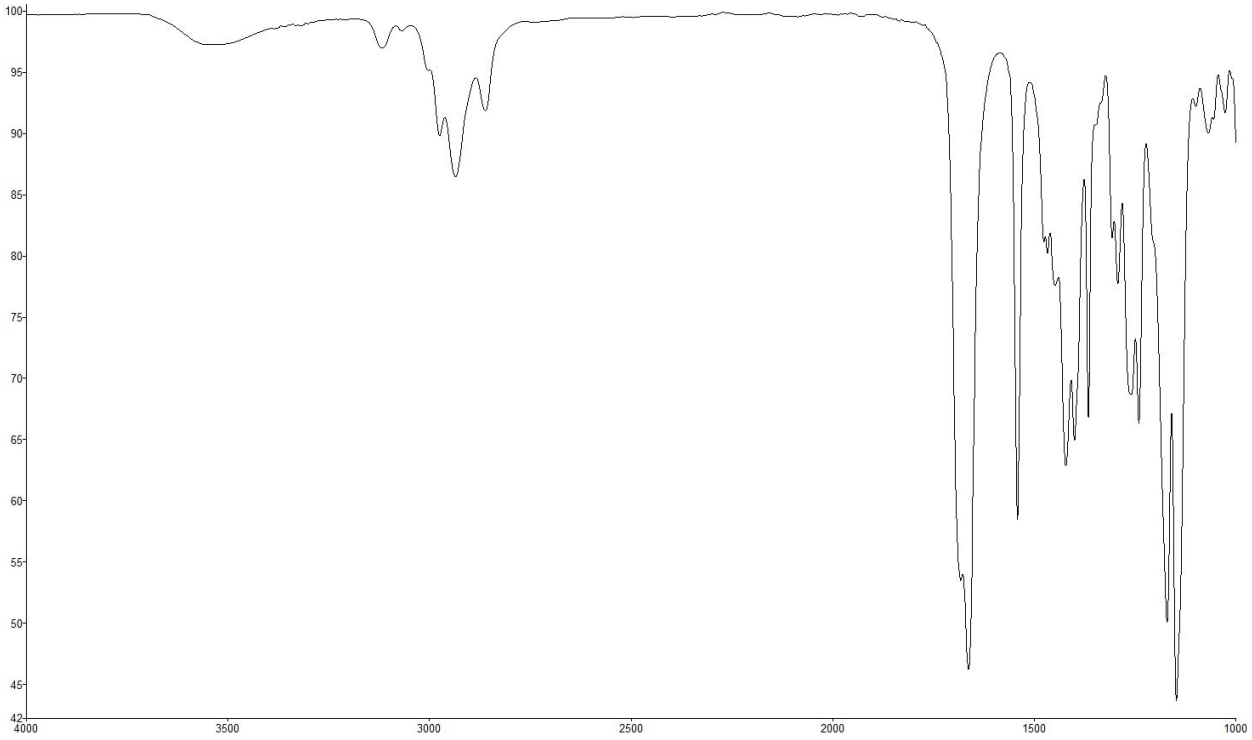

Figure 4.48 Infrared spectrum of compound **4.18**.

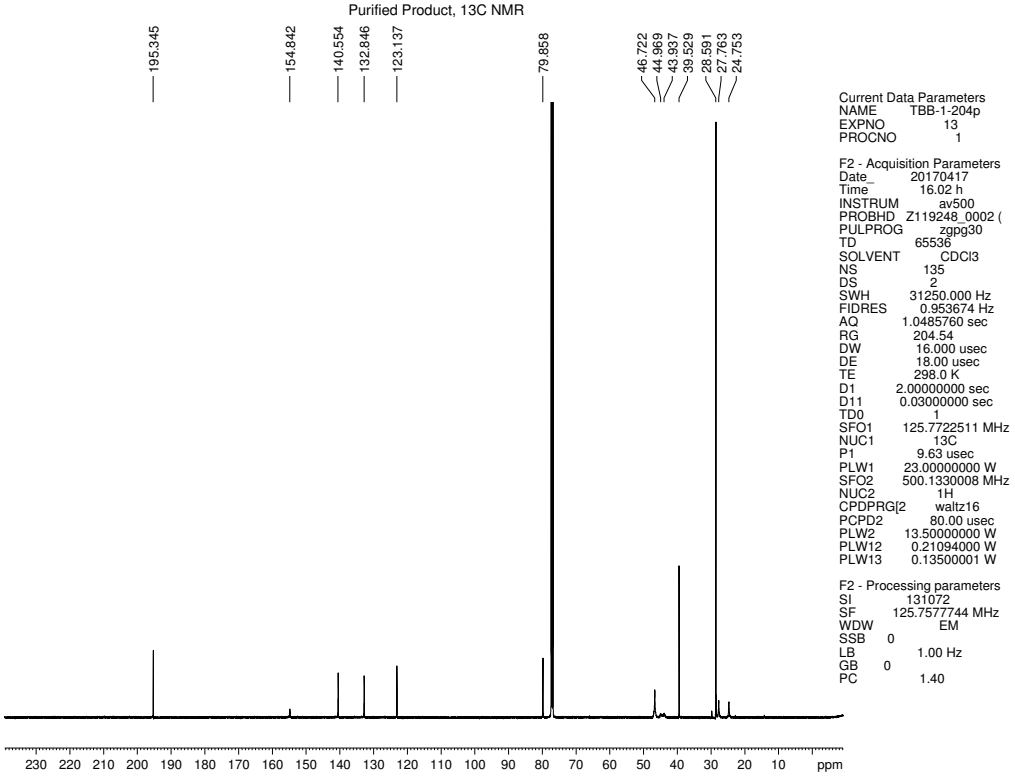

Figure 4.49 ^{13}C NMR (125 MHz, $CDCl_3$) of compound **4.18**.

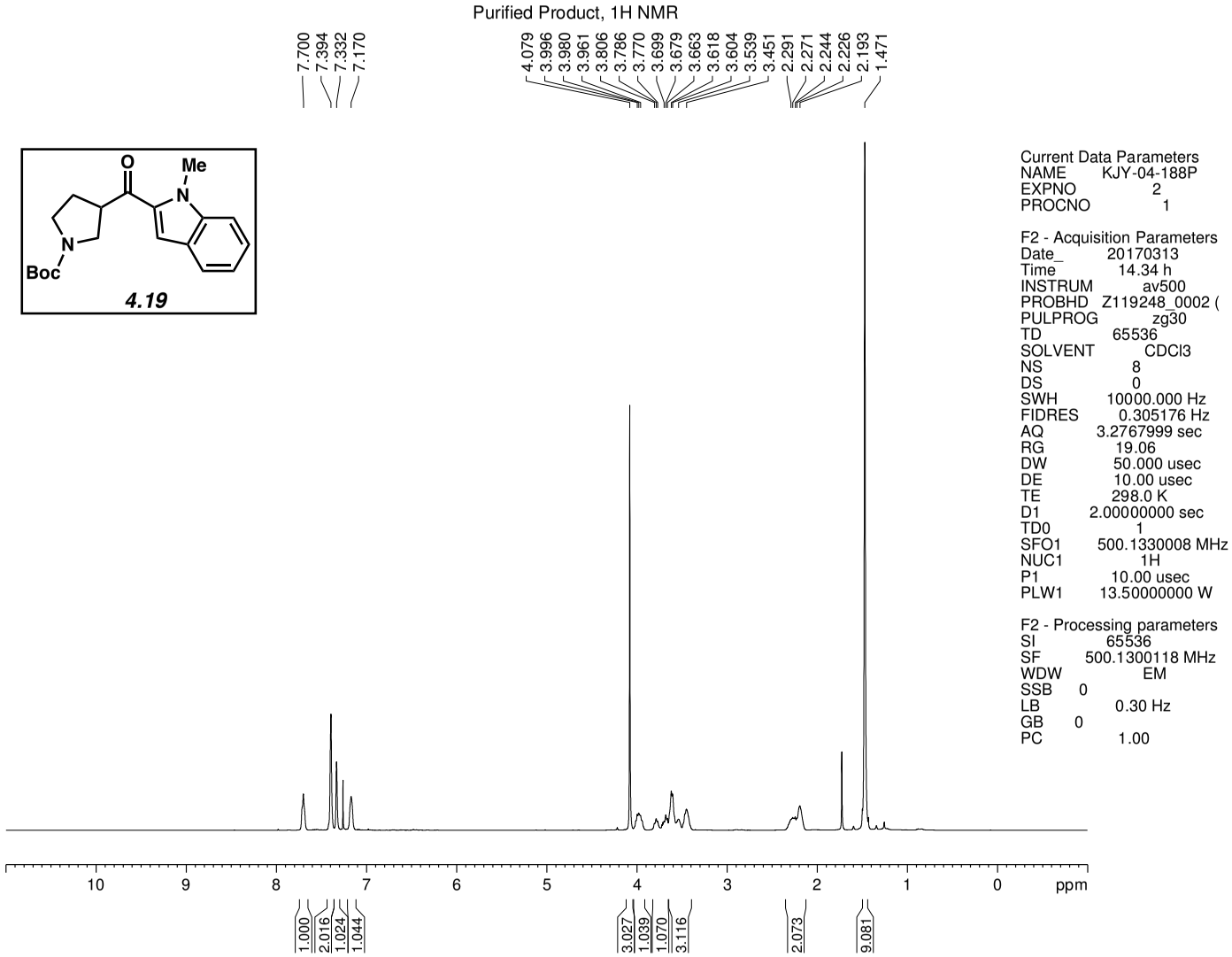

Figure 4.50 ^{1}H NMR (500 MHz, $CDCl_3$) of compound **4.19**.

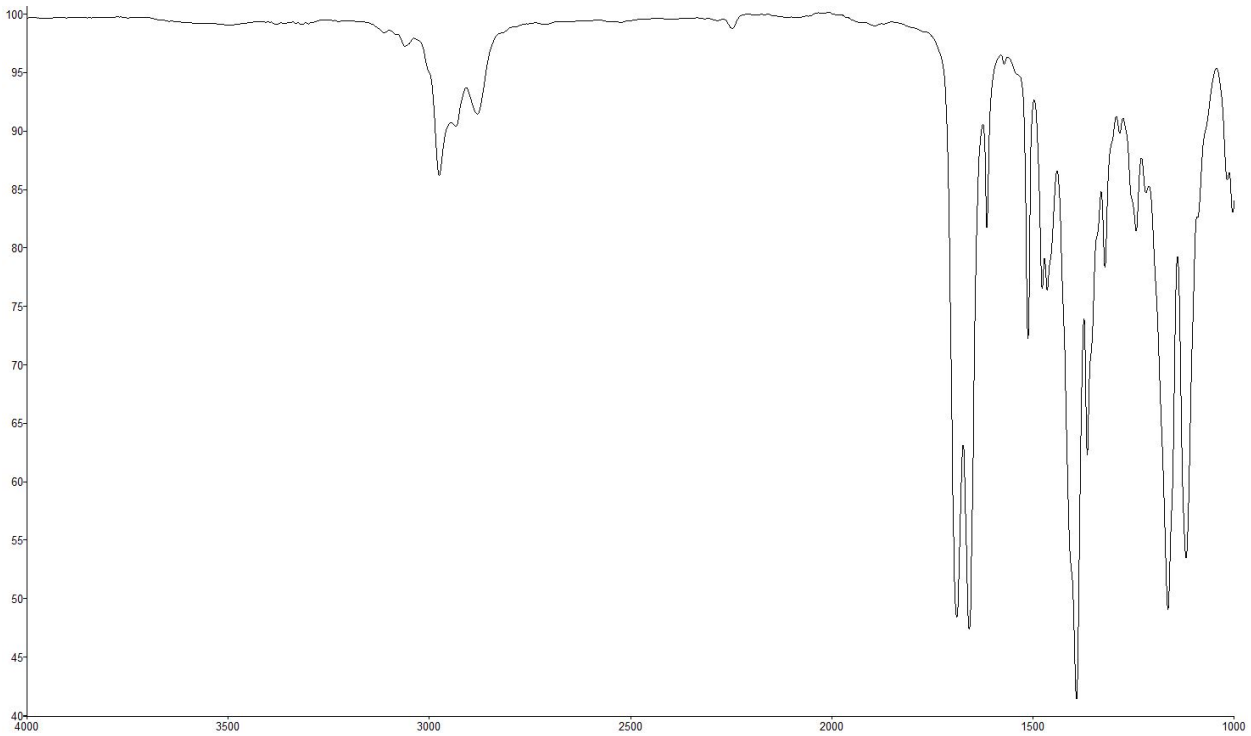

Figure 4.51 Infrared spectrum of compound **4.19**.

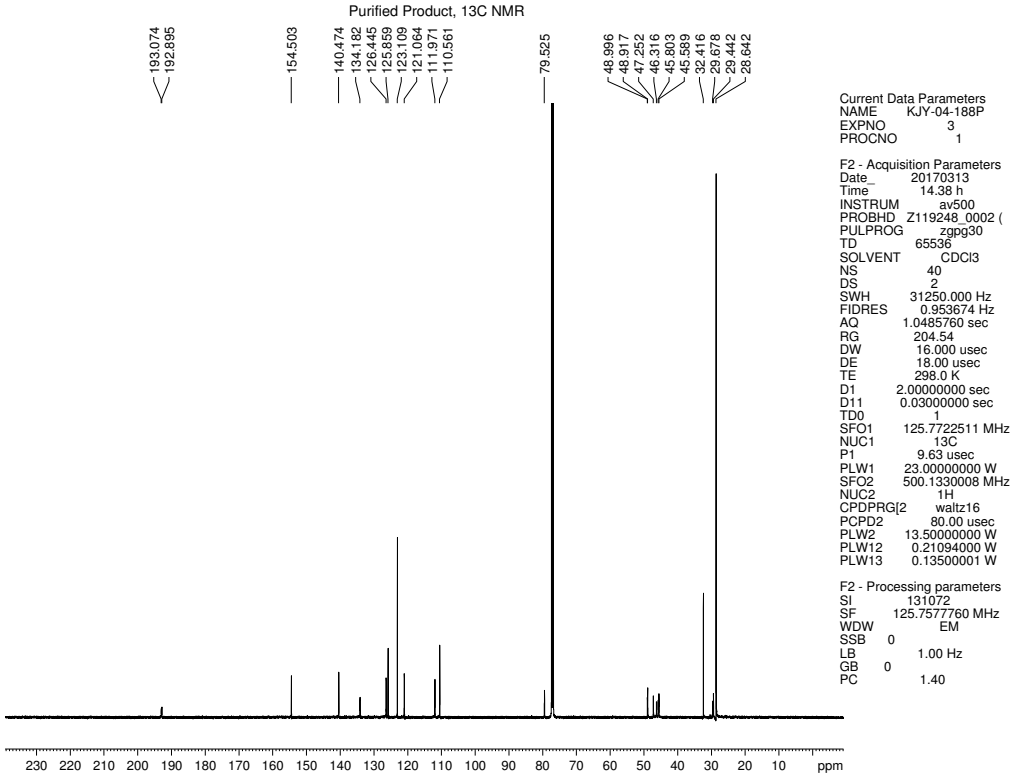

Figure 4.52 ^{13}C NMR (125 MHz, $CDCl_3$) of compound **4.19**.

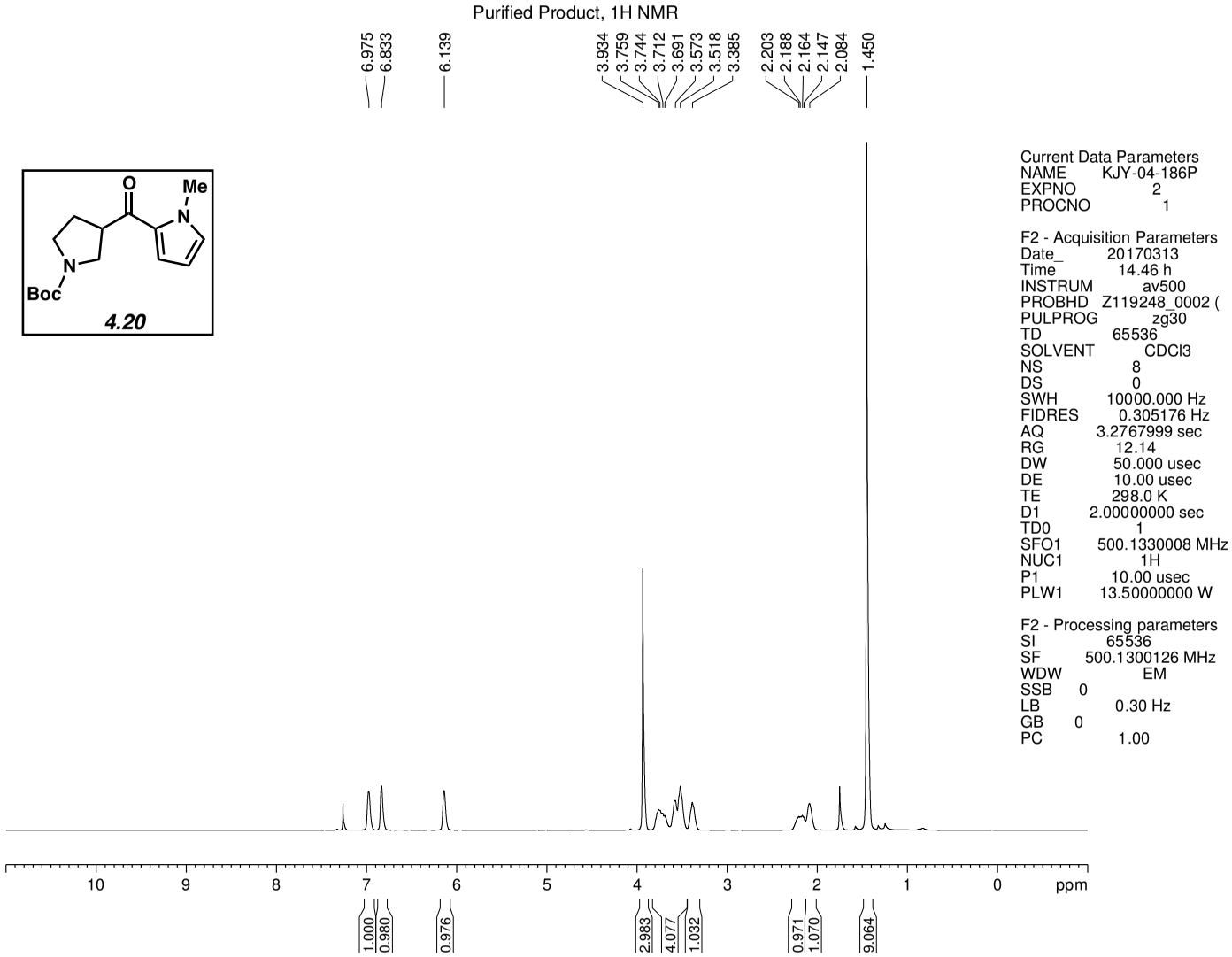

Figure 4.53 ^{1}H NMR (500 MHz, $CDCl_3$) of compound **4.20**.

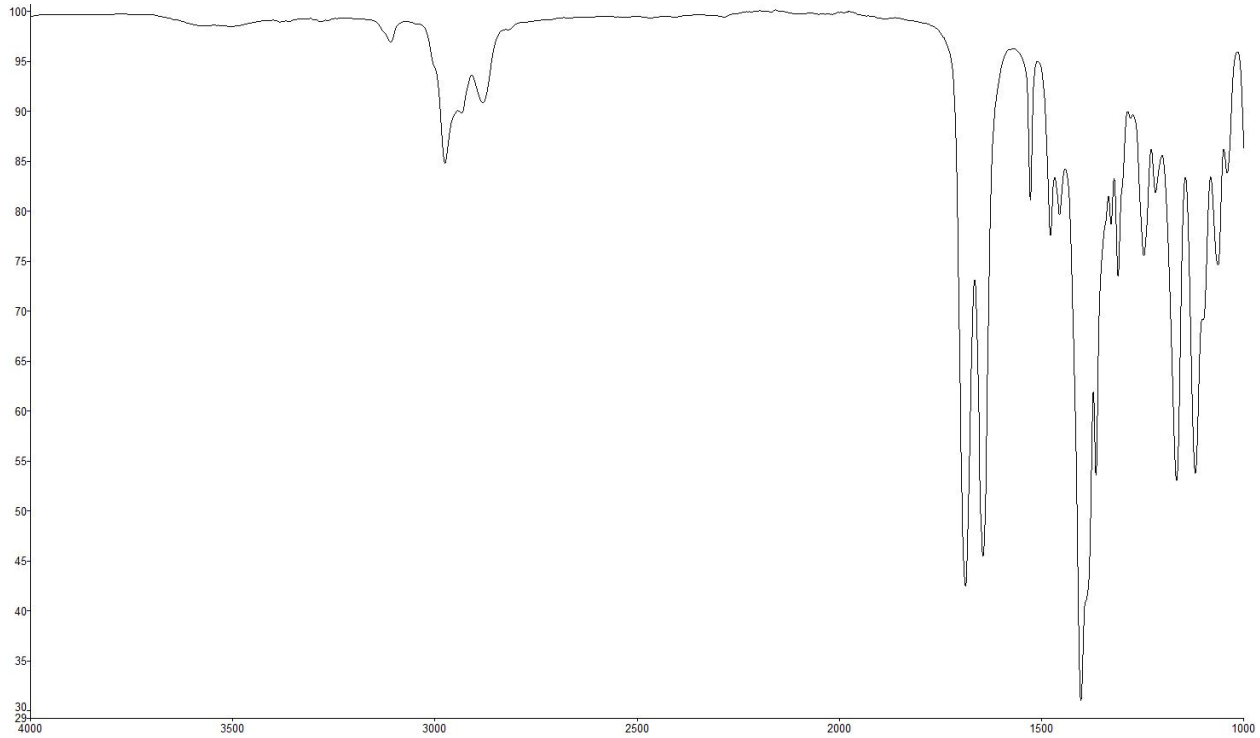

Figure 4.54 Infrared spectrum of compound **4.20**.

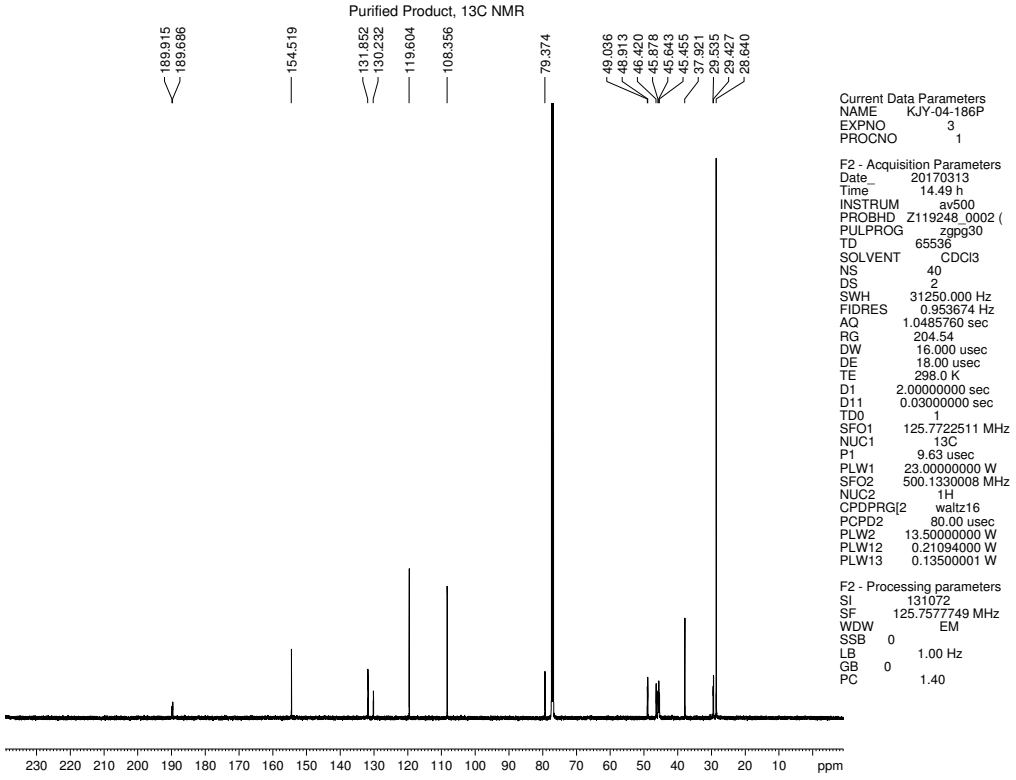

Figure 4.55 ^{13}C NMR (125 MHz, $CDCl_3$) of compound **4.20**.

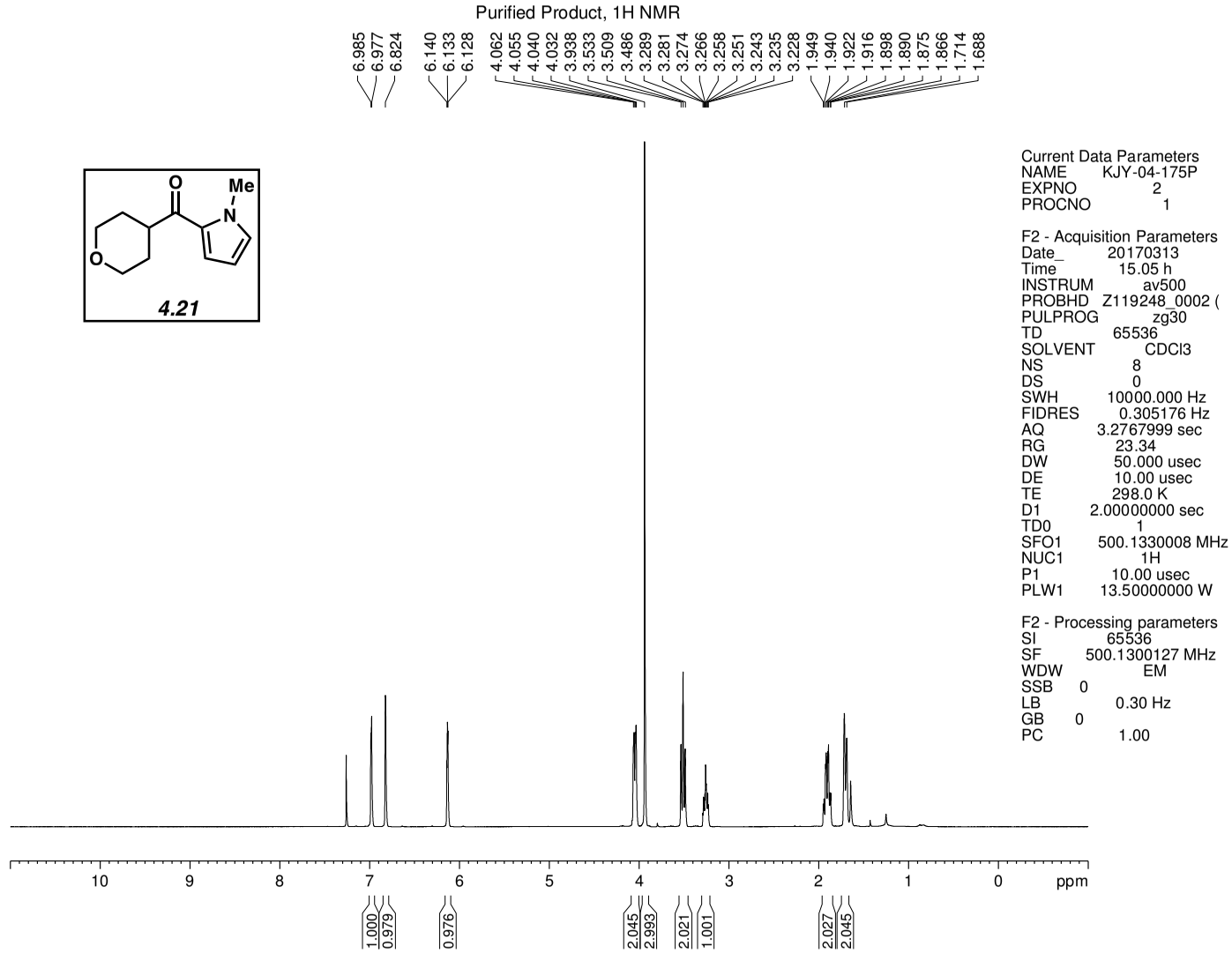

Figure 4.56 ^{1}H NMR (500 MHz, $CDCl_3$) of compound **4.21**.

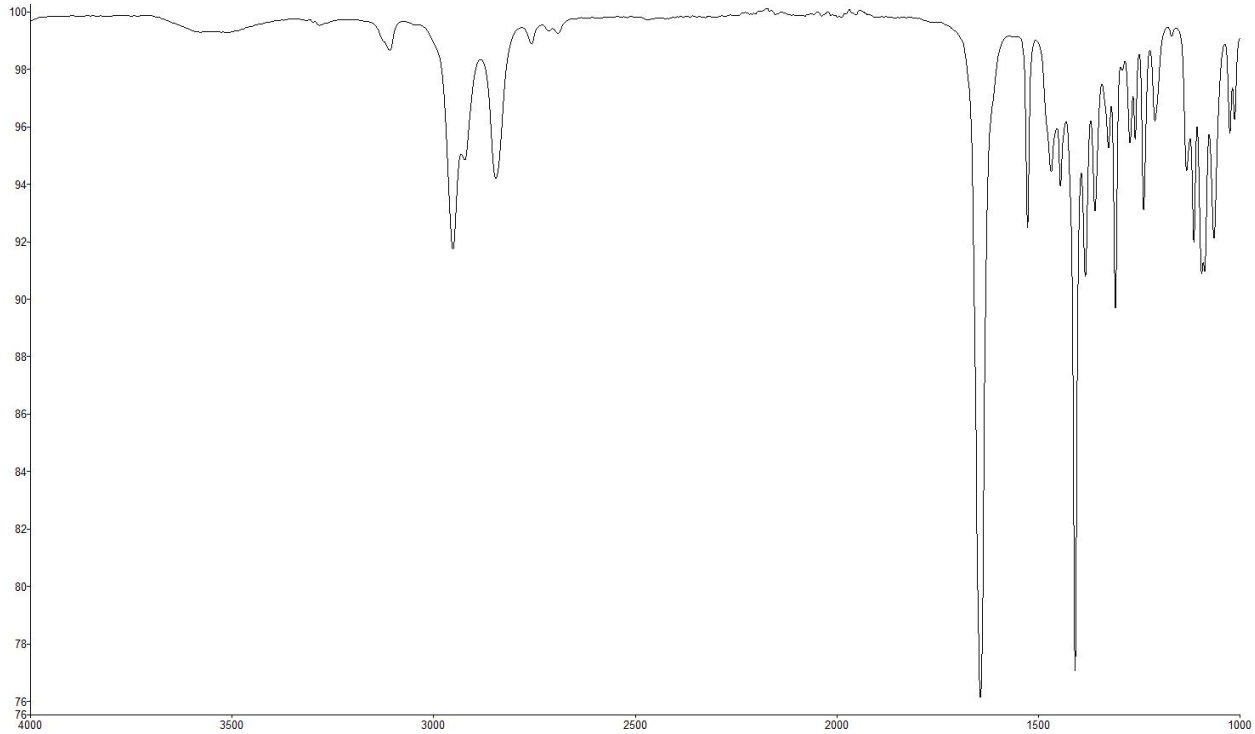

Figure 4.57 Infrared spectrum of compound **4.21**.

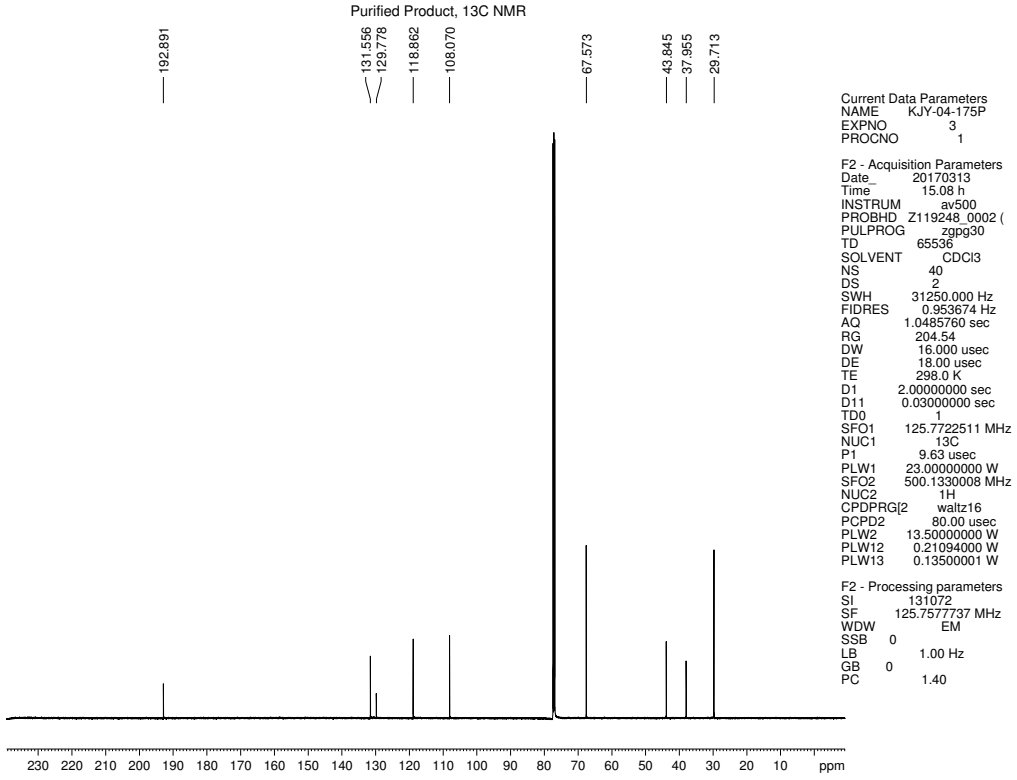

Figure 4.58 ^{13}C NMR (125 MHz, $CDCl_3$) of compound **4.22**.

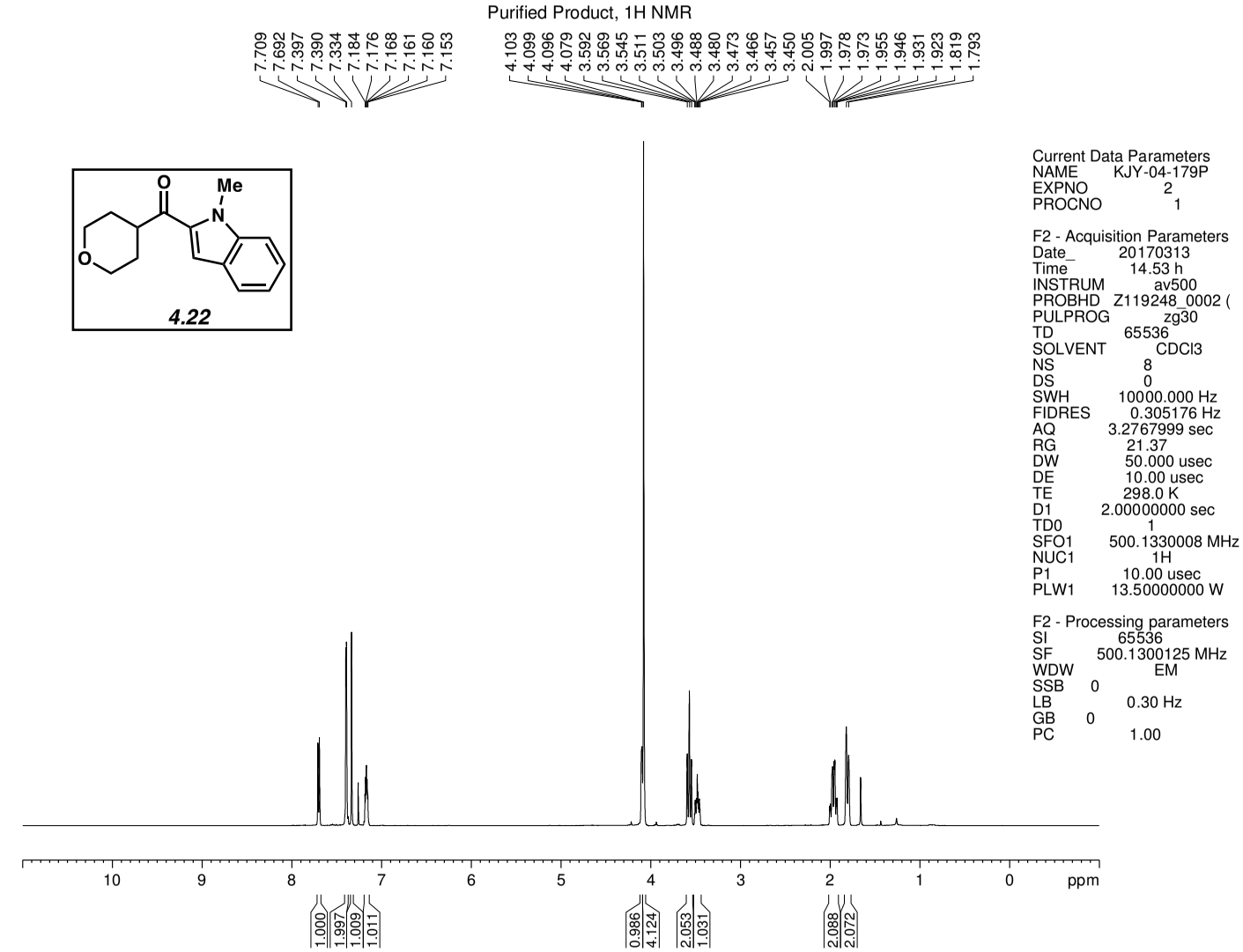

Figure 4.59 ^{1}H NMR (500 MHz, $CDCl_3$) of compound **4.22**.

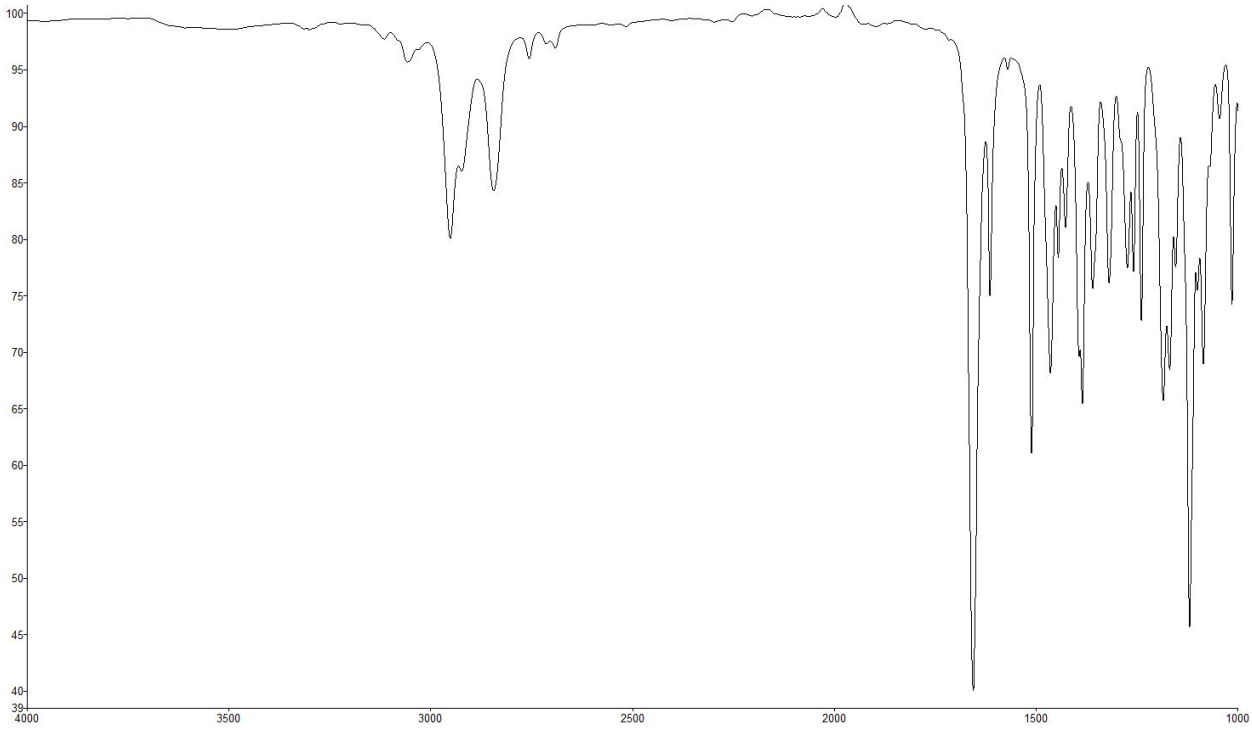

Figure 4.60 Infrared spectrum of compound **4.22**.

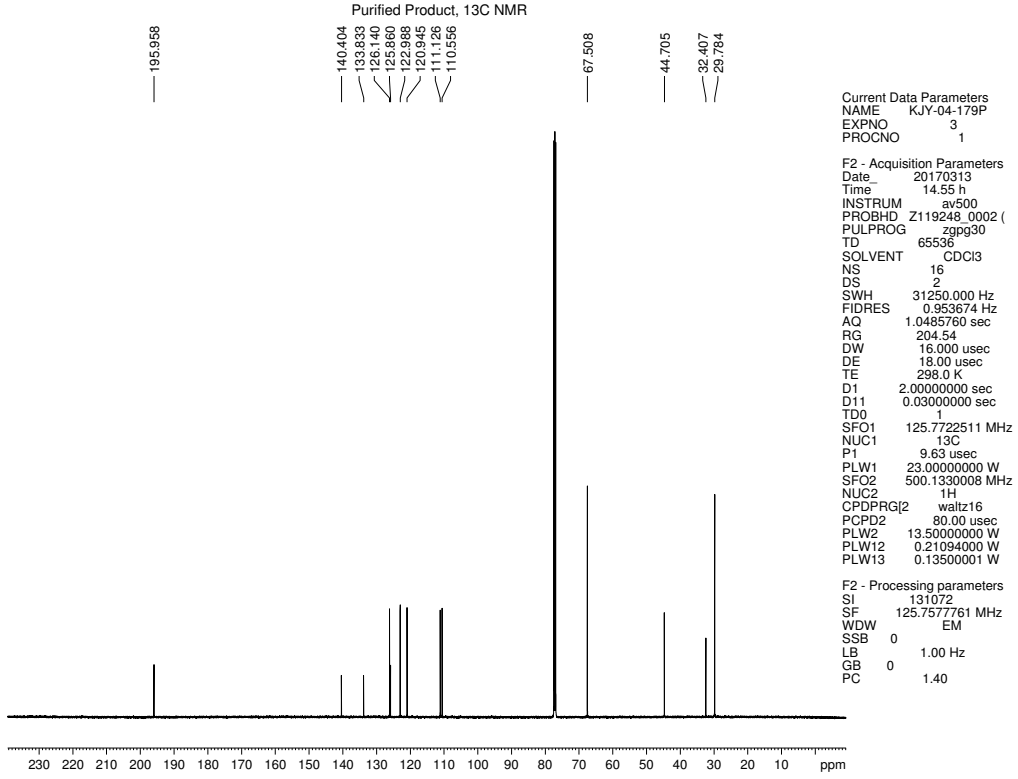

Figure 4.61 ^{13}C NMR (125 MHz, $CDCl_3$) of compound **4.22**.

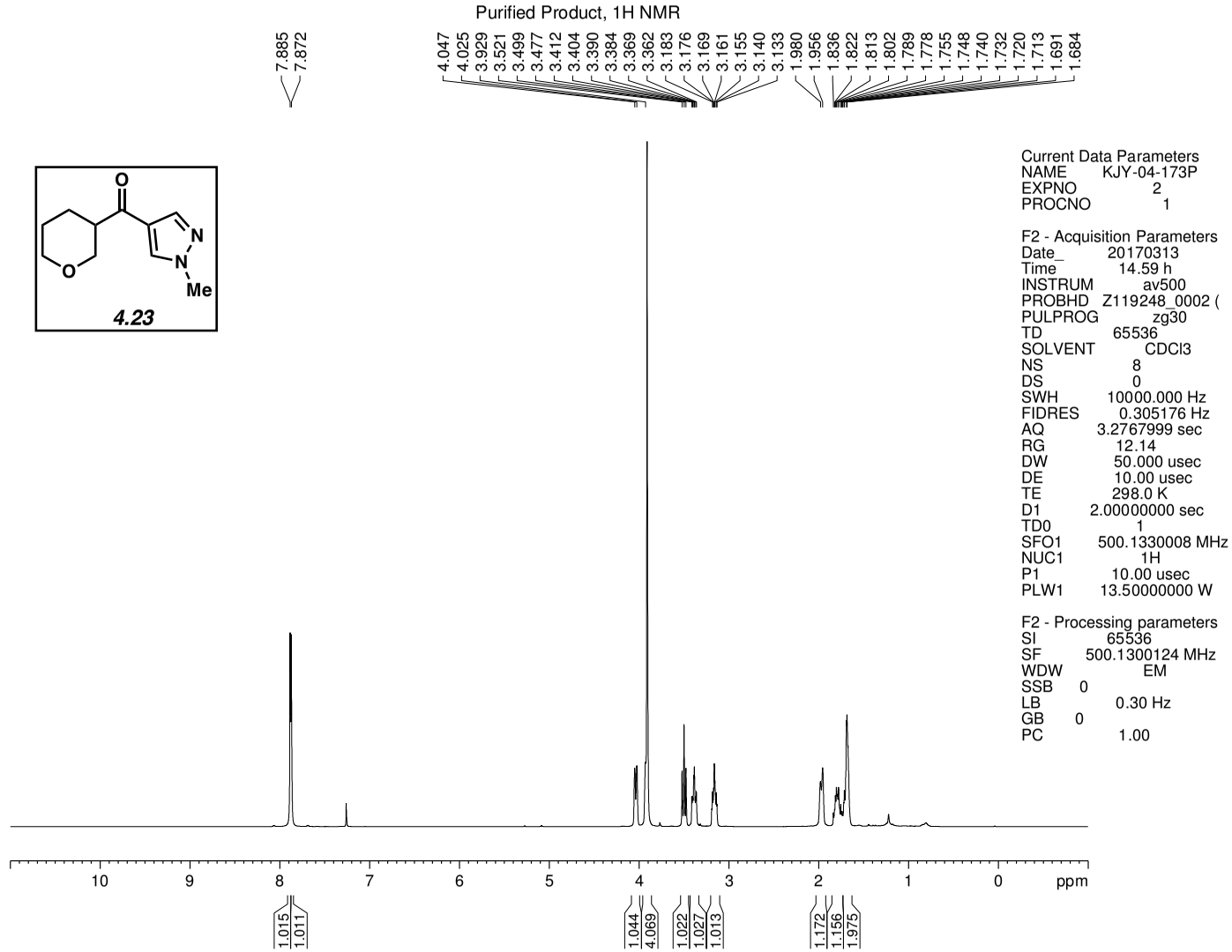

Figure 4.62 ^{1}H NMR (500 MHz, $CDCl_3$) of compound **4.23**.

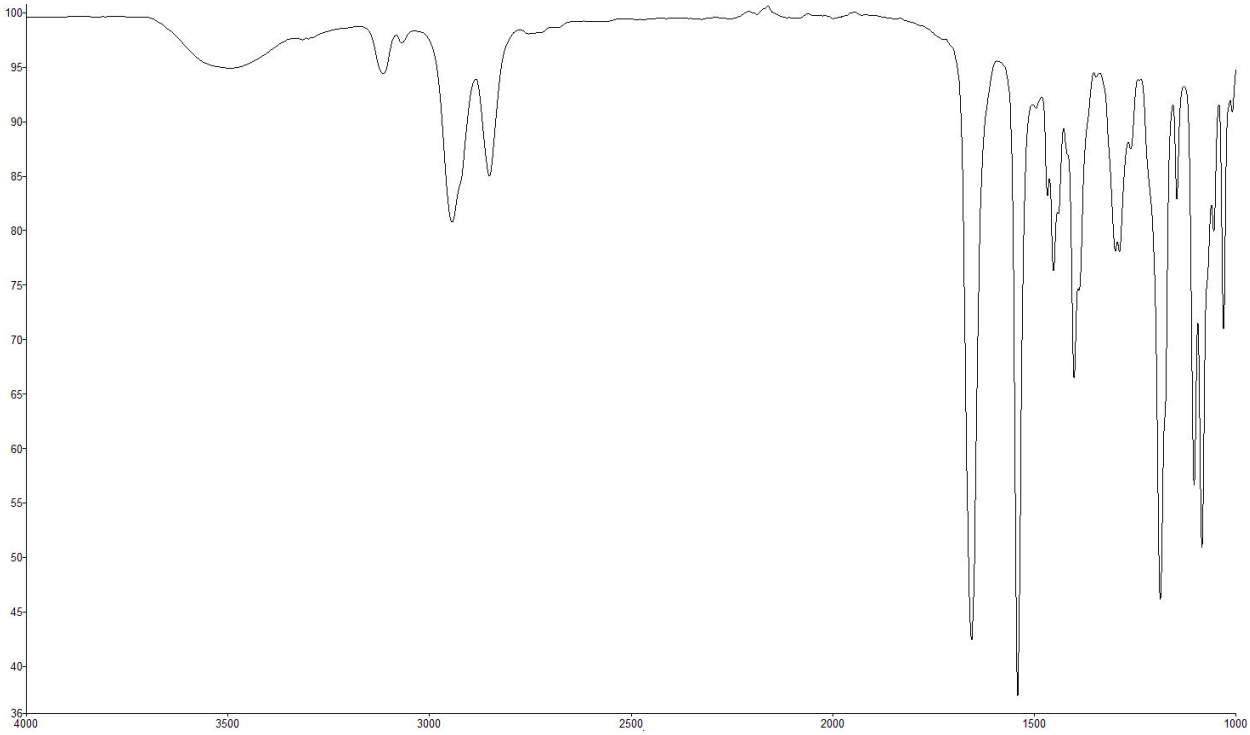

Figure 4.63 Infrared spectrum of compound **4.23**.

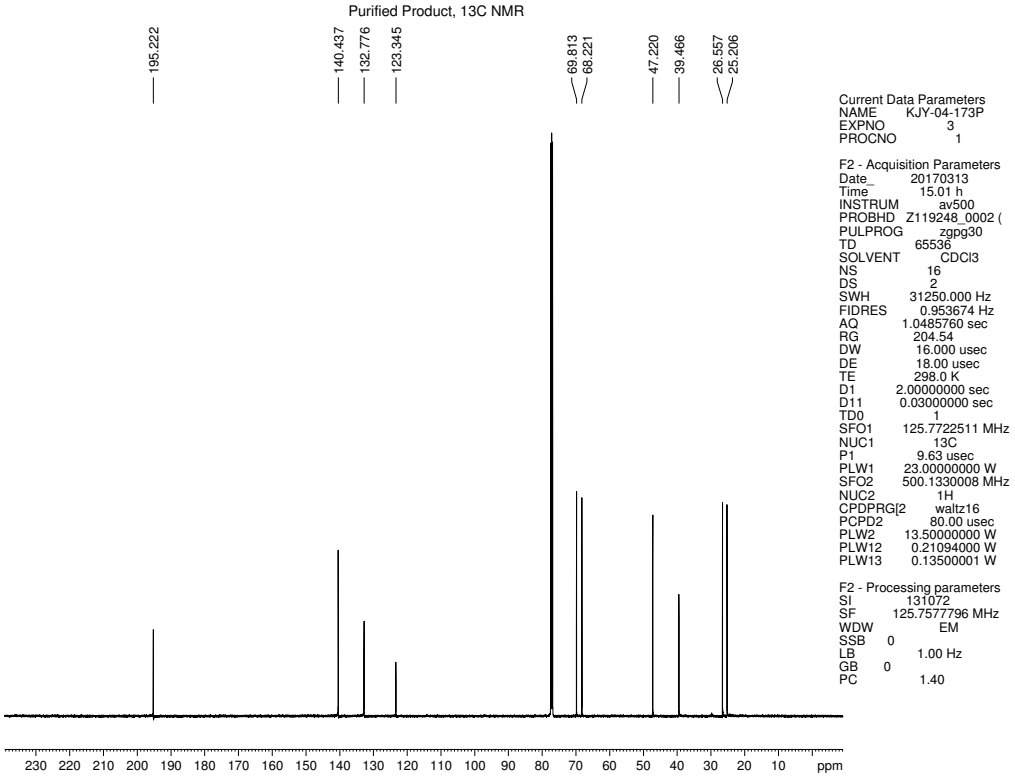

Figure 4.64 ^{13}C NMR (125 MHz, $CDCl_3$) of compound **4.23**.

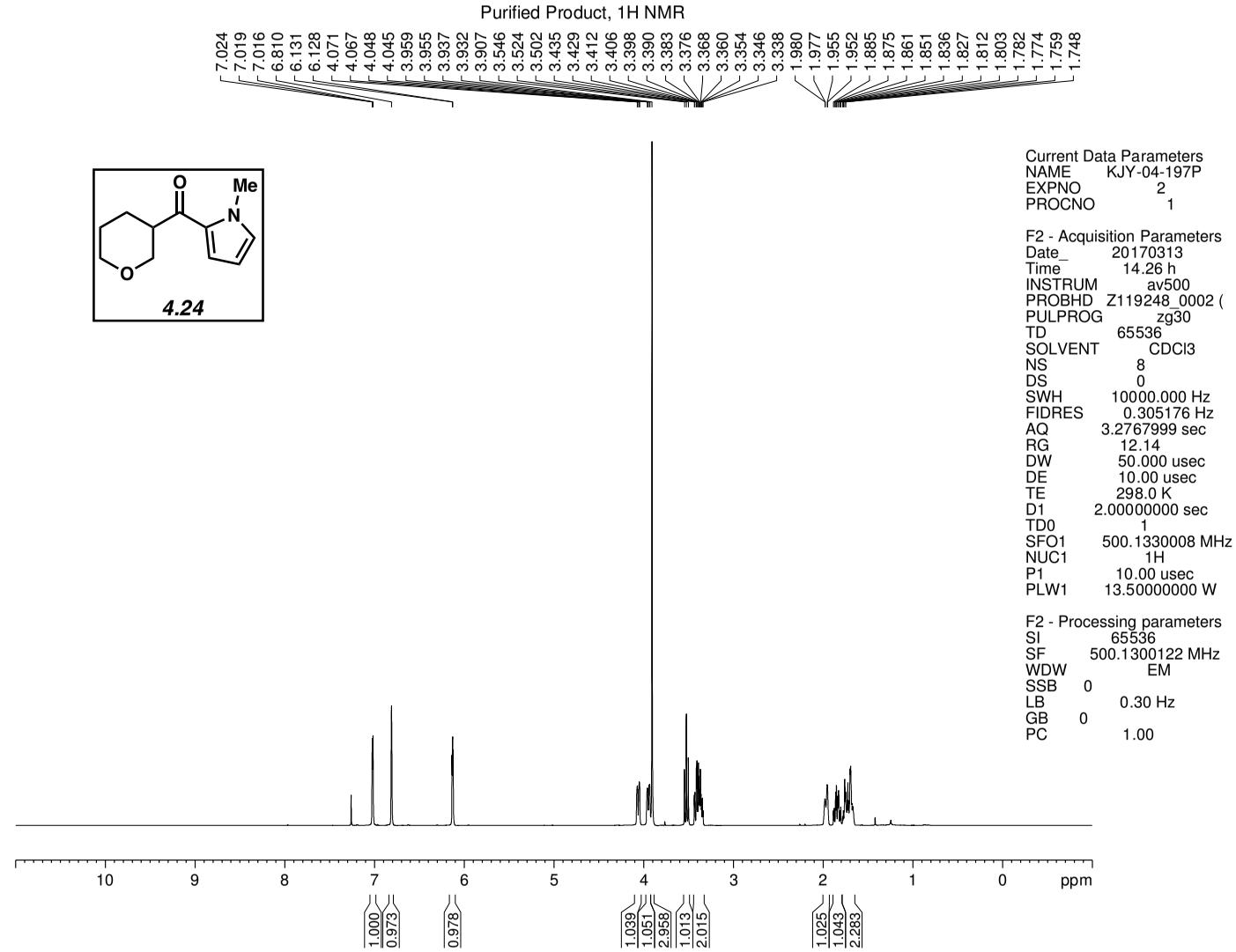

Figure 4.65 ^{1}H NMR (500 MHz, $CDCl_3$) of compound **4.24**.

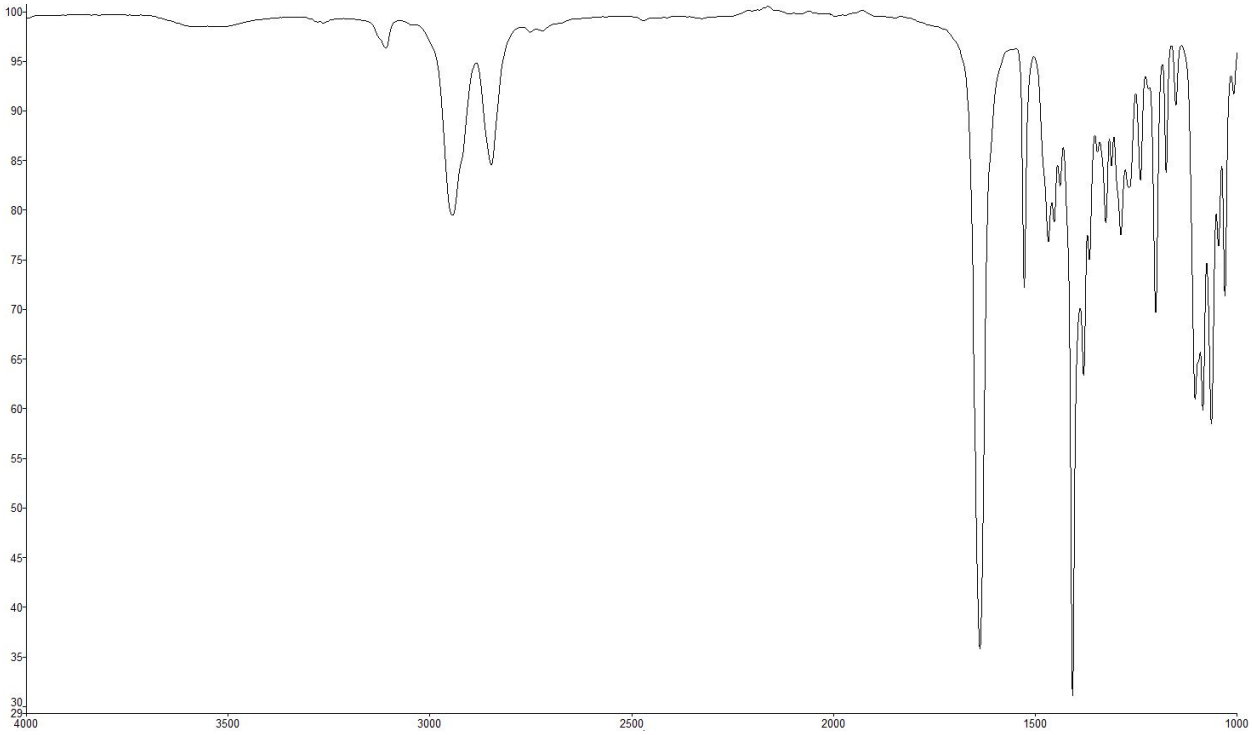

Figure 4.66 Infrared spectrum of compound **4.24**.

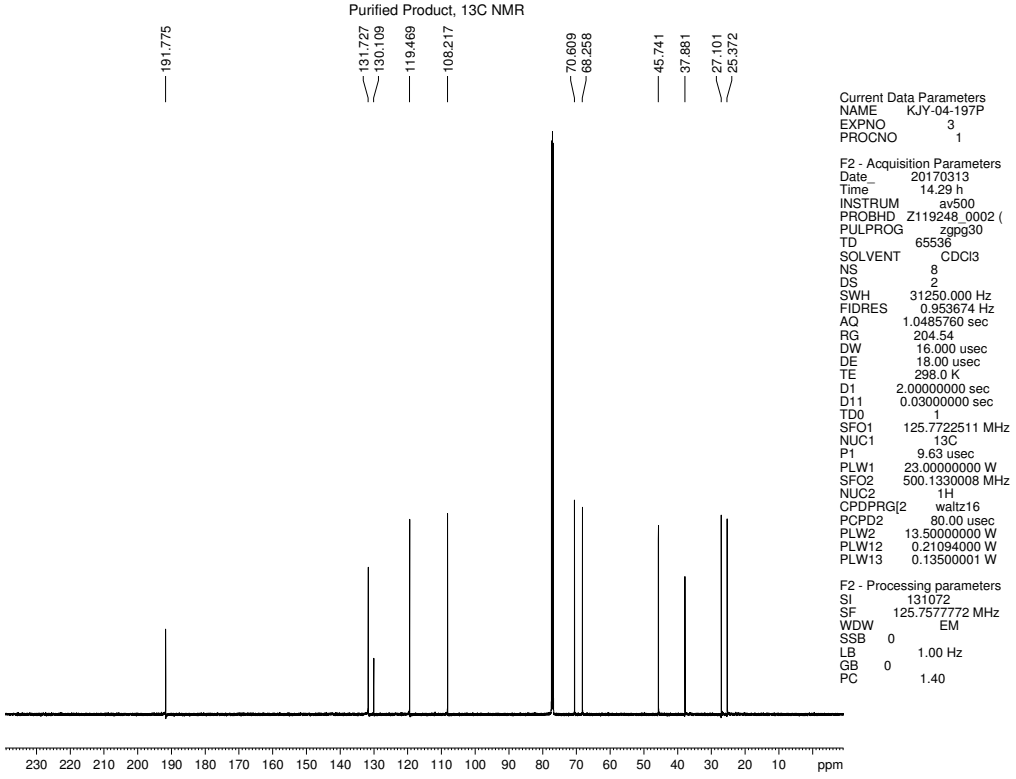

Figure 4.67 ^{13}C NMR (125 MHz, $CDCl_3$) of compound **4.24**.

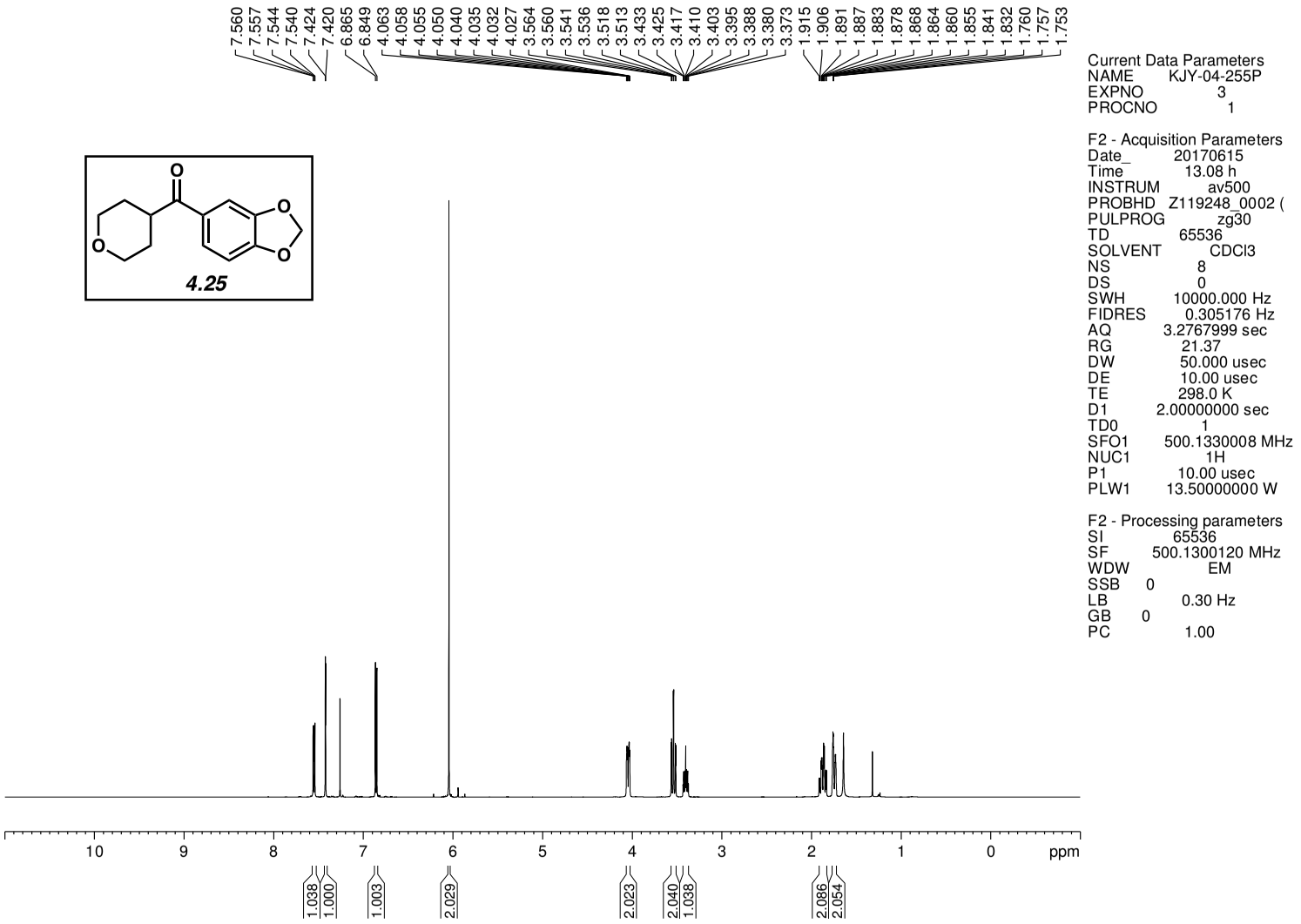

Figure 4.68 ^{1}H NMR (500 MHz, $CDCl_3$) of compound **4.25**.

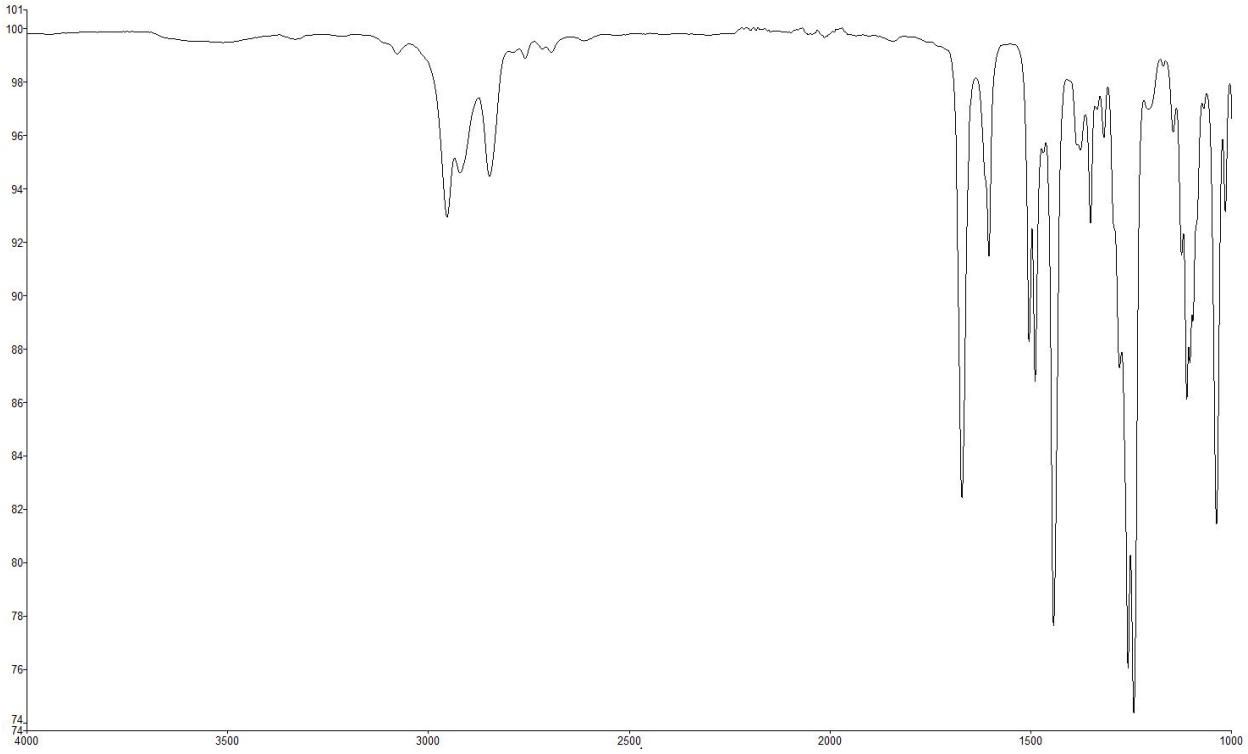

Figure 4.69 Infrared spectrum of compound **4.25**.

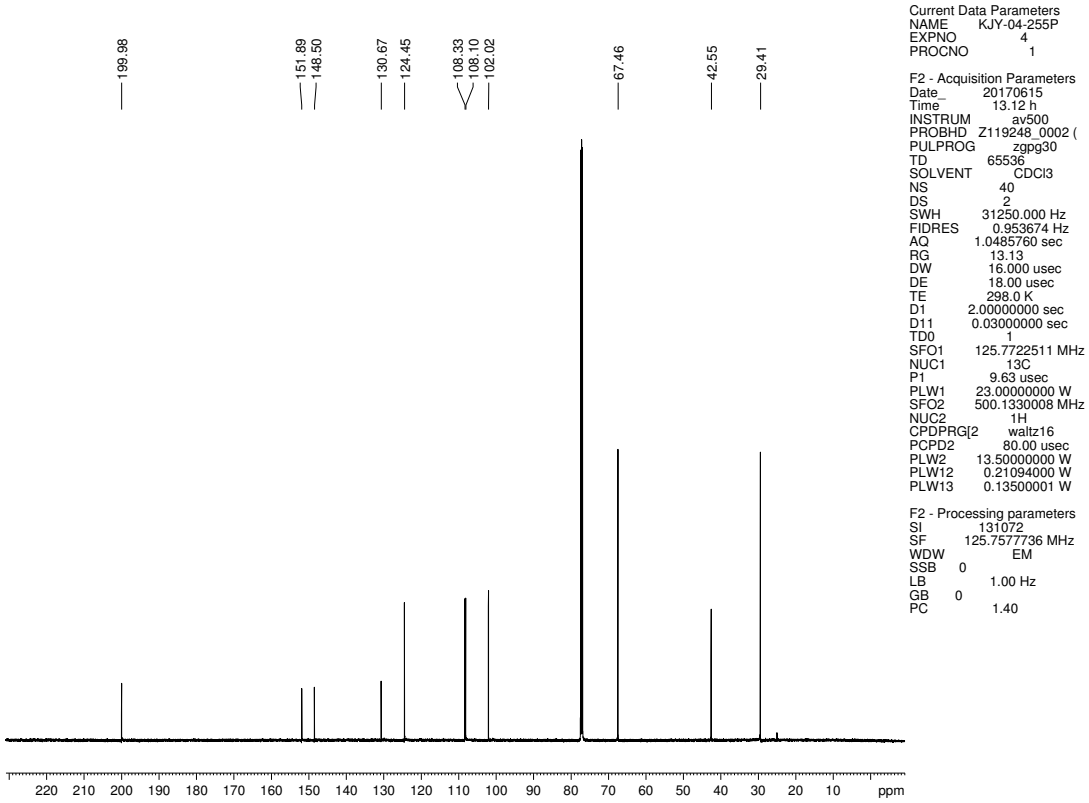

Figure 4.70 ^{13}C NMR (125 MHz, $CDCl_3$) of compound **4.25**.

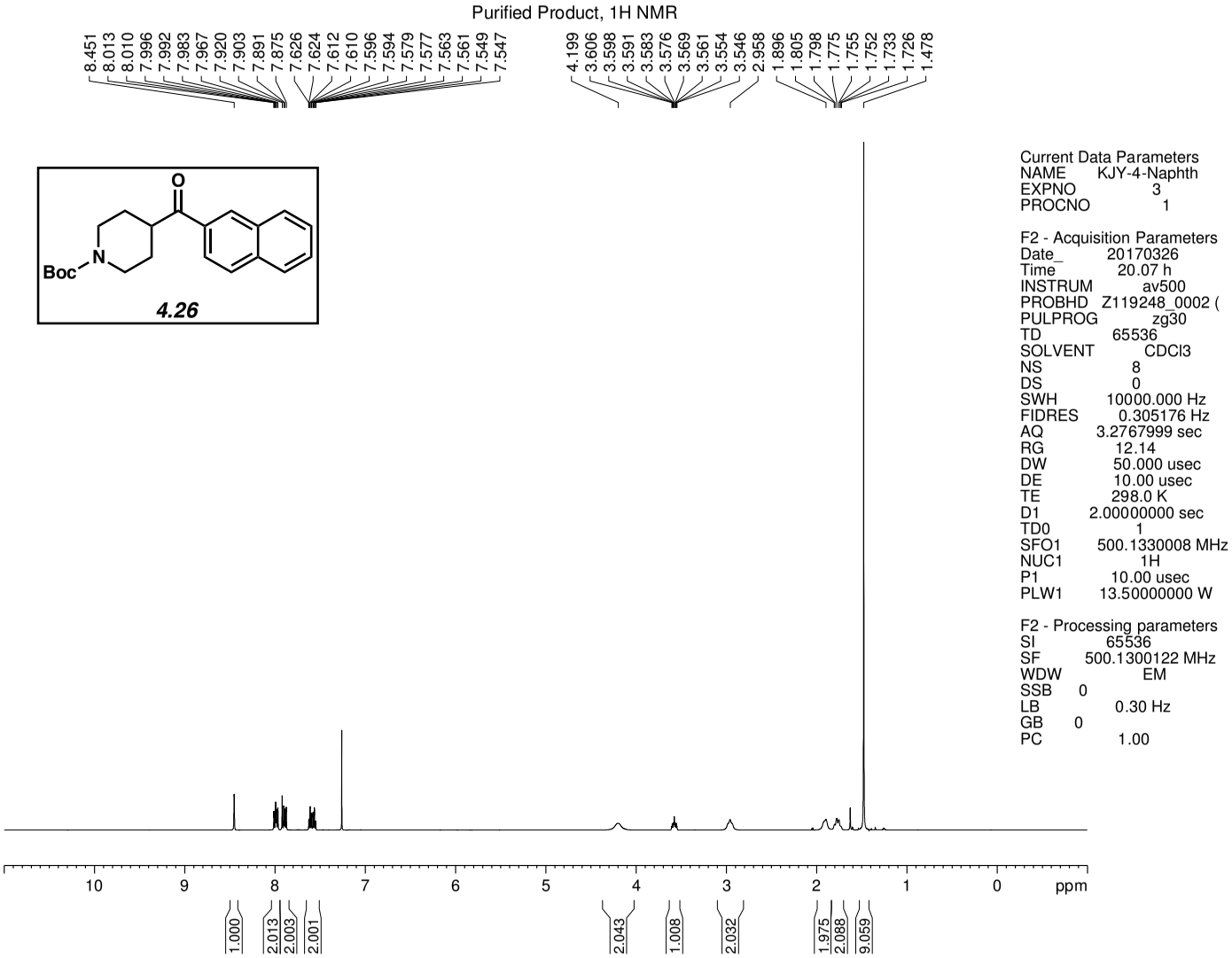

Figure 4.71 ^{1}H NMR (500 MHz, $CDCl_3$) of compound **4.26**.

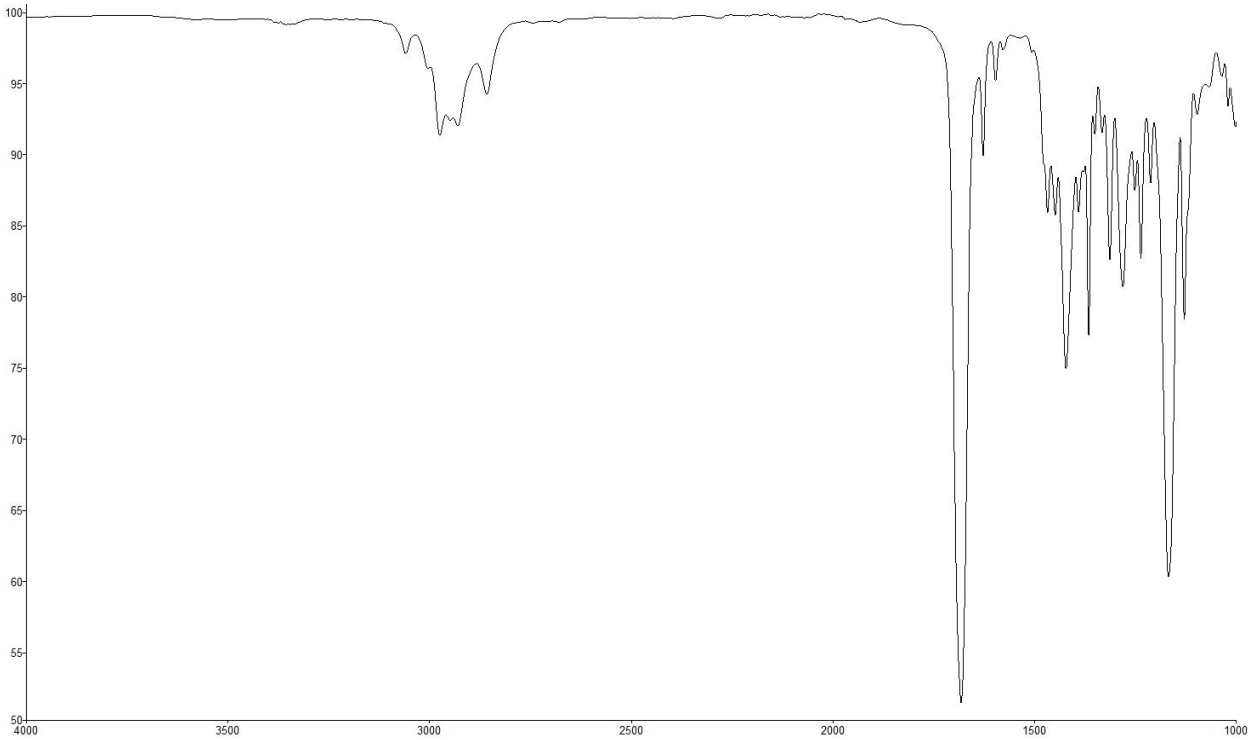

Figure 4.72 Infrared spectrum of compound **4.26**.

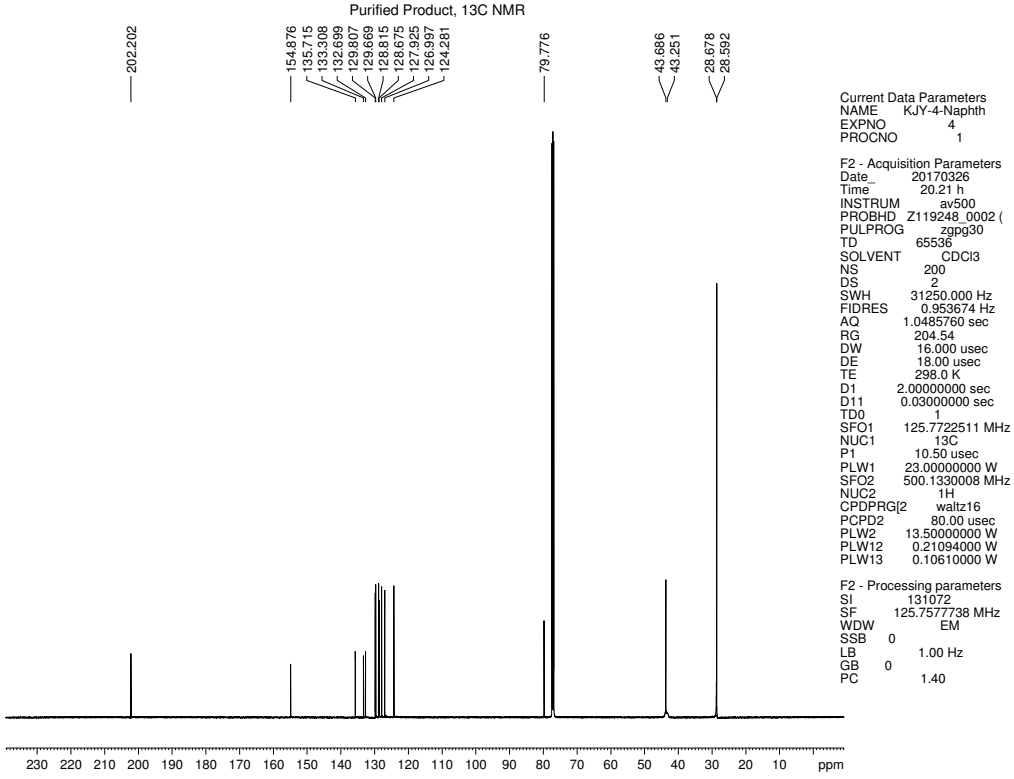

Figure 4.73 ^{13}C NMR (125 MHz, $CDCl_3$) of compound **4.26**.

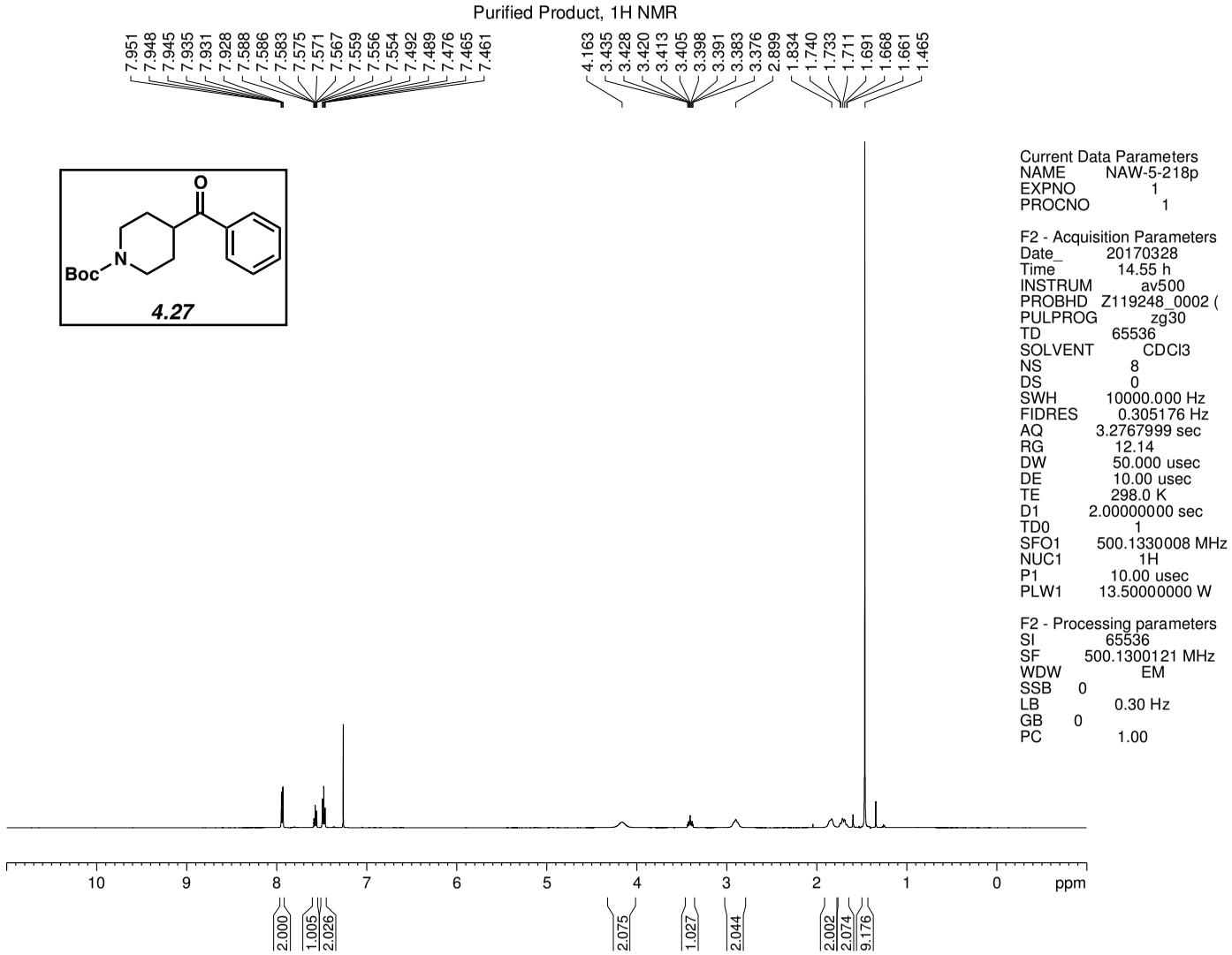

Figure 4.74 ^{1}H NMR (500 MHz, $CDCl_3$) of compound **4.27**.

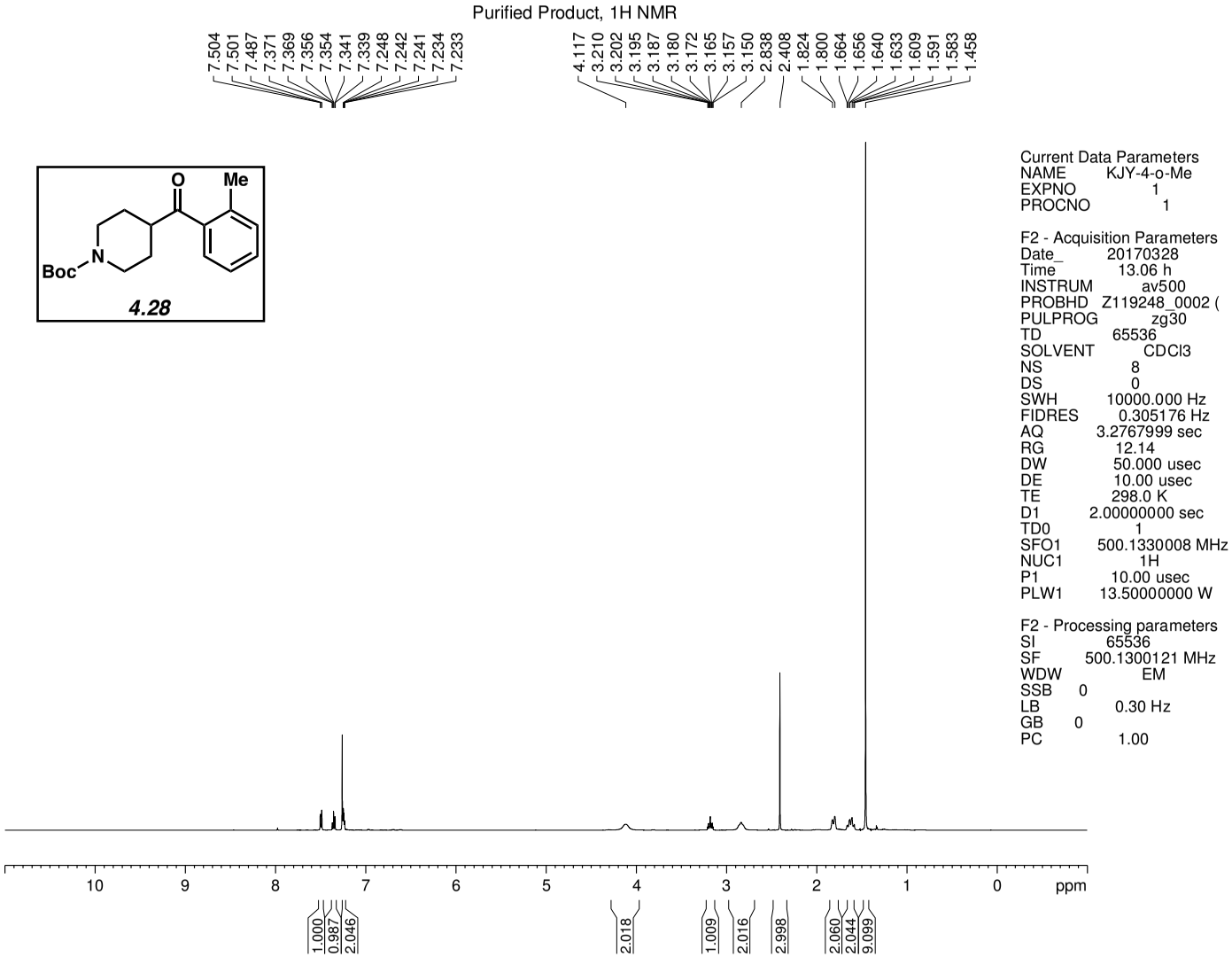

Figure 4.75 ^{1}H NMR (500 MHz, $CDCl_3$) of compound **4.28**.

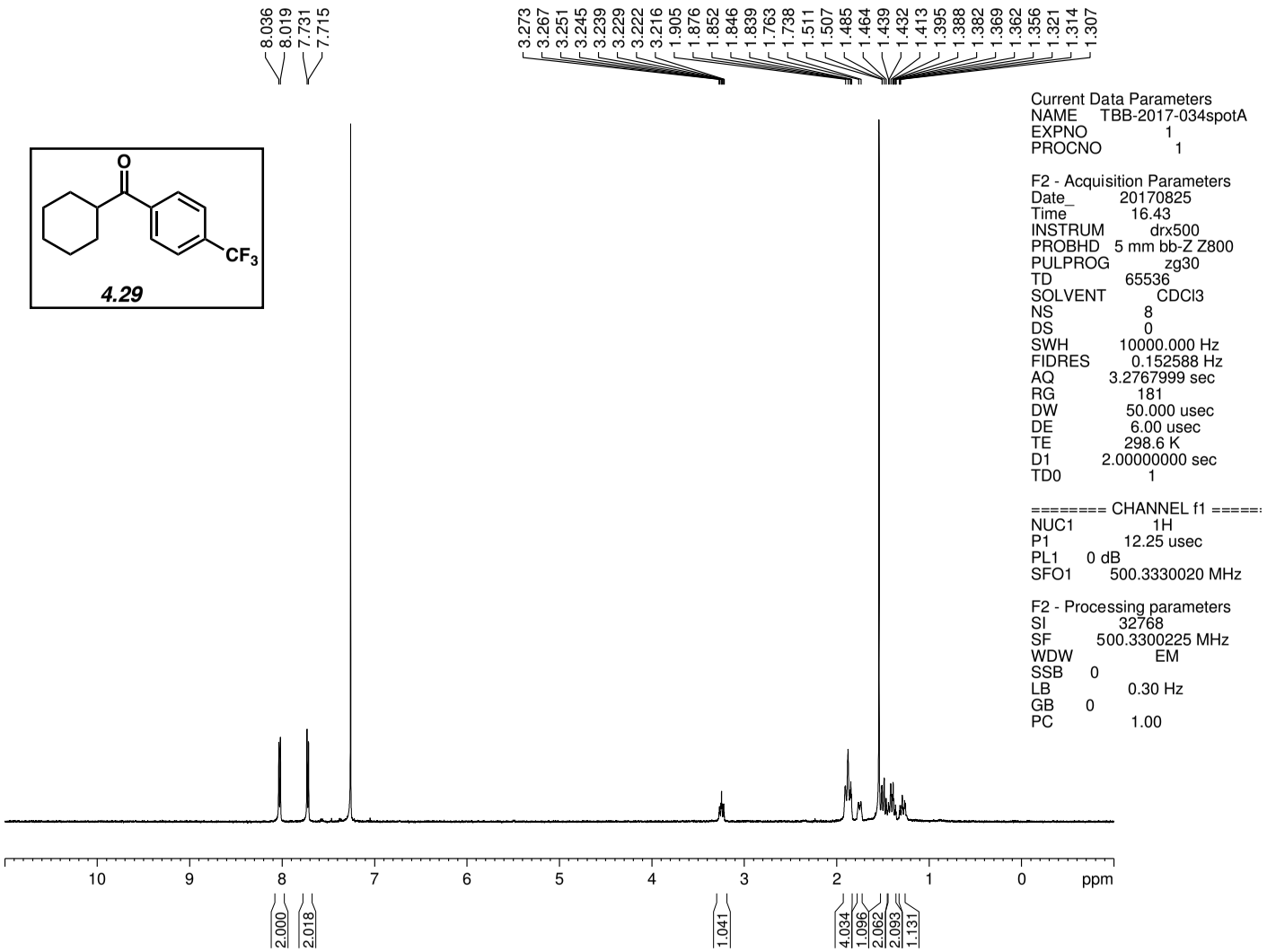

Figure 4.76 ^{1}H NMR (500 MHz, $CDCl_3$) of compound **4.29**.

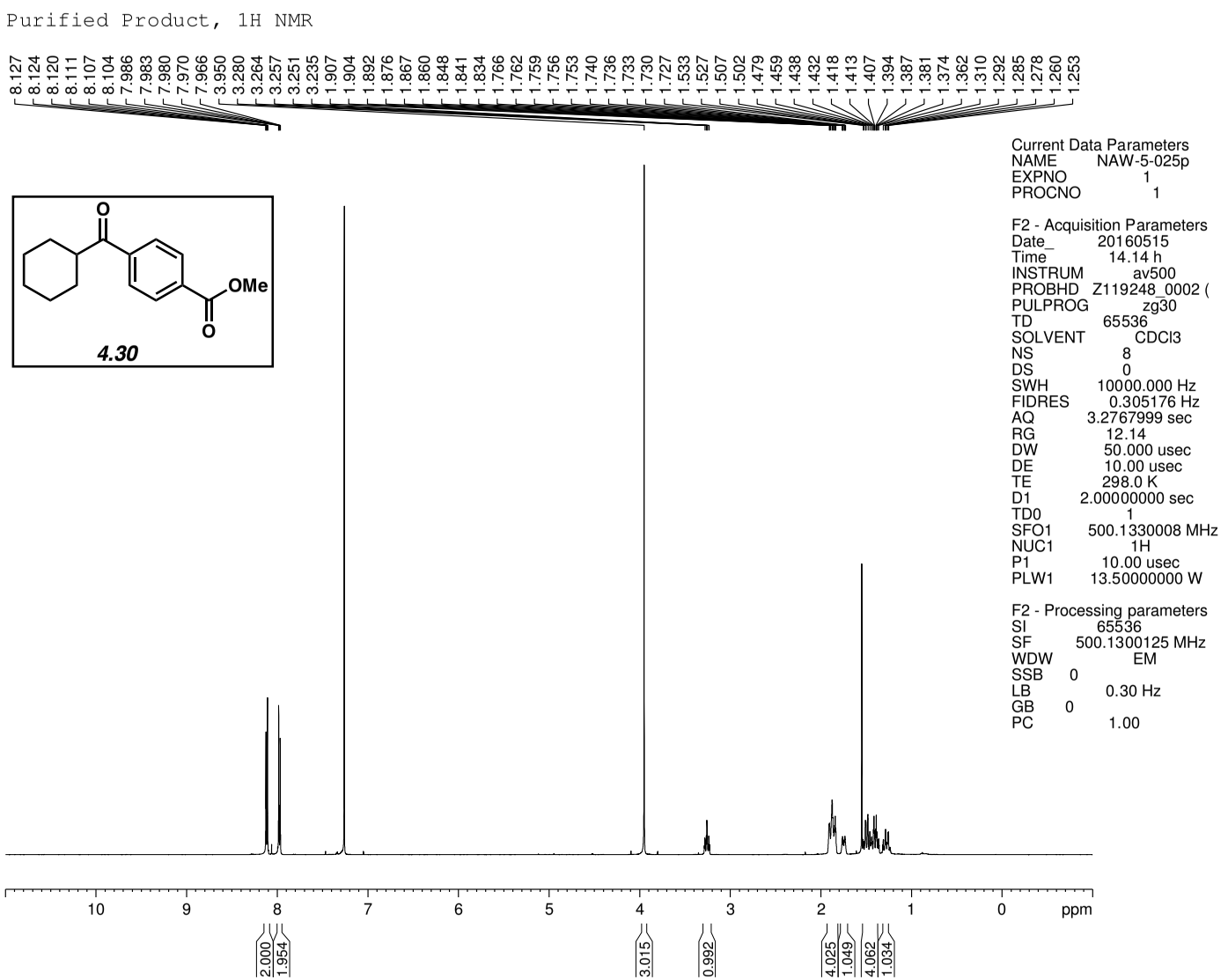

Figure 4.77 ^{1}H NMR (500 MHz, $CDCl_3$) of compound **4.30**.

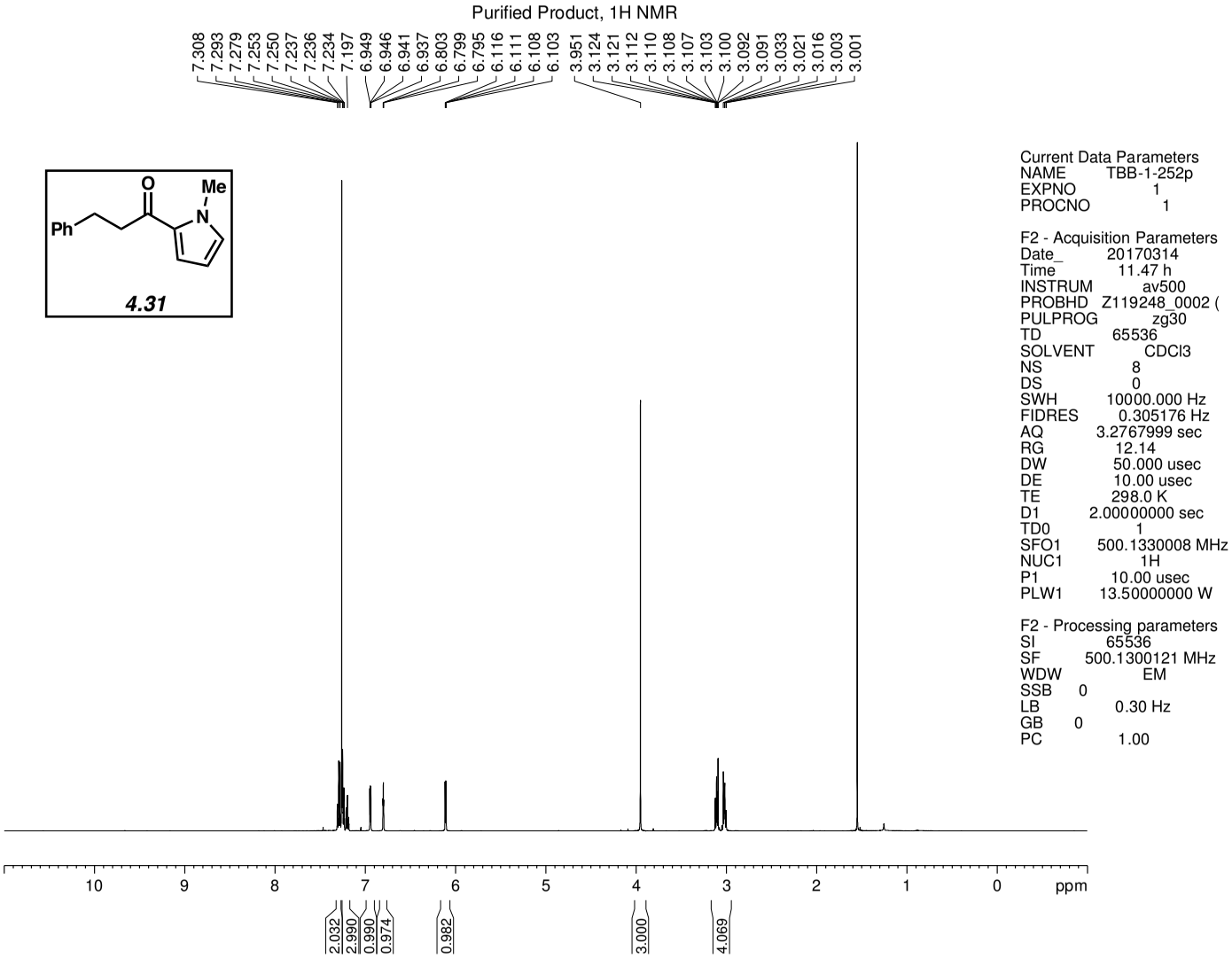

Figure 4.78 ^{1}H NMR (500 MHz, $CDCl_3$) of compound **4.31**.

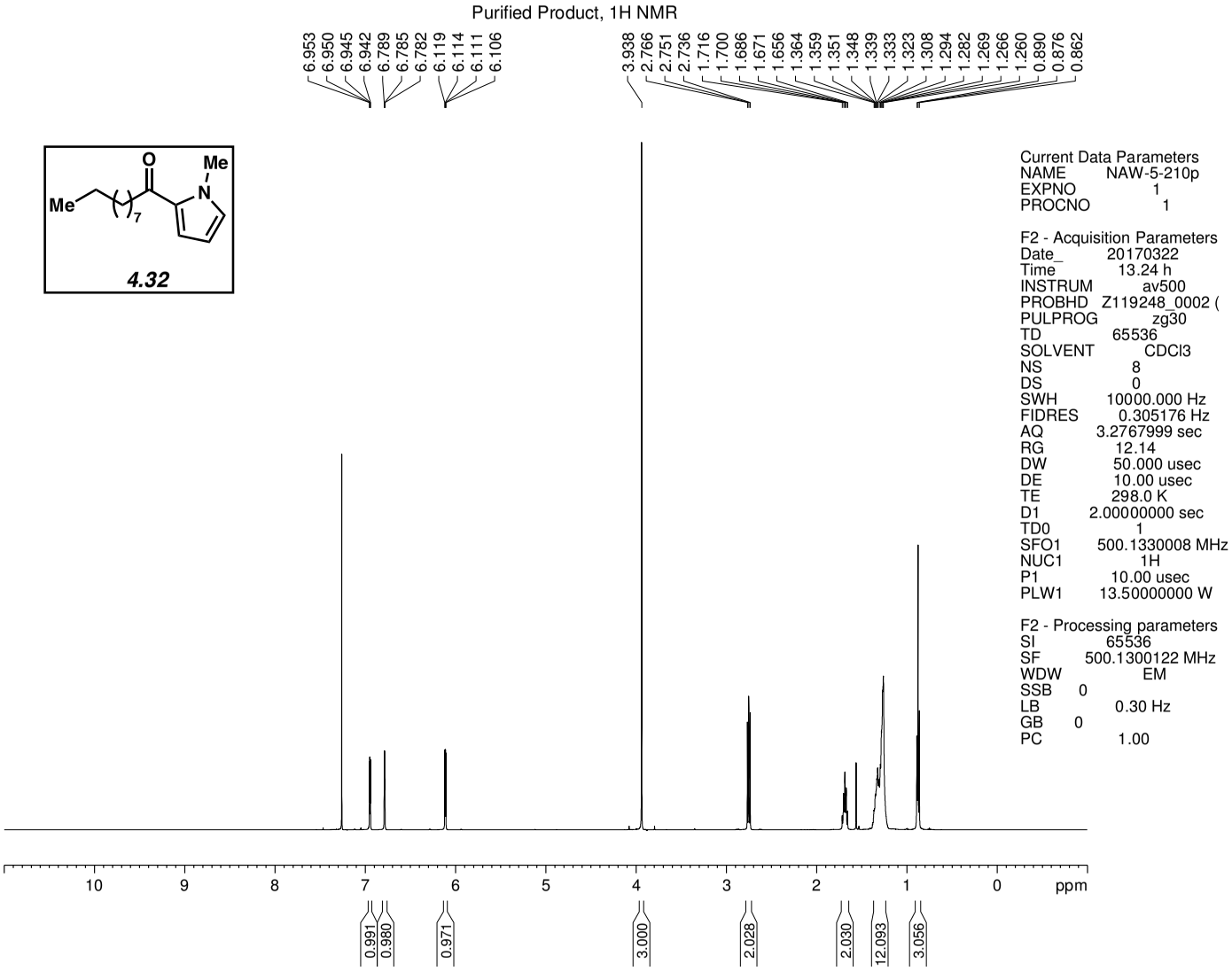

Figure 4.79 ^{1}H NMR (500 MHz, $CDCl_3$) of compound **4.32**.

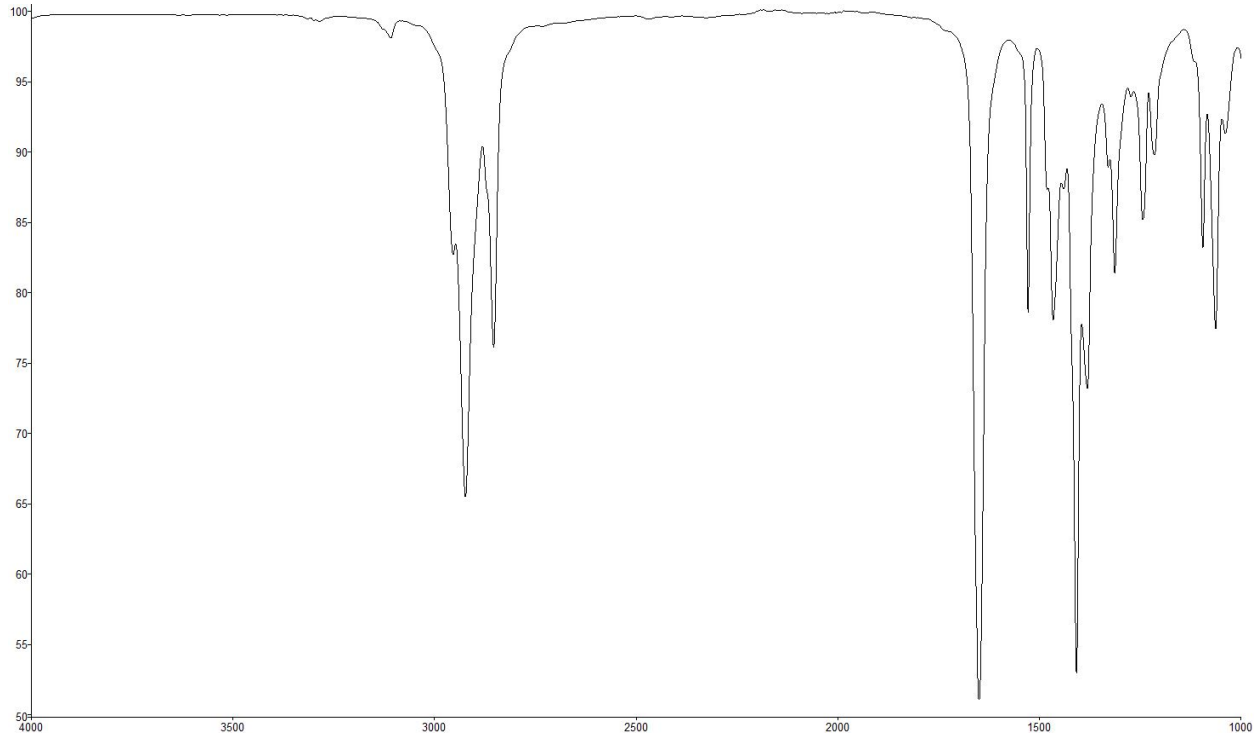

Figure 4.80 Infrared spectrum of compound **4.32**.

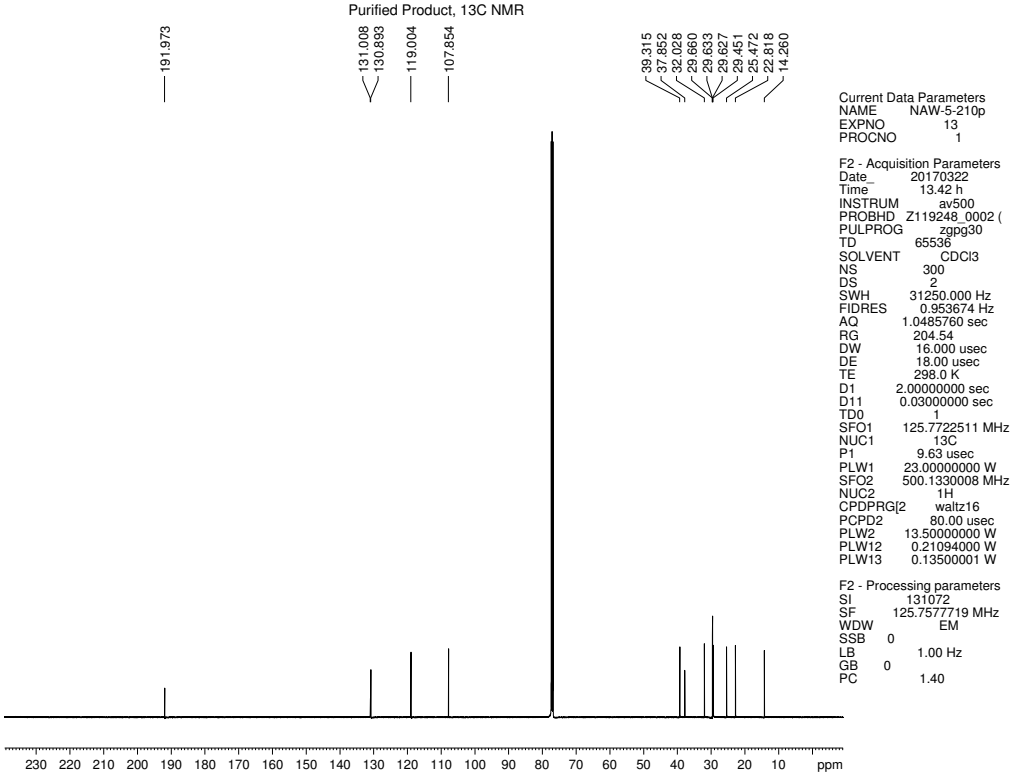

Figure 4.81 ^{13}C NMR (125 MHz, $CDCl_3$) of compound **4.32**.

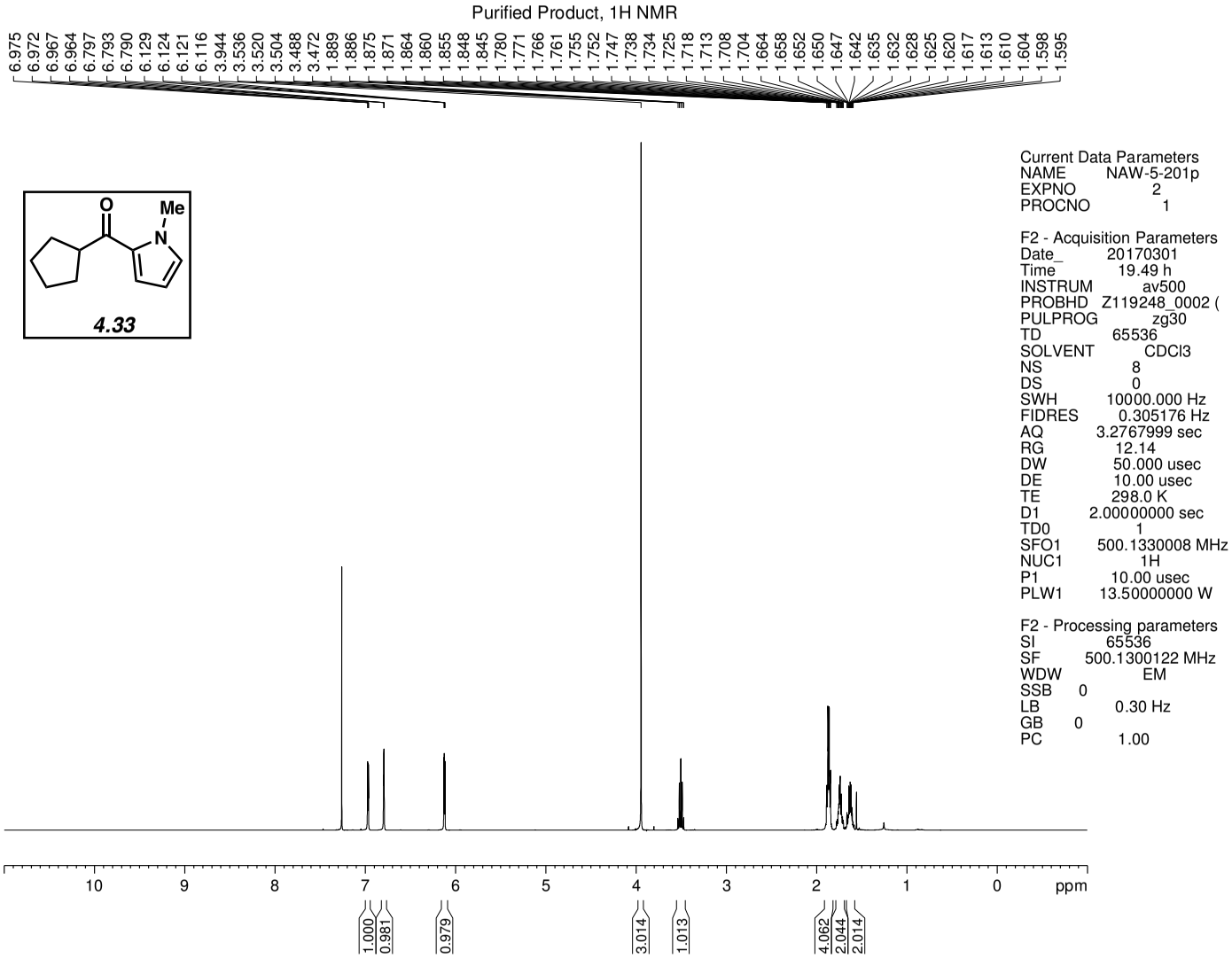

Figure 4.82 ^{1}H NMR (500 MHz, $CDCl_3$) of compound **4.33**.

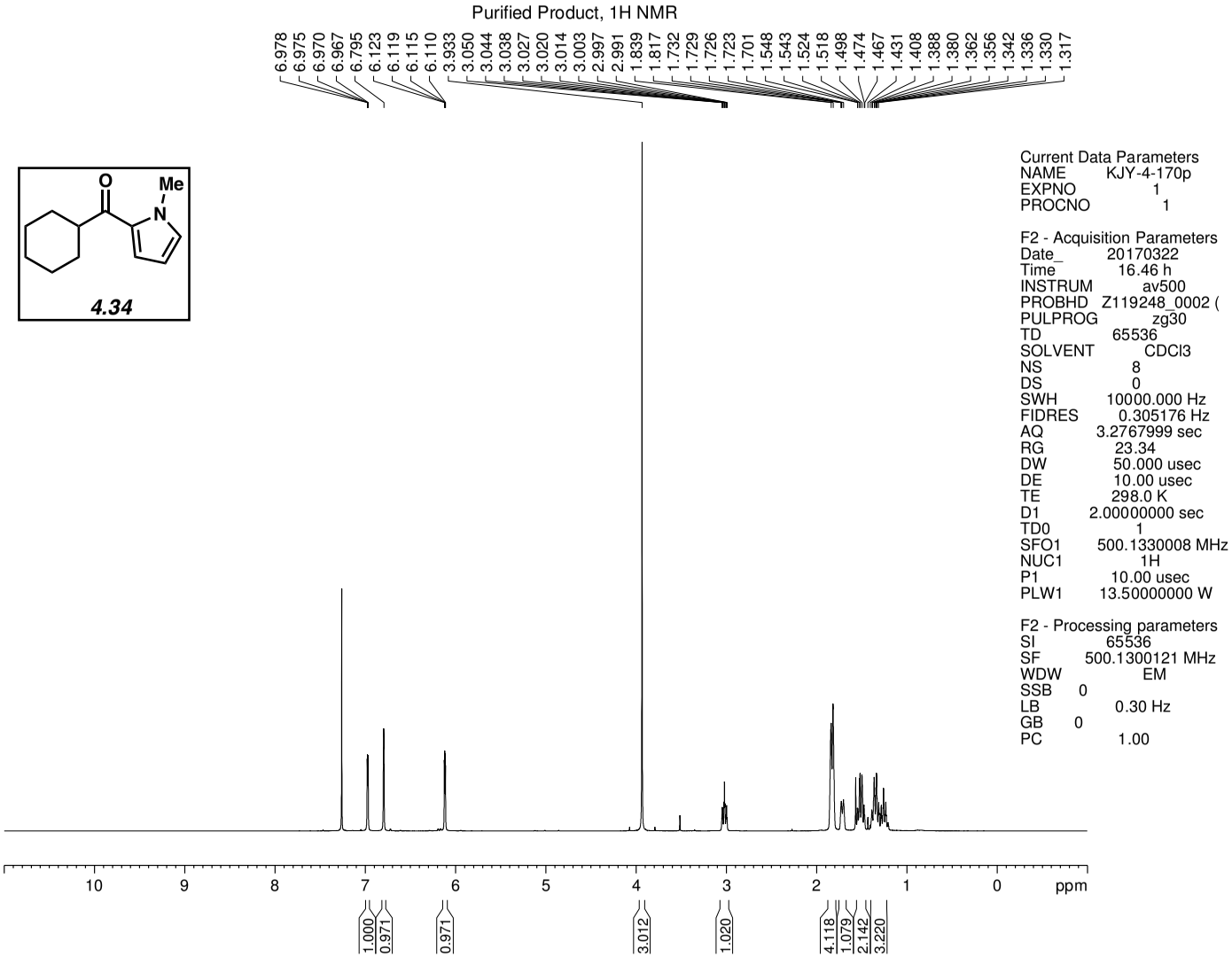

Figure 4.83 ^{1}H NMR (500 MHz, $CDCl_3$) of compound **4.34**.

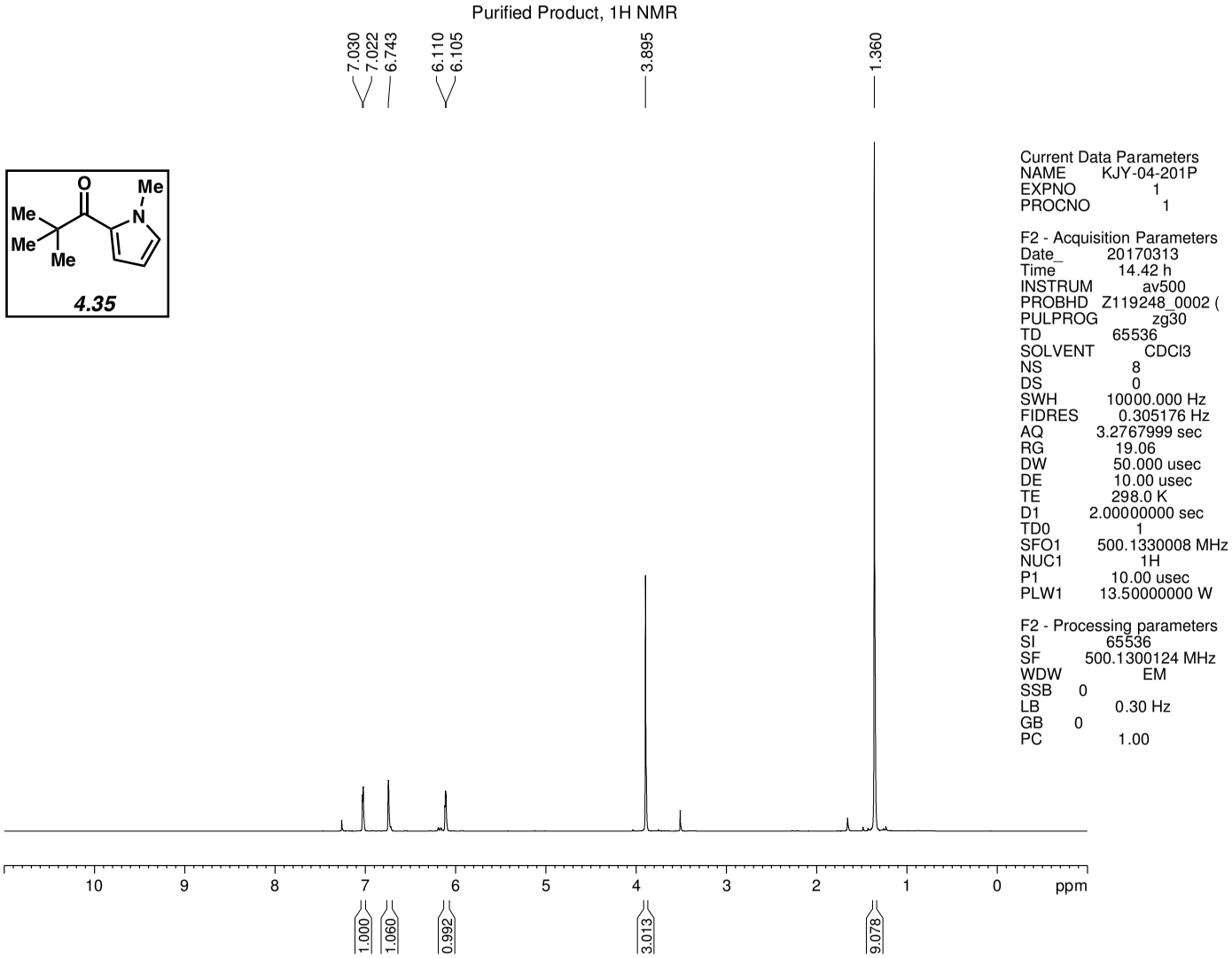

Figure 4.84 ^{1}H NMR (500 MHz, $CDCl_3$) of compound **4.35**.

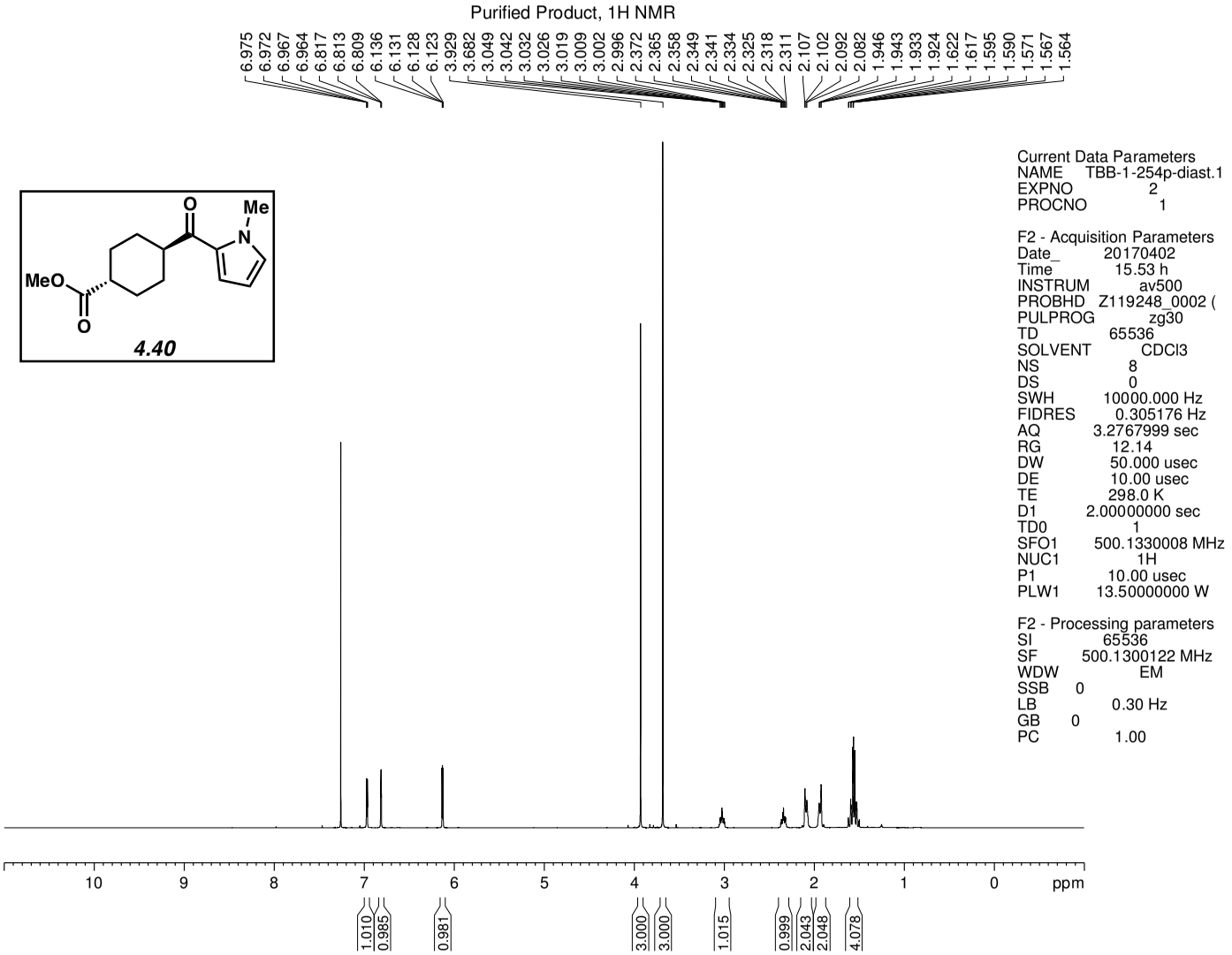

Figure 4.85 ^{1}H NMR (500 MHz, $CDCl_3$) of compound **4.40**.

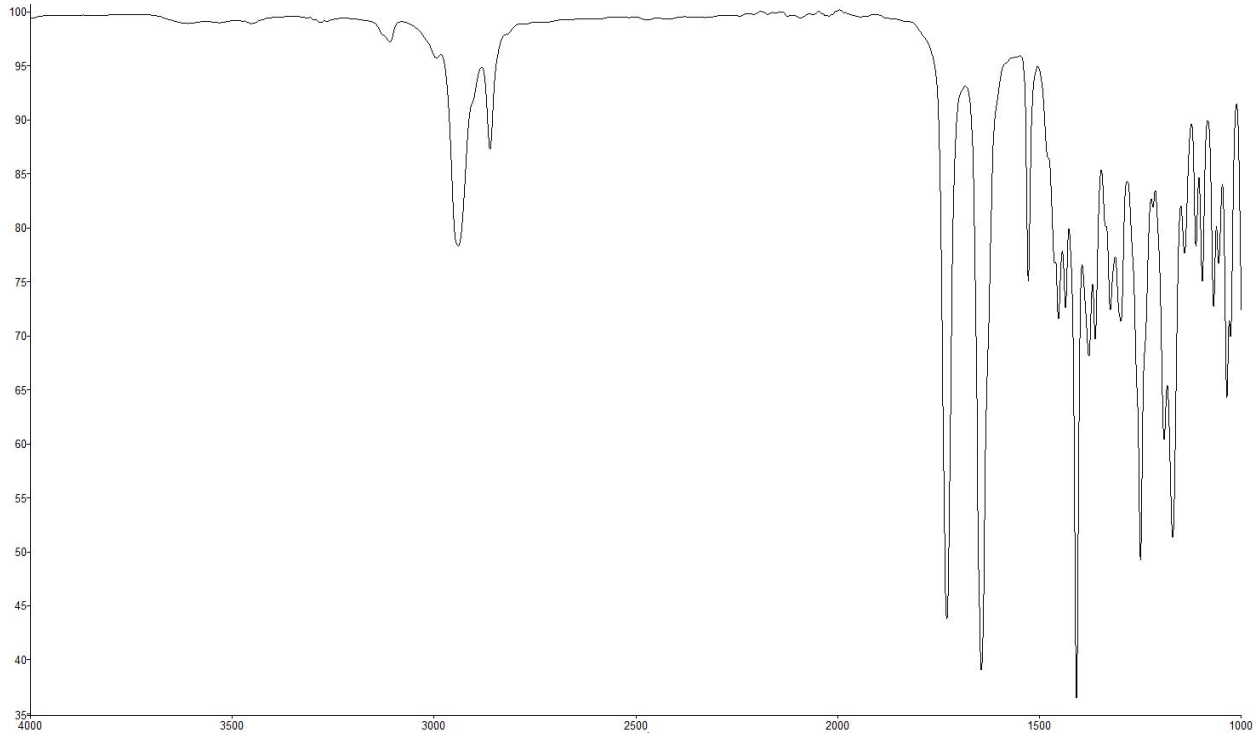

Figure 4.86 Infrared spectrum of compound **4.40**.

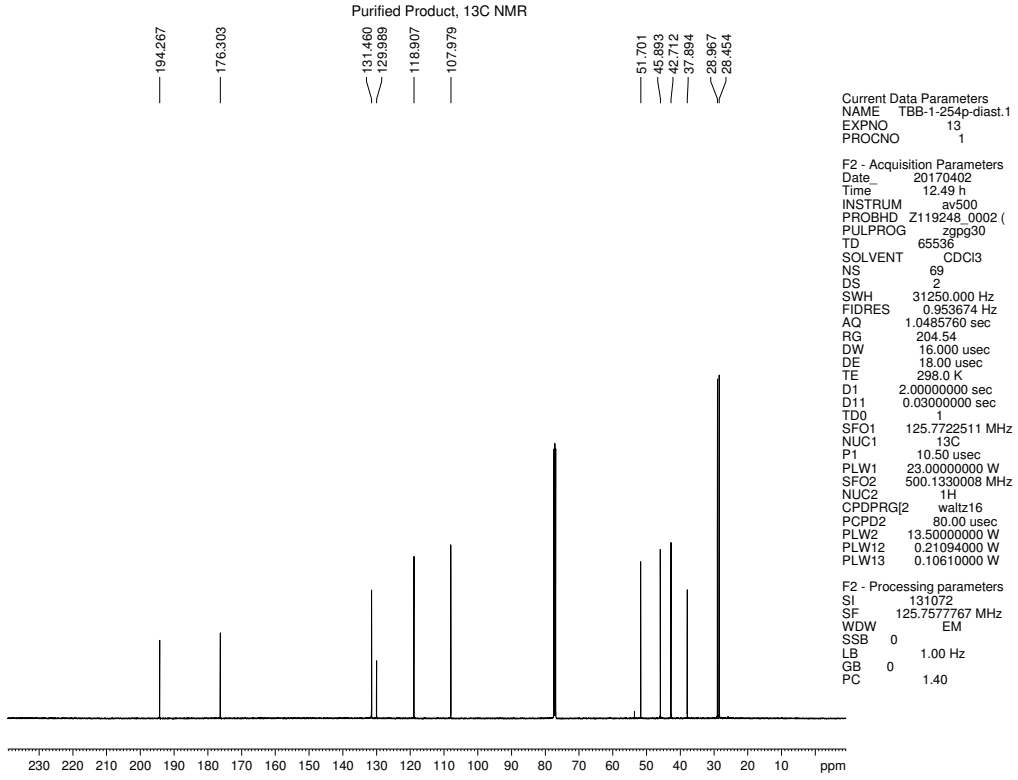

Figure 4.87 ^{13}C NMR (125 MHz, $CDCl_3$) of compound **4.40**.

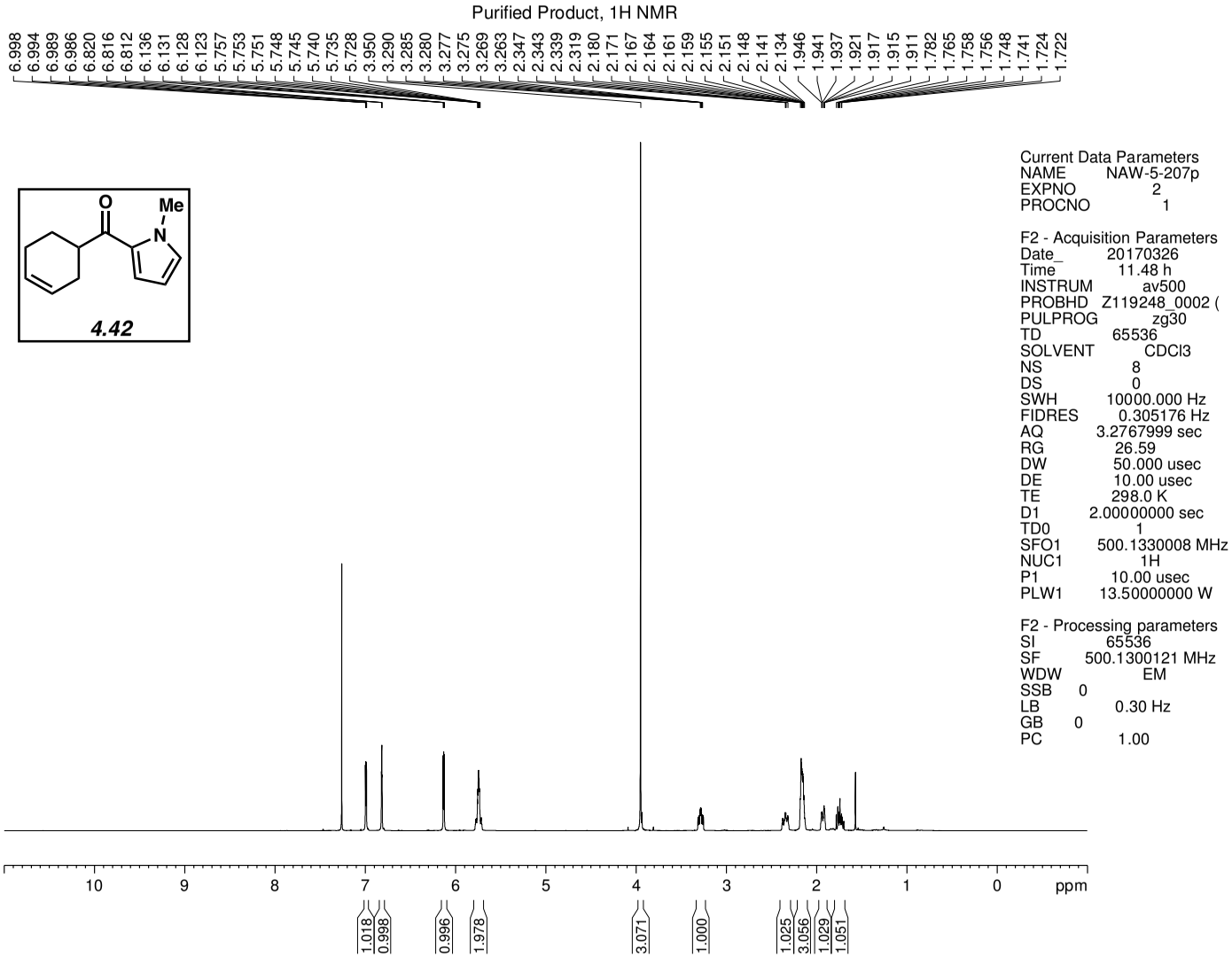

Figure 4.88 ^{1}H NMR (500 MHz, $CDCl_3$) of compound **4.42**.

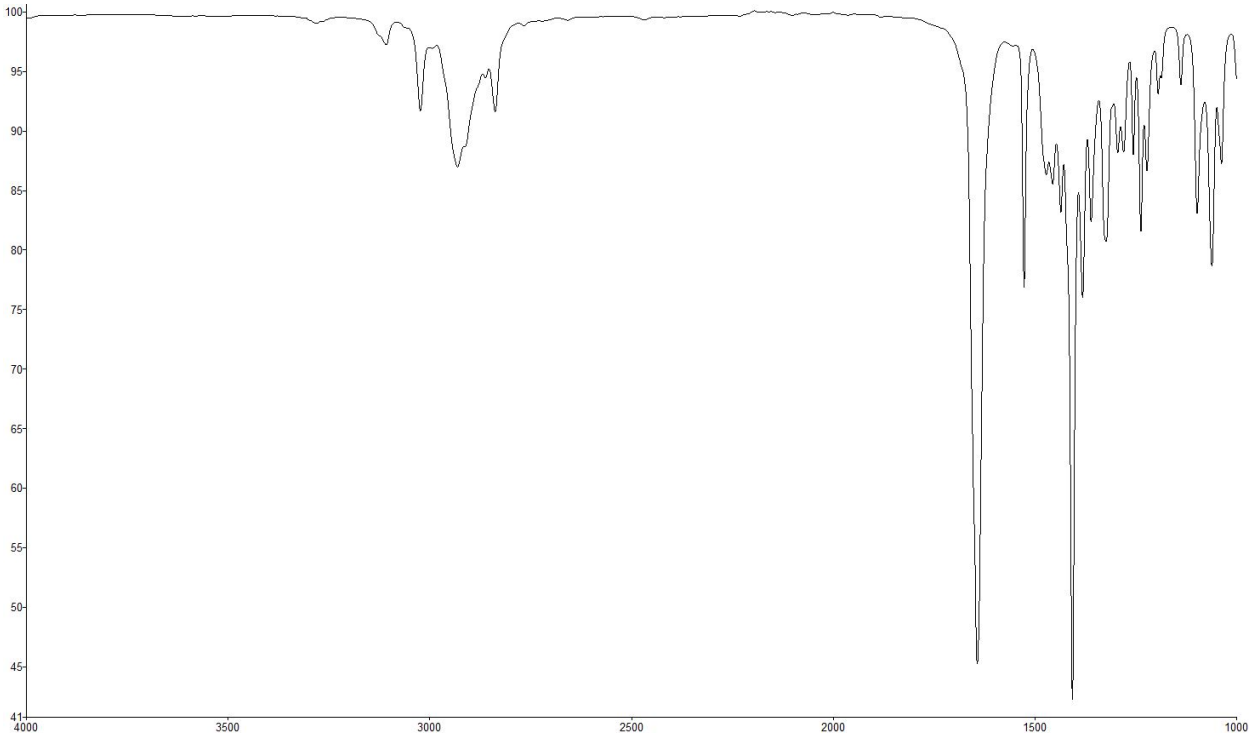

Figure 4.89 Infrared spectrum of compound **4.42**.

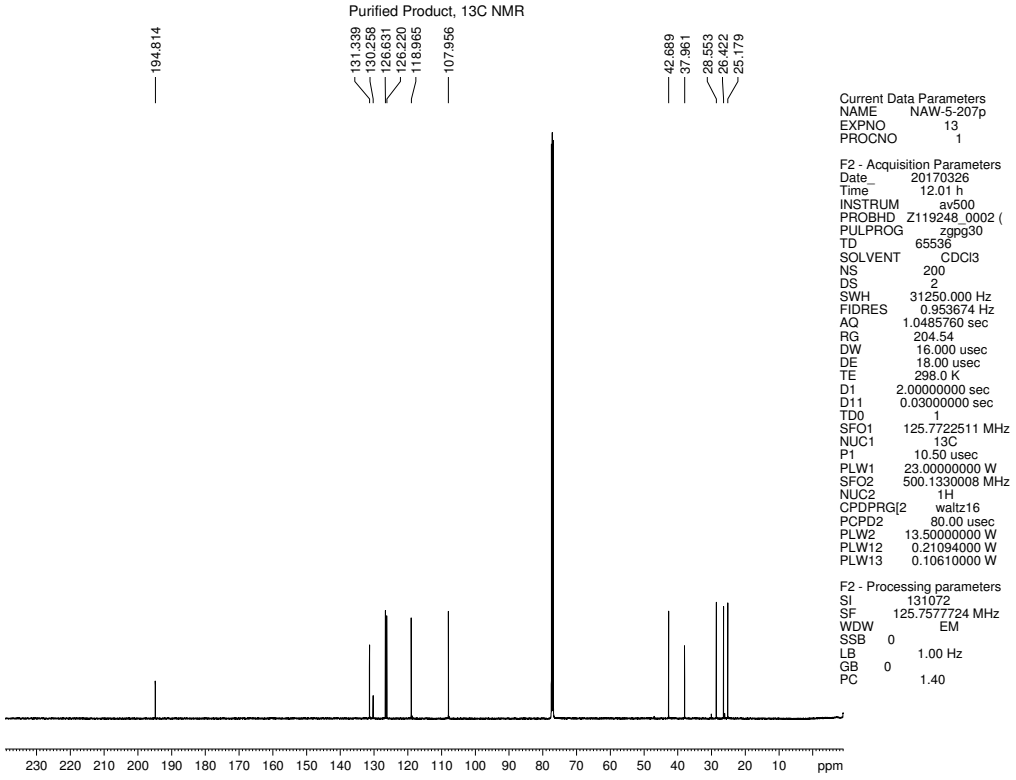

Figure 4.90 ^{13}C NMR (125 MHz, $CDCl_3$) of compound **4.42**.

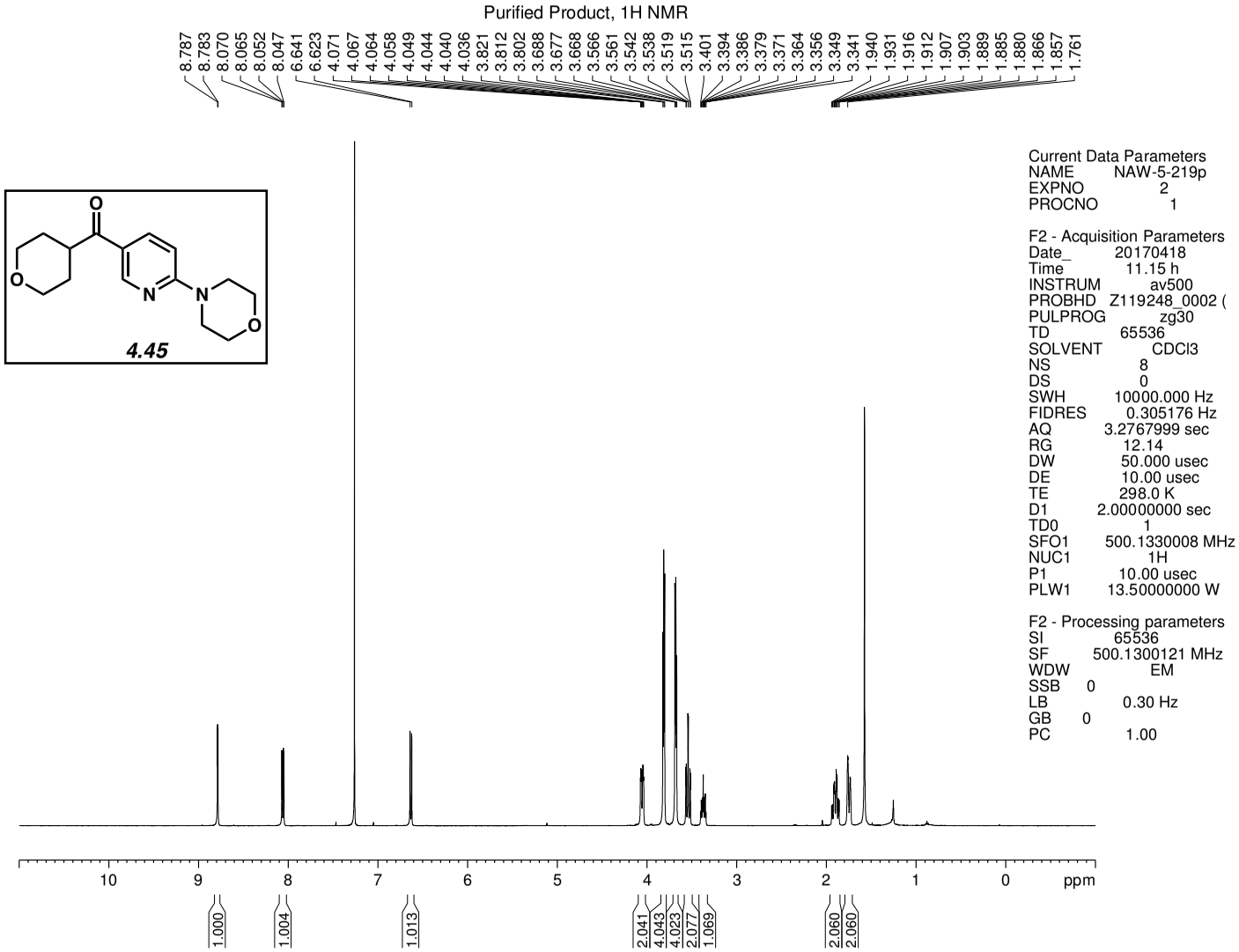

Figure 4.91 ^{1}H NMR (500 MHz, $CDCl_3$) of compound **4.45**.

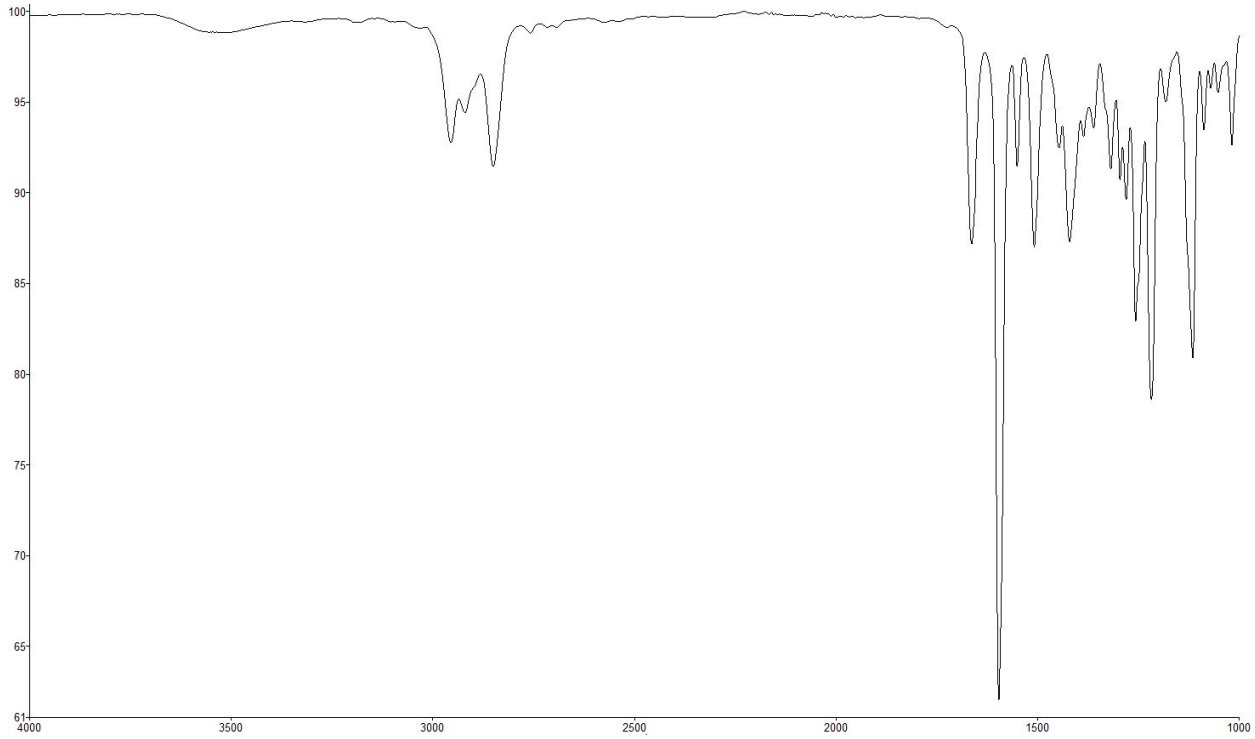

Figure 4.92 Infrared spectrum of compound **4.45**.

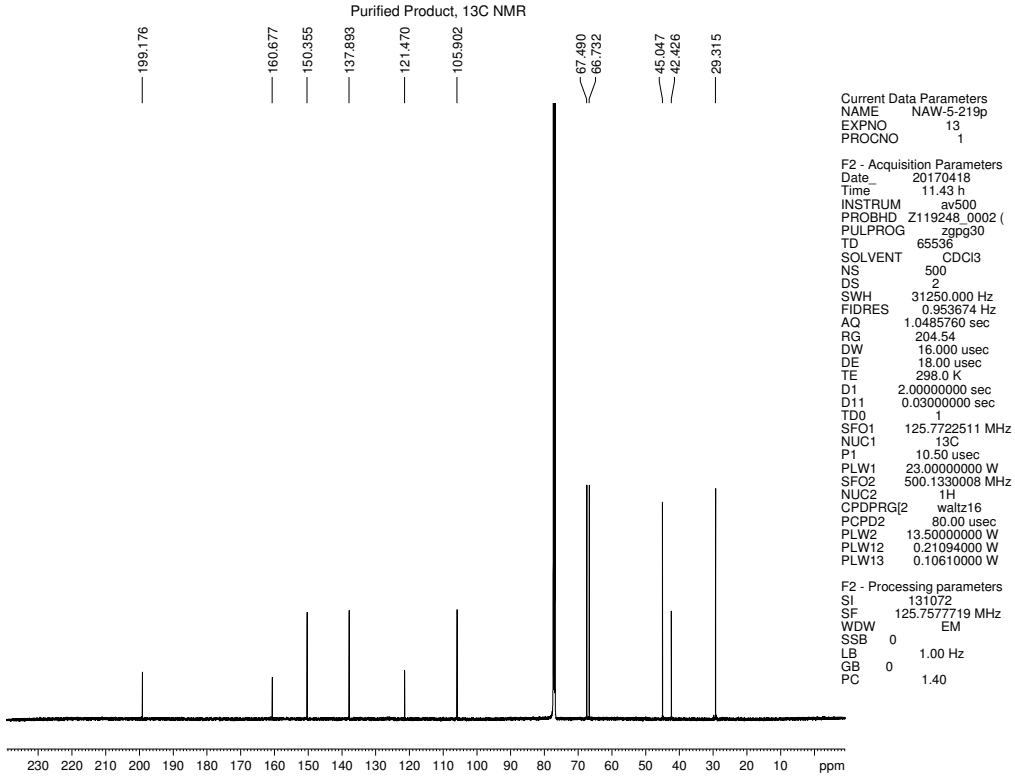

Figure 4.93 ^{13}C NMR (125 MHz, $CDCl_3$) of compound **4.45**.

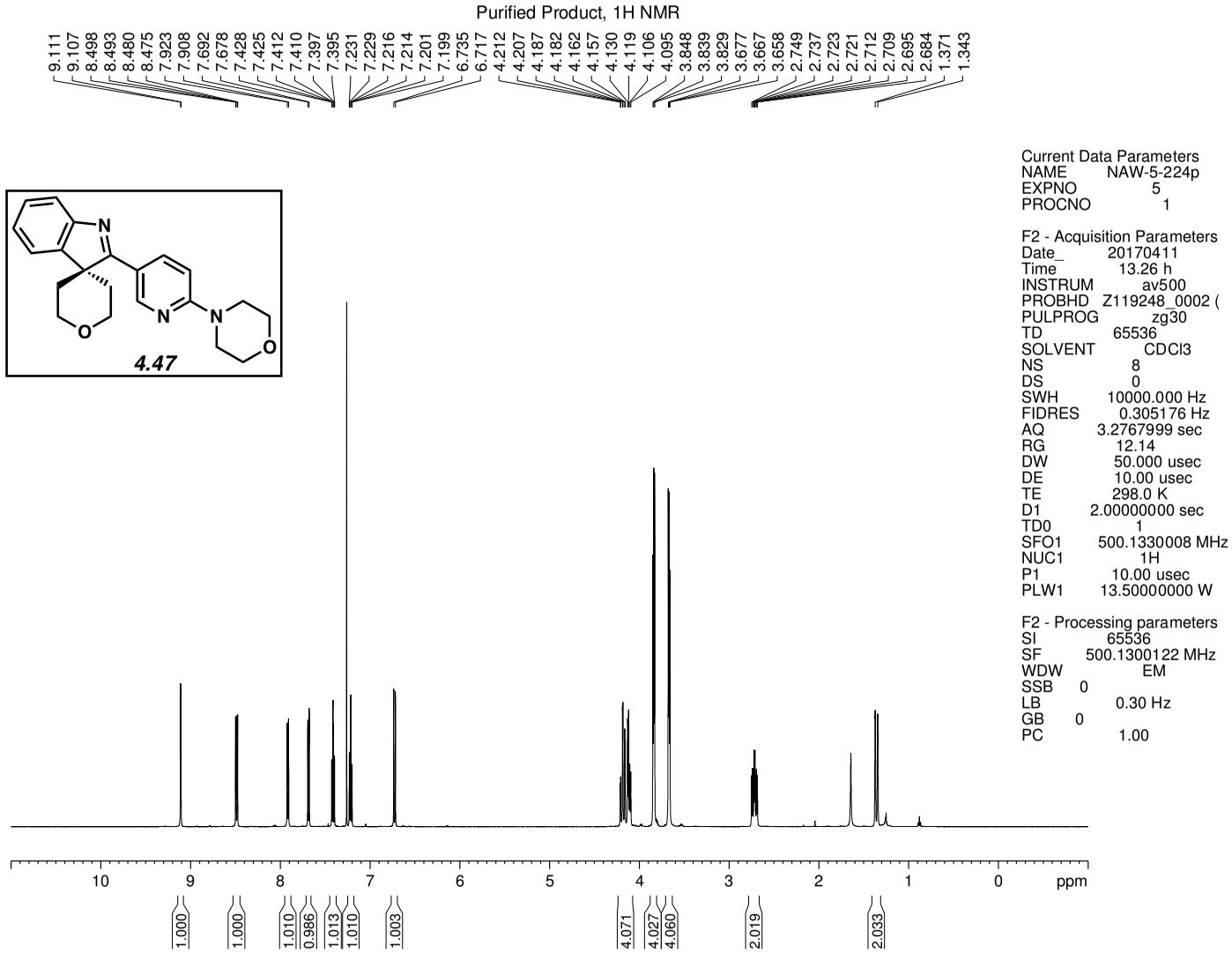

Figure 4.94 ^{1}H NMR (500 MHz, $CDCl_3$) of compound **4.47**.

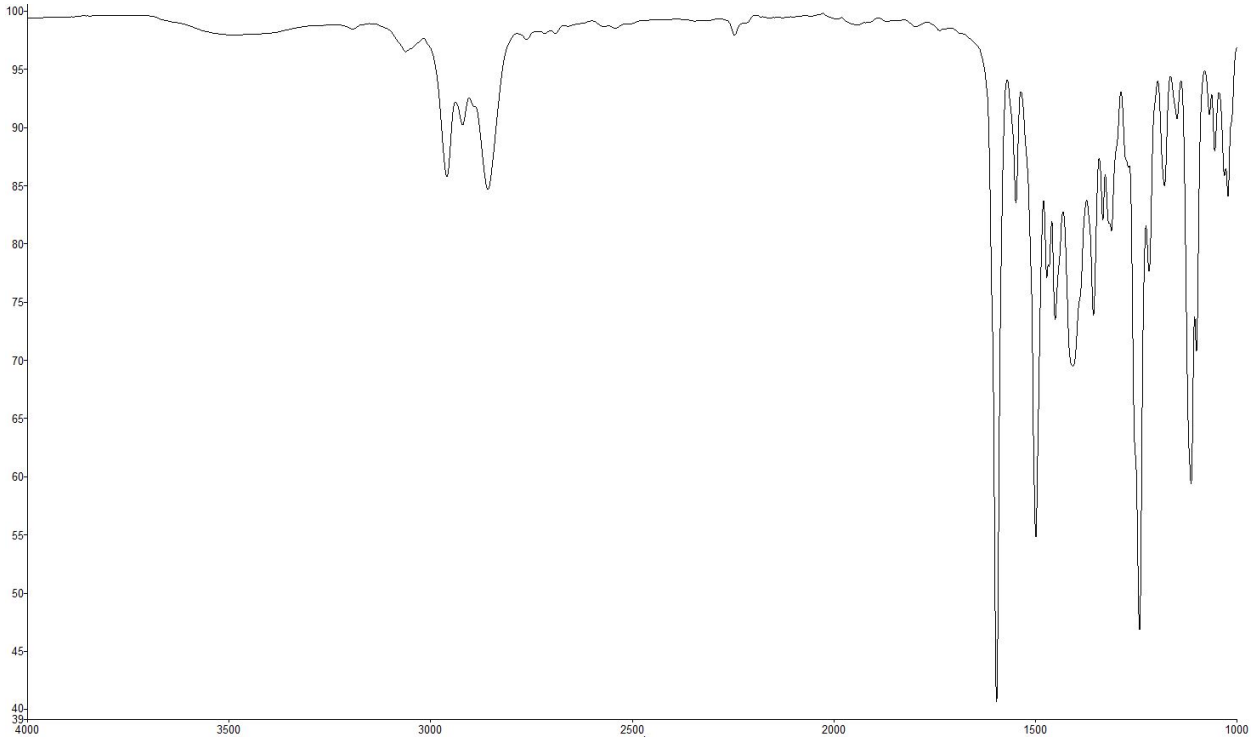

Figure 4.95 Infrared spectrum of compound **4.47**.

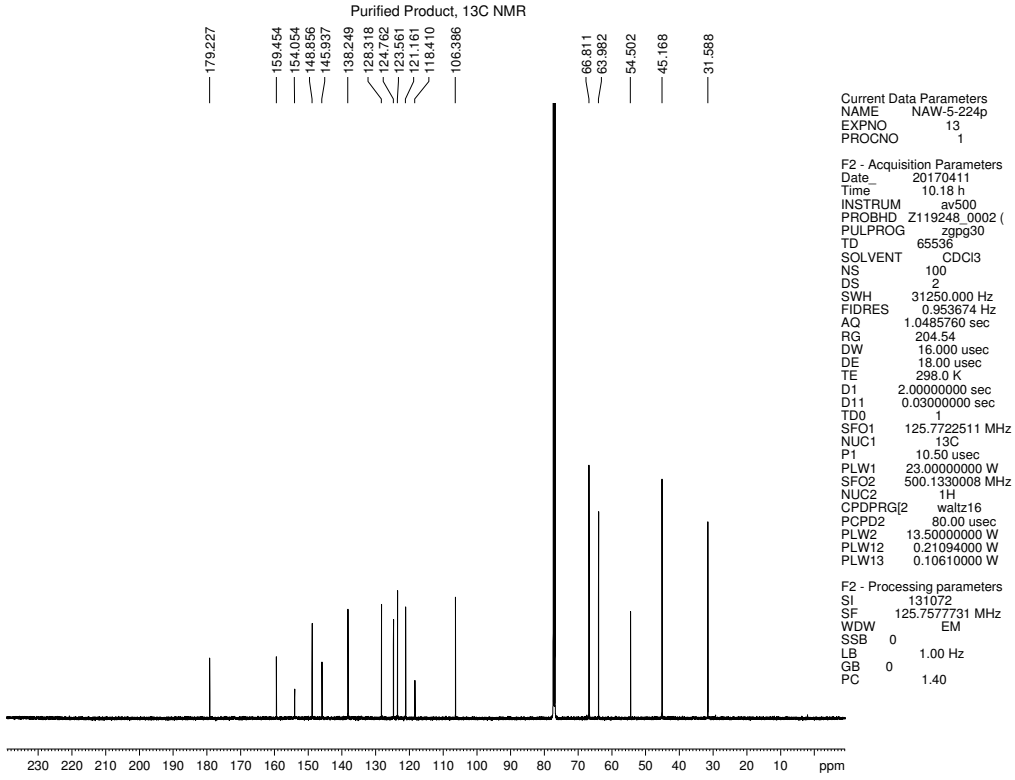

Figure 4.96 ^{13}C NMR (125 MHz, $CDCl_3$) of compound **4.47**.

4.12 Notes and References

(1) (a) Miyaura, N. In *Metal-Catalyzed Cross-Coupling Reactions*, 2nd ed.; de Meijere, A.; Diederich, F., Eds.; Wiley-VCH: Weinheim, 2004; Vol. 1, p. v–vi, 41. (b) Kotschy, A.; Timári, T. *Heterocycles from Transition Metal Catalysis: Formation and Functionalization*; Springer: Dordrecht, 2005; p 176. (c) Littke, A. In *Modern Arylation Methods*; Ackermann, L., Ed.; Wiley-VCH: Weinheim, 2009; p 29. (d) Schröter, S.; Stock, C.; Bach, T. *Tetrahedron* **2005**, *61*, 2245–2267.

(2) Recently, Szostak and Newman independently reported the Pd-catalyzed Suzuki–Miyaura coupling of phenol-derived esters. Both methods are highly focused on aryl esters, although four examples involving non-branched aliphatic substrates were disclosed in total between the two studies. One example utilizing an a-branched substrate was reported, albeit with some challenges noted by Newman. (a) Halima, T. B.; Zhang, W.; Yalaoui, T.; Hong, X.; Yang, Y.-F.; Houk, K. N.; Newman, S. G. *J. Am. Chem. Soc.* **2017**, *139*, 1311–1318. (b) Lei, R.; Meng, G.; Shi, S.; Ling, Y.; An, J.; Szostak, R.; Szostak, M. *Chem. Sci*. **2017**, *8*, 6525–6530.

(3) For additional non-decarbonylative transition metal-catalyzed reactions involving cleavage of the ester C–O bond, see: (a) Tatamidani, H.; Kakiuchi, F.; Chatani, N. *Org. Lett.* **2004**, *6*, 3597–3599. (b) Hie, L.; Fine Nathel, N. F.; Hong, X.; Yang, Y.-F.; Houk, K. N.; Garg, N. K. *Angew. Chem., Int. Ed.* **2016**, *55*, 2810–2814. (c) Yu, B.; Sun, H.; Xie, Z.; Zhang, G.; Xu, L.-W.; Zhang, W.; Gao, Z. *Org. Lett.* **2015**, *17*, 3298–3301. (d) LaBerge, N. A.; Love, J. A. *Eur. J. Org. Chem.* **2015,** 5546–5553. (e) Tatamidani, H.; Yokota, K.; Kakiuchi, F.; Chatani, N. *J. Org. Chem.* **2004**, *69*, 5615–5621. (f) Desnoyer, A. N.; Friese, F. W.; Chiu,

W.; Drover, M. W.; Patrick, B. O.; Love, J. A. *Chem. Eur. J.* **2016**, *22*, 4070–4077. (g) Shi, S.; Szostak, M. *Organometallics* **2017**, *36*, 3784–3789. (h) Dardir, A. H.; Melvin, P. R.; Davis, R. M.; Hazari, N.; Beromi, M. M. *J. Org. Chem*. **2018**, *83*, 469–477. (i) For a recent review, see: Takise, R.; Muto, K.; Yamaguchi, J. *Chem. Soc. Rev.* **2017**, *46*, 5864–5888.

(4) For nickel-catalyzed reactions involving cleavage of the amide C–N bond, see: (a) Hie, L.; Fine Nathel, N. F.; Shah, T.; Baker, E. L.; Hong, X.; Yang, Y.-F.; Liu, P.; Houk, K. N.; Garg, N. K. *Nature* **2015**, *524*, 79–83. (b) Weires, N. A.; Baker, E. L.; Garg, N. K. *Nat. Chem*. **2016**, *8*, 75–79. (c) Baker, E. L.; Yamano, M. M.; Zhou, Y.; Anthony, S. M.; Garg, N. K. *Nat. Commun*. **2016**, *7*, 11554–11558. (d) Simmons, B. J.; Weires, N. A.; Dander, J. E.; Garg, N. K. *ACS Catal*. **2016**, *6*, 3176–3179. (e) Dander, J. E.; Weires, N. A.; Garg, N. K. *Org. Lett*. **2016**, *18*, 3934–3936. (f) Shi, S.; Szostak, M. *Org. Lett.* **2016**, *18*, 5872–5875. (g) Shi, S.; Szostak, M. *Chem. Eur. J.* **2016**, *22*, 10420–10424. (h) Hie, L.; Baker, E. L.; Anthony, S. M.; Desrosiers, J.-N.; Senanayake, C.; Garg, N. K. *Angew. Chem., Int. Ed.* **2016**, *55*, 15129–15132. (i) Dey, A.; Sasmal, S.; Seth, K.; Lahiri, G. K.; Maiti, D. *ACS Catal.* **2017**, *7*, 433–437. (j) Ni, S.; Zhang, W.; Mei, H.; Han, J.; Pan, Y. *Org. Lett.* **2017**, *19*, 2536–2539. (k) Medina, J. M.; Moreno, J.; Racine, S.; Du, S.; Garg, N. K. *Angew. Chem., Int. Ed.* **2017**, *56*, 6567–6571. (l) Hu, J.; Wang, M.; Pu, X.; Shi, Z. *Nat. Commun.* **2017**, *8*, 14993–14999. (m) Weires, N. A.; Caspi, D. D.; Garg, N. K. *ACS Catal.* **2017**, *7*, 4381–4385. (n) Shi, S.; Szostak, M. *Synthesis* **2017**, *49*, 3602–3608. (o) Dander, J. E.; Baker, E. L.; Garg, N. K. *Chem. Sci.* **2017**, *8*, 6433–6438. (p) For a recent review, see: Dander, J. E.; Garg, N. K. *ACS Catal.* **2017**, *7*, 1413–1423.

(5) For nickel-catalyzed decarbonylative coupling reactions of amides, see: (a) Shi, S.; Meng, G.; Szostak, M. *Angew. Chem., Int. Ed.* **2016**, *55*, 6959–6963. (b) Hu, J.; Zhao, Y.; Liu, J.; Zhang, Y.; Shi, Z. *Angew. Chem., Int. Ed.* **2016**, *55*, 8718–8722. (c) Srimontree, W.; Chatupheeraphat, A.; Liao, H.-H.; Rueping, M. *Org. Lett*. **2017**, *19*, 3091–3094. (d) Liu, C.; Szostak, M. *Angew. Chem., Int. Ed.* **2017**, *56*, 12718–12722. (e) Yue, H.; Guo, L.; Liao, H.-H.; Cai, Y.; Zhu, C.; Rueping, M. *Angew. Chem., Int. Ed.* **2017**, *56*, 4282–4285. (f) Chatupheeraphat, A.; Liao, H.-H.; Lee, S.-C.; Rueping, M. *Org. Lett.* **2017**, *19*, 4255–4258. (g) Yue, H.; Guo, L.; Lee, S.-C.; Liu, X.; Rueping, M. *Angew. Chem., Int. Ed.* **2017**, *56*, 3972–3976. (h) Hu, J.; Wang, M.; Pu, X.; Shi, Z. *Nat. Commun.* **2017**, *8*, 14993–14999.

(6) For palladium-catalyzed C–C bond forming reactions of amides, see: (a) Li, X.; Zou, G. *Chem. Commun.* **2015**, *51*, 5089–5092. (b) Yada, A.; Okajima, S.; Murakami, M. *J. Am. Chem. Soc.* **2015**, 137, 8708–8711. (c) Meng, G.; Szostak, M. *Org. Biomol. Chem*. **2016**, *14*, 5690–5705. (d) Meng, G.; Szotak, M. *Angew. Chem., Int. Ed.* **2015**, *54*, 14518–14522. (e) Meng, G.; Szostak, M. *Org. Lett*. **2015**, *17*, 4364–4367. (f) Liu, C.; Meng, G.; Liu, Y.; Liu, R.; Lalancette, R.; Szostak, R.; Szostak, M. *Org. Lett.* **2016**, *18*, 4194–4197. (g) Lei, P.; Meng, G.; Szostak, M. *ACS Catal.* **2017**, *7*, 1960–1965. (h) Liu, C.; Liu, Y.; Liu, R.; Lalancette, R.; Szostak, R.; Szostak, M. *Org. Lett.* **2017**, *19*, 1434–1437. (i) Liu, C.; Meng, G.; Szostak, M. *J. Org. Chem.* **2016**, *81*, 12023–12030. (j) Meng, G.; Shi, S.; Szostak, M. *ACS Catal.* **2016**, *6*, 7335–7339. (k) Cui, M.; Wu, H.; Jian, J.; Wang, H.; Liu, C.; Stelck, D.; Zeng, Z. *Chem. Commun.* **2016**, *52*, 12076–12079. (l) Wu, H.; Li, Y.; Cui, M.; Jian, J.; Zeng, Z. *Adv. Synth. Catal.* **2016**, *358*, 3876–3880. (m) Shi, S.; Szostak, M. *Org. Lett*. **2017**, *19,* 3095–3098. (n) Lei, P.; Meng, G.; Ling, Y.; An, J.; Szostak, M. *J. Org. Chem.* **2017**, 82,

6638–6646. (o) Meng, G.; Szostak, R.; Szostak, M. *Org. Lett*. **2017**, *19*, 3596–3599. (p) Meng, G.; Lalancette, R.; Szostak, R.; Szostak, M. *Org. Lett.* **2017***, 19*, 4656–4659. (q) Osumi, Y.; Szostak, M. *Org. Biomol. Chem*. **2017**, *15*, 8867–8871. (r) Lei, P.; Meng, G.; Ling, Y.; An, J.; Nolan, S. P.; Szostak, M. *Org. Lett.* **2017**, *19*, 6510–6513.

(7) For examples of Pd-catalyzed Suzuki–Miyaura coupling of aliphatic amides, see: Li, X.; Zou, G. *J. Organomet. Chem*. **2015**, *794*, 136–145.

(8) The field of nickel-catalyzed cross-couplings itself has gained tremendous interest in recent years due not only to the high natural abundance, low cost, and low CO_2 footprint of nickel, but also because of its ability to effect new or challenging transformations, including those involving activation of the amide C–N bond. For pertinent reviews on nickel catalysis, see: (a) Rosen, B. M.; Quasdorf, K. W.; Wilson, D. A.; Zhang, N.; Resmerita, A.-M.; Garg, N. K.; Percec, V. *Chem. Rev*. **2011**, *111*, 1346−1416. (b) Tasker, S. Z.; Standley, E. A.; Jamison, T. F. *Nature* **2014**, *509*, 299−309. (c) Mesganaw, T.; Garg, N. K. *Org. Process Res. Dev.* **2013**, *17*, 29−39. (d) Ananikov, V. P. *ACS Catal*. **2015**, *5*, 1964−1971.

(9) Amani, J.; Alam, R.; Badir, S.; Molander, G. A. *Org. Lett.* **2017**, *19*, 2426–2429.

(10) Nahm, S.; Weinreb, S. M. *Tetrahedron Lett.* **1981**, *22*, 3815–3818.

(11) As Molander's methodology utilizes *alkyl* boron reagents (see ref 9), and ours uses *aryl* boron reagents, the two methods offer different strategic approaches to access ketone products.

(12) The less activated *N*-Bn,Boc amides used in the present study are not competent substrates in the Ir/Ni photoredox-mediated couplings of *N*-acyl succinimides (see ref 9).

(13) (a) Gooßen, L. J.; Ghosh, K. *Angew. Chem., Int. Ed.* **2001**, *40*, 3458–3460. (b) Gooßen, L. J.; Ghosh, K. *Eur. J. Org. Chem.* **2002**, 3254–3257. (c) Yang, H.; Li, H.; Wittenberg, R.; Egi, M.; Huang, W.; Liebeskind, L. S. *J. Am. Chem. Soc.* **2007**, *129*, 1132–1140. (d) Lovell, K. M.; Vasiljevik, T.; Araya, J. J.; Lozama, A.; Prevatt-Smith, K. M; Day, V. W.; Dersch, C. M.; Rothman, R. B.; Butelman, E. R.; Kreek, M. J.; Prisinzano, T. E. *Bioorg. Med. Chem.* **2012**, *20*, 3100–3110. (e) Haddach, M.; McCarthy, J. R. *Tetrahedron Lett.* **1999**, *40*, 3109–3112. (f) Nique, F.; Hebbe, S.; Triballeau, N.; Peixoto, C.; Lefrancois, J.-M.; Jary, H.; Alvey, L.; Manioc, M.; Housseman, C.; Klaassen, H.; Van Beeck, K.; Guedin, D.; Namour, F.; Minet, D.; Van Der Aar, E.; Feyen, J.; Fletcher, S.; Blanque, R.; Robin-Jagerschmidt, C.; Deprez, P. *J. Med. Chem.* **2012**, *55*, 8236–8247.

(14) The *N*-Bn,Boc amide derivatives employed in this study can be readily prepared from the corresponding carboxylic acids (i.e., benzyl amide formation, followed by treatment with Boc_2O) or directly from acid chlorides (i.e., using HN(Bn)Boc).

(15) For use of the Ni/ICy system in the Stille coupling of quaternary ammonium salts, see: Wang, D.-Y.; Kawahata, M.; Yang, Z.-K.; Miyamoto, K.; Komagawa, S.; Yamaguchi, K.; Wang, C.; Uchiyama, M. *Nat. Commun*. **2016**, *7*, 12937–12945.

(16) We attribute the improved competency of ligand **4.10** to its electron-rich nature, which ultimately renders oxidative addition more facile. For discussion of NHC ligands in transition metal catalysis, see: Hopkinson, M. N.; Richter, C.; Schedler, M.; Glorius, F. *Nature* **2014**, *510*, 485–496.

(17) For the relative nucleophilicities of substituted aryl boronates, see: (a) Barder, T. E.; Walker, S. D.; Martinelli, J. R.; Buchwald, S. L.; *J. Am. Chem. Soc.* **2005**, *127*, 4685–4696. (b) Billingsley, K. L.; Buchwald, S. L. *Angew. Chem., Int. Ed.* **2008**, *47*, 4695–4698.

(18) The underpinnings behind the modest catalyst turnover (i.e., Figure 4.4, entries 2 and 3) is not presently understood.

(19) In addition to esters, ketones, tertiary alcohols, secondary amides, carboxylic acids, and epoxides are tolerated in this methodology, as determined by a robustness screen (see Table 4.4).

(20) For bioactive spiroindolenines, see: (a) Weisbach, J. A.; Macko, E.; De Sanctis, N. J.; Cava, M. P.; Douglas, B. *J. Med. Chem*. **1964**, *7*, 735–739. (b) Fourtillan, J.-B.; Violeau, B.; Karam, O.; Jouannetaud, M.-P.; Fourtillan, M.; Jacquesy, J.-C. *Melatoninergic Agonist Spiro[indolepyrrolidine] Derivatives, Process for Their Preparation and Their Use as Medicinal Products*, 1998, US576347. (c) Chowdhury, S.; Fu, J.; Liu, S.; Qi, J. *Spiro-Condensed Indole Derivatives as Sodium Channel Inhibitors*, 2010, WO2010/53998. (d) Li, X.-N.; Cai, X.-H.; Feng, T.; Li, Y.; Liu, Y.-P.; Luo, X.-D. *J. Nat. Prod*. **2011**, *74*, 1073–1078. (e) Xu, Y.-J.; Pieters, L. *Mini. Rev. Med. Chem*. **2013**, *13*, 1056–1072. (f) Sweis, R. F.; Pliushchev, M.; Brown, P. J.; Guo, J.; Li, F.; Maag, D.; Petros, A. M.; Soni, N. B.; Tse, C.; Vedadi, M.; Michaelides, M. R.; Chiang, G. G.; Pappano, W. N. *ACS Med. Chem. Lett*. **2014**, *5*, 205–209.

(21) (a) Manske, R. H. F. *The Alkaloids, Chemistry and Physiology*, Academic Press, New York, 1981. (b) Cordell, G. A. *The Alkaloids: Chemistry and Biology*, Academic Press, San Diego, 1998. (c) Chadha, N.; Silakari, O. *Eur. J. Med. Chem.* **2017**, *134*, 159–184.

(22) For the classic Fischer indole synthesis, see: (a) Fischer, E.; Jourdan, F. *Ber. Dtsch. Chem. Ges.* **1883**, *16*, 2241−2245. (b) Fischer, E.; Hess, O.; *Ber. Dtsch. Chem. Ges.* **1884**, *17*, 559−568.

(23) Indolino-spirotetrahydropyrans have been pursued as kinase inhibitors of the P13K-Akt pathway, ion channel modulators, 5-HT_{2c} receptor agonists, HDAC inhibitors, and inhibitors of CMV DNA polymerase. (a) Gonzalez-Lopez de Turiso, F.; Shin, Y.; Brown, M.; Cardozo, M.; Chen, Y.; Fong, D.; Hao, X.; He, X.; Henne, K.; Hu, Y.-L.; Johnson, M. G.; Kohn, T.; Lohman, J.; McBride, H. J.; McGee, L. R.; Medina, J. C.; Metz, D.; Miner, K.; Mohn, D; Pattaropong, V.; Seganish, J.; Simard, J. L.; Wannberg, S.; Whittington, D. A.; Yu, G.; Cushing, T. D. *J. Med. Chem*. **2012**, 55, 7667–7685. (b) Brown, M.; Shin, Y.; Cushing, T. D.; Gonzalez-Lopez de Turiso, F.; He, X.; Kohn, T.; Lohman, J. W.; Pattaropong, V.; Seganish, J.; Shin, Y.; Simard, J. L. 2010, *Heterocyclic Compounds and Their Uses*, WO2010/151737. (c) Chen, G.; Cushing, T. D.; Fisher, B.; He, X.; Li, K.; Li, Z.; McGee, L. R.; Pattaropong, V.; Faulder, P.; Seganish, J. L.; Shin, Y. 2009, *Alkynyl Alcohols as Kinase Inhibitors*, WO2009/158011. (d) Padiya, K; Kamlesh, J; Nair, P. S.; Rivindra, R. R.; Chaure, G. S.; Gudade, G. B.; Parkale, S. S.; Manojkumar, V. L.; Swapnil, R. B.; Smita, A. B. *Spirocyclic Compounds as Voltage-Gated Sodium Channel Modulators*, 2012, WO2012/49555. (e) Semple, G.; Behan, D. P.; Feichtinger, K.; Glicklich, A.; Grottick, A. J.; Kam, M. M. S.; Kasem, M.; Lehmann, J.; Ren, A. S.; Schrader, T. O.; Shanahan, W. R.; Wong, A. S.-T.; Zhu, X. *5-HT_{2c} Receptor Agonists and Compositions and Methods of Use*, 2015, WO2015/66344. (f) Ng, P. Y.; Davis, H.; Bair, K. W.; Millan, D. S.; Rudintskaya, A.; Zheng, X.; Han, B.; Barczak, N.; Lancia Jr., D. *3-Spiro-7-Hydroxamic*

Acid Tetralins as HDAC Inhibitors, 2016, WO2016/168660; (g) Thibeault, C.; Rancourt, J.; Beaulieu, P. L.; Décor, A.; Grand-Maitre, C.; Kuhn, C.; Villemure, E.; Leblanc, M.; Lacoste, J.-E.; Moreau, B.; Jolicoeur, E.; Surprenant, S.; Hucke, O. *Inhibitors of Cytomegalovirus*, 2014, WO2014/70976.

(24) Fier, P. S.; Luo, J.; Hartwig, J. F. *J. Am. Chem. Soc.* **2013**, *135*, 2552–2559.

(25) Hie, L.; Baker, E. L.; Anthony, S. M.; Desrosiers, J. –N.; Senanayake, C.; Garg, N. K. *Angew. Chem., Int. Ed.* **2016**, *55*, 15129–15132.

(26) Weires, N. A.; Baker, E. L.; Garg, N. K. *Nat. Chem*. **2016**, *8*, 75–79.

(27) Dander, J. E.; Baker, E. L.; Garg, N. K. *Chem. Sci*. **2017**, *8*, 6433–6438.

(28) Allwood, D. M.; Blakemore, D. C.; Ley, S. V. *Org. Lett.* **2014**, *16*, 3064–3067.

(29) Takemiya, A.; Hartwig, J. F. *J. Am. Chem. Soc*. **2006**, *128*, 14800–14801.

(30) Bechara, W. S.; Pelletier, G.; Charette, A. B. *Nat. Chem*. **2012**, *4*, 228–234.

(31) Wakeham, R. J.; Taylor, J. E.; Bull, S. D.; Morris, J. A.; Williams, J. M. J. *Org. Lett.* **2013**, *15*, 702–705.

(32) Clerici, F.; Gelmi, M. L.; Rossi, L. M. *Synthesis* **1987**, 1025–1027.

(33) Barbero, M.; Cadamuro, S.; Degani, I.; Fochi, R.; Gatti, A.; Regondi, V. *J. Org. Chem.* **1988**, *53*, 2245–2250.

(34) Taylor, J. E.; Jones, M. D.; Williams, J. M. J.; Bull, S. D. *Org. Lett.* **2010**, *12*, 5740–5743.